

GEOLOGICA ULTRAIECTINA

Mededelingen van de  
Faculteit Aardwetenschappen  
Universiteit Utrecht

No. 153

**The depositional environment of Jurassic  
organic-rich sedimentary rocks in NW Europe.  
*A biomarker approach.***

**Heidy M.E. van Kaam-Peters**

GEOLOGICA ULTRAIECTINA

Mededelingen van de  
Faculteit Aardwetenschappen  
Universiteit Utrecht

No. 153

**The depositional environment of Jurassic  
organic-rich sedimentary rocks in NW Europe.  
*A biomarker approach.***

The depositional environment of Jurassic  
organic-rich sedimentary rocks in NW Europe.  
*A biomarker approach.*

Het afzettingsmilieu van Jurassische bitumineuze gesteenten  
in N.W. Europa.  
*Een studie met behulp van moleculaire fossielen.*

(met een samenvatting in het Nederlands)

Proefschrift ter verkrijging van de graad van doctor  
aan de Universiteit Utrecht  
op gezag van de Rector Magnificus, Prof. Dr. H.O. Voorma  
ingevolge het besluit van het College van Decanen  
in het openbaar te verdedigen  
op maandag 29 september 1997 des ochtends te 10:30 uur

door  
Helena Maria Elisabeth van Kaam-Peters  
geboren op 31 mei 1963, te Doesburg

Promotor: Prof. Dr. J.W. de Leeuw  
Co-promotor: Dr. Ir. J.S. Sinninghe Damsté



The investigations were (in part) supported by the Netherlands Geosciences Foundation (GOA) with financial aid from the Netherlands Organization for Scientific Research (NWO).

ISBN 90-5744-011-3

# Contents

<b>Summary</b>	7
<b>Samenvatting</b>	11
<b>Chapter 1.</b> Introduction	15
<b>Chapter 2.</b> Characterisation of an extremely organic sulfur-rich, 150 Ma old carbonaceous rock: Palaeoenvironmental implications.	29
<b>Chapter 3.</b> A high resolution biomarker study of different lithofacies of organic sulfur-rich carbonate rocks of a Kimmeridgian lagoon (French southern Jura).	65
<b>Chapter 4.</b> A molecular and carbon isotope biogeochemical study of biomarkers and kerogen pyrolysates of the Kimmeridge Clay Formation: Palaeoenvironmental implications.	105
<b>Chapter 5.</b> Palaeoclimatic control on the molecular and carbon isotopic composition of organic matter deposited in a Kimmeridgian euxinic shelf sea.	149
<b>Chapter 6.</b> Biomarker and compound-specific stable carbon isotope analysis of the Early Toarcian shales in SW Germany.	191
<b>Chapter 7.</b> Occurrence of two novel benzothiophene hopanoid families in sediments.	217
<b>Chapter 8.</b> The effect of clay minerals on diasterane/sterane ratios.	231
<b>Publications</b>	243
<b>Dankwoord</b>	245
<b>Curriculum Vitae</b>	247

---

## Summary

Information on the depositional environment of sediments and sedimentary rocks can be obtained in several ways, using e.g. sedimentological, palynological or (micro)palaeontological approaches. In this thesis, results are presented of molecular organic geochemical investigations, aimed at palaeoenvironmental reconstruction, of organic-rich sedimentary rocks of Jurassic age. Sample locations are in France, England and Germany. Particular attention has been paid to organic sulfur compounds, which have proven valuable biomarkers in earlier studies of Cretaceous and younger samples. The structural elucidation of the molecular fossils was performed by gas chromatography-mass spectrometry and thermal and chemical degradation techniques. Compound-specific stable carbon isotope analysis was applied to obtain additional information on the origin of molecular fossils (e.g. habitat of the source organism, way of carbon uptake of the source organism).

**Chapter 2** describes in detail the molecular composition of an organic sulfur-rich, laminated carbonate of the Upper Jurassic Calcaires en plaquettes Formation (CPF). This formation was deposited in a lagoonal environment and today crops out in the southern Jura mountains of France. Both bitumen and kerogen are dominated by intermolecularly sulfur-bound geomacromolecules, formed during early diagenesis by reaction of reduced inorganic sulfur species with functionalised biochemicals. Several novel homologous series of organic sulfur compounds were tentatively identified in the kerogen pyrolysate. The proportion of algal biopolymers in the kerogen is exceptionally small. Both free and sulfur-bound biomarkers in the bitumen are dominated by *n*-alkane and hopanoid carbon skeletons, whereas steroids are relatively minor. This suggests that cyanobacteria were more important primary producers than algae. Isorenieratene derivatives, indicating the occurrence of euxinic conditions in the lower part of photic zone, are relatively abundant. Based on these molecular data the depositional environment is interpreted to have been euxinic for most of the time.

Whilst Chapter 2 addresses the molecular composition of one 5 cm thick, laminated carbonate of the CPF, in **Chapter 3**, the different carbonate facies of the CPF are examined at the millimetre scale. Four carefully isolated laminae (light/parallel, dark/parallel, light/undulated, dark/undulated) and a massive limestone sample were analysed. The gross molecular composition of organic matter appeared similar in all samples. Extractable biomarkers are dominated by sulfur-bound *n*-alkane and hopanoid carbon skeletons. Derivatives of isorenieratene are relatively abundant. Kerogen pyrolysates are predominantly composed of organic sulfur compounds. The organic matter in the light-coloured, undulated lamina is distinguished from that in the other samples by differences in the concentrations and distributions of a number of biomarkers. These differences are ascribed to the periodic occurrence of benthic microbial mats. The vast majority of the OM in all samples, however, is derived from sulfur-bound planktonic lipids produced at times that bottom waters were euxinic and microbial mats were absent.

In **Chapter 4**, the structures and stable carbon isotopic compositions of biomarkers and kerogen pyrolysis products in three lithologically different samples of the Upper Jurassic Kimmeridge Clay Formation (KCF) in Dorset (UK) were studied. The aromatic hydrocarbon fractions of all three samples are dominated by isorenieratene derivatives,

providing the first evidence for photic zone euxinia in the KCF palaeoenvironment. Huc et al. (1992) in their study of the Dorset KCF reported a positive correlation between the total organic carbon (TOC) content and the stable carbon isotopic composition of TOC ( $\delta^{13}\text{C}_{\text{TOC}}$ ). Our samples meet this TOC- $\delta^{13}\text{C}_{\text{TOC}}$  relationship. Since the  $\delta^{13}\text{C}$  values of primary production markers vary only slightly among the samples, variations in  $\delta^{13}\text{C}_{\text{TOC}}$  cannot have resulted from changes in the  $^{13}\text{C}$  content or concentration of dissolved inorganic carbon as suggested previously. Based on the increasing abundance of organic sulfur with increasing TOC (and  $\delta^{13}\text{C}_{\text{TOC}}$ ) it is suggested that  $\delta^{13}\text{C}_{\text{TOC}}$  is controlled by the degree of sulfurisation.

A supplementary study of the KCF is reported in **Chapter 5**. To verify our hypothesis that  $\delta^{13}\text{C}_{\text{TOC}}$  is related to the degree of sulfurisation, thirteen samples, covering all different lithologies, were studied using bulk and molecular geochemical and microscopical techniques. The positive correlation between TOC and  $\delta^{13}\text{C}_{\text{TOC}}$  reported for shales (Huc et al., 1992) was found to also hold for (coccolithic) limestones if a correction is made for the dilution by carbonate. In agreement with earlier results (Chapter 4), the  $\delta^{13}\text{C}$  values of algal biomarkers in both bitumen and kerogen pyrolysate exhibit only small changes among the samples, which implies that changes in the  $^{13}\text{C}$  content or concentration of dissolved inorganic carbon cannot account for the differences in  $\delta^{13}\text{C}_{\text{TOC}}$ . The relative abundance of carbon isotopically heavy, linear,  $\text{C}_1$ - $\text{C}_3$  alkylated thiophenes in the kerogen pyrolysate increases with increasing  $\delta^{13}\text{C}_{\text{TOC}}$ . These thiophenes are probably partly derived from sulfurised carbohydrates linked *via* C-S bonds to the kerogen, rather than from thiophene moieties in the kerogen. Since algal carbohydrates are enriched in  $^{13}\text{C}$  by several per mil compared to algal lipids, differences in  $\delta^{13}\text{C}_{\text{TOC}}$  may be explained by different proportions of sulfurised carbohydrates in the kerogen. The increasing proportion of thiophenes in the kerogen pyrolysate with increasing  $\delta^{13}\text{C}_{\text{TOC}}$  is coupled with an increasing Rock Eval Sulfur Index (mg kerogen S/g TOC) and an increasing proportion of orange, organic sulfur-rich, amorphous organic matter as observed by microscopy. Thus, our data suggest that an increasing sulfurisation of organic matter was accompanied by an increasing sulfurisation of carbohydrates, which due to their relatively high  $^{13}\text{C}$  contents caused an increase in  $\delta^{13}\text{C}_{\text{TOC}}$ . Differences in the degree of sulfurisation probably resulted from both differences in the supply of reactive iron and differences in primary production.

**Chapter 6** addresses the negative isotope excursion of organic and inorganic carbon in the Early Toarcian shales in SW Germany. Jenkyns (1988) explained the global occurrence of the Early Toarcian shales by an Oceanic Anoxic Event (OAE). This hypothesis was based on the positive carbon isotope excursion of Early Toarcian limestones in several of the Tethyan sections. Through the burial of large amounts of organic matter, which is rich in  $^{12}\text{C}$ , the global carbon reservoir would have become relatively enriched in  $^{13}\text{C}$ , explaining the increase in  $\delta^{13}\text{C}$  of the limestones. Our biomarker and compound-specific stable carbon isotope data indicate that the negative carbon isotope excursion of organic matter in the SW German Toarcian shales is due to changes in  $\delta^{13}\text{C}$  of  $\text{CO}_2$  or  $[\text{CO}_2]_{\text{aq}}$  in the photic zone. As suggested previously by Küspert (1982), the negative excursion of  $\delta^{13}\text{C}_{\text{TOC}}$  probably resulted from the mixing of isotopically light  $\text{CO}_2$ , derived from the bacterial decomposition of organic matter, in anoxic bottom waters with the atmospheric-derived  $\text{CO}_2$  in the surface waters. Thus, unless the effect on  $\delta^{13}\text{C}_{\text{TOC}}$  of organic-derived  $\text{CO}_2$  recycling

into the photic zone exceeded by far the effect on  $\delta^{13}\text{C}_{\text{TOC}}$  of global organic carbon burial, the Early Toarcian OAE was not a global event.

The two final chapters discuss structural and diagenetic information derived from the studies described in chapters 2 through 6. **Chapter 7** reports the occurrence of two novel benzothiophene hopanoid families in sediments. Structural assignments were made on the basis of mass spectral data, desulfurisation experiments and gas chromatographic retention times. Quantitative data suggest a precursor-product relationship between thiophene hopanoids and benzothiophene hopanoids.

In **Chapter 8**, clay minerals are shown to significantly influence diasterane/sterane ratios in sedimentary organic matter. In two different sample sets, a positive correlation is found between clay/TOC and diasterane/sterane ratios. Quantitative data suggest that in the sedimentary environment, diasterenes are partly reduced to diasteranes and partly degraded, in a ratio largely dependent on the availability of clay minerals. The hydrogen atoms required for reduction of the diasterenes are probably (partly) derived from the water in the interlayers of clay minerals.



## Samenvatting

Informatie over het afzettingsmilieu van sedimenten en sedimentaire gesteenten kan op verschillende manieren verkregen worden, bijvoorbeeld via de sedimentologie, de palynologie of de (micro)palaeontologie. In dit proefschrift worden de resultaten beschreven van een op moleculair niveau uitgevoerd organisch geochemisch onderzoek naar de afzettingscondities van bitumineuze gesteenten van Jurassische ouderdom. De bestudeerde secties bevinden zich in Frankrijk, Engeland en Duitsland. In het bijzonder is aandacht besteed aan organische zwavelverbindingen, welke waardevolle moleculaire fossielen zijn gebleken bij eerdere milieureconstructie studies van Kretaceïsche en jongere afzettingen. De structuuropheldering van de moleculaire fossielen vond plaats met behulp van gaschromatografie-massaspectrometrie en thermische en chemische degradatietechnieken. Door toepassing van verbindingsspecifieke stabiele koolstofisotopenanalyse werd additionele informatie verkregen omtrent de oorsprong van de moleculaire fossielen (b.v. leefomgeving van het oorspronkelijke organisme, manier van koolstofopname van het oorspronkelijke organisme).

In **Hoofdstuk 2** wordt in detail de moleculaire samenstelling beschreven van een gelamineerde kalksteen met een hoog gehalte aan organisch zwavel, afkomstig van de Boven-Jurassische Calcaires en plaquettes Formatie (CPF). Deze formatie werd afgezet in een lagune en is thans ontsloten in het zuiden van de Franse Jura. Zowel het bitumen als het kerogeen worden gedomineerd door intermoleculair zwavelgebonden geomacromoleculen, gevormd tijdens de vroege diagenese door reactie van gereduceerde anorganische zwavelverbindingen met gefunctionaliseerde verbindingen. Verscheidene nieuwe homologe reeksen van organische zwavelverbindingen werden geïdentificeerd in het pyrolysaat van het kerogeen. De hoeveelheid biopolymeren in het kerogeen is uitzonderlijk klein. De moleculaire fossielen in het bitumen, zowel vrij als zwavelgebonden, hebben hoofdzakelijk lineaire en hopanoïde koolstofskeletten; steroïden zijn kwantitatief onbelangrijk. Dit suggereert dat cyanobacteriën belangrijkere primaire producenten waren dan algen. Derivaten van isoreniërateen, duidend op anoxische condities in het onderste deel van de fotische zone, zijn aanwezig in betrekkelijk hoge concentraties. Op basis van deze moleculaire data wordt voorgesteld dat het afzettingsmilieu gedurende het merendeel van de tijd euxinisch was.

Terwijl in Hoofdstuk 2 de moleculaire samenstelling beschreven wordt van een 5 cm dikke gelamineerde kalksteen van de CPF, worden in **Hoofdstuk 3** de verschillende kalkige faciës van de CPF onderzocht op millimeter niveau. Vier zorgvuldig geïsoleerde laagjes (licht/parallel, donker/parallel, licht/gegolfd, donker/gegolfd) en een ongelamineerde kalksteen werden geanalyseerd. Over het geheel genomen is de moleculaire samenstelling van het organisch materiaal vrijwel hetzelfde in alle monsters. Het extraheerbare organisch materiaal bestaat hoofdzakelijk uit lineaire en hopanoïde koolstofskeletten. Derivaten van isoreniërateen zijn in ruime mate aanwezig. De pyrolysat van de kerogenen worden gedomineerd door organische zwavelverbindingen. Het organisch materiaal in het lichtgekleurde gegolfde laagje wijkt af van dat in de andere monsters door verschillen in de concentratie en distributie van een aantal verbindingen. Deze verschillen worden toegeschreven aan het periodiek voorkomen van bentische microbiële matten. Het

overgrote deel van het organisch materiaal is echter afkomstig van zwavelgebonden lipiden van planktonische organismen, geproduceerd tijdens perioden dat het bodemwater euxinisch was en microbiële matten afwezig waren.

In **Hoofdstuk 4** worden de structuren en stabiele koolstofisotopensamenstellingen beschreven van extraheerbare organische verbindingen en pyrolyseproducten van het kerogeen aanwezig in drie lithologisch verschillende gesteenten van de Boven-Jurassische Kimmeridge Clay Formatie (KCF) in Dorset (UK). De aromatische koolwaterstoffracties van de drie monsters worden gedomineerd door derivaten van isoreniërateen, waarmee voor het eerst wordt aangetoond dat ten tijde van afzetting van de KCF er vrij  $H_2S$  aanwezig was in de fotische zone. Huc et al. (1992) vonden in hun monsterset van de KCF in Dorset een positief verband tussen het gehalte aan organisch koolstof (TOC) en de stabiele koolstofisotopensamenstelling van TOC ( $\delta^{13}C_{TOC}$ ). Onze monsters laten deze relatie tussen TOC en  $\delta^{13}C_{TOC}$  ook zien. Omdat de  $\delta^{13}C$ -waarden van lipiden van primaire producenten slechts weinig verschillen tussen de monsters, kunnen de variaties in  $\delta^{13}C_{TOC}$  niet veroorzaakt zijn door veranderingen in de  $\delta^{13}C$ -waarde of concentratie van opgelost anorganisch koolstof, zoals eerder werd gesuggereerd. Op grond van de toenemende hoeveelheid organisch zwavel met toenemende TOC (en  $\delta^{13}C_{TOC}$ ) wordt voorgesteld dat  $\delta^{13}C_{TOC}$  gerelateerd is aan de mate van verzwaveling.

In **Hoofdstuk 5** wordt over een aanvullend onderzoek van de KCF gerapporteerd. Ter verificatie van bovengenoemde hypothese werden dertien monsters, die alle verschillende lithologische eenheden van de KCF vertegenwoordigen, onderzocht met behulp van bulk geochemische, moleculair geochemische en microscopische methoden. De relatie tussen TOC en  $\delta^{13}C_{TOC}$  zoals aanwezig in de schalies (Huc et al., 1992), bestaat ook voor (coccoliet-rijke) kalkstenen, mits er wordt gecorrigeerd voor de verdunning door carbonaat. De moleculaire fossielen van algen, zowel in het bitumen als in het pyrolysaat van het kerogeen, hebben vrijwel dezelfde  $\delta^{13}C$ -waarde in alle monsters. Dit betekent dat, in overeenstemming met eerdere resultaten (Hoofdstuk 4), de verschillen in  $\delta^{13}C_{TOC}$  niet het gevolg kunnen zijn van veranderingen in de  $\delta^{13}C$ -waarde of concentratie van opgelost anorganisch koolstof. De relatieve hoeveelheid thiofenen met lineaire  $C_5$ - $C_7$  koolstofskeletten en hoge  $\delta^{13}C$ -waarden in het pyrolysaat van het kerogeen vertoont een positief verband met  $\delta^{13}C_{TOC}$ . Deze thiofenen zijn waarschijnlijk afkomstig van verzwavelde koolhydraten die gebonden zijn aan het kerogeen *via* C-S bindingen, en niet van thiofeeneenheden als zodanig aanwezig in het kerogeen. Omdat de  $\delta^{13}C$ -waarden van koolhydraten typisch 5-10% hoger liggen dan die van lipiden, kunnen de verschillen in  $\delta^{13}C_{TOC}$  verklaard worden door verschillen in de hoeveelheid zwavelgebonden koolhydraten in het kerogeen. Behalve de hoeveelheid thiofenen in het pyrolysaat van het kerogeen, laten ook de "Rock Eval Sulfur Index" (mg zwavel in het kerogen/g TOC) en de hoeveelheid oranje organisch-zwavel-rijk amorf organisch materiaal zoals microscopisch waargenomen, een positief verband zien met  $\delta^{13}C_{TOC}$ . Onze data suggereren dat een toenemende mate van verzwaveling van organisch materiaal gepaard ging met een toenemende verzwaveling van koolhydraten, welke door hun relatief hoog gehalte aan  $^{13}C$  een stijging veroorzaakten van  $\delta^{13}C_{TOC}$ . Verschillen in de mate van verzwaveling werden waarschijnlijk veroorzaakt door verschillen in de aanvoer van reactieve ijzermineralen en verschillen in primaire productie.

**Hoofdstuk 6** behandelt de negatieve stabiele koolstofisotopenexcursie van organisch en anorganisch koolstof in Onder-Toarcien schalies in Z.W. Duitsland. Jenkyns (1988) verklaarde het wereldwijd voorkomen van bitumineuze schalies tijdens het Vroeg-Toarcien door een anoxische toestand van de oceaan (“Oceanic Anoxic Event”) aan te nemen. Deze hypothese was gebaseerd op een positieve excursie in de koolstofisotopensamenstelling van Onder-Toarcien kalkstenen in een aantal secties langs de vroegere Tethys. Door het afzetten van grote hoeveelheden organisch materiaal, rijk aan  $^{12}\text{C}$ , zou het mondiale koolstofreservoir relatief zijn verrijkt met  $^{13}\text{C}$ , wat de toename in  $\delta^{13}\text{C}$  van de kalkstenen zou verklaren. Onze data betreffende het voorkomen van verschillende moleculaire fossielen en hun  $\delta^{13}\text{C}$ -waarden geven aan dat de negatieve excursie van  $\delta^{13}\text{C}_{\text{TOC}}$  in de Z.W. Duitse Toarcien schalies samenhangt met veranderingen in  $\delta^{13}\text{C}$  van  $\text{CO}_2$  of  $[\text{CO}_2]_{\text{aq}}$  in de fotische zone. Zoals eerder werd voorgesteld door Küspert (1982), is de negatieve excursie van  $\delta^{13}\text{C}_{\text{TOC}}$  waarschijnlijk het gevolg van menging van relatief isotopisch licht  $\text{CO}_2$  (dat vrijkomt bij de bacteriële afbraak van organisch materiaal) in anoxisch bodemwater met relatief isotopisch zwaar  $\text{CO}_2$  (dat in evenwicht is met  $\text{CO}_2$  in de atmosfeer) in het oppervlaktewater. Tenzij de recycling van isotopisch licht  $\text{CO}_2$  een veel groter effect heeft op  $\delta^{13}\text{C}_{\text{TOC}}$  dan het wereldwijd afzetten van grote hoeveelheden organisch materiaal, betekent dit dat de Vroeg-Toarcien “Oceanic Anoxic Event” geen mondiale gebeurtenis was.

De twee laatste hoofdstukken bevatten structurele en diagenetische informatie verkregen via de onderzoeken besproken in de hoofdstukken 2 t/m 6. **Hoofdstuk 7** vermeldt de aanwezigheid in sedimenten van twee nieuwe families hopanoïde benzothiofenen. De structuuropheldering vond plaats op basis van massaspectrometrische gegevens, ontzwavelingsexperimenten en gaschromatografische retentietijden. Kwantitatieve gegevens doen vermoeden dat hopanoïde benzothiofenen gevormd worden door cyclisatie en aromatisering van hopanoïde thiofenen.

In **Hoofdstuk 8** wordt aangetoond dat kleimineralen een aanzienlijk effect hebben op diasteraan/steraan ratio's in sedimentair organisch materiaal. In twee verschillende monstersets werd een positief verband gevonden tussen de klei/TOC ratio en de diasteraan/steraan ratio. De concentraties van de verschillende steroïden suggereren dat diasterenen onder sedimentaire omstandigheden gedeeltelijk worden gereduceerd tot diasteranen en gedeeltelijk worden afgebroken. De verhouding waarin dit gebeurt is afhankelijk van de beschikbaarheid van kleimineralen. De waterstofatomen die nodig zijn voor reductie van de diasterenen zijn waarschijnlijk (deels) afkomstig van water aanwezig tussen de laagvlakken van kleimineralen.

# Chapter 1

## Introduction

### Sedimentary organic matter

Large quantities of organic matter (OM) are biosynthesised every day by primary producers like plants, algae and photoautotrophic bacteria. The vast majority of this OM passes through the food chain and is ultimately recycled by bacteria. Nevertheless, ca. 0.1-0.5% of the biomass escapes from biodegradation and is stored in sediments and sedimentary rocks. Since different organic compounds are biodegraded at different rates and to different extents, the composition of this sedimentary OM is substantially different from that of the biota. Polysaccharides and proteins are among the first to be mineralised, leading to a relative enrichment of lipids. But also certain lipids are more likely to be degraded than others, causing the sedimentary OM to be a highly biased part of the original biomass (de Leeuw and Largeau, 1993; de Leeuw et al., 1995).

Approximately 5% of the sedimentary OM consists of bitumen, the part extractable by organic solvents. The bitumen contains a myriad of compounds. Despite the sometimes severe chemical transformations undergone during diagenesis, many of these compounds are still diagnostic of particular source organisms. Hence, these compounds are "molecular fossils" or "biomarkers" (Peters and Moldowan, 1993). Technically, it is more difficult to elucidate the structure and trace back the origin of the 95% of insoluble OM, the so-called kerogen. According to the neogenesis model of Tissot and Welte (1984), kerogens are largely made up of macromolecules formed from the random polymerisation and condensation of biodegradation products of polysaccharides and proteins. Later, the recognition and identification of highly resistant, aliphatic biomacromolecules in higher plant cuticles and cell walls of fresh-water algae (e.g. Nip et al., 1986; Largeau et al., 1986; Goth et al., 1988), led to the proposition of the selective preservation model (e.g. Tegelaar et al., 1989). In this model, kerogens are considered mixtures of highly resistant, sometimes partly altered, biopolymers. Although these biopolymers are only minor constituents of living organisms, it is believed that in the long term their refractory nature causes them to accumulate in sediments. Recently, the identification of resistant aliphatic biomacromolecules in cell walls of several marine microalgae (Gelin et al., 1996) provided further evidence for a major contribution of such biopolymers to marine kerogens.

Generally, organic-rich deposits are associated with anoxic depositional environments (Demaison and Moore, 1980; Wignall, 1994; Tyson, 1996). However, whether anoxia is a cause of OM preservation (due to inefficient OM mineralisation), or a result of high primary production (and thus high oxygen demand by bacterial decomposers), is a matter of debate (Pedersen and Calvert, 1990; Tyson and Pearson, 1991; Pedersen et al., 1992; Canfield, 1994). Regardless the efficiency of OM mineralisation, anoxic, sulfate-reducing conditions can sometimes lead to enhanced OM preservation through the reactions of biochemicals with hydrogen sulfide or polysulfides (Sinninghe Damsté et al., 1989). By incorporating one or more sulfur atoms (see below), otherwise labile compounds obtain a

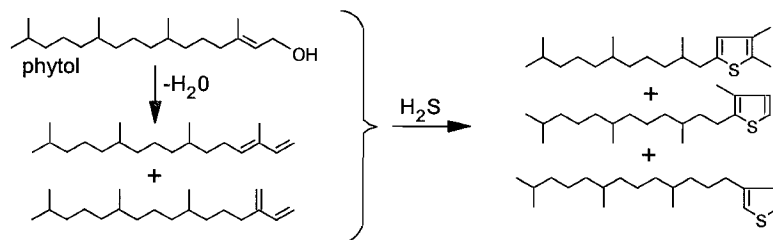


**Fig. 1.1.** Precursor-product relationships between phytol, phytadiene and sulfur-bound phytane.

better resistance against biodegradation and are more likely to be preserved in the sedimentary record.

Another factor which may exert control on the quality and quantity of OM in sediments is the affinity of biochemicals to mineral surfaces. Keil et al. (1994b) have shown that relatively labile OM can be preserved for hundreds of years in the sediment, but is rapidly decomposed once desorbed from the mineral matrix. In several coastal deposits, the mineral surface area is correlated with both concentration and composition of OM, presumably due to the selective adsorption of biochemicals (Keil et al., 1994a; Bergamaschi et al., 1997). Thus, in recent sediments, preferential adsorption to mineral surfaces accounts for another bias in the composition of sedimentary OM.

### Low-molecular-weight (LMW) biomarkers

Although LMW ( $M_w < 800$ ) organic compounds constitute only a minor part of the sedimentary OM, they can contain valuable information concerning depositional conditions, the composition of palaeobiota, and the degree of maturation of sediments (e.g. Peters and Moldowan, 1993; de Leeuw et al., 1995). Some biochemicals, and their fossil counterparts (biomarkers), are more specific than others. Bacteriohopanetetrol (**I**, see Appendix) is a ubiquitous component found in major groups of bacteria and cyanobacteria (Rohmer et al., 1993). The pigment isorenieratene (**II**), on the other hand, is highly specific, since it is exclusively biosynthesised by the brown strain of Chlorobiaceae (photosynthetic green sulfur bacteria). The value of a biomarker, however, is not determined singly by the specificity of its carbon skeleton. For example, the ratio of di- to triunsaturated  $n$ - $C_{37}$  methylketones (**III-IV**), compounds biosynthesised by some Prymnesiophyte algae, can be used to assess surface seawater temperature in the palaeoenvironment (Brassell et al., 1986a). Also, relative proportions of mono-, di- and trimethylated 2-methyl-2-(4,8,12-trimethyltridecyl)chromans (**V**), compounds of as yet unknown origin, can give an indication of the salinity of the palaeowater column (Sinninghe Damsté et al., 1987, 1993a).

As mentioned briefly above, in anoxic, sulfate-reducing environments, biochemicals may react with reduced inorganic sulfur species yielding organic sulfur compounds (OSC). In contrast to non-sulfur containing biomarkers, OSC carry information on the positions of functional groups (e.g. double bonds) in the precursor molecules, since it is only at these "reactive sites" that sulfur can be incorporated (Sinninghe Damsté et al., 1989; de Graaf et

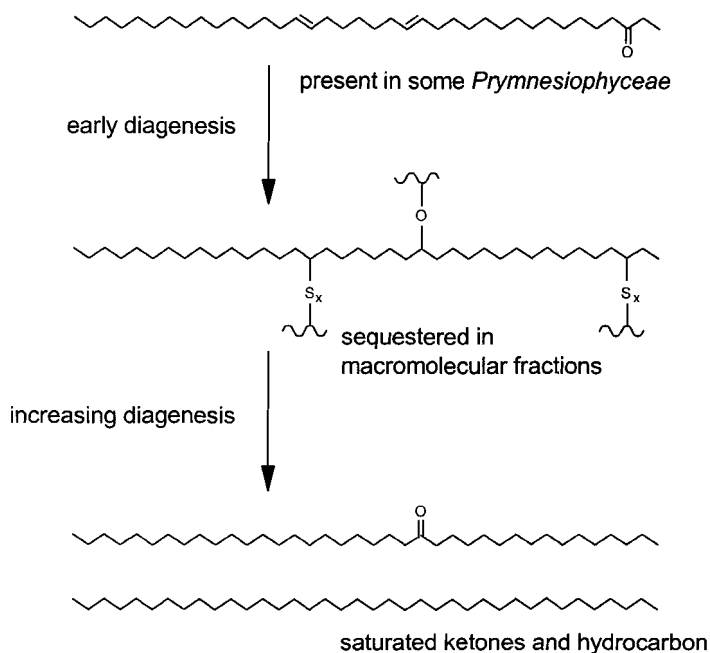


**Fig. 1.2.** Diagenetic scheme of  $n$ -C<sub>38</sub> di-unsaturated ketones (after Koopmans et al., 1997). Formation of 1,2-di- $n$ -alkylbenzenes and 2,5-di- $n$ -alkylthiophenes is not shown.

al., 1992; Schouten et al., 1993, 1994). For example, phytane skeletons with thiophene moieties at or near the end of the carbon chain, are likely formed by sulfur incorporation into phytol and phytadienes, degradation products of chlorophyll-a (Fig. 1.1; Brassell et al., 1986b; Schouten et al., 1994). Phytane skeletons with mid-chain thiophene moieties (e.g. VI), however, must be derived from other precursors.

### High-molecular-weight (HMW) biomarkers

HMW ( $M_w > 800$ ) compounds are not amenable to gas chromatographic analysis, which hampers their structural elucidation. This can be overcome by rapid thermal degradation of the macromolecule (pyrolysis), resulting in the release of characteristic LMW compounds that can be analysed by GC-MS (gas chromatography-mass spectrometry). Reconstruction of these pyrolysis products gives insight into the structure of the components in kerogens and other HMW organic matter. Alternatively, macromolecules can be cleaved using specific chemical degradation techniques, or be analysed by non-destructive techniques like <sup>13</sup>C NMR and FT-IR.

HMW biomarkers may be divided into two groups: (i) Compounds originally biosynthesised as macromolecules, and (ii) compounds which became macromolecularly bound during diagenesis. Examples of the first group are lignins and tannins (polyphenolic constituents of vascular plants), polycadinenes (present in resins), cutans and suberans

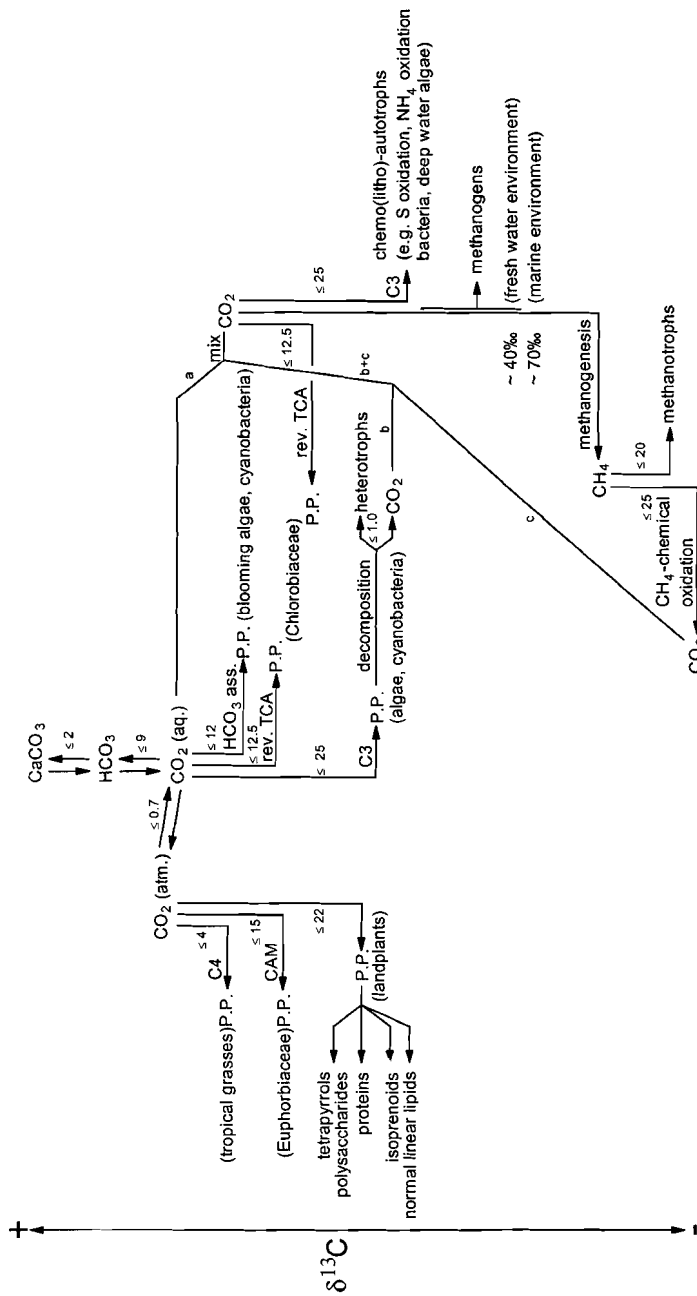


**Fig. 1.3.** Overview of  $\delta^{13}\text{C}$  fractionation in the biosphere (after de Leeuw et al., 1995). P.P., primary producers; atm, atmosphere; aq, aqueous; ass, assimilation; rev. TCA, reverse tricarboxylic acid cycle.

(aliphatic biopolymers in higher plants) and algaenans (aliphatic biopolymers in algal cell walls) (for a review see de Leeuw and Largeau, 1993). Major compounds of the second group are intermolecularly sulfur-bound and/or oxygen-bound LMW biomarkers (Mycke et al., 1987; Sinninghe Damsté et al., 1989; Kohnen et al., 1991a; Richnow et al., 1993; Schouten et al., 1995; Koopmans et al., 1997). Cross-linking of biochemicals by sulfur and oxygen (Fig. 1.2) is believed to take place during an early stage of diagenesis. Depending on the type and positions of functional groups, some compounds are more prone to cross-linking than others. With increasing diagenesis, sulfur- and oxygen-bound biomarkers are released from the macromolecular fractions (Fig. 1.2).

### Compound-specific stable carbon isotope analysis

The information inferred from the molecular structure of a biomarker may be supplemented by its stable carbon isotopic composition. Stable carbon isotopic compositions are usually expressed in  $\delta^{13}\text{C}$  (‰):

$$\delta^{13}\text{C} = \left( \frac{{}^{13}\text{C}/{}^{12}\text{C}_{\text{compound}}}{{}^{13}\text{C}/{}^{12}\text{C}_{\text{standard}}} - \frac{{}^{13}\text{C}/{}^{12}\text{C}_{\text{standard}}}{{}^{13}\text{C}/{}^{12}\text{C}_{\text{standard}}} \right) \times 1000$$

The primary standard used for reporting  $\delta^{13}\text{C}$  values is a marine limestone (PDB) with a  ${}^{13}\text{C}/{}^{12}\text{C}$  ratio of 0.0112372 (Craig, 1957). Organic compounds are usually depleted in  ${}^{13}\text{C}$  relative to PDB and have negative  $\delta^{13}\text{C}$  values. "Higher" or "less negative"  $\delta^{13}\text{C}$  values indicate higher  ${}^{13}\text{C}$  contents.

The  $\delta^{13}\text{C}$  values of biomarkers are determined by GC-IRMS (gas chromatography-isotope ratio mass spectrometry), a technique that became commercially available seven years ago (Freeman et al., 1990). To interpret molecular  $\delta^{13}\text{C}$  values, knowledge of the various controlling factors is required. The  $\delta^{13}\text{C}$  value of a biomarker depends on: (i) the  $\delta^{13}\text{C}$  value of the carbon source used in photosynthesis (in the case of heterotrophs:  $\delta^{13}\text{C}$  of the food), (ii) isotope effects associated with carbon uptake, metabolism and biosynthesis, and (iii) isotope effects associated with chemical alterations during diagenesis (e.g. Hayes, 1993; Freeman et al., 1994a). The extent to which  $\delta^{13}\text{C}$  values are determined by each of these factors may vary and is not always known.

In principle, differences in the pathway of carbon fixation and differences in  $\delta^{13}\text{C}$  of the carbon source utilised can account for the range of  $\delta^{13}\text{C}$  values observed in the biosphere (Fig. 1.3). The highest  $\delta^{13}\text{C}$  values are found in C4 plants and primary producers living under  $\text{CO}_2$  stress (due to low concentrations of  $\text{CO}_2$ , discrimination against  ${}^{13}\text{C}$  is reduced, which results in relatively high  $\delta^{13}\text{C}$  values of the biomass). At the low end of the range are methanotrophic organisms, which feed on isotopically light methane produced by methanogens (Fig. 1.3). The picture is further complicated by the fact that closely related compounds produced by a single organism may have different isotopic compositions. For example,  $\delta^{13}\text{C}$  values of *n*-alkanes in a single leaf were found to differ by up to 6‰, probably due to differences in biosynthesis (Collister et al., 1994). In spite of this and other complicating factors, compound-specific stable carbon isotope analysis has already shown many applications in palaeoenvironmental reconstruction (e.g. Hayes et al., 1987, 1989;



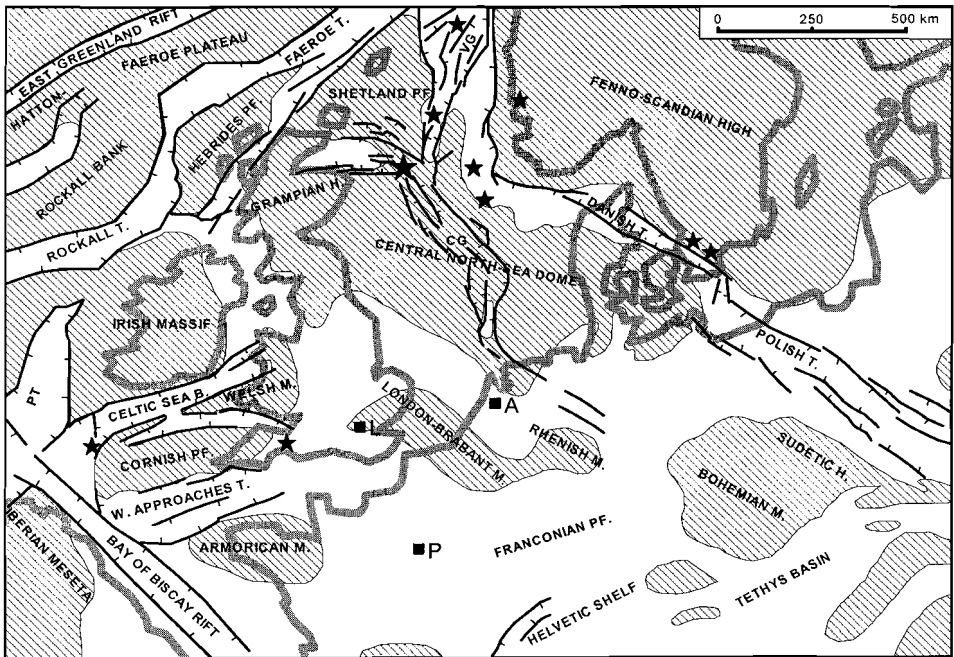
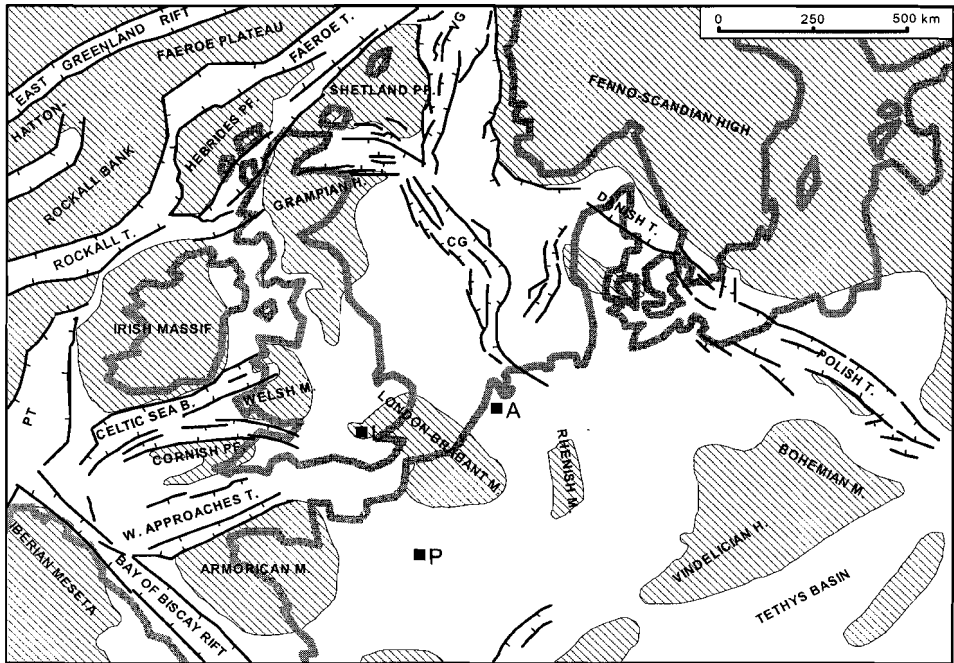


**Fig. 1.4.** Palaeogeography of NW Europe in the (a) (above) Early Jurassic, (b) (below) Middle Jurassic (after Ziegler, 1981). For legend see Fig. 1.5.

Freeman et al., 1994b; Collister et al., 1992; Kohnen et al., 1992; Jasper et al., 1994; Schoell et al., 1994; Kenig et al., 1995; this thesis).

### The Jurassic of NW Europe

In Jurassic times, the latitude of NW Europe was approximately 40°N (Parrish and Curtis, 1982; Hallam, 1984). In the absence of polar ice caps, equator-to-pole temperature gradients were relatively weak, and deep oceanic circulation was not as forceful as observed today. Throughout most of the Jurassic, the climate was warm and humid; only at the very end of this period (Late Tithonian), conditions became semi-arid (Hallam, 1984, 1985; Wignall and Ruffell, 1990; Hallam et al., 1991).

In terms of plate tectonics, the Jurassic setting of NW Europe (Fig. 1.4) can be described as that of a sub-plate of the Pangean megacontinent that was bordered to the

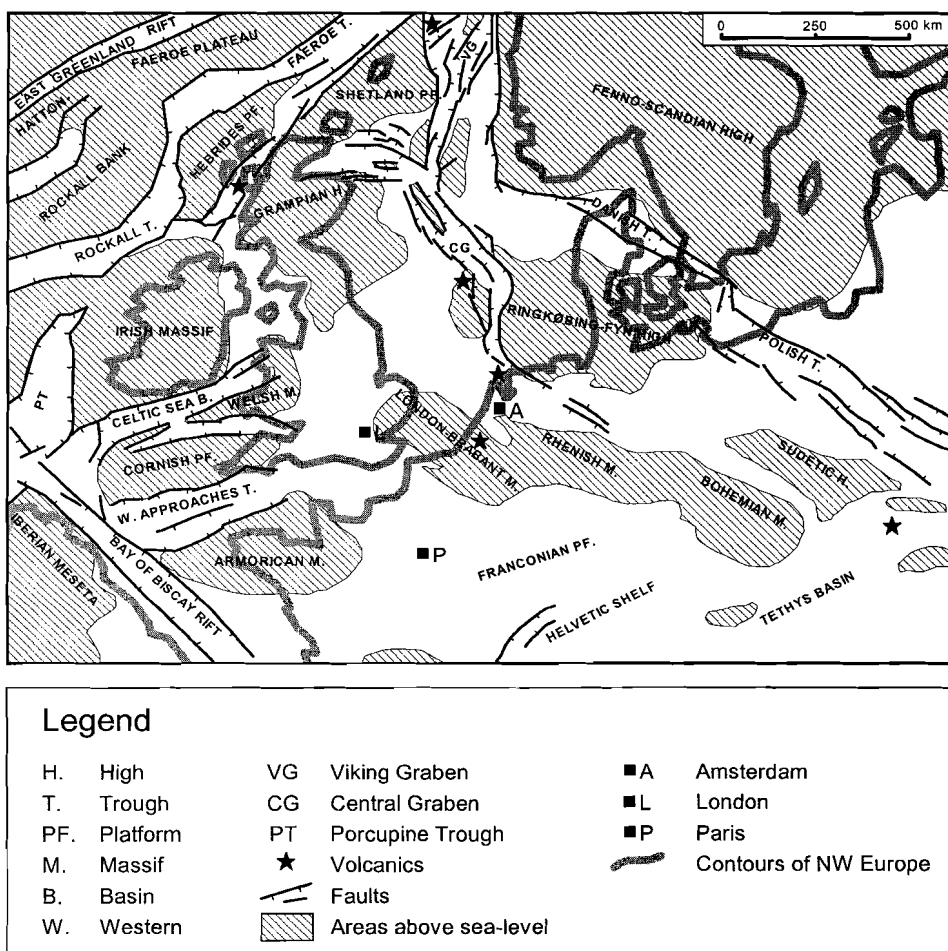


Fig. 1.5. Palaeogeography of NW Europe in the Late Jurassic (after Ziegler, 1981).

northeast against the stable Fennoscandian-Russian Platform by the Polish-Danish Rift, and to the northwest and the south by the large, active rift systems of the Arctic-North Atlantic and the Tethys (Ziegler, 1981). During the Early Jurassic, a number of interrupted, eustatic sea-level rises (Hallam, 1981), led to the inundation of large parts of NW Europe and the connection of the Tethys and the Arctic seas (Fig. 1.4a). As a result, TOC-poor shales and carbonates were deposited in the relatively shallow seas of western Europe, and future oil source rocks were formed in some of the deeper epicontinental basins (e.g. Paris Basin).

In the early Middle Jurassic, the tectonic activity along the Arctic-North Atlantic Rift caused the first break-up of the Pangean megacontinent by failure of the continental crust in the Central Atlantic (Ziegler, 1981). However, it was not until the Early Tertiary that the North Atlantic was opened. Roughly coincident with the first break-up of Pangea, sea-floor spreading started in the western Tethys, and a large rift dome was uplifted in the central North Sea (Fig. 1.4b) (Biju-Duval et al., 1977; Laubscher and Bernoulli, 1977; Ziegler, 1981). These tectonic events, which were connected with a eustatic lowering of the sea level, resulted in the development of volcanic centres at various places in the North Sea rift systems (Fig. 1.4b). The Early Jurassic and older sediments of the North Sea rift dome were deeply eroded and deposited in the surrounding grabens.

By the late Middle Jurassic, volcanic activity had ceased and the North Sea rift dome was subsiding (Ziegler, 1981). The sea level was rising, and by Late Jurassic times a sea-way was opened again through the central North Sea area (Fig. 1.5). The Viking Graben and the Central Graben became the dominant rift systems of the North Sea, and together with the Western Approaches-Celtic Sea grabens and the Polish-Danish Trough represented the major structural elements in NW Europe (Fig. 1.5). The Rockall-Faeroe rift zone was gradually uplifted, giving rise to minor volcanic centres alongside. In large parts of the central and northern North Sea, where subsidence rates exceeded sedimentation rates, Late Jurassic strata consist of organic-rich shales, some of which are important oil source rocks. In the Danish Trough, however, shales are organic-lean. Where sedimentation rates were in balance with subsidence rates and eustatic sea level changes, e.g. in the Polish Trough and the Paris Basin, carbonates and shales show the characteristics of shallow-water deposits.

### **Scope and framework of the thesis**

In recent years, organic sulfur geochemistry has been successfully applied in palaeoenvironmental reconstruction (e.g. de Leeuw and Sinninghe Damsté, 1990; Sinninghe Damsté and de Leeuw, 1990; Sinninghe Damsté et al., 1990, 1993b; Kohlen et al., 1991b). These reconstructions, however, all pertained to sediments and sedimentary rocks not older than the Upper Cretaceous. One objective of the present study, therefore, was to extend the use of OSC in molecular palaeontology to sedimentary rocks of Jurassic age. The other objective was to further explore the potential of compound-specific stable carbon isotope analysis in solving questions about ancient depositional environments.

The main part of the thesis deals with the palaeoenvironmental reconstruction of Jurassic organic-rich rocks from three different locations in NW Europe. In **Chapters 2 and 3** a detailed account is given of OM composition and its implications for depositional conditions, in carbonate rocks from the Upper Jurassic Calcaires en plaquettes Formation

(CPF). The CPF has not been buried deeply, and is thermally immature. The vast majority of biomarkers in the CPF is present in a sulfur-bound form. This demonstrates that sulfur-bound biomarkers are stable over a time-span of at least 150 million years, provided they are not exposed to elevated temperatures during burial. **Chapters 4 and 5** describe the analyses of samples from the Upper Jurassic Kimmeridge Clay Formation (KCF). Distributions and carbon isotopic compositions of biomarkers and kerogen pyrolysis products provided new insights into the KCF depositional environment. Evidence is presented that the molecular and carbon isotopic composition of OM in the KCF was largely controlled by palaeoclimatic changes. Furthermore, it is shown that large amounts of polysaccharide carbon were preserved through the incorporation of sulfur. In **Chapter 6** the negative carbon isotope excursion of the Early Toarcian shales in SW Germany is investigated. Molecular carbon isotope data and the composition of LMW and HMW biomarkers indicate that this excursion resulted from changes in the dissolved inorganic carbon system. It is proposed that, in the time of the carbon isotope excursion, waters in the SW German sea were frequently anoxic at depths below 10 to 20 meters.

The second part of the thesis reports additional results that emanated from the central task of reconstructing depositional environments. In **Chapter 7** the identification of two novel families of OSC (**VII** and **VIII**) is reported, and pathways of their formation are proposed. **Chapter 8** addresses the interaction between clay minerals and mono-unsaturated, rearranged steroids. The data suggest that water molecules in the interlayers of clay minerals can be important donors of hydrogen atoms to unsaturated organic compounds.

## References

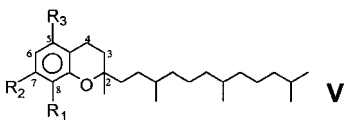
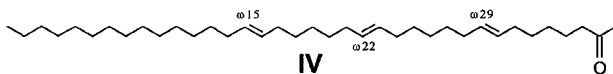
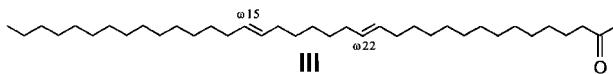
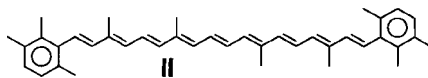
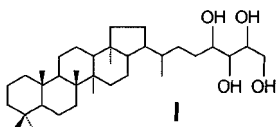
- Bergamaschi B.A., Tsamakidis E., Keil R.G., Eglinton T.I., Montluçon D.B. and Hedges J.I. (1997) The effect of grain size and surface area on organic matter, lignin and carbohydrate concentration, and molecular compositions in Peru Margin sediments. *Geochim. Cosmochim. Acta* **61**, 1247-1260.
- Biju-Duval B., Dercourt J. and Le Pichon X. (1977) From the Tethys ocean to the Mediterranean seas: A plate tectonic model of the evolution of the western Alpine system. In *Structural History of the Mediterranean Basins* (ed. B. Biju-Duval and L. Montadert), pp. 143-164. Editions Technip, Paris.
- Brassell S.C., Eglinton G., Marlowe I.T., Pflaumann U. and Sarnthein M. (1986a) Molecular stratigraphy: A new tool for climatic assessment. *Nature* **320**, 129-133.
- Brassell S.C., Lewis C.A., de Leeuw J.W., de Lange F. and Sinninghe Damsté J.S. (1986b) Isoprenoid thiophenes: Novel products of sediment diagenesis? *Nature* **320**, 160-162.
- Canfield D.E. (1994) Factors influencing organic carbon preservation in marine sediments. *Chem. Geol.* **114**, 315-329.
- Collister J.W., Summons R.E., Lichtfouse E. and Hayes J.M. (1992) An isotopic biogeochemical study of the Green River oil shale. *Org. Geochem.* **19**, 265-276.
- Collister J.W., Rielely G., Stern B., Eglinton G. and Fry B. (1994) Compound-specific  $\delta^{13}\text{C}$  analyses of leaf lipids from plants with differing carbon dioxide metabolisms. *Org. Geochem.* **21**, 619-627.
- Craig H. (1957) Isotopic standards for carbon and oxygen and correction factors for mass-spectrometric analysis of carbon dioxide. *Geochim. Cosmochim. Acta* **12**, 133-149.
- Demaison G.J. and Moore G.T. (1980) Anoxic environments and oil bed genesis. *Am. Assoc. Petr. Geol. Bull.* **64**, 1179-1209.
- Freeman K.H., Hayes J.M., Trendel J.-M. and Albrecht P. (1990) Evidence from carbon isotope measurements for diverse origins of sedimentary hydrocarbons. *Nature* **343**, 254-256.

- Freeman K.H., Boreham C.J., Summons R.E. and Hayes J.M. (1994a) The effect of aromatization on the isotopic compositions of hydrocarbons during early diagenesis. *Org. Geochem.* **21**, 1037-1049.
- Freeman K.H., Wakeham S.G. and Hayes J.M. (1994b) Predictive isotopic biogeochemistry: Hydrocarbons from anoxic marine basins. *Org. Geochem.* **21**, 629-644.
- de Graaf W., Sinninghe Damsté J.S. and de Leeuw J.W. (1992) Laboratory simulation of natural sulfurization I. Formation of monomeric and oligomeric isoprenoid polysulphides by low-temperature reactions of inorganic polysulphides with phytol and phytadienes. *Geochim. Cosmochim. Acta* **56**, 4321-4328.
- Gelin F., Boogers I., Noordeloos A.A.M., Sinninghe Damsté J.S., Hatcher P.G. and de Leeuw J.W. (1996) Novel, resistant microalgal polyethers: An important sink of organic carbon in the marine environment? *Geochim. Cosmochim. Acta* **60**, 1275-1280.
- Goth K., de Leeuw J.W., Püttmann W. and Tegelaar E.W. (1988) Origin of Messel Oil Shale kerogen. *Nature* **336**, 759-761.
- Hallam A. (1981) A revised sea-level curve for the Early Jurassic. *J. Geol. Soc. London* **138**, 735-743.
- Hallam A. (1984) Continental humid and arid zones during the Jurassic and Cretaceous. *Palaeogeogr. Palaeoclimatol. Palaeoecol.* **47**, 195-223.
- Hallam A. (1985) A review of Mesozoic climates. *J. Geol. Soc. London* **142**, 433-445.
- Hallam A., Grose J.A. and Ruffell A.H. (1991) Palaeoclimatic significance of changes in clay mineralogy across the Jurassic-Cretaceous boundary in England and France. *Palaeogeogr. Palaeoclimatol. Palaeoecol.* **81**, 173-187.
- Hayes J.M. (1993) Factors controlling  $^{13}\text{C}$  contents of sedimentary organic compounds: Principles and evidence. *Mar. Geol.* **113**, 111-125.
- Hayes J.M., Takigiku R., Ocampo R., Callot H.J. and Albrecht P. (1987) Isotopic compositions and probable origins of organic molecules in the Eocene Messel shale. *Nature* **329**, 48-51.
- Hayes J.M., Popp B.N., Takigiku R. and Johnson M.W. (1989) An isotopic study of biogeochemical relationships between carbonates and organic carbon in the Greenhorn Formation. *Geochim. Cosmochim. Acta* **53**, 2961-2972.
- Jasper J.P., Hayes J.M., Mix A.C. and Prah F.G. (1994) Photosynthetic fractionation of  $^{13}\text{C}$  and concentrations of dissolved  $\text{CO}_2$  in the central equatorial Pacific during the last 255,000 years. *Paleoceanography* **9**, 781-798.
- Keil R.G., Tsamakis E., Bor Fuh C., Giddings J.C. and Hedges J.I. (1994a) Mineralogical and textural controls on the organic composition of coastal marine sediments: Hydrodynamic separation using SPLITT-fractionation. *Geochim. Cosmochim. Acta* **58**, 879-893.
- Keil R.G., Montluçon D.B., Prah F.G. and Hedges J.I. (1994b) Sorptive preservation of labile organic matter in marine sediments. *Nature* **370**, 549-552.
- Kenig F., Sinninghe Damsté J.S., Frewin N.L., Hayes J.M. and de Leeuw J.W. (1995) Molecular indicators for palaeoenvironmental change in a Messinian evaporitic sequence (Vena del Gesso, Italy). II: High-resolution variations in abundances and  $^{13}\text{C}$  contents of free and sulphur-bound carbon skeletons in a single marl bed. *Org. Geochem.* **23**, 485-526.
- Kohnen M.E.L., Sinninghe Damsté J.S., Kock-van Dalen A.C. and de Leeuw J.W. (1991a) Di- or polysulphide-bound biomarkers in sulphur-rich geomacromolecules as revealed by selective chemolysis. *Geochim. Cosmochim. Acta* **55**, 1375-1394.
- Kohnen M.E.L., Sinninghe Damsté J.S. and de Leeuw J.W. (1991b) Biases from natural sulphurization in palaeoenvironmental reconstruction based on hydrocarbon biomarker distributions. *Nature* **349**, 775-778.
- Kohnen M.E.L., Schouten S., Sinninghe Damsté J.S., de Leeuw J.W., Merritt D.A. and Hayes J.M. (1992) Recognition of paleobiochemicals by a combined molecular sulfur and isotope geochemical approach. *Science* **256**, 358-362.
- Koopmans M.P., Schaeffer-Reiss C., de Leeuw J.W., Lewan M.D., Maxwell J.R., Schaeffer P. and Sinninghe Damsté J.S. (1997) Sulphur and oxygen sequestration of  $n\text{-C}_{37}$  and  $n\text{-C}_{38}$  unsaturated ketones in an immature kerogen and the release of their carbon skeletons during early stages of thermal maturation. *Geochim. Cosmochim. Acta* **61**, 2397-2408.

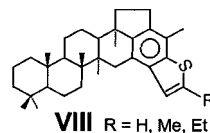
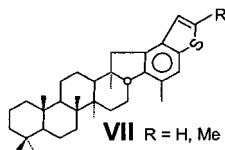
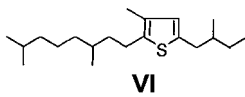
- Largeau C., Derenne S., Casadevall E., Kadouri A. and Sellier N. (1986) Pyrolysis of immature torbanite and of the resistant biopolymer (PRB A) isolated from the extant alga *Botryococcus braunii*. Mechanism for the formation and structure of torbanite. In *Advances in Organic Geochemistry 1985* (ed. D. Leythausser and J. Rullkötter). *Org. Geochem.* **10**, 1023-1032.
- Laubscher H. and Bernoulli D. (1977) Mediterranean and Tethys. In *Structural History of the Mediterranean Basins* (ed. B. Bijou-Duval and L. Montadert), pp. 129-132. Editions Technip, Paris.
- de Leeuw J.W. and Largeau C. (1993) A review of macromolecular organic compounds that comprise living organisms and their role in kerogen, coal, and petroleum formation. In *Organic Geochemistry, Principles and Applications* (ed. M.H. Engel and S.A. Macko), pp. 23-72. Plenum Press, New York.
- de Leeuw J.W. and Sinninghe Damsté J.S. (1990) Organic sulfur compounds and other biomarkers as indicators of palaeosalinity. In *Geochemistry of Sulfur in Fossil Fuels* (ed. W.L. Orr and C.M. White), *ACS Symposium Series 429*, pp. 417-443. Amer. Chem. Soc., Washington.
- de Leeuw J.W., Frewin N.L., van Bergen P.F., Sinninghe Damsté J.S. and Collinson M.E. (1995) Organic carbon as a palaeoenvironmental indicator in the marine realm. In *Marine Palaeoenvironmental Analysis from Fossils*. (ed. D.W.J. Bosence and Allison P.A.), pp. 43-71. *Geol. Soc. Spec. Publ.* **83**.
- Mycke B., Narjes F. and Michaelis W. (1987) Bacterioplanetol from chemical degradation of an oil shale kerogen. *Nature* **326**, 179-181.
- Nip M., Tegelaar E.W., de Leeuw J.W., Schenck P.A. and Holloway P.J. (1986) A new non-saponifiable highly aliphatic and resistant biopolymer in plant cuticles: Evidence from pyrolysis and <sup>13</sup>C-NMR analysis of present day and fossil plants. *Naturwissenschaften* **73**, 579-585.
- Parrish J.T. and Curtis R.L. (1982) Atmospheric circulation, upwelling, and organic-rich rocks in the Mesozoic and Cenozoic eras. *Palaeogeogr. Palaeoclimatol. Palaeoecol.* **40**, 31-66.
- Pedersen T.F. and Calvert S.E. (1990) Anoxia vs. productivity: What controls the formation of organic-carbon-rich sediments and sedimentary rocks? *Am. Assoc. Petr. Geol. Bull.* **74**, 454-466.
- Pedersen T.F., Shimmield G.B. and Price N.B. (1992) Lack of enhanced preservation of organic matter in sediments under the oxygen minimum on the Oman Margin. *Geochim. Cosmochim. Acta* **56**, 545-551.
- Peters K.E. and Moldowan J.M. (1993) *The Biomarker Guide: Interpreting Molecular Fossils in Petroleum and Ancient Sediments*. Prentice Hall, New Jersey.
- Richnow H.H., Jenisch A. and Michaelis W. (1993) The chemical structure of macromolecular fractions of a sulfur-rich oil. *Geochim. Cosmochim. Acta* **57**, 2767-2780.
- Rohmer M., Bissere P. and Neunlist S. (1993) The hopanoids, prokaryotic triterpenoids and precursors of ubiquitous molecular fossils. In *Biological Markers in Sediments and Petroleum* (ed. J.M. Moldowan, P. Albrecht and R.P. Philp), Prentice-Hall, Inc., New Jersey, U.S.A., pp. 1-17.
- Schoell M., Schouten S., Sinninghe Damsté J.S., de Leeuw J.W. and Summons R.E. (1994) A molecular organic carbon isotope record of Miocene climate changes. *Science* **263**, 1122-1125.
- Schouten S., van Driel G.B., Sinninghe Damsté J.S. and de Leeuw J.W. (1993) Natural sulphurization of ketones and aldehydes: A key reaction in the formation of organic sulphur compounds. *Geochim. Cosmochim. Acta* **57**, 5111-5116.
- Schouten S., de Graaf W., Sinninghe Damsté J.S., van Driel G.B. and de Leeuw J.W. (1994) Laboratory simulation of natural sulfurization II. Reaction of multifunctionalized lipids with inorganic polysulphides at low temperatures. In *Advances in Organic Geochemistry 1993* (ed. N. Telnæs, G. van Graas and K. Øygaard). *Org. Geochem.* **22**, 825-834.
- Schouten S., Sinninghe Damsté J.S., Baas M., Kock-van Dalen A.C., Kohnen M.E.L. and de Leeuw J.W. (1995) Quantitative assessment of mono- and polysulphide-linked carbon skeletons in sulphur-rich macromolecular aggregates present in bitumens and oils. *Org. Geochem.* **23**, 765-775.
- Sinninghe Damsté J.S. and de Leeuw J.W. (1990) Analysis, structure and geochemical significance of organically-bound sulphur in the geosphere: State of the art and future research. In *Advances in Organic Geochemistry 1989* (ed. B. Durand and F. Behar). *Org. Geochem.* **16**, 1077-1101.

- Sinninghe Damsté J.S., Kock-van Dalen A.C., de Leeuw J.W., Schenck P.A., Guoying S. and Brassell S.C. (1987) The identification of mono-, di- and trimethyl 2-methyl-2-(4,8,12-trimethyltridecyl)chromans and their occurrence in the geosphere. *Geochim. Cosmochim. Acta* **51**, 2393-2400.
- Sinninghe Damsté J.S., Rijpstra W.I.C., de Leeuw J.W. and Schenck P.A. (1988) Origin of organic sulphur compounds and sulphur-containing high molecular weight substances in sediments and immature crude oils. In *Advances in Organic Geochemistry 1987* (ed. L. Mattavelli and L. Novelli). *Org. Geochem.* **13**, 593-606.
- Sinninghe Damsté J.S., Rijpstra W.I.C., Kock-van Dalen A.C., de Leeuw J.W. and Schenck P.A. (1989) Quenching of labile functionalised lipids by inorganic sulphur species: Evidence for the formation of sedimentary organic sulphur compounds at the early stages of diagenesis. *Geochim. Cosmochim. Acta* **53**, 1343-1355.
- Sinninghe Damsté J.S., Kohnen M.E.L. and de Leeuw J.W. (1990) Thiophenic biomarkers for palaeoenvironmental assessment and molecular stratigraphy. *Nature* **345**, 609-611.
- Sinninghe Damsté J.S., Keely B.J., Betts S.E., Baas M., Maxwell J.R. and de Leeuw J.W. (1993a) Variations in abundances and distributions of isoprenoid chromans and long-chain alkylbenzenes in sediments of the Mulhouse Basin: a molecular sedimentary record of palaeosalinity. *Org. Geochem.* **20**, 1201-1215.
- Sinninghe Damsté J.S., Wakeham S.G., Kohnen M.E.L., Hayes J.M. and de Leeuw J.W. (1993b) A 6,000-year sedimentary molecular record of chemocline excursions in the Black Sea. *Nature* **362**, 827-829.
- Tegelaar E.W., de Leeuw J.W., Derenne S. and Largeau C. (1989) A reappraisal of kerogen formation. *Geochim. Cosmochim. Acta* **53**, 3103-3106.
- Tissot and Welte (1984) *Petroleum Formation and Occurrence*, 2nd edition. Springer, Heidelberg.
- Tyson R.V. and Pearson T.H. (1991) Modern and ancient continental shelf anoxia: An overview. In *Modern and Ancient Continental Shelf Anoxia* (ed. Tyson R.V. and Pearson T.H.), Geol. Soc. Lond. Spec. Publ. **58**, 1-24.
- Tyson R.V. (1996) Sequence stratigraphical interpretation of organic facies variations in marine siliciclastic systems: General principles and application to the onshore Kimmeridge Clay Formation, UK. In *Sequence Stratigraphy in British Geology* (ed. Hesselbo S. and Parkinson N.), Geol. Soc. Lond. Spec. Publ. **103**, 75-96.
- Wignall P.B. (1994) *Black Shales*. Clarendon Press, Oxford. pp. 127.
- Wignall P.B. and Ruffell A.H. (1990) The influence of a sudden climatic change on marine deposition in the Kimmeridgian of northwest Europe. *J. Geol. Soc. London* **147**, 365-371.
- Ziegler P.A. (1981) Evolution of sedimentary basins in North-West Europe. In *Petroleum Geology of the Continental Shelf of North-West Europe* (ed. L.V. Illing and G.D. Hobson), pp. 3-39. The Institute of Petroleum, London.

# Appendix



- a**  $R_1 = \text{CH}_3, R_2 = \text{H}, R_3 = \text{H}$       8-Me-MTTC
- b**  $R_1 = \text{CH}_3, R_2 = \text{H}, R_3 = \text{CH}_3$     5,8-diMe-MTTC
- c**  $R_1 = \text{CH}_3, R_2 = \text{CH}_3, R_3 = \text{H}$       7,8-diMe-MTTC
- d**  $R_1 = \text{CH}_3, R_2 = \text{CH}_3, R_3 = \text{CH}_3$    5,7,8-triMe-MTTC





## Chapter 2

### Characterisation of an extremely organic sulfur-rich, 150 Ma old carbonaceous rock: Palaeoenvironmental implications.

#### Abstract

An extremely organic sulfur-rich coccolithic limestone of the Upper Jurassic Calcaires en plaquettes Formation (southern Jura, France) was analysed for its molecular composition using several wet-chemical and instrumental methods and techniques. The bitumen accounts for 19% of the total organic matter, and predominantly consists of high-molecular-weight sulfur-bound constituents, which ended up in the asphaltene and polar fractions. *n*-Alkane and hopanoid carbon skeletons, together accounting for the majority of compounds in the polar and apolar fractions, mainly occur in a sulfur-bound form as thiophenes, dithiophenes, cyclic sulfides and compounds that are intermolecularly sulfur-bound. A series of C<sub>18</sub>-C<sub>32</sub> 9-methylalkanes, components of as yet unknown origin, is exclusively present in a sulfur-bound form. Sulfur incorporation into the aromatic carotenoid isorenieratene gave rise to a large variety of thiophenic and sulfidic aryl and diaryl isoprenoids. Although steroids are only minor constituents of the bitumen, it is noteworthy that 24-methyl-5 $\alpha$ ,14 $\beta$ ,17 $\beta$ (H)-cholestanes are more abundant than their 14 $\alpha$ ,17 $\alpha$ (H)-counterparts, and that a series of C<sub>27</sub>-C<sub>29</sub> steradienes was detected with unknown positions of the double bonds.

Like the bitumen, the kerogen and asphaltene pyrolysates are dominated by organic sulfur compounds. In addition to thiophenes and benzothiophenes, compounds that are common to pyrolysates of organic sulfur-rich macromolecules, several novel homologous series of sulfur-containing pyrolysis products were found. Based on mass spectral data and desulfurisation products, these were tentatively identified as alkylbithiophenes, dialkylbithiophenes, alkylphenylthiophenes, alkyl(methylphenyl)thiophenes and components possessing both a thiophene and a benzothiophene moiety.

The abundant sulfurisation of organic matter and the presence of isorenieratene derivatives indicate that the depositional environment was euxinic most of the time. Since the hopanoid biomarkers are outnumbering the steroids by far, and since the contribution of algal biopolymers to the kerogen is low, it is believed that the organic matter was largely sourced by cyanobacteria.

#### Introduction

The early diagenetic sulfurisation of organic matter (OM) was first evidenced at the molecular level by the identification of a C<sub>35</sub> thiophene hopanoid in immature sediments (Valisolalao, 1984), and many S-bound biomarkers have been identified since (e.g. Adam, 1991; Brassell et al., 1986; Cyr et al., 1986; van Kaam-Peters et al., 1995; Kohnen et al., 1991a; de Lemos Scofield, 1990; Schaeffer, 1993; Schaeffer et al., 1995; Schmid, 1986; Schouten et al., 1995b; Sinninghe Damsté et al., 1987c, 1989b). Reduced inorganic sulfur species can thus react with functionalised lipids, leading to a large variety of organic sulfur

compounds (OSC). In this way, otherwise labile organic compounds acquire a resistance against biodegradation, and are more likely to be preserved in the sedimentary record (Sinninghe Damsté and de Leeuw, 1990). Sulfur may be incorporated in an intramolecular fashion, or the sulfur atoms may form linkages between individual compounds, creating a macromolecular network (e.g. Schouten et al., 1995a; Sinninghe Damsté et al., 1988b). The OSC have a good biomarker potential. Firstly, as with non sulfur-containing biomarkers, the carbon skeleton itself may be specific to certain source organisms. Secondly, the positions of the C-S bonds indicate where original functionalities of the precursor molecule were located (Sinninghe Damsté et al., 1989a). And thirdly, though equally well applied to other compounds, their  $^{13}\text{C}$  content may help to determine the origin of OSC with little if any structural particularity.

Although organic sulfur-rich deposits can be traced back until the Precambrian, the Upper Jurassic limestone discussed in this study is among the oldest containing plentiful OSC in the bitumen. The sample was taken from a quarry near Orbagnoux (France), which has been exploited since 1843 to produce mineral oil used for agricultural and pharmaceutical products. Active ingredients in these products mostly are sulfur-containing compounds, which are distilled directly from the shale oil. The sedimentary OM was thus anticipated to be rich in organic sulfur, and taken together with its immature character ( $R_o = 0.3$ ; Kohnen, pers. comm.), seemed well-suited to study early diagenetic sulfur incorporation.

An extensive stratigraphical, micropalaeontological and sedimentological study of the Kimmeridgian sedimentation in the southern Jura mountains was performed by Bernier (1984). During the late Kimmeridgian, the Orbagnoux area was part of a carbonate platform with a north-south oriented barrier-reef at its outer boundary. Over an area of approximately 300 km<sup>2</sup>, in a confined lagoonal setting west of the barrier-reef, the Calcaires en plaquettes Formation (CPF) was deposited. This sedimentary sequence is composed of limestones with alternating light and dark coloured laminae of less than a millimetre to several centimetres thick. In a one to two kilometre wide zone along the reef carbonates, the CPF is more organic-rich than elsewhere, and in this zone the quarry is located. On the basis of sedimentological characteristics the bituminous laminated rocks in this region, including our sample, were interpreted to be deposited in an euxinic environment (Bernier, 1984). By contrast, in a more recent study dealing with the CPF (Tribovillard et al., 1992), it was proposed that OM preservation had resulted from the presence of microbial mats. The mats would have acted as a barrier separating an oxygenated water column from anoxic conditions in the sediment. Particulate OM settling on the sea-floor would be protected from oxidation by the microbial mats, and large amounts of OM would accumulate.

Here we describe in detail the molecular composition of the OM in one of the varved bituminous rocks of the CPF. The extractable OM was fractionated into an asphaltene, a polar and an apolar fraction. Polar and apolar fractions were analysed for their biomarker content, both qualitatively and quantitatively. The asphaltene fraction and the kerogen were examined using Curie-point pyrolysis-gas chromatography-mass spectrometry, and in the case of the kerogen an additional off-line pyrolysis experiment was performed. The off-line pyrolysate was fractionated and several novel homologous series of OSC were tentatively identified in one of the fractions. Altogether, the data provide the framework for a

palaeoenvironmental reconstruction, which is in line with the earlier interpretation of Bernier (1984) that sedimentation took place in an euxinic environment.

## Material and methods

*Sample description.* The sample was taken from a quarry near Orbagnoux, a small village located in the southern Jura mountains of France. The rock is predominantly composed of coccoliths and exhibits varves of generally less than a millimetre thickness. Depending on the concentration of OM in the individual laminae, these varves appear as various shades of brown. The OM is highly immature ( $R_o = 0.3$ ; Kohnen, pers. comm.), and its Rock Eval Hydrogen Index (HI) amounts to 766. The approximately 5 cm thick sample has a total organic carbon content (TOC) of 6.2%.

*Extraction and fractionation.* The powdered sample (ca. 100 g) was Soxhlet extracted with methanol (MeOH)/dichloromethane (DCM) (1:7.5; v/v) for 24 h. Asphaltenes were precipitated in *n*-heptane. An aliquot of the maltene fraction (ca. 250 mg), to which a mixture of four standards was added for quantitative analysis (Kohnen et al., 1990), was separated into two fractions using a column (20 cm x 2 cm; column volume ( $V_0$ ) = 35 ml) packed with alumina (activated for 2.5 h at 150°C) by elution with hexane/DCM (9:1, v/v; 150 ml; “apolar fraction”) and DCM/MeOH (1:1, v/v; 150 ml; “polar fraction”). An aliquot (ca. 10 mg) of the apolar fraction was further separated by argentation TLC (thin layer chromatography) using hexane as developer. The  $Ag^+$ -impregnated silica plate (20 x 20 cm; thickness 0.25 mm) was prepared by immersion into a solution of 1%  $AgNO_3$  in MeOH/ $H_2O$  (4:1; v/v) for 45 s and subsequent activation at 120°C for 1 h. Four fractions (A1,  $R_f = 0.82-1$ ; A2,  $R_f = 0.34-0.82$ ; A3,  $R_f = 0.10-0.34$ ; A4,  $R_f = 0-0.10$ ) were scraped off the TLC plate and ultrasonically extracted with ethyl acetate. All four fractions were analysed by GC and GC-MS, and subsequently the A2, A3 and A4 fractions were desulfurised (see below). Four A4 fractions prepared in this way were combined, and this combined fraction was further separated by TLC, using an activated silica plate with hexane as the eluents, and three subfractions were obtained (A4a,  $R_f = 0.62-1$ ; A4b,  $R_f = 0.38-0.62$ ; A4c,  $R_f = 0-0.38$ ).

*n*-Alkanes were removed from the A1 fraction (and from the desulfurised A4 fraction) using a 5 Å molecular sieve (8-12 mesh, Baker). The molecular sieve was extracted with DCM and activated at 400°C over night. Five grains were added for each mg of sample, and the mixture was refluxed in dry cyclohexane for 24 h. Recovery of the non-adduct was performed by removal of the cyclohexane followed by warm cyclohexane rinses of the sieves. All rinses were combined to yield the non-adduct. Subsequently, the *n*-alkanes were obtained by refluxing the sieves in hexane for 24 h. The non-adduct was further separated using a small column (5 cm x 0.5 cm;  $V_0 = 1$  ml) packed with  $AgNO_3$  impregnated (20% w/w; activated for 16 h at 120°C) silicagel (Merck, Silicagel 60, 70-230 mesh ASTM) by elution with hexane (saturated hydrocarbons) and ethyl acetate (stripping). The adduct and the saturated hydrocarbon fraction of the non-adduct were analysed by GC-IRMS.

*Raney nickel desulfurisation and hydrogenation.* The A2, A3 and A4 fractions obtained by argentation TLC were dissolved in 4 ml ethanol together with 0.5 ml of a suspension of

Raney nickel (0.5 g/ml ethanol) and heated under reflux for 1.5 h. In the case of the polar fraction, a known amount (ca. 20 µg) of standard (2,3-dimethyl-5-(1,1-dideuterohexadecyl)thiophene) was added to an aliquot (ca. 15 mg). The desulfurisation products were isolated by centrifugation and subsequent extraction with DCM (x4) of the precipitate. The combined extracts were washed (x3) with NaCl-saturated, bidistilled H<sub>2</sub>O and dried with MgSO<sub>4</sub>. The hydrocarbons formed were isolated using a small column (5 cm x 0.5 cm; V<sub>0</sub> = 1 ml) packed with alumina (activated for 2.5 h at 150°C) by elution with hexane/DCM (9:1, v/v). The fraction was evaporated to dryness and dissolved in 4 ml ethyl acetate. Two drops of pure acetic acid and a pinch of PtO<sub>2</sub> were added as catalysts. Hydrogen gas was bubbled through for 1 h, after which the solution was stirred for 24 h. The catalysts were removed using a small column packed with Na<sub>2</sub>CO<sub>3</sub> and MgSO<sub>4</sub>. The fraction was evaporated to dryness and dissolved in a small volume of hexane (2 mg/ml) to be analysed by GC and GC-MS.

*Off-line pyrolysis and fractionation.* Off-line pyrolysis was performed with 1 g of decarbonated (6N HCl), ultrasonically extracted rock, which was heated (400°C) for 1 h in a sample boat positioned in a glass tube in a cylindrical oven under a nitrogen flow. The volatile products generated were trapped in two successive cold traps containing hexane/DCM (9:1, v/v). The first trap was at room temperature; the second trap was cooled with solid CO<sub>2</sub>/acetone. The off-line pyrolysate (combined products of both traps) was fractionated by column chromatography (Al<sub>2</sub>O<sub>3</sub>; 15 cm x 1 cm; V<sub>0</sub> = 8 ml) into an apolar and polar fraction by elution with 32 ml hexane/DCM (9:1, v/v) and 32 ml MeOH/DCM (1:1, v/v), respectively. The apolar fraction was further separated using a column as described for the apolar/polar separation, by eluting with 48 ml hexane and, respectively, 8, 4, 4 and 16 ml hexane/DCM (9:1, v/v). The fractions obtained were analysed by GC and GC-MS, and subsequently the last eluting fraction (P5) was desulfurised. Desulfurisation of the P5 fraction was principally the same as outlined above for the TLC fractions, except that the hydrocarbons formed were not concentrated by evaporation, but to minimise loss of volatiles, were concentrated by distillation instead. Desulfurisation products were analysed by GC and GC-MS.

*Flash pyrolysis.* Pyrolysis (10 s) was performed with a FOM-3LX unit. The decarbonated (6N HCl) and ultrasonically extracted sample was applied to a ferromagnetic wire with a Curie temperature of 610°C.

*Gas chromatography (GC).* GC was performed using a Carlo Erba 5300 or a Hewlett-Packard 5890 instrument, both equipped with an on-column injector. A fused silica capillary column (25 m x 0.32 mm) coated with CP-Sil 5 (film thickness 0.12 µm) was used with helium as carrier gas. The effluent of the Carlo Erba 5300 was monitored by a flame ionisation detector (FID). The effluent of the Hewlett-Packard 5890 was monitored by both a flame ionisation detector (FID) and a sulfur-selective flame photometric detector (FPD), applying a stream-splitter with a split ratio of FID:FPD = ca. 1:2. Fractions of the off-line pyrolysate were analysed applying the following temperature program: 30°C (5 min),

3°C/min to 310°C (5 min). Fractions of the extract were injected at 70°C, after which the temperature was raised at 20°C/min to 130°C, and at 4°C/min to 320°C (15 min).

For analysing the flash pyrolysate, separation was achieved using a CP-Sil 5 capillary column (25 m x 0.32 mm) with a film thickness of 0.4 µm. The gas chromatograph, equipped with a cryogenic unit, was programmed from 0°C (5 min) to 310°C (5 min) at a rate of 3°C/min.

*Gas chromatography-mass spectrometry (GC-MS).* GC-MS was carried out on a Hewlett-Packard 5890 gas chromatograph interfaced to a VG Autospec Ultima Q mass spectrometer operated at 70 eV with a mass range  $m/z$  50-800 and a cycle time of 1.8 s (resolution 1000). The gas chromatograph was equipped with a CP-Sil 5 capillary column (25 m x 0.32 mm) with a film thickness of 0.12 µm. Helium was used as carrier gas. The flash pyrolysate and fractions of the off-line pyrolysate were analysed applying the same temperature program as for GC. Fractions of the extract were injected at 60°C, after which the temperature was raised at 20°C/min to 130°C, and at 4°C/min to 320°C (15 min).

*Gas chromatography-isotope ratio mass spectrometry (GC-IRMS).* The DELTA-C GC-IRMS-system used is in principal similar to the DELTA-S system described by Hayes et al. (1990). The gas chromatograph (Hewlett-Packard 5890) was equipped with an on-column injector and a fused silica capillary column (25 m x 0.32 mm) coated with CP-Sil 5 (film thickness 0.12 µm). Helium was used as the carrier gas. The oven temperature was programmed from 70°C to 130°C at 20°C/min, from 130°C to 310°C at 4°C/min and maintained at 310°C for 15 min. The  $\delta^{13}\text{C}$  values (vs. PDB) were calculated by integrating the mass 44, 45 and 46 ion currents of the  $\text{CO}_2$  peaks produced by combustion of the column effluent and those of  $\text{CO}_2$  spikes with a known  $^{13}\text{C}$ -content which were directly led into the mass spectrometer at regular intervals. The  $\delta^{13}\text{C}$  values reported are averages of at least two measurements.

*Quantification.* Free *n*-alkanes and *n*-alkanes released upon desulfurisation of the A2, A4, polar and asphaltene fractions were quantified by determining their peak areas in the  $m/z$  57 mass chromatogram, and relating these to the peak area of the internal standard (3-methyl-6-dideutero-henicosane) in the same chromatogram. To account for the different responses of FID and MS, concentrations were multiplied by the following correction factors: *n*- $\text{C}_{16}$  till *n*- $\text{C}_{27}$ , 0.88; *n*- $\text{C}_{28}$ , 0.90; *n*- $\text{C}_{29}$ , 0.93; *n*- $\text{C}_{30}$ , 0.98; *n*- $\text{C}_{31}$ , 1.04; *n*- $\text{C}_{32}$ , 1.14; *n*- $\text{C}_{33}$ , 1.26; *n*- $\text{C}_{34}$ , 1.41; *n*- $\text{C}_{35}$ , 1.60; *n*- $\text{C}_{36}$ , 1.85; *n*- $\text{C}_{37}$ , 2.20; *n*- $\text{C}_{38}$ , 2.51; *n*- $\text{C}_{39}$ , 2.71; *n*- $\text{C}_{40}$ , 2.93. In the case of the desulfurised A3 fraction the most abundant *n*-alkanes were quantified by comparing their peak areas in the FID-trace to that of the internal standard (2-methyl-2-(4,8,12-trimethyltridecyl)chroman). The remaining *n*-alkane homologues in this fraction were quantified by integration of their peaks in the  $m/z$  57 mass chromatogram and comparison with peak areas of *n*-alkanes with a known concentration.

Pristane, phytane and (22R)-17 $\alpha$ ,21 $\beta$ (H)-pentakishomohopane in the desulfurised A2, A4 and polar fractions, and free pristane, phytane, 17 $\alpha$ ,21 $\beta$ (H)-hopane, (22S)-homohop-17(21)-ene, benzohopanes **I** (see Appendix),  $\text{C}_{31}$  benzohopane **IIa**,  $\text{C}_{35}$  hopanoid benzothiophene **IIIb** and  $\text{C}_{34}$  hopanoid benzothiophene **IVb** were quantified by relating their

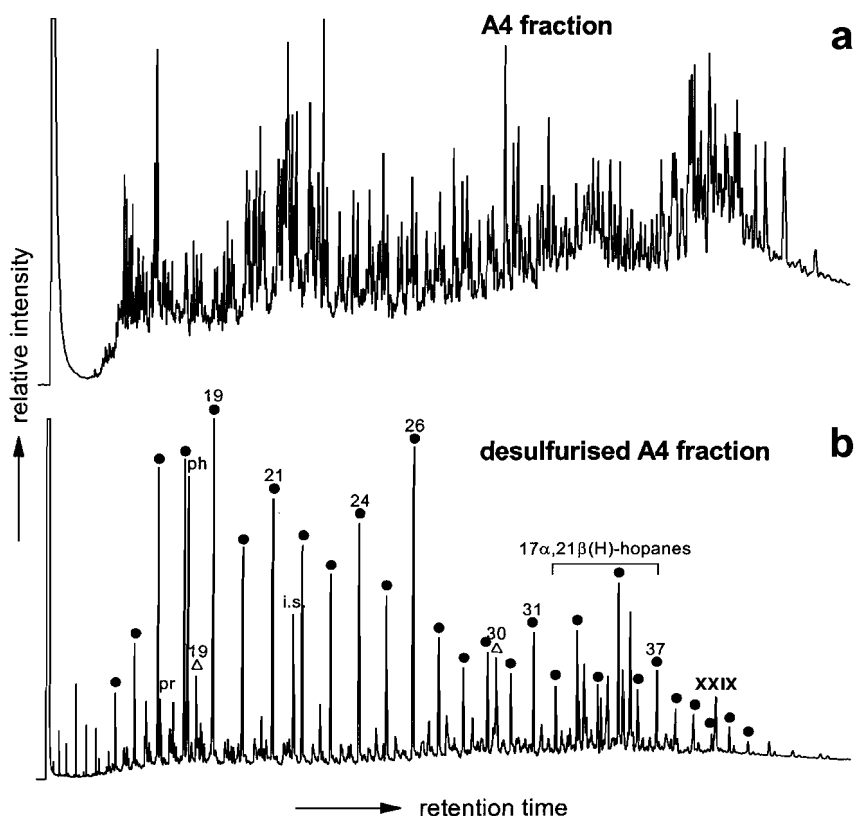


**Fig. 2.1.** GC-FID traces of (a) A4 fraction (b) desulfurised A4 fraction. Roman numbers refer to structures indicated in the Appendix; filled circles indicate *n*-alkanes; open triangles indicate 9-methylalkanes; numbers correspond to number of carbon atoms; pr = pristane; ph = phytane; i.s. = internal standard.

peak areas in the FID-trace to that of the internal standard. Other hopanoids were quantified by integration of their peaks in relevant mass chromatograms ( $m/z$  191, 367,  $M^+$  or  $M^+-15$ ) and comparison with peak areas of hopanoids whose concentrations were established using the FID-signal.

The 2,3-dimethylthiophene over (1,2-dimethylbenzene + *n*-non-1-ene) ratio was calculated from the peak areas concerned in the total ion current. The 2-methylthiophene over toluene ratio was determined by integration of the relevant peaks in the  $m/z$  97 + 98 and  $m/z$  91 + 92 mass chromatograms.

## Results and discussion

The extraction yield of the sample was very high, amounting to 0.19 g per g TOC. 38% of the extractable OM precipitated in *n*-heptane (asphaltene fraction). Chromatographic separation of the maltene fraction yielded a polar and an apolar fraction, amounting to 53

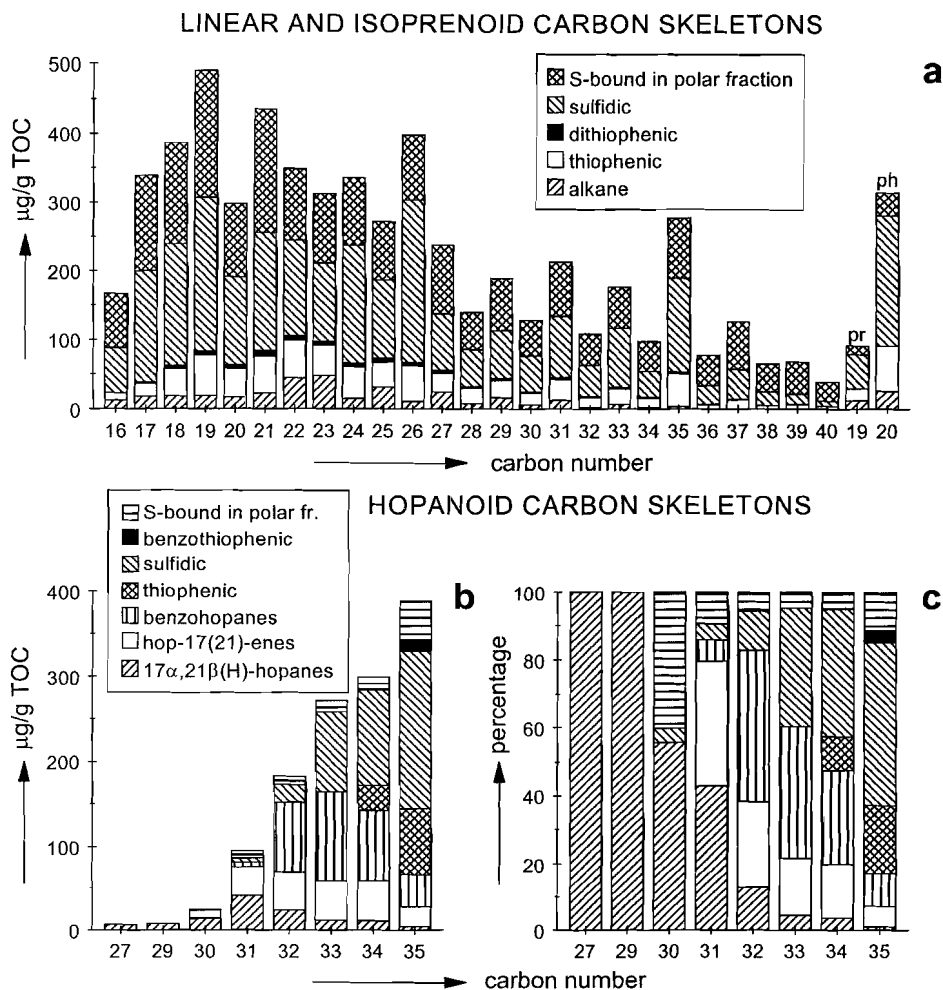


**Fig. 2.2.** TOC-normalised concentrations of (a) pristane (pr), phytane (ph) and *n*-alkane carbon skeletons and (b) hopanoid carbon skeletons. (c) Contribution of hopanoid carbon skeletons expressed as a percentage of their total.

and 24% w/w of the starting material, respectively. All fractions contain abundant OSC. In order to quantify several classes of OSC in the apolar fraction, thiophenic sulfur compounds were separated from sulfidic sulfur compounds using argentation TLC, and the individual fractions were desulfurised, resulting in a marked drop in complexity of the chromatograms (e.g. Fig. 2.1). Subsequently, *n*-alkanes, isoprenoid alkanes and hopanes released upon desulfurisation were quantified using an internal standard. The contribution of OSC to the polar fraction, consisting predominantly of high-molecular-weight (HMW) OSC and/or low-molecular-weight (LMW) sulfoxides, was determined by quantifying the desulfurisation products of this fraction. To determine to which extent these products were derived from

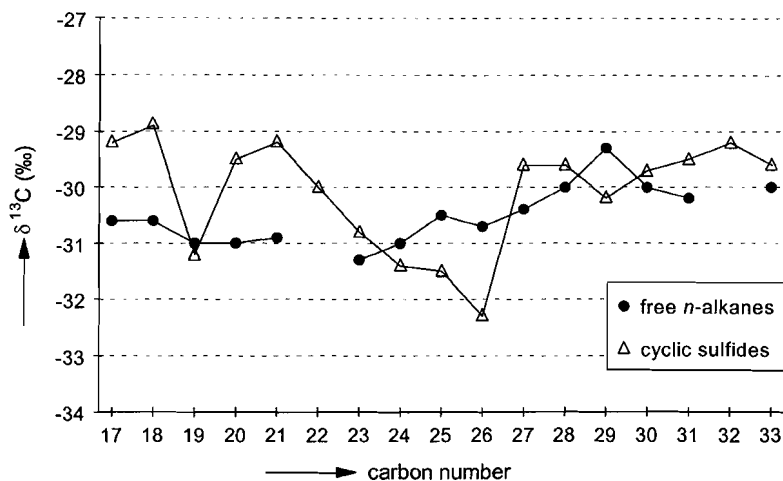


**Fig. 2.3.** Stable carbon isotopic composition of free *n*-alkanes (except for *n*-C<sub>22</sub>, which was contaminated) and *n*-alkanes released upon desulfurisation of the A4 fraction. Standard deviations are typically 0.3‰.

sulfoxides, the polar fraction was subjected to LiAlH<sub>4</sub> reduction (Payzant et al., 1986; Schouten et al., 1995c).

#### *Carbon skeletons in the bitumen*

*n*-Alkane skeletons. More than 90% of the *n*-alkane carbon skeletons are present in a S-bound form (Fig. 2.2a). Distributions of free *n*-alkanes maximise at *n*-C<sub>23</sub> and show a slight odd-over-even carbon number predominance of the C<sub>23+</sub> homologues, suggesting a small input from terrestrial plant waxes. The δ<sup>13</sup>C values of free C<sub>17</sub>-C<sub>24</sub> *n*-alkanes are stable at -31‰, whereas the higher homologues are slightly more enriched in <sup>13</sup>C (Fig. 2.3).

In the A2 fraction components with *n*-alkane backbones consist of 2-*n*-alkyl- and 2,5-di-*n*-alkylthiophenes. The distribution of *n*-alkanes released upon desulfurisation of the A2 fraction shows (sub)maxima at *n*-C<sub>19</sub>, *n*-C<sub>21</sub>, *n*-C<sub>24</sub>, *n*-C<sub>26</sub> and *n*-C<sub>35</sub>. In the case of *n*-C<sub>19</sub> the distribution of the corresponding thiophenes exhibits a relatively abundant 2-*n*-butyl-5-*n*-undecylthiophene (Fig. 2.4a). Distributions of C<sub>24</sub> and C<sub>26</sub> thiophenes are characterised by relatively high concentrations of mid-chain thiophenes, i.e. 2,5-di-*n*-alkylthiophenes with *n*-alkyl chains comprising more than six carbon atoms. Other thiophenes with linear carbon skeletons show distributions that are not notably different from each other.

The distribution of *n*-alkanes released upon desulfurisation of the A3 fraction maximises at *n*-C<sub>21</sub>. Although concentrations are low and no pure mass spectra could be obtained, in the original A3 fraction these *n*-alkane skeletons were probably present as dithiophenes. The isotope distributions and masses of the molecular ions pointed to the presence of two thiophene moieties, and the fragment ions indicated that the two thienyl



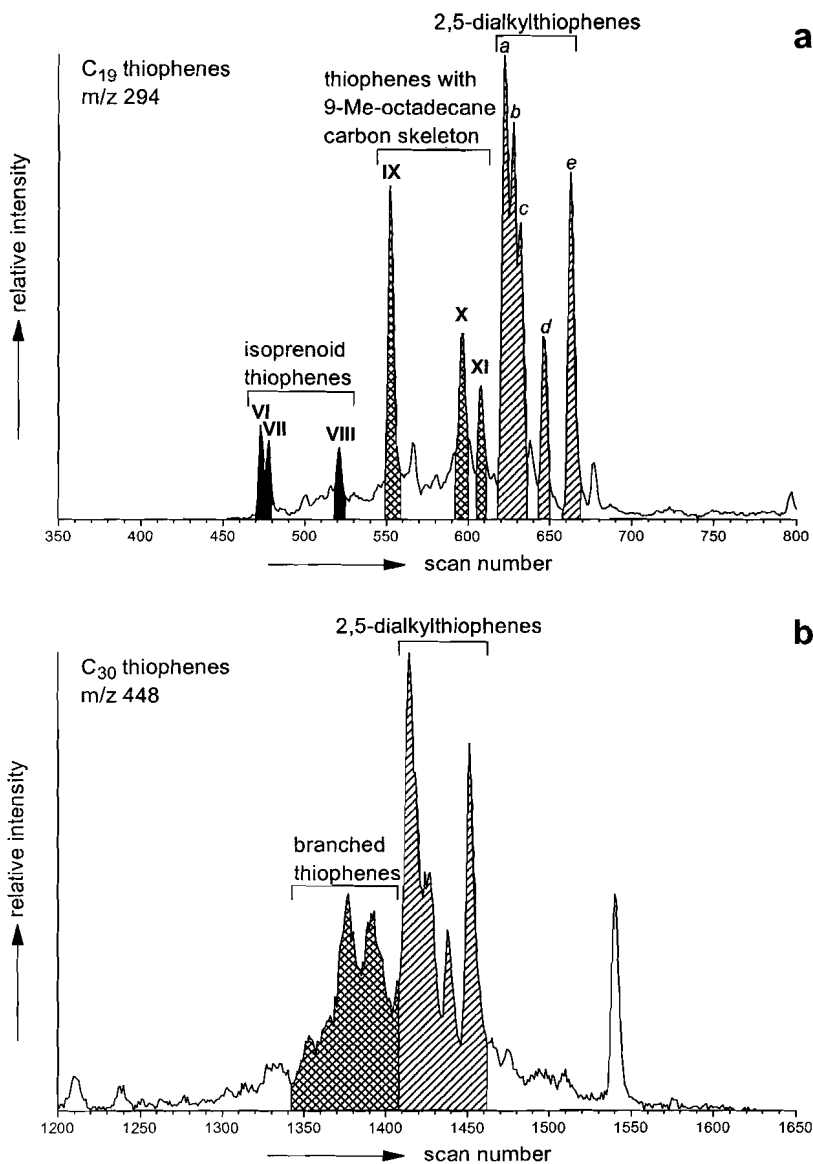


**Fig. 2.4.** Distributions of (a) C<sub>19</sub> thiophenes and (b) C<sub>30</sub> thiophenes as shown by partial mass chromatograms of the respective molecular ions. Roman numbers refer to structures indicated in the Appendix; *a* = 2-*n*-butyl-5-*n*-undecylthiophene, *b* = 2-*n*-propyl-5-*n*-dodecylthiophene, *c* = 2-ethyl-5-*n*-tridecylthiophene, *d* = 2-methyl-5-*n*-tetradecylthiophene, *e* = 2-*n*-pentadecylthiophene.

moieties were separated from each other by one or more carbon atoms (Schmid, 1986; Sinnighe Damsté et al., 1987c).

The cyclic sulfides with linear carbon skeletons eluting in the A4 fraction, comprise a complicated mixture of 2-*n*-alkylthiolanes, 2,5-di-*n*-alkylthiolanes, 2-*n*-alkylthianes and 2,6-di-*n*-alkylthianes, and form the largest sink of *n*-alkyl skeletons (Fig. 2.2a). Like the *n*-alkanes in the desulfurised A2 fraction, *n*-alkanes in the desulfurised A4 fraction are characterised by relatively abundant C<sub>19</sub>, C<sub>21</sub>, C<sub>24</sub>, C<sub>26</sub> and C<sub>35</sub> members. As regards *n*-C<sub>19</sub>, the distribution of the corresponding sulfides shows a prominent 2-*n*-propyl-6-*n*-undecylthiane. In addition, distributions of C<sub>19</sub>, C<sub>24</sub> and C<sub>26</sub> sulfides reveal relatively large contributions of 2,6-di-*n*-alkylthianes with side chains of at least five carbon atoms. Markedly, the C<sub>19</sub>, C<sub>24</sub> and C<sub>26</sub> *n*-alkanes in the desulfurised fraction not only deviate by their abundances and corresponding sulfide distributions, but also by their relatively low <sup>13</sup>C-contents as compared to other *n*-alkanes released (Fig. 2.3). No significant differences were observed among the distributions of other sulfides with linear carbon skeletons.

A long series of *n*-alkanes (C<sub>15</sub>-C<sub>44</sub>), maximising at *n*-C<sub>19</sub> and *n*-C<sub>21</sub>, was obtained after desulfurisation of the polar fraction. Like in the desulfurised A2 and A4 fractions, *n*-C<sub>35</sub> is the most abundant C<sub>27+</sub> *n*-alkane. LiAlH<sub>4</sub> reduction of the polar fraction yielded only trace amounts of sulfides, indicating that the contribution of *n*-alkane carbon skeletons that are present as sulfoxides, is extremely low (Payzant et al., 1986; Schouten et al., 1995c). The vast majority of *n*-alkanes in the desulfurised polar fraction are thus derived from intermolecularly S-bound skeletons forming macromolecules.

*Pristane and phytane skeletons.* Like the *n*-alkane skeletons, pristane and phytane skeletons are largely S-bound (Fig. 2.2). Pristane and phytane in the desulfurised A2 fraction derive from several C<sub>19</sub> and C<sub>20</sub> isoprenoid thiophenes. Thiophenes with a phytane skeleton are highly dominated by 2,3-dimethyl-5-(2,6,10-trimethylundecyl)-thiophene (**V**), identified by comparison of its mass spectrum and relative retention time with those reported (Sinninghe Damsté et al., 1986, 1987a). By contrast, there are three equally abundant thiophenes with a pristane skeleton (Fig. 2.4a). Based on mass spectral data (Sinninghe Damsté et al., 1986; Koopmans et al., 1997), these were tentatively identified as 5-(2,6-dimethylheptyl)-2-(3-methylbutyl)-3-methyl-thiophene (**VI**), 5-(3,7-dimethyloctyl)-2-(2-methylpropyl)-4-methyl-thiophene (**VII**) and 5-(2,6,10-trimethylundecyl)-3-methyl-thiophene (**VIII**). Pristane and phytane in the desulfurised A4 fraction originate from C<sub>19</sub> and C<sub>20</sub> isoprenoid thiolanes or thianes. The m/z 298 and m/z 312 mass chromatograms of the A4 fraction indicate the presence of at least two different sulfides with a pristane skeleton, and a complex mixture of sulfides with a phytane skeleton. Due to coelution no pure mass spectra of these compounds could be obtained. Pristane and phytane in the desulfurised polar fraction had been mainly bound in a macromolecular fashion, as concluded from the presence of only trace amounts of sulfoxides, obtained by LiAlH<sub>4</sub> reduction of the polar fraction.

Pristane/phytane ratios amount to 0.26, 0.26 and 0.38 in the desulfurised A2, A4 and polar fractions, respectively, which is consistently lower than the 0.48 in the saturated hydrocarbon fraction. Thus, sulfur incorporation favoured the preservation of the phytane skeleton over that of the pristane skeleton. S-bound phytane most likely originates from natural sulfurisation of phytol or derivatives thereof (Brassell et al., 1986; Sinninghe Damsté and de Leeuw, 1987). The relatively abundant pristane in the desulfurised fractions (Fig. 2.2) suggests a significant contribution of precursors other than tocopherols (Goossens et al.,

1984), a finding also reported for the Cretaceous Ghareb Formation (Koopmans et al., 1997). Koopmans et al. (1997) suggested S-bound pristane, during diagenesis ultimately yielding free pristane, to originate from sulfur incorporation into mono-, di- and tri-unsaturated pristenes, which occur in zooplankton (Blumer and Thomas, 1965; Blumer et al., 1969).

The  $\delta^{13}\text{C}$  values of free and S-bound phytane, probably reflecting  $\delta^{13}\text{C}$  of the average algal lipid, and the  $\delta^{13}\text{C}$  value of free pristane are virtually identical, amounting to -30.6 or -30.5‰ (Table 2.1). Since heterotrophs generally bear a close carbon isotopic resemblance to their diets (Fry and Sherr, 1984), it cannot be decided between a phytoplanktonic or zooplanktonic origin for pristane based on its stable carbon isotopic composition.

**Table 2.1.** Stable carbon isotopic composition of different biomarkers.

	$\delta^{13}\text{C}$ value (‰)
pristane <sup>1</sup>	-30.6 ± 0.1
phytane <sup>1</sup>	-30.5 ± 0.1
phytane <sup>2</sup>	-30.6 ± 0.4
9-methyloctadecane <sup>2</sup>	-28.1 ± 0.1
9-methylnonacosane <sup>2</sup>	-24.7 ± 0.3
17 $\alpha$ ,21 $\beta$ (H)-hopane <sup>1</sup>	-30.3 ± 0.4
(22S)-homohop-17(21)-ene <sup>1</sup>	-30.1 ± 0.3
(22R)-homohop-17(21)-ene <sup>1</sup>	-32.8 ± 0.5
(22R)-bishomohop-17(21)-ene <sup>1</sup>	-33.0 ± 1.6
(22R)-trishomohop-17(21)-ene <sup>1</sup>	-32.2 ± 0.8
(22S)-tetrakishomohop-17(21)-ene <sup>1</sup>	-28.7 ± 0.3
(22R)-tetrakishomohop-17(21)-ene <sup>1</sup>	-30.1 ± 0.5
(22S)-17 $\alpha$ ,21 $\beta$ (H)-tetrakishomohopane <sup>2</sup>	-29.7 ± 0.5
(22R)-17 $\alpha$ ,21 $\beta$ (H)-tetrakishomohopane <sup>2</sup>	-31.2 ± 0.3
(22S)-17 $\alpha$ ,21 $\beta$ (H)-pentakishomohopane <sup>2</sup>	-31.4 ± 0.5
(22R)-17 $\alpha$ ,21 $\beta$ (H)-pentakishomohopane <sup>2</sup>	-29.6 ± 0.2
C <sub>32</sub> benzohopane <b>I</b>	-32.6 ± 0.2
C <sub>33</sub> benzohopane <b>I</b>	-33.0 ± 0.4
C <sub>34</sub> benzohopane <b>I</b>	-30.6 ± 0.4
C <sub>35</sub> benzohopane <b>I</b>	-30.3 ± 0.6
C <sub>35</sub> benzothiophene hopanoid <b>IIIb</b>	-33.5 ± 0.3
<b>L</b> or <b>LI</b>	-28.7 ± 0.4
<b>LII</b> or <b>LIII</b>	-29.8 ± 0.2
diMe-MTTCs ( <b>LVIIb,c</b> )	-31.6 ± 0.8
triMe-MTTC ( <b>LVIId</b> )	-32.6 ± 0.2
isorenieratane ( <b>XXIX</b> )	-19.0 ± 0.8
<b>LVI</b>	-23.5 ± 0.6
<b>XLVII</b> <sup>3</sup>	-19.2 ± 0.3
<b>XLVIII</b> <sup>3</sup>	-21.2 ± 0.5
<b>XLIX</b> <sup>3</sup>	-19.6 ± 0.6

<sup>1</sup> non-adduct of A1 fraction

<sup>2</sup> desulfurised A4 fraction

<sup>3</sup> A4c fraction

*9-Methylalkane skeletons.* A series of C<sub>18</sub>-C<sub>32</sub> 9-methylalkanes maximising at C<sub>19</sub> and C<sub>30</sub> is present in the desulfurised A2, A3, A4 and polar fractions (Fig. 2.5). The series was not

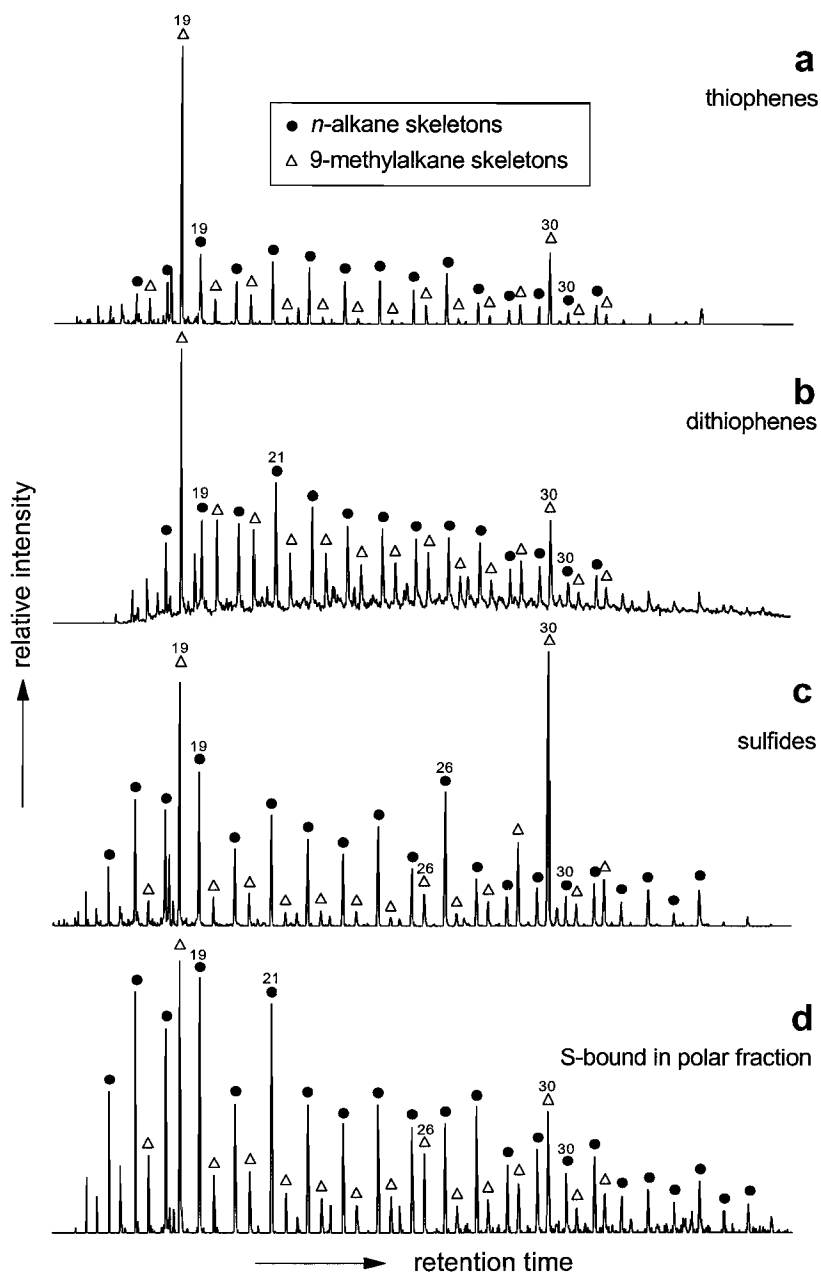


**Fig. 2.5.** Distributions of (a) thiophenic (b) dithiophenic (c) sulfidic and (d) macromolecularly S-bound 9-methylalkanes, as expressed by the  $m/z$  140 mass chromatograms of the different fractions after desulfurisation. Numbers correspond to number of carbon atoms.

detected in the saturated hydrocarbon fraction. Identification is based on the characteristic  $m/z$  140 and  $m/z$   $M^+ - 112$  fragment ions in their mass spectra, resulting from C-C bond cleavage adjacent to the tertiary carbon atom, accompanied by a hydrogen rearrangement (McCarthy et al., 1968; Holzer et al., 1979). The Kováts Index of the 9-methylpentacosane is 2538, which is not significantly different from 2536 reported for synthetic 9-methylpentacosane (Pomonis et al., 1989).

Detection of these 9-methylalkanes in the various desulfurised fractions implies the presence in the extract of thiophenes, dithiophenes, cyclic sulfides and macromolecularly S-bound moieties with such a skeleton. Thiophenes with the 9-methyloctadecane skeleton are dominated by 2-butyl-5-(2'-undecyl)-thiophene (**IX**), 2,5-diheptyl-3-methyl-thiophene (**X**) and 2-methyl-5-(4-methyltridecyl)-thiophene (**XI**) (Fig. 2.4), as identified by comparison of their mass spectra and relative retention times with those reported (Sinninghe Damsté et al., 1989a). By contrast, thiophenes with the 9-methylnonacosane skeleton exhibit a more random position of the thiophene moiety in the carbon chain, as deduced from the absence of distinct peaks in the appropriate region of the  $m/z$  448 mass chromatogram (Fig. 2.4b). The precise structures of the dithiophenes and sulfides with the 9-methylalkane skeleton could not be identified due to the relatively low abundance of dithiophenes in the A3 fraction, and the complexity of the sulfide fraction. 9-Methylalkanes in the desulfurised polar fraction are almost exclusively derived from macromolecular aggregates, as concluded from their almost absence in the  $\text{LiAlH}_4$  treated polar fraction. The desulfurisation method used does not allow for determination of the original position(s) of the sulfur-bond(s) within the molecules.

Although the origin of the series is unknown, there are several reasons to believe it derives from two different source organisms at least. Firstly, since the distribution of 9-methylalkanes is dominated by both an odd carbon number homologue and an even carbon number homologue, it is unlikely that there is a biosynthetic relationship between the two, since chain elongation generally proceeds with two carbon atoms at a time. Secondly, the thiophenes with the 9-methyloctadecane skeleton are highly dominated by three specific isomers, whereas the distribution of the branched  $\text{C}_{30}$  thiophenes shows no distinct peaks (Fig. 2.4). This indicates that the original functionalities of the 9-methylnonacosane were located at several carbon atoms throughout the molecule, whereas in the case of 9-methyloctadecane functionalities were limited to specific sites. Thirdly, 9-methyloctadecane is significantly depleted in  $^{13}\text{C}$  compared to 9-methylnonacosane (Table 2.1). However, it is recognised that this difference in isotopic composition on its own is no proof of a different provenance (Summons et al., 1994).

*Hopanoid skeletons.* Depending on carbon number, 15 to 80% of the extended hopanoids are present in a S-bound form (Fig. 2.2c). The non-sulfur containing hopanoids comprise series of  $\text{C}_{27}$ - $\text{C}_{35}$  (22S)- and (22R)-17 $\alpha$ ,21 $\beta$ (H)-hopanes exclusive of the  $\text{C}_{28}$  member,  $\text{C}_{31}$ - $\text{C}_{35}$  (22S)- and (22R)-hop-17(21)-enes,  $\text{C}_{32}$ - $\text{C}_{35}$  benzohopanes **I** and  $\text{C}_{31}$ - $\text{C}_{32}$  benzohopanes **II**. Since benzohopanes **II** are relatively low (for details see van Kaam-Peters et al., 1995), in Figs. 2.2b,c the summed concentrations of **I** and **II** are shown. Thiophene hopanoids, eluting in the A2 fraction, are almost exclusively composed of **XII**, **XIII** and **XIV**, which are  $\text{C}_{34}$  and  $\text{C}_{35}$  members with the thiophene moiety in the side chain (Sinninghe Damsté et al.,

1989b; Köster et al., 1997). A small contribution of C<sub>36</sub> ring A methylated thiophene hopanoid **XV** was detected as well. In the A3 fraction benzothiophene hopanoids **III**, **IV** and **XVI** are present in relatively low amounts (for details see van Kaam-Peters et al., 1995). In Figs. 2.2b,c the summed concentrations of **III** and **IV** are shown. The mixture of hopanoids eluting in the A4 fraction is extremely complex, but upon desulfurisation only 17 $\alpha$ ,21 $\beta$ (H)-hopanes were formed, which are easier to quantify. Hopanoid sulfides **XVII-XXII** were tentatively identified in the A4 fraction based on the mass spectral data reported in literature (Cyr et al., 1986; Kohnen et al., 1991a; Schaeffer, 1993; Schaeffer et al., 1995). The tentative identification of **XXIII** and **XXIV** is discussed elsewhere (Köster et al., 1997). Desulfurisation of the polar fraction yielded a series of C<sub>30</sub>-C<sub>35</sub> 17 $\alpha$ ,21 $\beta$ (H)-hopanes maximising at C<sub>35</sub> (Figs. 2.2b,c).

The distributions of free and S-bound hopanoids, indicate that by sulfur sequestration the C<sub>35</sub> hopane skeleton is selectively preserved over hopane skeletons with smaller side chains, which is in agreement with previous reports (de Leeuw and Sinninghe Damsté, 1990; Sinninghe Damsté et al., 1995). In addition, a correlation was established between the types of hopanoid sulfides formed and the homohopane 22S/22R epimer ratios. This effect of sulfur incorporation is discussed in detail elsewhere (Köster et al., 1997).

The hopanoid  $\delta^{13}\text{C}$  values measured vary between -33.5‰ and -28.7‰, and differences between pairs of 22S and 22R isomers are as large as 2.7‰ in the case of homohop-17(21)-enes (Table 2.1). Such a wide range of  $\delta^{13}\text{C}$  values was also reported for free and S-bound hopanoids in the Jurf ed Darawish oil shale (Sinninghe Damsté et al., 1995). On the basis of molecular mechanic calculations these authors have shown that the diagenetic pathways of bacteriohopanepolyol derivatives are extremely complex, and that even pairs of 22S and 22R isomers not necessarily derive from one bacteriohopanepolyol precursor. The wide range of  $\delta^{13}\text{C}$  values measured in this study is in agreement with this, probably reflecting the multiple origin of the different hopanoid species.

*Steroid skeletons.* Steroids are only minor constituents of the bitumen, and their concentrations could not be accurately determined. Nevertheless, distributions of desmethyl steroids are rather peculiar and warrant a description. 5 $\alpha$ -Cholestane and 24-ethyl-5 $\alpha$ -

**Table 2.2.** Steranes indicated in Fig. 2.6.

Peak	Sterane
1	5 $\beta$ -cholestane
2	(20R)-5 $\alpha$ ,14 $\beta$ ,17 $\beta$ (H)-cholestane
3	(20S)-5 $\alpha$ ,14 $\beta$ ,17 $\beta$ (H)-cholestane
4	5 $\alpha$ -cholestane
5	24-methyl-5 $\beta$ -cholestane
6	(20R)-24-methyl-5 $\alpha$ ,14 $\beta$ ,17 $\beta$ (H)-cholestane
7	(20S)-24-methyl-5 $\alpha$ ,14 $\beta$ ,17 $\beta$ (H)-cholestane
8	24-methyl-5 $\alpha$ -cholestane
9	24-ethyl-5 $\beta$ -cholestane
10	(20R)-24-ethyl-5 $\alpha$ ,14 $\beta$ ,17 $\beta$ (H)-cholestane
11	(20S)-24-ethyl-5 $\alpha$ ,14 $\beta$ ,17 $\beta$ (H)-cholestane
12	24-ethyl-5 $\alpha$ -cholestane

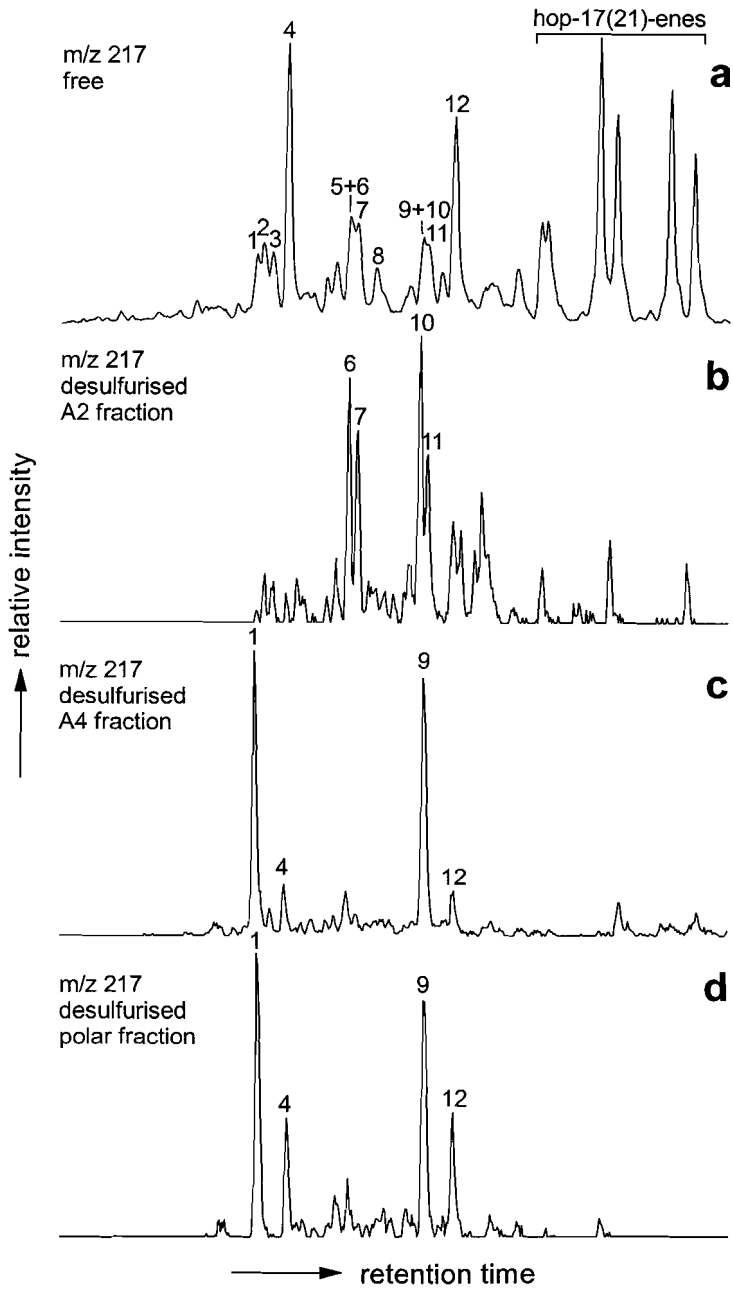


**Fig. 2.6.** Partial m/z 217 mass chromatograms of (a) A1 fraction (b) desulfurised A2 fraction (c) desulfurised A4 fraction and (d) desulfurised polar fraction. Numbers refer to steranes listed in Table 2.2.

cholestane are the dominant steranes in the saturated hydrocarbon fraction (Fig. 2.6a). Markedly, not 24-methyl-5 $\alpha$ -cholestane, but 24-methyl-5 $\alpha$ ,14 $\beta$ ,17 $\beta$ (H)-cholestanes are the next dominant steranes. The 5 $\alpha$ ,14 $\beta$ ,17 $\beta$ (H)-cholestanes and 24-ethyl-5 $\alpha$ ,14 $\beta$ ,17 $\beta$ (H)-cholestanes also occur, but their concentrations are well below those of 5 $\alpha$ -cholestane and 24-ethyl-5 $\alpha$ -cholestane. A series of C<sub>27</sub>-C<sub>29</sub> 5 $\beta$ -steranes is present as well (Fig. 2.6a). C<sub>28</sub>-C<sub>30</sub> 4-methyl steranes are present in trace amounts.

In the m/z 217 mass chromatogram of the desulfurised A2 fraction both 24-methyl-5 $\alpha$ ,14 $\beta$ ,17 $\beta$ (H)-cholestanes and 24-ethyl-5 $\alpha$ ,14 $\beta$ ,17 $\beta$ (H)-cholestanes surpass the other steranes in intensity (Fig. 2.6b). These 14 $\beta$ ,17 $\beta$ (H)-steranes most likely derive from the desulfurisation of steroid thiophenes **XXV**, identified by comparison of their mass spectra with those reported (Schmid, 1986). In addition to steroid thiophenes **XXV**, small amounts of unknown C<sub>27</sub>-C<sub>29</sub> steradienes were detected in the A2 fraction. Mass spectra of the unknown steradienes are characterised by a base peak at m/z M<sup>+</sup>-15, a next intense molecular ion, and fragment ions at m/z M<sup>+</sup>-43, m/z M<sup>+</sup>-56, m/z 253, m/z 213 and m/z 171.

Steranes in the desulfurised A4 fraction and in the desulfurised polar fraction are highly dominated by 5 $\beta$ -cholestane and 24-ethyl-5 $\beta$ -cholestane (Figs. 2.6c,d). The only steroid sulfides detected in the A4 fraction are **XXVI** and **XXVII**, identified by comparison of their mass spectra with those reported (Behrens et al., 1997; Schouten, 1995). Considering the stereochemistry at C-5, it is thought that 5 $\beta$ -steranes in the desulfurised A4 fraction predominantly derive from **XXVII**. It is noted, however, that due to the complexity of the A4 fraction, the presence of other steroid sulfides may have been overlooked. Steranes released upon desulfurisation of the polar fraction must have been macromolecularly S-bound, since no steroid sulfides were obtained upon LiAlH<sub>4</sub> reduction of the polar fraction.

The presence of 14 $\beta$ ,17 $\beta$ (H)-steranes in samples with an otherwise immature character (presence of 5 $\beta$ -steranes) has been ascribed to the early diagenetic transformation of  $\Delta^7$  5 $\alpha$ -sterols via  $\Delta^7$ ,  $\Delta^{8(14)}$  and  $\Delta^{14}$  5 $\alpha$ -sterenes and  $\Delta^{13(17)}$  5 $\alpha$ -spirosterenes (ten Haven et al., 1986; Peakman and Maxwell, 1988; Peakman et al., 1989). However, to our knowledge 14 $\beta$ ,17 $\beta$ (H)-steranes have as yet not been reported to exceed their 14 $\alpha$ ,17 $\alpha$ (H)-counterparts in concentration. Possibly, this is related to the unknown steradienes, which, like the sterenes mentioned above, might also be transformed into 14 $\beta$ ,17 $\beta$ (H)-steranes already in an early stage of diagenesis.

*Aryl- and diaryl isoprenoids.* Two series of aryl isoprenoids are present in the A2 fraction (Fig. 2.7a). On the basis of relative retention times the earlier respectively later eluting series were assigned the 2,3,6- and 2,3,4-trimethyl substitution pattern with respect to the isoprenoid chain (Summons and Powell, 1987). The 1-alkyl-2,3,6-trimethylbenzenes are probably largely derived from isorenieratene (**XXVIII**), a carotenoid exclusively biosynthesised by the strictly anaerobic brown strains of Chlorobiaceae (Schmidt, 1978), since its saturated analogue, isorenieratane (**XXIX**) is relatively abundant in the A3 and desulfurised A4 and polar fractions (Figs. 2.7b-d). The presence of isorenieratane was confirmed by coinjection with an authentic standard. Its relatively high  $\delta^{13}\text{C}$  value (Table 2.1) is in agreement with an origin from Chlorobiaceae, since these photosynthetic bacteria use the reverse tricarboxylic acid cycle for fixation of CO<sub>2</sub> (Sirevåg and Ormerod, 1970),



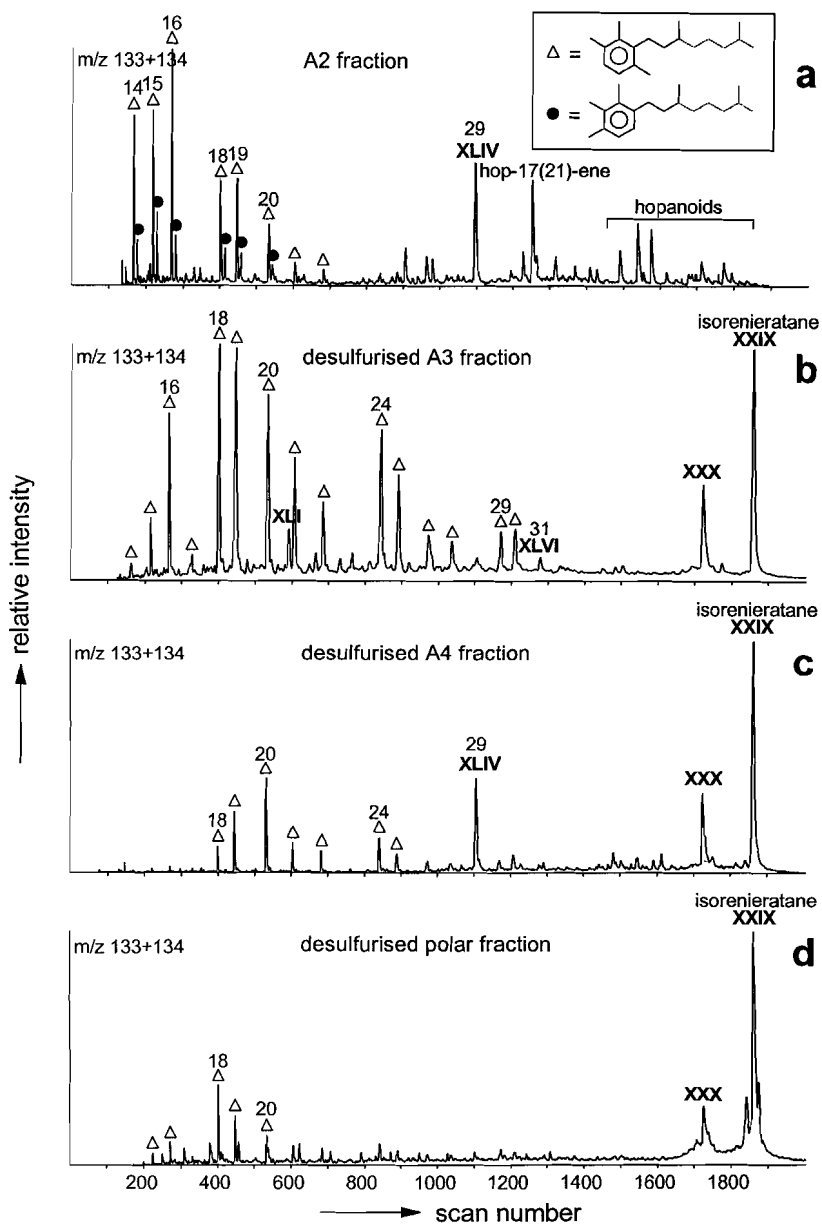


**Fig. 2.7.** M/z 133 + 134 mass chromatograms of (a) A2 fraction (b) desulfurised A3 fraction (c) desulfurised A4 fraction (d) desulfurised polar fraction. Roman numbers refer to structures indicated in the Appendix; numbers correspond to number of carbon atoms. The peaks directly before and after the peak of isorenieratane in (d) are 'mono-unsaturated isorenieratanes' resulting from incomplete hydrogenation of the desulfurisation products.

causing their biomass to be anomalously enriched in  $^{13}\text{C}$  relative to the algal OM (Quandt et al., 1977; Sirevåg et al., 1977).

The origin of the 1-alkyl-2,3,4-trimethylbenzenes in the A2 fraction is not clear. Possibly, these compounds are derived from the same precursor as the  $\text{C}_{40}$  aryl isoprenoid (XXX) in the A3 and desulfurised A4 and polar fractions (Figs. 2.7b-d). The identification of XXX is based on its mass spectrum only and inconclusive as to the substitution pattern of the aromatic ring. Up to now, however, only the 2,3,6- and 2,3,4-trimethyl substituted compounds are known (Schmidt, 1978; Schaeffer et al., 1997). Alternatively, the 1-alkyl-2,3,4-trimethylbenzenes are derived from okenone (XXXI), a monoaromatic carotenoid confined to the Chromatiaceae (Schmidt, 1978). This would explain why only short-chain 1-alkyl-2,3,4-trimethylbenzenes are found and not perhydro okenone, since in the work-up procedure employed LMW compounds possessing a keto or methoxy group would end up in the polar part of the desulfurised polar fraction. Further analysis of this fraction, however, indicated no such compounds.

Although two series of free aryl isoprenoids were detected, only the 2,3,6-trimethyl substituted series was found in the desulfurised fractions (Figs. 2.7b-d). Nevertheless, the sulfur-containing aryl isoprenoids comprise a complicated mixture (e.g. Fig. 2.8a), since sulfur incorporation can take place at many positions of the conjugated double bond system

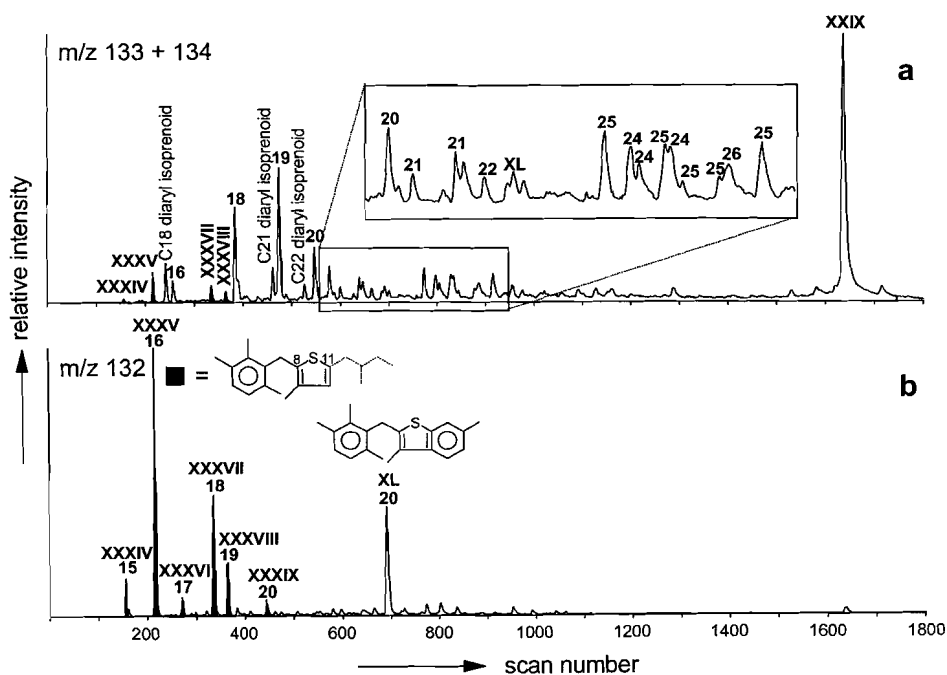


**Fig. 2.8.**  $m/z$  133 + 134 (a) and  $m/z$  132 (b) mass chromatograms of the A3 fraction showing the presence of thiophenic and benzothiophenic aryl isoprenoids. Roman numbers refer to structures referred in the Appendix; numbers correspond to number of carbon atoms.

of the isoprenoid chain in isorenieratene. Moreover, prior to the incorporation of sulfur there may have been expulsion of *m*-xylene or toluene from isorenieratene (Koopmans et al., 1996a), giving rise to C<sub>32</sub> or C<sub>33</sub> "carotenoids" with different methyl substitution patterns of the carbon chain (XXXII, XXXIII). The only sulfur-containing aryl isoprenoids that could be tentatively identified on the basis of mass spectra, relative retention times, FPD response and desulfurisation products, are those possessing a thiophenic sulfur between C-8 and C-11 of the isoprenoid chain (Fig. 2.8b). Mass spectra of these compounds are characterised by a base peak at m/z 132 (Koopmans et al., 1996a), and fragment ions indicating the presence of a thiophene or benzothiophene moiety (XXXIV-XL; Table 2.3). The distribution of aryl isoprenoids with a thiophene moiety (XXXIV-XXXIX) is characterised by a low C<sub>17</sub> member (Fig. 2.8b), in agreement with the common distribution of free aryl isoprenoids (cf. Summons and Powell, 1987). Desulfurisation of XL yields the C<sub>20</sub> diaryl isoprenoid XLI, eluting just before the C<sub>21</sub> aryl isoprenoid (Fig. 2.7b). It should be noted that there is no firm evidence for the position of the methyl substituent on the additional aromatic ring, since the mass spectra of XL and its desulfurisation product XLI, are also met by XLII and its desulfurisation product XLIII. Compound XLII, however, can only have formed from sulfuration, cyclisation, aromatisation and C-C bond cleavage of C<sub>33</sub> diaryl isoprenoid XXXIII, in its turn resulting from the expulsion of toluene from isorenieratene. On the other hand, compound XL can be directly produced by sulfuration, cyclisation, aromatisation and C-C bond cleavage of isorenieratene, rendering XL the more likely structure.

**Table 2.3.** Mass spectral characteristics of several OSC identified.

Structure	Formula	M <sup>+</sup>	Characteristic fragment ions (intensity)
XXXIV	C <sub>15</sub> H <sub>18</sub> S	230(22)	215(7), 133(12), 132(100), 117(12)
XXXV	C <sub>16</sub> H <sub>20</sub> S	244(22)	229(5), 133(12), 132(100), 111(12)
XXXVII	C <sub>18</sub> H <sub>24</sub> S	272(22)	243(7), 133(14), 132(100), 111(15)
XXXVIII	C <sub>19</sub> H <sub>26</sub> S	286(35)	243(59), 153(19), 133(18), 132(100), 111(25)
XXXIX	C <sub>20</sub> H <sub>28</sub> S	300(33)	243(71), 167(33), 133(17), 132(100), 111(47)
XL	C <sub>20</sub> H <sub>22</sub> S	294(31)	279(8), 175(9), 162(6), 133(11), 132(100)
XLV	C <sub>29</sub> H <sub>50</sub> S	430(70)	205(100), 177(36), 165(70)
XLVII	C <sub>40</sub> H <sub>60</sub> S	572(19)	355(50), 151(8), 137(9), 134(14), 133(100), 111(7)
XLVIII	C <sub>40</sub> H <sub>60</sub> S	572(27)	397(4), 299(9), 151(5), 137(5), 134(13), 133(100), 125(14), 111(6)
XLIX	C <sub>40</sub> H <sub>60</sub> S	572(37)	383(5), 327(4), 314(3), 313(3), 137(11), 134(14), 133(100), 125(24), 111(8)

The C<sub>29</sub> aryl isoprenoids in the A2 and in the desulfurised A4 fraction have a mass spectrum similar to that of the C<sub>29</sub> aryl isoprenoid in the desulfurised A3 fraction [m/z 400(17), 147(5), 134(80), 133(100), 119(7)], but their Kováts Indices differ considerably (2728, 2820). The earlier eluting compound (Figs. 2.7a,c) has been identified as trimethyl-(3,7,11,15-tetramethylhexadecyl)-benzene (XLIV) (Sinninghe Damsté et al., 1988a). XLIV in the desulfurised A4 fraction most likely derives from thiochroman XLV (Table 2.3), reported by Adam (1991), which is present in the A4 fraction. The elution behaviour of the C<sub>29</sub> aryl isoprenoid in the desulfurised A3 fraction suggests that this compound possesses the usual carotenoid side chain. Like the other C<sub>14</sub>-C<sub>30</sub> aryl isoprenoids in this fraction, it is probably largely derived from isorenieratene. The C<sub>31</sub> aryl isoprenoid (XLVI) in the

desulfurised A3 fraction (Fig. 2.7b) is most likely derived from the same precursor as **XXX**, since its formation from isorenieratene implies C-C bond cleavage adjacent to the aromatic ring, which is generally not favoured.

Although many different sulfur-containing isorenieratene derivatives can be formed (Koopmans et al., 1996a), the isorenieratane skeleton present in the desulfurised A4 fraction (Fig. 2.7c) is mainly derived from components **XLVII-XLIX** (Table 2.3; see also Koopmans et al., 1996a), which are by far the most abundant isorenieratene derivatives in the A4 fraction. Also, the thiophenic aryl isoprenoids with the sulfur atom between C-8 and C-11, i.e. those yielding the characteristic  $m/z$  132 fragment ion, are less abundant than aryl isoprenoids possessing thiophene moieties elsewhere in the carbon chain. Many of these latter components, however, do not show up very well in the  $m/z$  133 + 134 mass chromatogram, due to an intense cleavage  $\beta$  to the thiophene moiety.

*Other compounds.* Des-A-ferna-5,7,9-triene (**L**) (or des-A-arbora-5,7,9-triene; **LI**) and 25-norferna-5,7,9-triene (**LII**) (or 25-norarbora-5,7,9-triene; **LIII**), identified by comparison of their mass spectra with those published (Hauke et al., 1992a,b), are the most prominent components in the A2 fraction. Since the ferna-5,7,9-trienes are mirror-images of the corresponding arbora-5,7,9-trienes, and thus their mass spectra are identical, it is not clear whether these compounds derive from fern-9(11)-en-3 $\beta$ -ol (**LIV**) or from arbor-9(11)-en-3 $\beta$ -ol (**LV**), components mainly occurring in terrestrial plants. Regardless their actual precursor molecules, it is suggested that **L-LIII** have a non-terrestrial origin, since any other higher-plant triterpenoids are absent and long-chain odd-numbered  $n$ -alkanes derived from epicuticular plant waxes are low. The terrestrial origin of arborane/fernane derivatives in sediments has been questioned before (Hauke et al., 1992b, and references therein). The  $\delta^{13}\text{C}$  values of **L-LIII** are slightly enriched in  $^{13}\text{C}$  relative to average hopanoid values (Table 2.1), and are inconclusive as to their origin.

The most abundant compound in the A3 fraction is **LVI**, which may have formed from cyclisation, aromatisation and C-C bond cleavage of isorenieratene (Koopmans et al., 1996a). However, its  $\delta^{13}\text{C}$  value is 4.5‰ lower than that of isorenieratane (Table 2.1), suggesting it is partly derived from a precursor other than isorenieratene. Recently, it was shown that aryl isoprenoids with a 2,3,6-trimethyl substitution pattern of the aromatic ring can be formed from  $\beta$ -carotene, a carotenoid produced by the vast majority of photosynthetic organisms and thus much depleted in  $^{13}\text{C}$  relative to isorenieratene (Koopmans et al., 1996b). Similarly, **LVI** may have partly formed from  $\beta$ -carotene, although there is no further evidence for this. Alternatively, a fraction of **LVI** is derived from the precursor of **XXX**.

Methylated chromans (**LVII**), compounds of as yet unknown origin, are highly dominated by the trimethyl substituted member, suggesting that the salinity of the photic zone was not elevated relative to normal sea water (Sinninghe Damsté et al., 1987b, 1993a). Assuming **LVII** to be derived from photoautotrophs, their  $\delta^{13}\text{C}$  values, which fall within the range of hopanoid  $\delta^{13}\text{C}$  values (Table 2.1), point to an origin from organisms that assimilate carbon *via* the Calvin-cycle.

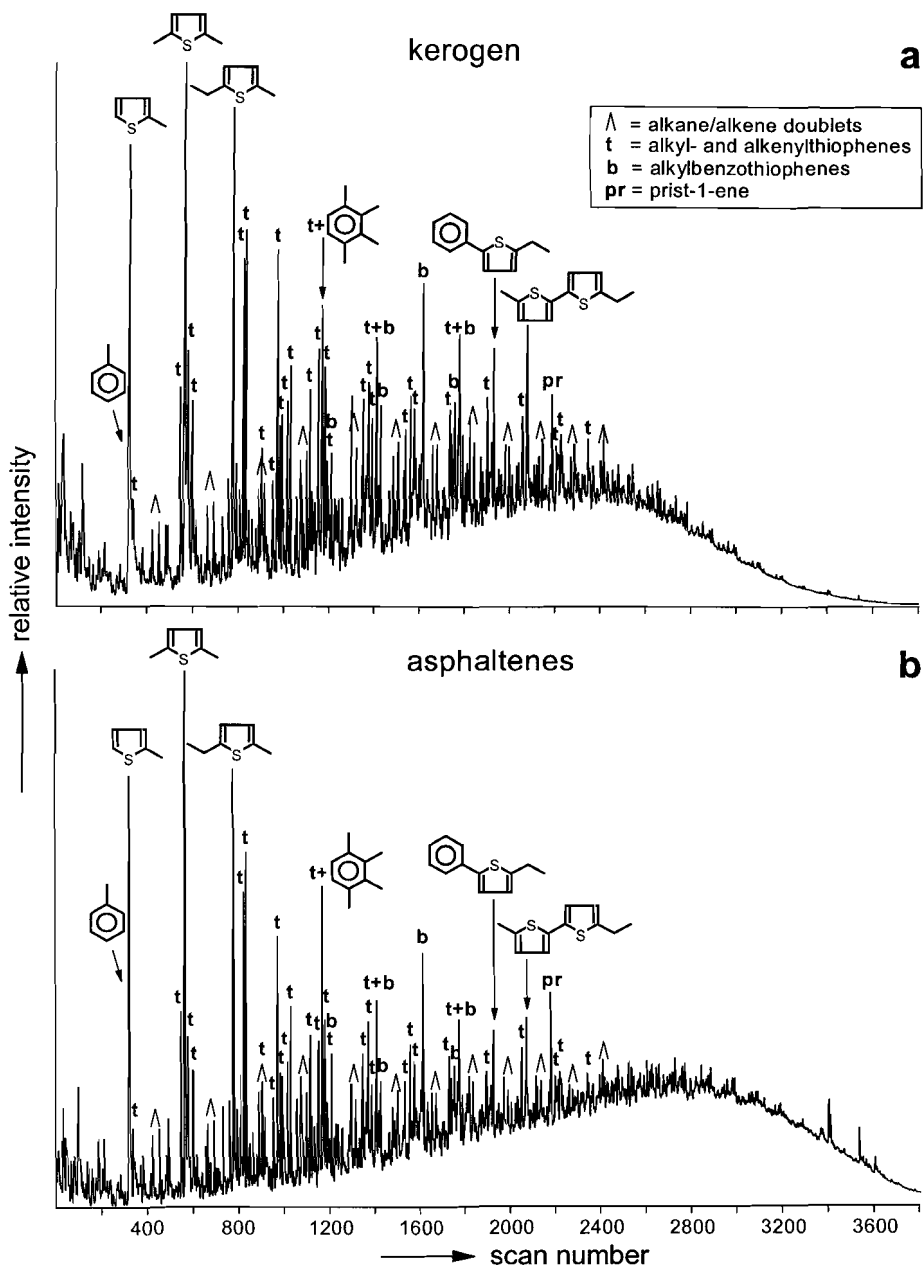


**Fig. 2.9.** Total ion current traces of the flash pyrolysates (Curie temperature of 610°C) of (a) kerogen and (b) asphaltenes.

**Table 2.4.** Results GSA-analysis.

	SS1 <sup>a</sup>	SS2 <sup>b</sup>	SS3 <sup>c</sup>	S(total) <sup>d</sup>	T <sub>max</sub> (S) <sup>e</sup>	SI <sup>f</sup>
	mg S/g rock	mg S/g rock	mg S/g rock	mg S/g rock	(°C)	mg S/g TOC
Orbagnoux	2.61	37.92	0.00	40.53	456	612

<sup>a</sup> Thermally extractable sulfur at 300°C for 3 minutes

<sup>b</sup> Pyrolysable organic sulfur (600°C)

<sup>c</sup> Pyrolysable mineral sulfur (600°C)

<sup>d</sup> SS1 + SS2 + SS3

<sup>e</sup> Temperature for maximum generation of pyrolysable organic sulfur

<sup>f</sup> Sulfur Index (mg SS2\*100/g TOC)

### Kerogen

The kerogen was analysed using both Curie-point pyrolysis and off-line pyrolysis. Py-GC-MS indicates that the vast majority of pyrolysis products are sulfur-containing components, especially alkylthiophenes, alkenylthiophenes and alkylbenzothiophenes (Fig. 2.9a). The 2,3-dimethylthiophene over (1,2-dimethylbenzene + *n*-non-1-ene) ratio (TR ratio) and the 2-methylthiophene over toluene ratio in the pyrolysate amount to 1.27 and 4.13, respectively, suggesting the atomic S<sub>org</sub>/C ratio of the kerogen to be higher than 0.09 (Eglinton et al., 1990, 1994). The atomic S<sub>org</sub>/C ratio calculated from the organic sulfur content measured by the Geoelf Sulfur Analyser (GSA, Table 2.4) (Bjørøy et al., 1993), adds up to the exceptionally high value of 0.24. This value of 0.24, however, would imply the presence of one sulfur atom to every four carbon atoms, which seems unrealistic.

Several novel series of sulfur compounds were tentatively identified in the kerogen pyrolysate, on the basis of mass spectral data and products released upon desulfurisation. By means of chromatographic separation a fraction of the off-line pyrolysate was prepared in which these series dominate (Fig. 2.10a). Mass chromatograms of their major fragment ions point to the presence of long homologous series (Figs. 2.10b-h). Desulfurisation of the fraction yielded almost exclusively *n*-alkanes, *n*-alkylbenzenes and di-*n*-alkylbenzenes (Fig. 2.11).

It is suggested that the homologous series dominating the *m/z* 179 + 180, *m/z* 193 + 194 and *m/z* 207 + 208 mass chromatograms (Figs. 2.10b-d) are indicative of 5-*n*-alkyl-2,2'-bithiophenes (LVIII), 5-*n*-alkyl-5'-methyl-2,2'-bithiophenes (LIX) and 5-*n*-alkyl-5'-ethyl-2,2'-bithiophenes (LX), respectively<sup>1</sup>, which upon desulfurisation are converted into *n*-alkanes, the most abundant compound class formed (Fig. 2.11a). The major fragment ions in their mass spectra exhibit a mass deficiency compared to hydrocarbon fragments with a similar mass, and an isotope distribution, indicating the presence of two sulfur atoms (e.g. Figs. 2.12a-c). Further evidence for the bithiophenic structure of the series is provided by the library mass spectrum of 2,2'-bithiophene (LVIIIa), since both this spectrum and the spectra of LVIII-LX exhibit small fragment ions at *m/z* 121 and *m/z* 134 (e.g. Figs. 2.12a-c). Moreover, the mass spectrum of LX is characterised by a fragment ion at *m/z* 192 resulting from β-cleavage on both sides of the bithiophene moiety. Any other position of the alkyl substituents in LVIII-LX would have resulted in the formation of branched alkanes upon

<sup>1</sup> C<sub>11</sub> members of series LIX and LX are in fact the same compounds.

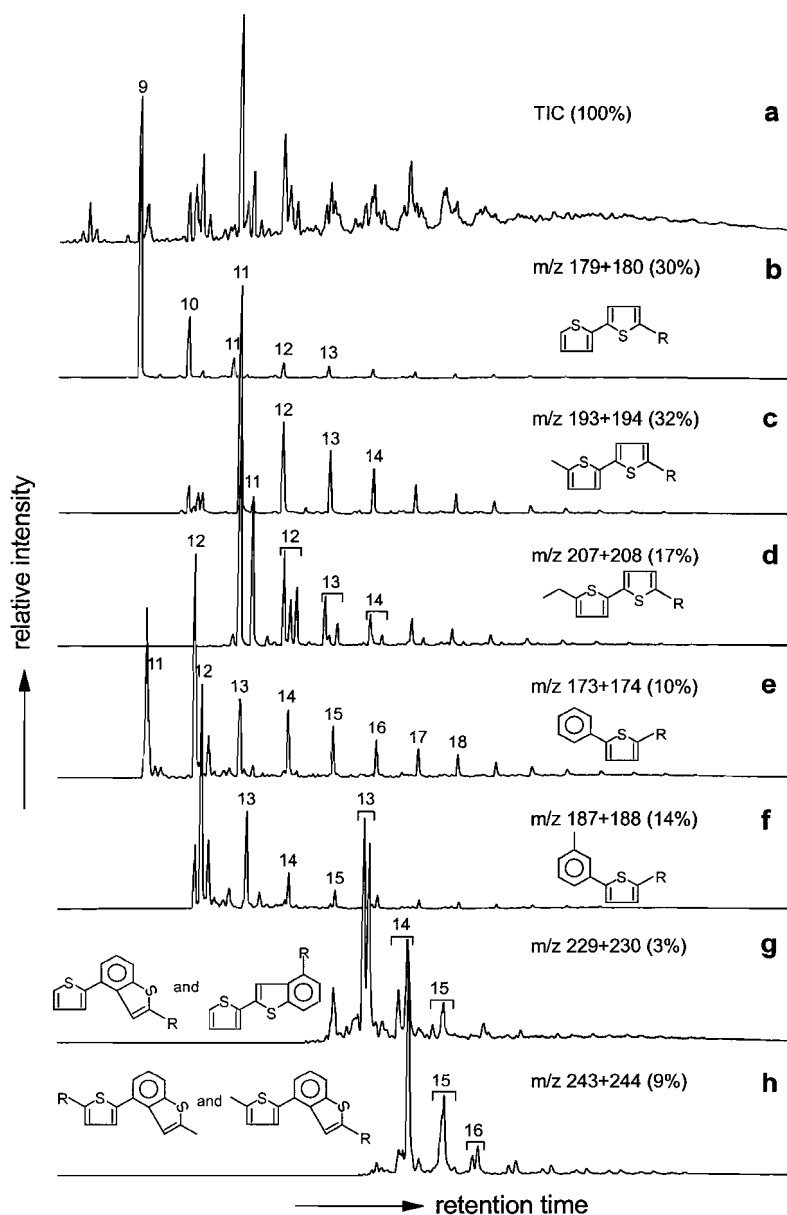


**Fig. 2.10.** Total ion current (TIC) trace (a) and mass chromatograms of  $m/z$  179 + 180 (b),  $m/z$  193 + 194 (c),  $m/z$  207 + 208 (d),  $m/z$  173 + 174 (e),  $m/z$  187 + 188 (f),  $m/z$  229 + 230 (g) and  $m/z$  243 + 244 (h) of P5 fraction of the off-line pyrolysate of the kerogen. Numbers correspond to number of carbon atoms. Each trace is identified with the intensity of the base peak expressed as a percentage relative to the intensity of the base peak in the TIC trace.

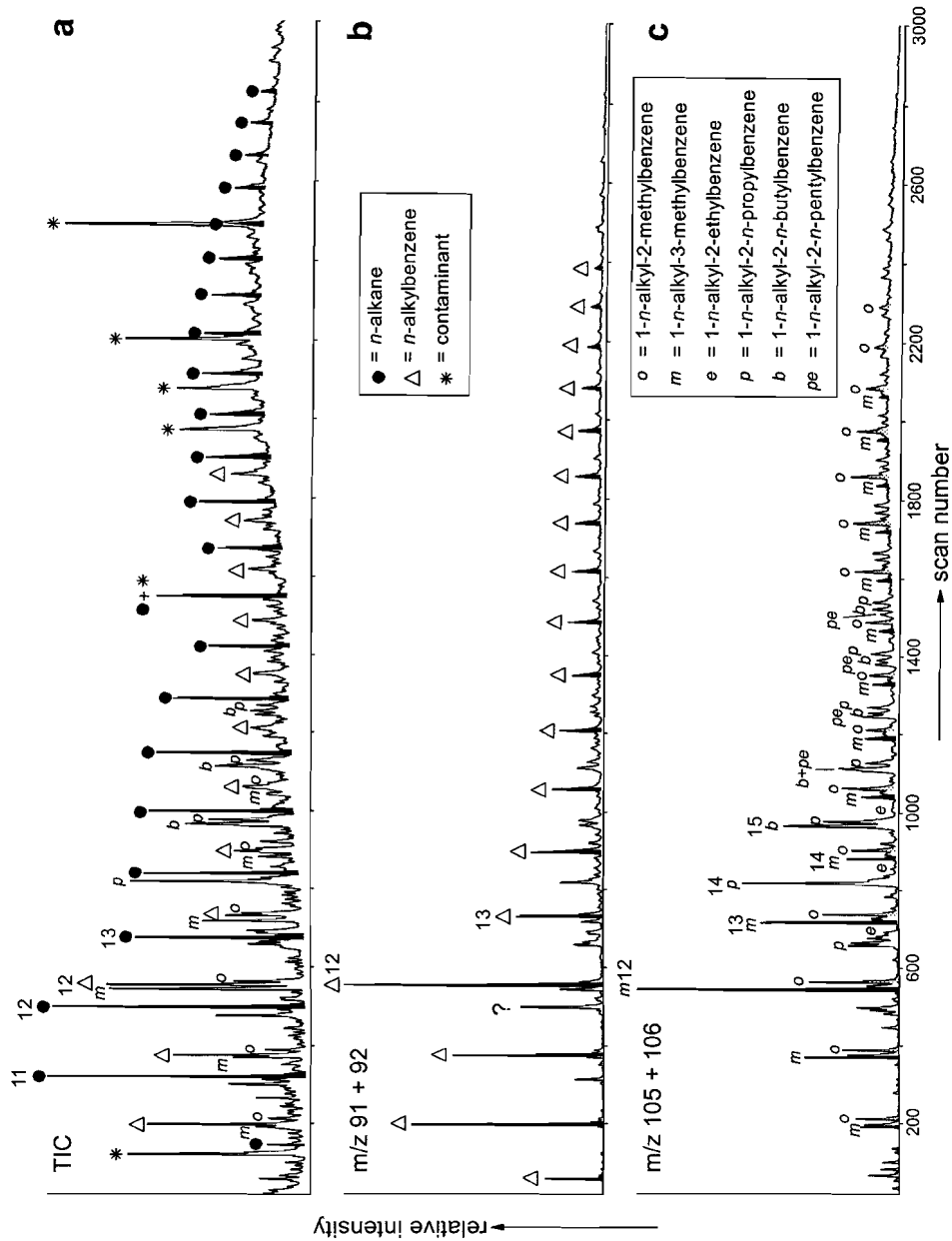


**Fig. 2.11.** Total ion current trace (a) and mass chromatograms of  $m/z$  91 + 92 (b) and  $m/z$  105 + 106 (c) of desulfurised P5 fraction of the off-line pyrolysate of the kerogen. Numbers correspond to number of carbon atoms. Alkylbenzenes were identified using the mass spectral data and relative retention times reported by Sinnighe Damsté et al. (1991).



desulfurisation, and these were not detected. However, the presence of two additional, less prominent, homologous series in the  $m/z$  207 + 208 mass chromatogram (Fig. 2.10d), indicates that bithiophenes with a non-linear carbon skeleton do occur.

The homologous series dominating the  $m/z$  173 + 174 mass chromatogram (Fig. 2.10e) is thought to represent 2-*n*-alkyl-5-phenylthiophenes (**LXI**), yielding *n*-alkylbenzenes upon desulfurisation (Figs. 2.11b and 2.13). The accurate masses and isotope distributions of the major fragment ions in their mass spectra allow for one sulfur atom (e.g. Fig. 2.12d). Furthermore, the mass spectra resemble that of 2-phenylthiophene (**LXIa**) in that they show small fragment ions at  $m/z$  115 and  $m/z$  128. The distribution of **LXI** is dominated by the C<sub>12</sub> member (Fig. 2.10e), in accordance with the distribution of *n*-alkylbenzenes obtained after desulfurisation (Fig. 2.11b). Apart from **LXI**, also 1-*n*-alkyl-2-(2'-thienyl)benzenes

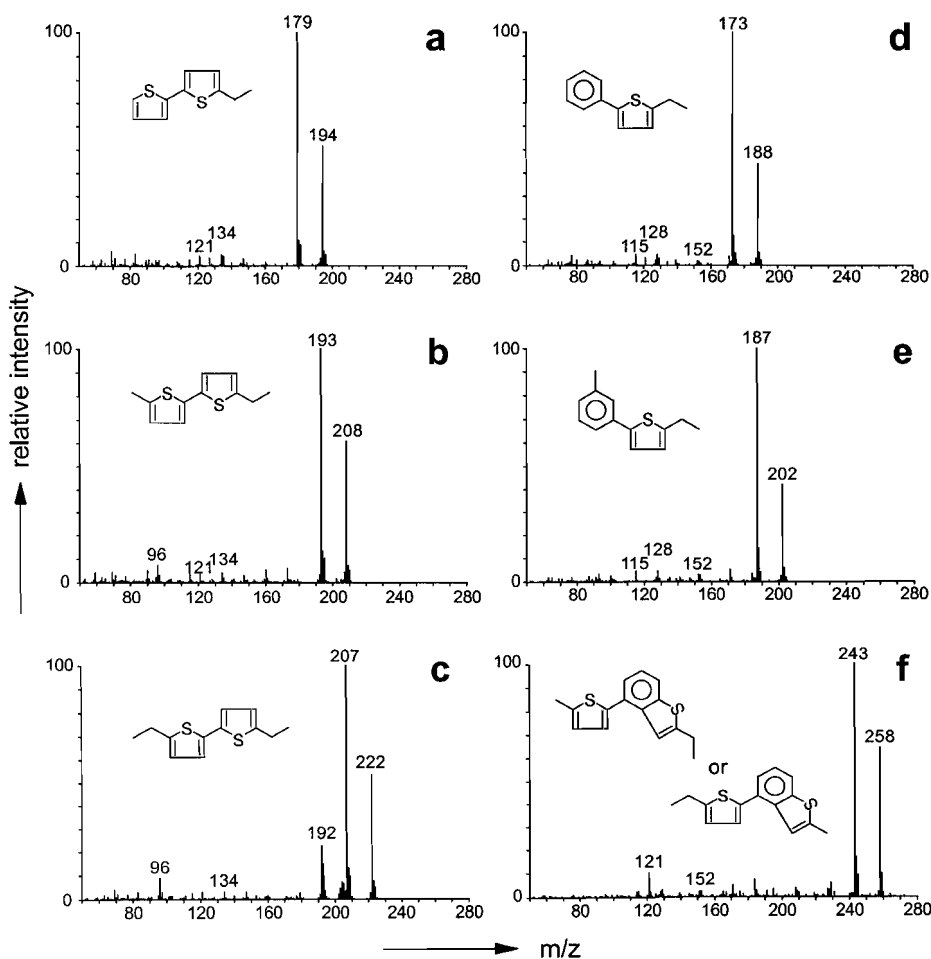


**Fig. 2.12.** Mass spectra of tentatively identified OSC in P5 fraction of kerogen pyrolysate.

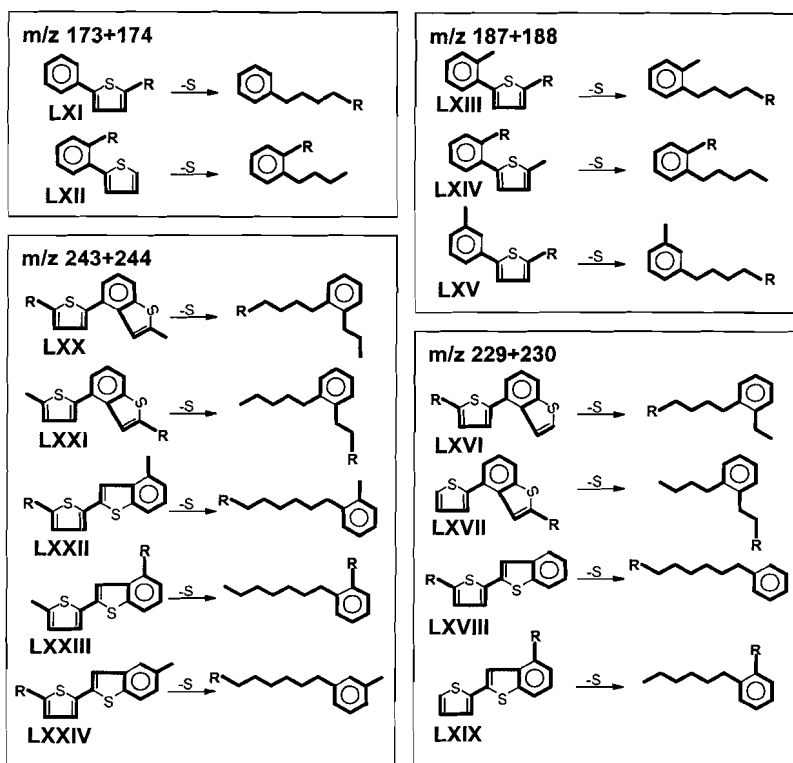


Fig. 2.13. OSC meeting the mass spectral data mentioned in the text, and their desulfurisation products.

(LXII) meet the mass spectral data. Upon desulfurisation, however, LXII would yield a series of 1-*n*-alkyl-2-butylbenzenes (Fig. 2.13). Since in the desulfurised fraction, 1-*n*-alkyl-2-butylbenzenes are relatively low, and moreover they maximise at C<sub>15</sub> (Fig. 2.11c), LXII is rejected as a likely structure for the homologous series.

Like LXI, the homologous series with major fragment ions at *m/z* 187 (Figs. 2.10f and 2.12e) is believed to possess a 2-phenylthiophene moiety. The accurate masses and isotope distributions of the major fragment ions point to the presence of one sulfur atom, and the signals at *m/z* 115 and *m/z* 128 are in agreement with such a structure (e.g. Fig. 2.12e). Assuming that the components were formed by cyclisation, aromatisation and sulfuration of linear carbon chains, the mass spectra are met only by 2-*n*-alkyl-5-(*o*-methylphenyl)thiophenes (LXIII) and 1-*n*-alkyl-2-(2'-(5'-methylthienyl))benzenes (LXIV). Upon desulfurisation LXIII and LXIV are converted into 1-*n*-alkyl-2-methylbenzenes and 1-*n*-alkyl-2-pentylbenzenes, respectively (Fig. 2.13). However, these dialkylbenzenes are not particularly abundant in the desulfurised fraction, neither do their distributions show a distinct maximum at C<sub>12</sub> (Fig. 2.11c), like observed in the *m/z* 187 + 188 mass chromatogram (Fig. 2.10f). Hence, the novel phenylthiophenes were probably formed by cyclisation, aromatisation and sulfuration of a branched carbon skeleton. It is suggested

that they are 2-*n*-alkyl-5-(*m*-methylphenyl)thiophenes (LXV), which are retrieved as 1-*n*-alkyl-3-methylbenzenes after desulfurisation (Fig. 2.13). The 1-*n*-alkyl-3-methylbenzenes are relatively abundant components of the desulfurised fraction (Fig. 2.11a), and their distribution is similar to that of LXV (Figs. 2.10f and 2.11c).

The *m/z* 229 + 230 mass chromatogram (Fig. 2.10g) is believed to represent 2-*n*-alkyl-5-(4'-benzo[*b*]thienyl)thiophenes (LXVI), 2-*n*-alkyl-4-(2'-thienyl)benzo[*b*]thiophenes (LXVII), 2-*n*-alkyl-5-(2'-benzo[*b*]thienyl)thiophenes (LXVIII) and/or 4-*n*-alkyl-2-(2'-thienyl)benzo[*b*]thiophenes (LXIX). Upon desulfurisation these compounds are converted into *n*-alkyl- and 1,2-di-*n*-alkylbenzenes (Fig. 2.13). The *m/z* 243 + 244 mass chromatogram (Fig. 2.10h) is ascribed to related series of compounds, i.e. 2-*n*-alkyl-5-(4'-(2'-methyl)-benzo[*b*]thienyl)-thiophenes (LXX), 2-*n*-alkyl-4-(2'-(5'-methyl)-thienyl)-benzo[*b*]thiophenes (LXXI), 2-*n*-alkyl-5-(2'-(4'-methyl)-benzo[*b*]thienyl)-thiophenes (LXXII), 4-*n*-alkyl-2-(2'-(5'-methyl)-thienyl)-benzo[*b*]thiophenes (LXXIII) and/or 2-*n*-alkyl-5-(2'-(5'-methyl)-benzo[*b*]thienyl)-thiophenes (LXXIV), yielding 1,2-di-*n*-alkylbenzenes and 1-*n*-alkyl-3-methylbenzenes upon desulfurisation (Fig. 2.13). Due to coelution only a reasonably pure mass spectrum of one of the C<sub>15</sub> members could be obtained (Fig. 2.12f). The mass deficiency and isotope distribution of the major fragment ion indicate the presence of two sulfur atoms, and the doubly ionised fragment ion at *m/z* 121.5 attests to the aromatic nature of the compound (Fig. 2.12f). Mass spectra of the *m/z* 229 + 230 series show identical features, albeit with a doubly ionised fragment at 114.5 and a base peak at *m/z* 229. Taking into account the limited variety of desulfurisation products (*n*-alkanes and alkylbenzenes), the only homologous series containing two sulfur atoms and leading to a base peak at *m/z* 229 are LXVI-LXIX. In the case of LXX-LXXIV however, it is recognised that solely on the basis of mass spectral data and desulfurisation products, there is no evidence for the position of the methyl substituent. Still, since the dialkylbenzenes in the desulfurised fraction predominantly consist of 1,2-di-*n*-alkylbenzenes and 1-*n*-alkyl-3-methylbenzenes (Fig. 2.11c), structures LXX-LXXIV are the most likely (Fig. 2.13).

Obviously, with the current data we can only speculate about which of the series LXVI-LXXIV is actually dominating the *m/z* 229 + 230 and *m/z* 243 + 244 mass chromatograms (Figs. 2.10g,h). Nevertheless, two observations are believed worthy of note. Firstly, the summed *m/z* 229 + 230 + 243 + 244 mass chromatogram is dominated by C<sub>14</sub> components, and from there peak areas gradually decrease with increasing carbon number. This is in agreement with the distribution of mid-chain 1,2-di-*n*-alkylbenzenes in the desulfurised fraction (Fig. 2.11c), components which cannot have resulted from desulfurisation of the homologous series shown in Figs. 2.10b-f. It, therefore, seems likely that the mid-chain di-*n*-alkylbenzenes are derived from LXVII and LXIX-LXXI. Secondly, series LXVI cannot be present in large amounts, since only trace amounts of its desulfurisation products, 1-*n*-alkyl-2-ethylbenzenes, were found (Fig. 2.11c).

The most abundant non-sulfur containing pyrolysis products are the doublets of *n*-alkenes and *n*-alkanes (Fig. 2.9). Given the low amount of terrestrial biomarkers in the extractable OM, these pyrolysate *n*-alkenes and *n*-alkanes are probably not derived from higher plant biopolymers like for example cutans (Nip et al., 1986) or suberans (Collinson et al., 1994; Tegelaar et al., 1995). They more likely derive from algaenans, the insoluble non-

hydrolysable biomacromolecules present in algal cell walls (de Leeuw et al., 1991). Up to now marine algaenans were shown present only in microalgae of the classes Chlorophyceae and Eustigmatophyceae (Derenne et al., 1992; Gelin et al., 1996). However, since the extractable OM is highly dominated by extended hopanoids, a cyanobacterial origin of the *n*-alkene/*n*-alkane doublets in the pyrolysate seems perhaps more likely. To the best of our knowledge, however, there has been only one report on a resistant cyanobacterial biopolymer (Chalansonnet et al., 1988), and doubts are thrown upon the validity of the isolation procedure employed (Allard et al., 1997). The presence of abundant coccoliths in the rock suggests there may be a contribution of Prymnesiophyte biomass to the kerogen, but as far as algaenans are concerned, these were not detected in the classes of Prymnesiophyceae analysed so far (*Emiliana huxleyi* and *Phaeocystis* sp.) (Gelin et al., 1997). Weighing one against another, the *n*-alkene/*n*-alkane doublets probably originate from marine algaenan(s).

Since two series of aryl isoprenoids were detected in the bitumen, and the C<sub>40</sub> carotenoid derivatives possibly all have the 2,3,6-trimethyl substitution pattern of the aromatic ring, it was decided to look for carotenoid derivatives in the kerogen pyrolysate. Using the mass spectral data and pseudo Kováts indices reported by Hartgers et al. (1994), both 1-ethyl-2,3,6-trimethylbenzene and 1-ethyl-2,3,4-trimethylbenzene were identified in a ratio similar to that of the free aryl isoprenoids. This suggests that the precursors of both series of aryl isoprenoids are partly sequestered in the kerogen.

### *Asphaltenes*

The flash pyrolysate of the asphaltene fraction is nearly identical to that of the kerogen (Fig. 2.9). Pyrolysis products are highly dominated by thiophenes, benzothiophenes and the novel series of OSC mentioned above (LVIII-LXXIV). Compound distributions are similar to those in the kerogen pyrolysate. The TR ratio and the 2-methylthiophene over toluene ratio in the asphaltene pyrolysate amount to 1.09 and 3.20, respectively. Although these values are somewhat lower than those measured for the kerogen, they still point to an S<sub>org</sub>/C ratio exceeding 0.09 (Eglinton et al., 1990, 1994). The large resemblance of asphaltene and kerogen pyrolysates suggests that the major characteristic distinguishing these two fractions is the degree of intermolecular sulfur cross-linking, in agreement with other studies of S-rich macromolecules (Sinninghe Damsté et al., 1990; Kohnen et al., 1991b).

### *Palaeoenvironmental assessment*

Although the sample is from a lagoonal and thus relatively near-shore setting, fluvial and eolian input of organic matter were low, as revealed by the small amounts of long-chain odd-numbered *n*-alkanes and the absence of higher-plant triterpenoids in the bitumen. Two relatively abundant arborane/fernane derivatives are present, but as pointed out above these probably have a non-terrestrial origin. The scarcity of terrestrial biomarkers not necessarily means that the climate was dry. The chroman (LVII) distribution points to a normal marine salinity of the photic zone (Sinninghe Damsté et al., 1987b, 1993a), indicating that at least evaporation was not exceeding precipitation by far. Markedly, the bitumen is almost devoid

of steroids, and biomarkers are highly dominated by homohopanoids and *n*-alkanes. This strongly suggests that, despite the presence of abundant coccoliths, inorganic remains of Prymnesiophyte algae, cyanobacteria were more important primary producers of organic matter than algae. The small relative contribution of *n*-alkanes and *n*-alkenes to the kerogen pyrolysate, most likely deriving from marine microalgae, is in agreement with this. The presence of isorenieratene derivatives indicates that at least periodically, anoxia was extending into the photic zone (Repeta, 1993; Sinninghe Damsté et al., 1993b; Koopmans et al., 1996a). Consistent with the periodic development of photic zone anoxia, the bitumen and kerogen pyrolysate are predominantly composed of OSC, which attests to the extensive sulfurisation of OM during early diagenesis.

Interestingly, there is only an 11.5‰ difference between the  $\delta^{13}\text{C}$  value of isorenieratane and that of phytane (Table 2.1), the latter presumably reflecting the  $^{13}\text{C}$  content of the average primary producer lipid. This sharply contrasts to the rather constant difference of 15‰ between the  $\delta^{13}\text{C}$  values of isorenieratane and algal biomarkers in 6 different samples of different age reported by Koopmans et al. (1996a). Considering the relatively shallow setting of our sample, it is suggested that in the lower part of the photic zone, where the Chlorobiaceae have their habitat, isotopically light  $\text{CO}_2$ , evolving from the mineralisation of OM settled on the sea floor, was mixed with the largely atmospheric-derived  $\text{CO}_2$  of the surface water. This would lower  $\delta^{13}\text{C}$  of DIC available to the Chlorobiaceae, in its turn lowering the  $\delta^{13}\text{C}$  of their biomass.

Our depositional model is at variance with that of Tribouillard et al. (1992). These authors suggested that microbial mats had played a role in the preservation of OM, by acting as a barrier between the oxygenated water column and the anoxic sediment, which would prevent the particulate OM deposited from oxidation. However, euxinic conditions and the inherent abundant sulfurisation of OM cannot be reconciled with the steep microgradients of oxygen and sulfide in a microbial mat (van Gemerden, 1993). The sulfide produced by sulfate-reducing bacteria in the deepest layers of the mat, are reoxidised to sulfate by colorless and purple sulfur bacteria in the intermediate layers. The top layers of the mat, composed of oxygenic phototrophs, are devoid of sulfide during the day, and only minor amounts of sulfide may diffuse out of the mat at night (Canfield and Des Marais, 1993).

## Conclusions

In the Upper Jurassic palaeolagoon of the Orbagnoux area euxinic conditions led to the formation of extremely organic sulfur-rich deposits. The extractable OM largely consists of compounds with *n*-alkane or homohopanoid backbones, whereas steroids are relatively minor. This suggests that cyanobacteria were more important primary producers than algae. More than 90% of the *n*-alkane carbon skeletons, and, depending on the length of their side-chain, 15 to 80% of the extended hopanoids, are present in a S-bound form. Novel series of  $\text{C}_{18}\text{-C}_{32}$  9-methylalkanes, components of as yet unknown origin, are present in the various desulfurised fractions, but absent in the saturated hydrocarbon fraction. This indicates that their precursor molecules, possessing multiple functional groups, rapidly reacted with reduced inorganic sulfur species during early diagenesis. Also isorenieratene, a pigment with a large conjugated double bond system, reacted with sulfur giving rise to a large variety of

OSC. Structural elucidation was only possible for a limited amount of these compounds. Nevertheless, the presence of isorenieratene derivatives per sé, indicates that at least periodically euxinic conditions existed within the lower part of the photic zone.

Steroids, both free and S-bound, manifest themselves by their unusual distributions. As for steranes, following 5 $\alpha$ -cholestane and 24-ethyl-5 $\alpha$ -cholestane, the next dominant steranes are (20S)- and (20R)-24-methyl-5 $\alpha$ ,14 $\beta$ ,17 $\beta$ (H)-cholestane. This is probably the first time that 14 $\beta$ ,17 $\beta$ (H)-steranes are reported to be more abundant than the corresponding 14 $\alpha$ ,17 $\alpha$ (H)-steranes, and this might be related to the unknown steradienes detected.

Not just the bitumen, but also the kerogen is extremely rich in organic sulfur, as revealed by the large predominance of OSC in the kerogen pyrolysate. The TR ratio and the 2-methylthiophene over toluene ratio of the kerogen pyrolysate (Eglinton et al., 1990, 1994) point to an atomic S<sub>org</sub>/C ratio exceeding 0.09. Apart from the more frequently occurring alkylthiophenes, alkenyl thiophenes and benzothiophenes, several novel homologous series of sulfur-containing pyrolysis products occur, comprising bithiophenes and components with both a thiophene and a benzene or benzothiophene moiety. *n*-Alkane/*n*-alkene doublets in the pyrolysate are relatively low and probably derive from marine microalgae. There is a striking similarity between the kerogen pyrolysate and the pyrolysate of the asphaltene fraction, the only difference being that the dominance of OSC is somewhat less pronounced in the asphaltene pyrolysate. This suggests that kerogen and asphaltenes have rather similar molecular compositions, and differ mainly in the degree of intermolecular cross-linking.

**Acknowledgements.** We thank the Netherlands Organization for Scientific Research (NWO) for the PIONIER grant to JSSD and the studentship of HMEvKP. We thank Shell International Petroleum Maatschappij BV for financial support for the GC-IRMS facility. Dr. M.E.L. Kohnen (Koninklijke/Shell Exploratie en Productie Laboratorium) kindly provided the sample. We acknowledge Dr. S. Schouten for measuring the molecular carbon isotope ratios. W. Pool and M. Dekker are thanked for analytical assistance.

## References

- Adam P. (1991) Nouvelles structures organo-soufrées d'intérêt géochimique: Aspects moléculaires et macromoléculaires. PhD thesis, Université Louis Pasteur, 237 pp.
- Allard B., Templier J. and Largeau C. (1997) Artifactual origin of mycobacterial bacteran. Formation of melanoidin-like artifactual macromolecular material during the usual isolation process. *Org. Geochem.* Submitted.
- Behrens A., Schaeffer P. and Albrecht P. (1997) 14 $\beta$ ,22R-Epithiosteranes, a novel series of fossil steroids widespread in sediments. *Tetrahedron Lett.* In press.
- Bernier P. (1984) Les formations carbonatées du Kimméridgien et du Portlandien dans le Jura méridional. Stratigraphie, micropaléontologie, sédimentologie. *Docum. Lab. Géol. Lyon* **92**, 803 pp.
- Bjørøy M., Jensen H., Connan J., Hall K. and Ferriday I.L. (1993) Geoelf Sulphur Analyser (GSA), a new instrument for rapid determination of organic and inorganic sulphur in sediments and coals. In *Organic geochemistry: Poster sessions from the 16th International Meeting on Organic Geochemistry, Stavanger 1993* (ed. K. Øygard), pp. 773-778. Falch Hurtigtrykk, Oslo.
- Blumer M. and Thomas D.W. (1965) "Zamene", isomeric C<sub>19</sub> monoolefins from marine zooplankton, fishes and mammals. *Science* **148**, 370-371.

- Blumer M., Robertson J.C., Gordon J.E. and Sass J. (1969) Phytol-derived C<sub>19</sub> di- and triolefinic hydrocarbons in marine zooplankton and fishes. *Biochemistry* **8**, 4067-4074.
- Brassell S.C., Lewis C.A., de Leeuw J.W., de Lange F. and Sinninghe Damsté J.S. (1986) Isoprenoid thiophenes: Novel products of sediment diagenesis? *Nature* **320**, 160-162.
- Canfield D.E. and Des Marais D.J. (1993) Biogeochemical cycles of carbon, sulfur, and free oxygen in a microbial mat. *Geochim. Cosmochim. Acta* **57**, 3971-3984.
- Chalansonnet S., Largeau C., Casadevall E., Berkaloff C., Peniguel G. and Couderc R. (1988) Cyanobacterial resistant biopolymers. Geochemical implications of the properties of *Schizothrix* sp. resistant material. In *Advances in Organic Geochemistry 1987* (ed. L. Mattavelli and L. Novelli). *Org. Geochem.* **13**, 1003-1010.
- Collinson M.E., van Bergen P.F., Scott A.C. and de Leeuw J.W. (1994) The oil-generating potential of plants from coal and coal-bearing strata through time: a review with new evidence from Carboniferous plants. In *Coal and Coal-bearing Strata as Oil-prone Source Rocks?* (ed. A.C. Scott and A.J. Fleet). *Geol. Soc. Spec. Publ.* **77**, 31-70.
- Cyr T.D., Payzant J.D., Montgomery D.S. and Strausz O.P. (1986) A homologous series of novel hopane sulfides in petroleum. *Org. Geochem.* **9**, 139-143.
- Derenne S., Largeau C., Berkaloff C., Rousseau B., Wilhelm C. and Hatcher P.G. (1992) Non-hydrolysable macromolecular constituents from outer walls of *Chlorella fusca* and *Nanochlorum eucaryotum*. *Phytochemistry* **31**, 1923-1929.
- Eglinton T.I., Sinninghe Damsté J.S., Kohnen M.E.L. and de Leeuw J.W. (1990) Rapid estimation of the organic sulphur content of kerogens, coals and asphaltenes by pyrolysis-gas chromatography. *Fuel* **69**, 1394-1404.
- Eglinton T.I., Irvine J.E., Vairavamurthy A.V., Zhou W. and Manowitz B. (1994) Formation and diagenesis of macromolecular organic sulfur in Peru margin sediments. In *Advances in Organic Geochemistry 1993* (ed. N. Telnæs, G. van Graas and K. Øygard). *Org. Geochem.* **22**, 781-799.
- Fry B. and Sherr E.B. (1984)  $\delta^{13}\text{C}$  measurements as indicators of carbon flow in marine and freshwater ecosystems. *Contr. Mar. Sci.* **27**, 13-47.
- Gelin F., Boogers I., Noordeloos A.A.M., Sinninghe Damsté J.S., Hatcher P.G. and de Leeuw J.W. (1996) Novel, resistant microalgal polyethers: An important sink of organic carbon in the marine environment? *Geochim. Cosmochim. Acta* **60**, 1275-1280.
- Gelin F., Volkman J.K., Largeau C., Derenne S., Sinninghe Damsté J.S. and de Leeuw J.W. (1997) Distribution of aliphatic, non-hydrolysable biopolymers in marine microalgae. *Org. Geochem.* Submitted.
- van Gernerden H. (1993) Microbial mats: A joint venture. *Mar. Geol.* **113**, 3-25.
- Goossens H., de Leeuw J.W., Schenck P.A. and Brassell S.C. (1984) Tocopherols as likely precursors of pristane in ancient sediments and crude oils. *Nature* **312**, 440-442.
- Hartgers W.A., Sinninghe Damsté J.S., Requejo A.G., Allan J., Hayes J.M., Ling Y., Xie T., Primack J. and de Leeuw J.W. (1994) A molecular and carbon isotopic study towards the origin and diagenetic fate of diaromatic carotenoids. In *Advances in Organic Geochemistry 1993* (ed. N. Telnæs, G. van Graas and K. Øygard). *Org. Geochem.* **22**, 703-725.
- Hauke V., Graff R., Wehrung P., Trendel J.M. and Albrecht P. (1992a) Novel triterpene-derived hydrocarbons of arborane/fernane series in sediments. Part I. *Tetrahedron* **48**, 3915-3924.
- Hauke V., Graff R., Wehrung P., Trendel J.M., Albrecht P., Riva A., Hopfgartner G., Gülaçar F.O., Buchs A. and Eakin P.A. (1992b) Novel triterpene-derived hydrocarbons of arborane/fernane series in sediments: Part II. *Geochim. Cosmochim. Acta* **56**, 3595-3602.
- ten Haven H.L., de Leeuw J.W., Peakman T.M. and Maxwell J.R. (1986) Anomalies in steroid and hopanoid maturity indices. *Geochim. Cosmochim. Acta* **50**, 853-855.
- Hayes J.M., Freeman K.H., Popp B.N. and Hoham C.H. (1990) Compound-specific isotopic analyses: A novel tool for reconstruction of ancient biogeochemical processes. In *Advances in Organic Geochemistry 1989* (ed. B. Durand and F. Behar). *Org. Geochem.* **16**, 1115-1128.
- Holzer G., Oro J. and Tornabene T.G. (1979) Gas chromatographic-mass spectrometric analysis of neutral lipids from methanogenic and thermoacidophilic bacteria. *J. Chromatogr.* **186**, 795-809.
- van Kaam-Peters H.M.E., Köster J., de Leeuw J.W. and Sinninghe Damsté J.S. (1995) Occurrence of two novel benzothiophene hopanoid families in sediments. *Org. Geochem.* **23**, 607-616.

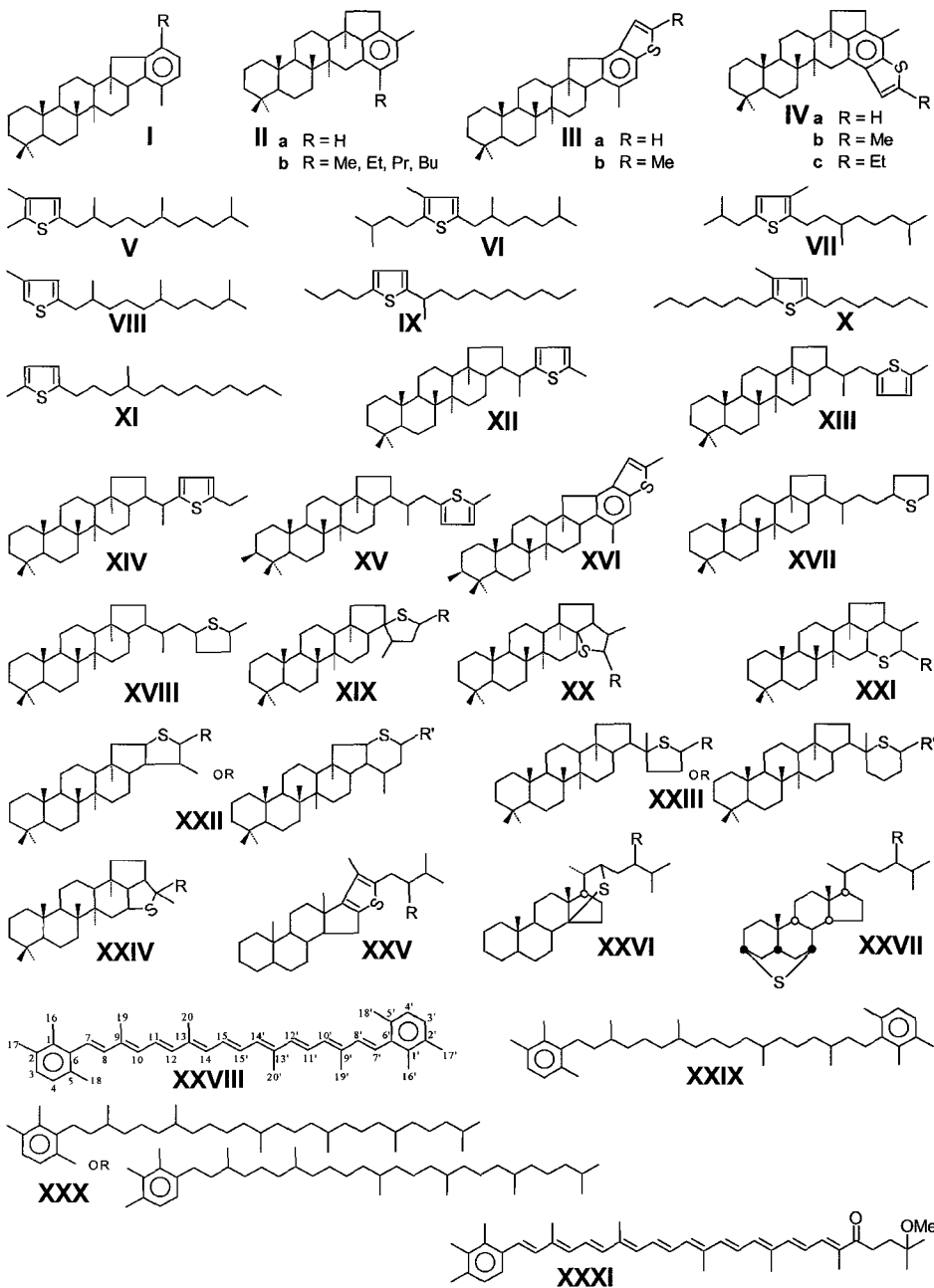
- Kohnen M.E.L., Sinninghe Damsté J.S., Rijpstra W.I.C. and de Leeuw J.W. (1990) Alkylthiophenes as sensitive indicators of palaeoenvironmental changes: A study of a Cretaceous oil shale from Jordan. In *Geochemistry of Sulfur in Fossil Fuels* (ed. W.L. Orr and C.M. White), *ACS Symposium Series 429*, pp. 444-485. Amer. Chem. Soc., Washington.
- Kohnen M.E.L., Sinninghe Damsté J.S., ten Haven H.L., Kock-van Dalen A.C., Schouten S. and de Leeuw J.W. (1991a) Identification and geochemical significance of cyclic di- and trisulphides with linear and acyclic isoprenoid carbon skeletons in immature sediments. *Geochim. Cosmochim. Acta* **55**, 3685-3695.
- Kohnen M.E.L., Sinninghe Damsté J.S., Kock-van Dalen A.C. and de Leeuw J.W. (1991b) Di- or polysulphide-bound biomarkers in sulphur-rich geomacromolecules as revealed by selective chemolysis. *Geochim. Cosmochim. Acta* **55**, 1375-1394.
- Koopmans M.P., Köster J., van Kaam-Peters H.M.E., Kenig F., Schouten S., Hartgers W.A., de Leeuw J.W. and Sinninghe Damsté J.S. (1996a) Dia- and catagenetic products of isorenieratene: Molecular indicators for photic zone anoxia. *Geochim. Cosmochim. Acta* **60**, 4467-4496.
- Koopmans M.P., Schouten S., Kohnen M.E.L. and Sinninghe Damsté J.S. (1996b) Restricted utility of aryl isoprenoids as indicators for photic zone anoxia. *Geochim. Cosmochim. Acta* **60**, 4873-4876.
- Koopmans M.P., Rijpstra W.I.C., Klapwijk M.M., de Leeuw J.W., Lewan M.D. and Sinninghe Damsté J.S. (1997) A thermal and chemical degradation approach to decipher pristane and phytane precursors in sedimentary organic matter. *Org. Geochem.* Submitted.
- Köster J., van Kaam-Peters H.M.E., Koopmans M.P., de Leeuw J.W. and Sinninghe Damsté J.S. (1997) Sulphurisation of homohopanoids: Effects on carbon number distribution, speciation and 22S/22R epimer ratios. *Geochim. Cosmochim. Acta* **61**, 2431-2452.
- de Leeuw J.W. and Sinninghe Damsté J.S. (1990) Organic sulfur compounds and other biomarkers as indicators of palaeosalinity. In *Geochemistry of Sulfur in Fossil Fuels* (ed. W.L. Orr and C.M. White), *ACS Symposium Series 429*, pp. 417-443. Amer. Chem. Soc., Washington.
- de Leeuw J.W., van Bergen P.F., van Aarssen B.G.K., Gatellier J.L.A., Sinninghe Damsté J.S. and Collinson M.E. (1991) Resistant biomacromolecules as major contributors to kerogen. *Phil. Trans. R. Soc. Lond.* **333**, 329-337.
- de Lemos Scofield (1990) Nouveaux marqueurs biologiques de sédiments et pétroles riches en soufre: Identification et mode de formation. PhD thesis, Université Louis Pasteur, 193 pp.
- McCarthy E.D., Han J. and Calvin M. (1968) Hydrogen atom transfer in mass spectrometric fragmentation patterns of saturated aliphatic hydrocarbons. *Anal. Chem.* **40**, 1475-1480.
- Nip M., Tegelaar E.W., de Leeuw J.W. and Schenck P.A. (1986) A new non-saponifiable and resistant biopolymer in plant cuticles. *Naturwissenschaften* **73**, 579-585.
- Payzant J.D., Montgomery D.S. and Strausz O.P. (1986) Sulfides in petroleum. *Org. Geochem.* **9**, 357-369.
- Peakman T.M. and Maxwell J.R. (1988) Acid-catalysed rearrangements of steroid alkenes-I. Rearrangement of 5 $\alpha$ -cholest-7-ene. *J. Chem. Soc., Perkin Trans. I*, 1065-1070.
- Peakman T.M., ten Haven H.L., Rechka J.R., de Leeuw J.W. and Maxwell J.R. (1989) Occurrence of (20R)- and (20S)- $\Delta^{8(14)}$  and  $\Delta^{14}$  5 $\alpha$ (H)-sterenes and the origin of 5 $\alpha$ (H),14 $\beta$ (H),17 $\beta$ (H)-steranes in an immature sediment. *Geochim. Cosmochim. Acta* **53**, 2001-2009.
- Pomonis J.G., Hakk H. and Fatland C.L. (1989) Synthetic methyl- and dimethylalkanes. Kováts Indices, [<sup>13</sup>C]NMR and mass spectra of some methylpentacosanes and 2,X-dimethylheptacosanes. *J. Chem. Ecol.* **15**, 2319-2333.
- Quandt I., Gottschalk G., Ziegler H. and Stichler W. (1977) Isotope discrimination by photosynthetic bacteria. *FEMS Microbiol. Lett.* **1**, 125-128.
- Repeta D.J. (1993) A high resolution historical record of Holocene anoxygenic primary production in the Black Sea. *Geochim. Cosmochim. Acta* **57**, 4337-4342.
- Schaeffer P. (1993) Marqueurs biologique de milieux évaporitiques. PhD thesis, Université Louis Pasteur, 339 pp.
- Schaeffer P., Reiss C., Trendel J.M., Adam P. and Albrecht P. (1995) A novel series of hopanoid sulphides; Evidence for ring A/B functionalised precursors. In *Organic Geochemistry*:

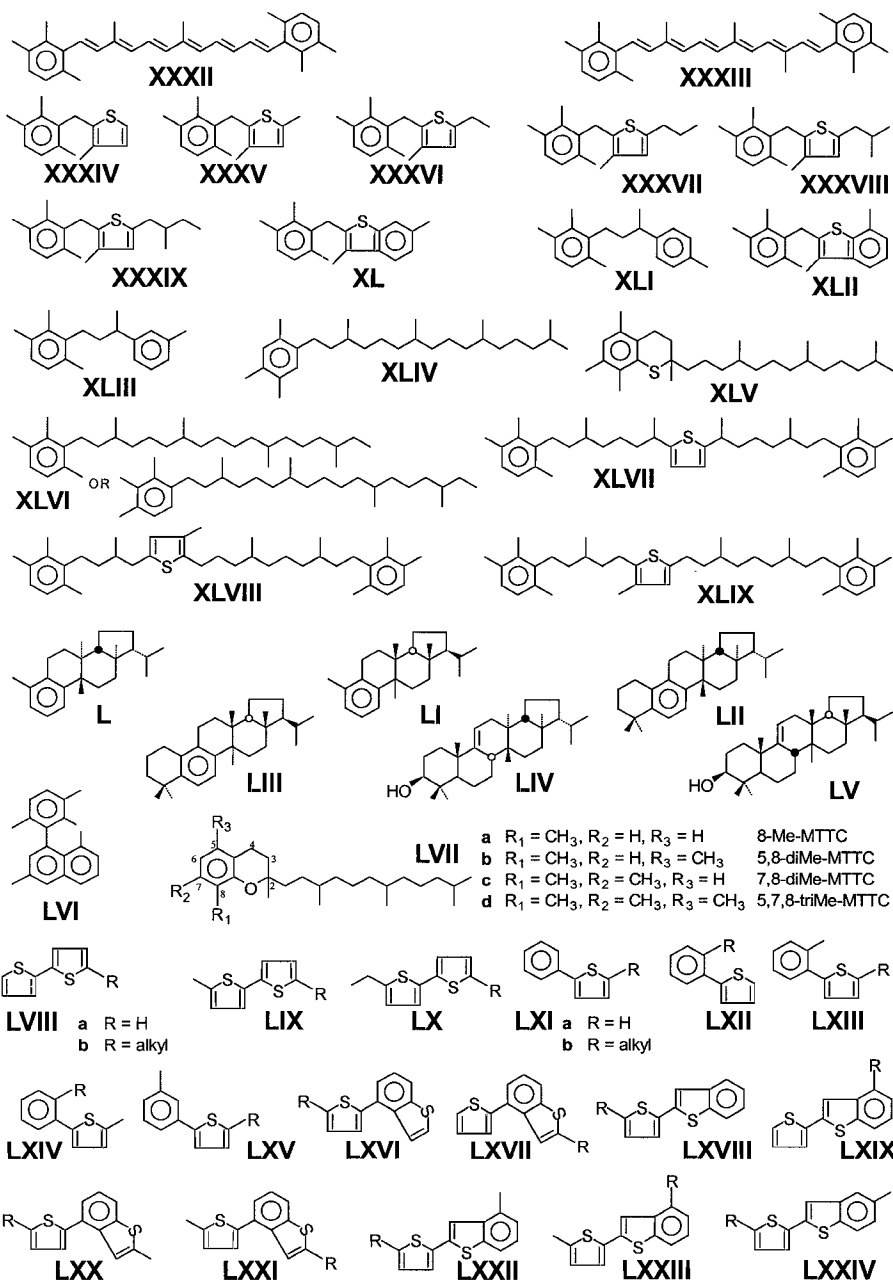


- Developments and applications to energy, climate, environment and human history* (ed. J.O. Grimalt et al.), pp. 1053-1054. A.I.G.O.A., Donostia-San Sebastián.
- Schaeffer P., Adam P., Wehrung P., Bernasconi S. and Albrecht P. (1997) Molecular and isotopic investigation of free and S-bound lipids from an actual meromictic lake (lake Cadagno, Switzerland). *Org. Geochem.* Submitted.
- Schmid J.-C. (1986) Marqueurs biologique soufrés dans les pétroles. PhD thesis, Université Louis Pasteur, 263 pp.
- Schmidt K. (1978) Biosynthesis of carotenoids. In *The Photosynthetic Bacteria* (ed. R.K. Clayton and W.R. Sistrom), pp. 729-750. Plenum Press, New York.
- Schouten (1995) Structural and stable carbon isotope studies of lipids in immature sulphur-rich sediments. PhD thesis, University of Groningen, 305 pp.
- Schouten S., Eglinton T.L., Sinninghe Damsté J.S. and de Leeuw J.W. (1995a) Influence of sulphur cross-linking on the molecular-size distribution of sulphur-rich macromolecules in bitumen. In *Geochemical Transformations of Sedimentary Sulfur* (ed. M.A. Vairavamurthy and M.A.A. Schoonen) *ACS Symposium Series 612*, 80-92.
- Schouten S., Sinninghe Damsté J.S. and de Leeuw J.W. (1995b) A novel triterpenoid carbon skeleton in immature sulphur-rich sediments. *Geochim. Cosmochim. Acta* **59**, 953-958.
- Schouten S., Sinninghe Damsté J.S. and de Leeuw J.W. (1995c) The occurrence and distribution of low-molecular-weight sulphoxides in polar fractions of sediment extracts and petroleum. *Org. Geochem.* **23**, 129-138.
- Sinninghe Damsté J.S. and de Leeuw J.W. (1987) The origin and fate of C-20 and C-15 isoprenoid sulphur compounds in sediments and oils. *Int. J. Environ. Anal. Chem.* **28**, 1-19.
- Sinninghe Damsté J.S. and de Leeuw J.W. (1990) Organically-bound sulphur in the geosphere: State of the art and future research. In *Advances in Organic Geochemistry 1989* (ed. B. Durand and F. Behar). *Org. Geochem.* **16**, 1077-1101.
- Sinninghe Damsté J.S., ten Haven H.L., de Leeuw J.W. and Schenck P.A. (1986) Organic geochemical studies of a Messinian evaporitic basin, northern Apennines (Italy)-II. Isoprenoid and *n*-alkyl thiophenes and thiolanes. In *Advances in Organic Geochemistry 1985* (ed. D. Leythaeuser and J. Rullkötter). *Org. Geochem.* **10**, 791-805.
- Sinninghe Damsté J.S., Kock-van Dalen A.C., de Leeuw J.W. and Schenck P.A. (1987a) The identification of 2,3-dimethyl-5-(2,6,10-trimethylundecyl)thiophene, a novel sulphur containing biological marker. *Tetrahedron Lett.* **28**, 957-960.
- Sinninghe Damsté J.S., Kock-van Dalen A.C., de Leeuw J.W., Schenck P.A., Guoying S. and Brassell S.C. (1987b) The identification of mono-, di- and trimethyl 2-methyl-2-(4,8,12-trimethyltridecyl)chromans and their occurrence in the geosphere. *Geochim. Cosmochim. Acta* **51**, 2393-2400.
- Sinninghe Damsté J.S., de Leeuw J.W., Kock-van Dalen A.C., de Zeeuw M.A., de Lange F., Rijpstra W.I.C. and Schenck P.A. (1987c) The occurrence and identification of series of organic sulphur compounds in oils and sediment extracts: I. A study of Rozel Point Oil (U.S.A.). *Geochim. Cosmochim. Acta* **51**, 2369-2391.
- Sinninghe Damsté J.S., Kock-van Dalen A.C. and de Leeuw J.W. (1988a) Identification of long-chain isoprenoid alkylbenzenes in sediments and crude oils. *Geochim. Cosmochim. Acta* **52**, 2671-2677.
- Sinninghe Damsté J.S., Rijpstra W.I.C., de Leeuw J.W. and Schenck P.A. (1988b) Origin of organic sulphur compounds and sulphur-containing high molecular weight substances in sediments and immature crude oils. In *Advances in Organic Geochemistry 1987* (ed. L. Mattavelli and L. Novelli). *Org. Geochem.* **13**, 593-606.
- Sinninghe Damsté J.S., Rijpstra W.I.C., Kock-van Dalen A.C., de Leeuw J.W. and Schenck P.A. (1989a) Quenching of labile functionalised lipids by inorganic sulphur species: Evidence for the formation of sedimentary organic sulphur compounds at the early stages of diagenesis. *Geochim. Cosmochim. Acta* **53**, 1343-1355.
- Sinninghe Damsté J.S., Rijpstra W.I.C., de Leeuw J.W. and Schenck P.A. (1989b) The occurrence and identification of series of organic sulphur compounds in oils and sediment extracts: II. Their presence in samples from hypersaline and non-hypersaline palaeoenvironments and possible

- application as source, palaeoenvironmental and maturity indicators. *Geochim. Cosmochim. Acta* **53**, 1323-1341.
- Sinninghe Damsté J.S., Eglinton T.I., Rijpstra W.I.C. and de Leeuw J.W. (1990) Characterization of organically bound sulfur in high-molecular-weight, sedimentary organic matter using flash pyrolysis and Raney Ni desulfurization. In *Geochemistry of Sulfur in Fossil Fuels* (ed. W.L. Orr and C.M. White), *ACS Symposium Series 429*, pp. 486-528. Amer. Chem. Soc., Washington.
- Sinninghe Damsté J.S., Kock-van Dalen A.C., Albrecht P.A. and de Leeuw J.W. (1991) Identification of long-chain 1,2-di-*n*-alkylbenzenes in Amposta crude oil from the Tarragona Basin, Spanish Mediterranean: Implications for the origin and fate of alkylbenzenes. *Geochim. Cosmochim. Acta* **55**, 3677-3683.
- Sinninghe Damsté J.S., Keely B.J., Betts S.E., Baas M., Maxwell J.R. and de Leeuw J.W. (1993a) Variations in abundances and distributions of isoprenoid chromans and long-chain alkylbenzenes in sediments of the Mulhouse Basin: A molecular sedimentary record of palaeosalinity. *Org. Geochem.* **20**, 1201-1215.
- Sinninghe Damsté J.S., Wakeham S.G., Kohnen M.E.L., Hayes J.M. and de Leeuw J.W. (1993b) A 6,000-year sedimentary molecular record of chemocline excursions in the Black Sea. *Nature* **362**, 827-829.
- Sinninghe Damsté J.S., van Duin A.C.T., Hollander D., Kohnen M.E.L. and de Leeuw J.W. (1995) Early diagenesis of bacteriohopanepolyol derivatives: Formation of fossil homohopanoids. *Geochim. Cosmochim. Acta* **59**, 5141-5147.
- Sirevåg R. and Ormerod J.G. (1970) Carbon dioxide fixation in green sulfur bacteria. *Biochem. J.* **120**, 399-408.
- Sirevåg R., Buchanan B.B., Berry J.A. and Troughton J.H. (1977) Mechanisms of CO<sub>2</sub> fixation in bacterial photosynthesis studied by the carbon isotope fractionation technique. *Arch. Microbiol.* **112**, 35-38.
- Summons R.E. and Powell T.G. (1987) Identification of aryl isoprenoids in source rocks and crude oils: Biological markers for the green sulphur bacteria. *Geochim. Cosmochim. Acta* **51**, 557-566.
- Summons R.E., Jahnke L.L. and Roksandic Z. (1994) Carbon isotopic fractionation in lipids from methanotrophic bacteria: Relevance for interpretation of the geochemical record of biomarkers. *Geochim. Cosmochim. Acta* **58**, 2853-2863.
- Tegelaar E.W., Hollman G., van der Vegt P., de Leeuw J.W. and Holloway P.J. (1995) Chemical characterization of the periderm tissue of some angiosperm species: Recognition of an insoluble, non-hydrolyzable, aliphatic biomacromolecule (suberan). *Org. Geochem.* **23**, 239-250.
- Tribovillard N., Gorin G. E., Belin S., Hopfgartner G. and Pichon R. (1992) Organic-rich biolaminated facies from a Kimmeridgian lagoonal environment in the French Southern Jura mountains - A way of estimating accumulation rate variations. *Palaeogeogr. Palaeoclimatol. Palaeoecol.* **99**, 163-177.
- Valisolalao J., Perakis N., Chappe B. and Albrecht P. (1984) A novel sulfur containing C<sub>35</sub> hopanoid in sediments. *Tetrahedron Lett.* **25**, 1183-1186.

# Appendix





## Chapter 3

### **A high resolution biomarker study of different lithofacies of organic sulfur-rich carbonate rocks of a Kimmeridgian lagoon (French southern Jura).**

#### **Abstract**

The Upper Jurassic Calcaires en plaquettes Formation (southern Jura, France), which was deposited in a lagoonal setting, reveals three lithofacies: limestones with fine-scale parallel laminations, limestones with undulated (stromatolite-type) laminations and massive limestones. It was examined, at the millimetre scale, if the lithological differences are accompanied by differences in the composition of OM, and if microbial mats played a role in the preservation of organic matter, as suggested previously. Four laminae of each type (light/parallel, dark/parallel, light/undulated, dark/undulated), and a massive limestone sample were analysed. The gross molecular composition of OM appeared similar in all samples, e.g.: (i) Extractable biomarkers are dominated by *n*-alkane and hopanoid carbon skeletons, predominantly in a sulfur-bound form. (ii) Isorenieratene derivatives, indicating anoxic conditions in the photic zone, are present in relatively large amounts. (iii) Kerogen pyrolysates are dominated by organic sulfur compounds. Notwithstanding the overall similarity in OM composition, also some significant differences were observed, e.g.: (i) Low-molecular-weight sulfur-bound hopanoids and steroids are relatively more abundant in TOC-lean, light-coloured samples than in TOC-rich, dark-coloured samples. This is probably related to differences in the degree of intermolecular sulfur cross-linking of the OM. (ii) The concentrations and distributions of several biomarkers in the light-coloured, undulated sample differ from those in the other samples. These differences are attributed to the periodic occurrence of microbial mats. Our data indicate that OM in the Calcaires en plaquettes Formation is predominantly composed of sulfur-bound lipids formed at times that bottom waters were euxinic. A periodic deepening of the oxic/anoxic interface, and of the light penetration depth, to below the sediment surface, allowed microbial mats to develop. Organic remains of the mats, however, are swamped by sulfur-bound planktonic lipids.

#### **Introduction**

The Upper Jurassic Calcaires en plaquettes Formation (CPF) was deposited over an area of approximately 300 km<sup>2</sup>, in a lagoonal environment alongside a barrier-reef (Bernier, 1984). The sedimentary sequence displays an alternation of laminated and massive limestones. Nearest to the barrier-reef, the CPF is most organic-rich, with total organic carbon contents (TOC) ranging up to 12% (Tribouvillard et al., 1992). The bituminous, laminated rocks of the CPF are known to be rich in organic sulfur, and since long, have been exploited for oil used in agricultural and pharmaceutical products.

Van Kaam-Peters and Sinninghe Damsté (1997) examined in detail the molecular composition of both soluble and insoluble organic matter (OM) in one of the finely

laminated, TOC-rich limestones of the CPF. Using wet-chemical techniques, the different types of organic sulfur compounds (OSC) in the bitumen (thiophenes, benzothiophenes, cyclic sulfides and intermolecularly sulfur-linked compounds) were separated, and subsequently, each fraction was desulfurised. Due to the desulfurisation, the complexity of the chromatograms was greatly reduced, and the most important compound classes, *n*-alkanes and hopanoids, were quantified. It appeared that the vast majority of *n*-alkane and hopanoid skeletons were present in a sulfur-bound (S-bound) form. Like the bitumen, the kerogen pyrolysate was found to be predominantly composed of OSC, some of which not reported before. Taken together the abundant sulfurisation of OM and the presence of, mainly S-bound, isorenieratene derivatives, the depositional environment was interpreted to have been euxinic for substantial periods of time.

The above interpretation of the depositional environment of the CPF is at variance with that of Tribouvillard et al. (1992). Based on bulk geochemical and optical examinations, these authors suggested that not the water column, but only pore waters were sulfidic, and that microbial mats formed a barrier between the oxygenated water column and the anoxic sediment. Particulate OM settling on the sea floor would be shielded from oxidation by the microbial mats, and depending on the sedimentation rates of organic and inorganic matter, light-coloured (TOC-lean) or dark-coloured (TOC-rich), parallel or undulated layers would develop.

Previously (van Kaam-Peters and Sinninghe Damsté, 1997), we studied the OM in a 5 cm thick limestone comprising tens of light- and dark-coloured parallel laminae, which implies that mainly the OM in the TOC-rich, dark-coloured layers was looked at. The objective of this study was to examine, at the millimetre scale, if the lithological differences are accompanied by changes in the molecular composition of the OM. We analysed the OM in four carefully isolated, approximately 1 mm thick laminae (light/parallel, dark/parallel, light/undulated, dark/undulated), and in a massive limestone sample of the CPF at Orbagnoux. Free and S-bound biomarkers in different fractions of the bitumen were analysed both qualitatively and quantitatively. The kerogens were studied by Curie-point pyrolysis-gas chromatography-mass spectrometry.

## Methods

*Extraction and fractionation.* The powdered samples (ca. 30 g) were Soxhlet extracted with methanol (MeOH)/dichloromethane (DCM) (1:7.5; v/v) for 24 h. Asphaltenes were precipitated in *n*-heptane. The maltene fractions, to which a mixture of four standards (3-methyl-6-dideutero-henicosane, 2,3-dimethyl-5-(1',1'-dideutero-hexadecyl)thiophene, 2-methyl-2-(4,8,12-trimethyldecyl)chroman and 2,3-dimethyl-5-(1',1'-dideutero-hexadecyl)thiolane) was added for quantitative analysis (Kohnen et al., 1990), were separated into two fractions using a column (20 cm x 2 cm; column volume ( $V_0$ ) = 35 ml) packed with alumina (activated for 2.5 h at 150°C) by elution with hexane/DCM (9:1, v/v; 150 ml; "apolar fraction") and DCM/MeOH (1:1, v/v; 150 ml; "polar fraction"). Aliquots (ca. 10 mg) of the apolar fractions were further separated by argentation TLC (thin layer chromatography) using hexane as developer. The Ag<sup>+</sup>-impregnated silica plates (20 x 20 cm; thickness 0.25 mm) were prepared by immersion into a solution of 1% AgNO<sub>3</sub> in

MeOH/H<sub>2</sub>O (4:1; v/v) for 45 s and subsequent activation at 120°C for 1 h. Four fractions (A1, R<sub>f</sub> = 0.82-1; A2, R<sub>f</sub> = 0.58-0.82; A3, R<sub>f</sub> = 0.11-0.58; A4, R<sub>f</sub> = 0-0.11) were scraped off the TLC plate and ultrasonically extracted with ethyl acetate. All TLC fractions were analysed by GC and GC-MS. The A3 fractions were analysed by GC-IRMS.

*n*-Alkanes were removed from the A1 fractions by elution over a small column (5 cm x 0.5 cm; V<sub>0</sub> = 1 ml) packed with a molecular sieve (silicalite) using cyclohexane as the eluents. The A1 non-adducts were analysed by GC-IRMS.

Following Raney nickel desulfurisation and hydrogenation (see below), the A2, A3 and A4 fractions were analysed by GC and GC-MS again. The desulfurised A4 fractions were further separated using a small column (5 cm x 0.5 cm; V<sub>0</sub> = 1 ml) packed with AgNO<sub>3</sub> impregnated (20% w/w; activated for 16 h at 120°C) silicagel (Merck, Silicagel 60, 70-230 mesh ASTM) by elution with hexane (saturated hydrocarbons) and ethyl acetate (stripping). Subsequently, the *n*-alkanes were removed from the hexane fractions as described above for the A1 fractions. The ethyl acetate fractions and the non-adducts of the hexane fractions were analysed by GC-IRMS.

*Raney nickel desulfurisation and hydrogenation.* The A2, A3 and A4 fractions obtained by argentation TLC were dissolved in 4 ml ethanol together with 0.5 ml of a suspension of Raney nickel (0.5 g/ml ethanol) and heated under reflux for 1.5 h. In the case of the polar fractions and the asphaltenes, a known amount (ca. 20 µg) of standard (2,3-dimethyl-5-(1,1-dideuterohexadecyl)thiophene) was added to an aliquot (ca. 15 mg). The desulfurisation products were isolated by centrifugation and subsequent extraction of the precipitate with DCM (x4). The combined extracts were washed (x3) with NaCl-saturated, bidistilled H<sub>2</sub>O and dried over MgSO<sub>4</sub>. The hydrocarbons formed were isolated using a small column (5 cm x 0.5 cm; V<sub>0</sub> = 1 ml) packed with alumina (activated for 2.5 h at 150°C) by elution with hexane/DCM (9:1, v/v). The fraction was evaporated to dryness and dissolved in 4 ml ethyl acetate. Two drops of pure acetic acid and a pinch of PtO<sub>2</sub> were added as catalysts. Hydrogen gas was bubbled through for 1 h, after which the solution was stirred for 24 h. The catalysts were removed using a small column packed with Na<sub>2</sub>CO<sub>3</sub> and MgSO<sub>4</sub>. The fraction was evaporated to dryness and dissolved in a small volume of hexane (2 mg/ml) to be analysed by GC and GC-MS.

*Gas chromatography (GC).* GC was performed using a Carlo Erba 5300 or a Hewlett-Packard 5890 instrument, both equipped with an on-column injector. A fused silica capillary column (25 m x 0.32 mm) coated with CP-Sil 5 (film thickness 0.12 µm) was used with helium as the carrier gas. The effluent of the Carlo Erba 5300 was monitored by a flame ionisation detector (FID). The effluent of the Hewlett-Packard 5890 was monitored by both a flame ionisation detector (FID) and a sulfur-selective flame photometric detector (FPD), applying a stream-splitter with a split ratio of FID:FPD = ca. 1:2. The samples were injected at 70°C and subsequently the oven was programmed to 130°C at 20°C/min and then at 4°C/min to 320°C, at which it was held for 15 min.

*Gas chromatography-mass spectrometry (GC-MS).* GC-MS was carried out on a Hewlett-Packard 5890 gas chromatograph interfaced to a VG Autospec Ultima Q mass spectrometer

operated at 70 eV with a mass range  $m/z$  50-800 and a cycle time of 1.8 s (resolution 1000). The gas chromatograph was equipped with a fused silica capillary column (25 m x 0.32 mm) coated with CP-Sil 5 (film thickness 0.12  $\mu\text{m}$ ). Helium was used as carrier gas. The samples were injected at 60°C and subsequently the oven was programmed to 130°C at 20°C/min and then at 4°C/min to 320°C, at which it was held for 15 min.

GC-MSMS was performed on a Hewlett-Packard 5890 gas chromatograph interfaced to a VG Autospec Ultima Q mass spectrometer. The gas chromatograph was equipped with a fused silica capillary column (60 m x 0.25 mm) coated with CP-Sil 5CB-MS (film thickness 0.25  $\mu\text{m}$ ). The carrier gas was helium. The gas chromatograph was programmed from 60°C to 200°C at a rate of 15°C/min and then at 1.5°C/min to 310°C (10 min). The mass spectrometer was operated at 70 eV with a source temperature of 250°C. Dissociation of the parent ions was induced by collision with argon (collision energy 18-20 eV). The parent ion to daughter ion transitions were analysed with 20 ms settling and 80-100 ms sampling periods. Total cycle time was 1020 ms.

*Gas chromatography-isotope ratio mass spectrometry (GC-IRMS).* The DELTA-C GC-IRMS-system used is in principal similar to the DELTA-S system described by Hayes et al. (1990). The gas chromatograph (Hewlett-Packard 5890) was equipped with an on-column injector and a fused silica capillary column (25 m x 0.32 mm) coated with CP-Sil 5 (film thickness 0.12  $\mu\text{m}$ ). Helium was used as the carrier gas. The oven temperature was programmed from 70°C to 130°C at 20°C/min, from 130°C to 310°C at 4°C/min and maintained at 310°C for 15 min. The  $\delta^{13}\text{C}$  values (vs PDB) were calculated by integrating the mass 44, 45 and 46 ion currents of the  $\text{CO}_2$  peaks produced by combustion of the column effluent and those of  $\text{CO}_2$  spikes with a known  $^{13}\text{C}$ -content which were directly led into the mass spectrometer at regular intervals.

*Curie-point pyrolysis-gas chromatography-mass spectrometry (Py-GC-MS).* Py-GC-MS was performed using a FOM-3LX pyrolysis unit, and a Hewlett-Packard 5890 gas chromatograph connected to a VG Autospec Ultima Q mass spectrometer. The isolated and extracted kerogens were applied to a ferromagnetic wire with a Curie temperature of 610°C. Kerogen isolation of the light-coloured, undulated layer went wrong, and therefore, for this sample the remnant of the extracted rock powder was pyrolysed. The gas chromatograph, equipped with a cryogenic unit, was programmed from 0°C (5 min) to 310°C (5 min) at a rate of 3°C/min. Separation was achieved using a CP-Sil 5 capillary column (25 m x 0.32 mm) with a film thickness of 0.4  $\mu\text{m}$ . Helium was used as the carrier gas. The mass spectrometer was operated at 70 eV with a mass range  $m/z$  50-800 and a cycle time of 1.8 s (resolution 1000).

*Identification.* Compounds were identified by comparison of mass spectra and retention times with those reported in literature. In addition, the presence of S-bound isorenieratane was confirmed by stable carbon isotope analysis. References to the relevant manuscripts are given throughout the text, where compounds are introduced. With the exception of one carotenoid derivative in the light-coloured, undulated layer, all compounds have been found in a sample of the CPF that was analysed earlier. In the paper describing the results of this



earlier study (van Kaam-Peters and Sinninghe Damsté, 1997), a more detailed account of the identifications is given.

*Quantification.* *n*-Alkanes, 9-methyloctadecane, and 9-methylnonacosane were quantified by determining their peak areas in the *m/z* 57 mass chromatogram, and relating these to the peak area of the (desulfurised) internal standard in the same chromatogram. To account for the different responses of FID and MS, concentrations were multiplied by the following correction factors: *n*-C<sub>16</sub> till *n*-C<sub>27</sub>, 0.88; *n*-C<sub>28</sub>, 0.90; *n*-C<sub>29</sub>, 0.93; *n*-C<sub>30</sub>, 0.98; *n*-C<sub>31</sub>, 1.04; *n*-C<sub>32</sub>, 1.14; *n*-C<sub>33</sub>, 1.26; *n*-C<sub>34</sub>, 1.41; *n*-C<sub>35</sub>, 1.60; *n*-C<sub>36</sub>, 1.85; *n*-C<sub>37</sub>, 2.20; *n*-C<sub>38</sub>, 2.51; *n*-C<sub>39</sub>, 2.71; *n*-C<sub>40</sub>, 2.93. In the case of 9-methyloctadecane and 9-methylnonacosane, correction factors of the corresponding *n*-alkanes were used.

Concentrations of steranes and 4-methyl steranes were determined by relating their peak areas in the *m/z* 217 respectively *m/z* 231 mass chromatograms to the peak area of the internal standard in the *m/z* 57 mass chromatogram, and multiplying by 1.9 to correct for the higher response if using FID. This factor of 1.9 ( $\pm$  0.2) was determined for C<sub>27</sub>-C<sub>29</sub> 5 $\beta$ ,14 $\alpha$ ,17 $\alpha$ (H)-steranes and C<sub>27</sub>-C<sub>29</sub> (20R)-5 $\alpha$ ,14 $\alpha$ ,17 $\alpha$ (H)-steranes using a sample of which the FID trace could also be integrated. Its use for quantification of C<sub>28</sub>-C<sub>30</sub> 4-methyl steranes is believed not to significantly enhance standard deviations.

Pristane, phytane, isorenieratane, benzohopanes I (see Appendix), C<sub>31</sub> benzohopane **IIa**, C<sub>35</sub> hopanoid benzothiophene **IIIb**, des-A-ferna-5,7,9-triene **IV** (or des-A-arbora-5,7,9-triene **V**), 25-norferna-5,7,9-triene **VI** (or 25-norarbora-5,7,9-triene **VII**), and non-coeluting hopenes and hopanes were quantified by integration of their peaks in the FID-trace and comparison with the FID peak area of the internal standard. Other hopanoids were quantified by integration of their peaks in relevant mass chromatograms (*m/z* 191, 367 or M<sup>+</sup>) and comparison with peak areas of hopanoids of which concentrations were established using the FID-signal. Chromans were quantified by integration of mass chromatograms of *m/z* 107 (fragment ion of chroman standard) + 121 + 135 + 149 using intensities of the fragment ions reported by Sinninghe Damsté et al. (1993b) to calculate total ion abundances. The 2-methylthiophene/toluene ratio (Eglinton et al., 1994) was calculated from the relevant peak areas in the *m/z* 97 + 98 and *m/z* 91 + 92 mass chromatograms.

## Results

### *Sample description and bulk data*

The rocks were sampled from a 4 m interval of the CPF near Orbagnoux, a small village in the southern Jura mountains of France. The lithology of this CPF section, is described in detail elsewhere (Tribovillard et al., 1992; Mongenot et al., 1997). In summary, the sedimentary column displays a succession of laminated and massive limestones, almost devoid of clay minerals. Morphologically the laminated rocks can be divided into a parallel type (Fig. 3.1a) and an undulated type (Fig. 3.1b). The thickness of the alternating light- and dark-coloured laminae ranges from less than a millimetre to more than a centimetre. Four, approximately 1 mm thick, laminae of each type were carefully scraped off some larger rock fragments. In addition, one massive limestone (M) was sampled. In massive limestone M

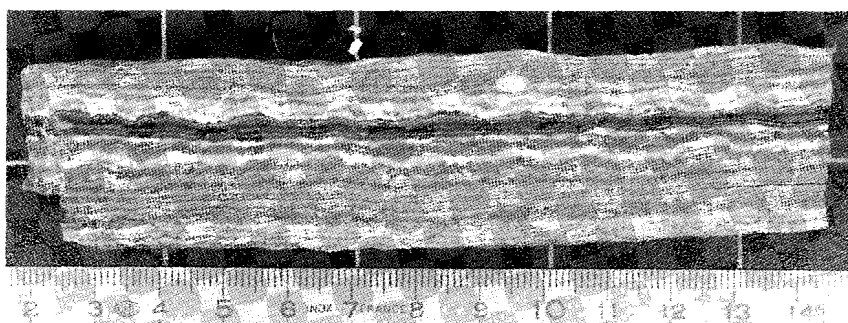
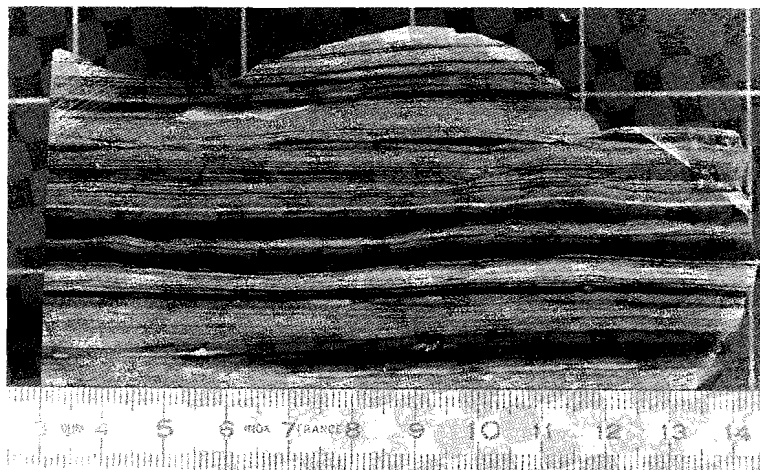


**Fig. 3.1.** (a) (above) Limestone with parallel laminae, and (b) (below) limestone with undulated laminae.

and in the light/parallel (LP), dark/parallel (DP) and dark/undulated (DU) laminae carbonate is largely composed of coccoliths. In the light/undulated (LU) lamina nannofossils are absent (Mongenot et al., 1997). Samples M, LP, DP, LU and DU, correspond to samples TM15, TM11, TM9sa, TM4c and TM4s, reported by Mongenot et al. (1997), respectively.

Bulk data of the samples are listed in Table 3.1. As anticipated from the colour of the samples, TOC values are lower in LP, LU and M (0.9-2.7%), than in DP and DU (7.2-8.6%). The Rock Eval Hydrogen Index (HI) ranges from 870 to 966, indicating that the kerogens are of Type I. The  $T_{max}$  values, ranging from 405 to 411°C, indicate that the OM is thermally immature. The  $\delta^{13}C$  values of the OM ( $\delta^{13}C_{TOC}$ ) are significantly higher in samples LU and DU (-23.9 and -23.5‰) than in the other samples (-28.1 to -26.4‰).

#### *Composition of the bitumen*

Extraction yields are very high in all samples, ranging from 0.25 to 0.47 g/g TOC (Table 3.1). A large part of the bitumen of sample LU, the sample with the highest proportion of

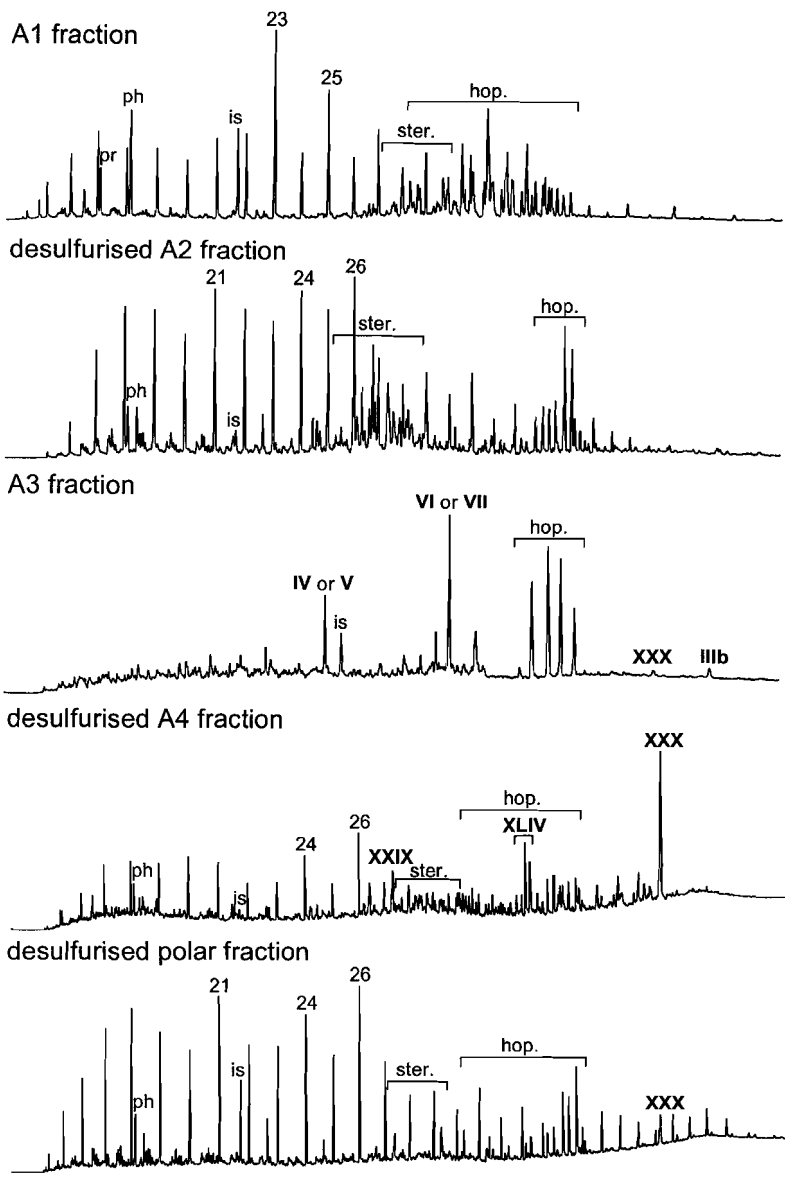


**Fig. 3.2.** FID-traces of different fractions of the bitumen of sample M. Note that hopanoids (hop.) are more important than steroids (ster.) in all but the desulfurised A2 fraction. Roman numbers refer to structures indicated in the Appendix; numbers denote chain lengths of *n*-alkanes; pr = pristane; ph = phytane; is = internal standard. Compounds XLIV (four epimers), recently identified by Poinso et al. (1997), survived desulfurisation.

**Table 3.1.** Bulk data and yields of the different fractions.

	LP	DP	LU	DU	M
TOC (%) <sup>a</sup>	2.7	7.2	0.9	8.6	2.2
T <sub>max</sub> (°C) <sup>a</sup>	411	409	405	408	410
HI (mg HC/g TOC) <sup>a</sup>	870	909	928	966	895
δ <sup>13</sup> C <sub>TOC</sub> (‰) <sup>a</sup>	-28.1	-26.4	-23.9	-23.5	-27.3
bitumen (g/g TOC)	0.25	0.31	0.47	0.29	0.25
asphaltenes (g/g TOC)	0.15	0.17	0.32	0.16	0.12
maltenes (g/g TOC)	0.13	0.16	0.18	0.16	0.14
polars (mg/g TOC)	62	81	69	83	62
apolars (mg/g TOC)	14	18	9.0	17	12
loss (%) <sup>b</sup>	42	37	57	38	47

<sup>a</sup> data from Mongenot et al. (1997)

<sup>b</sup> maltenes retained on column

bitumen, precipitated in *n*-heptane (asphaltene fraction), and as a result, the proportion of the maltene fraction shows no major differences among the samples. The polar and apolar fractions obtained by column chromatography, are slightly greater in samples DP and DU than in the other samples (Table 3.1).

To separate the different types of free and S-bound biomarkers, the apolar fractions of all samples were subjected to argentation TLC. In this way, four subfractions were obtained, comprising, in addition to other compounds, saturated hydrocarbons (A1), thiophenes (A2), benzothiophenes (A3) and sulfides (A4). Subsequently, the A2, A3 and A4 fractions were desulfurised (e.g. Fig. 3.2), and the major compound classes in the desulfurised fractions were quantified. Desulfurised A3 fractions appeared largely similar to the original A3 fractions, and are therefore not discussed.

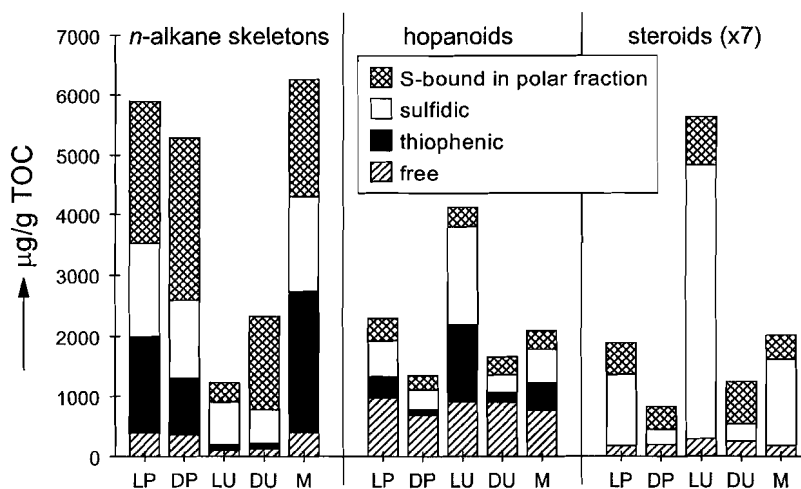


**Fig. 3.3.** Concentrations of free and S-bound *n*-alkanes, hopanoids and steroids in the different samples. In the case of the steroids, only the summed concentrations of desmethyl- and 4-methyl steroids of Fig. 3.9 are shown. Concentrations of D-ring aromatic 8,14-secohopanes are not included.

OSC in the polar fractions can potentially be composed of sulfoxides and intermolecularly S-bound biomarkers. To distinguish between these two types of OSC, the polar fractions were subjected to  $\text{LiAlH}_4$  reduction (Payzant et al., 1986; Schouten et al., 1995). In all instances, only trace amounts of sulfides were formed. This implies that compounds released upon desulfurisation of the polar fractions, hereafter referred to as compounds "S-bound in polar fraction", were intermolecularly linked *via* sulfur. Raney nickel desulfurisation of the asphaltene fractions yielded only trace amounts of hydrocarbons, and these are not discussed. The low yields of desulfurisation, however, do not imply that the asphaltene fractions are poor in sulfur. Desulfurisation was probably not very effective due to the fact that asphaltenes do not dissolve very well in ethanol, the reaction medium used.

*n*-Alkane skeletons. In all samples, the vast majority of *n*-alkane skeletons is present in a S-bound form, as thiophenes, sulfides and *n*-alkane skeletons that are macromolecularly S-bound (Fig. 3.3). Dithiophenic *n*-alkane skeletons, identified in the CPF sample analysed previously (van Kaam-Peters and Sinninghe Damsté, 1997), are absent. Concentrations of free and S-bound *n*-alkanes are consistently lowest in samples with undulated laminae (Fig. 3.3).

Except for sample LU, distributions of free *n*-alkanes are dominated by  $n\text{-C}_{23+}$ , and the  $\text{C}_{23+}$  *n*-alkanes show an odd-over-even carbon number predominance (Fig. 3.4). Free *n*-alkanes in sample LU are extremely low and maximise at  $n\text{-C}_{17}$ . Distributions of S-bound *n*-alkanes are considerably different from those of the free *n*-alkanes. In the desulfurised A2 fractions of all samples,  $\text{C}_{18}\text{-C}_{26}$  *n*-alkanes are significantly more abundant than  $\text{C}_{26+}$  *n*-alkanes, and (sub)maxima exist at  $n\text{-C}_{19}$ ,  $n\text{-C}_{21}$ ,  $n\text{-C}_{24}$  and  $n\text{-C}_{26}$  (Fig. 3.4b). In the desulfurised A4 and polar fractions, the (sub)maxima at  $n\text{-C}_{19}$ ,  $n\text{-C}_{21}$ ,  $n\text{-C}_{24}$ ,  $n\text{-C}_{26}$  are more pronounced, and in addition,  $\text{C}_{26+}$  *n*-alkanes maximise at  $n\text{-C}_{33}$  and  $n\text{-C}_{35}$  (Figs. 3.4c,d). The *n*-alkane distribution in the desulfurised A4 fraction of sample LU is markedly different from that of the other samples, since it is highly dominated by  $n\text{-C}_{17}$  and  $n\text{-C}_{18}$  (Fig. 3.4c).

*n*-Alkanes in the desulfurised A2 fractions resulted from the desulfurisation of 2-*n*-alkyl- and 2,5-di-*n*-alkylthiophenes. In agreement with previous results (van Kaam-Peters and Sinninghe Damsté, 1997),  $\text{C}_{19}$  thiophenes in all samples are characterised by a relatively abundant butyl-5-*n*-undecylthiophene, and  $\text{C}_{24}$  and  $\text{C}_{26}$  thiophenes show relatively high concentrations of mid-chain thiophenes, i.e. 2,5-di-*n*-alkylthiophenes with *n*-alkyl chains comprising more than six carbon atoms. Although, like  $n\text{-C}_{19}$ ,  $n\text{-C}_{24}$  and  $n\text{-C}_{26}$ , also  $n\text{-C}_{21}$  is relatively abundant in the desulfurised A2 fractions (Fig. 3.4b), the distribution of linear  $\text{C}_{21}$  thiophenes is not notably different from that of other, less abundant thiophenes with linear carbon skeletons.

The sulfides with linear carbon skeletons eluting in the A4 fraction, consist of 2-*n*-alkylthiolanes, 2,5-di-*n*-alkylthiolanes, 2-*n*-alkylthianes and 2,6-di-*n*-alkylthianes. The relatively abundant  $n\text{-C}_{19}$ ,  $n\text{-C}_{24}$  and  $n\text{-C}_{26}$  in the desulfurised A4 fractions of samples LP, DP, DU and M correspond to sulfide distributions that show relatively large proportions of 2,6-di-*n*-alkylthianes with side chains of more than four carbon atoms. In addition,  $\text{C}_{19}$  sulfides are characterised by a substantial 2-*n*-propyl-6-*n*-undecylthiane. Differences among the distributions of other sulfides are insignificant. The prominence of  $\text{C}_{19}$ ,  $\text{C}_{24}$  and  $\text{C}_{26}$  mid-

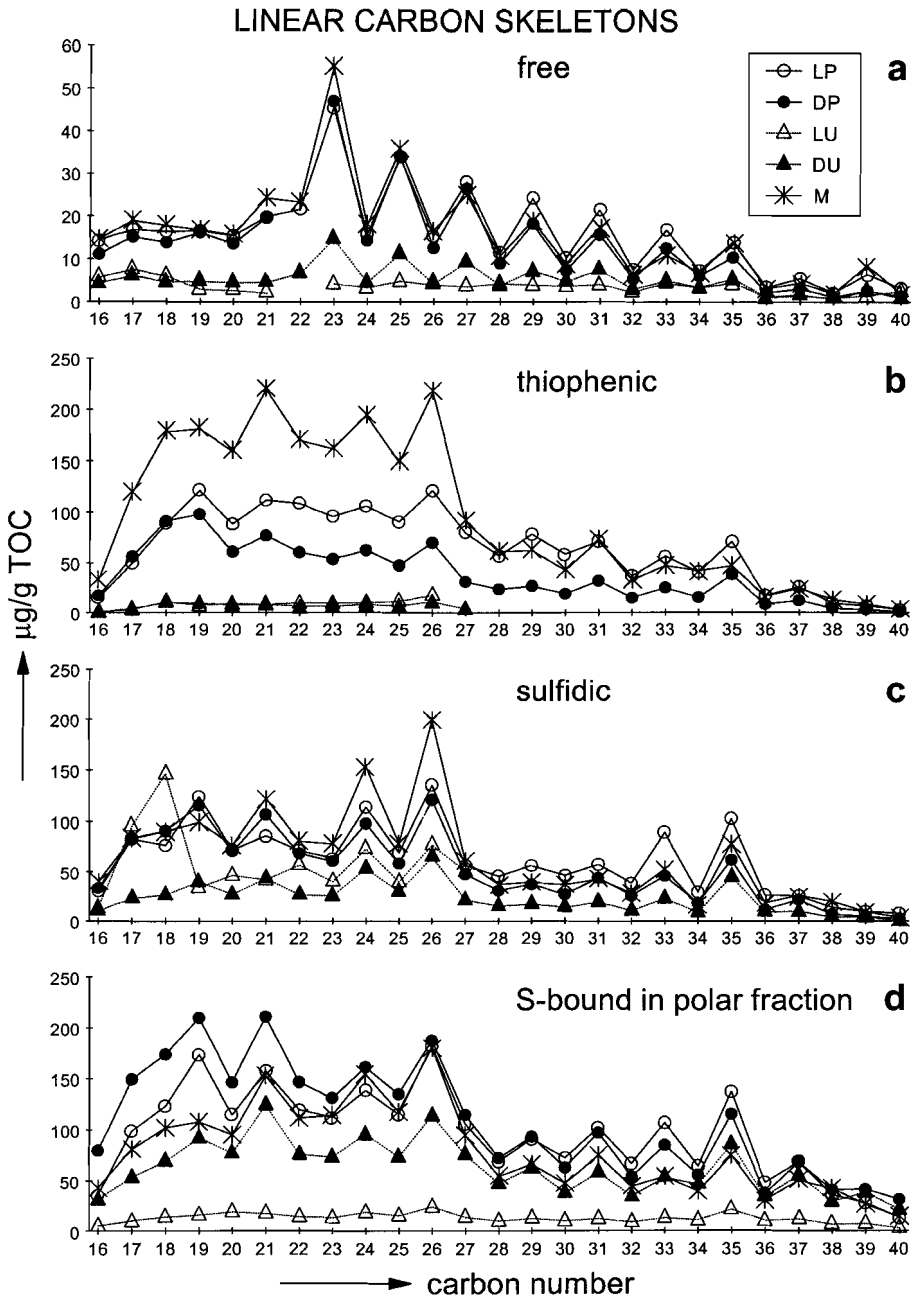


**Fig. 3.4.** Distributions of (a) free, (b) thiophenic, (c) sulfidic *n*-alkane skeletons, and of (d) *n*-alkane skeletons macromolecularly S-bound in the polar fractions.

chain thianes and 2-*n*-propyl-6-*n*-undecylthiane is consistent with the sulfide distribution of the CPF sample analysed by van Kaam-Peters and Sinninghe Damsté (1997). However, mid-chain thianes in samples LP, DP, DU and M, show equally abundant *cis* and *trans* isomers, whereas predominantly *trans* isomers occur in the CPF sample analysed earlier. In the sulfide fraction of sample LU, *n*-alkane skeletons are relatively minor, and their distribution could not be resolved.

**Table 3.2.** Concentrations ( $\mu\text{g/g}$  TOC) of selected biomarkers.

	LP	DP	LU	DU	M
pristane	18	19	4.0	10	14
phytane	33	36	8.8	22	32
phytane <sup>a</sup>	52	91	31	42	52
phytane <sup>b</sup>	58	98	110	80	59
phytane <sup>c</sup>	76	83	29	84	52
isorenieratane	10	11	13	9.1	8.6
isorenieratane <sup>b</sup>	850	430	800	390	530
isorenieratane <sup>c</sup>	130	150	120	170	52
Me-MTTC (XL <sub>a</sub> )	2.7	2.3	0.4	0.9	2.0
diMe-MTTCs (XL <sub>b,c</sub> )	17	12	3.4	7.9	12
triMe-MTTC (XL <sub>d</sub> )	26	22	9.0	21	20
<b>IV or V</b>	120	85	220	180	60
<b>VI or VII</b>	220	210	280	220	120

<sup>a</sup> desulfurised A2 fraction

<sup>b</sup> desulfurised A4 fraction

<sup>c</sup> desulfurised polar fraction

*Pristane and phytane skeletons.* Pristane and phytane were detected both in the saturated hydrocarbon fractions and in the desulfurised A2, A4 and polar fractions of all samples. Concentrations of free pristane and phytane and of S-bound phytane are listed in Table 3.2. Pristane in the desulfurised fractions could not be quantified, since in all instances it coeluted with 2,6,10-trimethyl-7-(3-methylbutyl)dodecane (C<sub>20</sub> HBI). Like the *n*-alkanes, phytane occurs predominantly in a S-bound form in all samples (Table 3.2).

The distribution of C<sub>19</sub> thiophenes reveals the presence of three thiophenes with a pristane skeleton, VIII-X (Sinninghe Damsté et al., 1986; Koopmans et al., 1997a). In sample LU, X is dominant over the other isomers, whereas in the rest of the samples, VIII-X are equally abundant. Thiophenes with a phytane skeleton in sample LU are dominated by XI and XII (Brassell et al., 1986; Sinninghe Damsté et al., 1986, 1987a), whereas in the other samples only XI is present in significant amounts. Due to the complexity of the A4 fractions, it was not possible to identify specific thiolanes or thianes with a pristane or phytane skeleton.

*9-Methylalkane skeletons.* Like in the CPF sample analysed before (van Kaam-Peters and Sinninghe Damsté, 1997), 9-methylalkanes (McCarthy et al., 1968; Holzer et al., 1979; Pomonis et al., 1989) are absent in the saturated hydrocarbon fractions, but series of C<sub>18</sub>-C<sub>32</sub> 9-methylalkanes, dominated by the C<sub>19</sub> and C<sub>30</sub> members, occur in the desulfurised A2, A4 and polar fractions of all samples. The proportion of 9-methylalkanes, as assessed from the

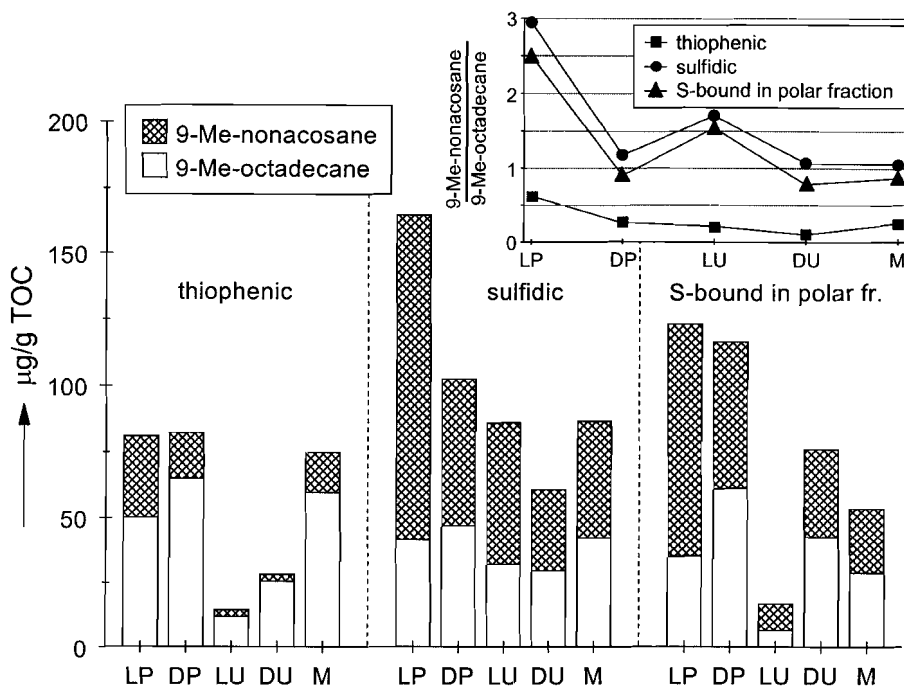


**Fig. 3.5.** Concentrations of 9-methyloctadecane and 9-methylnonacosane in the desulfurised A2 (thiophene), A4 (sulfide) and polar fractions. Insert shows the 9-methylnonacosane/9-methyloctadecane ratios in each of the fractions.

sum of the  $C_{19}$  and  $C_{30}$  members, is greatest in samples LP and DP (Fig. 3.5). In the desulfurised A2 fractions, the proportion of 9-methyloctadecane is always higher than that of 9-methylnonacosane (Fig. 3.5). In the desulfurised A4 and polar fractions, 9-methyloctadecane is either equally abundant or less abundant than 9-methylnonacosane (Fig. 3.5).

Consistent with previous results (van Kaam-Peters and Sinninghe Damsté, 1997), thiophenes with the 9-methyloctadecane skeleton consist of XIII-XV, dominated by XV, whereas thiophenes with the 9-methylnonacosane skeleton are not dominated by particular isomers.

*Hopanoïd skeletons.* In all samples, free and S-bound hopanoïds are important constituents of the bitumen (e.g. Fig. 3.2). The non-sulfur containing hopanoïds include  $C_{27}$  and  $C_{29}$ - $C_{35}$   $17\alpha,21\beta(H)$ -hopanes maximising at  $C_{31}$  (Fig. 3.6),  $C_{30}$ - $C_{35}$  hop-17(21)-enes maximising at  $C_{34}$  (Figs. 3.6 and 3.7g),  $C_{32}$ - $C_{35}$  benzohopanes I,  $C_{31}$ - $C_{35}$  benzohopanes II and small amounts of  $C_{29}$ - $C_{35}$  D-ring aromatic 8,14-sec-hopanoïds XVI (Hussler et al., 1984; Schaeffer et al., 1995; Köster et al., 1997).

Thiophene hopanoïds are mainly composed of  $C_{34}$ - $C_{35}$  members with the thiophene moiety in the side chain (XVII; Valisolalao et al., 1984; Sinninghe Damsté et al., 1989; Köster et al., 1997), of which XVIIa-b are dominant. The thiophene hopanoïd assemblages



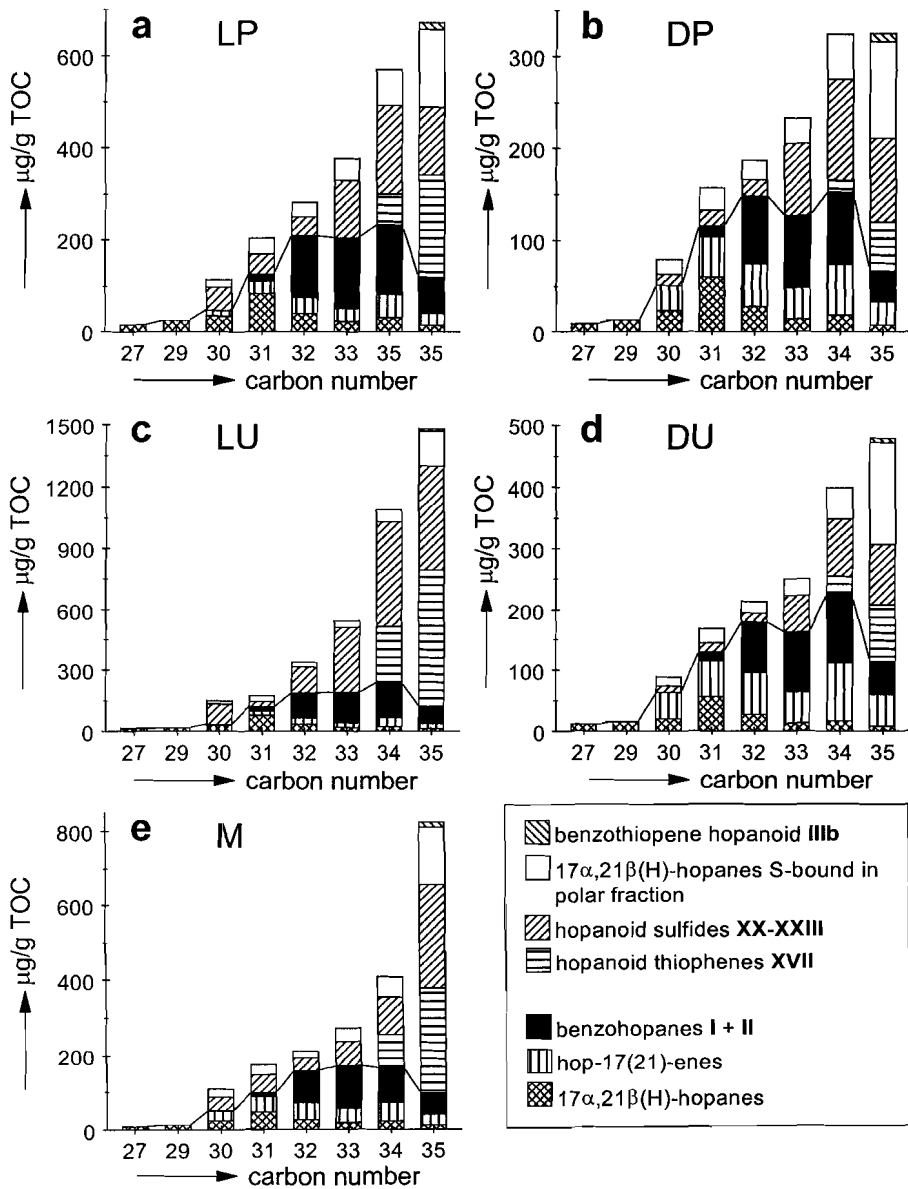
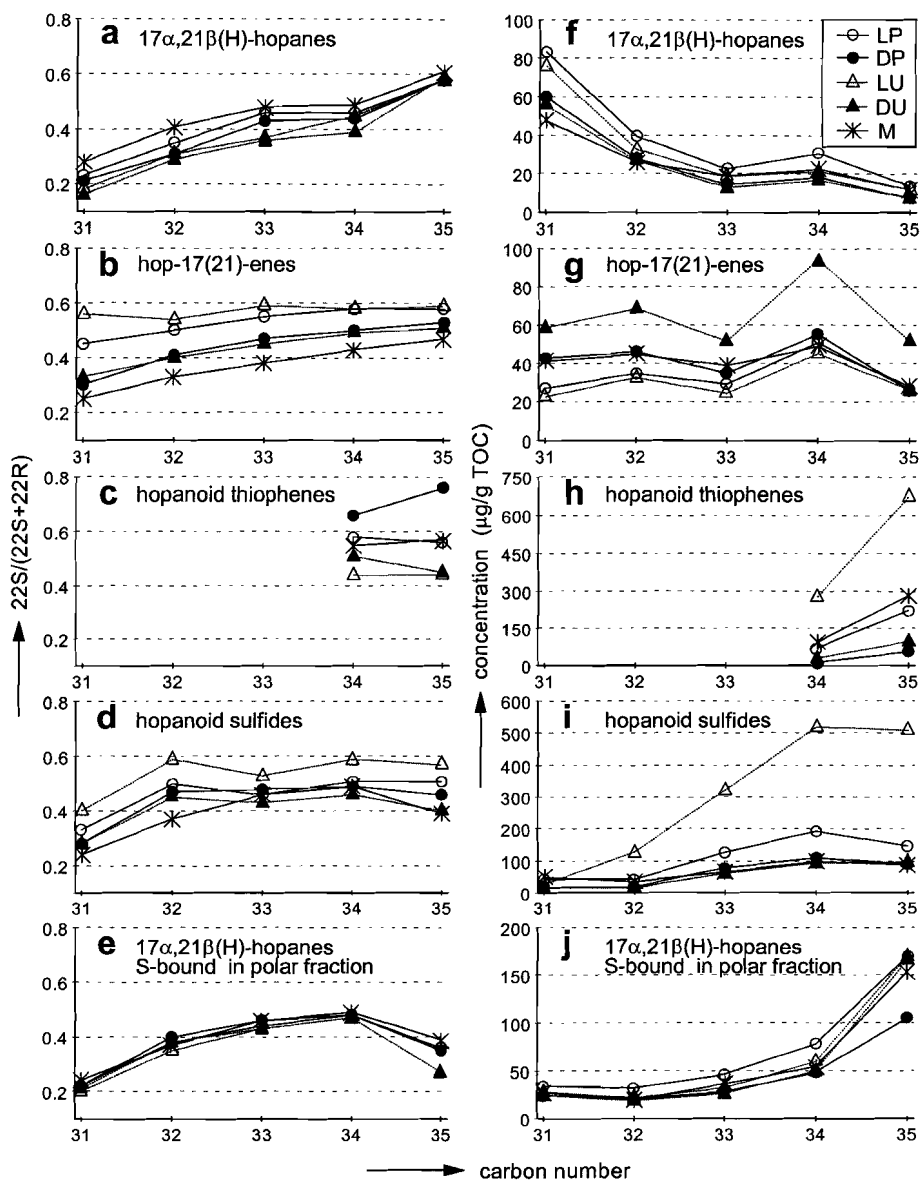


Fig. 3.6. TOC-normalised concentrations of hopanoid carbon skeletons.

in samples LU and LP differ from those in the other samples in that they show a relatively high XVIIa and a relatively low XVIIa, respectively. Upon desulfurisation of the thiophene hopanoids,  $\text{C}_{34}\text{-C}_{35}$   $17\alpha,21\beta(\text{H})$ -hopanes are formed, which are dominated by the  $\text{C}_{35}$  members (Fig. 3.7h).



**Fig. 3.7.** The 22S/(22S+22R) ratios (a-e) and distributions (f-j) of free and S-bound homohopanooids.

Benzothiophene hopanoids **III** and **XVIII** (van Kaam-Peters et al., 1995), were detected in the A3 fractions of all samples. Only **IIIb**, which in all instances is the dominant benzothiophene hopanoid, was quantified.

In contrast to the hopanoid sulfides in the CPF sample investigated previously (van Kaam-Peters and Sinninghe Damsté, 1997), hopanoid sulfides **XIXa-b**, with the sulfur

incorporated at or near the end of the side-chain (Kohnen et al., 1991; Köster et al., 1997), are absent. Hopanoid sulfides in all samples are composed of **XX-XXIII** (Schaeffer, 1993; Köster et al., 1997). Distributions of **XX** ( $C_{35} > C_{34} > C_{33} > C_{31} > C_{32}$ ), **XXI** ( $C_{31} > C_{34} > C_{35} \approx C_{33} \approx C_{32}$ ) and **XXII** ( $C_{34} > C_{31} \approx C_{32} \approx C_{33} \approx C_{35}$ ) are similar in all samples. Hopanoid sulfides **XXIII** consist of only  $C_{33}$ - $C_{35}$  members, but due to the large number of stereoisomers (Köster et al., 1997), they constitute a complex mixture. As deduced from the  $m/z$  115+129+143 mass chromatograms,  $C_{34}$  members dominate the distributions of **XXIII** in all samples. The distribution of stereoisomers of **XXIII** in sample LU, however, is different from that of the rest. Although each series of hopanoid sulfides exhibits a similar carbon number distribution in all samples, differences exist in the relative abundances of the series. The most conspicuous difference is the relatively high proportion of **XXI** in samples LP, LU and M. Desulfurisation of **XX-XXIII** yielded  $C_{30}$ - $C_{35}$   $17\alpha,21\beta$ (H)-hopanes maximising at  $C_{34}$  and  $C_{35}$  in all samples (Figs. 3.6 and 3.7i).

Fig. 3.6 gives an overview of the concentrations of the different hopanoid carbon skeletons in each of the samples. D-ring aromatic 8,14-secohopanes, present in relatively small amounts in all samples, are not included. Consistent with other observations (de Leeuw and Sinninghe Damsté, 1990; Sinninghe Damsté et al., 1995; Köster et al., 1997; van Kaam-Peters and Sinninghe Damsté, 1997), a positive correlation is observed between the length of the homohopane side-chain and the degree of sulfurisation. This selective preservation of the  $C_{35}$  hopane skeleton is most pronounced in the massive limestone sample M (Fig. 3.6e). Both relative to the non-sulfur containing hopanoids and absolutely, proportions of S-bound hopanoids are greatest in the TOC-lean, light coloured samples (LP, LU and M) (Fig. 3.3).

To examine whether a relationship exists between the different types of hopanoids and the isomerisation at C-22, as suggested by Köster et al. (1997), 22S/(22S+22R) ratios were determined of free and S-bound  $17\alpha,21\beta$ (H)-homohopanes and of homohop-17(21)-enes in all samples (Figs. 3.7a-e). The 22S/(22S+22R) ratio of free  $17\alpha,21\beta$ (H)-homohopanes gradually rises from ca. 0.2 to almost 0.6 with increasing carbon number (Fig. 3.7a). A less strong, and in the case of samples LU and LP weak, positive correlation is observed between carbon number and 22S/(22S+22R) ratio of homohop-17(21)-enes (Fig. 3.7b). The  $C_{34}$  and  $C_{35}$  hopanes released upon desulfurisation of the thiophene hopanoids exhibit 22S/(22S+22R) ratios between 0.44 and 0.76 (Fig. 3.7c). The 22S/(22S+22R) ratio of the  $C_{31}$  hopanes released upon desulfurisation of the A4 fraction is consistently lower than the 22S/(22S+22R) ratios of the  $C_{32}$ - $C_{35}$  hopanes in this fraction (Fig. 3.7d). Within the samples,  $C_{32}$ - $C_{35}$  hopanes in the desulfurised A4 fraction have very similar 22S/(22S+22R) ratios (Fig. 3.7d). The 22S/(22S+22R) ratios of homohopanes released upon desulfurisation of the polar fraction, gradually increase from 0.2 at  $C_{31}$  to almost 0.5 at  $C_{34}$  in all samples (Fig. 3.7e).  $C_{35}$  hopanes released from the polar fraction, exhibit 22S/(22S+22R) ratios between 0.27 (LU and DU) and 0.39 (Fig. 3.7e).

*Steroid skeletons.* Sterane mixtures in the saturated hydrocarbon fractions were analysed by GC-MS and GC-MSMS. The dominant desmethyl steranes in all samples are  $5\alpha$ -cholestane and 24-ethyl- $5\alpha$ -cholestane. Although the  $M^+$  to 217 transitions measured by GC-MSMS seem to indicate a dominance of  $5\alpha$ -cholestane over 24-ethyl- $5\alpha$ -cholestane (e.g. Fig. 3.8),

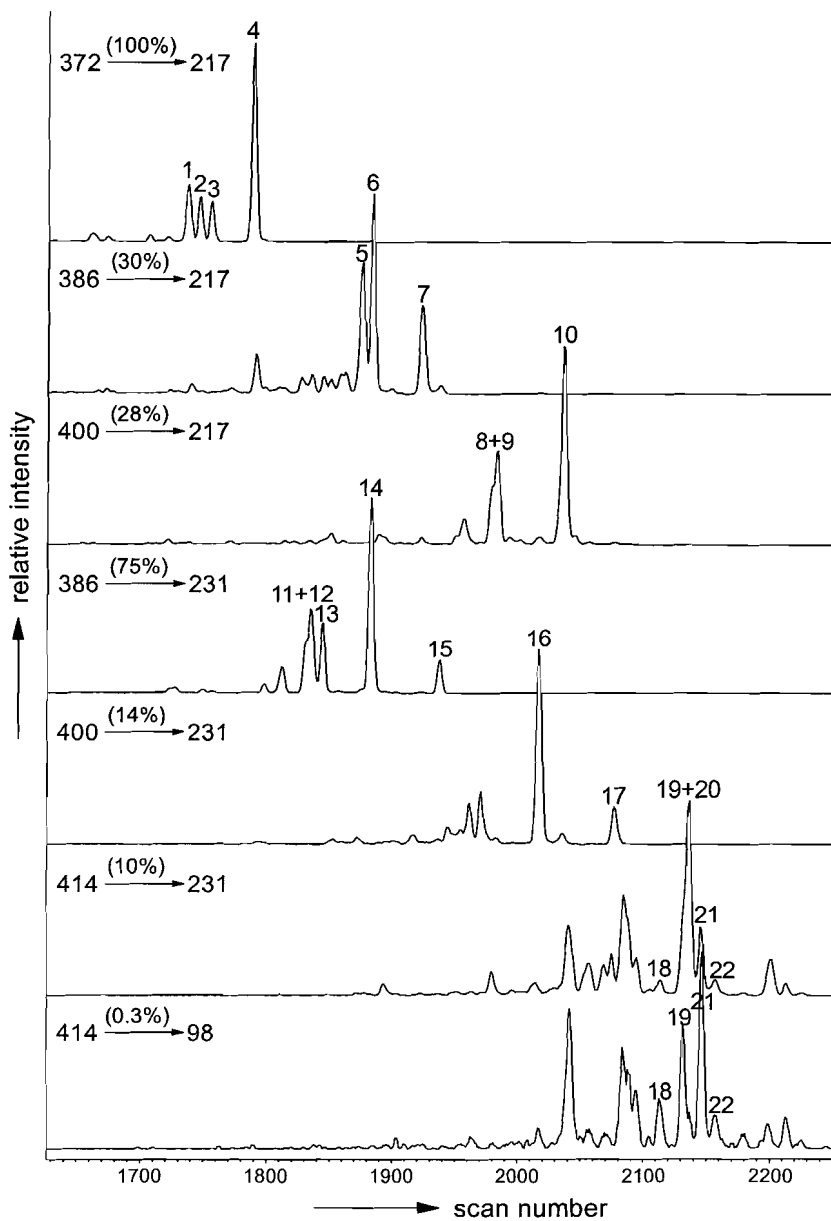


**Fig. 3.8.** Chromatograms showing desmethyl and 4-methyl sterane distributions in sample LU. The data were acquired by collisionally activated decomposition GC-MSMS. Each trace is identified with the masses of the parent and daughter ions, and the intensity of the base peak expressed as a percentage relative to the intensity of the 5 $\alpha$ -cholestane peak. Chromatograms were smoothed at 3 points of equal weight. Numbers refer to components listed in Table 3.3.

**Table 3.3.** Steranes identified.

peak <sup>a</sup>	structure assignment
1	5 $\beta$ -cholestane
2	(20R)-5 $\alpha$ ,14 $\beta$ ,17 $\beta$ (H)-cholestane
3	(20S)-5 $\alpha$ ,14 $\beta$ ,17 $\beta$ (H)-cholestane
4	5 $\alpha$ -cholestane
5	(20R)-24-methyl-5 $\alpha$ ,14 $\beta$ ,17 $\beta$ (H)-cholestane
6	(20S)-24-methyl-5 $\alpha$ ,14 $\beta$ ,17 $\beta$ (H)-cholestane
7	24-methyl-5 $\alpha$ -cholestane
8	(20R)-24-ethyl-5 $\alpha$ ,14 $\beta$ ,17 $\beta$ (H)-cholestane
9	(20S)-24-ethyl-5 $\alpha$ ,14 $\beta$ ,17 $\beta$ (H)-cholestane
10	24-ethyl-5 $\alpha$ -cholestane
11	4 $\alpha$ -methyl-5 $\beta$ -cholestane
12	4 $\alpha$ -methyl-(20R)-5 $\alpha$ ,14 $\beta$ ,17 $\beta$ (H)-cholestane
13	4 $\alpha$ -methyl-(20S)-5 $\alpha$ ,14 $\beta$ ,17 $\beta$ (H)-cholestane
14	4 $\alpha$ -methyl-5 $\alpha$ -cholestane
15	4 $\beta$ -methyl-5 $\alpha$ -cholestane
16	4 $\alpha$ ,24-dimethyl-5 $\alpha$ -cholestane
17	4 $\beta$ ,24-dimethyl-5 $\alpha$ -cholestane
18	4 $\alpha$ ,23S,24S-trimethyl-5 $\alpha$ -cholestane <sup>b</sup>
19	4 $\alpha$ ,23S,24R-trimethyl-5 $\alpha$ -cholestane <sup>b</sup>
20	4 $\alpha$ -methyl-24-ethyl-5 $\alpha$ -cholestane
21	4 $\alpha$ ,23R,24R-trimethyl-5 $\alpha$ -cholestane <sup>b</sup>
22	4 $\alpha$ ,23R,24S-trimethyl-5 $\alpha$ -cholestane <sup>b</sup>

<sup>a</sup> numbers refer to peaks indicated in Fig. 3.8

<sup>b</sup> stereochemistries at C-23 and C-24 after Moldowan (pers. comm., 1994)

integration of the  $m/z$  217 mass chromatograms shows that the concentration of 5 $\alpha$ -cholestane is actually similar to that of 24-ethyl-5 $\alpha$ -cholestane in all samples (Fig. 3.9a). Following 5 $\alpha$ -cholestane and 24-ethyl-5 $\alpha$ -cholestane, the next dominant desmethyl steranes are 24-methyl-5 $\alpha$ ,14 $\beta$ ,17 $\beta$ (H)-cholestanes. This extraordinarily abundance of C<sub>28</sub> 14 $\beta$ ,17 $\beta$ (H)-steranes (e.g. Fig. 3.8) was also observed in the CPF sample described previously (van Kaam-Peters and Sinninghe Damsté, 1997), and probably indicates a relatively large input of  $\Delta^7$ -sterols (Peakman et al., 1989).

Desmethyl steranes in the desulfurised A2 fractions of all samples are low, but their distributions are worth mentioning. Like in the saturated hydrocarbon fractions, C<sub>28</sub> 5 $\alpha$ ,14 $\beta$ ,17 $\beta$ (H)-steranes released upon desulfurisation of the A2 fractions, are more abundant than the C<sub>28</sub> 5 $\alpha$ ,14 $\alpha$ ,17 $\alpha$ (H)-steranes. The dominant desmethyl steranes in the desulfurised A2 fractions, however, are the C<sub>29</sub> 5 $\alpha$ ,14 $\beta$ ,17 $\beta$ (H)-steranes, which are thus also higher than their 14 $\alpha$ ,17 $\alpha$ (H)-counterparts. The only steroids eluting in the A2 fractions from which the 14 $\beta$ ,17 $\beta$ (H)-steranes could be derived, are steroid thiophenes **XXIV** (Schmid, 1986) and the unknown steradienes that were also reported by van Kaam-Peters and Sinninghe Damsté (1997).

Distributions of desmethyl steranes in the desulfurised A4 fractions are dominated by C<sub>27</sub>-C<sub>29</sub> 5 $\alpha$ ,14 $\alpha$ ,17 $\alpha$ (H)-steranes. Their concentrations vary widely among the samples (Fig. 3.9b). Within the samples, the C<sub>27</sub>-C<sub>29</sub> homologues are present in similar amounts (Fig.

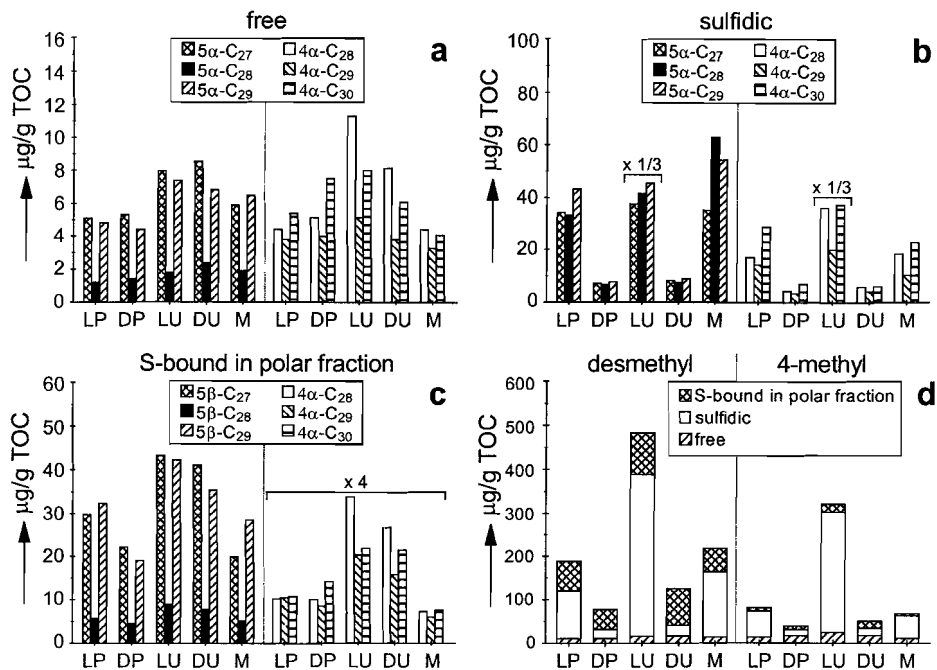


**Fig. 3.9.** Sterane distributions in (a) A1 fractions, (b) desulfurised A4 fractions and (c) desulfurised polar fractions. (d) Sum of  $C_{27}$ - $C_{29}$  desmethyl steranes and sum of  $C_{28}$ - $C_{30}$  4-methyl steranes per sample.  $5\alpha$ - $C_{27}$  =  $5\alpha$ -cholestane,  $5\alpha$ - $C_{28}$  = 24-methyl- $5\alpha$ -cholestane,  $5\alpha$ - $C_{29}$  = 24-ethyl- $5\alpha$ -cholestane,  $5\beta$ - $C_{27}$  =  $5\beta$ -cholestane,  $5\beta$ - $C_{28}$  = 24-methyl- $5\beta$ -cholestane,  $5\beta$ - $C_{29}$  = 24-ethyl- $5\beta$ -cholestane,  $4\alpha$ - $C_{28}$  =  $4\alpha$ -methyl- $5\alpha$ -cholestane,  $4\alpha$ - $C_{29}$  =  $4\alpha$ ,24-dimethyl- $5\alpha$ -cholestane,  $4\alpha$ - $C_{30}$  =  $4\alpha$ -methyl-24-ethyl- $5\alpha$ -cholestane.

3.9b).  $C_{27}$ - $C_{29}$   $5\alpha$ ,14 $\beta$ ,17 $\beta$ (H)-steranes are also present, but they never exceed the  $5\alpha$ ,14 $\alpha$ ,17 $\alpha$ (H)-steranes in concentration. Desmethyl steranes in the desulfurised A4 fractions mainly derive from **XXV** and **XXVI** (Schmid, 1986; Behrens et al., 1997), which are the only desmethyl steroid sulfides detected in the A4 fraction.

Desmethyl steranes in the desulfurised polar fractions mainly consist of  $5\beta$ ,14 $\alpha$ ,17 $\alpha$ (H)-isomers, of which  $C_{27}$  and  $C_{29}$  are dominant (Fig. 3.9c). The desulfurisation method used does not allow determination of the positions of the original C-S bonds.

In addition to the desmethyl steranes, 4-methyl steranes were detected in the saturated hydrocarbon fractions and desulfurised A4 and polar fractions of all samples. In all instances, the distributions are dominated by  $4\alpha$ -isomers (e.g. Fig. 3.8), and maximise at  $C_{28}$  and  $C_{30}$  (Figs. 3.9a-c). 4-Methyl steranes in the desulfurised A4 fractions resulted from the desulfurisation of **XXVII** and **XXVIII** (Schmid, 1986; Behrens et al., 1997), the only 4-methyl sterane sulfides detected. Generally, 4-methyl sterane distributions in samples LU and DU show a more pronounced  $4\alpha$ -methyl- $5\alpha$ -cholestane than observed in corresponding

fractions of the other samples (Figs. 3.9a-c). Four isomers of dinosterane were detected in the saturated hydrocarbon fractions of all samples (e.g. Fig. 3.8).

As with the S-bound hopanoids, S-bound desmethyl- and 4-methyl steroids are most abundant, both relative to the free steroids and absolutely, in the TOC-lean samples (LP, LU and M) (Figs. 3.3 and 3.9d). Distributions of monoaromatic steroids, which are major components of the A2 fractions of all samples (e.g. Fig. 3.2), have not been examined. As seen from their abundance relative to that of the thiophene hopanoids, which elute in the same fraction and which have been quantified, concentrations of monoaromatic steroids are greatest in sample LU, consistent with the higher relative abundance of steroids in this sample in general (Fig. 3.3).

*Aryl- and diaryl isoprenoids.* Two series of C<sub>18</sub>-C<sub>22</sub> aryl isoprenoids were detected in the A2 fractions of samples LU, DU and M. Based on relative retention times, the earlier eluting, dominant series is thought to have a 2,3,6-trimethyl substitution pattern of the aromatic ring, the other series a 2,3,4-trimethyl substitution pattern (Summons and Powell, 1987). C<sub>18</sub>-C<sub>22</sub> aryl isoprenoids are absent in sample DP, and only trace amounts of one series of C<sub>18</sub>-C<sub>22</sub> aryl isoprenoids were detected in sample LP. The C<sub>29</sub> aryl isoprenoid **XXIX** (Sinninghe Damsté et al., 1988a; van Kaam-Peters and Sinninghe Damsté, 1997), is relatively abundant in all samples.

Isorenieratane (**XXX**), eluting in the A3 fraction, is present in similar amounts in all samples (Table 3.2). Concentrations of free isorenieratane, however, are insignificant compared to those of isorenieratane released upon desulfurisation of the A4 and polar fractions (Table 3.2). Thiophenic aryl isoprenoids, found in the A3 fraction of the CPF sample examined previously (van Kaam-Peters and Sinninghe Damsté, 1997), are absent in all samples.

In general, distributions of aryl- and diaryl isoprenoids in the desulfurised A4 and polar fractions, are similar to those in the CPF sample described earlier (van Kaam-Peters and Sinninghe Damsté, 1997). In summary, these distributions show, in order of elution, a series of short-chain aryl isoprenoids with a 2,3,6-trimethyl substitution pattern of the aromatic ring, C<sub>29</sub> aryl isoprenoid **XXIX**, a C<sub>40</sub> aryl isoprenoid with a 2,3,4- or 2,3,6-trimethyl substitution pattern of the aromatic ring (**XXXI**; Schaeffer et al., 1997), and a dominant isorenieratane (**XXX**). The relative proportion of **XXXI** in the desulfurised polar fractions of samples LU and DU is somewhat higher than that observed in the other fractions. In the desulfurised A4 fraction of sample LU, an additional carotenoid-derived component (**XXXII**; Schaeffer et al., 1997) was found.

Isorenieratane in the desulfurised A4 fraction of sample LU, resulted from the desulfurisation of compounds **XXXVI** and **XXXVII** (Koopmans et al., 1996a). C<sub>40</sub> derivatives of isorenieratane in the A4 fractions of the other samples are composed of **XXXVI-XXXIX** (Koopmans et al., 1996a). Due to the complexity of the A4 fractions, no S-bound aryl isoprenoids could be identified.

*Other compounds.* Methylated 2-methyl-2-(4,8,12-trimethyltridecyl)chromans (MTTCs, **XL**) were detected in the A3 fractions of all samples. Their concentrations are significantly

lower in sample LU than in the other samples (Table 3.2). In all samples, chroman distributions are dominated by the trimethylated member **XLd** (Table 3.2).

Des-A-ferna-5,7,9-triene (**IV**) (or des-A-arbora-5,7,9-triene **V**), 25-norferna-5,7,9-triene (**VI**) (or 25-norarbora-5,7,9-triene **VII**) (Hauke et al., 1992a,b) are major components of the A3 fractions of all samples (e.g. Fig. 3.2). Although it is not known whether they derive from fern-9(11)-en-3 $\beta$ -ol (**XLI**) or from arbor-9(11)-en-3 $\beta$ -ol (**XLII**), these compounds are thought to have an aquatic origin (Hauke et al., 1992b; van Kaam-Peters and Sinninghe Damsté, 1997). Concentrations of **IV-VII**, in particular that of the tetracyclic compound (**IV** or **V**), are highest in samples LU and DU (Table 3.2).

The A4 fractions of all samples contain a series of OSC characterised by a major fragment ion at  $m/z$  169 in their mass spectra. These are probably the regular polycyclic isoprenoid sulfides recently identified by Poinot et al. (1997). The distributions are dominated by the C<sub>20</sub> and C<sub>30</sub> homologues (**XLIII-XLIV**).

#### *Stable carbon isotopic compositions of biomarkers*

Stable carbon isotopic compositions were determined for several biomarkers in the A1, A3 and desulfurised A4 fractions (Table 3.4). The  $\delta^{13}\text{C}$  values of free pristane and phytane amount to ca. -29‰ in sample LU, and to -31‰ in all other samples. The  $\delta^{13}\text{C}$  values of phytane in the desulfurised A4 fractions do not significantly differ among the samples, and average to -29.6‰.

The  $\delta^{13}\text{C}$  values of free C<sub>34</sub> 17 $\alpha$ ,21 $\beta$ (H)-hopanes, C<sub>33</sub>-C<sub>35</sub> 17 $\alpha$ ,21 $\beta$ (H)-hopanes in the desulfurised A4 fraction, and C<sub>32</sub>-C<sub>35</sub> benzohopanes **II** range from -32.9 to -28.7‰ (Table 3.4). In samples LP and M, C<sub>32</sub>-C<sub>35</sub> benzohopanes **II** and C<sub>33</sub>-C<sub>35</sub> 17 $\alpha$ ,21 $\beta$ (H)-homohopanes released upon desulfurisation of the A4 fraction, are depleted in  $^{13}\text{C}$  by 1 to 2‰ compared to identical homohopanooids in the other samples. Within each sample, C<sub>34</sub>-C<sub>35</sub> 17 $\alpha$ ,21 $\beta$ (H)-homohopanes in the desulfurised A4 fraction have similar  $\delta^{13}\text{C}$  values. C<sub>33</sub> 17 $\alpha$ ,21 $\beta$ (H)-homohopanes in the desulfurised A4 fraction, however, show  $\delta^{13}\text{C}$  values that are consistently 1 to 2‰ lower than those of higher homologues in the same fraction. Similarly, C<sub>33</sub> benzohopane **II** is always isotopically lighter than the other homologues in the same sample (Table 3.4).

The  $\delta^{13}\text{C}$  values of isorenieratane S-bound in the A4 fraction fall in a narrow range of -18.4 to -17.7‰. Compounds **IV** (or **V**) and **VI** (or **VII**) show  $\delta^{13}\text{C}$  values ranging from -30.4 to -28.7‰ (Table 3.4).

#### *Kerogen pyrolysates*

Differences among the flash pyrolysates of kerogens are small. In all pyrolysates, alkyl- and alkenylthiophenes, alkylbenzothiophenes, and linear alkylbithiophenes **XLV-XLVII** are the dominant constituents (e.g. Fig. 3.10). Other, less prominent, series of OSC in the pyrolysates are phenylalkylthiophenes **XLVIII** and **XLIX**. The identification of **XLV-XLIX** has been described elsewhere (van Kaam-Peters and Sinninghe Damsté, 1997). Non-sulfur containing pyrolysis products mainly consist of long homologous series of *n*-alkanes and *n*-alkenes, and series of alkylbenzenes, including 1,2,3,4-tetramethylbenzene (TMB). Phenols



**Table 3.4.** Stable carbon isotopic compositions,  $\delta^{13}\text{C}$  (‰)<sup>a</sup>, of different biomarkers.

	LP	DP	LU	DU	M
pristane <sup>b</sup>	-31.0 ± 0.1	-31.6 ± 0.9	-28.8 ± 0.5	-31.2 ± 0.3	-31.3 ± 0.4
phytane <sup>b</sup>	-31.1 ± 0.2	-31.2 ± 0.2	-29.6 ± 0.1	-30.8 ± 0.3	-31.6 ± 0.2
phytane <sup>c</sup>	-30.1 ± 0.7	-29.6 ± 0.2	-29.5 ± 1.0	-29.4 ± 0.2	-29.5 ± 0.2
(22S)-17 $\alpha$ ,21 $\beta$ (H)- tetrakishomohopane <sup>b</sup>	-29.8 ± 1.0	-31.8 ± 1.2	-30.1 ± 0.1	-28.9 ± 0.7	-29.4 ± 0.1
(22R)-17 $\alpha$ ,21 $\beta$ (H)- tetrakishomohopane <sup>b</sup>	-29.9 ± 0.9	-31.4 ± 1.2	-30.0 ± 0.3	-28.7 ± 0.7	-29.3 ± 0.3
(22S)-17 $\alpha$ ,21 $\beta$ (H)- trishomohopane <sup>c</sup>	-32.2 ± 0.1	-30.8 ± 0.1	-29.7 ± 1.0	-30.9 ± 0.3	-31.7 ± 0.7
(22R)-17 $\alpha$ ,21 $\beta$ (H)- trishomohopane <sup>c</sup>	-31.8 ± 0.1	-31.2 ± 0.1	-29.8 ± 0.8	-30.6 ± 0.6	-31.9 ± 0.2
(22S)-17 $\alpha$ ,21 $\beta$ (H)- tetrakishomohopane <sup>c</sup>	-30.7 ± 0.2	-29.2 ± 0.1	-28.7 ± 0.1	-29.6 ± 0.2	-30.3 ± 0.1
(22R)-17 $\alpha$ ,21 $\beta$ (H)- tetrakishomohopane <sup>c</sup>	-30.4 ± 0.1	-29.5 ± 0.1	-28.9 ± 0.1	-29.6 ± 0.1	-30.0 ± 0.1
(22S)-17 $\alpha$ ,21 $\beta$ (H)- pentakishomohopane <sup>c</sup>	-30.5 ± 0.2	-29.7 ± 0.1	-28.9 ± 0.1	-29.3 ± 0.1	-30.4 ± 0.2
(22R)-17 $\alpha$ ,21 $\beta$ (H)- pentakishomohopane <sup>c</sup>	-30.4 ± 0.2	-29.3 ± 0.1	-28.8 ± 0.1	-28.9 ± 0.1	-30.0 ± 0.1
C <sub>32</sub> benzohopane <b>II</b> <sup>d</sup>	-32.0 ± 0.4	-30.5 ± 0.3	-30.7 ± 0.5	-30.0 ± 0.1	-31.3 ± 0.3
C <sub>33</sub> benzohopane <b>II</b> <sup>d</sup>	-32.9 ± 0.3	-31.5 ± 0.9	-31.5 ± 0.1	-31.5 ± 0.5	-32.8 ± 0.3
C <sub>34</sub> benzohopane <b>II</b> <sup>d</sup>	-31.4 ± 0.3	-29.1 ± 0.9	-29.6 ± 0.4	-30.1 ± 0.7	-30.2 ± 0.2
C <sub>35</sub> benzohopane <b>II</b> <sup>d</sup>	-31.6 ± 0.4	-29.1 ± 1.2	-30.1 ± 0.1	-29.6 ± 1.8	-30.2 ± 0.3
<b>IV</b> or <b>V</b> <sup>d</sup>	-28.7 ± 0.4	n.d. <sup>f</sup>	-29.4 ± 0.2	-29.4 ± 0.4	-28.8 ± 0.1
<b>VI</b> or <b>VII</b> <sup>d</sup>	-30.3 ± 0.2	n.d. <sup>f</sup>	-30.1 ± 0.1	-29.4 ± 0.3	-30.4 ± 0.4
isorenieratane <sup>e</sup>	-18.3 ± 0.2	-18.1 ± 0.1	-18.3 ± 0.4	-18.4 ± 0.7	-17.7 ± 0.1

<sup>a</sup> indicated uncertainties are standard errors of means of 2 or 3 measurements

<sup>b</sup> non-adduct of A1 fraction

<sup>c</sup> non-adduct of saturated hydrocarbon fraction of desulfurised A4 fraction

<sup>d</sup> A3 fraction

<sup>e</sup> ethyl acetate fraction of desulfurised A4 fraction

<sup>f</sup> not determined because of contamination

and methoxyphenols, indicative of lignins (Saiz-Jimenez and de Leeuw, 1984), are present in trace amounts only.

Excluding 2-methylthiophene, the distributions of alkylthiophenes in the kerogen pyrolysates of the four laminated samples are the same. The abundance of 2-methylthiophene relative to the other thiophenes decreases slightly in the order LU, DP, DU, LP. Alkylthiophenes in the pyrolysate of sample M are characterised by relatively abundant C<sub>7+</sub> thiophenes, and a relatively high contribution of 2,3,5-trimethylthiophene. Distributions of alkenylthiophenes, alkylbenzothiophenes, alkylbithiophenes (**XLV-XLVII**) and phenylalkylthiophenes (**XLVIII-XLIX**) are similar in all but the pyrolysate of sample DU, in which the first one or two homologues of each series are relatively more pronounced. The pattern of *n*-alkene/*n*-alkane doublets (e.g. Fig. 3.10b) is similar in all pyrolysates. Alkylbenzene distributions differ mainly in the relative proportion of TMB. Compared to

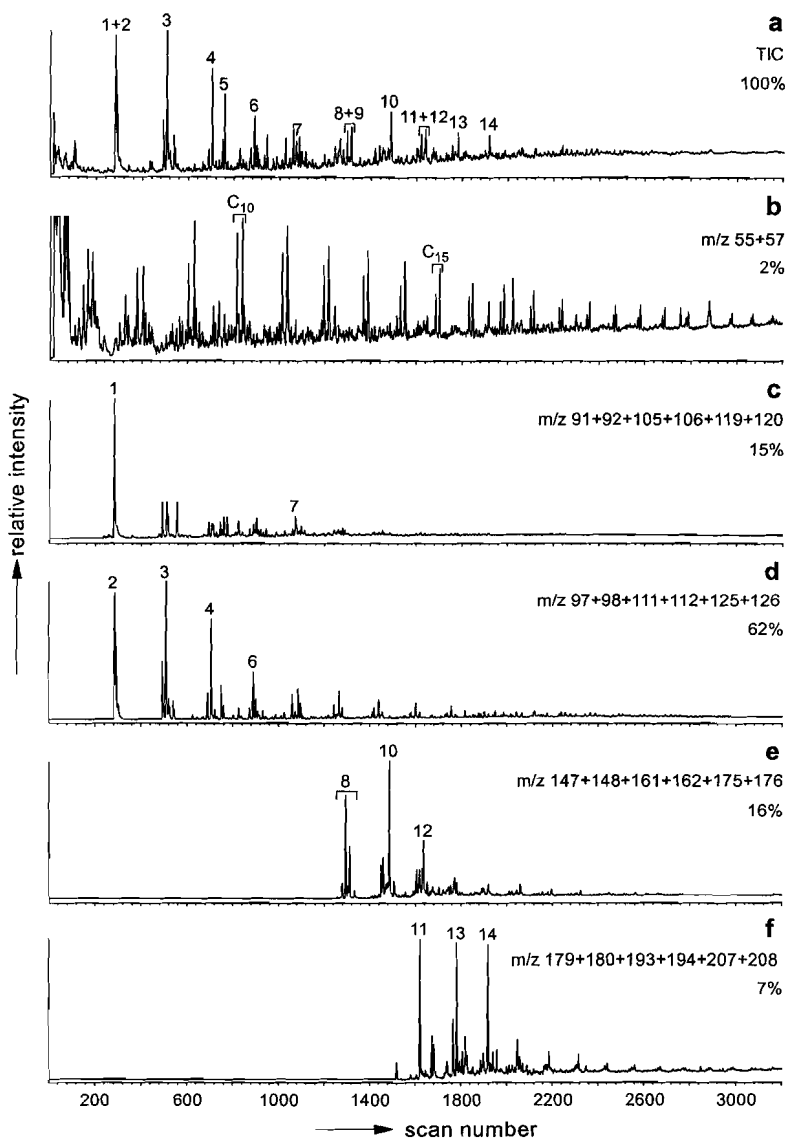


**Fig. 3.10.** Total ion current (TIC) trace (a) and mass chromatograms of characteristic fragment ions of *n*-alkenes and *n*-alkanes (b), alkylbenzenes (c), alkylthiophenes (d), alkylbenzothiophenes (e) and alkylbithiophenes (f) of kerogen pyrolysate of sample DU. Percentages indicate the intensities of the base peaks relative to the intensity of the base peak in the TIC trace. Key: 1 = toluene, 2 = 2-methylthiophene, 3 = 2,5-dimethylthiophene, 4 = 2-ethyl-5-methylthiophene, 5 = ethenylthiophene, 6 = 2-propyl-5-methylthiophene, 7 = 1,2,3,4-tetramethylbenzene, 8 = methylbenzothiophenes, 9 = acenaphthene, 10 = dimethylbenzothiophene, 11 = methylbithiophene, 12 = ethylmethylbenzothiophene, 13 = dimethylbithiophene, 14 = ethylmethylbithiophene.

toluene, TMB is most abundant in sample M, and far more abundant in the light-coloured samples than in the corresponding dark-coloured samples (LP > DP and LU > DU).

The 2-methylthiophene/toluene ratios (TR ratios) of the kerogen pyrolysates, reflecting the atomic  $S_{org}/C$  ratio of the kerogens (Eglinton et al., 1994), are extraordinarily high, amounting to 6.3 in samples DU and DP, and to 5.5, 4.0 and 3.9 in samples LU, M and LP, respectively. TR ratios of 1.0 were reported by Eglinton et al. (1994) for kerogens with  $S_{org}/C$  ratios between 0.07 and 0.09. Therefore, the kerogen  $S_{org}/C$  ratios of all our samples probably surpass 0.09.

## Discussion

### *Differences in OM composition*

The gross molecular composition of the OM is similar in all samples: Extractable biomarkers mainly consist of *n*-alkane and hopanoid carbon skeletons, and a large proportion of these is present in a S-bound form. Derivatives of isorenieratene, which are markers for photic zone euxinia (Repeta, 1993; Sinninghe Damsté et al., 1993c), are present in relatively large amounts. Free long-chain odd-numbered *n*-alkanes and other terrestrial plant markers are low. Finally, the kerogen pyrolysates are highly dominated by OSC (e.g. Fig. 3.10), and show trace amounts only of lignin-derived, phenolic compounds. Despite the overall similarity in OM composition, however, several qualitative and quantitative differences have been observed. These differences are summarised in Table 3.5. The most important differences in OM composition are discussed below.

*Degree of intermolecular sulfur cross-linking.* Artificial maturation studies of immature organic sulfur-rich sedimentary rocks indicate that sulfur incorporation into OM takes place almost exclusively in an intermolecular fashion, and that LMW OSC are generated from HMW fractions during diagenesis (Koopmans et al., 1995, 1996b, 1997b,c). Generation of LMW OSC already occurs at low levels of thermal maturation (i.e. when even the relatively thermally unstable 17 $\beta$ ,21 $\beta$ (H)-hopanes are still present; Koopmans et al., 1996b). In the CPF samples, 17 $\beta$ ,21 $\beta$ (H)-hopanes are absent and the 22S/(22S+22R) ratio of the C<sub>35</sub> 17 $\alpha$ ,21 $\beta$ (H)-hopanes approaches the thermodynamic equilibrium ratio of about 0.6 (Peters and Moldowan, 1993; Fig. 3.7a). This suggests that in the CPF the production of LMW OSC is already in a relatively advanced stage.

LMW S-bound hopanoids and steroids (thiophenes and cyclic sulfides) are more abundant in the light-coloured samples LP, LU and M than in samples DP and DU (Fig. 3.3). Also, though less clear, in the sample pairs LP/DP and LU/DU, concentrations of LMW S-bound *n*-alkanes are highest in the light-coloured laminae (Fig. 3.3). Apparently, the generation of LMW OSC from HMW fractions occurred more readily in light-coloured samples than in dark-coloured samples. This is most likely due to differences in the degree of intermolecular sulfur cross-linking of the OM, reflected by the different yields of polar and asphaltene fractions (Table 3.1). With increasing diagenesis, an increasing number of C-S bonds is cleaved and compounds enter fractions of a lower molecular weight (Koopmans et al., 1995, 1996b, 1997b,c). This implies that the amount of LMW OSC generated is

**Table 3.5.** Main differences in OM composition among the samples. The symbols --, -, +, and ++, in this order, stand for increasing values. Similar compound distributions are marked by the same symbols (◇, x, ○).

	LP	DP	LU	DU	M
<u>Abundance in bitumen of:</u>					
<i>n</i> -alkane skeletons <sup>a</sup>	+	+	--	-	+
9-methylalkane skeletons <sup>a</sup>	+	+	--	-	+
S-bound hopanoids <sup>a</sup>	+	-	++	-	+
S-bound steroids <sup>a</sup>	+	-	++	-	+
hop-17(21)-enes <sup>b</sup>	-	+	-	+	-
hopanoid sulfides <b>XXI</b> <sup>c</sup>	+	-	+	-	+
isorenieratane in desulfurised A4 fraction <sup>a</sup>	+	-	+	-	+
isorenieratane in desulfurised polar fraction <sup>a</sup>	-	+	-	+	-
<b>XXXI</b> in desulfurised polar fraction <sup>d</sup>	-	-	+	+	-
<b>XXXII</b> in desulfurised A4 fraction	n.d. <sup>e</sup>	n.d.	+	n.d.	n.d.
MTTCs ( <b>XL</b> ) <sup>a</sup>	+	+	-	+	+
<b>IV-VII</b> <sup>a</sup>	-	-	+	+	-
<u>Distribution in bitumen of:</u>					
<i>n</i> -alkanes in desulfurised A4 fraction	x	x	◇	x	x
thiophenes with pristane skeleton	x	x	◇	x	x
thiophenes with phytane skeleton	x	x	◇	x	x
isorenieratane skeletons in A4 fraction	x	x	◇	x	x
free and S-bound 4-methyl steranes	x	x	◇	◇	x
hopanoid thiophenes <b>XVII</b>	○	x	◇	x	x
<u>Ratios:</u>					
C <sub>30</sub> /C <sub>19</sub> 9-methylalkanes in bitumen	++	-	+	-	-
TR ratio in kerogen pyrolysate	-	++	+	++	-
TMB/toluene in kerogen pyrolysate	+	-	+	-	++
<u>Distribution in kerogen pyrolysate of:</u>					
alkylthiophenes	x	x	x	x	◇
alkenylthiophenes, alkylbenzothiophenes, alkylbithiophenes and phenylalkylthiophenes	x	x	x	◇	x
<sup>a</sup> relative to other samples	<sup>d</sup> relative to isorenieratane in same fraction				
<sup>b</sup> relative to other hopanoids within the sample	<sup>e</sup> not detected				
<sup>c</sup> relative to other hopanoids in same fraction					

directly related to the number of sulfur cross-links by which compounds are bound in macromolecular fractions. Sample LU, characterised by the highest amounts of LMW S-bound hopanoids and steroids (Fig. 3.3), is distinguished also by a relatively large proportion of asphaltenes (Table 3.1). Probably, prior to any C-S bond cleaving during diagenesis, the number of intermolecular C-S bonds in sample LU was relatively low already. In other words, a relatively small kerogen fraction was formed and a relatively large amount of asphaltenes. Since the initial number of sulfur cross-links in the OM of sample LU was relatively low, more LMW OSC could be generated in this sample than in the others.

The highly variable concentrations of S-bound isorenieratane (Table 3.2), which is the dominant isorenieratene derivative, probably also partly result from differences in the

degree of OM cross-linking by sulfur. Concentrations of isorenieratane in the desulfurised A4 fraction are greatest in samples LP and LU, whereas concentrations of isorenieratane in the desulfurised polar fraction maximise in samples DP and DU (Table 3.5).

*Linear and branched alkane skeletons.* With exception of the *n*-alkane distribution in the desulfurised A4 fraction of sample LU, variations in the *n*-alkane distributions among the samples mainly concern the ratio of  $C_{26+}$  *n*-alkanes over  $C_{18}$ - $C_{26}$  *n*-alkanes in the desulfurised A2, A4 and polar fractions (Figs. 3.4b-d). Interestingly, these variations in the *n*-alkane distributions correspond to variations in the 9-methylnonacosane/9-methyloctadecane ratios (9M ratios). In the desulfurised A2 fractions,  $C_{18}$ - $C_{26}$  *n*-alkanes are dominant over  $C_{26+}$  *n*-alkanes (Fig. 3.4b), and 9M ratios equal 0.6 or less (Fig. 3.5). In the desulfurised A4 and polar fractions,  $C_{26+}$  *n*-alkanes are relatively more pronounced (Figs. 3.4c,d), and 9M ratios amount to ca. 1 or more (Fig. 3.5). Also, the highest 9M ratios, which occur in the desulfurised A4 and polar fractions of sample LP (Fig. 3.5), correspond to the greatest proportions of  $C_{26+}$  *n*-alkanes relative to that of  $C_{18}$ - $C_{26}$  *n*-alkanes (Figs. 3.4c,d). These data may suggest that the *n*-alkanes and 9-methylalkanes in the desulfurised fractions are derived from similar source organisms. Further evidence for this hypothesis is provided by the concentrations of *n*-alkanes and 9-methylalkanes. In the desulfurised polar fraction of LU and in the desulfurised A2 fractions of LU and DU, both *n*-alkanes and 9-methylalkanes are extremely low (Figs. 3.4b,d and 3.5). In our previous study of the CPF (van Kaam-Peters and Sinninghe Damsté, 1997), we suggested that the  $C_{18}$ - $C_{32}$  9-methylalkanes were derived from two different source organisms at least. The present results are in agreement with this, since concentrations of 9-methyloctadecane and  $C_{18}$ - $C_{26}$  *n*-alkanes vary independently of those of 9-methylnonacosane and  $C_{26+}$  *n*-alkanes. Unfortunately, the source of all these compounds is unknown, but considering the abundant homohopanoids in all samples, a cyanobacterial origin seems likely.

*Hopanoïd skeletons.* The carbon number distributions of the different types of free hopanoïds and of hopanes in the desulfurised fractions, are similar in all samples (Figs. 3.7f-j). The summed concentrations of hopanoïd carbon skeletons (Fig. 3.6), however, show the selective preservation of  $C_{35}$  hopanoïds to be more pronounced in sample M than in the other samples. This indicates that homohopanoïd side-chain shortening reactions (Ourisson and Albrecht, 1992), which may occur prior to sulfurisation (Köster et al., 1997), were relatively unimportant during deposition of sample M. This may be explained by differences in the composition of the precursor bacteriohopanepolyol derivatives, or by differences in the oxicity of the palaeoenvironment (Peters and Moldowan, 1993; Sinninghe Damsté et al., 1995; Köster et al., 1997).

Markedly, hopanoïd sulfides **XXI** are relatively more abundant in light-coloured than in dark-coloured samples, whereas for the hop-17(21)-enes it is the other way round (Table 3.5; Fig. 3.6). Considering the position of the sulfur atom in **XXI** (between C-17 and C-23), it may be that **XXI** and hop-17(21)-enes have similar precursor hopanoïds, of which a greater part became macromolecularly S-bound and was released later as a LMW sulfide in the case of light-coloured samples.

Recently, Köster et al. (1997) postulated that the incorporation of sulfur may significantly influence the homohopanoid 22S/(22S+22R) ratios. During maturation, hopanoids with the sulfur atom between one carbon atom of the side-chain (exclusive of C-22) and one carbon atom of the D- or E-ring (condensed-type) will preserve their original 22R configuration, whereas hopanoids with the sulfur atom between two carbon atoms of the side-chain will isomerise to their thermodynamic equilibrium ratio. This equilibrium ratio is slightly dependent on the length of the hopanoid side-chain, and ranges from 0.57 to 0.62 (Seifert and Moldowan, 1980; van Duin et al., 1997). The formation of S-bound hopanoids of the side-chain type (free isomerisation at C-22) is structurally limited to the C<sub>32+</sub> homologues. Therefore, C<sub>32+</sub> hopanes obtained by desulfurisation will generally have higher 22S/(22S+22R) ratios than C<sub>31</sub>-C<sub>32</sub> hopanes obtained by desulfurisation (Köster et al., 1997). Since the free homohopanoids were probably partly generated from S-bound homohopanoids during diagenesis, the 22S/(22S+22R) ratios of the free homohopanoids will also show a positive relationship with carbon number (Köster et al., 1997). Indeed, in agreement with Köster et al. (1997), the 22S/(22S+22R) ratios of free and S-bound homohopanoids are consistently lowest at C<sub>31</sub> and generally highest at C<sub>34</sub> and C<sub>35</sub> (Figs. 3.7a-e). At higher levels of thermal maturity, when the release of hopanoids has ended, the isomerisation at C-22 will probably reach equilibrium values for all homologues.

Although generally the 22S/(22S+22R) ratios show similar trends in all samples, some differences clearly exist. For example, homohop-17(21)-enes in samples LP and LU (Fig. 3.7b) and homohopanoid sulfides in sample LU (Fig. 3.7d) have higher 22S/(22S+22R) ratios than the corresponding homologues in the other samples. Furthermore, the 22S/(22S+22R) ratios of C<sub>34</sub>-C<sub>35</sub> 17 $\alpha$ ,21 $\beta$ (H)-hopanes released upon desulfurisation of thiophene hopanoids XVII, vary widely (0.44-0.76, Fig. 3.7c). These thiophene hopanoids all have the thiophene moiety in their side-chain, implying that isomerisation at C-22 was not hindered. This indicates that stereochemistry at C-22 can be significantly influenced by factors other than maturation and sulfurisation.

The C<sub>31</sub> 17 $\alpha$ ,21 $\beta$ (H)-hopanes in the desulfurised A4 fraction probably largely derive from XXI and XXII, hopanoid sulfides with relatively abundant C<sub>31</sub> members. Hopanoid sulfides XXI are of the type presumed to mainly possess the 22R configuration (Köster et al., 1997). Notably, XXI is relatively most abundant in the light-coloured samples (Table 3.5), and the C<sub>31</sub> 22S/(22S+22R) ratio is highest in one of these (LU) (Fig. 3.7d). This may suggest that the generally low 22S/(22S+22R) ratios of the C<sub>31</sub> hopanoids cannot be explained solely by restricted isomerisation due to the condensed-type of sulfur incorporation.

*Steroid skeletons.* The distributions of free desmethyl steranes and of desmethyl steranes in the desulfurised A2 and polar fractions of all samples are similar to those in the CPF sample analysed before, and are discussed elsewhere (van Kaam-Peters and Sinninghe Damsté, 1997). Desmethyl steranes in the desulfurised A4 fractions of all samples are dominated by C<sub>27</sub>-C<sub>29</sub> 5 $\alpha$ -isomers. This sharply contrasts to the distribution of desmethyl steranes in the desulfurised A4 fraction of the CPF sample described earlier (van Kaam-Peters and Sinninghe Damsté, 1997), which is dominated by C<sub>27</sub> and C<sub>29</sub> 5 $\beta$ -isomers. These 5 $\beta$ -steranes were thought to be mainly derived from steroid sulfide L (Schouten, 1995) detected in the

A4 fraction. In agreement with this, L is absent in the A4 fractions of the present sample set, and only steroid sulfides XXV and XXVI, which can have both 5 $\alpha$  and 5 $\beta$  configurations, are present.

Distributions of free and S-bound 4-methyl steranes exhibit only minor differences among the samples (Figs. 3.9a-c). It is noted, however, that 4 $\alpha$ -methyl-5 $\alpha$ -cholestane is more pronounced in samples LU and DU than in the other samples. Since distributions of dinoflagellate sterols are characterised by the absence or low amounts of 4-methylcholesterol, distributions of 4-methyl steranes including dinosterane and maximising at C<sub>28</sub>, are thought to have a multiple origin, and a precursor derived from blooming algae has been suggested for 4-methyl-cholestane (van Kaam-Peters et al., 1997c). Apparently, these algae were relatively most abundant during deposition of samples LU and DU.

*Kerogen pyrolysates.* The compositional differences of the extractable OM are not reflected in the kerogen pyrolysates. In all pyrolysates, *n*-alkanes and *n*-alkenes are dwarfed by OSC (e.g. Fig. 3.10). This indicates that only a small part of the kerogen is composed of resistant aliphatic biomacromolecules. To date, insoluble non-hydrolysable aliphatic biopolymers have been found in higher plants (Nip et al., 1986; van Bergen et al., 1994; Tegelaar et al., 1995) and in cell walls of marine and fresh-water (micro)algae (Largeau et al., 1984, 1986; Goth et al., 1988; Derenne et al., 1992; Gelin et al., 1996). The one resistant cyanobacterial biopolymer reported (Chalansonnet et al., 1988), was recently shown to be an artefact (Allard et al., 1997). Considering the small amounts of terrestrial biomarkers in the bitumen and the virtual absence of lignin-derived products in the kerogen pyrolysates, the pyrolysate *n*-alkanes and *n*-alkenes are most likely derived from marine algaenans (insoluble non-hydrolysable algal biopolymers).

In contrast to the *n*-alkanes and *n*-alkenes, OSC in the pyrolysates could (partly) be derived from source organisms other than algae. Therefore, considering the abundant homohopanooids in the bitumen, it may be that part of the OSC in the kerogen pyrolysates is derived from S-bound cyanobacterial OM. The distributions of alkenylthiophenes, alkylbenzothiophenes, alkylbithiophenes and phenylalkylthiophenes in the pyrolysate of sample DU, and the distribution of alkylthiophenes in sample M differ from those in the other samples. This indicates that the composition of S-bound macromolecules in the kerogens of samples DU and M is different from that in the other samples. The nature of these differences, however, is not known.

The HI values of our samples are very high (870-966, Table 3.1). Such high HI values are generally associated with hydrogen-rich but sulfur-poor kerogens (Type I), deposited in lacustrine environments and having a good potential to produce high quality oils (Tissot and Welte, 1984). Kerogens that are both hydrogen- and sulfur-rich (Type I-S) were discovered in lacustrine basins in Catalonia (Sinninghe Damsté et al., 1993a). As regards the CPF, the dominant OSC in the kerogen pyrolysates (e.g. Fig. 3.10) suggest that the high HI values are largely due to the sulfur-richness and not to the hydrogen-richness of the kerogens. Despite their marine origin, these kerogens are also best classified as Type I-S.

*Stable carbon isotopic composition.* The OM in samples LU and DU is enriched in <sup>13</sup>C by 3 to 5‰ relative to OM in the other samples (Table 3.1). Because of the almost absence of

terrestrial markers in both bitumen and kerogen pyrolysates of all samples, these variations in  $\delta^{13}\text{C}_{\text{TOC}}$  cannot be ascribed to different proportions of terrestrial and marine OM. Consequently, the different  $\delta^{13}\text{C}_{\text{TOC}}$  values can only have resulted from changes in the composition of marine OM or from changes in the  $^{13}\text{C}$  content or concentration of dissolved inorganic carbon (DIC) in the photic zone. If the variations in  $\delta^{13}\text{C}_{\text{TOC}}$  originate from differences in the concentration of DIC or  $\delta^{13}\text{C}$  of DIC ( $\delta^{13}\text{C}_{\text{DIC}}$ ), the  $^{13}\text{C}$  contents of primary production markers must vary accordingly. Pristane and phytane are thought to mainly derive from tocopherols (Goossens et al., 1984) and chlorophyll-a (Volkman and Maxwell, 1986), respectively, which makes them fairly reliable markers of primary production. In several samples of the Kimmeridge Clay Formation, pristane and phytane have been found to predominantly derive from specific carbon isotopically heavy source(s) (van Kaam-Peters et al., 1997b), but the samples concerned are also characterised by relatively abundant norpristane and 2,6,10-trimethyldecane, a feature not observed in the CPF samples. Pristane and phytane have similar  $\delta^{13}\text{C}$  values in all but sample LU (Table 3.4). The  $\delta^{13}\text{C}$  values of S-bound phytane, which is believed to originate from phytol or derivatives thereof (Brassell et al., 1986; Sinninghe Damsté and de Leeuw, 1987), do not significantly differ among the samples (Table 3.4). Therefore, the relatively high  $\delta^{13}\text{C}_{\text{TOC}}$  values of both sample LU and sample DU, have probably not resulted from a higher  $^{13}\text{C}$  content or lower concentration of DIC in the photic zone.

Since the Chlorobiaceae use the reverse tricarboxylic acid cycle for fixation of  $\text{CO}_2$  (Sirevåg and Ormerod, 1970), the  $\delta^{13}\text{C}$  values of their biomass are independent of the concentration of DIC. Hence, the narrow range of  $\delta^{13}\text{C}$  values of S-bound isorenieratane (Table 3.4), indicates that at the lower boundary of the photic zone, where Chlorobiaceae have their habitat,  $\delta^{13}\text{C}$  of DIC was similar in all samples. This strengthens our inference above that the different  $\delta^{13}\text{C}_{\text{TOC}}$  values are not related to differences in the inorganic carbon system.

Samples LU and DU are characterised not only by relatively high  $\delta^{13}\text{C}_{\text{TOC}}$  values but also by relatively small amounts of free and S-bound *n*-alkane skeletons in the bitumen (Fig. 3.3). This suggests that differences in  $\delta^{13}\text{C}_{\text{TOC}}$  might be related to different contributions of *n*-alkane skeletons to the OM. However, the large resemblance of the kerogen pyrolysates of all samples, argue against compositional differences being the cause of variations in  $\delta^{13}\text{C}_{\text{TOC}}$ . In addition, hopanoid  $\delta^{13}\text{C}$  values are no higher than -28.7‰ (Table 3.4), and steroid  $\delta^{13}\text{C}$  values, although not measured, are not likely to exceed by far the  $\delta^{13}\text{C}$  values of pristane and phytane (-31.6 to -28.8‰). This implies that even if *n*-alkane skeletons would be absent, the resulting relatively enhanced proportions of steroids and hopanoids could not account for the  $\delta^{13}\text{C}_{\text{TOC}}$  values of -23.9 and -23.5‰ measured for samples LU and DU, respectively. A large contribution of isorenieratene derivatives, which have  $\delta^{13}\text{C}$  values of ca. -18‰ (Table 3.4), could account for such high  $\delta^{13}\text{C}_{\text{TOC}}$  values. However, despite the fact that isorenieratene derivatives can be major components of bitumen and kerogen pyrolysates, their presence is unaccompanied by any other significant organic remains of their source organisms (Chlorobiaceae), and hence their effect on  $\delta^{13}\text{C}_{\text{TOC}}$  is negligible (Hartgers et al., 1994).

Recently, van Kaam-Peters et al. (1997b) presented evidence that not only lipid carbon, but also substantial amounts of carbohydrate carbon may be preserved through



sulfurisation. Since carbohydrates are enriched in  $^{13}\text{C}$  by several permil compared to lipids, variations in  $\delta^{13}\text{C}_{\text{TOC}}$  can potentially be explained by differences in the proportion of carbohydrate carbon preserved. However, the relative abundance of linear  $\text{C}_1\text{-C}_3$  alkylated thiophenes in the kerogen pyrolysate, which to a certain extent reflects the contribution of sulfurised carbohydrates to the kerogen (van Kaam-Peters et al., 1997b), does not significantly differ among the samples. This suggests that different contributions of carbohydrate carbon to the kerogen cannot account for the variations in  $\delta^{13}\text{C}_{\text{TOC}}$  either.

Finally, the  $\delta^{13}\text{C}$  values of the hopanoids vary independently of those of pristane and phytane. The reasons for this are not evident, since there are many precursor bacteriohopanepolyol derivatives, and these are subject to different diagenetic pathways, causing wide ranges of  $\delta^{13}\text{C}$  values sometimes even for pairs of 22S and 22R epimers (Sinninghe Damsté et al., 1995).

### *Depositional environment*

Although the samples were deposited in a lagoonal environment, and thus in close proximity to the hinterland, terrestrial input of OM was low, as deduced from the relatively small amounts of higher plant markers in both bitumen and kerogen pyrolysates. The fact that terrestrial biomarkers are scarce, does not mean that the climate was dry. The chroman distributions, dominated by the trimethyl-MTTC (**XLd**), point to a normal salinity of the photic zone (Sinninghe Damsté et al., 1993b), implying that the water balance was at least not very negative. The abundant homohopanoids in the bitumen suggest that cyanobacteria significantly contributed to the planktonic and/or benthic community. The presence of isorenieratene derivatives and the abundant OSC in both bitumen and kerogen indicate that the depositional environment was euxinic for substantial periods of time.

Despite the presence of abundant coccoliths in samples LP, DP, DU and M, there is no direct evidence for organic remains of their source organisms (Prymnesiophyceae). To date, prymnesiophyte algae have not been reported to biosynthesise algaenans (Gelin et al., 1997; Koopmans et al., 1997c), but a few of them produce  $\text{C}_{37}\text{-C}_{39}$  linear unsaturated ketones (Brassell, 1993; Volkman et al., 1995), which, during early diagenesis, can be linked to the kerogen by both sulfur and oxygen bonds (Koopmans et al., 1997c). However, thermal degradation products of such sequestered  $\text{C}_{37}\text{-C}_{39}$  unsaturated ketones are absent (mid-chain ketones) or low ( $\text{C}_{37}\text{-C}_{39}$  *n*-alkanes and mid-chain thiophenes) in the extracts and kerogen pyrolysates of all samples.

The molecular data thus show that free  $\text{H}_2\text{S}$  was present in the water column during deposition of all types of rock, and these euxinic conditions led to the abundant sulfurisation, and hence a better preservation, of OM (Sinninghe Damsté and de Leeuw, 1990). Therefore, it is unlikely that the sulfurisation of planktonic OM settling on the sea floor, resulted from the presence of a microbial mat, as suggested by Tribovillard et al. (1992). The  $\text{H}_2\text{S}$  produced by sulfate reducing bacteria in the deepest layers of a mat, is oxidised by colourless and purple sulfur bacteria within the mat, and only at night minor amounts of  $\text{H}_2\text{S}$  may diffuse out (Nicholson et al., 1987; Canfield and Des Marais, 1993; van Gemerden, 1993). In this way, the photosynthetic microbes in the top layers of a mat are protected from

the poisonous H<sub>2</sub>S produced by sulfate reduction below. Consequently, OM deposited on top of a living microbial mat has almost no opportunity to react with sulfide.

Although the abundant sulfurisation of OM cannot have resulted from the presence of a microbial mat, this does not imply that microbial mats were absent all the time. The lithological differences as such indicate that sedimentary conditions have varied. The alternating light- and dark-coloured parallel laminae can be explained by seasonal variations in the fluxes of OM and particularly carbonate (largely coccoliths) in a calm depositional environment. Besides the substantial difference in water depth, this type of sedimentation is comparable to that in the present-day Black Sea (Hay, 1988). Massive limestones may reflect periods in time in which calcifying algae were relatively abundant and were not fully replaced by only organic-walled species. The small-scale, capricious, undulations of samples LU and DU (Fig. 3.1b), however, are hard to explain from the sedimentation of OM and carbonate produced in the surface waters. Also, sample LU is the only sample in which coccoliths and other nanofossils are absent (Mongenot et al., 1997). Therefore, it is suggested that the light-coloured undulated layers are "templates" of microbial mats, resulting from the precipitation of carbonate induced by benthic micro-organisms (cf. Riding, 1991). Like most microbial carbonates, these "templates" are poor in TOC. The dark-coloured undulated layers, composed of coccoliths and sulfur-rich OM deposited at times that bottom waters were frequently sulfidic, are moulded on the light-coloured undulated layers.

From the biomarker distributions there is some circumstantial evidence indeed, that the undulated rocks owe their structure to the periodic appearance of microbial mats. Sample LU is the only sample in which the *n*-alkanes obtained by desulfurisation of the A4 fraction, show a pronounced *n*-C<sub>17</sub> and *n*-C<sub>18</sub> (Fig. 3.4c). C<sub>17</sub>-C<sub>20</sub> mono- and di-unsaturated hydrocarbons are present up to 10 cm depth in recent microbial mat systems in Baja California (Boon and de Leeuw, 1987). The prominent *n*-C<sub>17</sub> and *n*-C<sub>18</sub> in the desulfurised A4 fraction of sample LU, may thus be explained by the sulfurisation of C<sub>17</sub> and C<sub>18</sub> *n*-alkadienes (at least two double bonds are required to form a cyclic sulfide) within the microbial mat. Although *n*-C<sub>17</sub> and *n*-C<sub>18</sub> are no specific biomarkers at all, the fact that in our sample set they are dominant only in sample LU, might be an indication for an origin from microbial mats.

Sample LU is distinguished not only by its different distribution of *n*-alkanes in the desulfurised A4 fraction, but also by some other features (Table 3.5). For example, distributions in sample LU of thiophenes with a pristane skeleton and thiophenes with a phytane skeleton differ from those in the other samples. Since sulfur incorporation selectively takes place at sites in the molecule where functional groups are located (Sinninghe Damsté et al., 1988b), these different distributions can be explained by differences in the composition of precursor compounds. Furthermore, sample LU is characterised by a relatively small contribution of MTTCs. Also, sample LU stands out by its different distribution of S-bound isorenieratane skeletons in the A4 fraction, the reason for this being not clear.

Most of the differences between LU and the other samples, could be related to the presence of a microbial mat. However, the presence of isorenieratene derivatives seems at odds with a benthic microbial mat system. Isorenieratene is exclusively biosynthesised by

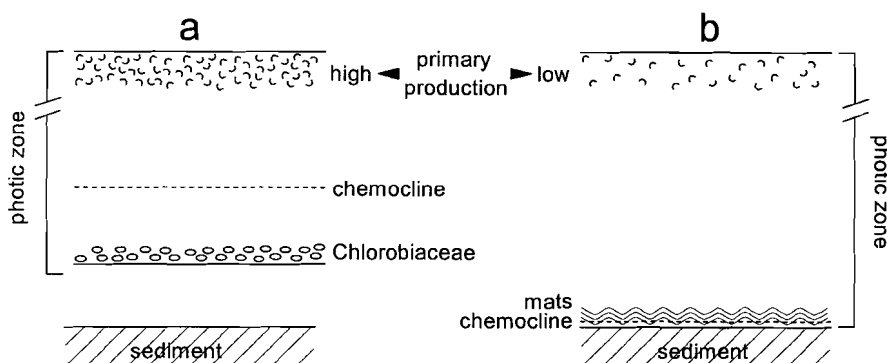


Fig. 3.11. Depositional conditions of (a) samples LP, DP, M and DU (b) sample LU.

the brown strain of Chlorobiaceae (Schmidt, 1978), bacteria which, in contrast to the green Chlorobiaceae, do not tolerate the diurnal variations in the oxygen regime of a microbial mat (van Gernerden, pers. comm. 1997). Therefore, it is thought that OM in sample LU is "contaminated" with isorenieratene derivatives from the adjoining TOC-rich laminae. These laminae are intimately associated with the precipitated carbonate. "Contamination" of sample LU may have taken place already in the depositional environment or during isolation of the lamina. Since the overall composition of OM in sample LU is similar to that in the other samples, it seems indeed that the mat-derived OM is overprinted by the planktonic-derived OM deposited (and sulfurised) under euxinic conditions. In addition, the stable carbon isotopic composition of S-bound isorenieratane is similar in all samples (Table 3.4). If the isorenieratene derivatives in sample LU were derived from Chlorobiaceae living in a microbial mat, their  $^{13}\text{C}$  contents would probably be higher than those of isorenieratene derivatives in the other samples, since  $\delta^{13}\text{C}_{\text{TOC}}$  values of microbial mats in Solar Lake and Gavish Sabkha are as high as -5.7 and -10.0‰, respectively (Schidlowski et al., 1984).

Although the exact sediment accumulation rates are unknown, the light- and dark-coloured undulated layers seem to alternate on a timescale of years to decades. Thus, the transition from microbially-induced carbonate precipitation (light-coloured undulated layers) to preservation of OM under euxinic conditions (dark-coloured undulated layers), and *vice versa*, took place within relatively short periods of time. It is noted that a layer of precipitated carbonate is likely to represent a shorter time interval than an equally thick, organic-rich layer. Considering the sulfur-richness of the OM in all samples, the following depositional conditions are proposed: Most of the time, the chemocline was situated in the photic zone at small distance above the sediment surface, and microbial mats were absent (Fig. 3.11a). These euxinic conditions prevailed during deposition of samples LP, DP, M and DU. Periodically, the chemocline may have been situated in the sediment, but not long enough to allow microbial mats to develop. At times that bottom waters were oxygenated for somewhat longer periods of time, microbial mats developed (Fig. 3.11b) and caused the precipitation of carbonate. Since the mat-building organisms require light intensities much higher than those demanded by the brown Chlorobiaceae, oxygenation of the bottom waters

must have been accompanied by a deepening of the light penetration depth. This may have been realised by a diminished primary production in the upper part of the photic zone (Fig. 3.11b). Given the extremely low light intensities required by the Chlorobiaceae on the one hand, and the shallow water setting as deduced from the presence of microbial carbonates on the other hand, the turbidity of the photic zone must have been rather high during deposition of samples LP, DP, M and DU.

## Conclusions

The limestones of the Upper Jurassic Calcaires en plaquettes Formation were deposited in a lagoonal environment under frequently euxinic conditions. The presence of hydrogen sulfide and polysulfides led to the incorporation of high amounts of sulfur into OM. The bitumen in all samples is predominantly composed of S-bound *n*-alkane and hopanoid carbon skeletons, whereas steroids are relatively minor. This suggests that cyanobacteria were more important primary producers than algae, which is in agreement with the relatively small contribution of *n*-alkene/*n*-alkane doublets, derived from algal biopolymers, to the kerogen pyrolysates. The abundant OSC in the kerogen pyrolysates may derive from both algal and cyanobacterial sources.

Changing fluxes of biogenic carbonate and OM, probably controlled by seasonal and climatical variations, resulted in alternating light-coloured and dark-coloured layers on a submillimetre to centimetre scale. The prolonged occurrence of abundant calcifying algae led to the formation of massive limestones. Occasionally, bottom waters were oxygenated for sufficiently long periods of time to allow for the development of microbial mats. The mat-building organisms induced the precipitation of carbonate (light-coloured undulated laminae). Nevertheless, although microbial mats left their morphological imprint, the OM preserved is predominantly derived from planktonic organisms thriving at times the water column was euxinic.

The  $\delta^{13}\text{C}_{\text{TOC}}$  values of the undulated type laminae are 3 to 5‰ higher than those of the other samples. These differences cannot be explained by mixing of marine and terrestrial OM, neither by differences in the concentration or  $^{13}\text{C}$  content of DIC in the photic zone. Although the composition of the bitumen in the undulated type laminae differs from that in the other samples, it is not clear how this could account for the differences in  $\delta^{13}\text{C}_{\text{TOC}}$ .

LMW OSC are relatively more abundant in TOC-lean, light-coloured samples than in TOC-rich, dark-coloured samples. This is probably related to differences in the degree of intermolecular sulfur cross-linking of the OM. The bitumen in the undulated type laminae differs from that in the other samples by a relatively small proportion of free and S-bound *n*-alkanes. This is attributed to differences in the composition of the biota. Differences in the sources of OM are not evident from the kerogen pyrolysates.

**Acknowledgements.** We thank the Netherlands Organization for Scientific Research (NWO) for the PIONIER grant to JSSD and the studentship of HMEvKP. We thank Shell International Petroleum Maatschappij BV for financial support for the GC-IRMS facility. We thank Th. Mongenot and Dr. N.-P. Tribouvillard (Université Paris Sud) for sample preparation and providing the photographs. We are grateful to Dr. P. de Boer (University of

Utrecht) for fruitful discussions. We thank Dr. S. Schouten (NIOZ) for measuring the molecular carbon isotope ratios. We thank M. Baas, M. Dekker and W. Pool (NIOZ) for analytical assistance.

## References

- Allard B., Templier J. and Largeau C. (1997) Artfactual origin of mycobacterial bacteran. Formation of melanoidin-like artfactual macromolecular material during the usual isolation process. *Org. Geochem.* Submitted.
- Behrens A., Schaeffer P. and Albrecht P. (1997) 14 $\beta$ ,22R-Epithiosteranes, a novel series of fossil steroids widespread in sediments. *Tetrahedron Lett.* In press.
- van Bergen P.F., Collinson M.E., Sinninghe Damsté J.S. and de Leeuw J.W. (1994) Chemical and microscopical characterization of inner seed coats of fossil water plants. *Geochim. Cosmochim. Acta* **58**, 231-239.
- Bernier P. (1984) Les formations carbonatées du Kimméridgien et du Portlandien dans le Jura méridional. Stratigraphie, micropaléontologie, sédimentologie. *Docum. Lab. Géol. Lyon* **92**, 803 pp.
- Brassell S.C. (1993) Applications of biomarkers for delineating marine paleoclimatic fluctuations during the Pleistocene. In *Organic Geochemistry: Principles and Applications* (ed. M.H. Engel and S.A. Macko), pp. 699-738. Plenum Press, New York.
- Brassell S.C., Lewis C.A., de Leeuw J.W., de Lange F. and Sinninghe Damsté J.S. (1986) Isoprenoid thiophenes: Novel products of sediment diagenesis? *Nature* **320**, 160-162.
- Boon J.J. and de Leeuw J.W. (1987) Organic geochemical aspects of cyanobacterial mats. In *The Cyanobacteria* (ed. P. Fay and C. van Baalen), pp. 471-492. Elsevier Science.
- Canfield D.E. and Des Marais D.J. (1993) Biogeochemical cycles of carbon, sulfur, and free oxygen in a microbial mat. *Geochim. Cosmochim. Acta* **57**, 3971-3984.
- Chalansonnet S., Largeau C., Casadevall E., Berkaloff C., Peniguel G. and Couderc R. (1988) Cyanobacterial resistant biopolymers. Geochemical implications of the properties of *Schizothrix* sp. resistant material. In *Advances in Organic Geochemistry 1987* (ed. L. Mattavelli and L. Novelli). *Org. Geochem.* **13**, 1003-1010.
- Derenne S., Largeau C., Berkaloff C., Rousseau B., Wilhelm C. and Hatcher P.G. (1992) Non-hydrolysable macromolecular constituents from outer walls of *Chlorella fusca* and *Nanochlorum eucaryotum*. *Phytochemistry* **31**, 1923-1929.
- van Duin A.C.T., Sinninghe Damsté J.S., Koopmans M.P., van de Graaf B. and de Leeuw J.W. (1997) A kinetic calculation method of homohopanoïd maturation: Applications in the reconstruction of burial histories of sedimentary basins. *Geochim. Cosmochim. Acta* **61**, 2409-2429.
- Eglinton T.I., Irvine J.E., Vairavamurthy A.V., Zhou W. and Manowitz B. (1994) Formation and diagenesis of macromolecular organic sulfur in Peru margin sediments. In *Advances in Organic Geochemistry 1993* (ed. N. Telnæs, G. van Graas and K. Øygaard). *Org. Geochem.* **22**, 781-799.
- Erba E. (1991) Deep mid-water bacterial mats from anoxic basins of the Eastern Mediterranean. *Mar. Geol.* **100**, 83-101.
- Gelin F., Boogers I., Noordeloos A.A.M., Sinninghe Damsté J.S., Hatcher P.G. and de Leeuw J.W. (1996) Novel, resistant microalgal polyethers: An important sink of organic carbon in the marine environment? *Geochim. Cosmochim. Acta* **60**, 1275-1280.
- Gelin F., Volkman J.K., Largeau C., Derenne S., Sinninghe Damsté J.S. and de Leeuw J.W. (1997) Distribution of aliphatic, non-hydrolysable biopolymers in marine microalgae. *Org. Geochem.* Submitted.
- van Gemerden H. (1993) Microbial mats: A joint venture. *Mar. Geol.* **113**, 3-25.
- Goossens H., de Leeuw J.W., Schenck P.A. and Brassell S.C. (1984) Tocopherols as likely precursors of pristane in ancient sediments and crude oils. *Nature* **312**, 440-442.

- Goth K., de Leeuw J.W., Püttmann W. and Tegelaar E.W. (1988) Origin of Messel Oil Shale kerogen. *Nature* **336**, 759-761.
- Hartgers W.A., Sinninghe Damsté J.S., Requejo A.G., Allan J., Hayes J.M., Ling Y., Xie T., Primack J. and de Leeuw J.W. (1994) A molecular and carbon isotopic study towards the origin and diagenetic fate of diaromatic carotenoids. In *Advances in Organic Geochemistry 1993* (ed. N. Telnæs, G. van Graas and K. Øygard). *Org. Geochem.* **22**, 703-725.
- Hauke V., Graff R., Wehrung P., Trendel J.M. and Albrecht P. (1992a) Novel triterpene-derived hydrocarbons of arborane/fernane series in sediments. Part I. *Tetrahedron* **48**, 3915-3924.
- Hauke V., Graff R., Wehrung P., Trendel J.M., Albrecht P., Riva A., Hopfgartner G., Gülaçar F.O., Buchs A. and Eakin P.A. (1992b) Novel triterpene-derived hydrocarbons of arborane/fernane series in sediments: Part II. *Geochim. Cosmochim. Acta* **56**, 3595-3602.
- Hay B.J. (1988) Sediment accumulation in the central western Black Sea over the past 5100 years. *Paleoceanography* **3**, 491-508.
- Hayes J.M., Freeman K.H., Popp B.N. and Hoham C.H. (1990) Compound-specific isotopic analyses: A novel tool for reconstruction of ancient biogeochemical processes. In *Advances in Organic Geochemistry 1989* (ed. B. Durand and F. Behar). *Org. Geochem.* **16**, 1115-1128.
- Holzer G., Oro J. and Tornabene T.G. (1979) Gas chromatographic-mass spectrometric analysis of neutral lipids from methanogenic and thermoacidophilic bacteria. *J. Chromatogr.* **186**, 795-809.
- Hussler G., Connan J. and Albrecht P. (1984) Novel families of tetra- and hexacyclic aromatic hopanoids predominant in carbonate rocks and crude oils. *Org. Geochem.* **6**, 39-49.
- van Kaam-Peters H.M.E. and Sinninghe Damsté J.S. (1997) Characterisation of an extremely organic sulfur-rich, 150 Ma old carbonaceous rock: Palaeoenvironmental implications. *Org. Geochem.* Accepted.
- van Kaam-Peters H.M.E., Köster J., de Leeuw J.W. and Sinninghe Damsté J.S. (1995) Occurrence of two novel benzothiophene hopanoid families in sediments. *Org. Geochem.* **23**, 607-616.
- van Kaam-Peters H.M.E., Köster J., van der Gaast S.J., Sinninghe Damsté J.S. and de Leeuw J.W. (1997a) The effect of clay minerals on diasterane/sterane ratios. In prep.
- van Kaam-Peters H.M.E., Schouten S., Köster J. and Sinninghe Damsté J.S. (1997b) Palaeoclimatic control on the molecular and carbon isotopic composition of organic matter deposited in a Kimmeridgian euxinic shelf sea. *Geochim. Cosmochim. Acta*. Submitted.
- van Kaam-Peters H.M.E., Schouten S., de Leeuw J.W. and Sinninghe Damsté J.S. (1997c) A molecular and carbon isotope biogeochemical study of biomarkers and kerogen pyrolysates of the Kimmeridge Clay Formation: Palaeoenvironmental implications. *Org. Geochem.* Accepted.
- Kohnen M.E.L., Sinninghe Damsté J.S., Rijpstra W.I.C. and de Leeuw J.W. (1990) Alkylthiophenes as sensitive indicators of palaeoenvironmental changes: A study of a Cretaceous oil shale from Jordan. In *Geochemistry of Sulfur in Fossil Fuels* (ed. W.L. Orr and C.M. White), *ACS Symposium Series 429*, pp. 444-485. Amer. Chem. Soc., Washington DC.
- Kohnen M.E.L., Sinninghe Damsté J.S., ten Haven H.L., Kock-van Dalen A.C., Schouten S. and de Leeuw J.W. (1991) Identification and geochemical significance of cyclic di- and trisulphides with linear and acyclic isoprenoid carbon skeletons in immature sediments. *Geochim. Cosmochim. Acta* **55**, 3685-3695.
- Koopmans M.P., Sinninghe Damsté J.S., Lewan M.D. and de Leeuw J.W. (1995) Thermal stability of thiophene biomarkers as studied by hydrous pyrolysis. *Org. Geochem.* **23**, 583-596.
- Koopmans M.P., Köster J., van Kaam-Peters H.M.E., Kenig F., Schouten S., Hartgers W.A., de Leeuw J.W. and Sinninghe Damsté J.S. (1996a) Dia- and catagenetic products of isorenieratene: Molecular indicators for photic zone anoxia. *Geochim. Cosmochim. Acta* **60**, 4467-4496.
- Koopmans M.P., de Leeuw J.W., Lewan M.D. and Sinninghe Damsté J.S. (1996b) Impact of dia- and catagenesis on sulphur and oxygen sequestration of biomarkers as revealed by artificial maturation of an immature sedimentary rock. *Org. Geochem.* **25**, 391-426.
- Koopmans M.P., Rijpstra W.I.C., Klapwijk M.M., de Leeuw J.W., Lewan M.D. and Sinninghe Damsté J.S. (1997a) A thermal and chemical degradation approach to decipher pristane and phytane precursors in sedimentary organic matter. *Org. Geochem.* Submitted.

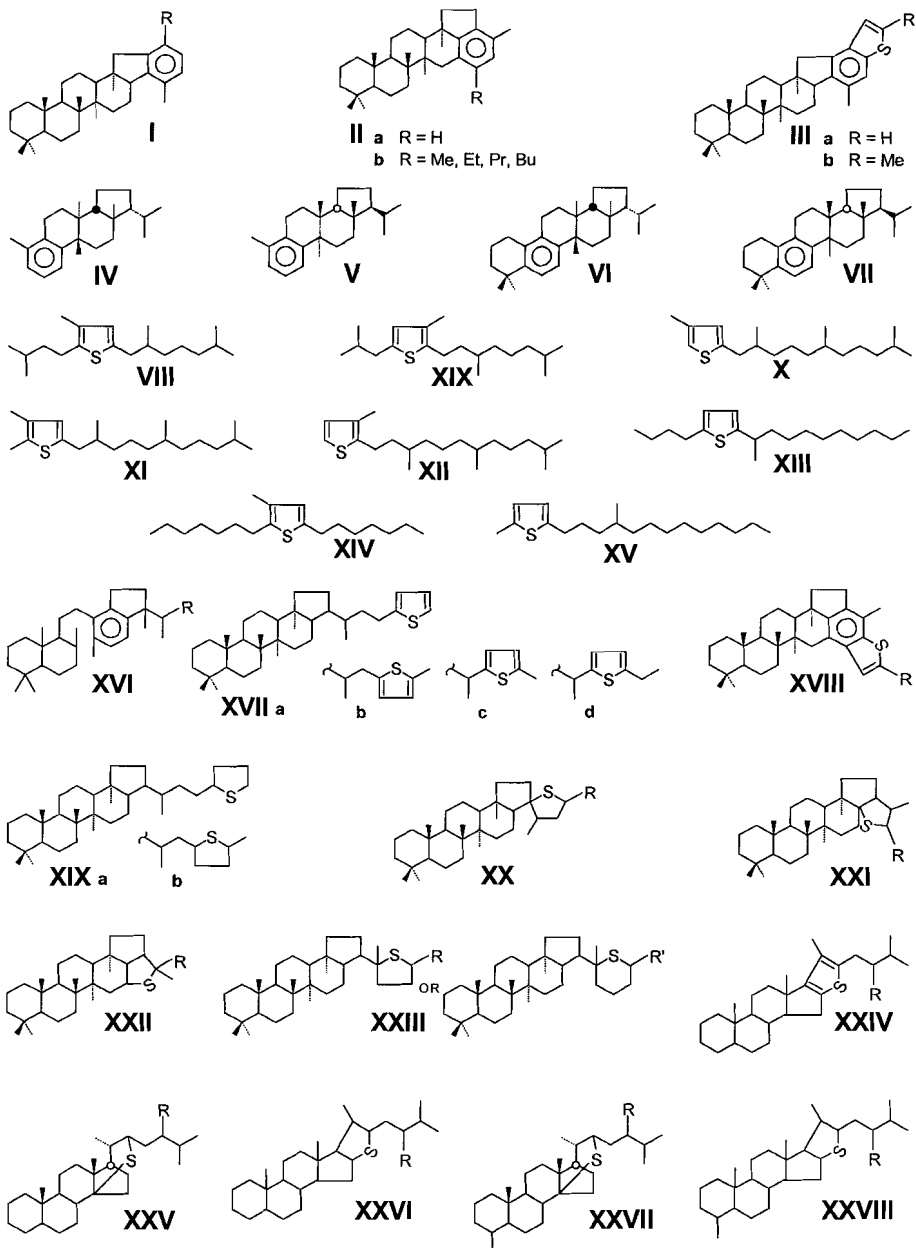
- Koopmans M.P., Rijpstra W.I.C., de Leeuw J.W., Lewan M.D. and Sinninghe Damsté J.S. (1997b) Artificial maturation of an immature sulphur- and oxygen-rich limestone from the Ghareb Formation, Jordan. *Org. Geochem.* Submitted.
- Koopmans M.P., Schaeffer-Reiss C., de Leeuw J.W., Lewan M.D., Maxwell J.R., Schaeffer P. and Sinninghe Damsté J.S. (1997c) Sulphur and oxygen sequestration of *n*-C<sub>37</sub> and *n*-C<sub>38</sub> unsaturated ketones in an immature kerogen and the release of their carbon skeletons during early stages of thermal maturation. *Geochim. Cosmochim. Acta* **61**, 2397-2408.
- Köster J., van Kaam-Peters H.M.E., Koopmans M.P., de Leeuw J.W. and Sinninghe Damsté J.S. (1997) Sulphurisation of homohopanooids: Effects on carbon number distribution, speciation and 22S/22R epimer ratios. *Geochim. Cosmochim. Acta* **61**, 2431-2452.
- Largeau C., Casadevall E., Kadouri A. and Metzger P. (1984) Comparative study of immature torbanite and of the extant alga *Botryococcus braunii*. In *Advances in Organic Geochemistry 1983* (ed. P.A. Schenck, J.W. de Leeuw and G.W.M. Lijmbach). *Org. Geochem.* **6**, 327-332.
- Largeau C., Derenne S., Casadevall E., Kadouri A. and Sellier N. (1986) Pyrolysis of immature torbanite and of the resistant biopolymer (PRB A) isolated from the extant alga *Botryococcus braunii*. Mechanism for the formation and structure of torbanite. In *Advances in Organic Geochemistry 1985* (ed. D. Leythaeuser and J. Rullkötter). *Org. Geochem.* **10**, 1023-1032.
- de Leeuw J.W. and Sinninghe Damsté J.S. (1990) Organic sulfur compounds and other biomarkers as indicators of palaeosalinity. In *Geochemistry of Sulfur in Fossil Fuels* (ed. W.L. Orr and C.M. White), *ACS Symposium Series* **429**, pp. 417-443. Amer. Chem. Soc., Washington DC.
- McCarthy E.D., Han J. and Calvin M. (1968) Hydrogen atom transfer in mass spectrometric fragmentation patterns of saturated aliphatic hydrocarbons. *Anal. Chem.* **40**, 1475-1480.
- Mongenot Th., Tribouvillard N.-P., Arbey F., Lallier-Vergès E., Derenne S., Largeau C. and Connan J. (1997) Microbial mat development and iron deficiency: Intertwined key factors in the formation of organic sulphur-rich deposits. *Sed. Geol.* Submitted.
- Nicholson J.M., Stolz J.F. and Pierson B.K. (1987) Structure of a microbial mat at Great Sippewissett Marsh, Cape Cod, Massachusetts. *FEMS Microbiol. Ecol.* **45**, 343-364.
- Nip M., Tegelaar E.W., de Leeuw J.W., Schenck P.A. and Holloway P.J. (1986) A new non-saponifiable highly aliphatic and resistant biopolymer in plant cuticles: Evidence from pyrolysis and <sup>13</sup>C-NMR analysis of present day and fossil plants. *Naturwissenschaften* **73**, 579-585.
- Ouirsson G. and Albrecht P. (1992) Hopanooids. 1. Geohopanooids: The most abundant natural products on earth? *Acc. Chem. Res.* **25**, 398-402.
- Payzant J.D., Montgomery D.S. and Strausz O.P. (1986) Sulfides in petroleum. *Org. Geochem.* **9**, 357-369.
- Peakman T.M., ten Haven H.L., Rechka J.R., de Leeuw J.W. and Maxwell J.R. (1989) Occurrence of (20R)- and (20S)- $\Delta^{8(14)}$  and  $\Delta^{14}$  5 $\alpha$ (H)-sterenes and the origin of 5 $\alpha$ (H),14 $\beta$ (H),17 $\beta$ (H)-steranes in an immature sediment. *Geochim. Cosmochim. Acta* **53**, 2001-2009.
- Peters K.E. and Moldowan J.M. (1993) The biomarker guide. Interpreting molecular fossils in petroleum and ancient sediments. Prentice Hall, New Jersey. pp. 363.
- Poinsot J., Schneckenburger P., Adam P., Schaeffer P., Trendel J.M. and Albrecht P. (1997) Novel polycyclic polyprenic sulfides in sediments. *Tetrahedron Lett.* Submitted.
- Pomonis J.G., Hakk H. and Fatland C.L. (1989) Synthetic methyl- and dimethylalkanes. Kováts Indices, [<sup>13</sup>C]NMR and mass spectra of some methylpentacosanes and 2,X-dimethylheptacosanes. *J. Chem. Ecol.* **15**, 2319-2333.
- Repeta D.J. (1993) A high resolution historical record of Holocene anoxygenic primary production in the Black Sea. *Geochim. Cosmochim. Acta* **57**, 4337-4342.
- Riding R. (1991) Calcified cyanobacteria. In *Calcareous Algae and Stromatolites* (ed. R. Riding), pp. 55-87. Springer-Verlag, Berlin.
- Saiz-Jimenez C. and de Leeuw J.W. (1984) Pyrolysis-gas chromatography-mass spectrometry of isolated, synthetic and degraded lignins. In *Advances in Organic Geochemistry 1983* (ed. P.A. Schenck, J.W. de Leeuw and G.W.M. Lijmbach). *Org. Geochem.* **6**, 417-422.
- Saiz-Jimenez C. and de Leeuw J.W. (1986) Lignin pyrolysis products: Their structures and their significance as biomarkers. In *Advances in Organic Geochemistry 1985* (ed. D. Leythaeuser and J. Rullkötter). *Org. Geochem.* **10**, 869-876.

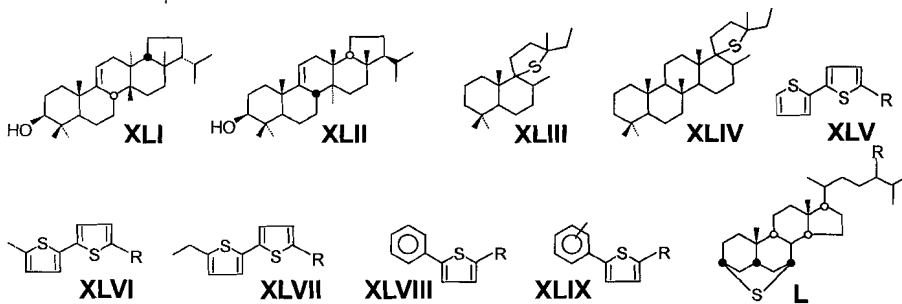
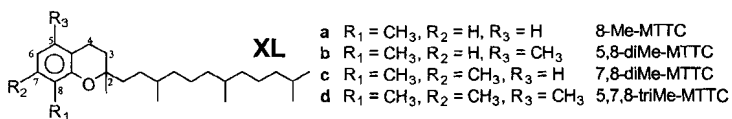
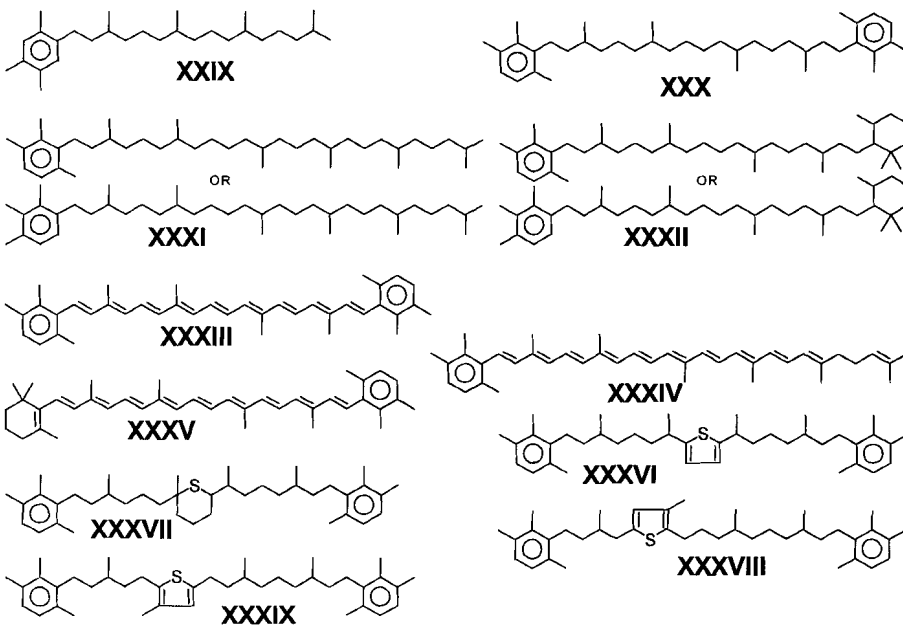
- Schaeffer P. (1993) Marqueurs biologique de milieux évaporitiques. PhD thesis, Université Louis Pasteur, 339 pp.
- Schaeffer P., Adam P., Trendel J.-M., Albrecht P. and Connan J. (1995) A novel series of benzohopanes widespread in sediments. *Org. Geochem.* **23**, 87-89.
- Schaeffer P., Adam P., Wehrung P., Bernasconi S. and Albrecht P. (1997) Molecular and isotopic investigation of free and S-bound lipids from an actual meromictic lake (lake Cadagno, Switzerland). *Org. Geochem.* Submitted.
- Schidlowski M., Matzigkeit U. and Krumbein W.E. (1984) Superheavy organic carbon from hypersaline microbial mats. *Naturwissenschaften* **71**, 303-308.
- Schmid J.-C. (1986) Marqueurs biologique soufrés dans les pétroles. PhD thesis, Université Louis Pasteur, 263 pp.
- Schmidt K. (1978) Biosynthesis of carotenoids. In *The Photosynthetic Bacteria* (ed. R.K. Clayton and W.R. Sistrom), pp. 729-750. Plenum Press, New York.
- Schouten (1995) Structural and stable carbon isotope studies of lipids in immature sulphur-rich sediments. PhD thesis, University of Groningen, 305 pp.
- Schouten S., Sinninghe Damsté J.S. and de Leeuw J.W. (1995) The occurrence and distribution of low-molecular-weight sulphoxides in polar fractions of sediment extracts and petroleum. *Org. Geochem.* **23**, 129-138.
- Seifert W.K. and Moldowan J.M. (1980) The effect of thermal stress on source-rock quality as measured by hopane stereochemistry. In *Advances in Organic Geochemistry 1979* (ed. A.G. Douglas and J.R. Maxwell), pp. 229-237. Pergamon, Oxford.
- Sinninghe Damsté J.S. and de Leeuw J.W. (1987) The origin and fate of C-20 and C-15 isoprenoid sulphur compounds in sediments and oils. *Int. J. Environ. Anal. Chem.* **28**, 1-19.
- Sinninghe Damsté J.S. and de Leeuw J.W. (1990) Organically-bound sulphur in the geosphere: State of the art and future research. In *Advances in Organic Geochemistry 1989* (ed. B. Durand and F. Behar). *Org. Geochem.* **16**, 1077-1101.
- Sinninghe Damsté J.S., ten Haven H.L., de Leeuw J.W. and Schenck P.A. (1986) Organic geochemical studies of a Messinian evaporitic basin, northern Apennines (Italy)-II. Isoprenoid and *n*-alkyl thiophenes and thiolanes. In *Advances in Organic Geochemistry 1985* (ed. D. Leythaeuser and J. Rullkötter). *Org. Geochem.* **10**, 791-805.
- Sinninghe Damsté J.S., Kock-van Dalen A.C., de Leeuw J.W. and Schenck P.A. (1987a) The identification of 2,3-dimethyl-5-(2,6,10-trimethylundecyl)-thiophene, a novel sulphur containing biological marker. *Tetrahedron Lett.* **28**, 957-960.
- Sinninghe Damsté J.S., Kock-van Dalen A.C., de Leeuw J.W., Schenck P.A., Guoying S. and Brassell S.C. (1987b) The identification of mono-, di- and trimethyl 2-methyl-2-(4,8,12-trimethyltridecyl)chromans and their occurrence in the geosphere. *Geochim. Cosmochim. Acta* **51**, 2393-2400.
- Sinninghe Damsté J.S., Kock-van Dalen A.C. and de Leeuw J.W. (1988a) Identification of long-chain isoprenoid alkylbenzenes in sediments and crude oils. *Geochim. Cosmochim. Acta* **52**, 2671-2677.
- Sinninghe Damsté J.S., Rijpstra W.I.C., de Leeuw J.W. and Schenck P.A. (1988b) Origin of organic sulphur compounds and sulphur-containing high molecular weight substances in sediments and immature crude oils. In *Advances in Organic Geochemistry 1987* (ed. L. Mattavelli and L. Novelli). *Org. Geochem.* **13**, 593-606.
- Sinninghe Damsté J.S., Rijpstra W.I.C., de Leeuw J.W. and Schenck P.A. (1989) The occurrence and identification of series of organic sulphur compounds in oils and sediment extracts: II. Their presence in samples from hypersaline and non-hypersaline palaeoenvironments and possible application as source, palaeoenvironmental and maturity indicators. *Geochim. Cosmochim. Acta* **53**, 1323-1341.
- Sinninghe Damsté J.S., de las Heras F.X.C., van Bergen P.F. and de Leeuw J.W. (1993a) Characterization of Tertiary Catalan lacustrine oil shales: Discovery of extremely organic sulfur-rich Type I kerogens. *Geochim. Cosmochim. Acta* **57**, 389-415.
- Sinninghe Damsté J.S., Keely B.J., Betts S.E., Baas M., Maxwell J.R. and de Leeuw J.W. (1993b) Variations in abundances and distributions of isoprenoid chromans and long-chain alkylbenzenes



- in sediments of the Mulhouse Basin: A molecular sedimentary record of palaeosalinity. *Org. Geochem.* **20**, 1201-1215.
- Sinninghe Damsté J.S., Wakeham S.G., Kohnen M.E.L., Hayes J.M. and de Leeuw J.W. (1993c) A 6,000-year sedimentary molecular record of chemocline excursions in the Black Sea. *Nature* **362**, 827-829.
- Sinninghe Damsté J.S., van Duin A.C.T., Hollander D., Kohnen M.E.L. and de Leeuw J.W. (1995) Early diagenesis of bacteriohopanepolyol derivatives: Formation of fossil homohopanoids. *Geochim. Cosmochim. Acta* **59**, 5141-5147.
- Sirevåg R. and Ormerod J.G. (1970) Carbon dioxide fixation in green sulphur bacteria. *Biochem. J.* **120**, 399-408.
- Summons R.E. and Powell T.G. (1987) Identification of aryl isoprenoids in source rocks and crude oils: Biological markers for the green sulphur bacteria. *Geochim. Cosmochim. Acta* **51**, 557-566.
- Tegelaar E.W., Hollman G., van der Vegt P., de Leeuw J.W. and Holloway P.J. (1995) Chemical characterization of the periderm tissue of some angiosperm species: recognition of an insoluble, non-hydrolyzable, aliphatic biomacromolecule (Suberan). *Org. Geochem.* **23**, 239-250.
- Tissot and Welte (1984) *Petroleum Formation and Occurrence*, 2nd edition. Springer, Heidelberg.
- Tribouvillard N., Gorin G. E., Belin S., Hopfgartner G. and Pichon R. (1992) Organic-rich biolaminated facies from a Kimmeridgian lagoonal environment in the French Southern Jura mountains - A way of estimating accumulation rate variations. *Palaeogeogr. Palaeoclimatol. Palaeoecol.* **99**, 163-177.
- Volkman J.K. and Maxwell J.R. (1986) Acyclic isoprenoids as biological markers. In *Biological Markers in the Sedimentary Record* (ed. R.B. Johns), pp. 1-42. Elsevier, New York.
- Volkman J.K., Barrett S.M., Blackburn S.I. and Sikes E.L. (1995) Alkenones in *Gephyrocapsa oceanica*: Implications for studies of paleoclimate. *Geochim. Cosmochim. Acta* **59**, 513-520.

# Appendix





## Chapter 4

### **A molecular and carbon isotope biogeochemical study of biomarkers and kerogen pyrolysates of the Kimmeridge Clay Formation: Palaeoenvironmental implications.**

#### **Abstract**

Structures and carbon isotopic compositions of biomarkers and kerogen pyrolysis products of a dolomite, a bituminous shale and an oil shale of the Kimmeridge Clay Formation (KCF) in Dorset were studied in order to gain insight into (i) the type and extent of water column anoxia and (ii) changes in the concentration and isotopic composition of dissolved inorganic carbon (DIC) in the palaeowater column. The samples studied fit into the curve of increasing  $\delta^{13}\text{C}$  of the kerogen ( $\delta^{13}\text{C}_{\text{TOC}}$ ) with increasing TOC, reported by Huc et al. (1992). Their hypothesis, that the positive correlation between TOC and  $\delta^{13}\text{C}_{\text{TOC}}$  is the result of differing degrees of organic matter (OM) mineralisation in the water column, was tested by measuring the  $\delta^{13}\text{C}$  values of primary production markers. These  $\delta^{13}\text{C}$  values were found to differ on average by only 1‰ among the samples, implying that differences in the extent of OM mineralisation cannot fully account for the 3‰ difference in  $\delta^{13}\text{C}_{\text{TOC}}$ . The extractable OM in the oil shale differs from that in the other sediments due to both differences in maturity, and differences in the planktonic community. These differences, however, are not likely to have significantly influenced  $\delta^{13}\text{C}_{\text{TOC}}$  either. All three sediments contain abundant derivatives of isorenieratene, indicating that periodically euxinia was extending into the photic zone. The sediments are rich in organic sulfur, as revealed by the abundant sulfur compounds in the pyrolysates. The prominence of  $\text{C}_1$ - $\text{C}_3$  alkylated thiophenes over *n*-alkanes and *n*-alkenes is most pronounced in the pyrolysate of the sediment richest in TOC. This suggests that sulfurisation of OM may have played an important role in determining the TOC- $\delta^{13}\text{C}_{\text{TOC}}$  relationship reported by Huc et al. (1992).

#### **Introduction**

The OM-rich Kimmeridge Clay facies (KCF) was deposited in a series of basins that extended from eastern Greenland and Canada to offshore Norway, and south to the English Channel (Doré et al., 1985). On shore the sediments display a cyclic sedimentation of shales, bituminous shales, oil shales and carbonates (TOC 0-60%), but individual cycles vary in thickness and are not always complete (Tyson, 1989). The KCF is the presumed source rock of most North Sea oils, which explains the large interest in these sediments. Indeed, the KCF has been the subject of numerous investigations (e.g. Irwin et al., 1977; Tyson et al., 1979; Williams and Douglas, 1980, 1983; Cox and Gallois, 1981; Farrimond et al., 1984; Oschmann, 1988, 1991; Eglinton et al., 1988; Tyson, 1989, 1996; Wignall, 1989; Miller, 1990; Bertrand et al., 1990; Boucher et al., 1990; Huc et al., 1992; Bertrand and Lallier-

Vergès, 1993; Herbin et al., 1993; Hollander et al., 1993a; Ramanampisoa and Disnar, 1994; Tribouvillard et al., 1994; Boussafir et al., 1995; Cooper et al., 1995).

Our interest in studying the KCF was twofold. Firstly, in most depositional models for the KCF (e.g. Tyson et al., 1979; Tyson, 1985; Oschmann, 1988, 1991) anoxia of the palaeowater column plays an important role. In the KCF anoxia has mainly been established by palaeoecological methods (i.e. study of palaeo macro- and microbenthos) or has been assumed from geochemical bulk parameters such as elevated Rock Eval hydrogen indices. Recently, a wide variety of diagenetic products of isorenieratene derived from green sulfur bacteria has been identified (Koopmans et al., 1996). Since green sulfur bacteria require both light and hydrogen sulfide for photosynthesis, the presence of isorenieratene derivatives indicates photic zone euxinia (i.e. the presence of hydrogen sulfide in the photic zone). It was thought that a search for these components in the KCF could shed further light on the type and extent of anoxia in the KCF palaeoenvironment. Secondly, Huc et al. (1992) in their study of the KCF in Dorset (UK) found a positive correlation between the total organic carbon (TOC) content and the stable carbon isotopic composition of TOC ( $\delta^{13}\text{C}_{\text{TOC}}$ ). They proposed that the low  $^{13}\text{C}$  contents of OM-lean samples were due to a relatively abundant reworking of biomass in the water column. Hollander et al. (1993a) hypothesised that accumulation of TOC-rich sediments occurred at times when dissolved  $\text{CO}_2$  concentrations in surface waters were lowest, most likely due to increased primary productivity. These hypotheses can easily be tested by documenting changes in the  $^{13}\text{C}$  content of molecular fossils derived from organisms living at specific depths in the water column (cf. Collister et al., 1992; Freeman et al., 1994b; Kenig et al., 1995; Schouten et al., 1997). Such data much more accurately reflect the changes in DIC in the water column than  $\delta^{13}\text{C}_{\text{TOC}}$ , since TOC is a complex mixture of potentially carbon isotopically distinct sources (e.g. terrestrial vs. aquatic) influenced by a wide variety of diagenetic reactions.

To this end we examined on a molecular level the OM in three lithologically different rocks of the Lower Kimmeridge Clay at its type locality in Dorset (Table 4.1). The identification of a suite of isorenieratene derivatives, which dominate the aromatic hydrocarbon fractions, provides the first evidence for photic zone euxinia in the Kimmeridge Clay palaeoenvironment. We also tested the hypotheses of Huc et al. (1992) and Hollander et al. (1993a) by measuring the stable carbon isotopic composition of individual biomarkers and kerogen pyrolysis products. Our data indicate, in disagreement with the Huc and Hollander hypotheses, that the concentration and isotopic composition of DIC both in the upper water column and at the chemocline were probably rather constant. It seems more likely that  $\delta^{13}\text{C}_{\text{TOC}}$  was controlled by the degree of sulfurisation. A preliminary account of this work has been published previously (van Kaam-Peters et al., 1995).

## Experimental

*Sample descriptions.* Rocks were sampled from the exposed upper part of the Lower Kimmeridge Clay in Kimmeridge Bay, Dorset. Three lithologically different samples were taken within a 10 m interval: a ferroan dolomite (2.4% TOC), a bituminous shale (7.9% TOC) and an oil shale (28.9% TOC).

*Mineralogical content.* X-ray powder diffraction (XRD) was carried out with a Philips PW1050/25 goniometer, using  $\text{CoK}\alpha$  radiation (40kV, 40mA) from a long fine focus tube, a graphite monochromator in the diffracted beam, and a vacuum/helium device to minimise the absorption of the X-rays by air (Van der Gaast and Vaars, 1981). The instrument was equipped with a variable divergence slit. The slit settings were: 12 mm irradiated specimen length; receiving slit, 0.1 mm; antiscatter slit, 0.5°; counting time, 2 s/ 0.02° 2 $\theta$ . Approximately 10 mg sample material was pressed into a 0.5 mm deep depression in a low-background sample holder (Si-wafer). The specimens were measured at 50% relative humidity. Patterns were corrected for the Lorentz and polarisation factor and for the irradiated specimen volume.

Carbonate contents were determined by weighing the dry sediments before and after decalcification (6N HCl). Complete carbonate dissolution was checked by analysing the residues by XRD. Quartz was quantified using XRD with  $\text{CaF}_2$  as an external standard. Samples were mixed with 20%  $\text{CaF}_2$  and the standard and the peak area of the quartz base peak were compared to a calibration curve. The contribution of clay minerals to the sediment was determined by difference after determination of the total carbonate, quartz and OM contents. Given the relatively low pyrite concentrations (<2 wt.%), this is a reasonable assumption.

*Extraction and fractionation.* The powdered samples (ca. 70 g) were Soxhlet extracted with methanol (MeOH)/dichloromethane (DCM) (1:7.5, v/v) for 24 h. Asphaltenes were removed from the extracts by precipitation in *n*-heptane. Aliquots of the maltene fractions (ca. 250 mg), to which a mixture of four standards (3-methyl-6-dideutero-henicosane, 2,3-dimethyl-5-(1',1'-dideutero-hexadecyl)thiophene, 2-methyl-2-(4,8,12-trimethyldecyl)chroman and 2,3-dimethyl-5-(1',1'-dideutero-hexadecyl)thiolane) was added for quantitative analysis (Kohnen et al., 1990), were separated into two fractions using a column (20 cm x 2 cm; column volume ( $V_0$ ) = 35 ml) packed with alumina (activated for 2.5 h at 150°C) by elution with hexane/DCM (9:1, v/v; 150 ml; "apolar fraction") and DCM/ MeOH (1:1, v/v; 150 ml; "polar fraction"). Aliquots (ca. 10 mg) of the apolar fractions were further separated by argentation TLC (thin layer chromatography) using hexane as developer. The  $\text{Ag}^+$ -impregnated silica plates (20 x 20 cm; thickness 0.25 mm) were prepared by immersion into a solution of 1%  $\text{AgNO}_3$  in MeOH/ $\text{H}_2\text{O}$  (4:1, v/v) for 45 s and subsequent activation at 120°C for 1 h. Four fractions (A1,  $R_f$  = 0.85-1.00; A2,  $R_f$  = 0.35-0.85; A3,  $R_f$  = 0.06-0.35; A4,  $R_f$  = 0-0.06) were scraped off the TLC plate and ultrasonically extracted with ethyl acetate (x3).

*n*-Alkanes were removed from the A1 fractions using a 5 Å molecular sieve (8-12 mesh, Baker). The molecular sieve was extracted with DCM and activated at 400°C overnight. Five grains were added for each mg of sample, and the mixture was refluxed in dry cyclohexane for 24 h. Recovery of the non-adduct was performed by removal of the cyclohexane followed by warm cyclohexane rinses of the sieves. All rinses were combined to yield the non-adduct. Subsequently, the *n*-alkanes were obtained by refluxing the sieves in hexane for 24 h. The A1 non-adducts were further separated using a small column (5 cm x 0.5 cm;  $V_0$  = 1 ml) packed with  $\text{AgNO}_3$  impregnated (20% w/w; activated for 16 h at 120°C)

silicagel (Merck, Silicagel 60, 70-230 mesh ASTM) by elution with hexane (saturated hydrocarbons) and ethyl acetate (mono-unsaturated hydrocarbons).

*Raney nickel desulfurisation and hydrogenation.* A weighed amount (ca. 15 mg) of polar fraction with a known amount (ca. 20  $\mu\text{g}$ ) of internal standard (2,3-dimethyl-5-(1,1-dideuterohexadecyl)thiophene) was dissolved in 4 ml ethanol together with 0.5 ml of a suspension of Raney nickel (0.5 g/ml ethanol) and heated under reflux for 1.5 h. The desulfurisation products were isolated by centrifugation and subsequent extraction of the precipitate with DCM (x4). The combined extracts were washed (x3) with NaCl-saturated, bidistilled  $\text{H}_2\text{O}$  and dried with  $\text{MgSO}_4$ . The hydrocarbons liberated were isolated using a small column (5 cm x 0.5 cm;  $V_0 = 1$  ml) packed with alumina (activated for 2.5 h at  $150^\circ\text{C}$ ) by elution with hexane/DCM (9:1, v/v). The fraction was evaporated to dryness and dissolved in 4 ml ethyl acetate. Two drops of pure acetic acid and a pinch of  $\text{PtO}_2$  were added as catalysts. Hydrogen gas was bubbled through for 1 h, after which the solution was stirred for 24 h. The catalysts were removed using a small column packed with  $\text{Na}_2\text{CO}_3$  and  $\text{MgSO}_4$ . The fraction was evaporated to dryness and dissolved in a small volume of hexane (2 mg/ml) to be analysed by GC and GC-MS.

*HI-treatment of kerogen.* A weighed amount of extracted sediment, equivalent to ca. 150 mg organic carbon, with a known amount (ca. 40  $\mu\text{g}$ ) of internal standard (2,3-dimethyl-5-(1,1-dideuterohexadecyl)thiophene) was dissolved in 4 ml 57% HI-solution (in  $\text{H}_2\text{O}$ ) and heated under reflux for 1 h. After cooling and centrifugation the supernatant was transferred into a separatory funnel. Hexane and bidistilled  $\text{H}_2\text{O}$  were added to obtain two layers. The hexane layer was washed with bidistilled  $\text{H}_2\text{O}$  (3x),  $\text{Na}_2\text{S}_2\text{O}_3$  (5% w/w in  $\text{H}_2\text{O}$ ) (1x) and bidistilled  $\text{H}_2\text{O}$  (2x), dried with  $\text{MgSO}_4$  and evaporated to dryness. Apolar products released (as iodides) were isolated using a small column (5 cm x 0.5 cm;  $V_0 = 1$  ml) packed with alumina (activated for 2.5 h at  $150^\circ\text{C}$ ) by elution with hexane/DCM (9:1, v/v). The resultant fraction was evaporated to dryness, dissolved in 4 ml 1,4-dioxane together with 50-100 mg  $\text{LiAlH}_4$ , and heated under reflux for 1.5 h. After cooling 1 ml ethyl acetate was added to deactivate the  $\text{LiAlH}_4$ . After cooling and centrifugation the supernatant was transferred into a separatory funnel. Hexane and bidistilled  $\text{H}_2\text{O}$  were added to obtain two layers. The hexane layer was washed once with bidistilled  $\text{H}_2\text{O}$ . The fraction was dried with  $\text{MgSO}_4$ , weighed and dissolved in hexane (2 mg/ml) to be analysed by GC.

*Off-line pyrolysis and fractionation.* Off-line pyrolysis was performed with 0.5 g decarbonated (6N HCl), ultrasonically extracted rock samples which were heated ( $400^\circ\text{C}$ ) for 1 hr in a glass tube positioned in a cylindrical oven under a nitrogen flow. The volatile products generated were trapped in two successive cold traps containing hexane/DCM (9:1, v/v). The first trap was at room temperature; the second trap was cooled with solid  $\text{CO}_2$ /acetone. The off-line pyrolysate (combined products of both traps) was fractionated by column chromatography ( $\text{Al}_2\text{O}_3$ ; 15 cm x 1 cm;  $V_0 = 8$  ml) into an apolar and polar fraction by elution with 32 ml hexane/DCM (9:1, v/v) and 32 ml MeOH/DCM (1:1, v/v), respectively. The apolar fraction was further separated into three fractions using a column (8 cm x 1 cm;  $V_0 = 3$  ml) packed with  $\text{AgNO}_3$  impregnated (20% w/w; activated for 16 h at

120°C) silicagel (Merck, Silicagel 60, 70-230 mesh ASTM) by elution with 7.5 ml hexane (saturated hydrocarbons), 6 ml hexane/ethyl acetate (9:1, v/v; mono-unsaturated hydrocarbons, low-molecular-weight aromatics and low-molecular-weight thiophenes) and 12 ml ethyl acetate (stripping). The hexane fraction was carefully distilled until a concentration was reached suitable for GC-IRMS analysis of the *n*-alkanes. The *n*-alkenes were analysed by GC-IRMS after the aromatic components and thiophenes had been removed from the hexane/ethyl acetate fraction. This was achieved using a column packed with alumina (8 cm x 1 cm;  $V_0 = 3$  ml) by elution with 9 ml *n*-heptane (ethyl acetate removed by distillation). The eluent was carefully distilled until a concentration was reached suitable for GC and GC-IRMS analysis of the *n*-alkenes.

*Gas chromatography (GC).* GC was performed using a Carlo Erba 5300 or a Hewlett-Packard 5890 instrument, both equipped with an on-column injector. A fused silica capillary column (25 m x 0.32 mm) coated with CP-Sil 5 (film thickness 0.12  $\mu\text{m}$ ) was used with helium as carrier gas. The effluent of the Carlo Erba 5300 was monitored by a flame ionisation detector (FID). The effluent of the Hewlett-Packard 5890 was monitored by both a flame ionisation detector (FID) and a sulfur-selective flame photometric detector (FPD), applying a stream-splitter with a split ratio of FID:FPD = ca. 1:2. The samples were injected at 70°C and the oven was programmed to 130°C at 20°C/min and then at 4°C/min to 320°C, at which it was held for 15 min.

*Gas chromatography-mass spectrometry (GC-MS).* GC-MS was carried out on a Hewlett-Packard 5890 gas chromatograph interfaced to a VG Autospec Ultima Q mass spectrometer operated at 70 eV with a mass range  $m/z$  50-800 and a cycle time of 1.8 s (resolution 1000). The gas chromatograph was equipped with a fused silica capillary column (25 m x 0.32 mm) coated with CP-Sil 5 (film thickness 0.12  $\mu\text{m}$ ). Helium was used as carrier gas. The samples were injected at 60°C and the oven was programmed to 130°C at 20°C/min and then at 4°C/min to 320°C, at which it was held for 15 min.

GC-MSMS was performed on a Hewlett-Packard 5890 gas chromatograph interfaced to a VG Autospec Ultima Q mass spectrometer. The gas chromatograph was equipped with a fused silica capillary column (60 m x 0.25 mm) coated with CP-Sil 5CB-MS (film thickness 0.25  $\mu\text{m}$ ). The carrier gas was helium. The gas chromatograph was programmed from 60°C to 200°C at a rate of 15°C/min and then at 1.5°C/min to 310°C (10 min). The mass spectrometer was operated at 70 eV with a source temperature of 250°C. Dissociation of the parent ions was induced by collision with argon (collision energy 18-20 eV). The parent ion to daughter ion transitions were analysed with 20 ms settling and 80-100 ms sampling periods. Total cycle time was 1020 ms.

*Gas chromatography-isotope ratio mass spectrometry (GC-IRMS).* The DELTA-C GC-IRMS-system used is in principle similar to the DELTA-S system described by Hayes et al. (1990). The gas chromatograph (Hewlett-Packard 5890) was equipped with an on-column injector and a fused silica capillary column (25 m x 0.32 mm) coated with CP-Sil 5 (film thickness 0.12  $\mu\text{m}$ ). Helium was used as the carrier gas. The fractions of the off-line pyrolysate were injected at 35°C and subsequently the oven temperature was raised at 4°C/min to 310°C with a final hold time of 5 min. For analysis of the TLC fractions the



oven temperature was programmed from 70°C to 130°C at 20°C/min, from 130°C to 310°C at 4°C/min and maintained at 310°C for 15 min. The  $\delta^{13}\text{C}$  values (vs. PDB) were calculated by integrating the mass 44, 45 and 46 ion currents of the  $\text{CO}_2$  peaks produced by combustion of the column effluent and those of  $\text{CO}_2$  spikes with a known  $^{13}\text{C}$  content which were directly led into the mass spectrometer at regular intervals. The  $\delta^{13}\text{C}$  values reported are averages of at least two measurements.

*Curie-point pyrolysis-gas chromatography (Py-GC).* Py-GC was performed with a Hewlett-Packard 5890 gas chromatograph using a FOM-3LX unit for pyrolysis. Extracted and decarbonated (6N HCl) sediments were applied to a ferromagnetic wire. The Curie temperature was 610°C. The gas chromatograph, equipped with a cryogenic unit, was programmed from 0°C (5 min) to 310°C (5 min) at a rate of 3°C/min. Separation was achieved using a fused silica capillary column (25 m x 0.32 mm) coated with CP-Sil 5 (film thickness 0.4  $\mu\text{m}$ ). Helium was used as the carrier gas.

Curie-point pyrolysis-gas chromatography-mass spectrometry (Py-GC-MS) was performed using the same equipment and conditions as described above for the Py-GC in addition to a VG Autospec Ultima mass spectrometer operated at 70 eV with a mass range  $m/z$  50-800 and a cycle time of 1.8 s (resolution 1000).

*Quantification.* Pristane, phytane, chromans and derivatives of isorenieratene were quantified by integration of their peaks and the peak of the internal standard in the FID-trace. Free *n*-alkanes and  $\text{C}_{35}$  hopanes were quantified by integration of their peaks in the  $m/z$  57 and  $m/z$  191 mass chromatograms, respectively, and comparison with the peak area of the internal standard in the  $m/z$  57 mass chromatogram. To account for the different responses of FID and MS, concentrations were multiplied by formerly established correction factors.

## Results and discussion

Three lithologically different samples of the Lower Kimmeridge Clay at its type locality in Dorset were studied. Bulk properties of these samples are listed in Table 4.1. From the extractable OM, polar and apolar fractions were obtained, and the latter were further separated into several subfractions (see Experimental). These subfractions were analysed

**Table 4.1.** Bulk data.

	dolomite	bituminous shale	oil shale
TOC (% w/w)	2.4	7.9	28.9
HI (mg HC/g TOC)	616	678	713
$R_o$ (%)	n.d. <sup>a</sup>	n.d. <sup>a</sup>	0.42 <sup>b</sup>
carbonate (% w/w)	78	4.3	5.6
quartz (% w/w)	3	16	7
clay (% w/w) <sup>c</sup>	15	68	44
clay/TOC	6.3	8.6	1.5

<sup>a</sup> not determined

<sup>b</sup> inferred from Pristane Formation Index (Goossens *et al.*, 1988)

<sup>c</sup> by difference

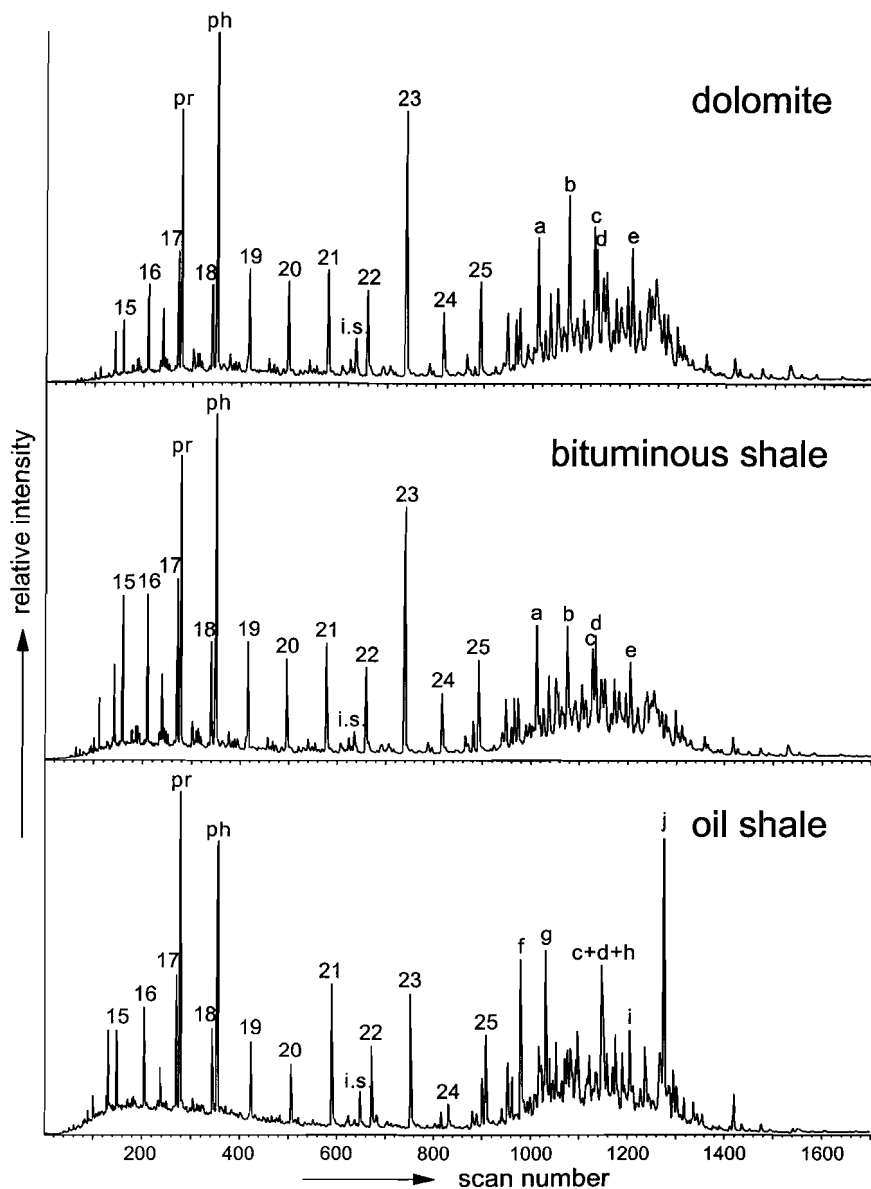


**Fig. 4.1.** Total ion current traces of the saturated hydrocarbon fractions of three lithologically different samples of the KCF. Numbers indicate chain length of *n*-alkanes. Key: pr = pristane, ph = phytane, i.s. = internal standard, a = 2-methyl-hexacosane, b = 5 $\alpha$ -cholestane, c = 4 $\alpha$ -methyl-5 $\alpha$ -cholestane, d = 3-isopropyl-hexacosane, e = 24-ethyl-5 $\alpha$ -cholestane, f = (20S)-4-methyldiacholest-13(17)-ene, g = (20R)-4-methyldiacholest-13(17)-ene, h = 4,23,24-trimethyldiacholest-13(17)-ene, i = 29-norneohop-13(18)-ene, j = neohop-13(18)-ene.

**Table 4.2.** Stable carbon isotopic composition of different biomarkers.

	$\delta^{13}\text{C}$ (‰)		
	dolomite	bituminous shale	oil shale
pristane	-31.3 ± 0.2	-31.4 ± 0.2	-30.0 ± 0.3
phytane	-31.2 ± 0.2	-30.9 ± 0.2	-30.1 ± 0.5
C <sub>27</sub> iso-alkane	-14.8 ± 0.8	-14.1 ± 0.1	
5 $\alpha$ -cholestane	-29.3 ± 0.2	-30.1 ± 0.6	-29.1 ± 0.7
(20S)-13 $\beta$ ,17 $\alpha$ (H)-diacholestane	-29.1 ± 0.1	-30.1 ± 0.1	
(20R)-13 $\beta$ ,17 $\alpha$ (H)-diacholestane	-28.9 ± 0.9	-30.6 ± 0.6	
(20S)-diacholest-13(17)-ene			-30.1 ± 0.9
(20R)-diacholest-13(17)-ene			-31.7 ± 0.5
24-ethyl-5 $\alpha$ -cholestane	-29.9 ± 1.8		-29.2 ± 0.2
(20R)-4 $\beta$ -methyl-5 $\alpha$ -cholestane			-26.2 ± 0.1
(20S)-4 $\beta$ -methyl-diacholest-13(17)-ene			-25.3 ± 0.5
(20R)-4 $\beta$ -methyl-diacholest-13(17)-ene			-24.8 ± 0.2
cluster of 4 $\alpha$ - and 4 $\beta$ -methyl-24-ethyl-5 $\alpha$ -cholestane and the 6 latest eluting 4,23,24-trimethyl-5 $\alpha$ -cholestanes	-28.3 ± 0.5	-28.6 ± 0.6	
one of the 4,23,24-trimethyl-diacholest- 13(17)-enes			-28.1 ± 0.1
hop-17(21)-ene			-26.3 ± 0.2
neohop-13(18)-ene		-26.0 ± 0.2	-26.5 ± 0.1
(22R)-17 $\alpha$ ,21 $\beta$ (H)-homohopane			-26.8 ± 0.7
(22R)-17 $\beta$ ,21 $\beta$ (H)-homohopane			-26.9 ± 0.4
di-Me MTTCs ( <b>XLIIb,c</b> )	-32.1 ± 1.1		
tri-Me MTTC ( <b>XLIIId</b> )	-33.1 ± 0.5	-32.9 ± 0.5	

using GC, GC-MS, GC-MSMS and GC-IRMS. Polar fractions were desulfurised and components released were studied by GC and GC-MS. In order to study the insoluble OM, the residues after extraction were subjected to both Curie-point pyrolysis and off-line pyrolysis.

#### *Free acyclic hydrocarbons*

Pristane and phytane are the dominant components of the saturated hydrocarbon fractions (Fig. 4.1); pristane/phytane ratios are 0.78, 0.87 and 1.16 in the dolomite, bituminous shale and oil shale, respectively. The  $\delta^{13}\text{C}$  values of pristane and phytane are similar and range from -31.4 to -30.0‰ (Table 4.2). This similarity in  $^{13}\text{C}$  content is not surprising, since both pristane and phytane, originating mainly from tocopherols (Goossens et al., 1984) and chlorophyll-a, respectively, are predominantly derived from algal and cyanobacterial primary production.

The distributions of the *n*-alkanes in the dolomite and bituminous shale are dominated by *n*-C<sub>23</sub>, whereas that in the oil shale maximises both at *n*-C<sub>23</sub> and at *n*-C<sub>21</sub> (Figs. 4.1, 4.2) as previously noted by Williams and Douglas (1980, 1983) and Farrimond et al. (1984) in other KCF samples. The *n*-C<sub>23</sub> in all three samples and the *n*-C<sub>21</sub> in the oil shale are significantly enriched in  $^{13}\text{C}$  relative to other *n*-alkanes (Fig. 4.2). These isotope excursions

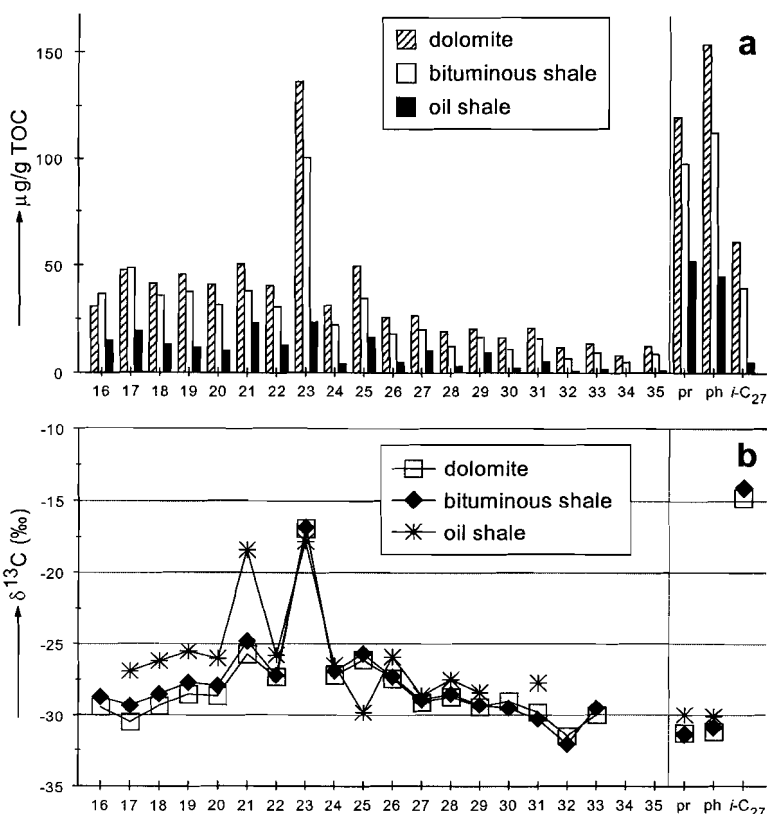


**Fig. 4.2.** (a) Quantities and (b) stable carbon isotopic composition of *n*-alkanes, pristane (pr), phytane (ph) and 2-methylhexacosane (*i*-C<sub>27</sub>).

can only be explained by invoking different source organisms for these *n*-alkanes. The fact that the dominant *n*-alkanes have the highest δ<sup>13</sup>C values indicate that there was an input of carbon isotopically heavy *n*-alkanes on top of the *n*-alkanes with relatively low <sup>13</sup>C contents (ca. -28‰). The organism(s) responsible for the high δ<sup>13</sup>C value of *n*-C<sub>23</sub> may have also produced the abundant C<sub>27</sub> iso-alkane (Fig. 4.1), since it is even more enriched in <sup>13</sup>C than *n*-C<sub>23</sub> (Table 4.2, Fig. 4.2) and their concentrations are positively correlated. The δ<sup>13</sup>C value of *n*-C<sub>23</sub> can thus be explained by a 75% contribution of -14.4‰ (δ<sup>13</sup>C of *i*-C<sub>27</sub>) and a 25% background of ca. -28‰. The *n*-C<sub>21</sub> and *n*-C<sub>25</sub> in the bituminous shale and dolomite, are enriched in <sup>13</sup>C as well but not to the same extent (Fig. 4.2). These *n*-alkanes are the nearest odd-numbered homologues of *n*-C<sub>23</sub> and it is suggested that a fraction of *n*-C<sub>21</sub> and *n*-C<sub>25</sub> originates from the same source organism that produced the isotopically heavy *n*-C<sub>23</sub>. In that case, the source organism contributed less to *n*-C<sub>21</sub> and *n*-C<sub>25</sub> than to *n*-C<sub>23</sub>. In the oil shale *n*-C<sub>21</sub> is relatively more abundant and carbon isotopically more enriched than in the other samples, and it even approaches the abundance and <sup>13</sup>C content of *n*-C<sub>23</sub> (Fig. 4.2). Apparently, during deposition of the oil shale the earlier mentioned source organism(s)

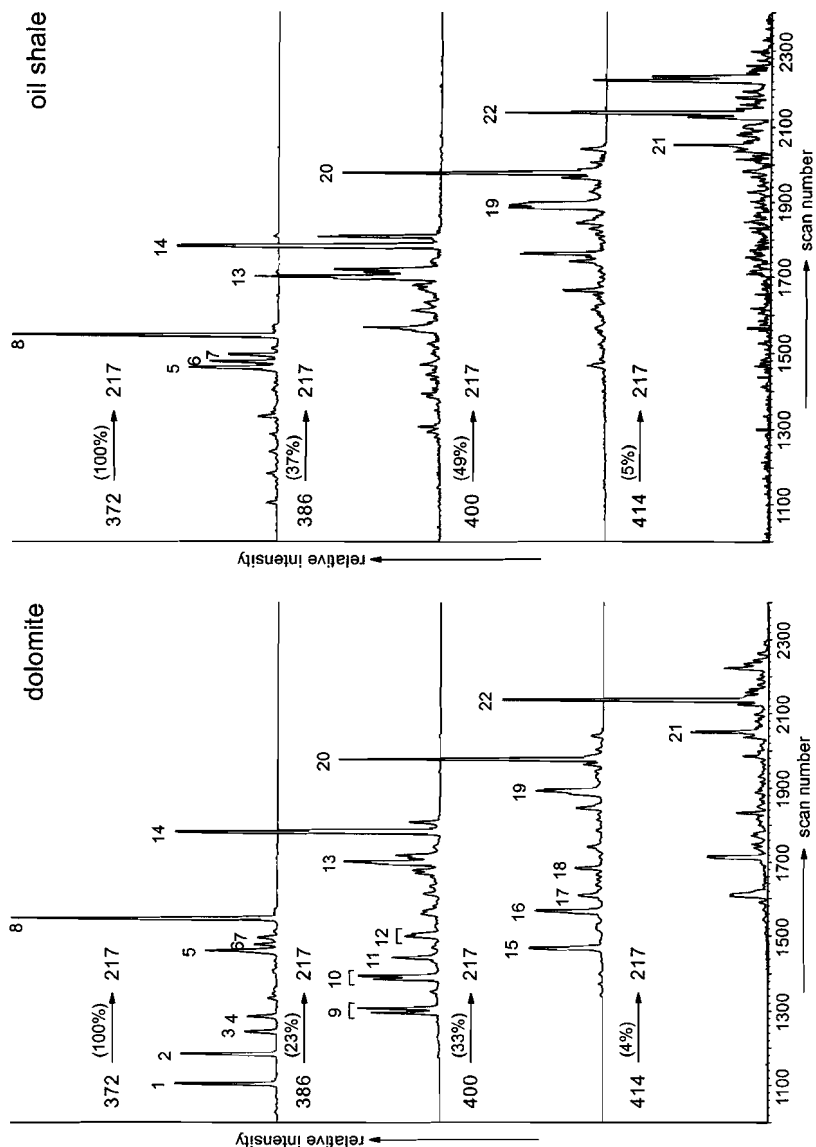


**Fig. 4.3.** Chromatograms showing desmethyl sterane distributions in the dolomite and oil shale. Distributions of desmethyl steranes in the bituminous shale are identical to those in the dolomite and are therefore not shown. The data were acquired by collisionally activated decomposition GC-MSMS. Each trace is identified with the masses of the parent and daughter ions, and the intensity of the base peak expressed as a percentage relative to the intensity of the 5 $\alpha$ -cholestane peak. Chromatograms were smoothed at 3 points of equal weight. Numbers refer to components listed in Table 4.3.

biosynthesised the  $n$ -C<sub>21</sub> and  $n$ -C<sub>23</sub> precursors in an almost 1:1 ratio, assuming no selective loss during diagenesis. The preferred biosynthesis of the  $n$ -C<sub>23</sub> precursor during deposition of the other sediments may be due to different environmental conditions.

3-Isopropylhexacosane, recently identified by Schouten et al. (1997), was detected in relatively high amounts in all three samples (Fig. 4.1). This compound is biosynthetically related to the  $n$ -C<sub>23</sub> and  $i$ -C<sub>27</sub> alkanes (Schouten et al., 1997), and it is probably one of the unknown branched alkanes reported by Farrimond et al. (1984). Its  $\delta^{13}\text{C}$  value could not be determined due to coelution problems.

### *Steroids*

The steranes comprise a complicated mixture of isomers (e.g. Fig. 4.1), which could only be fully resolved by GC-MSMS (Figs. 4.3, 4.4). The distributions of steranes in the dolomite and bituminous shale are in general quite similar. Therefore, only data of the dolomite and oil shale are shown. In order to obtain relatively simple fractions for determination of  $\delta^{13}\text{C}$  values of steranes, saturated and mono-unsaturated hydrocarbons present in the non-adducts of the A1 fractions were separated using argentation column chromatography (see Experimental). Since the fractions obtained were still complex, only a limited number of  $\delta^{13}\text{C}$  values of steranes could be obtained (Table 4.2). The diasterenes present in the bituminous shale and in the dolomite partly eluted in the A2 fractions, and due to the isotopic fractionation associated with chromatographic separation, their  $^{13}\text{C}$  contents could not be established.

*Desmethyl steroids.* (20R)-5 $\alpha$ ,14 $\alpha$ ,17 $\alpha$ (H)-Steranes have similar distributions in all three samples, i.e. C<sub>27</sub> > C<sub>29</sub> > C<sub>28</sub>. Also, as revealed by the  $m/z$  414 to  $m/z$  217 transition measured by GC-MSMS (Fig. 4.3), each sample contains small amounts of 24-propyl-5 $\alpha$ -cholestane, an indicator of marine sedimentary environments (Moldowan et al., 1990). Desmethyl sterenes and steradienes were not detected.

In the oil shale, small amounts of C<sub>27</sub>-C<sub>29</sub> spirosterenes were detected. These are intermediates in the early diagenetic isomerisation of  $\Delta^7$ -sterols, and ultimately most of them are transformed into 20S and 20R 14 $\beta$ ,17 $\beta$ (H)-steranes (Peakman et al., 1989). Indeed, GC-MS and GC-MSMS analyses revealed the presence of 5 $\alpha$ ,14 $\beta$ ,17 $\beta$ (H)-cholestanes in all three samples (Fig. 4.3), relatively most abundant in the oil shale. The 5 $\alpha$ ,14 $\beta$ ,17 $\beta$ (H)-steranes in these samples cannot have resulted from the isomerisation of 5 $\alpha$ ,14 $\alpha$ ,17 $\alpha$ (H)-steranes upon maturation, because (20S)-5 $\alpha$ ,14 $\alpha$ ,17 $\alpha$ (H)-steranes are absent and the thermodynamically unstable 5 $\beta$ ,14 $\alpha$ ,17 $\alpha$ (H)-steranes are present in relatively large amounts (Fig. 4.3). The fact that 14 $\beta$ ,17 $\beta$ (H)-cholestanes with both stereochemistries at C-20 are relatively most abundant in the oil shale (Fig. 4.3) is thus not related to differences in maturity, but to different proportions of organisms producing  $\Delta^7$ -sterols.

The  $\delta^{13}\text{C}$  values of 5 $\alpha$ -cholestane, representing the "average" stable carbon isotope composition of algal lipids, do not differ more than 1‰ between the samples (Table 4.2). This also holds for the  $\delta^{13}\text{C}$  values of 24-ethyl-5 $\alpha$ -cholestanes, although they could only be determined in two samples (Table 4.2). In all samples 5 $\alpha$ -cholestane is enriched in  $^{13}\text{C}$  by ca. 1‰ compared to pristane and phytane. This may be explained by a contribution of

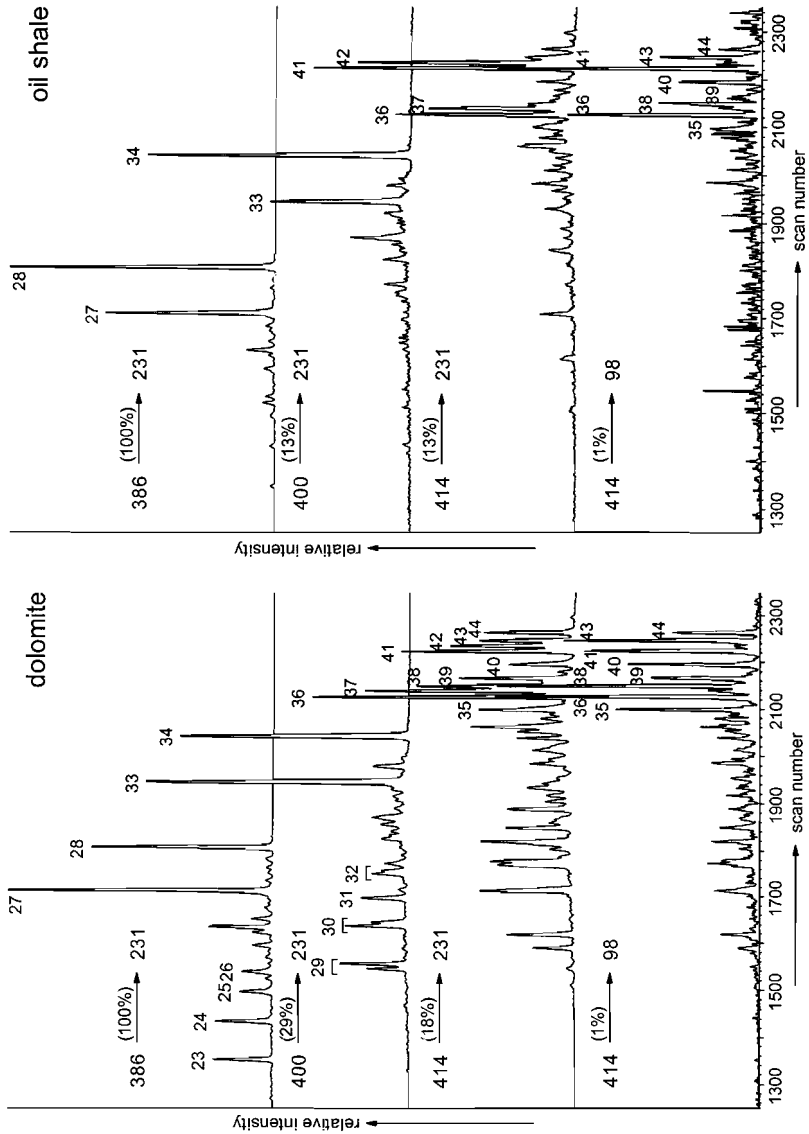


**Fig. 4.4.** Chromatograms showing 4-methyl sterane distributions in the dolomite and oil shale. Distributions of 4-methyl steranes in the bituminous shale are identical to those in the dolomite and are therefore not shown. The data were acquired by collisionally activated decomposition GC-MSMS. Each trace is identified with the masses of the parent and daughter ions, and the intensity of the base peak expressed as a percentage relative to the intensity of the 4-methyl-5 $\alpha$ -cholestane peak. Chromatograms were smoothed at 3 points of equal weight. Numbers refer to components listed in Table 4.3.

pristane and phytane derived from cyanobacteria relatively depleted in  $^{13}\text{C}$ , to the pristane and phytane derived from algae.

*4-Methyl steroids.* In the dolomite and bituminous shale,  $4\alpha$ -methyl steranes are only slightly lower than their desmethyl equivalents (Fig. 4.1, e.g. compounds b and c), and together with the  $4\beta$ -isomers they exceed their desmethyl counterparts in concentration. In the oil shale, both  $4\alpha$ - and  $4\beta$ -methylcholestane dominate over cholestane, but  $\text{C}_{29}$  and  $\text{C}_{30}$  4-methyl steranes are minor compared to their desmethyl counterparts. The transitions of  $m/z$  414 to  $m/z$  231 and  $m/z$  414 to  $m/z$  98 (Fig. 4.4) reveal the presence of  $4\alpha$ - and  $4\beta$ ,23,24-trimethyl- $5\alpha$ -cholestanes (dinosteranes) in all three samples. Four side chain epimers are present of both  $4\alpha$ - and  $4\beta$ -methyl dinosterane. The C-23 and C-24 diastereomers of  $5\alpha$ -dinosterane were synthesised by Stoilov et al. (1992, 1994), and their elution order was established (J.M. Moldowan, pers. comm., 1994). On the basis of these reports the dinosterane stereochemistries at C-23 and C-24 were assigned (Table 4.3).

In the oil shale, the dinosteranes are highly dominated by the 23S,24R-isomers, whereas in the dolomite (and bituminous shale) there is a more uniform distribution of side chain epimers (Fig. 4.4). Possible explanations for this discrepancy are:

(i) Different precursors are involved. For example, dehydration and hydrogenation of 4,23,24-trimethylcholestan- $3\beta$ -ol (dinostanol) does not alter the stereochemistry at C-23 and C-24 and will lead to 4,23,24-trimethylcholestanes possessing the original side chain stereochemistry of the precursor. On the other hand, dehydration and hydrogenation of 4,23,24-trimethylcholest-22E-en- $3\beta$ -ol (dinosterol) may yield all eight epimers produced by isomerisation of the chiral centres at C-4, C-23 and C-24. This explanation infers the presence of organisms that biosynthesised dinostanols in much higher quantities than dinosterols. Although in most algae stanols are minor compared to sterols, in the marine dinoflagellate *Gonyaulax polygramma* both free and esterified 4-methyl steroids are dominated by dinostanol (Volkman et al., 1984).

(ii) The isomer distribution of dinosterane reflects a certain isomerisation stage. From the 22S/(22S+22R) ratio and the relative abundance of  $17\beta$ , $21\beta$ (H)-hopanes (see below) it is clear that the OM has a more "immature" biomarker distribution in the oil shale than in the other sediments. Thus, the dominant side-chain configuration of dinosterane encountered in the oil shale is possibly that of the original precursor, and the additional isomers may have formed during diagenesis.

4-Methylcholestane (and 4-methyldiacholestenes) in the oil shale is on average enriched in  $^{13}\text{C}$  by 4‰ compared to the desmethyl steroids (Table 4.2). This points to the presence of organisms biosynthesising isotopically distinct 4-methylcholesterol in much larger quantities than any desmethyl steroid. Dinoflagellates are a well-known source of 4-methyl sterols and of the characteristic dinosterols (de Leeuw et al., 1983; Summons et al., 1987, 1992). Their presence in the KCF has been revealed by micro-palaeontological studies (e.g., Downie, 1957), and in the samples investigated this is confirmed by the abundant dinosteranes. However, distributions of dinoflagellate sterols reported in literature so far, are characterised by the absence or low amounts of 4-methylcholesterol (e.g., Kokke et al., 1981; Wengrovitz et al., 1981, de Leeuw et al., 1983; Volkman et al., 1984; Withers et al., 1978; Withers, 1987). Since 4-methylcholestanes are the dominant homologues in the



**Table 4.3.** Steranes identified.

peak <sup>a</sup>	structure assignment	peak <sup>a</sup>	structure assignment
1	(20S)-13 $\beta$ ,17 $\alpha$ (H)-diacholestane <sup>b</sup>	23	(20S)-4 $\alpha$ -methyl-13 $\beta$ ,17 $\alpha$ (H)-diacholestane <sup>c</sup>
2	(20R)-13 $\beta$ ,17 $\alpha$ (H)-diacholestane <sup>b</sup>	24	(20R)-4 $\alpha$ -methyl-13 $\beta$ ,17 $\alpha$ (H)-diacholestane <sup>c</sup>
3	(20R)-13 $\alpha$ ,17 $\beta$ (H)-diacholestane <sup>b</sup>	25	(20R)-4 $\alpha$ -methyl-13 $\alpha$ ,17 $\beta$ (H)-diacholestane <sup>c</sup>
4	(20S)-13 $\alpha$ ,17 $\beta$ (H)-diacholestane <sup>b</sup>	26	(20S)-4 $\alpha$ -methyl-13 $\alpha$ ,17 $\beta$ (H)-diacholestane <sup>c</sup>
5	5 $\beta$ -cholestane	27	4 $\alpha$ -methyl-5 $\alpha$ -cholestane
6	(20R)-5 $\alpha$ ,14 $\beta$ ,17 $\beta$ (H)-cholestane	28	4 $\beta$ -methyl-5 $\alpha$ -cholestane
7	(20S)-5 $\alpha$ ,14 $\beta$ ,17 $\beta$ (H)-cholestane	29	(20S)-4 $\alpha$ ,24-dimethyl-13 $\beta$ ,17 $\alpha$ (H)-diacholestane <sup>c</sup>
8	5 $\alpha$ -cholestane	30	(20R)-4 $\alpha$ ,24-dimethyl-13 $\beta$ ,17 $\alpha$ (H)-diacholestane <sup>c</sup>
9	(20S)-24-methyl-13 $\beta$ ,17 $\alpha$ (H)-diacholestane <sup>c</sup>	31	(20R)-4 $\alpha$ ,24-dimethyl-13 $\alpha$ ,17 $\beta$ (H)-diacholestane <sup>c</sup>
10	(20R)-24-methyl-13 $\beta$ ,17 $\alpha$ (H)-diacholestane <sup>c</sup>	32	(20S)-4 $\alpha$ ,24-dimethyl-13 $\alpha$ ,17 $\beta$ (H)-diacholestane <sup>c</sup>
11	(20R)-24-methyl-13 $\alpha$ ,17 $\beta$ (H)-diacholestane <sup>c</sup>	33	4 $\alpha$ ,24-dimethyl-5 $\alpha$ -cholestane
12	(20S)-24-methyl-13 $\alpha$ ,17 $\beta$ (H)-diacholestane <sup>c</sup>	34	4 $\beta$ ,24-dimethyl-5 $\alpha$ -cholestane
13	24-methyl-5 $\beta$ -cholestane	35	4 $\alpha$ ,23S,24S-trimethyl-5 $\alpha$ -cholestane <sup>d</sup>
14	24-methyl-5 $\alpha$ -cholestane	36	4 $\alpha$ ,23S,24R-trimethyl-5 $\alpha$ -cholestane <sup>d</sup>
15	(20S)-24-ethyl-13 $\beta$ ,17 $\alpha$ (H)-diacholestane <sup>c</sup>	37	4 $\alpha$ -methyl-24-ethyl-5 $\alpha$ -cholestane
16	(20R)-24-ethyl-13 $\beta$ ,17 $\alpha$ (H)-diacholestane <sup>c</sup>	38	4 $\alpha$ ,23R,24R-trimethyl-5 $\alpha$ -cholestane <sup>d</sup>
17	(20R)-24-ethyl-13 $\alpha$ ,17 $\beta$ (H)-diacholestane <sup>c</sup>	39	4 $\alpha$ ,23R,24S-trimethyl-5 $\alpha$ -cholestane <sup>d</sup>
18	(20S)-24-ethyl-13 $\alpha$ ,17 $\beta$ (H)-diacholestane <sup>c</sup>	40	4 $\beta$ ,23S,24S-trimethyl-5 $\alpha$ -cholestane <sup>d</sup>
19	24-ethyl-5 $\beta$ -cholestane	41	4 $\beta$ ,23S,24R-trimethyl-5 $\alpha$ -cholestane <sup>d</sup>
20	24-ethyl-5 $\alpha$ -cholestane	42	4 $\beta$ -methyl-24-ethyl-5 $\alpha$ -cholestane
21	24-propyl-5 $\beta$ -cholestane	43	4 $\beta$ ,23R,24R-trimethyl-5 $\alpha$ -cholestane <sup>d</sup>
22	24-propyl-5 $\alpha$ -cholestane	44	4 $\beta$ ,23R,24S-trimethyl-5 $\alpha$ -cholestane <sup>d</sup>

<sup>a</sup> numbers refer to peaks indicated in Figs. 4.3 and 4.4

<sup>b</sup> stereochemistry at C-20 after Sieskind et al. (1995)

<sup>c</sup> assuming the elution order to be similar to that of the diacholestanes

<sup>d</sup> stereochemistries at C-23 and C-24 after Moldowan (pers. comm., 1994)

samples studied, the 4-methyl steroids probably have a multiple origin. This is in agreement with the fact that the  $\delta^{13}\text{C}$  value of 4-methylcholestane (and 4-methyldiacholestenes) significantly differs from that of the cluster of 4-methyl-24-ethylcholestane and 4,23,24-trimethylcholestane isomers (Table 4.2). Unless these differences are due to an isotope effect resulting from the side chain alkylation step in biosynthesis (Withers et al., 1979), which is deemed unlikely, this implies that 4-methyl sterols were produced by two isotopically distinct sources at least. Differences in  $\delta^{13}\text{C}$  values of otherwise similar algal lipids are not unusual, since lipid  $^{13}\text{C}$  contents are affected by numerous factors including growth rate and cell size of the algae (Goericke et al., 1994; Laws et al., 1995). Still, care should be taken when inferring isotopically distinct sources, since carbon isotopic differences as high as 10‰ were measured between co-occurring hopan-29-ol and 3 $\beta$ -methylhopan-29-ol in methanotrophic bacteria (Summons et al., 1994). The prominence of 4-methylcholestanes over the longer-chain homologues is most pronounced in the oil shale, indicating that species composition during its deposition was different from that of the other samples. It should be noted that in a marl of the Tertiary Mulhouse Basin the  $\delta^{13}\text{C}$  values of 4-methylcholestane and dinosterane differ by 4.6‰ (Hollander et al., 1993b), also suggesting multiple origins of the 4-methyl steroids.

*Methylococcus capsulatus* is known to produce 4-methylcholesterol and 4,4-dimethylcholesterol (Bird et al., 1971), but it is probably not the source of the 4-methyl steroids in the samples studied since 4,4-dimethyl steroids are absent. Also, since *M. capsulatus* is a methylotrophic bacterium, its sterols cannot have  $\delta^{13}\text{C}$  values as heavy as those measured (Summons et al., 1994). Some prymnesiophyte microalgae can also biosynthesise 4-methyl steroids, but these do not comprise  $\text{C}_{28}$  members (Volkman et al., 1990). Recently, abundant 4-methylcholestanol and a small amount of dinosterol were identified in a plankton tow and in a freshly deposited fluff layer on the abyssal plain in the Gulf of Biscay (de Leeuw, unpublished results). This suggests that these compounds derive from a blooming algal source.

*Rearranged steroids.* Diasterenes and diasteranes have similar carbon number distributions as the regular steranes ( $\text{C}_{27} > \text{C}_{29} > \text{C}_{28}$ ), expressing their diagenetic relationship. Similarly, 4-methyl diasterenes and 4-methyl diasteranes show distributions identical to that of the 4-methyl steranes ( $\text{C}_{28} > \text{C}_{29} > \text{C}_{30}$ ). The saturated rearranged steroids are relatively abundant in the dolomite and bituminous shale, but in the oil shale they could hardly be detected (Figs. 4.3, 4.4). The rearrangement of steroids is believed to be catalysed by clay minerals (Rubinstein et al., 1975; Sieskind et al., 1979) and diasteranes/steranes ratios typically reflect sediment mineralogy with high ratios reflecting clay-rich sediments (e.g. Peters and Moldowan, 1993). Surprisingly, the clay content in the oil shale is significantly higher than that of the dolomite (Table 4.1), in disagreement with this general observation. Sieskind et al. (1979) reported that formation of diasteranes from sterols proceeds faster with kaolinite than with montmorillonite, suggesting a control on diasterane formation by clay mineral composition. However, the clay mineral composition as revealed by XRD appeared the same in all three samples (Fig. 4.5). The clay/TOC ratio is four to six times lower in the oil shale than in the other sediments (Table 4.1). This would suggest that, due to the low availability of clay minerals to the OM, lower amounts of rearranged steroids could be formed in the oil

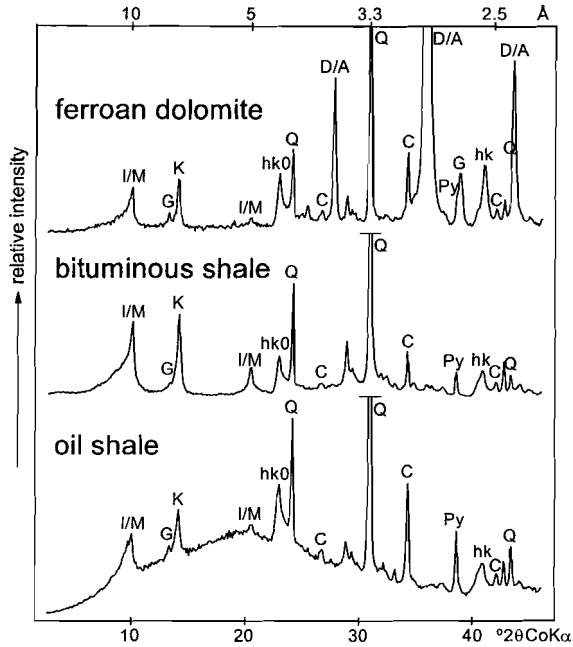


**Fig. 4.5.** X-ray powder diffractograms of the three lithologically different samples, showing similar assemblages of clay minerals. Key: A = ankerite, C = calcite, D = dolomite, G = gypsum, I = illite, K = kaolinite, M = mica, Py = pyrite, Q = quartz. Patterns were smoothed at 5 points of equal weight.

shale. However, if the unsaturated rearranged steroids are also taken into account, this is no longer valid, for diasterenes and 4-methyl diasterenes are extremely abundant in the oil shale (Fig. 4.1). Therefore, in agreement with van Kaam-Peters et al. (1997a), it seems more likely that the hydrogenation of the rearranged sterenes (leading to formation of diasterenes) depends on the amounts of clay available.

Remarkably, while both 4 $\alpha$ -methyl and 4 $\beta$ -methyl steranes are present, only one C-4 epimer is present for the corresponding diasterenes (Fig. 4.4). Based on their relative retention times in comparison with those of 4-methyl diasterenes in samples where 4 $\beta$ -methyl steranes are absent (van Kaam-Peters et al., 1997b), it is thought that these are 4 $\alpha$ -methyl isomers. The pairs of the 24-methyl and 4 $\beta$ ,24-dimethyldiacholestanes (Figs. 4.3, 4.4) are thought to represent 24S and 24R isomers. Since these isomers are almost equally abundant it is suggested that they, at least partly, formed from 24-methylene sterols like 24-methylene-cholesterol (**I**, see Appendix) and 4 $\alpha$ -methyl-24-methylene-cholesta-8(14)-en-3 $\beta$ -ol (amphisterol, **II**), though it is known that 24-methyl sterols with both the 24S and 24R configuration are biosynthesised (Withers, 1987). Amphisterol is the major sterol in many species of the dinoflagellate genus *Amphidinium* (Withers, 1987). It is not clear whether the 24S and 24R isomers of the 24-ethylidiacholestanes are coeluting or only one of these isomers is present (Fig. 4.3).

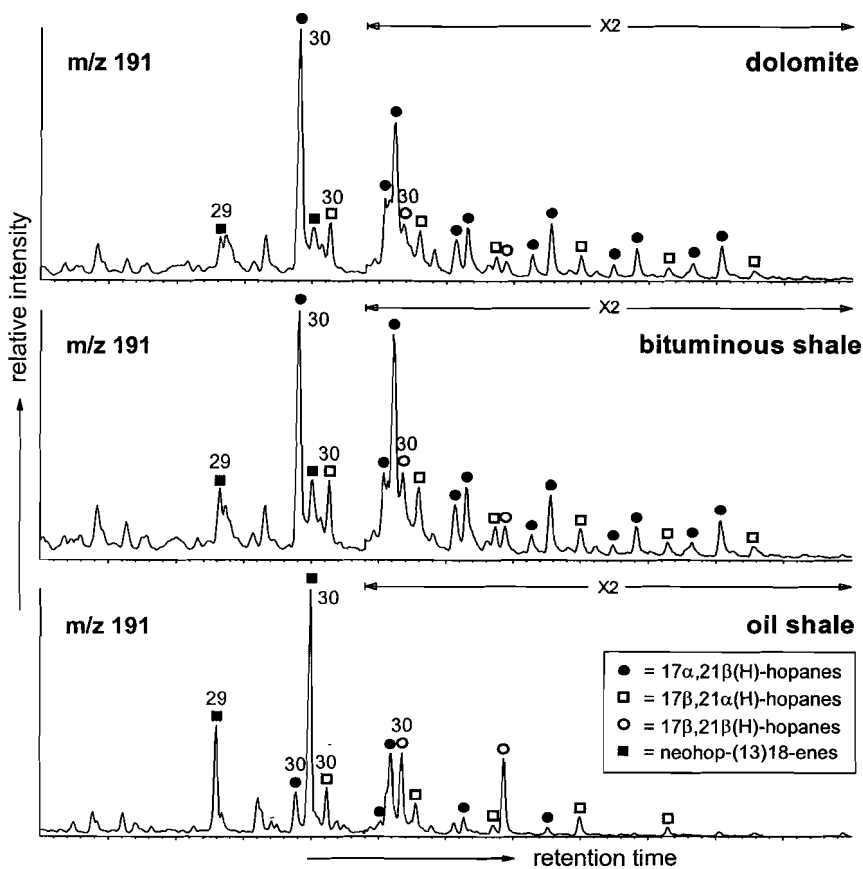


**Fig. 4.6.**  $m/z$  191 mass chromatograms showing hopanoid distributions in the saturated hydrocarbon fractions.

In the dolomite and bituminous shale,  $\delta^{13}\text{C}$  values of the diacholestanes do not differ significantly from that of cholestane (Table 4.2). Apparently, the eventual isotopic fractionation accompanying diagenetic rearrangement is minor. This is in accordance with the findings of Freeman et al. (1994a), showing that the diagenetic aromatisation of hydrocarbons, which implies the removal of hydrogen or methyl groups, does not significantly alter the original  $^{13}\text{C}$  content.

### *Hopanoids*

The distributions of hopanoids in the bituminous shale and dolomite, as revealed by the  $m/z$  191 mass chromatograms (Figs. 4.6a,b), are virtually identical.  $17\alpha,21\beta(\text{H})$ -Hopanes are dominated by the  $\text{C}_{30}$  member. The  $22\text{S}/(22\text{S}+22\text{R})$  ratio of the homohopanes, is on average 0.25. The presence of the thermodynamically unstable  $17\beta,21\alpha(\text{H})$ -hopanes and  $17\beta,21\beta(\text{H})$ -hopanes indicates that the samples are relatively immature. 29-Norneohop-

**Table 4.4.** Quantities of different (groups of) compounds.

	concentration ( $\mu\text{g/gTOC}$ )		
	dolomite	bituminous shale	oil shale
$C_{16}$ - $C_{35}$ <i>n</i> -alkanes	690	540	190
pristane	120 (1.2) <sup>a</sup>	98 (1.1)	52 (3.0)
phytane	150 (2.8)	110 (2.6)	45 (8.4)
$C_{35}$ hopanes	3.2 (0.6)	1.9 (0.6)	<0.1 (2.1)
isorenieratane (IV)	48 (8.8)	40 (7.9)	33 (3.8)
sum of V, VIII, XII, XIIIa, XIIIb, XIVa, XV, XVI	120	130	110
8-Me MTTC (XLIa)	4.4	<0.1	<0.1
di-Me MTTCs (XLIb,c)	10	5.9	<0.1
tri-Me MTTC (XLIId)	45	35	5.1

<sup>a</sup> values between parentheses indicate quantities sulfur-bound in the polar fraction

13(18)-ene and neohop-13(18)-ene, clearly present in the oil shale, are low in the dolomite and bituminous shale. The distribution of hopanoids in the oil shale is dominated by the  $C_{29}$ - $C_{30}$  neohop-13(18)-enes (Fig. 4.6c). The  $22S/(22S+22R)$  ratio of the  $17\alpha,21\beta(H)$ -hopanes approaches zero in the oil shale, and the  $C_{30}$   $\beta\beta/(\alpha\beta+\beta\beta)$  ratio is much higher than in the other samples (Fig. 4.6).

Although the rocks have probably experienced the same burial history, the  $22S/(22S+22R)$  ratio of the extended hopanes and the  $C_{30}$   $\beta\beta/(\alpha\beta+\beta\beta)$  ratio indicate that in the oil shale the OM is thermally less mature than in the other two samples. This is also evident from the concentrations of the free and sulfur-bound hopanoids (Table 4.4).  $C_{35}$  hopanes are only trace components in the saturated hydrocarbon fraction of the oil shale (Fig. 4.6), but they are released upon desulfurisation of its polar fraction (Table 4.4) and are dominated by the  $17\beta,21\beta(H)$ -isomer. Hence, the degree of maturation of the oil shale was insufficient to release most of the hopanoids sequestered *via* sulfur linkages in the polar fraction (Köster et al., 1997). By contrast, the dolomite and bituminous shale do contain free  $C_{35}$  hopanes (Fig. 4.6, Table 4.4), and  $C_{35}$  hopanes released upon desulfurisation of the polar fractions are less abundant and comprise the  $17\alpha,21\beta(H)$ -isomers. Apparently, degree of sulfurisation and possibly other aspects in addition to burial depth and time, play a role in the distribution of hopanoid isomers (cf. Sinninghe Damsté et al., 1995b).

The hopanoids are enriched in  $^{13}\text{C}$  compared to most of the steroids (Table 4.2), which may partly be explained by differences in biosynthesis (Kenig et al., 1995). Variations in  $\delta^{13}\text{C}$  values amongst the individual hopanoids are insignificant (Table 4.2). Consequently,  $C_{29}$ - $C_{30}$  hopanoids cannot be conclusively assigned a different origin than the extended hopanes. However, the varying abundance of neohop-13(18)-enes relative to the other hopanoids (Fig. 4.6) suggest that at least two sources are involved.

#### *Derivatives of isorenieratene*

Isorenieratene (III) is a carotenoid uniquely biosynthesised by the brown-coloured subgroup of the photosynthetic green sulfur bacteria (Chlorobiaceae). These are strict anaerobes which live under an extremely low light intensity and require  $\text{H}_2\text{S}$ . Their presence points to an

anoxic water column that extended into the photic zone (e.g. Sinninghe Damsté et al., 1993c; Repeta, 1993). Chlorobiaceae fix their carbon through the reverse tricarboxylic acid cycle (Sirevåg and Ormerod, 1970) and consequently their biomass is anomalously enriched in  $^{13}\text{C}$  relative to the algal OM (Quandt et al., 1977; Sirevåg et al., 1977). Upon diagenesis isorenieratene may be transformed into different molecular structures, but these products retain their original elevated  $^{13}\text{C}$  content, thereby betraying their origin (e.g. Summons and Powell, 1987; Kohnen et al., 1992; Sinninghe Damsté et al., 1995a; Koopmans et al., 1996).

Whilst isorenieratane (IV) may be produced in sediments by the hydrogenation of isorenieratene (Schaefflé, 1977; Hartgers et al., 1994), many other derivatives result from more complicated transformations of isorenieratene. Cyclisation of a part of the acyclic isoprenoid chain *via* an intramolecular Diels-Alder reaction followed by aromatisation of the newly formed ring yields the triaromatic compounds V and VI (Koopmans et al., 1996). The  $\text{C}_{32}$  and  $\text{C}_{33}$  diaryl isoprenoids (VII and VIII) are produced from isorenieratene by the expulsion of *m*-xylene and toluene, respectively, prior to hydrogenation. The expulsion of *m*-xylene and toluene has long been known from the thermal degradation of  $\beta$ -carotene (Byers and Erdman, 1981), but only recently it was shown applicable to sedimentary  $\beta$ -carotene and isorenieratene (Jiang and Fowler, 1986; Schoell et al., 1994; Koopmans et al., 1996, 1997). Subsequent expulsion of fragments is not a favoured process. Instead, cyclisation and subsequent aromatisation lead to many structures and structural isomers (Koopmans et al., 1996). Moreover, cleavage of C-C bonds takes place, leading to an even larger variety of short-chain derivatives.

In addition to expulsion, cyclisation and aromatisation reactions, sulfur incorporation into isorenieratene also takes place during diagenesis. The anoxic water column, prerequisite for the presence of isorenieratene, and the top layers of the sediment are rich in reduced inorganic sulfur species and these readily react with the nine conjugated double bonds of isorenieratene (Schouten et al., 1994; Kok et al., 1995). Actually, a large fraction of isorenieratene was shown to be sulfur-bound in geomacromolecules in recent Black Sea sediments (cf. Sinninghe Damsté et al., 1993c; Repeta, 1993; Wakeham et al., 1995). Intramolecular sulfur incorporation, yielding among others the compounds IX-XI, also plays a role in the diagenetic pathway of isorenieratene (Koopmans et al., 1996).

Derivatives of isorenieratene are present in the A2, A3, A4 and desulfurised polar fractions of all three KCF samples. The A2 fractions contain a series of  $\text{C}_{13}$ - $\text{C}_{22}$  aryl isoprenoids exhibiting the usual distribution pattern with the low  $\text{C}_{17}$  member (cf. Summons and Powell, 1987). In the A3 and A4 fractions the majority of compounds derives from isorenieratene (Figs. 4.7, 4.8). Concentrations of isorenieratane and the sum of concentrations of major other isorenieratene derivatives (V, VIII, XIIIa, XIIIb, XII, XVI, XV, XIVa) are listed in Table 4.4. Quantities are lowest in the oil shale, but concentrations (in  $\mu\text{g/g}$  TOC) of other biomarkers are also lowest in the oil shale (Table 4.4). Desulfurisation of the polar fractions yielded isorenieratane (IV) as the major product, but also small quantities of aryl isoprenoids and compounds V-VIII were released.

In addition to the numerous isorenieratene derivatives identified by Koopmans et al. (1996), we tentatively identified some additional derivatives of isorenieratene (see below). Although this does not contribute to establishing the presence of Chlorobiaceae in the depositional environment, differences in types and distributions of isorenieratene derivatives

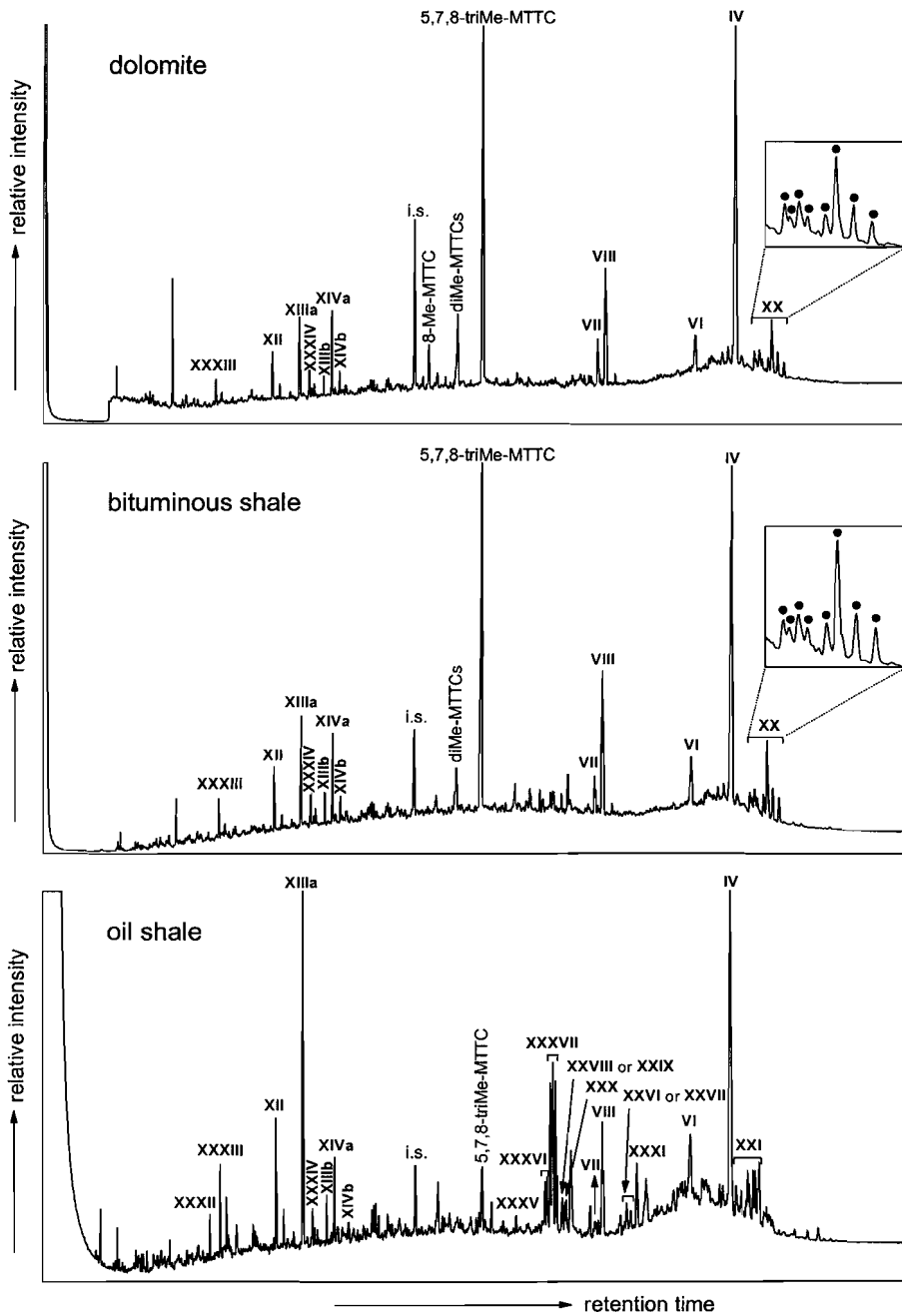


**Fig. 4.7.** Gas chromatograms of the A3 fractions. Roman numerals refer to components indicated in the Appendix. Insets show isomer distributions of XX.





**Table 4.5.** Stable carbon isotopic composition of diagenetic derivatives of isorenieratene.

	$\delta^{13}\text{C}$ (‰)		
	dolomite	bituminous shale	oil shale
<b>IV</b>	-16.9 ± 0.2	-17.7 ± 0.3	-16.6 ± 0.3
<b>V</b>	-17.2 ± 0.2	-18.0 ± 0.2	-16.3 ± 0.2
<b>VI</b>	-17.3 ± 0.3		
<b>VIII</b>	-16.5 ± 0.4	-16.8 ± 0.5	-15.9 ± 0.3
<b>XI</b>			-22.0 ± 0.3
<b>XII</b>			-16.5 ± 0.3
<b>XIIIa</b>	-17.6 ± 1.6		-16.3 ± 0.2
<b>XIVa</b>	-18.6 ± 1.8		
<b>XV</b>			-15.3 ± 0.5
<b>XV + XVI</b>		-17.5 ± 0.7	
<b>XVI</b>			-14.7 ± 0.5
<b>XVIII</b>			-19.0 ± 0.2
<b>XX</b>	-18.0 ± 0.4		
<b>XXI</b>			-18.2 ± 1.6
<b>XXIII + XXXVIII</b>	-17.9 ± 0.4		
<b>XXXVI + XXXVII</b>		-16.5 ± 1.0	
<b>XXXVII</b>	-17.7 ± 0.8		-18.0 ± 0.7
<b>XXXIX + XL</b>	-19.9 ± 1.4	-19.9 ± 0.6	

may be related to differences in diagenesis/catagenesis. In this respect it is noteworthy that, like the rearranged steroids, isorenieratene derivatives in the oil shale are less saturated than those in the other sediments, possibly due to the low clay/TOC ratio in the oil shale (Table 4.1).

*C*<sub>40</sub> derivatives of isorenieratene with an additional aromatic ring. The presence of isorenieratane (**IV**) was established by coinjection with an authentic standard. The structures of other products were determined from mass spectral data (Koopmans et al., 1996), stable carbon isotopic data (Table 4.5) and the presence of atropisomers producing characteristic distribution patterns upon GC and GC-MS analyses. Atropisomers contain an axially chiral centre which, in combination with other chiral centres in the molecule, results in two or more diastereomers that can be separated on a normal GC column (Koopmans et al., 1996). The two stable configurations of an atropisomer are almost equally abundant, which can be recognised in GC traces and mass chromatograms.

Theoretically, from isorenieratene five diaryl isoprenoids with an additional aromatic ring can be formed (**V**, **VI**, **XVII**, **XVIII** and **XIX**; Sinnighe Damsté et al., 1995a). Compounds **V** and **VI** (Koopmans et al., 1996), are abundantly present in the samples studied (Figs. 4.7, 4.8). Furthermore, two additional compounds with mass spectra suggesting that they are diaryl isoprenoids with an additional aromatic ring were detected, albeit in relatively low amounts. They eluted after compound **V** in the A4 fractions (Fig. 4.8). It is proposed that these are **XVII** [*m/z* 538(12), 173(10), 147(46), 134(38), 133(100), 119(13)] and **XVIII** [*m/z* 538(13), 134(57), 133(100), 119(12)], eluting in this order. Compound **XIX** is rejected, because its mass spectrum, likewise that of compound **V** [*m/z* 538(20), 173(12), 134(36), 133(100), 119(22)], is expected to show a *m/z* 119 fragment

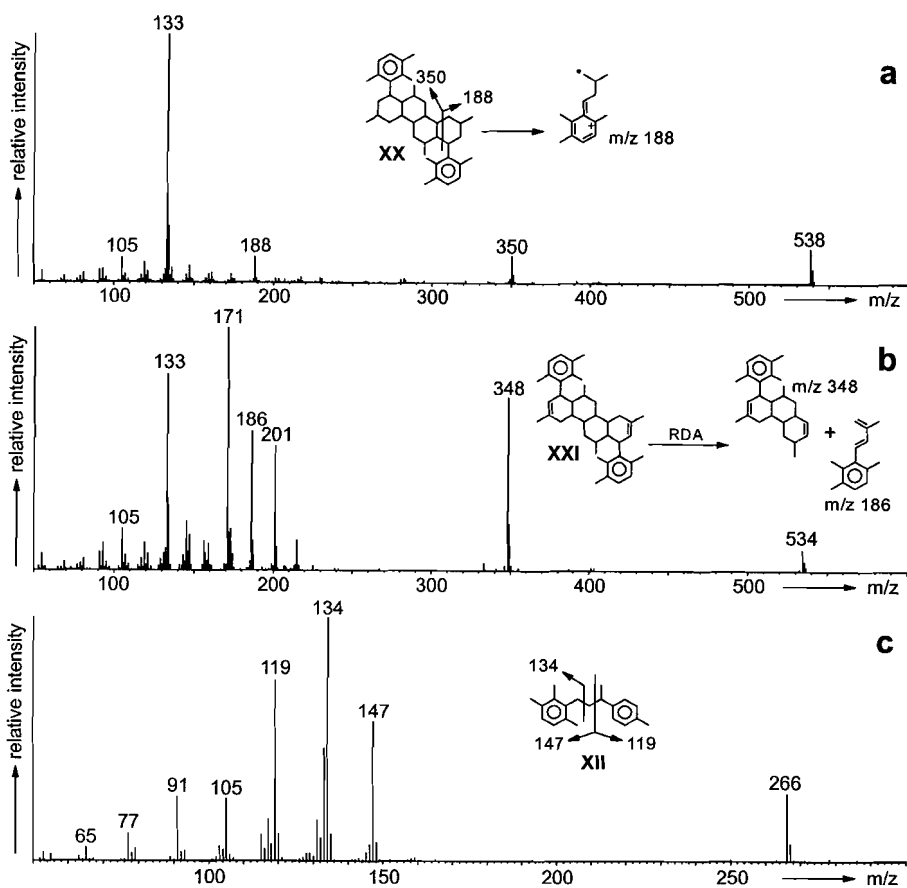


**Fig. 4.9.** Mass spectra of tentatively identified derivatives of isorenieratene. Stable carbon isotopic compositions of these compounds are listed in Table 4.5.

significantly higher than that in the mass spectrum of isorenieratene [ $m/z$  546(29), 134(91), 133(100), 119(10)], due to  $\beta$ -cleavage on both sides of its dialkylphenyl moiety. In addition, cyclisation of isorenieratene (**III**) involving C-20 to C-14' is not regarded a likely process since C-20 is  $sp^3$  hybridised and is not part of the conjugated system (Koopmans et al., 1996). In compound **XVII** the position of the additional aromatic ring is such that on one side of this ring the  $\beta$ -cleavage coincides with the cleavage  $\gamma$  to the terminal trimethylalkylphenyl group. This probably causes a more intense fragment at  $m/z$  147 than in case of compound **XVIII**, and consequently **XVIII** is thought to be the later eluting compound. Note that **XVIII** is significantly enriched in  $^{13}\text{C}$  (Table 4.5) relative to the algal signal (Table 4.2), which strengthens its origin from isorenieratene.

*Derivatives of isorenieratene with cyclohexyl moieties.* The compounds **XX** and **XXI** eluting after isorenieratene (**IV**) (Fig. 4.7) have been tentatively identified on the basis of mass spectral data, stable carbon isotopic composition and hydrogenation experiments. The  $^{13}\text{C}$

contents were determined on peak clusters comprising several isomers (Table 4.5, Fig. 4.7), because the individual isomers are not base-line separated. As the peaks arise from a hump the  $\delta^{13}\text{C}$  values largely depend on the integration method used, and the standard deviations are large. Despite the uncertainties associated with methods used for peak integration, **XX** and **XXI** are significantly enriched in  $^{13}\text{C}$  relative to the algal signal, providing evidence for an origin from the Chlorobiaceae. The intense fragment ions at  $m/z$  133 in their mass spectra and the presence of many isorenieratene derived products in the samples suggest that these components represent diagenetic products of isorenieratene.

The mass spectrum of **XX** (Fig. 4.9a) is characterised by a base peak at  $m/z$  133, radical ions at  $m/z$  188 and 350, and a molecular ion at  $m/z$  538. The accurate mass of the molecular ion points to a deficit of eight hydrogen atoms in the elemental composition in comparison with isorenieratane (**IV**). This deficit cannot be explained by an additional aromatic ring, for such a triaromatic compound can only have four diastereomers, and gas chromatography indicates at least eight structural isomers of **XX** (see insets in Fig. 4.7). Moreover, the four diastereomers of compound **V**, identified by Sinninghe Damsté et al. (1995a) by NMR, are represented by a single peak in the gas chromatogram. **XX** is not susceptible to hydrogenation ( $\text{PtO}_2/\text{H}_2$ , ethyl acetate), and in order to explain the deficit of eight hydrogen atoms as compared with isorenieratane, it is proposed that four additional saturated rings are present. Assuming that these are six-membered rings, which is the case for nearly all isorenieratene derived products (Koopmans et al., 1996), only structure **XX** can be proposed on the basis of the isorenieratene carbon skeleton. This structure can account for the characteristic fragment ions in the mass spectrum (Fig. 4.9a), and for the cluster of eight isomers in the chromatogram. If we assume an all-trans configuration for the saturated ring system and equatorial positions for the trimethylphenyl groups, which considerably reduces the number of possible isomers, eight diastereomers can be envisaged. These can be explained by the four methyl bearing chiral carbon atoms, because the all-trans saturated ring system has no plane of symmetry.

Additional evidence for the structural assignment of **XX** was obtained from hydrogenation ( $\text{PtO}_2/\text{H}_2$ , ethyl acetate) of the A3 fraction of the oil shale. Hydrogenation yielded compound **XX**, which was absent in the original fraction (Fig. 4.7), and there was a concomitant decrease in the concentration of component **XXI**. Apparently, component **XXI** was transformed into component **XX** by incorporation of four hydrogen atoms. The position of the double bonds was tentatively determined from the mass spectrum of **XXI**, displaying intense fragment ions at  $m/z$  186 and 348 probably resulting from a retro Diels-Alder reaction (Fig. 4.9b). The fully aromatised counterpart of **XX**, component **XXII**, has been tentatively identified by Koopmans et al. (1996).

Figs. 4.10c-f show several novel products of isorenieratene with both additional cyclohexyl and benzene rings. These compounds were tentatively identified on the basis of mass spectral data and by the fact that they are not susceptible to hydrogenation ( $\text{PtO}_2/\text{H}_2$ , ethyl acetate). Unfortunately, it was not possible to measure the carbon isotopic composition of these compounds. Mass spectra of the  $\text{C}_{40}$  diaryl isoprenoids with three additional aromatic rings (**XVI** and **XXIII**) and mass spectra of the  $\text{C}_{32}$  'carotenoids' with two additional aromatic rings (**XXIV** and **XXV**) (Koopmans et al., 1996), are shown in Figs. 4.10a and b, respectively, in order to demonstrate their resemblance with the mass spectra in

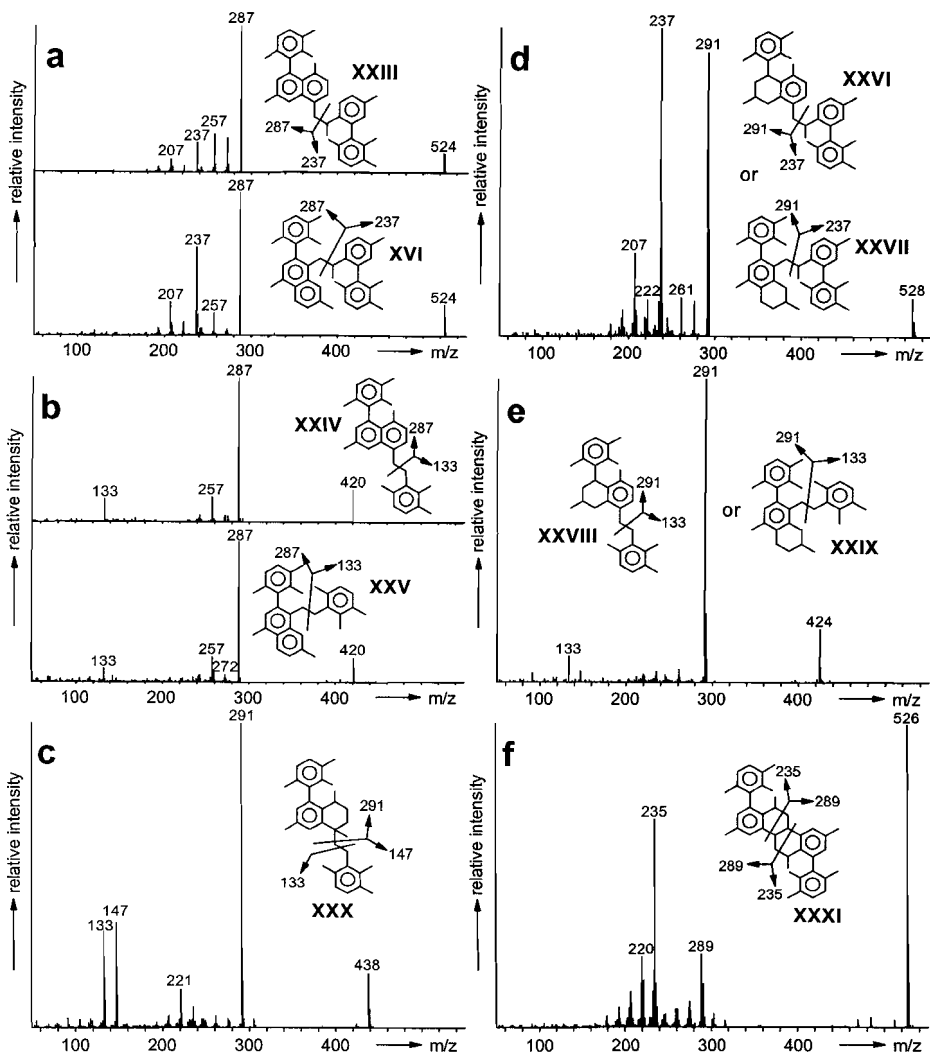


**Fig. 4.10.** Mass spectra and structures of (a, b) previously identified (Koopmans et al., 1996) and (c, d, e, f) newly tentatively identified derivatives of isorenieratene.

Figs. 4.10d and e. The differences between the spectra almost exclusively concern the fragments at  $m/z$  287,  $m/z$  272,  $m/z$  257 and the molecular ions, which all shifted four mass units. Apparently, instead of a naphthyl moiety a tetrahydronaphthyl moiety is present. From the mass spectra alone, however, it is impossible to distinguish between XXVI and XXVII, and between XXVIII and XXIX (Figs. 4.10d,e). The mass spectra shown in Figs. 4.10c,f are ascribed to compounds XXX and XXXI, probably deriving from the  $C_{33}$  'carotenoid' and isorenieratene, respectively. Note that XXXI is easily envisaged to be formed by the aromatisation of component XXI.

The presence of diaryl isoprenoids with saturated cyclohexyl moieties in sediments shows that cyclisation of isorenieratene is not necessarily coupled with aromatisation. However, it is not known if aromatisation and hydrogenation are competitive processes during diagenesis/catagenesis, since it cannot be excluded that sulfur was incorporated and later upon its release led to the formation of derivatives possessing saturated rings. Sulfur incorporation into isorenieratene *per sé* certainly took place, as indicated by the presence of components **IX**, **X** and **XI** in the A3 and A4 fractions (Figs. 4.7, 4.8), and by the isorenieratane released upon desulfurisation of the polar fractions (Table 4.4).

*Short-chain derivatives of isorenieratene.* Short-chain derivatives of isorenieratene are thought to result mainly from the cleavage of C-C bonds occurring more or less simultaneously with the cyclisation and aromatisation of isorenieratene (Koopmans et al., 1996). The C-C bond cleavage preferentially takes place adjacent to the newly formed ring. It was demonstrated that the formation of an additional aromatic ring involving C-7 to C-12 or C-11 to C-15' in isorenieratene (**III**) is much more favourable than that comprising other carbon atoms of the backbone (Koopmans et al., 1996). Indeed, **V** and **VI** are highly dominant over **XVII** and **XVIII**, and the abundant compound **XIIIa** probably is a cleavage product of the C<sub>40</sub> precursor of **V**. However, **XII**, a C<sub>20</sub> aryl isoprenoid with an additional aromatic ring, present in significant quantities (Fig. 4.7), cannot have resulted from C-C bond cleavage in the C<sub>40</sub> precursor of either **V** or **VI**. This short-chain derivative of isorenieratene was tentatively identified using mass spectral (Fig. 4.9c) and carbon isotopic data (Table 4.5). The McLafferty rearrangement yielding the m/z 134 fragment (Fig. 4.9c), is considerably enhanced compared to that of isorenieratane. This is explained by the fact that in case of **XII**, the hydrogen atom concerned, i.e. the one  $\gamma$  to the trimethylalkylphenyl group, is also  $\beta$  to the second aromatic ring, thus promoting its transfer. Obviously, the position of the methyl group of the additional aromatic ring cannot be established from the mass spectrum (Fig. 4.9c). But regardless the position of this methyl group, **XII** cannot derive from cleavage of one of the C<sub>32</sub>, C<sub>33</sub> or C<sub>40</sub> precursors of major isorenieratene derivatives. Nevertheless, **XII** is abundant in the samples studied, and it is probably the same compound with M<sup>+</sup> = 266 observed in the Permian Kupferschiefer (Schwark and Püttmann, 1990). Possibly, the C<sub>40</sub> precursor of **XVII**, which is the only isorenieratene derivative having cyclised at the energetically unfavourable C-10 and C-15 positions, upon C-C bond cleavage yielded **XII**. But if so, it remains unclear why component **XII** is so abundant, whereas **XVII** is present in only small amounts.

### *Chromans*

Methylated 2-methyl-2-(4,8,12-trimethyltridecyl)chromans (MTTCs; **XLII**) are present in all three samples in relatively high concentrations (Table 4.4). They are dominated by 5,7,8-trimethyl MTTC, indicating a normal marine salinity of the photic zone (Sinninghe Damsté et al., 1987, 1993b). Their <sup>13</sup>C content (Table 4.2) is in agreement with their presumed algal origin (Sinninghe Damsté et al., 1993b).

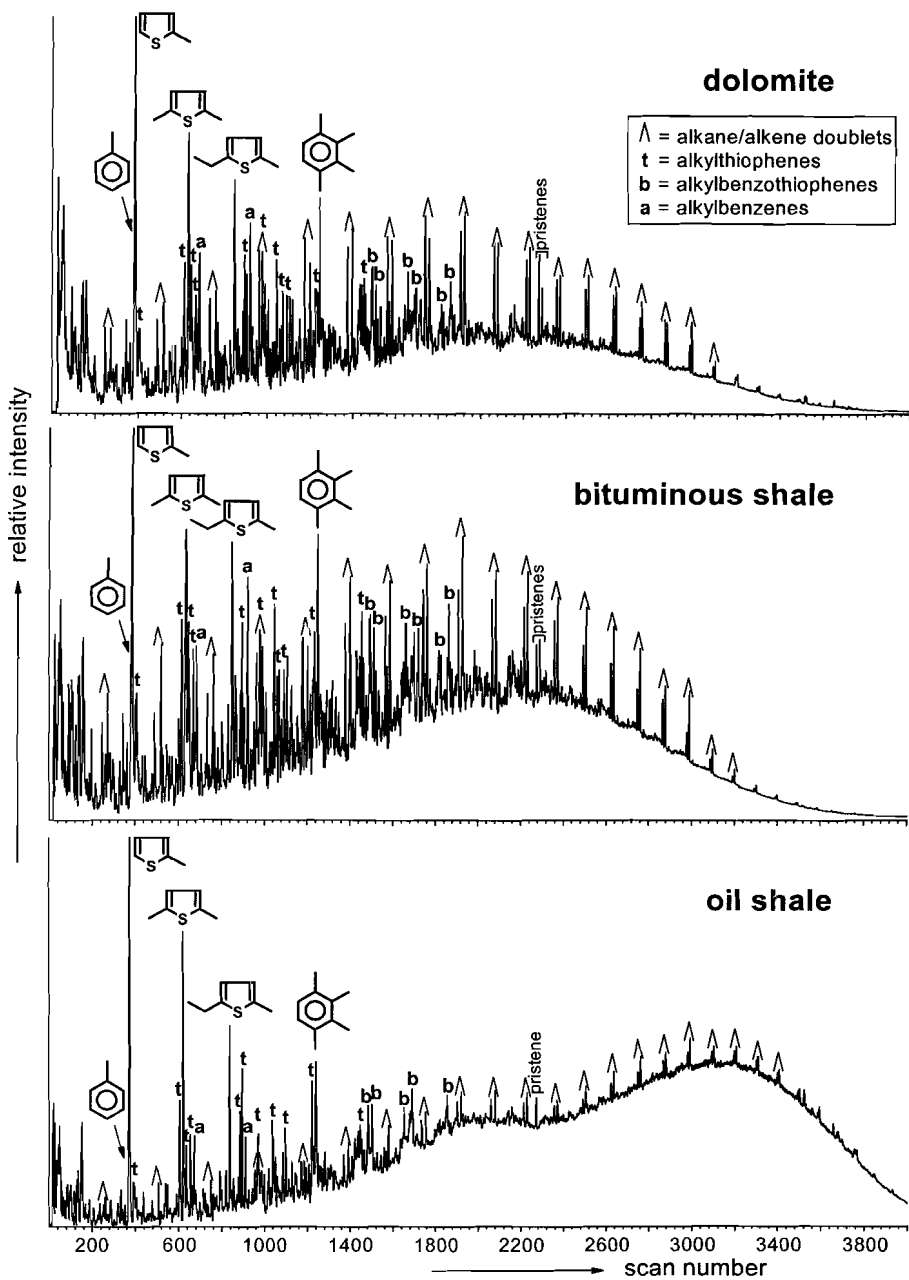


**Fig. 4.11.** Total ion current traces of flash pyrolysates of the kerogens at a Curie temperature of 610°C. The unresolved complex mixtures were not produced by the evaporation of low-molecular-weight compounds, because thermal extraction at 358°C did not yield any product.

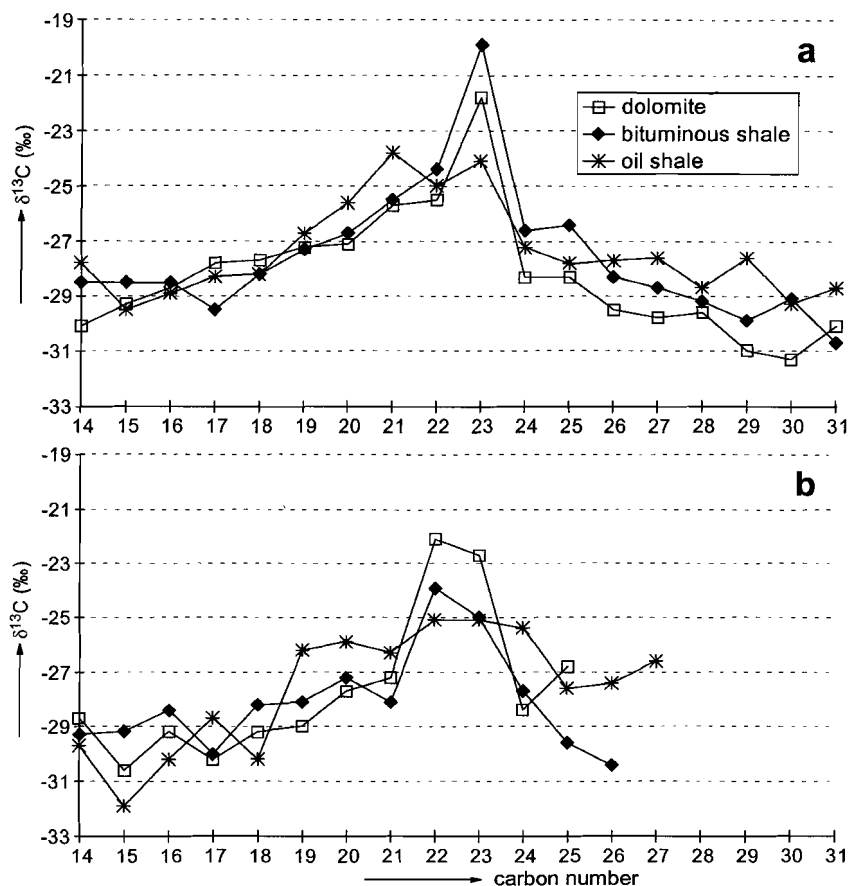


**Fig. 4.12.** Stable carbon isotopic compositions of (a)  $n$ -alkanes and (b)  $n$ -alkenes released upon pyrolysis of the different kerogens. The standard deviation of  $\delta^{13}\text{C}$  of  $\text{C}_{14}$ - $\text{C}_{25}$   $n$ -alkanes is typically 0.3‰;  $\delta^{13}\text{C}$  of  $\text{C}_{25+}$   $n$ -alkanes and  $\delta^{13}\text{C}$  of  $n$ -alkenes have a standard deviation of typically 0.8‰.

### *Kerogens*

Py-GC-MS of the kerogens (Fig. 4.11) revealed pairs of  $n$ -alkanes and  $n$ -alkenes, large quantities of sulfur compounds and an abundant 1,2,3,4-tetramethylbenzene (TMB) probably originating from sequestered isorenieratene (Hartgers et al., 1994), although other sources cannot be excluded (Hoefs et al., 1995). Phenolic pyrolysis products are minor, indicating that the contribution of lignins or biodegraded lignins to the kerogens is very small (Saiz-Jimenez and de Leeuw, 1984, 1986). The compound classes are the same in each of the pyrolysates, but the dominance of sulfur compounds, particularly that of  $\text{C}_1$ - $\text{C}_3$  alkylated thiophenes, over  $n$ -alkanes and  $n$ -alkenes is most pronounced in the oil shale. It should also be noted that the magnitude and shape of the UCMs (unresolved complex mixtures) differ considerably (Fig. 4.11). Because thermal extraction of the kerogens at

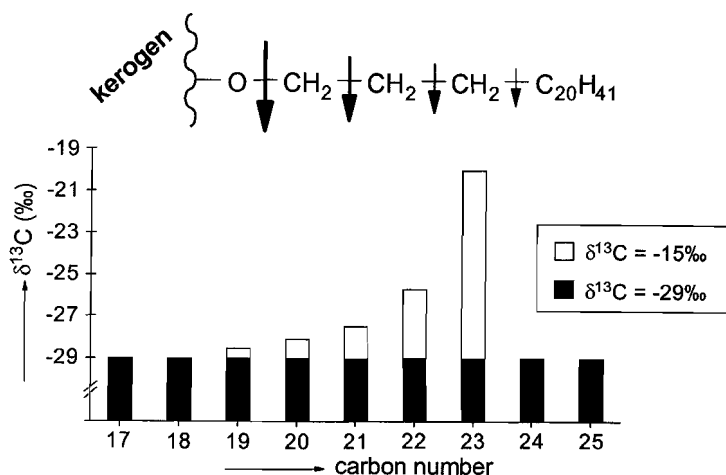


**Fig. 4.13.** Hypothetical scheme showing how the presence of a carbon isotopically heavy, ether-linked  $n\text{-C}_{23}$  may affect the isotopic composition of  $n\text{-alkanes}$  formed upon pyrolysis of kerogen.

358°C did not yield any products, these UCMs were not produced by the evaporation of low-molecular-weight compounds. In order to determine the relative amounts of  $n\text{-alkanes}$  released, their peak areas and the total area of pyrolysis products were integrated. The ratios of total pyrolysate versus total  $n\text{-alkanes}$  thus obtained (37, 39 and 160 in the dolomite, bituminous shale and oil shale, respectively), suggest that the relative contribution of  $n\text{-alkanes}$  to the pyrolysates decreases with increasing TOC. This is in accordance with the amounts of free  $n\text{-alkanes}$  in the extracts (Fig. 4.2), which are lowest in the oil shale and highest in the dolomite. The kerogens were also subjected to off-line pyrolysis, enabling compound-specific stable carbon isotope analysis of the  $n\text{-alkanes}$  and  $n\text{-alkenes}$ , discussed in detail below.

*Stable carbon isotopic composition of  $n\text{-alkanes}$  and  $n\text{-alkenes}$ .* The stable carbon isotopic compositions of  $n\text{-alkanes}$  and  $n\text{-alkenes}$  present in the off-line pyrolysates do not differ significantly among the samples, but there are large variations in  $\delta^{13}\text{C}$  among the different homologues (Fig. 4.12). The  $\delta^{13}\text{C}$  values of  $n\text{-alkanes}$  in the pyrolysates of the bituminous shale and dolomite show a distinct maximum at  $n\text{-C}_{23}$  (Fig. 4.12a). From this maximum there is a sharp drop towards the higher homologues, whereas in the direction of the lower homologues there is a more gradual decrease in  $\delta^{13}\text{C}$ . This pattern may be explained by the presence in the kerogen of a carbon isotopically heavy  $n\text{-C}_{23}$  moiety terminally linked to a heteroatom. Release of this moiety upon pyrolysis would then be favoured over the cleavage of one of its C-C bonds since the bond energies of C-S and C-O bonds are c. 70 and 40 kJ/mol smaller than that of a C-C bond (Claxton et al., 1993). Consequently, the moiety largely ends up as an  $n\text{-C}_{23}$  in the pyrolysate, causing the isotope excursion (Fig. 4.13). Obviously, the  $^{13}\text{C}$  content of the  $n\text{-C}_{23}$  moiety must be higher than that of  $n\text{-C}_{23}$  in the pyrolysate, because the latter is also derived from material more depleted in  $^{13}\text{C}$ . Since the recombination of two radicals formed upon pyrolysis was shown to be an insignificant



process (Hartgers et al., 1991), the  $C_{23}$   $n$ -alkanes in the pyrolysate probably originate from sources other than the  $C_{23}$  moiety. This explains the earlier mentioned sharp drop in  $\delta^{13}C$  for these  $n$ -alkanes. The gradual decrease in  $\delta^{13}C$  when going from  $n$ - $C_{23}$  to  $n$ - $C_{18}$  (Fig. 4.12a) is explained by a diminishing contribution of  $n$ -alkanes produced from the isotopically heavy  $n$ - $C_{23}$  moiety (Fig. 4.13). Thus, besides release of this moiety, cleavage of its C-C bonds does occur. Moreover, the closer the C-C bond to the heteroatom the more likely it is cleaved. Similar preferred cleavages are also apparent from the distribution of  $n$ -alkanes (and  $n$ -alkenes) in the pyrolysate of the oxygen cross-linked algaenan of the alga *Nannochloropsis salina* (Gelin et al., 1996). The maxima in these distributions, like the isotope excursions shown in Fig. 4.12a, are characterised by a gradual rise and a steep descent, although the feature is somewhat blurred due to additional alkyl groups in the algaenan. It is noteworthy that, although absolute  $\delta^{13}C$  values are 3‰ lighter,  $n$ -alkanes in several Central Graben oils also show a maximum  $^{13}C$  content at  $n$ - $C_{23}$  and a gradual decrease of  $\delta^{13}C$  with decreasing chain length (Bjørøy et al., 1994). This suggests a similar  $n$ - $C_{23}$  contribution to the kerogens of Kimmeridgian North Sea source rocks.

The  $\delta^{13}C$  values of  $n$ -alkanes in the pyrolysate of the oil shale show maxima both at  $n$ - $C_{21}$  and at  $n$ - $C_{23}$  (Fig. 4.12a), but these are less distinct than the maxima in the other samples. It is suggested that in the oil shale kerogen, along with the isotopically enriched  $n$ - $C_{23}$  moiety, an  $n$ - $C_{21}$  moiety is present which is also enriched in  $^{13}C$  and possibly linked *via* a heteroatom. This is supported by the fact that  $n$ -alkanes in the extract of the oil shale show more pronounced but similar isotope excursions (Fig. 4.2).

Interestingly,  $\delta^{13}C$  values of  $n$ -alkenes in the kerogen pyrolysates of the bituminous shale and dolomite are highest at  $n$ - $C_{22}$  and slightly lower at  $n$ - $C_{23}$  (Fig. 4.12b). Apparently, upon pyrolysis of the  $^{13}C$  enriched  $n$ - $C_{23}$  moiety in the kerogen, formation of the  $C_{22}$   $n$ -alkene is slightly favoured over that of the  $C_{23}$   $n$ -alkene. This is in accordance with the distribution of  $n$ -alk-1-enes released upon pyrolysis of silicon-bound  $n$ -octadecane (Hartgers et al., 1991), which is dominated by the  $C_{17}$   $n$ -alkene. It is noted that the  $n$ - $C_{22}$  alkene isotope excursion is less pronounced in the pyrolysate of the bituminous shale than in the pyrolysate of the dolomite (Fig. 4.12b), whereas the opposite holds for the isotope excursion of their  $n$ - $C_{23}$  alkanes (Fig. 4.12a). This is possibly related to the fact that in case of the bituminous shale measurements of  $\delta^{13}C$  were performed on clusters of  $n$ -alk-1-enes and  $n$ -alk-2-enes, whereas in the pyrolysate of the dolomite only  $n$ -alk-1-enes were measured. Isotope excursions of  $n$ -alkenes in the pyrolysate of the oil shale kerogen are obscure (Fig. 4.12b). Nevertheless,  $^{13}C$  contents are highest at  $n$ - $C_{20}$  and at  $n$ - $C_{22}$ , showing that  $n$ -alkenes released upon pyrolysis of the earlier mentioned isotopically heavy  $n$ - $C_{21}$  and  $n$ - $C_{23}$  alkane moieties, are dominated by  $n$ - $C_{20}$  and  $n$ - $C_{22}$ , respectively.

Although the kerogens are very rich in sulfur (Fig. 4.11), the moieties of  $n$ - $C_{23}$  and  $n$ - $C_{21}$  mentioned above are probably not sulfur-bound. In that case,  $n$ -alkanes released upon desulfurisation of the polar fractions are expected to show a relatively high abundance and high  $^{13}C$  content of  $n$ - $C_{23}$ , and in case of the oil shale also of  $n$ - $C_{21}$ . Due to low amounts  $\delta^{13}C$  values could not be determined, but the distributions of sulfur-bound  $n$ -alkanes neither maximise at  $n$ - $C_{21}$  nor at  $n$ - $C_{23}$ . On the contrary,  $n$ -alkanes released upon HI-treatment of the oil shale kerogen, by which ether bonds are selectively cleaved, did maximise at  $n$ - $C_{21}$  and  $n$ - $C_{23}$ . This suggests that the  $^{13}C$  enriched moieties of  $n$ - $C_{21}$  and  $n$ - $C_{23}$  are macromolecularly

**Table 4.6.** Stable carbon isotopic composition of bulk organic matter.

	$\delta^{13}\text{C}$ (‰)		
	dolomite	bituminous shale	oil shale
kerogen	-25.4 ± 0.2	-25.4 ± 0.2	-22.5 ± 0.2
non-volatile part of kerogen pyrolysate	-25.4 ± 0.2	-25.1 ± 0.2	-22.4 ± 0.2
residual kerogen after pyrolysis	-24.7 ± 0.2	-24.6 ± 0.2	-21.8 ± 0.2

linked *via* oxygen. Unfortunately, amounts of these *n*-alkanes were too low to determine  $^{13}\text{C}$  contents.

*Stable carbon isotopic composition of bulk OM.* In all three samples the kerogen and the non-volatile part of the pyrolysate (off-line) have similar stable carbon isotopic compositions, and the residual kerogen after pyrolysis is enriched in  $^{13}\text{C}$  by 0.7‰ compared to the original kerogen (Table 4.6). Thus, despite the release upon pyrolysis of different amounts of compositionally different OM (Fig. 4.11), the 2.9‰ difference between  $\delta^{13}\text{C}$  of the oil shale kerogen and  $\delta^{13}\text{C}$  of the other kerogens, is still present in the kerogen residues. This is not too surprising, as these residues amount to ca. 80% of the original kerogen. Since the  $\delta^{13}\text{C}$  values of the (non-volatile) pyrolysates are similar to those of the kerogens (Table 4.6), the enrichment in  $^{13}\text{C}$  of the residual kerogen after pyrolysis (Table 4.6) is probably caused by the release of gases depleted in  $^{13}\text{C}$  (e.g. methane). Also, since the (non-volatile) pyrolysates have  $^{13}\text{C}$  contents similar to those of the kerogens, and most of the  $\text{C}_{15}$ , *n*-alkanes and *n*-alkenes are depleted in  $^{13}\text{C}$  relative to the kerogen (Fig. 4.12), the contribution of these *n*-alkanes and *n*-alkenes to the pyrolysate is probably minor. This is in accordance with the results obtained by flash pyrolysis (Fig. 4.11), showing that the UCM constitutes the largest part of the pyrolysate.

### Palaeoenvironmental implications

The presence of a large suite of derivatives of isorenieratene in the three KCF samples indicates that at least periodically sedimentation took place in an euxinic water column that extended into the photic zone. This is a new finding, which may have important implications for our understanding of the formation of the KCF. Anoxia has been inferred to have played a major role in the depositional models for the KCF, but the presence of benthic macrofauna in mudstones containing very high amounts of OM (up to 10%; see Wignall, 1990) has been interpreted to indicate "recurrent periodic or seasonal but not continuous bottom water anoxia (Oschmann, 1988, 1991; Tyson, 1989)" (Tyson, 1996). This fits the actualistic model for the origin of OM-rich facies deposited in ancient epeiric seas (Tyson and Pearson, 1991), which is based on an analysis of anoxia in modern shelf seas. In this model a seasonal thermal stratification of the shallow waters in the epeiric seas, formed during major transgressions, is proposed, and the duration of the seasonal stratification period is thought to be dependent on astronomically forced, climatic variations. Our results indicate that during stratification the bottom waters have become completely devoid of oxygen, and hydrogen sulfide was generated by sulfate-reducing bacteria and was subsequently oxidised by phototrophic green sulfur bacteria residing at the chemocline, situated in the photic zone. It is not possible to determine the duration of these periods. The high concentrations of

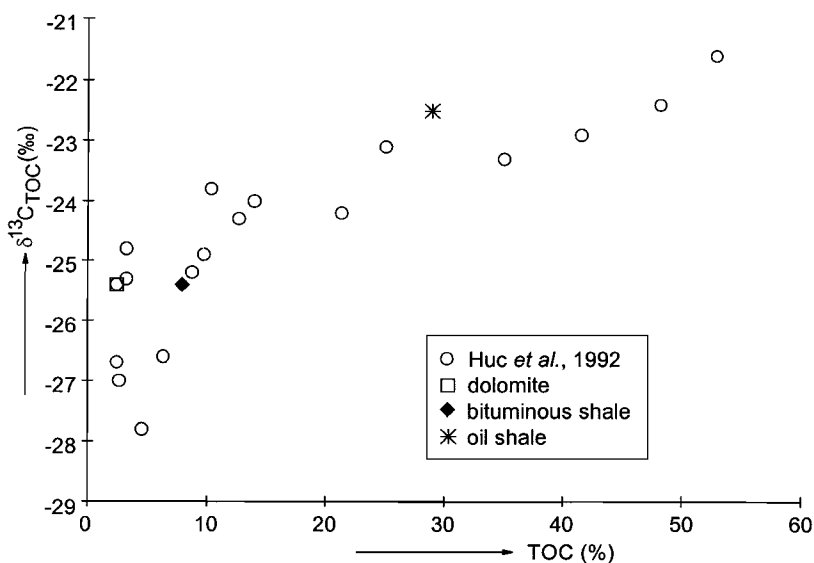


**Fig. 4.14.** Relationship between TOC and  $\delta^{13}\text{C}_{\text{TOC}}$  (after Huc *et al.*, 1992). Data from this study fit into the trend reported by Huc *et al.* (1992).

isorenieratene derivatives, which exceed the concentration of chlorophyll-derived phytane, seem to indicate that green sulfur bacteria were important organisms in the palaeoenvironment, suggesting that a more or less permanent stratification existed. Although the presence of benthos in the KCF indicates oxygenation events, there is no indication that oxic conditions were established for prolonged periods of time. Given the large amounts of OM preserved in the sediments, it seems more likely that oxic periods were relatively short-lived.

Huc *et al.* (1992) in their study of the KCF in Dorset found a positive correlation between TOC and  $\delta^{13}\text{C}_{\text{TOC}}$ . Our samples agree with this trend (Fig. 4.14): the dolomite and bituminous shale are depleted in  $^{13}\text{C}$  by 2.9‰ relative to the oil shale and have lower TOC contents. Huc *et al.* (1992) tentatively explained this trend by extensive reworking of biomass in the water column during deposition of the TOC-lean sediments. OM degradation would lead to release of  $\text{CO}_2$  relatively depleted in  $^{13}\text{C}$ , and its return to the surface water would decrease the  $^{13}\text{C}$  content of  $\text{CO}_2$  available for primary producers. The OM that is subsequently produced from the assimilation of this light  $\text{CO}_2$  would have a relatively low  $\delta^{13}\text{C}$ . Hollander *et al.* (1993a) reached a different conclusion with respect to the causes of high  $\delta^{13}\text{C}_{\text{TOC}}$  values of TOC-rich samples of the KCF. In their sample set, the  $\delta^{13}\text{C}$  values of primary carbonate varied from +1.2 to -2.2‰, but  $\delta^{13}\text{C}_{\text{TOC}}$  values varied much more (-21.6 to -28.0‰). Therefore, the decreasing  $\Delta\delta^{13}\text{C}_{\text{carbonate-kerogen}}$  with increasing Hydrogen Index (and TOC) was interpreted to suggest that “the accumulation of TOC-rich sediments occurred at a time when concentration of dissolved  $\text{CO}_2$  in surface waters was lowest, probably controlled by increasing productivity in surface waters which were  $\text{CO}_2$  limited”.

Although we do not have  $\delta^{13}\text{C}$  values of primary carbonate in our samples, both explanations seem in conflict with our molecular data. Pristane and phytane are derived predominantly from tocopherols (Goossens et al., 1984) and chlorophyll-a, respectively, and therefore, are good general indicators for  $\delta^{13}\text{C}$  values of lipids biosynthesised by primary producers. Their  $\delta^{13}\text{C}$  values, however, differ only 0.8-1.4‰ among the samples (Table 4.2). Similarly,  $\delta^{13}\text{C}$  values of cholestane, representing the “average”  $^{13}\text{C}$  content of algal steroids, do not differ more than 1‰ among the samples (Table 4.2). This implies that differences in  $\delta^{13}\text{C}$  of DIC ( $\delta^{13}\text{C}_{\text{DIC}}$ ), caused by changes in the extent of biological reworking in the water column (Huc et al., 1992), or differences in  $[\text{CO}_2]_{\text{aq}}$ , caused by changes in primary productivity (Hollander et al., 1993a), cannot fully account for the 3‰ difference in  $\delta^{13}\text{C}_{\text{TOC}}$ . This interpretation is supported by (i) similar  $\delta^{13}\text{C}$  values of *n*-alkanes in the off-line pyrolysates (Fig. 4.12), indicating similar  $\delta^{13}\text{C}$  values of algaenans biosynthesised in the upper part of the photic zone and (ii) similar  $\delta^{13}\text{C}$  values of isorenieratane indicating similar  $\delta^{13}\text{C}_{\text{DIC}}$  values at the chemocline (during fixation of  $\text{CO}_2$  by green sulfur bacteria there is hardly any fractionation relative to DIC, and therefore,  $\delta^{13}\text{C}$  values of their biomass are almost independent of  $[\text{CO}_2]_{\text{aq}}$ ; see Sinninghe Damsté et al., 1993c).

Assuming 1‰ of the 3‰ variation in  $\delta^{13}\text{C}_{\text{TOC}}$  to result from changes in  $\delta^{13}\text{C}_{\text{DIC}}$  and  $[\text{CO}_2]_{\text{aq}}$ , still 2‰ must be accounted for by other factors. Huc et al. (1992) considered the possibility of differences in the amount of terrestrial and marine OM as causes for the variations in TOC content and HI (which could also effect  $\delta^{13}\text{C}_{\text{TOC}}$ ) but concluded that this was unlikely. Differences in our smaller sample set are probably not caused by different contributions of terrestrial OM either since (i) HI values are relatively high and differ only slightly and (ii) py-GC-MS analyses indicate only small contributions from lignins or modified lignins. Therefore, the different sources of sedimentary OM have to be aquatic in origin.

Although extractable biomarkers cannot with certainty be used to identify the major sources of OM (Sinninghe Damsté et al., 1993a), they can be used to infer sources with distinct  $^{13}\text{C}$  contents that may have contributed to changes in  $\delta^{13}\text{C}_{\text{TOC}}$ . Steroid and hopanoid distributions in the oil shale differ from those in the other samples (Figs. 4.3, 4.4, 4.6), and this variation cannot be explained solely by diagenetic processes. Therefore, during deposition of the oil shale, the biota was of a different composition than during deposition of the other samples. However, this difference is not associated with increased abundances of isotopically heavy components (cf. Table 4.2), and therefore, is unlikely to account for the observed range of  $\delta^{13}\text{C}_{\text{TOC}}$  values. In the extracts, two groups of isotopically heavy lipids were recognised, which, if their source organisms would also contribute significantly to TOC, could explain differences of several per mil in  $\delta^{13}\text{C}_{\text{TOC}}$ . These groups are (i) isorenieratene derivatives with an average  $\delta^{13}\text{C}$  value of -17‰ and (ii) *n*- $\text{C}_{23}$  (in the oil shale also *n*- $\text{C}_{21}$ ) and *i*- $\text{C}_{27}$ , presumed to derive from the same unknown organism, with a  $\delta^{13}\text{C}$  value of ca. -14‰.

Indeed, the flash pyrolysates of the kerogens contain relatively large amounts of 1,2,3,4-TMB, which may be derived from sequestered isorenieratane skeletons in the kerogen (Hartgers et al., 1994). A quantitative study of a kerogen from the Duvernay Formation, of which the pyrolysate was completely dominated by 1,2,3,4-TMB, indicated

that an exceedingly high amount (ca. 1%) of TOC is derived from derivatives of diaromatic carotenoids, suggesting a large contribution of carbon isotopically heavy residue of biomass from green sulfur bacteria to  $C_{org}$ . (Hartgers et al., 1994). The  $\delta^{13}C_{TOC}$  was, however, close to that expected for purely algal debris, indicating that the large contribution of diaromatic carotenoids was unaccompanied by any other significant organic remains of green sulfur bacteria. Since the Duvernay kerogen should be considered as an endmember, it is unlikely that varying contributions of isorenieratene derivatives are the cause for changes in the  $^{13}C$  content of the KCF kerogens. This is also suggested by the similar concentrations of isorenieratene derivatives in the extracts (Table 4.4) and similar abundances of 1,2,3,4-TMB in the kerogen pyrolysates (Fig. 4.11).

The second carbon isotopically heavy source of lipids recognised in the extracts ( $n$ - $C_{23}$ ,  $n$ - $C_{21}$  and  $i$ - $C_{27}$ ) are also apparent, at least partially, from the enhanced  $\delta^{13}C$  values of  $C_{19}$ - $C_{23}$   $n$ -alkanes and  $n$ -alkenes in the pyrolysates (Fig. 4.12). Although these components are quantitatively unimportant contributors to  $C_{org}$ , variations in contributions of as yet unrecognised residues of biomass derived from the unknown precursor organism(s) could explain variations in the  $^{13}C$  content of the KCF kerogens. However, the stable carbon isotopic compositions of the  $C_{19}$ - $C_{23}$   $n$ -alkanes and  $n$ -alkenes in the pyrolysate (which probably represent a mixture derived from algaenan(s) with a  $\delta^{13}C$  value of ca. -29‰ and the specific source with a  $\delta^{13}C$  value of ca. -14‰) indicate that the contribution of the  $^{13}C$  enriched  $n$ -alkanes and  $n$ -alkenes to the pyrolysate of the oil shale is not more substantial than that of the other samples.

Since the extractable lipids do not provide a clue to the origin of the differences in the  $^{13}C$  content of the KCF kerogens, attention has to be focused on their pyrolysates. Bulk carbon isotopic compositions of the (non-volatile) off-line pyrolysates indicate that they are representative of the kerogen as a whole (Table 4.6). As already noted, the prominence of organic sulfur compounds and the large UCM are the major characteristics which distinguish the oil shale pyrolysate from the pyrolysates of the other samples (Fig. 4.11). Abundant alkylated thiophenes in kerogen pyrolysates are indicative of their richness in organic sulfur (Sinninghe Damsté et al., 1988, 1989, 1990; Eglinton et al., 1990). A positive correlation between TOC and the abundance of sulfur-rich OM in sediments of the KCF was also reported by Boussafir et al. (1995), although the differences in the abundance of thiophenes in the pyrolysates were not as pronounced as in our sample set. These authors attributed the variations in TOC to differences in primary production, and suggested that during periods with high phytoplankton productivity there would be enhanced sulfate reduction and enhanced preservation of lipids through sulfurisation of OM. However, our data indicate that also during deposition of the TOC-lean sediments, sulfide was present in the photic zone. Therefore, changes in phytoplankton productivity were probably not the principal cause of the euxinic conditions.

In summary, our analyses of samples of the Lower Kimmeridge Clay indicate that deposition took place in an environment in which there was photic zone anoxia for substantial periods of time. Sulfurisation was abundant even in the most organic-lean sample. The positive correlation between TOC and  $\delta^{13}C_{TOC}$  (Huc et al., 1992) cannot be explained by large changes in the concentration and isotopic composition of DIC as

previously proposed, and seems to be related to an increasing amount of organic sulfur with increasing TOC.

## Conclusions

1. Biomarker distributions in the KCF reveal that primary producers and other organisms that contributed to the OM in the oil shale, were of a different composition than those present during deposition of the dolomite and bituminous shale. The oil shale is also distinguished from the other sedimentary rocks in that it contains almost no rearranged steranes. This is probably due to the decreased clay/TOC ratio (four to six times lower) compared to the other samples.
2. Large amounts of isorenieratane and other diagenetic derivatives of isorenieratene, which testify to the presence of photosynthetic green sulfur bacteria, were found in three lithologically different samples of the KCF. This implies that, at least periodically, photic zone euxinia occurred in the KCF depositional environment.
3. An  $n$ -C<sub>23</sub> moiety, enriched in <sup>13</sup>C and probably terminally linked *via* oxygen, is present in the kerogens of the samples studied. The trend in  $\delta^{13}\text{C}$  of pyrolysis released  $n$ -alkanes is similar to those reported by Bjorøy et al. (1994) of  $n$ -alkanes in several Central Graben oils. This suggests the presence of a carbon isotopically heavy  $n$ -C<sub>23</sub> moiety in the kerogens of Kimmeridgian North Sea source rocks.
4. Irrespective of TOC, abundant sulfurisation of OM has taken place, as revealed by substantial amounts of organic sulfur compounds, including the sulfur-containing UCM, released upon pyrolysis of the kerogens. The dominance of C<sub>1</sub>-C<sub>3</sub> alkylated thiophenes over  $n$ -alkanes and  $n$ -alkenes is most pronounced in the pyrolysate of the most OM-rich sample.
5. Compound-specific stable carbon isotope data indicate that the positive correlation between TOC and  $\delta^{13}\text{C}_{\text{TOC}}$  of the KCF cannot be explained by differences in the extent of biological reworking in the water column (Huc et al., 1992), nor by varying [CO<sub>2</sub>]<sub>aq</sub> caused by changes in productivity (Hollander et al., 1993a). Concentrations and <sup>13</sup>C contents of lipid biomarkers, though different among themselves, do not differ substantially among the samples. Therefore, compositional changes in planktonic communities are not thought to have notably influenced  $\delta^{13}\text{C}_{\text{TOC}}$  either. Since not only  $\delta^{13}\text{C}_{\text{TOC}}$  but also the abundance of organic sulfur is positively correlated with TOC,  $\delta^{13}\text{C}_{\text{TOC}}$  is thought to be related to the degree of sulfurisation.

**Acknowledgements.** We thank the Netherlands Organization for Scientific Research (NWO) for the PIONIER grant to JSSD and the studentship of HMEvKP. We thank Shell International Petroleum Maatschappij BV for financial support for the GC-IRMS facility. Drs. R.V. Tyson, S.G. Wakeham and J.W. Collister are gratefully acknowledged for their comments on an earlier version of this paper. Samples were kindly provided by Dr. M.E.L. Kohnen (Koninklijke/Shell Exploratie en Productie Laboratorium). We thank R. Suijker, W. Pool and M. Dekker for analytical assistance. We are grateful to S.J. van der Gaast and R. Kloosterhuis for performing X-ray powder-diffraction and determining  $\delta^{13}\text{C}$  of bulk organic matter, respectively.

## References

- Bertrand P. and Lallier-Vergès E. (1993) Past sedimentary organic matter accumulation and degradation controlled by productivity. *Nature* **364**, 786-788.
- Bertrand P., Lallier-Vergès E., Martinez L., Pradier B., Tremblay P., Huc A., Jouhannel R. and Tricart J.P. (1990) Examples of spatial relationships between organic matter and mineral groundmass in the microstructure of the organic-rich Dorset Formation rocks, Great Britain. In *Advances in Organic Geochemistry 1989* (ed. B. Durand and F. Behar). *Org. Geochem.* **16**, 661-675.
- Bird C.W., Lynch J.M., Pirt F.J., Reid W.W., Brooks C.J.W. and Middleditch B.S. (1971) Steroids and squalene in *Methylococcus capsulatus* grown on methane. *Nature* **230**, 473-474.
- Bjorøy M., Hall P.B. and Moe R.P. (1994) Stable carbon isotope variation of *n*-alkanes in Central Graben oils. In *Advances in Organic Geochemistry 1993* (ed. N. Telnæs, G. van Graas and K. Øygard). *Org. Geochem.* **22**, 355-381.
- Boucher R.J., Standen G., Patience R.L. and Eglinton G. (1990) Molecular characterisation of kerogen from the Kimmeridge clay formation by mild selective chemical degradation and solid state <sup>13</sup>C-NMR. In *Advances in Organic Geochemistry 1989* (ed. B. Durand and F. Behar). *Org. Geochem.* **16**, 951-958.
- Boussafir M., Gelin F., Lallier-Vergès E., Derenne S., Bertrand P. and Largeau C. (1995) Electron microscopy and pyrolysis of kerogens from the Kimmeridge Clay Formation, UK: Source organisms, preservation processes, and origin of microcycles. *Geochim. Cosmochim. Acta* **59**, 3731-3747.
- Byers J.D. and Erdman J.G. (1981) Low temperature degradation of carotenoids as a model for early diagenesis in recent sediments. In *Advances in Organic Geochemistry 1981* (ed. M. Bjorøy et al.), 725-735. John Wiley, Chichester.
- Claxton M.J., Patience R.L. and Park P.J.D. (1993) Molecular modelling of bond energies in potential kerogen sub-units. In *Organic geochemistry: Poster sessions from the 16th international meeting on organic geochemistry, Stavanger 1993* (ed. K. Øygard et al.), pp. 198-201. Falch Hurtigtrykk, Oslo.
- Collister J.W., Summons R.E., Lichtfouse E. and Hayes J.M. (1992) An isotopic biogeochemical study of the Green River oil shale. *Org. Geochem.* **19**, 265-276.
- Cooper B.S., Barnard P.C. and Telnæs N. (1995) The Kimmeridge Clay Formation of the North Sea. In *Petroleum Source Rocks* (ed. B.J. Katz), pp. 89-110. Springer, Berlin.
- Cox B.M. and Gallois R.W. (1981) The stratigraphy of the Kimmeridge Clay of the Dorset type area and its correlation with some other Kimmeridgian sequences. *Rep. Inst. Geol. Sci.*, **80/4**, 1-44.
- Doré A.G., Vollset J. and Hamar G.P. (1985) Correlation of the off shore sequences referred to the Kimmeridge Clay Formation: Relevance to the Norwegian Sector. In *Petroleum Geochemistry in Exploration on the Norwegian Shelf* (Thomas B.M., ed.), Graham & Trotham, London, pp. 27-37.
- Downie C. (1957) Microplankton from the Kimmeridge Clay. *Q. J. Geol. Soc. London* **112**, 413-434.
- Eglinton T.I., Philp R.P. and Rowland S.J. (1988) Flash pyrolysis of artificially matured kerogens from the Kimmeridge Clay, U.K. *Org. Geochem.* **12**, 33-41.
- Eglinton T.I., Sinninghe Damsté J.S., Kohnen M.E.L. and de Leeuw J.W. (1990) Rapid estimation of the organic sulfur content of kerogens, coals and asphaltenes by pyrolysis-gas chromatography. *Fuel* **69**, 1394-1404.
- Farrimond P., Comet P., Eglinton G., Evershed R.P., Hall M.A., Park D.W. and Wardroper A.M.K. (1984) Organic geochemical study of the Upper Kimmeridge Clay of the Dorset type area. *Mar. Petrol. Geol.* **1**, 340-354.
- Freeman K.H., Boreham C.J., Summons R.E. and Hayes J.M. (1994a) The effect of aromatization on the isotopic compositions of hydrocarbons during early diagenesis. *Org. Geochem.* **21**, 1037-1049.

- Freeman K.H., Wakeham S.G. and Hayes J.M. (1994b) Predictive isotopic biogeochemistry: Hydrocarbons from anoxic marine basins. *Org. Geochem.* **21**, 629-644.
- Gelin F., Boogers I., Noordeloos A.A.M., Sinninghe Damsté J.S., Hatcher P.G. and de Leeuw J.W. (1996) Novel, resistant microalgal polyethers: An important sink of organic carbon in the marine environment? *Geochim. Cosmochim. Acta* **60**, 1275-1280.
- Goericke R., Montoya J.P. and Fry B. (1994) Physiology of isotopic fractionation in algae and cyanobacteria. In *Stable Isotopes in Ecology and Environmental Science* (ed. K. Lajtha and R.H. Michener), pp. 187-221. Blackwell Scientific Publications, Oxford.
- Goossens H., de Leeuw J.W., Schenck P.A. and Brassell S.C. (1984) Tocopherols as likely precursors of pristane in ancient sediments and crude oils. *Nature* **312**, 440-442.
- Goossens H., Due A., de Leeuw J.W., van de Graaf B. and Schenck P.A. (1988) The Pristane Formation Index, a new molecular maturity parameter. A simple method to assess maturity by pyrolysis/evaporation-gas chromatography of unextracted samples. *Geochim. Cosmochim. Acta* **52**, 1189-1193.
- Hartgers W.A., Sinninghe Damsté J.S. and de Leeuw J.W. (1991) Flash pyrolysis of silicon-bound hydrocarbons. *J. Anal. Appl. Pyrol.* **20**, 141-150.
- Hartgers W.A., Sinninghe Damsté J.S., Requejo A.G., Allan J., Hayes J.M., Ling Y., Xie T., Primack J. and de Leeuw J.W. (1994) A molecular and carbon isotopic study towards the origin and diagenetic fate of diaromatic carotenoids. In *Advances in Organic Geochemistry 1993* (ed. N. Telnæs, G. van Graas and K. Øygaard). *Org. Geochem.* **22**, 703-725.
- Hayes J.M., Freeman K.H., Popp B.N. and Hoham C.H. (1990) Compound-specific isotopic analyses: A novel tool for reconstruction of ancient biogeochemical processes. In *Advances in Organic Geochemistry 1989* (ed. B. Durand and F. Behar). *Org. Geochem.* **16**, 1115-1128.
- Herbin J.P., Müller C., Geyssant J.R., Mélières F., Penn I.E. and the Yorkim Group (1993) Variation of the distribution of organic matter within a transgressive system tract: Kimmeridge Clay (Jurassic), England. In *Source Rocks in a Sequence Stratigraphic Framework* (ed. B.J. Katz and L.M. Pratt), *AAPG Studies in Geology* **37**, pp. 67-100. Amer. Assoc. of Petrol. Geol.
- Hoefs M.J.L., van Heemst J.D.H., Gelin F., Koopmans M.P., van Kaam-Peters H.M.E., Schouten S., de Leeuw J.W. and Sinninghe Damsté J.S. (1995) Alternative biological sources for 1,2,3,4-tetramethylbenzene in flash pyrolysates of kerogen. *Org. Geochem.* **23**, 975-979.
- Hollander D.J., McKenzie J.A., Hsu K.J. and Huc A.Y. (1993a) Application of an eutrophic lake model to the origin of ancient organic-carbon-rich sediments. *Global Biogeochem. Cycles* **7**, 157-179.
- Hollander D.J., Sinninghe Damsté J.S., Hayes J.M., de Leeuw J.W. and Huc A.Y. (1993b) Molecular and bulk isotopic analyses of organic matter in marls of the Mulhouse Basin (Tertiary, Alsace, France). *Org. Geochem.* **20**, 1253-1263.
- Huc A.Y., Lallier-Vergès E., Bertrand P., Carpentier B. and Hollander D.J. (1992) Organic Matter Response to Change of Depositional Environment in Kimmeridgian Shales, Dorset, U.K. In *Organic Matter: Productivity, Accumulation, and Preservation in Recent and Ancient Sediments* (ed. J.K. Whelan and J.W. Farrington), pp. 469-486. Columbia Univ. Press.
- Irwin H., Curtis C. and Coleman M. (1977) Isotopic evidence for source of diagenetic carbonates formed during burial of organic-rich sediments. *Nature* **269**, 209-213.
- Jiang Z.S. and Fowler M.G. (1986) Carotenoid-derived alkanes in oils from northwestern China. In *Advances in Organic Geochemistry 1985* (ed. D. Leythaeuser and J. Rullkötter). *Org. Geochem.* **10**, 831-839.
- van Kaam-Peters H.M.E., Köster J., van der Gaast S.J., Sinninghe Damsté J.S. and de Leeuw J.W. (1997a) The effect of clay minerals on diasterane/sterane ratios. In prep.
- van Kaam-Peters H.M.E., Schouten S., Schoell M. and Sinninghe Damsté J.S. (1997b) Biomarker and compound-specific stable carbon isotope analysis of the Early Toarcian shales in SW Germany. In prep.
- Kenig F., Sinninghe Damsté J.S., Hayes J.M. and de Leeuw J.W. (1995) Molecular indicators of palaeoenvironmental change in a Messinian evaporitic sequence (Vena del Gesso, Italy): II. High-resolution variations in abundances and <sup>13</sup>C contents of free and sulfur-bound carbon skeletons in a single marl bed. *Org. Geochem.* **23**, 485-526.



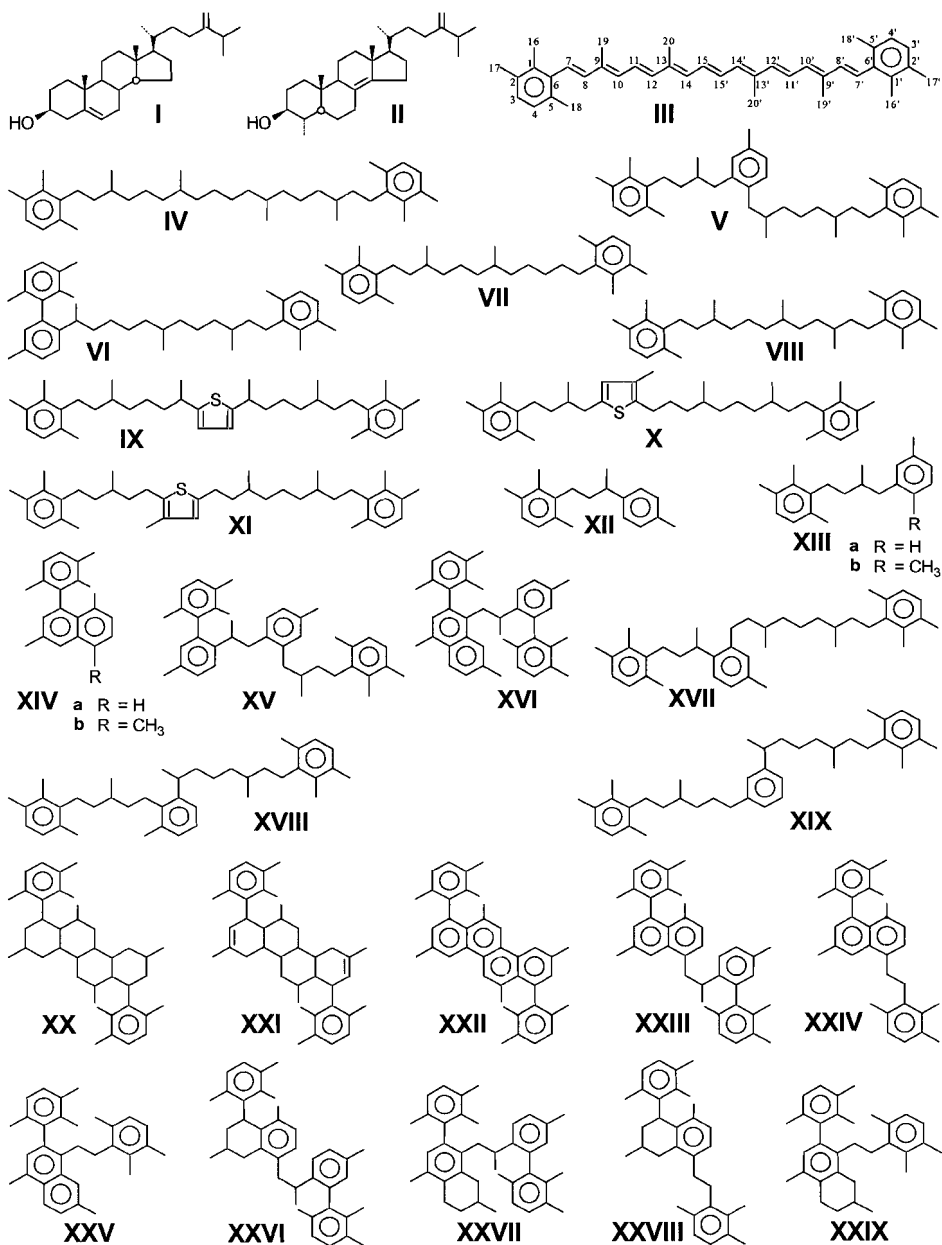
- Kohnen M.E.L., Sinninghe Damsté J.S., Rijpstra W.I.C. and de Leeuw J.W. (1990) Alkylthiophenes as sensitive indicators of palaeoenvironmental changes: A study of a Cretaceous oil shale from Jordan. In *Geochemistry of Sulfur in Fossil Fuels* (ed. W.L. Orr and C.M. White), *ACS Symposium Series 429*, pp. 444-485. Amer. Chem. Soc., Washington.
- Kohnen M.E.L., Schouten S., Sinninghe Damsté J.S., de Leeuw J.W., Merritt D.A. and Hayes J.M. (1992) Recognition of paleobiochemicals by a combined molecular sulfur and isotope geochemical approach. *Science* **256**, 358-362.
- Kok M.D., Schouten S. and Sinninghe Damsté J.S. (1995) Laboratory simulation of natural sulfurization: The reactivity of some functionalized model compounds and the catalytic influence of sediment. In *Organic Geochemistry: Developments and Applications to Energy, Climate, Environment and Human History* (ed. J.O. Grimalt et al.), pp. 1047-1049. A.I.G.O.A., Donostia-San Sebastián.
- Kokke W.C.M.C., Fenical W. and Djerassi C. (1981) Sterols with unusual nuclear unsaturation from three cultured marine dinoflagellates. *Phytochem.* **20**, 127-134.
- Koopmans M.P., Köster J., van Kaam-Peters H.M.E., Kenig F., Schouten S., Hartgers W.A., de Leeuw J.W. and Sinninghe Damsté J.S. (1996) Diagenetic and catagenetic products of isorenieratene: Molecular indicators for photic zone anoxia. *Geochim. Cosmochim. Acta.* **60**, 4467-4496.
- Koopmans M.P., de Leeuw J.W. and Sinninghe Damsté J.S. (1997) Novel cyclised and aromatised diagenetic products of b-carotene in the Green River Shale. *Org. Geochem.* In press.
- Köster J., van Kaam-Peters H.M.E., Koopmans M.P., de Leeuw J.W. and Sinninghe Damsté J.S. (1997) Sulphurisation of homohopanooids: Effects on carbon number distribution, speciation and 22S/22R epimer ratios. *Geochim. Cosmochim. Acta* **61**, 2431-2452.
- Laws E.A., Popp B.N., Bidigare R.R., Kennicutt M.C. and Macko S.A. (1995) Dependence of phytoplankton carbon isotopic composition on growth rate and  $[CO_2]_{aq}$ : Theoretical considerations and experimental results. *Geochim. Cosmochim. Acta* **59**, 1131-1138.
- de Leeuw J.W., Rijpstra W.I.C., Schenck P.A. and Volkman J.K. (1983) Free, esterified and residual bound sterols in Black Sea Unit 1 sediments. *Geochim. Cosmochim. Acta* **47**, 455-465.
- Miller R.G. (1990) A paleo-oceanographic approach to the Kimmeridge Clay Formation. In *Deposition of organic facies* (ed. A.Y. Huc), *AAPG Studies in Geology* **30**, pp. 13-26. Amer. Assoc. of Petrol. Geol.
- Moldowan J.M., Fago F.J., Lee C.J., Jacobson S.R., Watt D.S., Slougui N.-E., Jeganathan A. and Young D.C. (1990) Sedimentary 24-n-propylcholestanes, molecular fossils diagnostic of marine algae. *Science* **247**, 309-312.
- Oschmann W. (1988) Kimmeridge Clay sedimentation - A new cyclic model. *Palaeogeogr. Palaeoclimatol. Palaeoecol.* **65**, 217-251.
- Oschmann W. (1991) Distribution, dynamics and palaeoecology of Kimmeridgian (Upper Jurassic) shelf anoxia in western Europe. In *Modern and Ancient Continental Shelf Anoxia* (ed. R.V. Tyson and T.H. Pearson), *Geological Society Special Publication* **58**, pp. 381-395.
- Peakman T.M., ten Haven H.L., Rechka J.R., de Leeuw J.W. and Maxwell J.R. (1989) Occurrence of (20R)- and (20S)- $\Delta^8(14)$  and  $\Delta^{14}$  5 $\alpha$ (H)-sterenes and the origin of 5 $\alpha$ (H),14 $\beta$ (H),17 $\beta$ (H)-steranes in an immature sediment. *Geochim. Cosmochim. Acta* **53**, 2001-2009.
- Peters K.E. and Moldowan J.M. (1993) *The Biomarker Guide*. Prentice-Hall, London. 363 pp.
- Quandt I., Gottschalk G., Ziegler H. and Stichler W. (1977) Isotope discrimination by photosynthetic bacteria. *FEMS Microbiol. Lett.* **1**, 125-128.
- Ramanampisoa L. and Disnar J.R. (1994) Primary control of paleoproduction on organic matter preservation and accumulation in the Kimmeridge rocks of Yorkshire (UK). *Org. Geochem.* **21**, 1153-1167.
- Repeta D.J. (1993) A high resolution historical record of Holocene anoxygenic primary production in the Black Sea. *Geochim. Cosmochim. Acta* **57**, 4337-4342.
- Rubinstein I., Sieskind O. and Albrecht P. (1975) Rearranged sterenes in a shale: Occurrence and simulated formation. *J. Chem. Soc., Perkin Trans. I*, 1833-1836.
- Saiz-Jimenez C. and de Leeuw J.W. (1984) Pyrolysis-gas chromatography-mass spectrometry of isolated, synthetic and degraded lignins. In *Advances in Organic Geochemistry 1983* (ed. P.A. Schenck, J.W. de Leeuw and G.W.M. Lijmbach). *Org. Geochem.* **6**, 417-422.

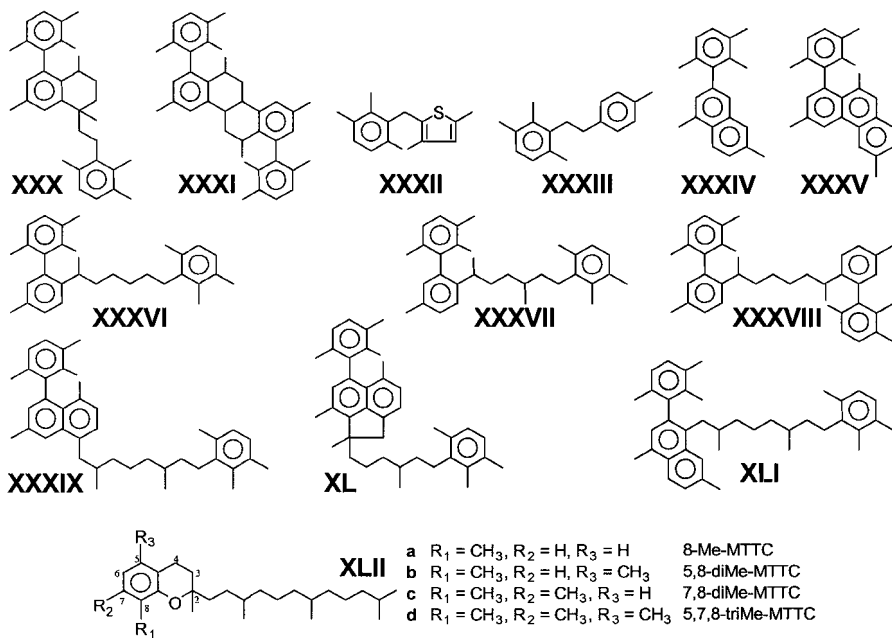
- Saiz-Jimenez C. and de Leeuw J.W. (1986) Lignin pyrolysis products: Their structures and their significance as biomarkers. In *Advances in Organic Geochemistry 1985* (ed. D. Leythaeuser and J. Rullkötter). *Org. Geochem.* **10**, 869-876.
- Schaefflé J., Ludwig B., Albrecht P. and Ourisson G. (1977) Hydrocarbures aromatiques d'origine géologique. II. Nouveaux caroténoïdes aromatiques fossiles. *Tetrahedron Lett.* **41**, 3673-3676.
- Schoell M., Hwang R.J., Carlson R.M.K. and Welton J.E. (1994) Carbon isotopic composition of individual biomarkers in gilsonites (Utah). *Org. Geochem.* **21**, 673-683.
- Schouten S., de Graaf W., Sinninghe Damsté J.S., van Driel G.B. and de Leeuw J.W. (1994) Laboratory simulation of natural sulfurization: II. Reaction of multi-functionalized lipids with inorganic polysulfides at low temperatures. In *Advances in Organic Geochemistry 1993* (ed. N. Telnæs, G. van Graas and K. Oygard). *Org. Geochem.* **22**, 825-834.
- Schouten S., Baas M., van Kaam-Peters H.M.E. and Sinninghe Damsté J.S. (1997) Long-chain 3-isopropylalkanes: A new class of sedimentary branched acyclic hydrocarbons. *Geochim. Cosmochim. Acta*. Submitted.
- Schouten S., Schoell M., Summons R.E., Sinninghe Damsté J.S. and Leeuw J.W. (1997) Molecular biogeochemistry of Monterey sediments Naples Beach, USA II: Carbon isotopic compositions of free and sulfur-bound carbon skeletons. In *The Monterey Formation: From rock to molecule* (ed. C.M. Isaacs and J. Rullkötter). Columbia Univ. Press. In press.
- Schwark L. and Püttmann W. (1990) Aromatic hydrocarbon composition of the Permian Kupferschiefer in the Lower Rhine Basin, NW Germany. In *Advances in Organic Geochemistry 1989* (ed. B. Durand and F. Behar). *Org. Geochem.* **16**, 749-761.
- Sieskind O., Joly G. and Albrecht P. (1979) Simulation of the geochemical transformation of sterols: superacid effect of clay minerals. *Geochim. Cosmochim. Acta* **43**, 1675-1679.
- Sieskind O., Kintzinger J.P., Metz B. and Albrecht P. (1995) Structure determination of diacholestanes. Their geochemical significance. *Tetrahedron* **51**, 2009-2022.
- Sinninghe Damsté J.S., Kock-van Dalen A.C., de Leeuw J.W., Guoying S. and Brassell S.C. (1987) The identification of mono-, di- and trimethyl 2-methyl-2-(4,8,12-trimethyltridecyl)chromans and their occurrence in the geosphere. *Geochim. Cosmochim. Acta* **51**, 2393-2400.
- Sinninghe Damsté J.S., Kock-van Dalen A.C., de Leeuw J.W. and Schenck P.A. (1988) Identification of homologous series of alkylated thiophenes, thiolanes, thianes and benzothiophenes present in pyrolysates of sulfur-rich kerogens. *J. Chromatogr.* **435**, 435-452.
- Sinninghe Damsté J.S., Eglinton T.I., de Leeuw J.W. and Schenck P.A. (1989) Organic sulfur in macromolecular sedimentary organic matter: I. Structure and origin of sulfur-containing moieties in kerogen, asphaltenes and coal as revealed by flash pyrolysis. *Geochim. Cosmochim. Acta* **53**, 873-889.
- Sinninghe Damsté J.S., Eglinton T.I., Rijpstra W.I.C. and de Leeuw J.W. (1990) Characterisation of sulfur-rich high molecular weight substances by flash pyrolysis and Raney Ni desulfurisation. In *Geochemistry of Sulfur in Fossil Fuels* (ed. W.L. Orr and C.M. White), *ACS Symposium Series* **429**, pp. 486-528. Amer. Chem. Soc., Washington.
- Sinninghe Damsté J.S., de las Heras F.X.C., van Bergen P.F. and de Leeuw J.W. (1993a) Characterization of Tertiary Catalan lacustrine oil shales: Discovery of extremely organic sulfur-rich Type I kerogens. *Geochim. Cosmochim. Acta* **57**, 389-415.
- Sinninghe Damsté J.S., Keely B.J., Betts S.E., Baas M., Maxwell J.R. and de Leeuw J.W. (1993b) Variations in abundances and distributions of isoprenoid chromans and long-chain alkylbenzenes in sediments of the Mulhouse Basin: a molecular sedimentary record of palaeosalinity. *Org. Geochem.* **20**, 1201-1215.
- Sinninghe Damsté J.S., Wakeham S.G., Kohlen M.E.L., Hayes J.M. and de Leeuw J.W. (1993c) A 6,000-year sedimentary molecular record of chemocline excursions in the Black Sea. *Nature* **362**, 827-829.
- Sinninghe Damsté J.S., Köster J., Baas M., Koopmans M.P., van Kaam-Peters H.M.E., Geenevasen J.A.J. and Kruk C. (1995a) Cyclisation and aromatisation of carotenoids during sediment diagenesis. *J. Chem. Soc., Chem. Commun.*, 187-188.

- Sinninghe Damsté J.S., van Duin A.C.T., Hollander D., Kohnen M.E.L. and de Leeuw J.W. (1995b) Early diagenesis of bacteriohopanepolyol derivatives: Formation of fossil homohopanooids. *Geochim. Cosmochim. Acta* **59**, 5141-5147.
- Sirevåg R. and Ormerod J.G. (1970) Carbon dioxide fixation in green sulfur bacteria. *Biochem. J.* **120**, 399-408.
- Sirevåg R., Buchanan B.B., Berry J.A. and Troughton J.H. (1977) Mechanisms of CO<sub>2</sub> fixation in bacterial photosynthesis studied by the carbon isotope fractionation technique. *Arch. Microbiol.* **112**, 35-38.
- Stoilov I., Kolaczowska E., Pyrek J.S., Brock C.P., Watt D.S., Carlson R.M.K. and Moldowan J.M. (1992) A synthesis of C-23 and C-24 diastereomers of 5 $\alpha$ -dinosterane. *Tetrahedron Lett.* **33**, No. 50, 7689-7692.
- Stoilov I., Smith S.L., Watt D.S., Carlson R.M.K., Fago F.J. and Moldowan J.M. (1994) <sup>1</sup>H and <sup>13</sup>C NMR analysis of C-23 and C-24 Diastereomers of 5 $\alpha$ -dinosterane. *Magn. Res. Chem.* **32**, 101-106.
- Summons R.E. and Powell T.G. (1987) Identification of aryl isoprenoids in source rocks and crude oils: Biological markers for the green sulfur bacteria. *Geochim. Cosmochim. Acta* **51**, 557-566.
- Summons R.E., Volkman J.K. and Boreham C.J. (1987) Dinosterane and other steroidal hydrocarbons of dinoflagellate origin in sediments and petroleum. *Geochim. Cosmochim. Acta* **51**, 3075-3082.
- Summons R.E., Thomas J., Maxwell J.R. and Boreham C.J. (1992) Secular and environmental constraints on the occurrence of dinosterane in sediments. *Geochim. Cosmochim. Acta* **56**, 2437-2444.
- Summons R.E., Jahnke L.L. and Roksandic Z. (1994) Carbon isotopic fractionation in lipids from methanotrophic bacteria: Relevance for interpretation of the geochemical record of biomarkers. *Geochim. Cosmochim. Acta* **58**, 2853-2863.
- Tribouillard N., Desprairies A., Lallier-Vergès E., Bertrand P., Moureau N., Ramdani A. and Ramanampisoa L. (1994) Geochemical study of organic-matter rich cycles from the Kimmeridge Clay Formation of Yorkshire (UK): productivity versus anoxia. *Palaeogeogr. Palaeoclimatol. Palaeoecol.* **108**, 165-181.
- Tyson R.V. (1985) *Palynofacies and Sedimentology of Some Late Jurassic Sediments from the British Isles and Northern North Sea*. Ph.D. thesis. The Open University, Milton Keynes. 623 pp.
- Tyson R.V. (1989) Late Jurassic palynofacies trends, Piper and Kimmeridge Clay Formations, UK onshore and northern North Sea. In *Northwestern European Micropalaeontology and Palynology* (ed. D.J. Batten and M.C. Keen), British Micropalaeontological Society Series, Ellis Horwood, Chichester, pp. 135-172.
- Tyson R.V. (1996) Sequence stratigraphical interpretation of organic facies variations in marine siliciclastic systems: General principles and application to the onshore Kimmeridge Clay Formation, UK. In *Sequence Stratigraphy in British Geology* (ed. S. Hesselbo and N. Parkinson), Geol. Soc. Lond. Spec. Publ. **103**, 75-96.
- Tyson R.V. and Pearson T.H. (1991) Modern and ancient continental shelf anoxia: An overview. In *Modern and Ancient Continental Shelf Anoxia* (ed. R.V. Tyson and T.H. Pearson), Geol. Soc. Lond. Spec. Publ. **58**, 1-24.
- Tyson R.V., Wilson R.C.L. and Downie C. (1979) A stratified water column environmental model for the type Kimmeridge Clay. *Nature* **277**, 377-380.
- van der Gaast S.J. and Vaars A.J. (1981) A method to eliminate the background in X-ray diffraction patterns of oriented clay mineral samples. *Clay Miner.* **16**, 383-393.
- van Kaam-Peters H.M.E., Schouten S., Leeuw J.W. de and Sinninghe Damsté J.S. (1995) The Kimmeridge clay formation: Biomarker and molecular stable carbon isotope analysis. In: *Organic Geochemistry: Developments and Applications to Energy, Climate, Environment and Human History*, (ed. J.A. Grimalt and C. Dorronsoro), A.I.G.O.A., San Sebastian, pp. 216-218.
- Volkman J.K., Gagosian R.B. and Wakeham S.G. (1984) Free and esterified sterols of the marine dinoflagellate *Gonyaulax polygramma*. *Lipids* **19**, 457-465.

- Volkman J.K., Kearney P. and Jeffrey S.W. (1990) A new source of 4-methyl sterols and 5 $\alpha$ (H)-stanols in sediments: prymnesiophyte microalgae of the genus *Pavlova*. *Org. Geochem.* **15**, 489-497.
- Wakeham S.G., Sinninghe Damsté J.S., Kohnen M.E.L. and de Leeuw J.W. (1995) Organic sulfur compounds formed during early diagenesis in Black Sea sediments. *Geochim. Cosmochim. Acta* **59**, 521-533.
- Wengrovitz P.S., Sanduja R. and Alam M. (1981) Dinoflagellate sterols-3: Sterol composition of the dinoflagellate *Gonyaulax monilata*. *Comp. Biochem. Physiol.* **69B**, 535-539.
- Wignall P.B. (1989) Sedimentary dynamics of the Kimmeridge Clay: tempests and earthquakes. *J. Geol. Soc. London* **146**, 273-284.
- Wignall P.B. (1990) *Benthic Palaeoecology of the Late Jurassic Kimmeridge Clay of England*. Special Papers in Palaeontology **43**.
- Williams P.F.V. and Douglas A.G. (1980) A preliminary organic geochemical investigation of the Kimmeridgian oil shales. In *Advances in Organic Geochemistry 1979* (ed. A.G. Douglas and J.R. Maxwell), pp. 531-545. Pergamon, Oxford.
- Williams P.F.V. and Douglas A.G. (1983) The effect of lithologic variation on organic geochemistry in the Kimmeridge Clay of Britain. In *Advances in Organic Geochemistry 1981* (ed. M. Bjorøy et al.), pp. 568-575. Wiley, Chichester.
- Withers N.W. (1987) Dinoflagellate sterols. In *The Biology of Dinoflagellates* (ed. F.J.R. Taylor), Chap. 9, pp. 316-359. Blackwell Scientific Publications, Oxford.
- Withers N.W., Tuttle R.C., Holz G.G., Beach D.H., Goad L.J. and Goodwin T.W. (1978) Dehydrodinosterol, dinosterone and related sterols of a non-photosynthetic dinoflagellate, *Cryptocodinium cohnii*. *Phytochem.* **17**, 1987-1989.
- Withers N.W., Tuttle R.C., Goad L.J. and Goodwin T.W. (1979) Dinosterol side chain biosynthesis in a marine dinoflagellate, *Cryptocodinium cohnii*. *Phytochemistry* **18**, 71-73.

# Appendix





## Chapter 5

### Palaeoclimatic control on the molecular and carbon isotopic composition of organic matter deposited in a Kimmeridgian euxinic shelf sea.

#### Abstract

Thirteen samples from the Kimmeridge Clay Formation (KCF) in Dorset, covering all different lithologies, were studied using bulk and molecular geochemical and microscopical techniques. Our data show that the positive correlation between TOC and  $\delta^{13}\text{C}_{\text{TOC}}$  reported for shales (Huc et al., 1992) also holds for other lithologies (e.g. limestones) if we correct for dilution by carbonate (TOC\*). Despite the wide range of  $\delta^{13}\text{C}_{\text{TOC}}$  values (-26.7 to -20.7‰), the  $\delta^{13}\text{C}$  values of individual biomarkers of algal and green sulfur bacterial origin and of kerogen pyrolysis products (i.e. *n*-alkanes) show in general only small changes (<2‰). This indicates that changes in the concentration of dissolved inorganic carbon (DIC) or  $\delta^{13}\text{C}$  of DIC ( $\delta^{13}\text{C}_{\text{DIC}}$ ) in the palaeowater column cannot account for the 6‰ difference in  $\delta^{13}\text{C}_{\text{TOC}}$ .

Kerogen pyrolysates indicated that with increasing TOC\*, and thus increasing  $\delta^{13}\text{C}_{\text{TOC}}$ , carbon isotopically heavy  $\text{C}_1$ - $\text{C}_3$  alkylated thiophenes with a linear carbon skeleton become increasingly abundant; in the case of the Blackstone Band kerogen (TOC\* = 63%) they dominate the pyrolysate. These thiophenes are probably derived from sulfur-bound carbohydrates in the kerogen. Algal carbohydrates are typically 5-10‰ heavier than algal lipids and differences in preservation of labile carbohydrate carbon through sulfuration may thus explain the range in  $\delta^{13}\text{C}_{\text{TOC}}$  values without the need to invoke any change in water column conditions. The increasing dominance of thiophenes in the kerogen pyrolysate with increasing TOC\* is consistent with the increasing Sulfur Index (mg kerogen S/g TOC) and the increasing dominance of orange amorphous organic matter produced by natural sulfuration.

The organic matter of all sediments was deposited under euxinic conditions as revealed by the occurrence of isorenieratene derivatives indicating (periodic) photic zone euxinia. At times of reduced run-off from the hinterland, represented by so-called condensed sections, the flux of reactive iron was relatively small compared to the flux of reactive organic matter, which resulted in the formation of relatively small amounts of pyrite and an excess of hydrogen sulfide capable of reacting with fresh organic matter. Within the condensed sections, variations in the degree of sulfuration of organic matter are probably due to both differences in primary production and differences in the supply of reactive iron.

In summary, our data demonstrate that climatic changes, probably driven by Milankovitch cycles, can have a large impact on the molecular and carbon isotopic compositions of the sedimentary organic matter in an otherwise relatively stable stratified basin. They also show that large amounts of relatively labile carbohydrate carbon may be preserved through sulfuration.

## Introduction

Since its first recognition as a discrete division by William Smith in the early nineteenth century (Cox and Gallois, 1981), the Upper Jurassic Kimmeridge Clay Formation (KCF) has received almost continuous attention of earth scientists. All the early work applies to the outcrops and subcrops in England (for references see Cox and Gallois, 1981). Today, the onshore KCF, including the type section in Kimmeridge Bay (Dorset), is known to be different from its equivalents in the graben systems of the North Sea and on the Norwegian Platform, which are important oil source rocks (Miller, 1990; Wignall, 1994; Cooper et al., 1995; Tyson, 1996). The frequently alternating lithologies of the onshore KCF (mudstones, bituminous shales, oil shales, carbonates) sharply contrast to the more homogeneous development of shales in the North Sea. Despite this poor resemblance with the offshore source rocks, the present-day studies also mainly concern the onshore sedimentary sequence (e.g. Farrimond et al., 1984; Oschmann, 1988, 1991; Eglinton et al., 1988; Wignall, 1989; Bertrand et al., 1990; Huc et al., 1992; Bertrand and Lallier-Vergès, 1993; Herbin et al., 1993; Ramanampisoa and Disnar, 1994; Tribovillard et al., 1994; Boussafir et al., 1995; Waterhouse, 1995; Tyson, 1996). This may partly be due to the onshore rocks being easier of access and better documented, but also due to the interest in the processes underlying the cyclic sedimentation. Various depositional models have been proposed, some of which described shortly below.

In order to explain the sedimentary sequence of bituminous shale-oil shale-coccolithic limestone, Tyson et al. (1979) suggested a rising chemocline in the palaeowater column. The non-bioturbated coccolithic limestone, being one endmember in this sequence, would represent the ultimate anaerobic facies. More recent studies (Tyson, 1985; Oschmann, 1988, 1991; Tyson and Pearson, 1991) indicate that anoxia in the Kimmeridgian epeiric basin is more likely to have resembled modern anoxia in eutrophic shelf seas, and an anaerobic facies was defined which does allow for oxygenated periods, provided that these periods are too short to support benthic life. In order to explain the onset and termination of anoxia, Oschmann (1988) proposed that a thermocline developed seasonally between arctic, cold, dense, southward-flowing, anoxic bottom waters and warm, less dense, northward-flowing surface waters. Miller (1990) postulated a seasonally stratified water column generated by the salinity contrast between northward-flowing, warm, saline bottom waters and southward-flowing cold surface waters. By contrast, Tyson and Pearson (1991) pointed out that large-scale circulation patterns are not essential for explaining the initiation, occurrence and termination of seasonal oxygen deficiency in the water column. They presented a model in which the changing sedimentary conditions are explained by astronomically forced climatic variations super-imposed on a longer term sea-level fluctuation, this latter in essence also astronomically forced.

Recently, the actualistic model of Tyson and Pearson (1991) was placed into a sequence-stratigraphic framework (Tyson, 1996), although it was recognised that locally the KCF sediment distribution does not really conform to the progradational infilling of basins assumed in the Exxon sequence stratigraphical model. The organic-rich beds of the *eudoxus* to *pectinatus* biozones, concentrated in five 5-30 m thick bands, appeared closely related to the MFS (maximum flooding surface, see Haq et al., 1987) intervals of Melnyk et al. (1992,



1994), which in their turn correspond to periods of onlap on the basin margin reported by Wignall (1991). This suggested that the bands were deposited during relatively high sea-level stands, and are relatively condensed (Tyson, 1996). The author denotes that the rapidly deposited coccolithic limestones, intercalated between the organic-rich beds, are not necessarily at odds with deposition in a condensed section (CS). In essence, the interpretation of a CS interval is related to the siliciclastic flux, and major components of the coccolithic limestones are of biogenic origin.

In the models above, differences in TOC are attributed to changing accumulation rates of detrital minerals and variations in bottom water oxygenation. By contrast, several workers consider primary production to play a major role in determining the amount of organic matter (OM) ultimately preserved. The KCF section in the Cleveland Basin (onshore UK) studied by Bertrand and Lallier-Vergès (1993) was ascribed to a deposition under continuously anoxic bottom-water conditions. From the total amount of reduced sulfur species the authors estimated the fraction of organic carbon that had been oxidised by sulfate reduction. It appeared that the 'sulfate reduction index', which is defined as the ratio of (organic carbon preserved + mineralised by sulfate reduction) to preserved organic carbon, was lowest in samples containing ca. 3% TOC. Starting from there, the ratio quasi-linearly increased both with decreasing and with increasing TOC (TOC not exceeding 12%). These data in combination with the mineralogical and inorganic geochemical composition of the sediments led the authors to explain the variations in TOC by different fluxes of different OM, and not by a varying dilution by detrital and/or biogenic minerals.

Boussafir et al. (1995) reported that the organic sulfur compounds (OSC) released upon pyrolysis of KCF kerogens probably derive from the orange (transmitted light), nanoscopically amorphous organic matter (AOM) seen by transmission electron microscopy (TEM). They also reported that the relative abundance of orange AOM increases with TOC. On the basis of these results a model was proposed in which a climatically induced growth of primary production would lead to enhanced sulfate reduction and thus to a better preservation of OM *via* the reaction of lipids with reduced inorganic sulfur species.

Huc et al. (1992) in their study of the KCF in Dorset found a positive correlation between TOC and  $\delta^{13}\text{C}_{\text{TOC}}$ . This TOC- $\delta^{13}\text{C}_{\text{TOC}}$  relationship was ascribed to a relatively extensive reworking of biomass in the water column during deposition of the OM-lean samples. Later, Hollander et al. (1993) hypothesised that the TOC-rich sediments had been deposited at a time when the concentration of DIC in the photic zone was lowest, presumably due to high primary production.

In a previous study of the Dorset KCF we investigated in detail the molecular and carbon isotopic composition of OM in three lithologically different rocks of the Lower Kimmeridge Clay (van Kaam-Peters et al., 1997c). The abundant isorenieratene derivatives, originating from photosynthetic green sulfur bacteria, in all three samples indicated that during deposition, the lower part of the photic zone had been euxinic at least periodically. Furthermore, differences among the samples in the  $^{13}\text{C}$  contents of extractable biomarkers and algaenans (resistant biomacromolecules present in algal cell walls) appeared much smaller than differences in  $\delta^{13}\text{C}_{\text{TOC}}$ , indicating that the positive correlation between TOC and  $\delta^{13}\text{C}_{\text{TOC}}$  (Huc et al., 1992) could not be explained by differences in  $\delta^{13}\text{C}_{\text{DIC}}$  or the concentration of DIC in the photic zone. Based on the increasing abundance of organic

sulfur with increasing TOC (and  $\delta^{13}\text{C}_{\text{TOC}}$ ), it was suggested that  $\delta^{13}\text{C}_{\text{TOC}}$  was controlled by the degree of sulfurisation.

Since our ideas were based on the analysis of three samples only, a supplementary study was performed, of which results are presented here. Thirteen samples of the Upper Kimmeridge Clay were analysed, comprising all different lithologies, including some coccolithic limestones. The coccolithic limestones play a crucial role in the apparent positive correlation between TOC and  $\delta^{13}\text{C}_{\text{TOC}}$ , since on the one hand they are believed to represent periods of severe oxygen deficiency (Tyson, 1985, 1996; Oschmann 1988, 1991), on the basis of which they are grouped with the high  $\delta^{13}\text{C}_{\text{TOC}}$  oil shales, whereas on the basis of TOC they plot with the low  $\delta^{13}\text{C}_{\text{TOC}}$  mudstones. The approach to our study, therefore, was to determine if our samples fit into the trend of increasing  $\delta^{13}\text{C}_{\text{TOC}}$  with increasing TOC (Huc et al., 1992), and to establish the contributions of the several carbon isotopically distinct compound classes to the OM. We examined the presence of isorenieratene derivatives, and verified our previous finding that individual biomarkers and algaenans have similar  $\delta^{13}\text{C}$  values, regardless of  $\delta^{13}\text{C}_{\text{TOC}}$ . Finally, we further substantiated our hypothesis that  $\delta^{13}\text{C}_{\text{TOC}}$  was controlled by the degree of sulfurisation, and examined if this was reflected by optical changes of the OM using thin sections for transmitted light observations, and polished sections for reflected light and fluorescence microscopy.

## Methods

*Mineralogical content.* X-ray powder diffraction (XRD) was carried out as described elsewhere (van Kaam-Peters et al., 1997c). Total organic carbon (TOC) and total sulfur ( $S_{\text{TOTAL}}$ ) contents were determined by a LECO C/S analyser. In addition, organic and inorganic sulfur contents were measured by the Geoelf Sulfur Analyser (GSA), an instrument which essentially consists of a specially designed injector for thermal extraction and pyrolysis of the sample connected to both a FID detector and a sulfur selective chemiluminescence detector (Bjørøy et al., 1993). Carbonate content was calculated from TOC of the untreated sediment and TOC of the decalcified (6M HCl) sediment (TOC\*). TOC\* was determined by LECO analysis of a weighed amount of decalcified sediment.

*Extraction and fractionation.* The powdered rocks (ca. 70 g) were Soxhlet extracted with methanol (MeOH)/dichloromethane (DCM) (1:7.5 v/v) for 24 h. Asphaltenes were removed from the extracts by precipitation in *n*-heptane. Aliquots of the maltene fractions (ca. 200 mg), to which a mixture of four standards was added for quantitative analysis (Kohnen et al., 1990), were separated into three fractions using a column [20 cm x 2 cm; column volume ( $V_0$ ) = 35 ml] packed with alumina (activated for 2.5 h at 150°C) by elution with hexane (150 ml; “saturated hydrocarbon fraction”), hexane/DCM (9:1 v/v; 150 ml; “aromatic hydrocarbon fraction”) and DCM/MeOH (1:1 v/v; 150 ml; “polar fraction”). Saturated hydrocarbon and aromatic hydrocarbon fractions were analysed by GC and GC-MS; saturated hydrocarbon fractions were analysed also by GC-MSMS. *n*-Alkanes were removed from aliquots (ca. 4 mg) of the saturated hydrocarbon fractions by elution over a small column (5 cm x 0.5 cm;  $V_0$  = 1 ml) packed with a molecular sieve (silicalite) using cyclohexane as the eluents. *n*-Alkanes were retrieved from the molecular sieve by dissolving

the sieve in HF, subsequently neutralising the solution with Na<sub>2</sub>CO<sub>3</sub>, and extraction with hexane (x3). Both adducts and non-adducts were analysed using GC-IRMS. Polar fractions were desulfurised as described elsewhere (van Kaam-Peters et al., 1997c). The desulfurisation products were separated over a small column packed with alumina (activated for 2.5 h at 150°C) by elution with respectively hexane and hexane/DCM (9:1, v/v). The hexane/DCM fraction was evaporated to dryness and dissolved in a small volume of hexane (2 mg/ml) to be analysed by GC, GC-MS and GC-IRMS.

*Off-line pyrolysis and fractionation.* Off-line pyrolysis was performed with a weighed amount of decarbonated (6N HCl), ultrasonically extracted rock sample, equivalent to ca. 100 mg organic carbon to which 100 µg standard (3-methyl-6-dideutero-henicosane) was added. Samples were heated (400°C) for 1.5 hr in a sample boat positioned in a glass tube in a cylindrical oven under a nitrogen flow. The volatile products generated were trapped in two successive cold traps containing hexane/DCM (9:1 v/v). The first trap was at room temperature; the second trap was cooled with solid CO<sub>2</sub>/acetone. A second standard (50 µg squalane) was added to the first trap. An aliquot of the pyrolysate (combined products of both traps plus the material condensed at the end of the glass tube) was taken for bulk stable carbon isotope analysis and GC-FID/FPD. The remainder of the pyrolysate was fractionated by column chromatography (Al<sub>2</sub>O<sub>3</sub>; 15 cm x 1 cm; V<sub>0</sub> = 8 ml) into a hexane fraction (20 ml), a hexane/DCM (9:1 v/v) fraction (32 ml), and a MeOH/DCM (1:1, v/v) fraction (32 ml). The hexane fraction was further separated into two fractions using a column (8 cm x 1 cm; V<sub>0</sub> = 3 ml) packed with AgNO<sub>3</sub> impregnated (20% w/w; activated for 16 h at 120°C) silicagel (Merck, Silicagel 60, 70-230 mesh ASTM) by elution with 9 ml hexane (saturated hydrocarbons) and 12 ml ethylacetate (stripping). The final hexane fraction was carefully distilled until a concentration was reached suitable for GC-IRMS analysis of the *n*-alkanes and acyclic isoprenoids. In the case of sample D4, a subsequent adduction was performed in order to remove the *n*-alkanes and determine the stable carbon isotopic composition of pristane and phytane. To determine δ<sup>13</sup>C of 1,2,3,4-tetramethylbenzene, an additional pyrolysate of sample D9 was prepared, which was fractionated into a hexane/DCM (9:1 v/v) fraction and a MeOH/DCM (1:1, v/v) fraction. The hexane/DCM fraction was concentrated and analysed by GC-IRMS. To determine δ<sup>13</sup>C of C<sub>1</sub>-C<sub>3</sub> alkylated thiophenes and benzenes, two additional off-line pyrolysis experiments were performed on samples D9 and D10. The combined products of both traps (not the condensed material) were concentrated and analysed by GC-IRMS.

*Instrumental analyses.* Gas chromatography (GC), gas chromatography-mass spectrometry (GC-MS), gas chromatography-mass spectrometry-mass spectrometry (GC-MSMS), Curie-point pyrolysis-gas chromatography (Py-GC) and Curie-point pyrolysis-gas chromatography-mass spectrometry (Py-GC-MS) were carried out as described elsewhere (van Kaam-Peters et al., 1997c). Gas chromatography-isotope ratio mass spectrometry (GC-IRMS) was performed using the Hewlett-Packard 5890 gas chromatograph interfaced to the Finnigan Mat DELTA-C IRMS-system. For measuring C<sub>1</sub>-C<sub>3</sub> alkylated thiophenes and benzenes in the off-line pyrolysate of the kerogen, the gas chromatograph was equipped with a fused silica capillary column (60 m x 0.25 mm) coated with CP-Sil 5CB-MS (film

thickness 0.25  $\mu\text{m}$ ), and the oven was programmed from 35°C (5 min) to 310°C at a rate of 4°C/min. Helium was used as the carrier gas. Measurements of other pyrolysis products and extractable biomarkers were performed using a fused silica capillary column (25 m x 0.32 mm) coated with CP-Sil 5 (film thickness 0.12  $\mu\text{m}$ ). The saturated hydrocarbon fractions of the off-line pyrolysate were injected at 35°C and the oven temperature was raised at 4°C/min to 310°C with a final hold time of 5 min. For analysis of fractions of the bitumen the oven was programmed from 70°C to 130°C at 20°C/min, from 130°C to 310°C at 4°C/min and maintained at 310°C for 15 min. The  $\delta^{13}\text{C}$  values (vs PDB) were calculated by integrating the mass 44, 45 and 46 ion currents of the  $\text{CO}_2$  peaks produced by combustion of the column effluent and those of  $\text{CO}_2$  spikes with a known  $^{13}\text{C}$ -content which were directly led into the mass spectrometer at regular intervals. The  $\delta^{13}\text{C}$  values reported are averages of at least two measurements.

*Microscopy.* Organic petrographical examination of the samples was carried out in reflected and ultraviolet light on polished blocks under oil immersion using a ZEISS Axioskop microscope system, equipped with a HBO 100W high pressure Hg vapor lamp, a 395-440 nm excitation filter and a 470 nm barrier filter for fluorescence microscopy. Observations were made with a 63x oil immersion objective. Petrographic thin sections were investigated under transmitted light using a ZEISS Universal standard petrographic microscope.

*Quantification.* Acyclic hydrocarbons, steranes, 4-methyl steranes, hopanes, diasterenes and neohop-13(18)-enes were quantified by integration of their peaks in the m/z 57, m/z 217, m/z 231, m/z 191, m/z 257 and m/z 191 mass chromatograms, respectively, and comparison with the peak area of the internal standard (3-methyl-6-dideutero-henicosane) in the m/z 57 mass chromatogram. Concentrations of *n*-alkanes and steranes were multiplied by formerly established correction factors (van Kaam-Peters et al., 1997b) to account for the different responses of FID and MS. Concentrations of hopanes, diasterenes and neohop-13(18)-enes were corrected for the different relative intensities of their fragment ions, using correction factors determined from mass spectra of pure compounds. Concentrations of branched alkanes were not corrected. 13 $\beta$ ,17 $\alpha$ (H)-Diacholestanes were quantified by correcting the 13 $\beta$ ,17 $\alpha$ (H)-diacholestanes/5 $\alpha$ -cholestane ratio, obtained by integration of the 372 to 217 transition using GC-MSMS, for the different intensities of the 372 to 217 transitions, and multiplying the ratio by the concentration of 5 $\alpha$ -cholestane. Aromatic hopanoids (**I-II**; see Appendix) and derivatives of isorenieratene (**III-XVIII**) were quantified by integration of mass chromatograms of relevant m/z values, and comparison with the peak area of the internal standard (2-methyl-2-(4,8,12-trimethyltridecyl)chroman) in the m/z 107+147 mass chromatogram. The peak areas obtained were converted into peak areas of total ion currents using fragment ion intensities determined from mass spectra of non-coeluting peaks: m/z 107+147: chroman standard (39%); m/z 346: **I** (11%); m/z 328: **II** (10%); m/z 133+134: **III** (39%), **IV** (49%), **V** + **VII** (58%), **VI** (46%), **VIII** (31%); m/z 237: **IX** + **X** (26%), **XI** (39%), **XII** (27%); m/z 287: **XIII** + **XIV** (20%), **XV** + **XVI** (23%), **XVII** + **XVIII** (19%). Chromans (**XIX**) were quantified by integration of mass chromatograms of m/z 107 (fragment ion of chroman standard) + 121 + 135 + 149 using intensities of the fragment ions reported by Sinninghe Damsté et al. (1993b) to calculate total ion abundances.

The 2,3-dimethylthiophene over (1,2-dimethylbenzene + *n*-non-1-ene) ratio (Eglinton et al., 1990a) was determined by integration of the appropriate peaks in the total ion current. The 2-methylthiophene over toluene ratio was determined by integration of the appropriate peaks in the *m/z* 97 + 98 and *m/z* 91 + 92 mass chromatograms. The 2,5-dimethylthiophene over (2-ethylthiophene + 2,4-dimethylthiophene + 2,3-dimethylthiophene) ratio was determined by integration of the relevant peaks in the *m/z* 97 + 98 + 111 + 112 mass chromatogram. The ratios of benzothiophenes over toluene, methylnaphthalenes over toluene, and methylindans over toluene were calculated from the peak area of the six most prominent C<sub>1</sub>-C<sub>2</sub> alkylated benzothiophenes in the *m/z* 147 + 148 + 161 + 162 mass chromatogram, the peak area of the two methylnaphthalenes in the *m/z* 142 mass chromatogram, the area of the five most prominent peaks in the *m/z* 117 mass chromatogram, and the area of the toluene peak in the *m/z* 91 + 92 mass chromatogram.

## Results

### *Bulk analyses*

Thirteen outcrop samples were taken of the type Kimmeridge Clay between Clavell's Hard and Freshwater Steps in Dorset (U.K.). The samples are from a 57 m interval situated in the *wheatleyensis*, *hudlestoni* and *pectinatus* ammonite zones (Cox and Gallois, 1981), and cover all different lithologies (Table 5.1). Bulk data are listed in Table 5.2. TOC values vary between 0.6 and 52.1%. With the exception of sample D2, the Hydrogen Index (HI) falls in the range of 500-850 mg HC/g TOC, typical of type II kerogens. The  $\delta^{13}\text{C}_{\text{TOC}}$  values widely fluctuate with depth, ranging from -26.7‰ to -20.7‰.

A positive correlation between TOC and  $\delta^{13}\text{C}_{\text{TOC}}$  was reported by Huc et al. (1992), for a section of the KCF partly overlapping our sampling interval. However, the alleged positive correlation is absent in our sample set (Fig. 5.1a). The  $\delta^{13}\text{C}_{\text{TOC}}$  of samples D1, D3

**Table 5.1.** Sample description.

sample	depth (m) <sup>a</sup>	Pectinatites biozone <sup>b</sup>	lithology <sup>b</sup>
D1	0	<i>pectinatus</i>	laminated coccolith-rich limestone (White Stone Band)
D2	19.3	<i>hudlestoni</i>	tabular cementstone (Basalt Stone Band)
D3	42.4	<i>hudlestoni</i>	coccolith-rich limestone
D4	42.6	<i>hudlestoni</i>	oil shale
D5	43.7	<i>hudlestoni</i>	bituminous mudstone
D6	44.3	<i>hudlestoni</i>	mudstone, undifferentiated
D7	45.6	<i>hudlestoni</i>	coccolith-rich limestone <sup>c</sup> (Rope Lake Head Stone Band)
D8	45.9	<i>hudlestoni</i>	coccolith-rich limestone
D9	50.6	<i>wheatleyensis</i>	oil shale (Blackstone Band)
D10	51.4	<i>wheatleyensis</i>	bituminous mudstone
D11	53.2	<i>wheatleyensis</i>	oil shale
D12	53.7	<i>wheatleyensis</i>	calcareous mudstone
D13	57.2	<i>wheatleyensis</i>	calcareous mudstone

<sup>a</sup> relative to sample D1

<sup>b</sup> according to Cox and Gallois (1981)

<sup>c</sup> XRD indicates mainly diagenetic carbonate

**Table 5.2.** Bulk data.

sample	TOC		HI	OI	SS1 <sup>a</sup>	SS2 <sup>b</sup>	SS3 <sup>c</sup>	SI <sup>d</sup>	S <sub>TOTAL</sub> <sup>e</sup>	S <sub>TOTAL</sub> <sup>f</sup>	TOC*	$\delta^{13}\text{C}_{\text{TOC}}$ (‰)	carbonate (%)	bitumen (mg/g TOC)
	(%)	T <sub>max</sub>							GSA	LECO				
D1	4.5	420	738	24	0.32	6.61	0.00	148	0.7	0.8	61.1	-22.3	93 <sup>h</sup>	79
D2	0.6	430	150	14	0.14	0.00	0.19	0	<0.1	0.4	2.6	-26.5	76 <sup>i</sup>	43
D3	7.0	420	756	13	0.33	4.32	0.00	62	0.5	2.1	48.1	-21.3	85 <sup>h</sup>	61
D4	24.1	423	832	9	0.60	25.0	2.48	104	2.8	4.1	26.8	-22.9	10 <sup>h</sup>	69
D5	18.2	426	721	7	0.50	10.8	1.11	59	1.2	3.5	18.2	-23.9	0 <sup>j</sup>	49
D6	6.2	427	576	9	0.24	1.56	1.45	25	0.3	2.2	6.9	-26.0	10 <sup>h</sup>	57
D7	2.1	424	619	32	0.07	0.79	0.13	38	0.1	0.8	14.7	-24.7	86 <sup>i</sup>	52
D8	10.7	421	772	13	0.75	7.17	0.77	67	0.9	1.3	36.6	-23.0	71 <sup>k</sup>	63
D9	52.1	425	768	9	2.93	83.9	0.53	161	8.7	8.0	62.8	-20.7	17 <sup>h</sup>	52
D10	4.8	429	536	14	0.32	1.95	1.40	41	0.4	2.0	6.2	-25.8	22 <sup>k</sup>	58
D11	10.8	427	691	10	0.32	4.89	2.17	45	0.7	3.0	14.3	-26.1	25 <sup>h</sup>	56
D12	3.7	427	517	14	0.31	2.40	4.53	65	0.7	2.2	5.0	-26.7	25 <sup>k</sup>	65
D13	7.4	425	651	11	0.26	5.13	3.01	69	0.8	2.3	10.7	-25.8	30 <sup>k</sup>	60

<sup>a</sup> Thermally extractable sulfur at 300°C for 3 minutes (mg S/g rock)

<sup>b</sup> Pyrolysable (600°C) organic sulfur (mg S/g rock)

<sup>c</sup> Pyrolysable (600°C) inorganic sulfur (mg S/g rock)

<sup>d</sup> Sulfur Index (mg SS2\*100/g TOC)

<sup>e</sup> (SS1+SS2+SS3)/10 (%)

<sup>f</sup> determined by LECO analysis (%)

<sup>g</sup> TOC after decalcification

<sup>h</sup> calcite

<sup>i</sup> mainly diagenetic carbonate, little calcite

<sup>j</sup> XRD indicates some calcite

<sup>k</sup> mainly calcite, little diagenetic carbonate

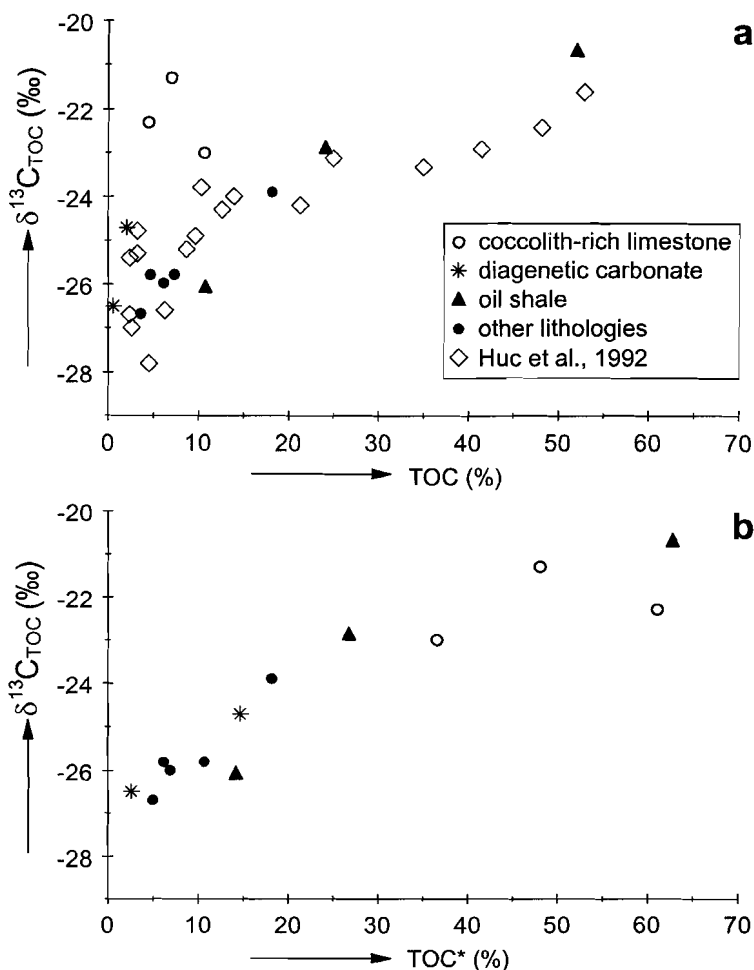


**Fig. 5.1.** Correlation between (a) TOC and  $\delta^{13}C_{TOC}$  (b) TOC\* and  $\delta^{13}C_{TOC}$ . Data from Huc et al. (1992) are plotted for reference.

and D8, which are coccolithic limestones, strongly deviate from the trend followed by the other samples (Fig. 5.1a). In order to compensate for the dilution of TOC by carbonate,  $\delta^{13}C_{TOC}$  was also plotted versus TOC of the decarbonated sediment (TOC\*). This resulted in a shift towards higher TOC values for all samples, especially for the coccolithic limestones D1, D3 and D8, and an almost linear relationship between TOC\* and  $\delta^{13}C_{TOC}$  was found (Fig. 5.1b). Note that, although its carbonate content is also high (Table 5.2), the diagenetic carbonate D2 is characterised by significantly lower TOC\* and  $\delta^{13}C_{TOC}$  values than the coccolithic limestones (Fig. 5.1b). Sample D7, a diagenetically altered coccolithic limestone, displays intermediate TOC\* values (Fig. 5.1b).

Total sulfur content ( $S_{TOTAL}$ ) measured by the LECO instrument is generally higher than  $S_{TOTAL}$  obtained by GSA analysis, particularly in the low  $\delta^{13}C_{TOC}$  samples (Table 5.2).

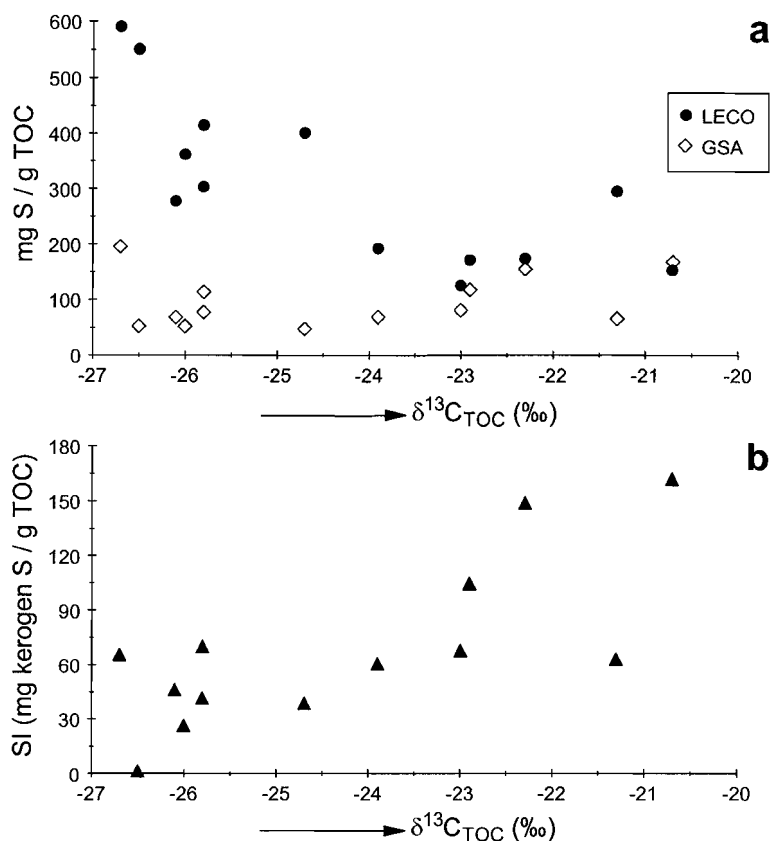


**Fig. 5.2.** (a) TOC-normalised total sulfur content obtained by LECO and GSA analyses as a function of  $\delta^{13}\text{C}_{\text{TOC}}$ . The inorganic sulfur content is systematically underestimated by GSA analysis. (b) The GSA Sulfur Index (SI) as a function of  $\delta^{13}\text{C}_{\text{TOC}}$ . The SI of sample D3 ( $\delta^{13}\text{C}_{\text{TOC}} = -21.3$ ‰) is probably erroneously low, since pyrite is minor in this sample (XRD data) and  $S_{\text{TOTAL}}$  determined by the LECO instrument (duplicate analysis) is four times higher than  $S_{\text{TOTAL}}$  measured by GSA analysis.

Given the inert atmosphere and the relatively low temperature (600°C) employed in GSA analysis, this method probably severely underestimates the inorganic sulfur content. For the LECO series, an inverse relationship exists between  $\delta^{13}\text{C}_{\text{TOC}}$  and total sulfur content normalised on TOC (Fig. 5.2a). The TOC-normalised sulfur contents calculated from the GSA data do not correlate with  $\delta^{13}\text{C}_{\text{TOC}}$  (Fig. 5.2a). The Sulfur Index (SI) is generally higher in high  $\delta^{13}\text{C}_{\text{TOC}}$  samples than in low  $\delta^{13}\text{C}_{\text{TOC}}$  samples (Fig. 5.2b). The SI of sample D3 ( $\delta^{13}\text{C}_{\text{TOC}} = -21.3$ ‰) is probably erroneously low (see figure legend).



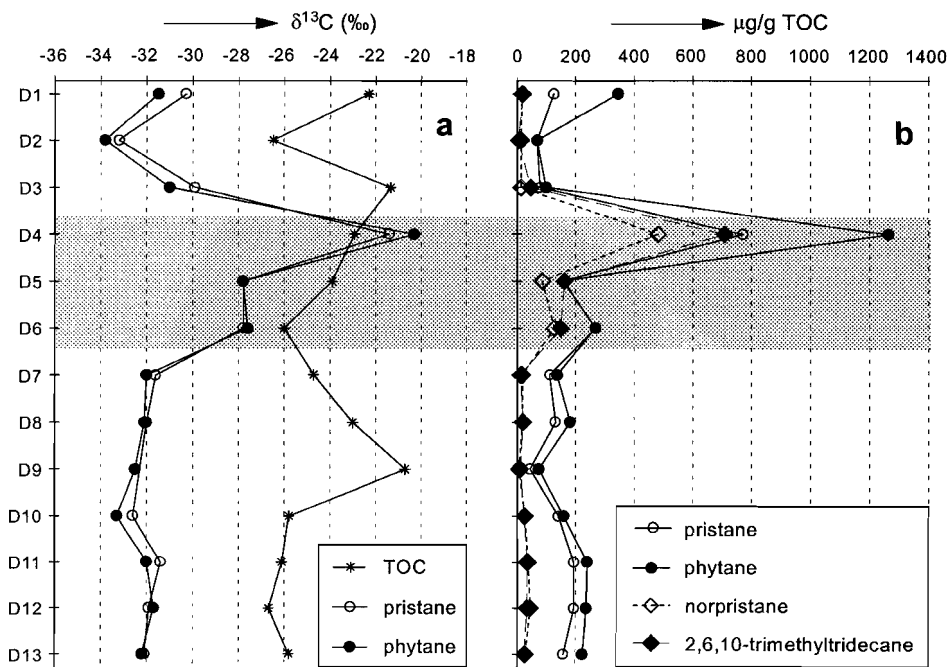


**Fig. 5.3.** (a) The  $\delta^{13}\text{C}$  values of TOC, pristane and phytane (b) concentrations of  $\text{C}_{16}$  and  $\text{C}_{18}\text{-C}_{20}$  regular isoprenoid alkanes versus depth.

### Extractable organic matter

*Free acyclic hydrocarbons.* The saturated hydrocarbon fractions of all samples are dominated by pristane and phytane. The  $\delta^{13}\text{C}$  values of pristane and phytane vary between -33‰ and -31‰ in most cases, but in the stratigraphic interval comprising samples D4-D6, significantly higher  $\delta^{13}\text{C}$  values are found, with a maximum of almost -20‰ in D4 (Fig. 5.3a). Coincident with this maximum in  $\delta^{13}\text{C}$ , there is a maximum in the concentrations of pristane and phytane. Furthermore, samples D4-D6 are characterised by relatively high concentrations of norpristane and 2,6,10-trimethyltridecane, which are only trace compounds in the other samples (Fig. 5.3b). Both compounds are enriched in  $^{13}\text{C}$  as well (Table 5.3).

In agreement with other reports (Williams and Douglas, 1980, 1983; Farrimond et al., 1984), distributions of free *n*-alkanes show distinct maxima at *n*- $\text{C}_{21}$  and *n*- $\text{C}_{23}$  in all samples (Fig. 5.4). These homologues differ from the other *n*-alkanes not only in their abundance but also in their  $^{13}\text{C}$  content, which is 6 to 15‰ higher than the isotopic composition of most *n*-alkanes (ca. -30‰). Other isotopically heavy alkanes, present in all samples, are 2-methyltetracosane, 2-methylhexacosane, 3-isopropyltetracosane and 3-isopropylhexacosane, with  $\delta^{13}\text{C}$  values between -20 and -16‰ (Table 5.3). The 3-isopropyl alkanes, recently identified by Schouten et al. (1997), probably represent the unknown branched alkanes reported by Farrimond et al. (1984).

**Table 5.3.** The  $\delta^{13}\text{C}$  values of different biomarkers.

compound	D1	D2	D3	D4	D5	D6	D7
pristane	-30.3 ± 0.7	-33.2 ± 0.3	-29.9 ± 0.4	-21.4 ± 0.5	-27.8 ± 0.2	-27.8 ± 0.1	-31.6 ± 0
phytane	-31.5 ± 0.1	-33.8 ± 0.3	-31.0 ± 0.1	-20.3 ± 0.2	-27.8 ± 0.2	-27.6 ± 0.1	-32.0 ± 0
2,6,10-trimethyl- tridecane				-17.3 ± 0.3	-21.0 ± 0.5		
norpristane				-20.2 ± 0.7		-24.7 ± 0.6	
2-methyltetracosane			-17.3 ± 0.8	-18.1 ± 0.6	-16.9 ± 0.9	-17.4 ± 0.2	-18.1 ± 0
3-isopropyl- tetracosane			-18.3 ± 0.6	-20.0 ± 0.6	-18.6 ± 0.9	-18.2 ± 0.4	-18.4 ± 0
2-methylhexacosane		-18.6 ± 0.4	-17.4 ± 0.2	-18.2 ± 0.1	-16.3 ± 0.5	-17.0 ± 0.1	-16.6 ± 0
3-isopropyl- hexacosane		-18.9 ± 0.3	-16.7 ± 0.8	-17.8 ± 0.1	-16.6 ± 0.6	-18.2 ± 0.1	-17.0 ± 0
isorenieratane <sup>a</sup>	-17.8 ± 0.8		-17.1 ± 0.8	-16.5 ± 0.1	-17.0 ± 0.3	-17.4 ± 0.5	-17.6 ± 0

<sup>a</sup> sulfur-bound in polar fraction**Table 5.3 continued.** The  $\delta^{13}\text{C}$  values of different biomarkers.

compound	D8	D9	D10	D11	D12	D13
pristane	-32.0 ± 0.3	n.d.	-32.6 ± 0.1	-31.4 ± 0.2	-31.9 ± 0.1	-32.1 ± 0.1
phytane	-32.1 ± 0.2	-32.5 ± 0.3	-33.3 ± 0.2	-32.0 ± 0.1	-31.7 ± 0.3	-32.2 ± 0.1
2,6,10-trimethyl- tridecane						
norpristane				-29.8 ± 0.5	-29.8 ± 0.2	
2-methyltetracosane	-17.0 ± 0.7					
3-isopropyl- tetracosane	-18.3 ± 1.3					
2-methylhexacosane	-15.9 ± 0.3	-17.3 ± 0.1	-16.6 ± 0.8	-16.9 ± 0.5	-18.0 ± 0.5	
3-isopropyl- hexacosane	-16.8 ± 0.4	-17.4 ± 0.4	-17.2 ± 0.1	-17.7 ± 0.1	-18.0 ± 0.2	
isorenieratane <sup>a</sup>	-16.6 ± 0.3	-17.3 ± 0.7	-17.7 ± 0.3	-17.0 ± 0.1	-17.9 ± 0.4	-16.9 ± 0.7

<sup>a</sup> sulfur-bound in polar fraction

*Steroids.* In addition to GC-MS analysis of the saturated hydrocarbon fractions, steranes were analysed using GC-MSMS by measuring the  $M^+$  to 217,  $M^+$  to 231 and 414 to 98 transitions, the latter characteristic of dinosterane. Sterane distributions were found to differ only slightly among the samples and resemble those reported previously for the Lower Kimmeridge Clay (van Kaam-Peters et al., 1997c). No significant differences were observed in the distributions of desmethyl steranes ( $C_{27} > C_{29} > C_{28}$ ). Distributions of 4-methyl steranes ( $C_{28} > C_{29} \cong C_{30}$ ) vary only in that the dominance of 4 $\alpha$ - and 4 $\beta$ -methyl-5 $\alpha$ -cholestane is not as pronounced in all samples. Eight isomers of 4,23,24-trimethylcholestane (dinosterane) are present in all samples. The striking similarity of sterane distributions in lithologically very different samples of the KCF in Dorset was also reported by Farrimond et al. (1984) and Huc et al. (1992). The former authors, however, reported the presence of 20S-5 $\alpha$ ,14 $\alpha$ ,17 $\alpha$ (H)-steranes, whereas all our samples, derived from the same stratigraphic interval and same location, contain 5 $\beta$ ,14 $\alpha$ ,17 $\alpha$ (H)-steranes and no 20S-5 $\alpha$ ,14 $\alpha$ ,17 $\alpha$ (H)-steranes.

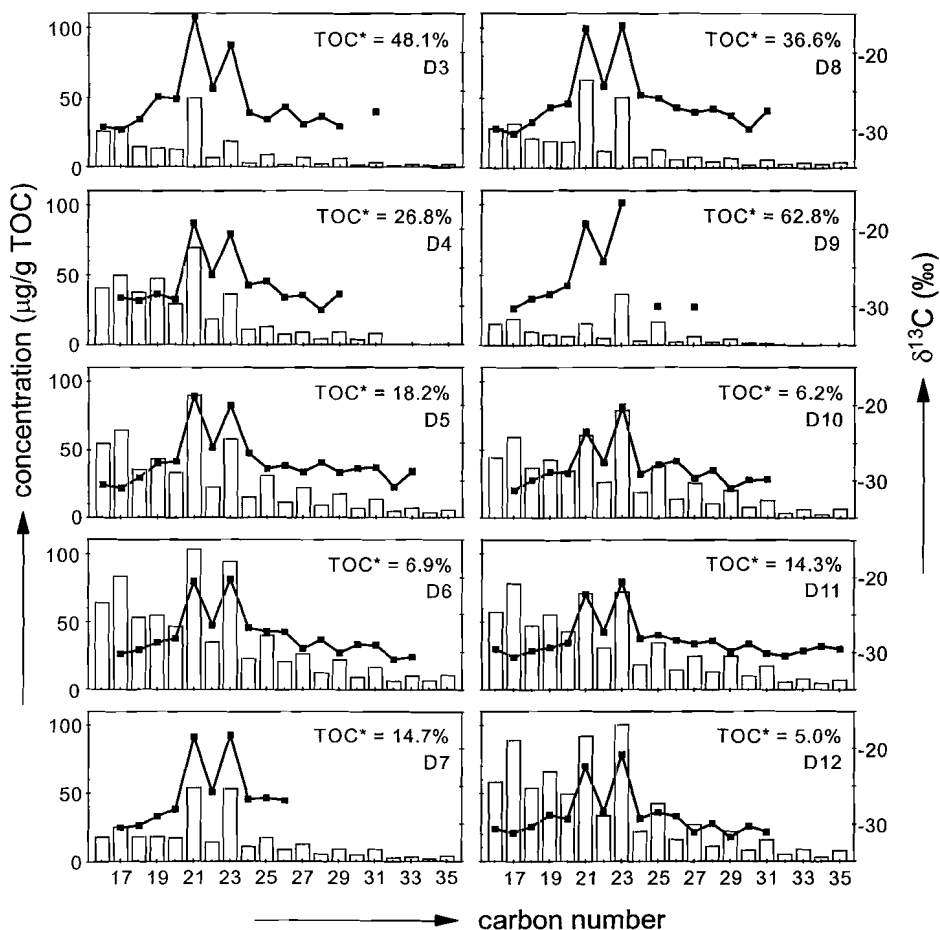


**Fig. 5.4.** Concentrations and  $\delta^{13}\text{C}$  values of *n*-alkanes in the saturated hydrocarbon fractions.

Although their distributions are similar, concentrations of desmethyl steranes show large differences among the samples, as illustrated in Fig. 5.5b by the concentrations of  $5\alpha$ -cholestane. 4-Methyl steranes are generally low, as can be concluded from the concentrations of 4-methyl- $5\alpha$ -cholestanes, which are the most abundant 4-methyl steranes in all samples (Fig. 5.5b). Differences in the 4-methyl sterane concentrations cannot really be assessed by looking at the concentrations of 4-methyl- $5\alpha$ -cholestanes only, since the distributions of 4-methyl steranes are not the same in all samples. It should be noted that the relatively abundant 4-methyl- $5\alpha$ -cholestanes, as compared to  $5\alpha$ -cholestane, in samples D5, D3 and D9 (Fig. 5.5b), correspond to 4-methyl sterane distributions with highly dominant 4-methyl- $5\alpha$ -cholestanes.

Distributions of rearranged steroids are similar to those of the regular steroids, but relative abundances of diasteranes, diasterenes and steranes are highly variable (not shown).

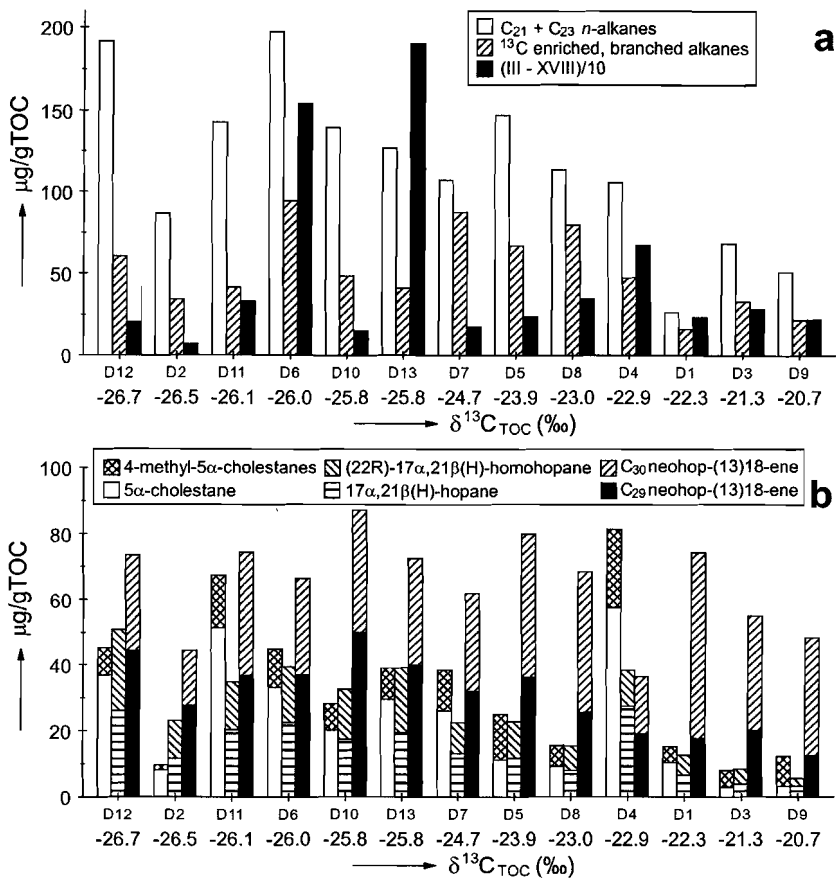


**Fig. 5.5.** Concentrations of (a) carbon isotopically heavy biomarkers (b) steroids and hopanoids versus  $\delta^{13}\text{C}_{\text{TOC}}$ .

The diasterane/sterane ratio was shown to be largely dependent on the clay/TOC ratio (van Kaam-Peters et al., 1997a).

*Hopanoids.* Distributions of hopanoids in the hexane fractions are dominated by C<sub>29</sub>-C<sub>30</sub> neohop-(13)18-enes and C<sub>30</sub>-C<sub>31</sub> hopanes. Except for samples D2, a diagenetic carbonate, and D4, which is also an outlier with respect to the concentrations of steroids (Fig. 5.5b) and acyclic isoprenoids (Fig. 5.3b), concentrations of hopanes decrease, and neohop-13(18)-ene becomes dominant over 29-norneohop-13(18)-ene with increasing  $\delta^{13}\text{C}_{\text{TOC}}$  (Fig. 5.5b). Concentrations of diaromatic (I) and triaromatic hopanoids (II), present in the aromatic hydrocarbon fractions, are highly variable (Table 5.4) and neither correlate with  $\delta^{13}\text{C}_{\text{TOC}}$  nor with the concentrations of other hopanoids.

*Derivatives of isorenieratene.* As in the Lower Kimmeridge Clay (van Kaam-Peters et al., 1997c), aromatic hydrocarbon fractions of all samples contain abundant derivatives of

**Table 5.4.** Concentrations ( $\mu\text{g/g TOC}$ ) of different aromatic biomarkers.

compound	D1	D2	D3	D4	D5	D6	D7	D8	D9	D10	D11	D12	D13
<b>I</b>	14	0	8	2	6	4	2	4	2	2	2	3	0
<b>II</b>	150	3	75	38	36	40	88	210	30	7	14	13	560
<b>III</b>	8	2	14	4	7	20	4	8	11	5	5	5	0
<b>IV</b>	20	3	34	9	21	81	16	43	22	8	30	10	450
<b>V</b>	10	5	25	96	27	180	18	25	10	15	24	17	36
<b>VI</b>	47	10	35	100	32	230	26	54	39	25	53	29	230
<b>VII</b>	67	12	54	250	48	430	43	73	49	43	68	61	98
<b>VIII</b>	14	4	21	29	10	130	0	40	21	0	42	9	1000
<b>IX</b>	4	1	8	7	7	25	5	7	4	4	6	4	0
<b>X</b>	21	8	44	36	31	110	22	31	27	15	26	17	0
<b>XI</b>	16	6	20	21	21	100	14	29	15	10	21	13	38
<b>XII</b>	11	5	13	84	15	95	10	13	8	10	15	15	16
<b>XIII</b>	2	1	3	2	3	12	2	4	3	1	4	2	0
<b>XIV</b>	1	0	2	1	1	6	1	2	2	1	2	1	0
<b>XV</b>	2	4	1	4	2	20	2	2	1	3	8	6	0
<b>XVI</b>	4	3	5	8	7	32	4	8	6	4	10	5	10
<b>XVII</b>	3	2	2	11	2	24	2	3	2	3	8	7	13
<b>XVIII</b>	4	2	4	16	7	45	5	7	3	4	10	6	13
<b>III-XVIII</b>	240	68	290	680	240	1500	170	350	220	150	330	210	1900
<b>XIXb,c</b>	2	3	1	3	3	4	3	2	1	3	4	5	6
<b>XIXd</b>	27	27	14	15	23	110	25	24	6	42	67	59	39

isorenieratene (e.g. Fig. 5.6). Distributions are similar in most, but not all of the samples (Table 5.4). Isorenieratene derivatives are biomarkers of the strictly anaerobic brown strain of Chlorobiaceae (Koopmans et al., 1996), whose presence points to an euxinic water

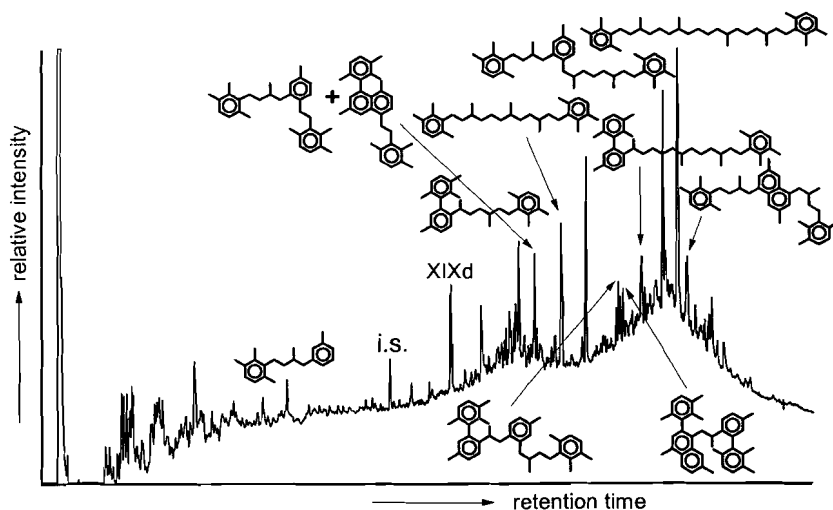


**Fig. 5.6.** GC-FID trace of the aromatic hydrocarbon fraction of sample D6.

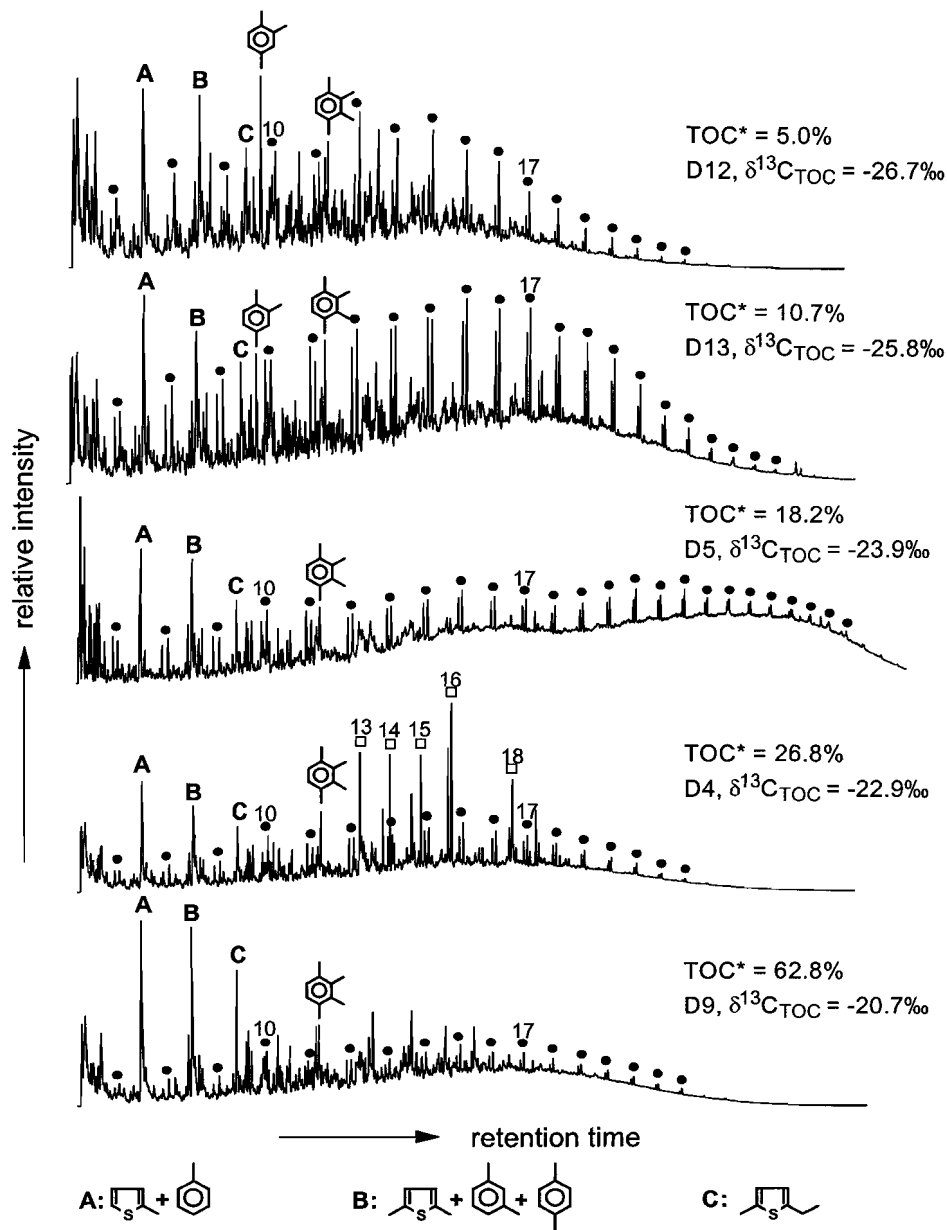


**Fig. 5.7.** Kerogen Py-GC-MS traces of five samples with different TOC\* values. Filled circles represent homologous series of *n*-alkane/*n*-alkene doublets. Open squares represent regular isoprenoids. Figures indicate the number of carbon atoms.

column extending into the photic zone. Since the Chlorobiaceae use the reverse TCA-cycle for fixation of CO<sub>2</sub> (Sirevåg and Ormerod, 1970), implying that they hardly discriminate

between  $^{12}\text{C}$  and  $^{13}\text{C}$ , their biomass is anomalously enriched in  $^{13}\text{C}$  compared to the average algal biomass. This is in agreement with the high  $\delta^{13}\text{C}$  values of isorenieratane released upon desulfurisation of the polar fractions (Table 5.3). Summed concentrations of isorenieratene derivatives are highly variable and do not show a correlation with  $\delta^{13}\text{C}_{\text{TOC}}$  (Fig. 5.5a).

*Chromans and OSC.* Chroman distributions in all samples are dominated by 5,7,8-trimethyl-MTTC (**XIXd**), suggesting that the surface waters were of a normal marine salinity (Sinninghe Damsté et al., 1987, 1993b). The OSC in the extracts ( $\text{C}_{11}\text{-C}_{15}$  thiolanes and  $\text{C}_{10}\text{-C}_{14}$  benzothiophenes) occur only in small amounts. The signal of the sulfur-selective FPD, however, indicated OSC to be abundant in the unresolved complex mixtures (UCMs) of both saturated and aromatic hydrocarbon fractions. These UCMs are particularly large in samples with the most  $^{13}\text{C}$ -enriched kerogens.

### *Kerogens*

*Flash-pyrolysis.* All kerogen pyrolysates are characterised by series of *n*-alkane/*n*-alkene doublets, abundant thiophenic and benzothiophenic OSC, and series of alkylbenzenes (Fig. 5.7). 1,2,3,4-Tetramethylbenzene is an abundant alkylbenzene, and is probably derived from sequestered isorenieratene in the kerogen (Hartgers et al., 1994; Hoefs et al., 1995), since it has a  $\delta^{13}\text{C}$  value of  $-17.8 \pm 0.2\text{‰}$  (sample D9), similar to isorenieratene sequestered in the polar fraction (Table 5.3). Also, isorenieratene derivatives are abundant in the aromatic hydrocarbon fractions and desulfurised polar fractions. Phenolic pyrolysis products, revealing the presence of lignins or diagenetically altered lignins (Saiz-Jimenez and de Leeuw, 1984, 1986), are present in trace amounts only in all samples.

Although the compound classes present in the pyrolysates are the same for all samples, significant differences are observed in their relative abundances. Firstly, the pyrolysate of sample D4 deviates from the other pyrolysates by its abundant acyclic isoprenoids (Fig. 5.7). This is the same sample that contains, in large concentrations,  $^{13}\text{C}$ -

**Table 5.5.** LMW OSC in flash pyrolysates of KCF kerogens.

Peak <sup>a</sup>	Compound
1	2-methylthiophene
2	3-methylthiophene
3	2-ethylthiophene
4	2,5-dimethylthiophene
5	2,4-dimethylthiophene
6	2,3-dimethylthiophene
7	2-propylthiophene
8	2-ethyl-5-methylthiophene
9	2-ethyl-4-methylthiophene
10	2,3,5-trimethylthiophene
11	2-methylbenzo[b]thiophene
12	4- and 3-methylbenzo[b]thiophene
13	2,4-dimethylbenzo[b]thiophene
14	2,3-dimethylbenzo[b]thiophene

<sup>a</sup> Numbers refer to peaks in Fig. 5.9

enriched C<sub>16</sub>-C<sub>20</sub> isoprenoids in its extract (Fig. 5.3). Secondly, OSC become increasingly important with increasing  $\delta^{13}\text{C}_{\text{TOC}}$ , as shown by the strong positive correlation of 2-methylthiophene over toluene and 2,3-dimethylthiophene over (1,2-dimethylbenzene + *n*-non-1-ene) ratios, both reflecting the kerogen atomic S<sub>org</sub>/C ratio (Eglinton et al., 1990a, 1994), with  $\delta^{13}\text{C}_{\text{TOC}}$  (Figs. 5.8a,b). Moreover, with increasing  $\delta^{13}\text{C}_{\text{TOC}}$  2-methylthiophene, 2,5-dimethylthiophene and 2-ethyl-5-methylthiophene, which all have linear carbon skeletons, become increasingly dominant over other thiophenes (Figs. 5.8c, 5.9a, Table 5.5). Like the thiophene ratios, the ratio of benzothiophenes over toluene is significantly enhanced

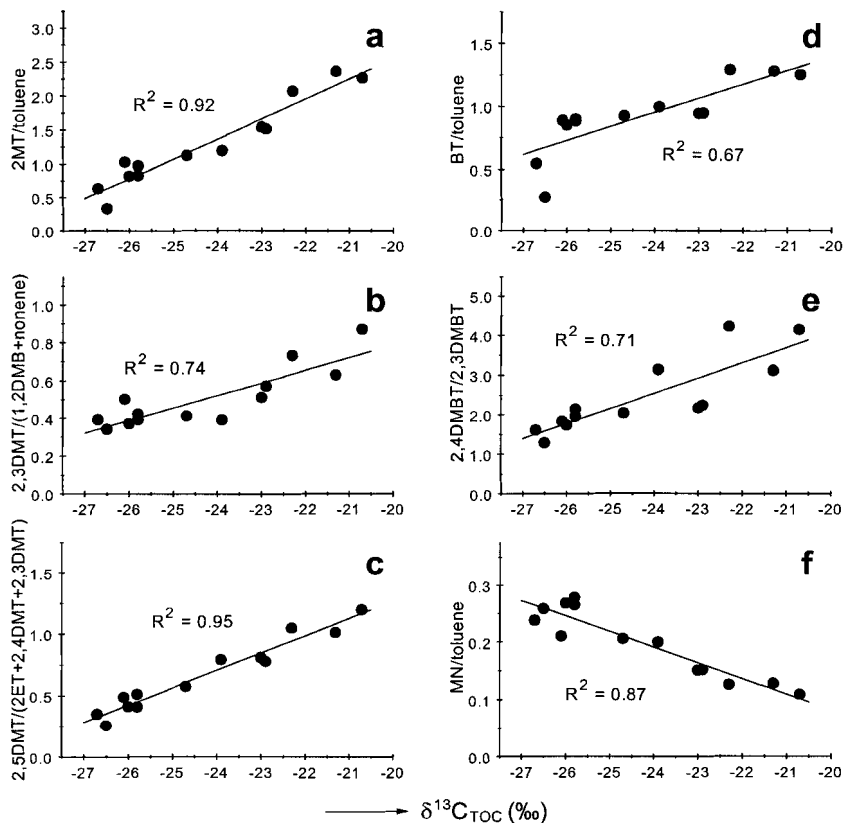


**Fig. 5.8.** Correlation between  $\delta^{13}\text{C}_{\text{TOC}}$  and ratio of (a) 2-methylthiophene over toluene, (b) 2,3-dimethylthiophene over (1,2-dimethylbenzene + *n*-non-1-ene), (c) 2,5-dimethylthiophene over (2-ethylthiophene + 2,4-dimethylthiophene + 2,3-dimethylthiophene), (d) benzothiophenes (i.e. six most prominent C<sub>1</sub>-C<sub>2</sub> alkylated benzothiophenes in the *m/z* 147 + 148 + 161 + 162 mass chromatogram) over toluene, (e) 2,4-dimethylbenzo[b]thiophene over 2,3-dimethylbenzo[b]thiophene, and (f) methylnaphthalenes over toluene in kerogen pyrolysates. MT = methylthiophene, DMT = dimethylthiophene, DMB = dimethylbenzene, ET = ethylthiophene, BT = benzothiophenes, DMBT = dimethylbenzo[b]thiophene, MN = methylnaphthalenes.



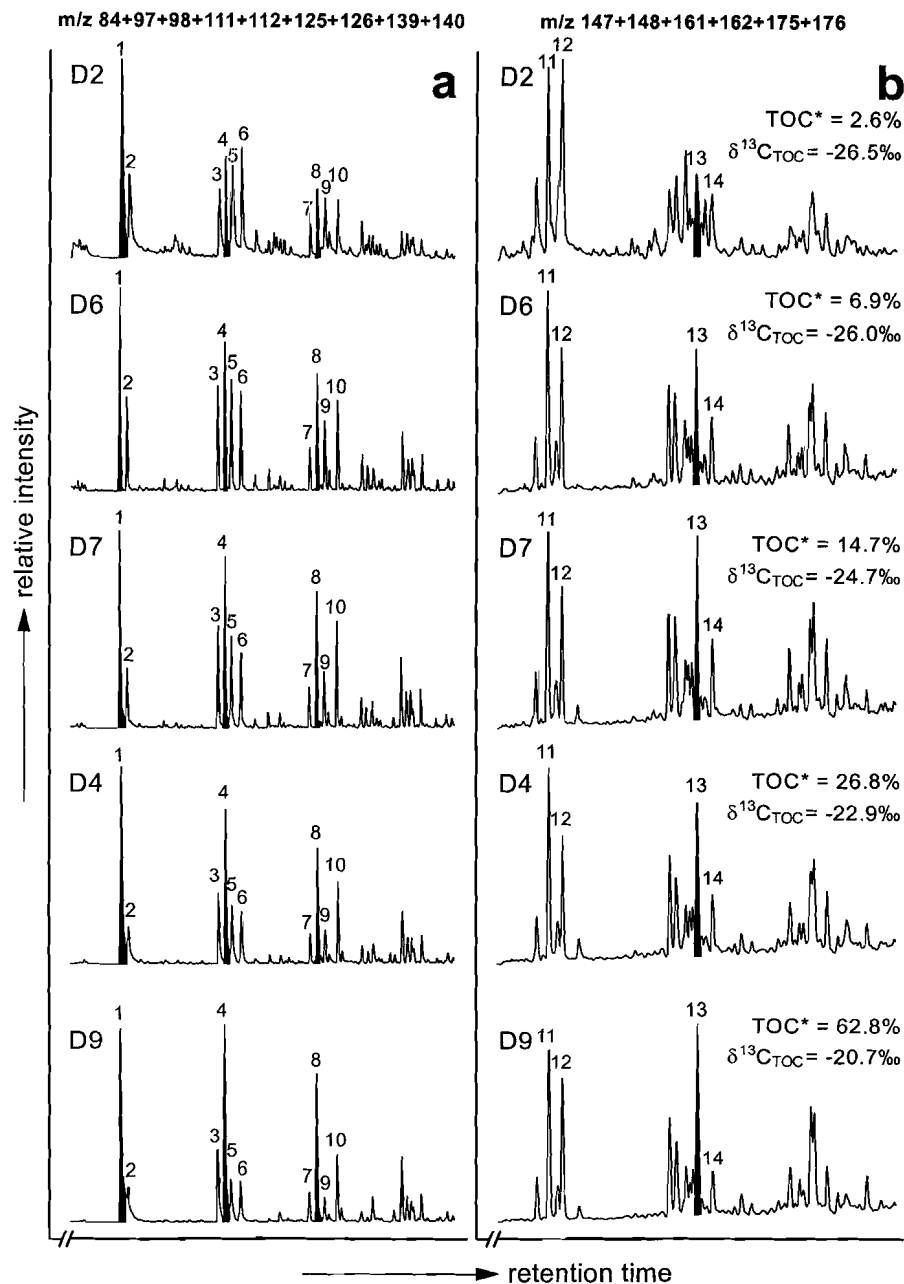


Fig. 5.9. Partial mass chromatograms showing distribution of (a) LMW alkylated thiophenes and (b) LMW alkylated benzo[b]thiophenes in pyrolysates of five samples with different TOC\* and  $\delta^{13}\text{C}_{\text{TOC}}$  values. Numbers refer to components listed in Table 5.5.

in samples with high  $\delta^{13}\text{C}_{\text{TOC}}$  (Fig. 5.8d), and 2,4-dimethylbenzo[b]thiophene, which has a linear carbon skeleton, becomes an increasingly abundant member of the  $\text{C}_2$  alkylated benzothiophene cluster (Figs. 5.8e, 5.9b, Table 5.5). On the other hand, distributions of non-sulfur compounds like methylnaphthalenes and methylindans are identical in all pyrolysates, and their abundances relative to that of toluene are negatively correlated with  $\delta^{13}\text{C}_{\text{TOC}}$  (e.g. Fig. 5.8f). Finally, the magnitude of the UCM is significantly enhanced in samples with a high  $\delta^{13}\text{C}_{\text{TOC}}$ , though this is not very clear from Fig. 5.7, since the pyrograms are normalised on their highest peak.

*Off-line pyrolysis.* The pyrolysis yield (i.e. fraction of organic carbon released upon pyrolysis) varies between 1 and 40% (Table 5.6), and correlates well with the HI determined by Rock Eval, for which samples are heated to a significantly higher temperature (Espitalié et al., 1977). Unfortunately, the recovery of the internal standard (calculated using the squalane standard, which was added after pyrolysis), was found to depend strongly on TOC\* (Table 5.6), suggesting the mineral matrix interferes with the evaporation of the standard. Pyrolysis products could thus not be quantified using this standard. As an alternative, *n*-alkanes were quantified using the external standard, implying that eventual losses during pyrolysis were not accounted for. Unexpectedly, summed concentrations of  $\text{C}_{11+}$  *n*-alkanes determined in this way are extremely low and of the same order of magnitude in all pyrolysates (0.5-2.5 mg/g TOC; Table 5.6). The size of the UCM in the off-line pyrolysates is positively correlated with  $\delta^{13}\text{C}_{\text{TOC}}$ . The presence of sulfur in the UCMs was confirmed by the FPD signal, which followed the shape of the UCMs on the FID-trace.

The  $\delta^{13}\text{C}$  values of the kerogen residues after pyrolysis are almost similar to the corresponding  $\delta^{13}\text{C}_{\text{TOC}}$  values (Table 5.6). The pyrolysates are consistently depleted in  $^{13}\text{C}$  by ca. 1‰ relative to the corresponding kerogens (Table 5.6). It should be noted that pyrolysates were evaporated to dryness to determine their  $\delta^{13}\text{C}$ , and gases have not been analysed.

The saturated hydrocarbon fractions of the pyrolysates were analysed using GC-IRMS. Like the free  $\text{C}_{21}$  and  $\text{C}_{23}$  *n*-alkanes, *n*- $\text{C}_{21}$  and *n*- $\text{C}_{23}$  alkanes released by pyrolysis appear more enriched in  $^{13}\text{C}$  than other *n*-alkanes (Fig. 5.10). The  $^{13}\text{C}$  contents of free *n*- $\text{C}_{21}$  and *n*- $\text{C}_{23}$  are higher than those of *n*- $\text{C}_{21}$  and *n*- $\text{C}_{23}$  in the pyrolysates, but if in the extract one of the two *n*-alkanes has a more pronounced isotope excursion than the other, this is also the case in the corresponding pyrolysate (Fig. 5.10).  $\text{C}_{11}$  to  $\text{C}_{20}$  acyclic, regular isoprenoids exclusive of the  $\text{C}_{12}$  and  $\text{C}_{17}$  members are abundant in the pyrolysate of sample D4. Not only are these isoprenoids significantly enriched in  $^{13}\text{C}$  relative to the *n*-alkanes (excluding *n*- $\text{C}_{21}$  and *n*- $\text{C}_{23}$ ), but also their  $^{13}\text{C}$  contents are higher than those of isoprenoids in the other samples (Fig. 5.10). The isoprenoids in D5 and D6, although only slightly more abundant than those in some of the other samples, also have significantly higher  $\delta^{13}\text{C}$  values than the average *i*- $\text{C}_{16}$  and *i*- $\text{C}_{18}$  alkanes (Fig. 5.10).

For samples D9 and D10, two additional pyrolysis experiments were performed in order to determine the  $^{13}\text{C}$  contents of the most abundant alkylthiophenes and alkylbenzenes. Due to the complexity of the pyrolysates only a limited number of  $\delta^{13}\text{C}$  values, including those of  $\text{C}_9$ - $\text{C}_{11}$  *n*-alkanes and *n*-alkenes, could be determined, and standard deviations are relatively large (Table 5.7). Both alkylthiophenes and alkylbenzenes and  $\text{C}_9$ - $\text{C}_{11}$  *n*-alkanes

**Table 5.6.** Off-line pyrolysis data.

sample	TOC* (%) <sup>a</sup>	pyrolysis yield (%)	% recovery of internal standard	C <sub>11+</sub> , <i>n</i> -alkanes (mg/g TOC)	δ <sup>13</sup> C (‰)				estimated carbohydrate carbon (%)
					kerogen	kerogen residue after pyrolysis	pyrolysate	linear algaenans	
D1	61.1	33.9	74	0.6	-22.3	-23.0	-23.6	-27.8	56
D2	2.6	0.6	10	1.0	-26.5	n.d. <sup>b</sup>	-27.2	n.d.	24
D3	48.1	33.2	56	0.5	-21.3	-21.5	-21.8	-25.3	55
D4	26.8	40.2	21	2.1	-22.9	-23.2	-23.3	-27.4	48
D5	18.2	27.5	17	1.8	-23.9	-23.8	n.d.	-27.3	37
D6	6.9	14.8	3	2.3	-26.0	-25.7	n.d.	-27.8	18
D7	14.7	23.9	24	2.2	-24.7	-24.7	n.d.	-27.6	30
D8	36.6	37.3	49	1.8	-23.0	-23.5	-23.5	-26.0	37
D9	62.8	37.0	65	0.9	-20.7	-20.8	-21.5	-26.7	69
D10	6.2	14.4	5	1.3	-25.8	-25.8	-26.9	-28.4	25
D11	14.3	21.6	7	2.2	-26.1	-26.6	-27.0	-28.4	22
D12	5.0	13.0	4	2.5	-26.7	-26.5	-27.6	-28.7	19
D13	10.7	18.8	5	1.3	-25.8	-25.7	n.d.	-29.2	31

<sup>a</sup> TOC after decalcification<sup>b</sup> not determined

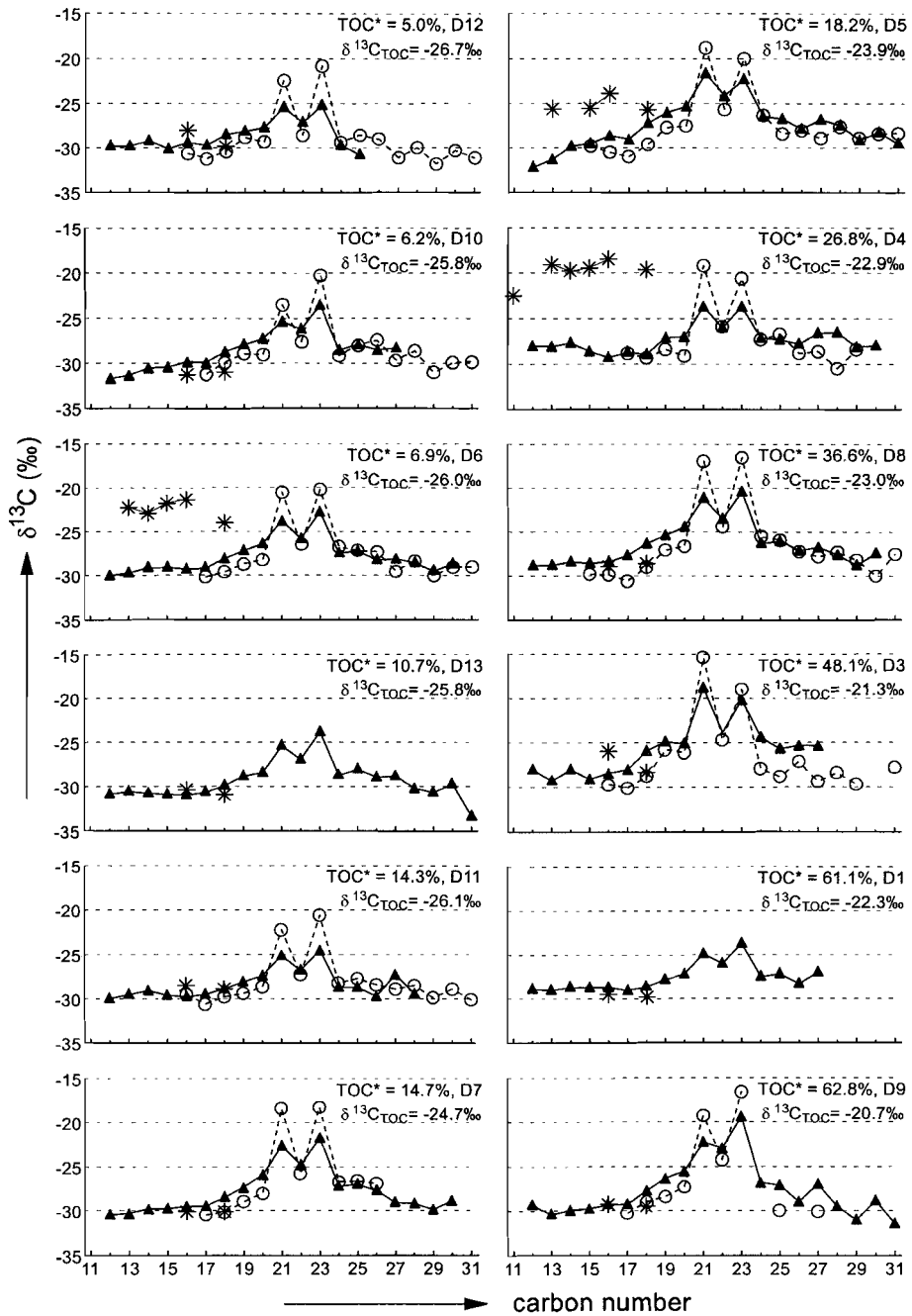


**Fig. 5.10.** Stable carbon isotopic compositions of *n*-alkanes (filled triangles) and regular isoprenoid alkanes (asterisks) released by off-line pyrolysis, and free *n*-alkanes (open circles).

and *n*-alkenes are 4 to 7‰ heavier in sample D9 than in D10. Within the samples, C<sub>9</sub>-C<sub>11</sub> *n*-alkanes and *n*-alkenes have similar δ<sup>13</sup>C values, and are significantly more depleted in <sup>13</sup>C than the other pyrolysis products (Table 5.7). Excluding 2-ethyl-5-methylthiophene, which is the most <sup>13</sup>C enriched compound in each of the pyrolysates, the δ<sup>13</sup>C values of the alkylthiophenes and alkylbenzenes are similar within the samples (Table 5.7).

**Table 5.7.** The δ<sup>13</sup>C values of different pyrolysis products of samples D9 and D10.

	D9	D10
toluene <sup>a</sup>	-22.7 ± 0.7	-27.3 ± 0.8
2-methylthiophene <sup>b</sup>	-22.1 ± 1.3	-26.3 ± 1.2
<i>n</i> -C <sub>9</sub> alkene + alkane <sup>c</sup>	-24.6 ± 0.3	
2,5-dimethylthiophene <sup>c</sup> + 1,3-dimethylbenzene + 1,4-dimethylbenzene	-20.8 ± 0.2	-27.6 ± 0.9
2,4-dimethylthiophene	-21.8 ± 0.5	-27.6 ± 0.8
2,3-dimethylthiophene	-19.8 ± 1.5	-25.7 ± 1.5
1,2-dimethylbenzene	-20.6 ± 0.5	-27.5 ± 1.7
<i>n</i> -C <sub>10</sub> alkene + alkane <sup>c</sup>	-25.7 ± 0.3	
2-ethyl-5-methylthiophene	-15.5 ± 1.6	-19.3 ± 1.1
2,3,5-trimethylthiophene	-21.3 ± 0.5	
1,2,4-trimethylbenzene	-21.6 ± 0.9	-27.7 ± 1.1
<i>n</i> -C <sub>11</sub> alkene + alkane <sup>c</sup>	-25.0 ± 1.1	

<sup>a</sup> not baseline separated from 2-methylthiophene

<sup>b</sup> not baseline separated from toluene

<sup>c</sup> coelution

### *Organic petrography*

The OM (except for samples D6 and D10) was optically examined in reflected, ultraviolet and transmitted light. The most TOC-rich and most <sup>13</sup>C enriched sample (D9, Blackstone Band) comprises more than 70% of strongly fluorescing, oval-shaped, internally unstructured bodies, about 200 μm in length and few μm in thickness. In transmitted light these appear as orange to red coloured transparent lenses. Based on their appearance these macerals are attributed to bituminite (Teichmüller, 1974). Other macerals in this sample are bituminite with inclusions of framboidal pyrite, strongly fluorescing, thin walled alginites, and liptodetrinite. In the coccolithic limestones (D1, D3, D8), which have the highest δ<sup>13</sup>C<sub>TOC</sub> values after sample D9, coccoliths and calcite crystals are embedded in bituminite (yellow fluorescing AOM). The OM in the other samples is largely present as organo-mineral matrix, but bituminite is also observed. Generally, the proportion of bituminite increases with increasing TOC.

Several types of alginites were observed, and they were grouped according to the thickness and colour of their cell walls as seen from fluorescence microscopy (thick walled alginites with strong to very strong yellow fluorescence, medium walled alginites, and thin walled alginites with weak brownish or strong to very strong yellow fluorescence). In samples D1, D3, D8 and D9, which are the four samples most enriched in <sup>13</sup>C, alginites constitute only a very small part of the OM (< 1%). Moreover, in these samples only thin

walled types were detected. The other samples, with the exception of D2 (Basalt Stone Band), contain both thin and thick walled alginites. Alginites of medium thickness were observed only in D4 and D11. The total contribution of alginites differs significantly among the samples, and reaches a maximum in D13 (7%).

The contribution of cuticles and other relatively well preserved plant tissues to the samples is generally low (< 0.5%). In most samples, inertinite (black woody material) adds to 1 or 2%, implying this maceral is relatively more abundant in the OM of TOC-lean samples. In samples D4 and D12 inertinite is more prominent than in the other samples (3 to 6%). Spores and pollen were not detected. Vitrinite is scarce in all samples, and often too small for reflectance measurement. Vitrinite reflectance values of 0.36 and 0.31 were reported by Park (1982, as cited in Farrimond et al., 1984) for the Whitestone Band and Blackstone Band, respectively. Black (transmitted light) AOM (as seen by TEM), reported by Boussafir et al. (1995) to be a minor constituent of their isolated kerogens of the *eudoxus* zone (Cleveland Basin, UK), was not observed in our sample set. However, since we have been studying the OM in polished sections to preserve the sediment structure, the black AOM, if present, may have been identified as vitrinite or inertodetrinite.

## Discussion

The coccolith-rich limestones D1, D3 and D8 do not fit into the TOC- $\delta^{13}\text{C}_{\text{TOC}}$  relationship reported by Huc et al. (1992) (Fig. 5.1a). On the basis of their relatively high  $\delta^{13}\text{C}_{\text{TOC}}$ , OM in these samples is more likely to resemble OM in the oil shales than that in shales poor in TOC. This would be in accordance with the models proposed by Tyson (1985, 1996) and Oschmann (1988, 1991), in which both coccolithic limestones and TOC-rich shales are thought to be deposited in frequently oxygen-depleted depositional environments. If we compensate for dilution of the sediment by carbonate, by expressing the organic carbon content as a weight percentage of the non-carbonate part of the rock (TOC\*), the coccolith-rich limestones indeed end up between the oil shales in Fig. 5.1b. This suggests that no coccolithic limestones are included in the sample set of Huc et al. (1992), and that the positive correlation between TOC and  $\delta^{13}\text{C}_{\text{TOC}}$  is in fact one between TOC\* and  $\delta^{13}\text{C}_{\text{TOC}}$ . Even the diagenetic carbonates D2 and D7 (D7 is a diagenetically altered coccolith-rich limestone), with their low respectively intermediate  $\delta^{13}\text{C}_{\text{TOC}}$ , comply with the almost linear relationship between TOC\* and  $\delta^{13}\text{C}_{\text{TOC}}$  (Fig. 5.1b).

Differences in  $\delta^{13}\text{C}_{\text{TOC}}$  can sometimes be explained by different contributions of terrestrial and marine OM. In the case of the KCF, however, optical examination has shown only a minor part of the OM to be terrestrially derived, and it has been examined by modelling that differences in  $\delta^{13}\text{C}_{\text{TOC}}$  resulting from the mixing of terrestrial and marine OM cannot account for the wide range of  $\delta^{13}\text{C}_{\text{TOC}}$  values observed (Huc et al., 1992). The microscopical data of our sample set and the generally high HI values (Table 5.2) are in agreement with this conclusion. Moreover, the kerogen pyrolysates of all samples indicate only minor contributions from lignins or modified lignins, and terrestrial biomarkers in the bitumen are low. The origin of the large fluctuations in  $\delta^{13}\text{C}_{\text{TOC}}$  must thus be due to changes in the marine component of the OM.

### Extractable biomarkers

It was examined if there were any trends in the molecular and stable carbon isotopic composition of the extractable OM that could be related to the positive correlation between TOC\* and  $\delta^{13}\text{C}_{\text{TOC}}$ . The similar  $\delta^{13}\text{C}$  values in all samples of  $\text{C}_{16}$ - $\text{C}_{18}$  *n*-alkanes (Fig. 5.4), components primarily derived from algae or cyanobacteria (Gelpi et al., 1970), and, in fact, most *n*-alkanes indicate that differences in  $\delta^{13}\text{C}_{\text{DIC}}$  and differences in the concentration of DIC in the photic zone were minor, confirming our previous suggestion (van Kaam-Peters et al., 1997c). This implies that the hypotheses of Huc et al. (1992) and Hollander et al. (1993), explaining the TOC\*- $\delta^{13}\text{C}_{\text{TOC}}$  relationship by changes in the degree of OM reworking or by changes in primary productivity, need to be reevaluated. Since the uptake of  $\text{CO}_2$  by Chlorobiaceae, the source organisms of the isorenieratene derivatives, is unaccompanied by significant isotopic fractionations, the stable carbon isotopic composition of their biomass is independent of the concentration of DIC. Therefore, the narrow range of  $\delta^{13}\text{C}$  values measured for macromolecularly sulfur-bound (S-bound) isorenieratene (Table 5.3), indicates that also at the chemocline, where Chlorobiaceae have their ecological niche,  $\delta^{13}\text{C}_{\text{DIC}}$  was invariably the same.

Assuming that pristane and phytane are mainly derived from tocopherols (Goossens et al., 1984) and chlorophyll-a (Volkman and Maxwell, 1986), respectively, one would expect their  $\delta^{13}\text{C}$  values to be more or less similar to those of the  $\text{C}_{16}$ - $\text{C}_{18}$  *n*-alkanes. This is clearly not the case, as in samples D4-D6 pristane and phytane exhibit a large isotope excursion (Fig. 5.3a). Since there were no large variations in  $\delta^{13}\text{C}_{\text{DIC}}$  and in the concentration of DIC, the isotopically heavy pristane and phytane in samples D4-D6 probably partly derive from yet an additional source. Unlike the other samples, D4-D6 also contain substantial amounts of isotopically heavy norpristane and 2,6,10-trimethyldecane (Fig. 5.3), and their kerogen pyrolysates are characterised by isotopically heavy, acyclic, regular isoprenoids (Figs. 5.7 and 5.10). This suggests that the pristane and phytane in samples D4-D6 partly derive from source organism(s) biosynthesising isoprenoid algaenan(s). Such isoprenoid algaenans may originate from marine algal equivalents of *Botryococcus braunii*, *L* race (Höld et al., 1997). It is not clear whether the free isoprenoid alkanes derive from low-molecular-weight (LMW) precursors, or were released from the isoprenoid algaenan(s) during diagenesis, or both scenarios apply. In the bitumens of samples D4-D6 pristane and phytane are more abundant than the  $\text{C}_{16}$  and  $\text{C}_{18}$  isoprenoids (Fig. 5.3), whereas in their kerogen pyrolysates the opposite is the case (Fig. 5.7). This suggests that, if the isoprenoid alkanes in the bitumen derive directly from the algaenan(s), less energy is involved in the release of pristane and phytane than in that of norpristane and 2,6,10-trimethyldecane.

Although extractable biomarkers may not be representative of the total OM (Sinninghe Damsté et al., 1993a; Sinninghe Damsté and Schouten, 1997), they can be used to differentiate between biomass from isotopically distinct sources, that may have contributed to the kerogen. In other words, increasing concentrations of isotopically heavy biomarkers with increasing TOC\*, may be accompanied by an increasing proportion of isotopically heavy biomass to the kerogen, which may explain the TOC\*- $\delta^{13}\text{C}_{\text{TOC}}$  relationship observed. Several compounds with  $\delta^{13}\text{C}$  values considerably higher than the ca. -30‰ of most *n*-alkanes (Fig. 5.4) and the ca. -32‰ of pristane and phytane (excluding

pristane and phytane of samples D4-D6 for reasons explained above) have been identified in the extracts. These are C<sub>21</sub> and C<sub>23</sub> *n*-alkanes ( $\delta^{13}\text{C}$  between -23.5‰ and -15.4‰, excluding *n*-C<sub>21</sub> in D2), 2-methyltetracosane, 2-methylhexacosane, 3-isopropyltetracosane and 3-isopropylhexacosane ( $\delta^{13}\text{C}$  between -20.0‰ and -15.9‰), all thought to derive from the same source (Schouten et al., 1997), and derivatives of isorenieratene ( $\delta^{13}\text{C} = -17 \pm 1\%$ ). The summed concentrations of isorenieratene derivatives and the summed concentrations of iso- and isopropyl- tetracosanes and hexacosanes do not correlate with  $\delta^{13}\text{C}_{\text{TOC}}$  (Fig. 5.5a), suggesting that high  $\delta^{13}\text{C}_{\text{TOC}}$  values cannot be ascribed to large contributions of these compounds, or associated kerogen fractions derived from their source organisms, to the OM. A similar reasoning can be applied to the summed concentrations of *n*-C<sub>21</sub> and *n*-C<sub>23</sub>, which to some extent are inversely related to  $\delta^{13}\text{C}_{\text{TOC}}$  (Fig. 5.5a).

Major compound classes in the bitumen other than isoprenoid and normal alkanes and derivatives of isorenieratene, are desmethyl and 4-methyl steroids, neohop-(13)18-enes and homohopanes. In the Lower Kimmeridge Clay,  $\delta^{13}\text{C}$  values of these compounds vary between -31.7‰ and -24.8‰, implying that changes in their relative abundances could not account for the  $\delta^{13}\text{C}_{\text{TOC}}$  of -22.5‰ measured for one of the samples (van Kaam-Peters et al., 1997c). In this study, no  $\delta^{13}\text{C}$  values were determined for these compounds. However, in analogy to the Lower Kimmeridge Clay, variations in their relative abundances (Fig. 5.5b) are unlikely to be associated with large differences in  $\delta^{13}\text{C}_{\text{TOC}}$ . The steroid and hopanoid biomarkers are largely derived from (i) the same algal and cyanobacterial source organisms as pristane, phytane and C<sub>16</sub>-C<sub>18</sub> *n*-alkanes, components with  $\delta^{13}\text{C}$  values between -32‰ and -30‰, and (ii) from heterotrophs grazing on these algae and cyanobacteria, and having lipid  $^{13}\text{C}$  contents similar to those of their food source (Fry and Sherr, 1984). Therefore, it is very unlikely that the steroid and hopanoid  $\delta^{13}\text{C}$  values are as high as -20‰, the lowest value that would be required to account for the range of  $\delta^{13}\text{C}_{\text{TOC}}$  values observed.

### *Kerogen pyrolysates*

Since the composition of the extractable OM provides no explanation for the large fluctuations in  $\delta^{13}\text{C}_{\text{TOC}}$ , attention is focused on the kerogen pyrolysates. The (non-volatile) off-line pyrolysates are consistently depleted in  $^{13}\text{C}$  by ca. 1‰ relative to the corresponding kerogens (Table 5.6). This suggests that, in agreement with the findings of Horsfield (1989), the pyrolysates are more or less representative of the kerogen as a whole. In addition, the  $\delta^{13}\text{C}$  values of the kerogen residues after pyrolysis are very similar to the corresponding  $\delta^{13}\text{C}_{\text{TOC}}$  values (Table 5.6). This is not surprising if pyrolysis yields are low, but for samples with yields higher than ca. 20% it may indicate that the pyrolysis does not particularly favour the release of certain isotopically distinct compounds. Theoretically,  $\delta^{13}\text{C}$  of the gases released can be calculated by difference, but this is only reliable for samples with high pyrolysis yields. Looking at the five samples with pyrolysis yields of more than 30% (Table 5.6), both the pyrolysates and the kerogen residues are depleted in  $^{13}\text{C}$  relative to the starting material, implying the gases are isotopically heavier than the corresponding kerogen.

The relatively high  $\delta^{13}\text{C}$  values of C<sub>21</sub> and C<sub>23</sub> *n*-alkanes in the kerogen pyrolysates (Fig. 5.10) are explained by the presence in the kerogen of carbon isotopically heavy *n*-C<sub>21</sub>



and  $n\text{-C}_{23}$  moieties that are terminally linked to the kerogen *via* oxygen (cf. van Kaam-Peters et al., 1997c). Upon pyrolysis these moieties will largely be released from the kerogen as  $n\text{-C}_{21}$  and  $n\text{-C}_{23}$  alkanes. In addition, some  $^{13}\text{C}$  enriched  $n$ -alkanes with slightly shorter chains are formed by cleavage of C-C bonds near the oxygen atom (van Kaam-Peters et al., 1997c). It is noted that the  $^{13}\text{C}$  contents of  $n\text{-C}_{21}$  and  $n\text{-C}_{23}$  in the bitumen are consistently higher than those of  $n\text{-C}_{21}$  and  $n\text{-C}_{23}$  released upon pyrolysis, and  $^{13}\text{C}$  contents of  $n\text{-C}_{18}$ ,  $n\text{-C}_{19}$  and  $n\text{-C}_{20}$  in the bitumen are consistently lower than the corresponding  $n$ -alkanes in the pyrolysate (Fig. 5.10). Therefore, part of the  $^{13}\text{C}$  enriched  $n$ -alkanes present in the bitumen was probably not released from the kerogen during diagenesis, but derives from LMW precursors biosynthesised by the same source organism(s) producing the  $^{13}\text{C}$  enriched  $n$ -alkane moieties in the kerogen. This scenario is in agreement with recent work of Gelin et al. (1996), who identified both alkyldiols and ether-linked macromolecules composed of alkyldiol carbon skeletons in the algal biomass of *Nannochloropsis salina*.

The  $\delta^{13}\text{C}$  patterns of  $n$ -alkanes in the kerogen pyrolysates (Fig. 5.10) can thus be ascribed to homologous series of  $n$ -alkanes derived from algaenans having a  $\delta^{13}\text{C}$  value of approximately -30‰, in addition to some  $\text{C}_{18}\text{-C}_{23}$   $n$ -alkanes derived from the isotopically heavy  $n\text{-C}_{21}$  and  $n\text{-C}_{23}$  moieties. The fact that the 'background'  $n$ -alkanes in the kerogen pyrolysates have similar  $\delta^{13}\text{C}$  values in all samples, again demonstrates that differences in  $\delta^{13}\text{C}_{\text{DIC}}$  and in the concentration of DIC were insignificant. The rather wide range of  $\delta^{13}\text{C}$  values of  $n\text{-C}_{21}$  and  $n\text{-C}_{23}$  in the pyrolysates (Fig. 5.10) shows that the contribution of isotopically heavy  $n\text{-C}_{21}$  and  $n\text{-C}_{23}$  moieties to the kerogen is variable, and in principle, this could (partly) account for the variation in  $\delta^{13}\text{C}_{\text{TOC}}$ . However, the magnitude of the  $n\text{-C}_{21}$  and  $n\text{-C}_{23}$  isotope excursions in the pyrolysates of D1, D4, D10, D11 and D13 is the same, whereas their  $\delta^{13}\text{C}_{\text{TOC}}$  varies between -26.1‰ and -22.3‰. This implies that differences in  $\delta^{13}\text{C}_{\text{TOC}}$  are not related to different proportions of the isotopically heavy  $n\text{-C}_{21}$  and  $n\text{-C}_{23}$  moieties. Similarly, differences in  $\delta^{13}\text{C}_{\text{TOC}}$  cannot be explained by different contributions of the isotopically heavy isoprenoid algaenans mentioned above. These algaenans are present only in samples D4-D6, and several other samples have higher  $\delta^{13}\text{C}_{\text{TOC}}$  values (Fig. 5.10).

#### *Possible carbohydrate origin for $\text{C}_1\text{-C}_3$ alkylated thiophenes in kerogen pyrolysates*

The relative abundance of OSC, and the size of the UCM, are the major characteristics of the kerogen pyrolysates distinguishing one sample from another. Most conspicuous are the highly variable proportions of alkylated thiophenes. Alkylated thiophenes have been proposed to be formed by  $\beta$ -cleavage of thiophene units present in the macromolecular matrix, which have been formed by sulfur incorporation into LMW or high-molecular-weight (HMW) lipids (Sinninghe Damsté et al., 1989, 1990; Douglas et al., 1991). Since it is likely that, analogous to the free lipids and algaenans, S-bound lipids have similar  $\delta^{13}\text{C}$  values in all samples, the different abundances of the alkylated thiophenes would still not be able to explain the differences in the  $^{13}\text{C}$  content of the KCF kerogens.

However, a major problem remains with the interpretation that alkylated thiophenes are derived from alkylthiophene moieties present in the kerogen. Eglinton et al. (1990a,b) have shown that upon both natural and artificial maturation the precursors of the alkylated thiophenes were lost from the kerogen earlier than those of the alkylated benzenes and  $n$ -

alkanes. This was rather surprising since the bond energy of the  $\beta$ -bond in alkylthiophenes is almost identical to that in alkylbenzenes (Claxton et al., 1993). Sinninghe Damsté et al. (1990) hypothesized that this may be related to the mode of bonding of the alkylthiophene moiety in the kerogen (e.g. by multiple weak S-C bonds) and suggested that during natural maturation these moieties were released as long-chain thiophenes. Subsequent studies of a sulfur-rich kerogen by micro-sealed vessel pyrolysis (Horsfield et al., 1989), which enables monitoring the produced LMW components, indicated, however, that LMW alkylated thiophenes are also the most important products if this kerogen is heated to temperatures as low as 150°C (Sinninghe Damsté and Horsfield, unpublished results). Furthermore, heating of a long-chain alkylthiophene at 300°C for 3 days yielded no LMW alkylthiophenes by cleavage of the relatively weak  $\beta$ -bond. Recently, several studies (Krein and Aizenshtat, 1994; Schouten et al., 1994; Koopmans et al., 1995; Tomic et al., 1995) have indicated that alkylthiophenes are stable thermal products formed at relatively low temperatures from carbon skeletons linked intermolecularly *via* several sulfur bridges. In addition, sulfur speciation studies with XANES spectroscopy of artificially matured kerogens indicated that the relative amounts of (poly)sulfide sulfur decreased significantly with increasing maturation temperature, whilst the relative amount of thiophenic sulfur remained relatively constant (Nelson et al., 1995). All these findings shed a new light on the origin of the LMW alkylthiophenes in pyrolysates. It seems likely to ascribe them, at least in part, to small (i.e. C<sub>5</sub>-C<sub>7</sub>), predominantly linear carbon skeletons, linked to the kerogen matrix by multiple (poly)sulfide linkages rather than to alkylthiophene moieties present as such. This would explain the early loss during maturation of the precursor moieties of the LMW alkylthiophenes (Eglinton et al., 1990a,b) since C-S bonds are relatively weak. In that case it would be logical to partly relate the alkylthiophenes to sulfurised monosaccharides since (i) they possess C<sub>5</sub>-C<sub>7</sub> linear carbon skeletons and (ii) they contain multiple functional groups, which allow reaction with inorganic reduced sulfur species during early diagenesis, possibly after dehydration. Such reactions are comparable to those occurring with bacteriohopanetetrol (containing a side-chain structurally similar to that of a monosaccharide), where sulfur is incorporated in the side-chain by up to four (poly)sulfide linkages (Richnow et al., 1992, 1993) leading to sequestration of the carbon skeleton in HMW OM fractions.

This hypothesis is supported by several results. First of all, it has been shown by laboratory studies that carbohydrates can react with hydrogen sulfide or polysulfides, yielding OSC which upon pyrolysis produce several thiophenes (Moers et al., 1988). Recently, flash pyrolysis of the alga *Phaeocystis sp.* collected during a bloom in the North Sea and the same material artificially sulfurised indicated that C<sub>1</sub>-C<sub>3</sub> alkylated thiophenes are only produced after sulfurisation (Kok et al., 1997a). Since *Phaeocystis sp.* contains large amounts of carbohydrates, it was assumed that sulfurisation of carbohydrates led to the thiophene precursors. Secondly, in agreement with our data (Table 5.7), alkylthiophenes in pyrolysates were found to be significantly enriched in <sup>13</sup>C relative to the *n*-alkanes derived from algaenan (Eglinton, 1994; Höld et al., 1995). Since carbohydrates are known to be enriched in <sup>13</sup>C by several per mil compared to lipids derived from the same organism (Park and Epstein, 1961; Degens et al., 1968; DeNiro and Epstein, 1978), this would be in favour of an origin for C<sub>1</sub>-C<sub>3</sub> alkylated thiophenes from sulfurised carbohydrates.

If a substantial fraction of the LMW thiophenes indeed represent sulfurised carbohydrates, variations in the contribution of these components may explain the different  $^{13}\text{C}$  contents of the KCF kerogens. Indeed, the abundance of LMW thiophenes is positively correlated with  $\delta^{13}\text{C}_{\text{TOC}}$  (Figs. 5.8a,b). Moreover, the dominance of 2-methylthiophene, 2,5-dimethylthiophene and 2-ethyl-5-methylthiophene (components with linear carbon skeletons and presumed to be derived from sulfurised carbohydrates) over other alkylthiophenes also increases with increasing  $\delta^{13}\text{C}_{\text{TOC}}$  (Fig. 5.8c). Still, in all instances the peak areas of the linear  $\text{C}_1\text{-C}_3$  alkylated thiophenes are rather small compared to the area of the total pyrolysate (e.g. Fig. 5.7), implying that additional  $^{13}\text{C}$ -enriched compounds are necessary to account for the different  $\delta^{13}\text{C}_{\text{TOC}}$  values. The benzothiophenes are believed to be potential candidates, since (i) Kok et al. (1997b) have shown that in the pyrolysates of the insoluble non-hydrolysable residues of (poly)saccharides sulfurised in the laboratory, not only short-chain, linear thiophenes are present but also other OSC, among which significant amounts of benzothiophenes, (ii) the relative abundance of benzothiophenes is positively correlated with  $\delta^{13}\text{C}_{\text{TOC}}$  (Fig. 5.8d), and (iii) analogous to the linear  $\text{C}_1\text{-C}_3$  alkylated thiophenes, 2,4-dimethylbenzo[b]thiophene (having a linear carbon skeleton) becomes increasingly dominant over other  $\text{C}_2$  alkylated benzothiophenes with increasing  $\delta^{13}\text{C}_{\text{TOC}}$  (Fig. 5.8e). Thus, it is suggested that benzothiophenes are also partly derived from sulfurised carbohydrates, although their pathway of formation is enigmatic.

Finally, considering the small quantities of *n*-alkanes in the off-line pyrolysates (Table 5.6), the UCM must play an important role in the isotopic mass balance. That is, except for the most OM-lean samples, the pyrolysates are predominantly composed of UCM, implying that  $\delta^{13}\text{C}$  of the UCM ( $\delta^{13}\text{C}_{\text{UCM}}$ ) must almost equal  $\delta^{13}\text{C}$  of the pyrolysate ( $\delta^{13}\text{C}_{\text{PYROLYSATE}}$ ). It is suggested that the UCM largely originates from the gradual decomposition upon gas chromatographic separation of S-bound macromolecules in the pyrolysate, in their turn cleaved off the kerogen. We suspect that the increasing proportion of carbohydrate derived thiophenes and benzothiophenes with increasing  $\delta^{13}\text{C}_{\text{TOC}}$  mentioned above, is accompanied by an increasing contribution of S-bound carbohydrates to the UCM. Obviously, it cannot be concluded that the carbohydrate carbon is the only isotopically heavy carbon pool in the UCM. It is possible that also certain S-bound  $^{13}\text{C}$ -enriched lipids become increasingly dominant constituents of the UCM with increasing  $\delta_{\text{UCM}}$ . But if so, one would expect such compounds to be present also in the desulfurised polar fractions. Although, with the exception of isorenieratane, the lipids released upon desulfurisation of the polar fractions were not analysed by GC-IRMS, they can be excluded as an important source of  $^{13}\text{C}$ , since none of these become increasingly abundant with increasing  $\delta^{13}\text{C}_{\text{TOC}}$ .

#### *Two endmember isotopic mixing model*

As outlined above, the KCF kerogens probably contain both lipid carbon and carbohydrate carbon, lipid biomarkers having similar  $^{13}\text{C}$  contents in all samples. In order to explain the differences in  $\delta^{13}\text{C}_{\text{TOC}}$ , therefore, a two endmember mixing model is proposed, with  $\delta^{13}\text{C}$  of lipids ( $\delta^{13}\text{C}_{\text{LIPIDS}}$ ) at the one end and  $\delta^{13}\text{C}$  of carbohydrates ( $\delta^{13}\text{C}_{\text{CARBOHYDRATES}}$ ) at the other end. Accordingly, the proportion of the two carbon pools can be calculated using:

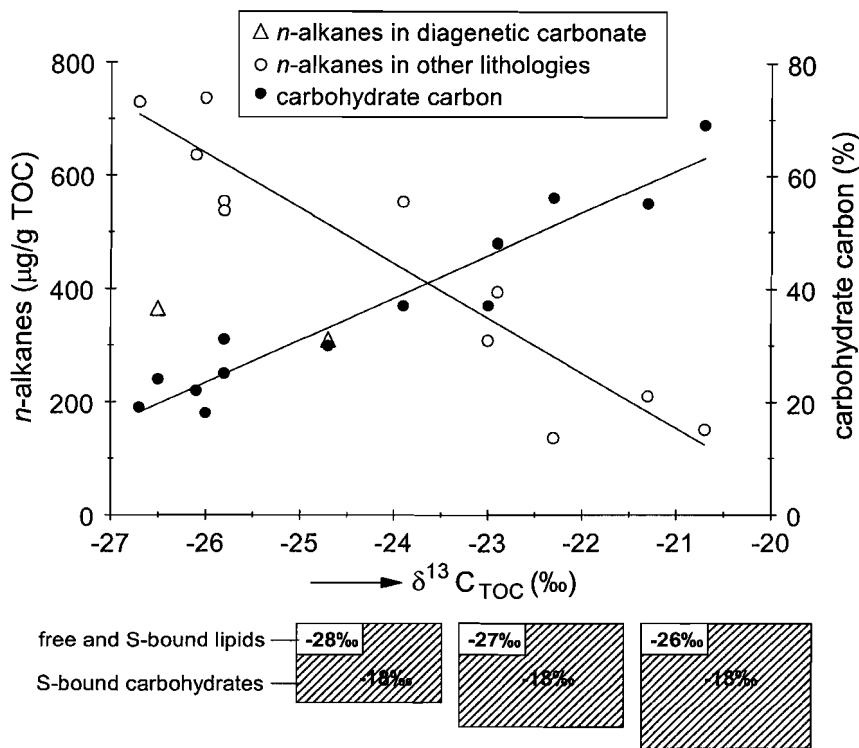


**Fig. 5.11.** Summed concentrations of  $C_{16}$ - $C_{35}$   $n$ -alkanes and relative abundance of carbohydrate carbon (calculated from carbon isotope data; Table 5.6, equation 1) as a function of  $\delta^{13}C_{TOC}$ . White and shaded rectangles represent proportions of lipid respectively carbohydrate carbon along the  $\delta^{13}C_{TOC}$  gradient (not to scale).

$$\delta^{13}C_{TOC} = X * \delta^{13}C_{LIPIDS} + Y * \delta^{13}C_{CARBOHYDRATES} \quad (1)$$

in which X and Y are the proportions of lipid respectively carbohydrate carbon. The quantitatively most important lipids identified are the algaenans. Therefore,  $\delta^{13}C_{LIPIDS}$  is thought to be best approximated by taking the weighed average of  $\delta^{13}C$  values of  $n$ -alkanes in the pyrolysate ( $\delta^{13}C_{ALGAENAN}$ ). The  $\delta^{13}C_{ALGAENAN}$  values show a positive correlation with  $\delta^{13}C_{TOC}$  (Table 5.6), caused by the varying contributions of isotopically heavy  $n$ - $C_{21}$  and  $n$ - $C_{23}$  alkanes. However, an increase in  $\delta^{13}C_{TOC}$  of 6‰ is accompanied by a rise in  $\delta^{13}C_{ALGAENAN}$  of only 3‰, and particularly in the high  $\delta^{13}C_{TOC}$  samples, additional amounts of isotopically heavy carbon, presumably derived from carbohydrates, are needed to account for the offset between  $\delta^{13}C_{TOC}$  and  $\delta^{13}C_{ALGAENAN}$ . Using  $\delta^{13}C_{LIPIDS} = \delta^{13}C_{ALGAENAN}$ , and  $\delta^{13}C_{CARBOHYDRATES} = -18\text{‰}$  (i.e. average  $\delta^{13}C$  value of 2,5-dimethylthiophene and 2-ethyl-5-methylthiophene in kerogen pyrolysate of sample D9; Table 5.7), the contribution of carbohydrate carbon to the kerogen was calculated (Table 5.6). The carbohydrate carbon content thus obtained is positively correlated with  $\delta^{13}C_{TOC}$  (Fig. 5.11).

Additional evidence for our mixing model arises from the fact that, excluding the diagenetic carbonates (D2 and D7), summed concentrations of *n*-alkanes show a strong, negative correlation with  $\delta^{13}\text{C}_{\text{TOC}}$  (Fig. 5.11). This inverse relationship with  $\delta^{13}\text{C}_{\text{TOC}}$  can be understood assuming an OM flux of which the labile compounds (particularly carbohydrates) become increasingly preserved through sulfurisation, thereby raising  $\delta^{13}\text{C}_{\text{TOC}}$  and decreasing the concentration of biomarkers if expressed relative to TOC. Sedimentary lipids are thus increasingly diluted by sulfurised carbohydrates with increasing  $\delta^{13}\text{C}_{\text{TOC}}$  (Fig. 5.11), consistent with the higher SI of the high  $\delta^{13}\text{C}_{\text{TOC}}$  samples (Fig. 5.2b). Note that there is a factor of 4.5 between the minimum and maximum *n*-alkane concentrations, which roughly corresponds to the factor of 3.5 between endmembers in the range of estimated carbohydrate carbon contents (Fig. 5.11). The low summed *n*-alkane concentrations in the diagenetic carbonates may be explained by the recently proposed mechanism for the formation of natural dolomite, in which bacteria are believed to play an active role (Vasconcelos et al., 1995). Possibly, the precursors of the *n*-alkanes (and of several other biomarkers; Fig. 5.5 and Table 5.4) were partly mineralised by these bacteria during post-depositional dolomite formation.

Further evidence for the mixing model is provided by microscopical data. Recently, the brown AOM in the KCF of Yorkshire was shown to consist of very thin lamellae when examined by transmission electron microscopy (TEM), whereas TEM observation of the orange AOM did not reveal any microstructure (Boussafir et al., 1995). In the same study, the authors reported the orange AOM to contain substantial amounts of organic sulfur, and to be predominant in kerogens of high TOC (= 10%) samples. Most likely, the internally unstructured, orange bituminite in our samples, which makes up an increasing part of the OM with increasing  $\delta^{13}\text{C}_{\text{TOC}}$ , corresponds to the orange AOM in the isolated kerogens of the Yorkshire KCF described by Boussafir et al. (1995). Thus, taking into account the dilution of the sediment by carbonate, the positive correlation between TOC and the proportion of orange, organic sulfur-rich AOM reported by Boussafir et al. (1995), can now be extrapolated to the range of TOC values of our samples. Considering the mixing model mentioned above, it is suggested that the orange AOM is composed of both S-bound lipids and S-bound carbohydrates, of which the latter become increasingly abundant with increasing TOC\*.

Finally, Lallier-Vergès et al. (1993) reported a decreasing sulfate reduction index (SRI), defined as (organic carbon preserved + organic carbon mineralised by sulfate reduction)/(organic carbon preserved), with increasing TOC for their shale samples of the KCF in Dorset. This SRI was calculated from TOC and total sulfur content, assuming the generalised reaction stoichiometry for sulfate reduction, whereby consumption of two moles of carbon yields one mole of  $\text{H}_2\text{S}$  (Berner and Raiswell, 1983), and assuming that a constant part of the  $\text{H}_2\text{S}$  was retained in the sediment as reduced inorganic or organic sulfur. Thus, the information encompassed in the SRI is in fact similar to that of the amount of sulfur per gram TOC. Indeed, in agreement with the negative trend of SRI versus TOC reported by Lallier-Vergès et al. (1993), the TOC-normalised concentrations of sulfur in our sample set, are inversely related to  $\delta^{13}\text{C}_{\text{TOC}}$  (and thus also to TOC\*) (LECO series, Fig. 5.2a). This suggests that in the high TOC\* samples a smaller part of the OM was mineralised by sulfate

reduction than in the low TOC\* samples, which is consistent with the greater proportions of carbohydrate carbon in the high TOC\* samples.

#### *Degree of OM sulfurisation*

As testified by the presence of isorenieratene derivatives in all samples, even during deposition of the most TOC-lean shales, at least periodically H<sub>2</sub>S was present in the photic zone. The duration of periods with photic zone euxinia (PZE) and the frequency of PZE conditions, however, may have varied. Biofacies studies have shown that the frequency at which bottom waters were oxygenated and/or the duration of these oxygenation events were at minimum during deposition of the oil shales and coccolithic limestones, and oxygenation generally increased with decreasing TOC of the shales (Oschmann 1988, 1991). In other words, the depositional environment of low TOC\* sediments was more frequently oxic than that of high TOC\* sediments. This does not imply, however, that during deposition of the low TOC\* sediments oxic periods were dominant. As a single oxygenation event may produce a several centimetre thick bioturbated layer, the sedimentary record will generally be biased towards more oxic conditions, at least in terms of sediment thickness. The fact that high amounts of OM were preserved in the sediments (except in D2) suggests that oxygenation events were rather short-lived, and that anoxic conditions prevailed even during deposition of relatively TOC-lean sediments (except D2).

Hoefs et al. (1997) have shown that the aerobic oxidation of kerogens in Madeira Abyssal Plain turbidites leads to preferential degradation of S-bound moieties and to a decrease in  $\delta^{13}\text{C}_{\text{TOC}}$ . Similarly, a more frequent oxygenation during deposition of the low TOC\* sediments could have caused the selective degradation of S-bound carbohydrates leading to relatively low concentrations of organic sulfur in the kerogen and relatively low  $\delta^{13}\text{C}_{\text{TOC}}$  values. However, this interpretation seems at conflict with the sulfur isotope data obtained for eight of our samples (D1, D4 and D8-D13) (Brüchert and van Kaam-Peters, 1997). Like  $\delta^{13}\text{C}_{\text{TOC}}$ , the isotopic composition of kerogen sulfur ( $\delta^{34}\text{S}_{\text{TOC}}$ ) is positively correlated with TOC\*. Selective degradation of S-bound carbohydrates, would not lead to such a relationship, unless <sup>32</sup>S is preferentially incorporated into lipids and not into carbohydrates, which seems highly unlikely.

Sequence stratigraphical data indicate that samples D3-D13 were deposited within the same CS interval, sample D1 was deposited in a younger CS interval, and sample D2 lies in between (Tyson, 1996). During deposition in a CS interval the overall accumulation rate of detrital minerals, and thus of reactive iron, is relatively low. Consequently, relatively large amounts of OM could react with reduced inorganic sulfur species (cf. Gransch and Posthuma, 1974; Berner, 1985; Orr, 1986). The CS intervals occur with a periodicity on a million year timescale controlled by sea-level changes (Tyson, 1996). The decimetre- to metre-scale variations in lithology, on the other hand, have a Milankovitch periodicity (House, 1985; Waterhouse, 1995). In principle, there are two ways in which the orbitally-forced climatic changes could account for the different degrees of OM sulfurisation observed in our sample set.

Firstly, since the Milankovitch cyclicity is connected with differences in the flux of eolian dust and run-off from the hinterland (Kroon et al., 1990; Hovan et al., 1991; Weltje

and de Boer, 1993; Tiedemann et al., 1994), OM sulfurisation may have been controlled by the supply of reactive iron to the sediment. Hydrogen sulfide, produced by sulfate-reducing bacteria, builds up in the pore waters only if it is formed at higher rates than that it is consumed by precipitation as iron sulfides. Recently, iron minerals potentially reactive toward sulfide were shown to differ greatly in their reaction rates (Canfield et al., 1992; Raiswell and Canfield, 1996), and it was suggested that in euxinic environments the incorporation of sulfur into OM is not controlled by the abundance of reactive iron (Raiswell et al., 1993). The most reactive iron phases (iron oxides/oxyhydroxides) are quickly sulfurised, but porewaters would still contain large concentrations of dissolved sulfide, and the next reactive iron phases (iron silicates) do not effectively compete with OM for dissolved sulfide (Canfield et al., 1992). However, it may be envisaged that, even if bottom waters are highly sulfidic, an instantaneous, relatively large supply of iron oxides to the sediment causes a drop in the concentration of sulfide in the top layers of the sediment. Still, such a drop in the sulfide concentration is not likely to persist very long, since sulfide will be quickly replenished by diffusion from above and below. If iron oxides continue to be deposited at enhanced rates, pore water sulfides may all be consumed by precipitation as iron sulfides and no longer diffuse out of the sediment. Under these circumstances, the availability of sulfide for reaction with OM is largely dependent on the proportion of iron oxides and OM. Thus, the influence of reactive iron on OM sulfurisation was greatest during periods of non-euxinia.

Secondly, the degree of OM sulfurisation may be related to climatically-controlled differences in primary production. The positive correlation between TOC\* and  $\delta^{34}\text{S}_{\text{TOC}}$  suggests that, due to high phytoplankton productivity, sulfate reduction was more intense in high TOC\* samples than in low TOC\* samples (a greater consumption of sulfate results in a greater  $^{34}\text{S}$  enrichment of dissolved sulfides) (Brüchert and van Kaam-Peters, 1997). Also, enhanced primary production may account for the extraordinary high proportions of carbohydrate carbon in the high  $\delta^{13}\text{C}_{\text{TOC}}$  samples (Table 5.6). It is known that in late stages of phytoplankton blooms, when nitrate and phosphate are depleted, excessive biosynthesis of storage carbohydrates takes place (Morris, 1980, and references therein). An increasing primary production with increasing  $\delta^{13}\text{C}_{\text{TOC}}$  is also consistent with the observation that in the samples most enriched in  $^{13}\text{C}$ , the variety of alginites is much reduced. High phytoplankton productivity (blooming) is generally accompanied by a low species diversity, and the species that bloom are usually low in non-blooming situations. Thus, apparently, with increasing  $\delta^{13}\text{C}_{\text{TOC}}$ , an increasing proportion of the OM is derived from blooming algae. This is also in agreement with the fact that the proportion of 4-methyl-5 $\alpha$ -cholestanes relative to that of the ubiquitous 5 $\alpha$ -cholestane, is generally greatest in high  $\delta^{13}\text{C}_{\text{TOC}}$  samples (Fig. 5.5b).

#### *Implications for other sedimentary environments*

Although the samples investigated are extremely rich in OM, it is believed that our findings have implications for organic geochemical interpretations of less OM-rich sediments as well. For example, variations in  $\delta^{13}\text{C}_{\text{TOC}}$  in the Peterborough Member of the Oxford Clay have been ascribed to variations in heterotrophic reworking (Kenig et al., 1994). However, also in these sediments variations in  $\delta^{13}\text{C}$  of pristane and phytane are minor (Kenig et al., 1994), and

organic S/C ratios are positively correlated with TOC (Chu et al., 1993). Thus, like in the KCF, differences in  $\delta^{13}\text{C}_{\text{TOC}}$  may well originate from different contributions of carbohydrate carbon to the kerogen.

Furthermore, the hypothesis that the areal extent of the shelf seas governs the global burial rate of organic carbon (Jenkyns, 1996), should be reconsidered. This hypothesis was based on the assumption that the widespread Cretaceous and Upper Jurassic (positive) carbon isotope excursions resulted from globally enhanced primary production. As most organic carbon is synthesised in shelf seas, the positive carbon isotope excursions were attributed to high sea-level stands. However, our KCF data show that within the condensed sections (high sea-level stands) considerable variations exist in  $\delta^{13}\text{C}_{\text{TOC}}$  of the sedimentary OM, resulting from differences in sulfurisation, and hence preservation, of labile OM.

## Conclusions

The positive correlation between TOC and  $\delta^{13}\text{C}_{\text{TOC}}$  reported by Huc et al. (1992) for their shale samples of the Dorset KCF, is absent in our sample set of this section, which comprises also carbonate rocks. However, by expressing the TOC content as a weight percentage of the non-carbonate part of the rock (TOC\*), an almost linear relationship is found between TOC\* and  $\delta^{13}\text{C}_{\text{TOC}}$ . The  $\delta^{13}\text{C}_{\text{TOC}}$  values widely vary between -26.7 and -20.7‰.

The terrestrial contribution to the OM is minor, which implies that differences in  $\delta^{13}\text{C}_{\text{TOC}}$  were not caused by mixing of terrestrial and marine OM. Molecular markers of green sulfur bacteria ( $\delta^{13}\text{C} = \text{ca. } -17\text{‰}$ ) and other primary producers ( $\delta^{13}\text{C} = \text{ca. } -31\text{‰}$ ) have similar  $\delta^{13}\text{C}$  values in all samples. This indicates that the TOC\*– $\delta^{13}\text{C}_{\text{TOC}}$  relationship cannot have resulted from differences in  $\delta^{13}\text{C}_{\text{CO}_2}$  or  $[\text{CO}_2]_{\text{aq}}$  in the photic zone. The  $\text{C}_{21}$  and  $\text{C}_{23}$  *n*-alkanes,  $\text{C}_{25}$  and  $\text{C}_{27}$  isoalkanes, and  $\text{C}_{27}$  and  $\text{C}_{29}$  isopropylalkanes, present in variable amounts in all samples, are significantly enriched in  $^{13}\text{C}$  compared to the average algal lipid. Other carbon isotopically heavy biomarkers present in all samples are derivatives of isorenieratene, which are markers for photic zone euxinia. Differences in the concentrations of isotopically distinct biomarkers do not correspond to differences in  $\delta^{13}\text{C}_{\text{TOC}}$ , suggesting that the TOC\*– $\delta^{13}\text{C}_{\text{TOC}}$  relationship cannot be explained by varying contributions of  $^{13}\text{C}$  enriched OM sources.

A mixture of linear algaenans and carbon isotopically heavy, probably ether-linked *n*- $\text{C}_{21}$  and *n*- $\text{C}_{23}$  moieties, is present in the kerogens of all samples. For each of the samples, the weighted average of  $\delta^{13}\text{C}$  of *n*-alkanes in the kerogen pyrolysate was calculated, and this was taken as an estimate of  $\delta^{13}\text{C}_{\text{ALGAENAN}}$ . The  $\delta^{13}\text{C}_{\text{ALGAENAN}}$  values are positively correlated with  $\delta^{13}\text{C}_{\text{TOC}}$ , and may account for 3‰ of the 6‰ difference in  $\delta^{13}\text{C}_{\text{TOC}}$ . A few kerogens were shown to contain also relatively large amounts of isotopically heavy, isoprenoid algaenans, but their presence is not associated with high  $\delta^{13}\text{C}_{\text{TOC}}$  values. Samples containing the isotopically heavy, isoprenoid algaenans are characterised also by relatively abundant,  $^{13}\text{C}$  enriched,  $\text{C}_{16}$  and  $\text{C}_{18}$ – $\text{C}_{20}$  regular isoprenoid alkanes in their extracts.

The proportion of OSC in the kerogen pyrolysate, the GSA Sulfur Index, and the proportion of orange, organic sulfur-rich AOM are positively correlated with  $\delta^{13}\text{C}_{\text{TOC}}$ . This



strongly suggests that  $\delta^{13}\text{C}_{\text{TOC}}$  is related to the degree of OM sulfurisation. Furthermore, a strong positive correlation exists between  $\delta^{13}\text{C}_{\text{TOC}}$  and the relative abundance of carbon isotopically heavy, linear,  $\text{C}_1\text{-C}_3$  alkylated thiophenes in the kerogen pyrolysate. These thiophenes are probably derived from S-bound carbohydrates in the kerogen. Since algal carbohydrates are substantially enriched in  $^{13}\text{C}$  compared to algal lipids, variations in  $\delta^{13}\text{C}_{\text{TOC}}$  can be explained by a two endmember isotopic mixing model with  $\delta^{13}\text{C}_{\text{LIPIDS}}$  at the one end, and  $\delta^{13}\text{C}_{\text{CARBOHYDRATES}}$  at the other end. Thus, the  $\text{TOC}^*\text{-}\delta^{13}\text{C}_{\text{TOC}}$  relationship may be explained by an increasing proportion of sulfurised carbohydrates in the kerogen with increasing  $\text{TOC}^*$ .

As indicated by the presence of isorenieratene derivatives in the extracts, the OM in the KCF was deposited under frequently euxinic conditions. Except for one OM-lean carbonate, the samples studied were deposited in a condensed section, implying a relatively small input of reactive iron to the sediment, which favours the occurrence of euxinia. The degree of sulfurisation of OM is highly variable even among samples from within the condensed sections, probably due to both differences in primary production and differences in the flux of reactive iron, controlled by orbitally-forced climatic changes.

**Acknowledgements.** We thank the Netherlands Organization for Scientific Research (NWO) for the PIONIER grant to JSSD and the studentship of HMEvKP. Shell International Petroleum Maatschappij BV financially supported the GC-IRMS facility. Dr. B.M. Cox kindly provided us with a detailed map of the Kimmeridge Bay area, which was very helpful during sampling. We thank V. Brüchert for his useful comments on the manuscript. We are grateful to M. Baas, R. Suijker, M. Dekker and W. Pool (NIOZ) and A. Schulz (TUC) for analytical assistance. S.J. van der Gaast and R. Kloosterhuis (NIOZ) are acknowledged for performing X-ray powder-diffraction and determining bulk  $\delta^{13}\text{C}$  values, respectively.

## References

- Berner R.A. and Raiswell R. (1983) Burial of organic carbon and pyrite sulfur in sediments over Phanerozoic time: a new theory. *Geochim. Cosmochim. Acta* **47**, 855-862.
- Berner R.A. (1985) Sulphate reduction, organic matter decomposition and pyrite formation. *Phil. Trans. Roy. Soc. London A* **315**, 25-38.
- Bertrand P. and Lallier-Vergès E. (1993) Past sedimentary organic matter accumulation and degradation controlled by productivity. *Nature* **364**, 786-788.
- Bertrand P., Lallier-Vergès E., Martinez L., Pradier B., Tremblay P., Huc A., Jouhannel R. and Tricart J.P. (1990) Examples of spatial relationships between organic matter and mineral groundmass in the microstructure of the organic-rich Dorset Formation rocks, Great Britain. In *Advances in Organic Geochemistry 1989* (ed. B. Durand and F. Behar). *Org. Geochem.* **16**, 661-675.
- Bjørøy M., Jensen H., Connan J., Hall K. and Ferriday I.L. (1993) Geoelf Sulphur Analyser (GSA), a new instrument for rapid determination of organic and inorganic sulphur in sediments and coals. In *Organic geochemistry: Poster sessions from the 16th International Meeting on Organic Geochemistry, Stavanger 1993* (ed. K. Øygard), pp. 773-778. Falch Hurtigtrykk, Oslo.
- Boussafir M., Gelin F., Lallier-Vergès E., Derenne S., Bertrand P. and Largeau C. (1995) Electron microscopy and pyrolysis of kerogens from the Kimmeridge Clay Formation, UK: Source organisms, preservation processes, and origin of microcycles. *Geochim. Cosmochim. Acta* **59**, 3731-3747.

- Brüchert V. and van Kaam-Peters H.M.E. (1997) Carbon and sulfur isotopic variation in the Kimmeridge Clay Formation: Implications for environmental reconstruction. In prep.
- Canfield D.E., Raiswell R. and Bottrell S. (1992) The reactivity of sedimentary iron minerals toward sulfide. *Am. J. Sci.* **292**, 659-683.
- Chu T., Bonnell L.M. and Anderson T.F. (1993) Speciation and isotopic composition of sulfur in the Oxford Clay Formation (Jurassic, U.K.). *Chem. Geol.* **107**, 443-445.
- Claxton M.J., Patience R.L. and Park P.J.D. (1993) Molecular modelling of bond energies in potential kerogen sub-units. In *Organic geochemistry: Poster sessions from the 16th international meeting on organic geochemistry, Stavanger 1993* (ed. K. Øygard et al.), pp. 198-201. Falch Hurtigtrykk, Oslo.
- Cooper B.S., Barnard P.C. and Telnæs N. (1995) The Kimmeridge Clay Formation of the North Sea. In *Petroleum Source Rocks* (ed. B.J. Katz), pp. 89-110. Springer, Berlin.
- Cox B.M. and Gallois R.W. (1981) The stratigraphy of the Kimmeridge Clay of the Dorset type area and its correlation with some other Kimmeridgian sequences. *Rep. Inst. Geol. Sci.*, **80/4**, 1-44.
- Degens E.T., Behrendt M., Gotthardt B. and Reppmann E. (1968) Metabolic fractionation of carbon isotopes in marine plankton-II. Data on samples collected off the coasts of Peru and Ecuador. *Deep Sea Research* **15**, 11-20.
- DeNiro M.J. and Epstein S. (1978) Influence of diet on the distribution of carbon isotopes in animals. *Geochim. Cosmochim. Acta* **42**, 495-506.
- Douglas A.G., Sinninghe Damsté J.S., Fowler M.G., Eglinton T.I. and de Leeuw J.W. (1991) Unique distributions of hydrocarbons and sulphur compounds released by flash pyrolysis from the fossilised alga *Gloeocapsomorpha prisca*, a major constituent in one of four Ordovician kerogens. *Geochim. Cosmochim. Acta* **55**, 275-291.
- Eglinton T.I., Philp R.P. and Rowland S.J. (1988) Flash pyrolysis of artificially matured kerogens from the Kimmeridge Clay, U.K. *Org. Geochem.* **12**, 33-41.
- Eglinton T.I., Sinninghe Damsté J.S., Kohnen M.E.L. and de Leeuw J.W. (1990a) Rapid estimation of the organic sulphur content of kerogens, coals and asphaltenes by pyrolysis-gas chromatography. *Fuel* **69**, 1394-1404.
- Eglinton T.I., Sinninghe Damsté J.S., Kohnen M.E.L., de Leeuw J.W., Larter S.R. and Patience R.L. (1990b) Analysis of maturity-related changes in the organic sulfur composition of kerogens by flash pyrolysis-gas chromatography. In *Geochemistry of Sulfur in Fossil Fuels* (ed. W.L. Orr and C.M. White), *ACS Symposium Series* **429**, pp. 529-565. Amer. Chem. Soc., Washington.
- Eglinton T.I., Irvine J.E., Vairavamurthy A.V., Zhou W. and Manowitz B. (1994) Formation and diagenesis of macromolecular organic sulfur in Peru margin sediments. In *Advances in Organic Geochemistry 1993* (ed. N. Telnæs, G. van Graas and K. Øygard). *Org. Geochem.* **22**, 781-799.
- Espitalié J., Madec M., Tissot B. and Leplat P. (1977) Source rock characterization method for petroleum exploration. *Offshore Technology Conference*, OTC 2935, Houston, Texas, May 2-5, 439-444.
- Farrimond P., Comet P., Eglinton G., Evershed R.P., Hall M.A., Park D.W. and Wardroper A.M.K. (1984) Organic geochemical study of the Upper Kimmeridge Clay of the Dorset type area. *Mar. Petrol. Geol.* **1**, 340-354.
- Fry B. and Sherr E.B. (1984)  $\delta^{13}\text{C}$  measurements as indicators of carbon flow in marine and freshwater ecosystems. *Contr. Mar. Sci.* **27**, 13-47.
- Gelin F., Boogers I., Noordeloos A.A.M., Sinninghe Damsté J.S., Hatcher P.G. and de Leeuw J.W. (1996) Novel, resistant microalgal polyethers: An important sink of organic carbon in the marine environment? *Geochim. Cosmochim. Acta* **60**, 1275-1280.
- Gelpi E., Schneider H., Mann J. and Oró J. (1970) Hydrocarbons of geochemical significance in microscopic algae. *Phytochem.* **9**, 603-612.
- Goossens H., de Leeuw J.W., Schenck P.A. and Brassell S.C. (1984) Tocopherols as likely precursors of pristane in ancient sediments and crude oils. *Nature* **312**, 440-442.
- Gransch J.A. and Posthuma J. (1974) On the origin of sulphur in crudes. In *Advances in Organic geochemistry 1973* (ed. B. Tissot and F. Bienner), pp. 727-739. Editions Technip, Paris.
- Haq B.U., Hardenbol J. and Vail P.R. (1987) Chronology of fluctuating sea levels since the Triassic. *Science* **235**, 1156-1167.

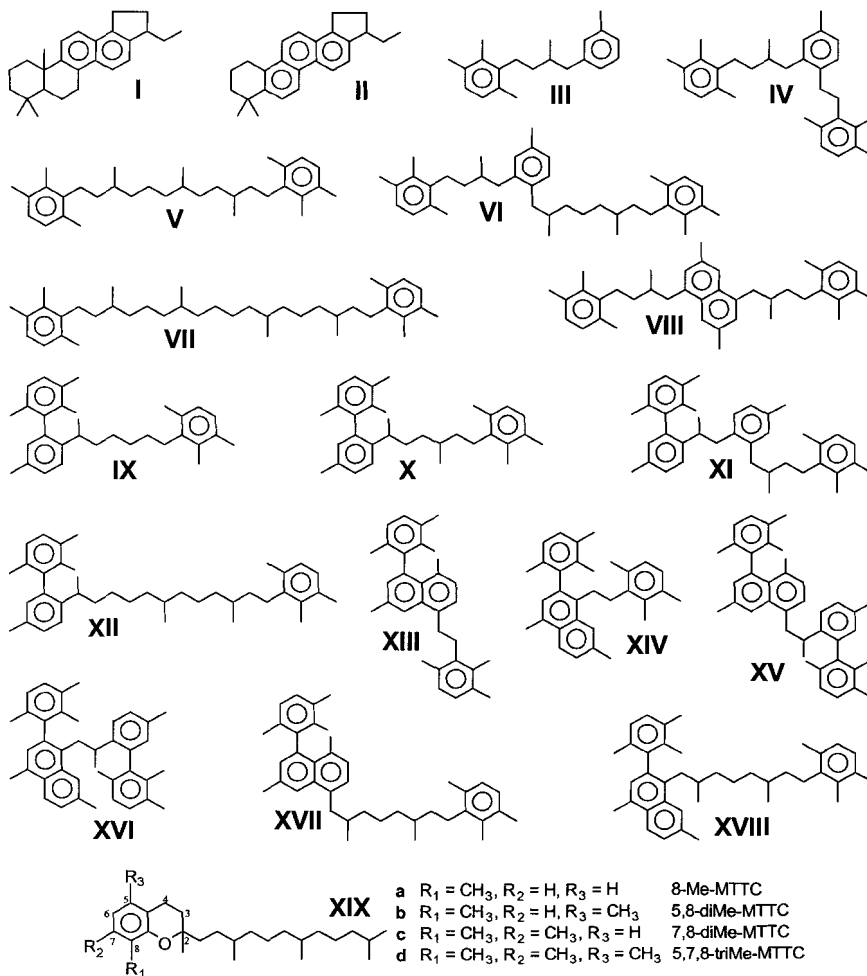
- Hartgers W.A., Sinninghe Damsté J.S., Requejo A.G., Allan J., Hayes J.M., Ling Y., Xie T., Primack J. and de Leeuw J.W. (1994) A molecular and carbon isotopic study towards the origin and diagenetic fate of diaromatic carotenoids. In *Advances in Organic Geochemistry 1993* (ed. N. Telnæs, G. van Graas and K. Øygaard). *Org. Geochem.* **22**, 703-725.
- Herbin J.P., Müller C., Geysant J.R., Mélières F., Penn I.E. and the Yorkim Group (1993) Variation of the distribution of organic matter within a transgressive system tract: Kimmeridge Clay (Jurassic), England. In *Source Rocks in a Sequence Stratigraphic Framework* (ed. B.J. Katz and L.M. Pratt), *AAPG Studies in Geology* **37**, pp. 67-100. Amer. Assoc. of Petrol. Geol.
- Hoefs M.J.L., van Heemst J.D.H., Gelin F., Koopmans M.P., van Kaam-Peters H.M.E., Schouten S., de Leeuw J.W. and Sinninghe Damsté J.S. (1995) Alternative biological sources for 1,2,3,4-tetramethylbenzene in flash pyrolysates of kerogen. *Org. Geochem.* **23**, 975-979.
- Hoefs M.J.L., Sinninghe Damsté J.S., de Lange G.J. and de Leeuw J.W. (1997) Changes in kerogen composition across an oxidation front in Madeira Abyssal Plain turbidites as revealed by pyrolysis GC-MS. *Proc. ODP, Sci. Results* **157** (ed. P.P.E. Weaver, H.-U. Schmincke, J.V. Firth and W. Duffield). In press.
- Höld I.M., Schouten S. and Sinninghe Damsté J.S. (1995) Multiple origins of pyrolysis products of kerogens as revealed by compound-specific carbon isotope analysis. In *Organic Geochemistry: Developments and applications to energy, climate, environment and human history* (ed. J.O. Grimalt et al.), pp. 956-959. A.I.G.O.A., Donostia-San Sebastián.
- Höld I.M., Schouten S., van Kaam-Peters H.M.E. and Sinninghe Damsté J.S. (1997) Recognition of *n*-alkyl and isoprenoid algaenans in marine sediments by stable carbon isotope analysis of pyrolysis products of kerogens. *Org. Geochem.* Submitted.
- Hollander D.J., McKenzie J.A., Hsu K.J. and Huc A.Y. (1993) Application of an eutrophic lake model to the origin of ancient organic-carbon-rich sediments. *Global Biogeochem. Cycles* **7**, 157-179.
- Horsfield B. (1989) Practical criteria for classifying kerogens: Some observations from pyrolysis-gas chromatography. *Geochim. Cosmochim. Acta* **53**, 891-901.
- Horsfield B., Disko U. and Leistner F. (1989) The micro-scale simulation of maturation: outline of a new technique and its potential applications. *Geol. Rundsch.* **78**, 361-374.
- House M.R. (1985) A new approach to an absolute timescale from measurements of orbital cycles and sedimentary microrhythms. *Nature* **315**, 721-725.
- Hovan S.A., Rea D.K. and Pisias N.G. (1991) Late Pleistocene continental climate and oceanic variability recorded in northwest Pacific sediments. *Paleoceanography* **6**, 349-370.
- Huc A.Y., Lallier-Vergès E., Bertrand P., Carpentier B. and Hollander D.J. (1992) Organic matter response to change of depositional environment in Kimmeridgian shales, Dorset, U.K. In *Organic Matter: Productivity, Accumulation, and Preservation in Recent and Ancient Sediments* (ed. J.K. Whelan and J.W. Farrington), pp. 469-486. Columbia Univ. Press.
- Jenkyns H.C. (1996) Relative sea-level change and carbon isotopes: data from the Upper Jurassic (Oxfordian) of central and southern Europe. *Terra Nova* **8**, 75-85.
- van Kaam-Peters H.M.E., Köster J., van der Gaast S.J., Sinninghe Damsté J.S. and de Leeuw J.W. (1997a) The effect of clay minerals on diasterane/sterane ratios. In prep.
- van Kaam-Peters H.M.E., Rijpstra W.I.C., de Leeuw J.W. and Sinninghe Damsté J.S. (1997b) A high resolution biomarker study of different lithofacies of organic sulfur-rich carbonate rocks of a Kimmeridgian lagoon (French southern Jura). *Org. Geochem.* Submitted.
- van Kaam-Peters H.M.E., Schouten S., de Leeuw J.W. and Sinninghe Damsté J.S. (1997c) A molecular and carbon isotope biogeochemical study of biomarkers and kerogen pyrolysates of the Kimmeridge Clay Formation: Palaeoenvironmental implications. *Org. Geochem.* Accepted.
- Kenig F., Hayes J.M., Popp B.N. and Summons R.E. (1994) Isotopic biogeochemistry of the Oxford Clay Formation (Jurassic), UK. *J. Geol. Soc. London* **151**, 139-152.
- Kohnen M.E.L., Sinninghe Damsté J.S., Rijpstra W.I.C. and de Leeuw J.W. (1990) Alkylthiophenes as sensitive indicators of palaeoenvironmental changes: A study of a Cretaceous oil shale from Jordan. In *Geochemistry of Sulfur in Fossil Fuels* (ed. W.L. Orr and C.M. White), *ACS Symposium Series* **429**, pp. 444-485. Amer. Chem. Soc., Washington.

- Kok M., Schouten S. and Sinninghe Damsté J.S. (1997a) Formation of insoluble, non-hydrolysable, sulfur-rich macromolecules by incorporation of inorganic sulfur species into algal sugars. In prep.
- Kok M., Schouten S. and Sinninghe Damsté J.S. (1997b) Sulfurisation of C<sub>5</sub> and C<sub>6</sub> sugars in a laboratory simulation experiment under mild aqueous conditions. In prep.
- Koopmans M.P., Sinninghe Damsté J.S., Lewan M.D. and de Leeuw J.W. (1995) Thermal stability of thiophene biomarkers as studied by hydrous pyrolysis. *Org. Geochem.* **23**, 583-596.
- Koopmans M.P., Köster J., van Kaam-Peters H.M.E., Kenig F., Schouten S., Hartgers W.A., de Leeuw J.W. and Sinninghe Damsté J.S. (1996) Dia- and catagenetic products of isorenieratene: Molecular indicators for photic zone anoxia. *Geochim. Cosmochim. Acta* **60**, 4467-4496.
- Krein E.B. and Aizenshtat Z. (1994) The formation of isoprenoid sulfur compounds during diagenesis: simulated sulfur incorporation and thermal transformation. *Org. Geochem.* **21**, 1015-1025.
- Kroon D., Beets K., Mowbray S., Shimmield G. and Steens T. (1990) Changes in northern Indian Ocean monsoonal wind activity during the last 500ka. *Mem. Soc. Geol. It.* **44**, 189-207.
- Lallier-Vergès E., Bertrand P., Huc A.Y., Bückel D. and Tremblay P. (1993) Control of the preservation of organic matter by productivity and sulphate reduction in Kimmeridgian shales from Dorset (UK). *Mar. Petr. Geol.* **10**, 600-605.
- Melnyk D.H., Athersuch J. and Smith D.G. (1992) Estimating the dispersion of biostratigraphic events in the subsurface by graphic correlation: an example from the Late Jurassic of the Wessex Basin, UK. *Marine and Petroleum Geology* **9**, 602-607.
- Melnyk D.H., Smith D.G. and Amiri-Garroussi (1994) Filtering and frequency mapping as tools in subsurface cyclostratigraphy, with examples from the Wessex Basin, U.K. In *Orbital Forcing and Cyclic Sequences* (ed. P.L. de Boer and D.G. Smith), Int. Assoc. Sedimentol. Spec. Publ. **19**, 35-46.
- Miller R.G. (1990) A paleo-oceanographic approach to the Kimmeridge Clay Formation. In *Deposition of organic facies* (ed. A.Y. Huc), *AAPG Studies in Geology* **30**, pp. 13-26. Amer. Assoc. of Petrol. Geol.
- Moers M.E.C., de Leeuw J.W., Cox H.C. and Schenck P.A. (1988) Interaction of glucose and cellulose with hydrogen sulphide and polysulphides. In *Advances in Organic Geochemistry 1987* (ed. L. Mattavelli and L. Novelli). *Org. Geochem.* **13**, 1087-1091.
- Morris I. (1980) Photosynthetic products, physiological state, and phytoplankton growth. In *The Physiological Ecology of Phytoplankton*. Studies in Ecology **7**, 83-102. Blackwell Scient. Publ., London.
- Nelson B.C., Eglinton T.I., Seewald J.S., Vairavamurthy M.A. and Miknis F.P. (1995) Transformations in organic sulphur speciation during maturation of Monterey shale: Constraints from laboratory experiments. In *Geochemical Transformations of Sedimentary Sulfur* (ed. M.A. Vairavamurthy and M.A.A. Schoonen), *ACS Symposium Series 612*, pp. 138-166. Amer. Chem. Soc., Washington.
- Orr W.L. (1986) Kerogen/asphaltene/sulfur relationships in sulfur-rich Monterey oils. In *Advances in Organic geochemistry 1985* (ed. D. Leythaeuser and J. Rullkötter). *Org. Geochem.* **10**, 499-516.
- Oschmann W. (1988) Kimmeridge Clay sedimentation - A new cyclic model. *Palaeogeogr. Palaeoclimatol. Palaeoecol.* **65**, 217-251.
- Oschmann W. (1991) Distribution, dynamics and palaeoecology of Kimmeridgian (Upper Jurassic) shelf anoxia in western Europe. In *Modern and Ancient Continental Shelf Anoxia* (ed. R.V. Tyson and T.H. Pearson), Geol. Soc. Lond. Spec. Publ. **58**, 381-395.
- Park D.W. (1982) A further study of the organic geochemistry of the Kimmeridge Clay. *BSc. thesis*, University of Bristol, UK.
- Park R. and Epstein S. (1961) Metabolic fractionation of <sup>13</sup>C & <sup>12</sup>C in plants. *Plant physiology* **36**, 133-138.
- Raiswell R. and Canfield D.E. (1996) Rates of reaction between silicate iron and dissolved sulfide in Peru Margin sediments. *Geochim. Cosmochim. Acta* **60**, 2777-2787.

- Raiswell R., Bottrell S.H., Al-Biatty H.J. and Tan M.Md. (1993) The influence of bottom water oxygenation and reactive iron content on sulfur incorporation into bitumens from Jurassic marine shales. *Am. J. Sci.* **293**, 569-596.
- Ramanampisoa L. and Disnar J.R. (1994) Primary control of paleoproduction on organic matter preservation and accumulation in the Kimmeridge rocks of Yorkshire (UK). *Org. Geochem.* **21**, 1153-1167.
- Richnow H.H., Jenisch A. and Michaelis W. (1992) Structural investigations of sulphur-rich macromolecular oil fractions and a kerogen by *sequential* chemical degradation. In *Advances in Organic Geochemistry 1991* (ed. C.B. Eckardt, J.R. Maxwell, S.R. Larter and D.A.C. Manning). *Org. Geochem.* **19**, 351-370.
- Richnow H.H., Jenisch A. and Michaelis W. (1993) The chemical structure of macromolecular fractions of a sulfur-rich oil. *Geochim. Cosmochim. Acta* **57**, 2767-2780.
- Saiz-Jimenez C. and de Leeuw J.W. (1984) Pyrolysis-gas chromatography-mass spectrometry of isolated, synthetic and degraded lignins. In *Advances in Organic Geochemistry 1983* (ed. P.A. Schenck, J.W. de Leeuw and G.W.M. Lijmbach). *Org. Geochem.* **6**, 417-422.
- Saiz-Jimenez C. and de Leeuw J.W. (1986) Lignin pyrolysis products: Their structures and their significance as biomarkers. In *Advances in Organic Geochemistry 1985* (ed. D. Leythaeuser and J. Rullkötter). *Org. Geochem.* **10**, 869-876.
- Schouten S., de Graaf W., Sinninghe Damsté J.S., van Driel G.B. and de Leeuw J.W. (1994) Laboratory simulation of natural sulphurization: II. Reaction of multi-functionalized lipids with inorganic polysulphides at low temperatures. In *Advances in Organic Geochemistry 1993* (ed. N. Telnæs, G. van Graas and K. Oygard). *Org. Geochem.* **22**, 825-834.
- Schouten S., Baas M., van Kaam-Peters H.M.E. and Sinninghe Damsté J.S. (1997) Long-chain 3-isopropylalkanes: A new class of sedimentary branched acyclic hydrocarbons. *Geochim. Cosmochim. Acta*. Submitted.
- Sinninghe Damsté J.S. and Schouten S. (1997) Is there evidence for a substantial contribution of prokaryotic biomass to organic carbon in Phanerozoic carbonaceous sediments? *Org. Geochem.* In press.
- Sinninghe Damsté J.S., Kock-van Dalen A.C., de Leeuw J.W., Schenck P.A., Guoying S. and Brassell S.C. (1987) The identification of mono-, di- and trimethyl 2-methyl-2-(4,8,12-trimethyltridecyl)chromans and their occurrence in the geosphere. *Geochim. Cosmochim. Acta* **51**, 2393-2400.
- Sinninghe Damsté J.S., Eglinton T.I., de Leeuw J.W. and Schenck P.A. (1989) Organic sulphur in macromolecular sedimentary organic matter: I. Structure and origin of sulphur-containing moieties in kerogen, asphaltenes and coal as revealed by flash pyrolysis. *Geochim. Cosmochim. Acta* **53**, 873-889.
- Sinninghe Damsté J.S., Eglinton T.I., Rijpstra W.I.C. and de Leeuw J.W. (1990) Characterisation of sulfur-rich high molecular weight substances by flash pyrolysis and Raney Ni desulfurisation. In *Geochemistry of Sulfur in Fossil Fuels* (ed. W.L. Orr and C.M. White), *ACS Symposium Series 429*, pp. 486-528. Amer. Chem. Soc., Washington.
- Sinninghe Damsté J.S., de las Heras F.X.C., van Bergen P.F. and de Leeuw J.W. (1993a) Characterization of Tertiary Catalan lacustrine oil shales: Discovery of extremely organic sulfur-rich Type I kerogens. *Geochim. Cosmochim. Acta* **57**, 389-415.
- Sinninghe Damsté J.S., Keely B.J., Betts S.E., Baas M., Maxwell J.R. and de Leeuw J.W. (1993b) Variations in abundances and distributions of isoprenoid chromans and long-chain alkylbenzenes in sediments of the Mulhouse Basin: a molecular sedimentary record of palaeosalinity. *Org. Geochem.* **20**, 1201-1215.
- Sirevåg R. and Ormerod J.G. (1970) Carbon dioxide fixation in green sulphur bacteria. *Biochem. J.* **120**, 399-408.
- Teichmüller M. (1974) Über neue Macerale der Liptinitgruppe und die Entstehung des Micrinit. *Fortschr. Geol. Rheinld. Westf.* **24**, 37-64.
- Tiedemann R., Sarnthein M. and Shackleton N.J. (1994) Astronomic timescale for the Pliocene Atlantic  $\delta^{18}\text{O}$  and dust flux records of Ocean Drilling Program site 659. *Paleoceanography* **9**, 619-638.

- Tomic J., Behar F., Vandenbroucke M. and Tang Y (1995) Artificial maturation of Monterey kerogen (Type II-S) in a closed system and comparison with Type II kerogen: implications on the fate of sulfur. *Org. Geochem.* **23**, 647-660.
- Tribovillard N., Desprairies A., Lallier-Vergès E., Bertrand P., Moureau N., Ramdani A. and Ramanampisoa L. (1994) Geochemical study of organic-matter rich cycles from the Kimmeridge Clay Formation of Yorkshire (UK): productivity versus anoxia. *Pal. Pal. Pal.* **108**, 165-181.
- Tyson R.V. (1985) *Palynofacies and Sedimentology of Some Late Jurassic Sediments from the British Isles and Northern North Sea*. Ph.D. thesis. The Open University, Milton Keynes. 623 pp.
- Tyson R.V. (1996) Sequence stratigraphical interpretation of organic facies variations in marine siliciclastic systems: General principles and application to the onshore Kimmeridge Clay Formation, UK. In *Sequence Stratigraphy in British Geology* (ed. Hesselbo S. and Parkinson N.), Geol. Soc. Lond. Spec. Publ. **103**, 75-96.
- Tyson R.V. and Pearson T.H. (1991) Modern and ancient continental shelf anoxia: An overview. In *Modern and Ancient Continental Shelf Anoxia* (ed. Tyson R.V. and Pearson T.H.), Geol. Soc. Lond. Spec. Publ. **58**, 1-24.
- Tyson R.V., Wilson R.C.L. and Downie C. (1979) A stratified water column environmental model for the type Kimmeridge Clay. *Nature* **277**, 377-380.
- Vasconcelos C., McKenzie J.A., Bernasconi S., Grujic D. and Tien A.J. (1995) Microbial mediation as a possible mechanism for natural dolomite formation at low temperatures. *Nature* **377**, 220-222.
- Volkman J.K. and Maxwell J.R. (1986) Acyclic isoprenoids as biological markers. In *Biological Markers in the Sedimentary Record* (ed. R.B. Johns), pp. 1-42. Elsevier, New York.
- Waterhouse H.K. (1995) High-resolution palynofacies investigation of Kimmeridgian sedimentary cycles. In *Orbital Forcing Timescales and Cyclostratigraphy* (ed. M.R. House and A.S. Gale), Geol. Soc. Lond. Spec. Publ. **85**, 75-114.
- Weltje G. and de Boer P.L. (1993) Astronomically induced paleoclimatic oscillations reflected in Pliocene turbidite deposits on Corfu (Greece): Implications for the interpretation of higher order cyclicity in ancient turbidite systems. *Geology* **21**, 307-310.
- Wignall P.B. (1989) Sedimentary dynamics of the Kimmeridge Clay: tempests and earthquakes. *J. Geol. Soc.* **146**, 273-284.
- Wignall (1991) Test of the concepts of sequence stratigraphy in the Kimmeridgian (Late Jurassic) of England and northern France. *Marine and Petroleum Geology* **8**, 430-441.
- Wignall P.B. (1994) Blackshales. Clarendon Press, Oxford. pp. 127.
- Williams P.F.V. and Douglas A.G. (1980) A preliminary organic geochemical investigation of the Kimmeridgian oil shales. In *Advances in Organic Geochemistry 1979* (eds. A.G. Douglas and J.R. Maxwell), pp. 531-545. Pergamon, Oxford.
- Williams P.F.V. and Douglas A.G. (1983) The effect of lithologic variation on organic geochemistry in the Kimmeridge Clay of Britain. In *Advances in Organic Geochemistry 1981* (eds. M. Bjorøy et al.), pp. 568-575. Wiley, Chichester.

## Appendix



## Chapter 6

### **Biomarker and compound-specific stable carbon isotope analysis of the Early Toarcian shales in SW Germany.**

#### **Abstract**

The Early Toarcian transgression is marked by the occurrence of organic carbon-rich shales in large parts of western Europe, and in some places in other parts of the world. Based on the positive carbon isotope excursion of pelagic limestones in the lower part of the *falciferum* Zone in several of the Tethyan sections, the widespread occurrence of the Early Toarcian shales was explained by an Oceanic Anoxic Event (OAE) (Jenkyns, 1988). The rapid burial of large amounts of organic carbon, which is rich in  $^{12}\text{C}$ , would have led to a relative enrichment in  $^{13}\text{C}$  of the global carbon reservoir, and hence to an increase in  $\delta^{13}\text{C}$  of the limestones. In SW Germany, however, both organic and inorganic carbon display a negative isotope excursion in the lower part of the *falciferum* Zone (Küspert, 1982; Moldowan et al., 1986).

The aim of our study was to examine if the negative carbon isotope excursion of organic matter (OM) in the SW German Toarcian shales, can be attributed to compositional changes of the OM, or if the excursion is related to variations in  $\delta^{13}\text{C}$  of  $\text{CO}_2$  ( $\delta^{13}\text{C}_{\text{CO}_2}$ ) or  $[\text{CO}_2]_{\text{aq}}$  in the photic zone. To this end, we analysed the molecular and (molecular) carbon isotopic composition of OM in ten samples spanning the Early Toarcian (TOC 2.5-10.5%; HI 364-689). Biomarker distributions and kerogen pyrolysates were found to differ only slightly among the samples, and  $\delta^{13}\text{C}$  values of primary production markers follow a trend similar to that of  $\delta^{13}\text{C}$  of the kerogen ( $\delta^{13}\text{C}_{\text{TOC}}$ ). This strongly suggests that differences in  $\delta^{13}\text{C}_{\text{TOC}}$  are related to differences in  $\delta^{13}\text{C}_{\text{CO}_2}$  or  $[\text{CO}_2]_{\text{aq}}$  in the photic zone. The presence of isorenieratane in all samples indicates that photic zone anoxia (PZA) was a common feature of the Early Toarcian sea in SW Germany. Although no relationship was found between  $\delta^{13}\text{C}_{\text{TOC}}$  and the concentration of isorenieratane, the negative excursion of  $\delta^{13}\text{C}_{\text{TOC}}$  is best explained by the occurrence of a shallow oxic/anoxic interface in the water column. In agreement with Küspert (1982), isotopically light, organic-derived  $\text{CO}_2$  in anoxic bottom waters, was probably mixed with the largely atmospheric-derived  $\text{CO}_2$  in the upper part of the photic zone. Our results indicate that, unless the recycling of organic-derived  $\text{CO}_2$  exceeded by far the effect on  $\delta^{13}\text{C}_{\text{TOC}}$  of global organic carbon burial, the Early Toarcian OAE was not a global event at all.

#### **Introduction**

The Liassic epicontinental basins of northern Europe, i.e. Yorkshire, NW German, SW German, Paris and Chalhac Basins, were intermittently open to the Arctic and Tethys oceans, depending on sea level fluctuations and changes in the connecting water-routes (Katz, 1995). During the Lower Toarcian, coincident with the peak of the Lower Jurassic



transgression (Hallam, 1981), highly bituminous shales were deposited in extensive parts of the European epicontinental seas and in parts of the Tethyan continental margins (Loh et al., 1986; Jenkyns et al., 1991; Farrimond et al., 1994). In addition, contemporaneous black shales are reported to occur in western Canada, Japan, Madagascar, Argentina, and on the Arctic Slope, and the global occurrence of the synchronous black shale facies led to the interpretation of the phenomenon as an OAE (Jenkyns, 1988). Traditionally, the occurrences in northern Europe are best documented. The most organic carbon-rich facies of the Lower Toarcian in Germany, the Posidonienschiefer (Posidonia Shale), has long been known for its excellently preserved vertebrate and invertebrate skeletons (for a historical overview see Oschmann, 1995). Equivalents in England and France are the equally renowned Jet Rock and Schistes Carton, respectively. Generally, the Lower Toarcian shales of northern Europe have a good or excellent oil-generation potential, but oil production is limited due to their low level of thermal maturity (Tissot et al., 1971; Barnard and Cooper, 1981; Espitalié et al., 1988).

Based on the assumption that the Tethyan outcrops are of identical age to those in northern Europe, which was demonstrated at one locality in Italy (Jenkyns et al., 1985), the most organic carbon-rich Toarcian shales occur in the lower part of the *falciferum* Zone, the *exaratum* Subzone (Jenkyns, 1988). In this Subzone, in several sections of the European continental margin of the Tethys, the stable carbon isotopic compositions of the pelagic limestones display a positive shift (Jenkyns and Clayton, 1986). Analogous to what was inferred from the Cenomanian-Turonian OAE (Schlanger et al., 1987), this positive carbon isotope excursion was explained by the severe removal of organic carbon, which is rich in  $^{12}\text{C}$ , from the global reservoir, through the rapid burial of organic carbon in black shales (Jenkyns, 1988). Originally, the Toarcian OAE was explained by an oxygen-minimum layer model (Jenkyns, 1985, 1988), but organic geochemical data indicate that, depending on the geographical position, the causes of black shale formation are variable (Farrimond et al., 1989; Hollander et al., 1991), thus casting doubt upon the true global nature of this OAE. A further complication stems from the fact that in the Italian Monte Brughetto section and in the SW German and Paris Basins, both organic and inorganic carbon exhibit a negative isotope excursion in the *exaratum* Subzone (Küspert, 1982; Moldowan et al., 1986; Jenkyns and Clayton, 1986; Hollander et al., 1991). In the case of the carbonates these negative isotope excursions may be explained by diagenetic overprinting, i.e. the incorporation of isotopically light  $\text{CO}_2$  derived from the post-depositional bacterial oxidation of OM (Jenkyns and Clayton, 1986). In the case of the kerogens, however, a diagenetic cause is not feasible, and changes in water column stratification (Küspert, 1982; Hollander et al., 1991) or changes in the planktonic community (Jenkyns and Clayton, 1986; Prauss and Riegel, 1989) have been invoked.

The aim of this study was to test if indeed the negative carbon isotope excursion of the kerogens of the SW German Posidonia Shale can be attributed to compositional changes of the nannoflora (Jenkyns and Clayton, 1986; Prauss and Riegel, 1989), or if isotopically light  $\text{CO}_2$ , derived from the bacterial decomposition of OM, was recycled into the photic zone from stagnant waters below (Küspert, 1982). To this end, ten samples spanning the Lower Toarcian were selected for organic geochemical and compound-specific stable carbon isotope analysis. Assuming that to a certain extent the carbon isotopic fractionation between

dissolved CO<sub>2</sub> and primary photosynthate was constant, the scenario of CO<sub>2</sub>-recycling leading to a decrease in δ<sup>13</sup>C of dissolved CO<sub>2</sub> (δ<sup>13</sup>C<sub>CO<sub>2</sub></sub>) implies a negative excursion in δ<sup>13</sup>C of photoautotrophic biomass. This was verified by measuring the stable carbon isotopic composition of primary production markers. The hypothesis that changes in δ<sup>13</sup>C of the kerogen (δ<sup>13</sup>C<sub>TOC</sub>) resulted from changes in the planktonic community, was verified by examining the molecular composition of bitumen and kerogen pyrolysate. Finally, particular attention was paid to the occurrence of isorenieratene derivatives. These are highly specific markers for photic zone anoxia (Repeta, 1993; Sinninghe Damsté et al., 1993), and depth profiles of these compounds can potentially provide important insights into the palaeoenvironmental and palaeoceanographic conditions during sediment deposition.

## Methods

*Extraction and fractionation.* The powdered samples (ca. 70 g) were Soxhlet extracted with methanol (MeOH)/dichloromethane (DCM) (1:7.5 v/v) for 24 h. Asphaltenes were removed from the extracts by precipitation in *n*-heptane. Aliquots of the maltene fractions (ca. 200 mg), to which a mixture of four standards was added for quantitative analysis (Kohnen et al., 1990), were separated over a column (20 cm x 2 cm; column volume (V<sub>0</sub>) = 35 ml) packed with alumina (activated for 2.5 h at 150°C) by elution with hexane/DCM (9:1 v/v; 150 ml; “apolar fraction”) and DCM/MeOH (1:1 v/v; 150 ml; “polar fraction”). Aliquots (ca. 10 mg) of the apolar fractions were further separated using a small column (5 cm x 0.5 cm; V<sub>0</sub> = 1 ml) packed with AgNO<sub>3</sub> impregnated (20% w/w; activated for 16 h at 120°C) silicagel (Merck, Silicagel 60, 70-230 mesh ASTM) by elution with hexane (saturated hydrocarbons) and ethylacetate (aromatic hydrocarbons). Saturated hydrocarbon fractions were analysed by GC and GC-MSMS. Aromatic hydrocarbon fractions were analysed by GC and GC-MS.

*n*-Alkanes were removed from the saturated hydrocarbon fractions by elution over a small column (5 cm x 0.5 cm; V<sub>0</sub> = 1 ml) packed with a molecular sieve (silicalite) using cyclohexane as the eluents. In the case of samples T11, T18, T23 and T27, *n*-alkanes were retrieved from the molecular sieve by dissolving the sieve in HF, subsequently neutralising the solution with Na<sub>2</sub>CO<sub>3</sub>, and extraction with hexane (x3). Both adducts and non-adducts were analysed using GC-IRMS.

*Gas chromatography (GC).* GC was performed using a Carlo Erba 5300 or a Hewlett-Packard 5890 instrument, both equipped with an on-column injector. A fused silica capillary column (25 m x 0.32 mm) coated with CP-Sil 5 (film thickness 0.12 μm) was used with helium as carrier gas. The effluent was monitored by a flame ionisation detector (FID). Samples were injected at 70°C and subsequently the oven was programmed to 130°C at 20°C/min and then at 4°C/min to 320°C, at which it was held for 15 min.

*Gas chromatography-mass spectrometry (GC-MS).* GC-MS was carried out on a Hewlett-Packard 5890 gas chromatograph interfaced to a VG Autospec Ultima Q mass spectrometer operated at 70 eV with a mass range *m/z* 50-800 and a cycle time of 1.8 s (resolution 1000). The gas chromatograph was equipped with a fused silica capillary column (25 m x 0.32 mm) coated with CP-Sil 5 (film thickness 0.12 μm). Helium was used as carrier gas. The samples

were injected at 60°C and subsequently the oven was programmed to 130°C at 20°C/min and then at 4°C/min to 320°C, at which it was held for 15 min.

*Gas chromatography-mass spectrometry-mass spectrometry (GC-MSMS).* GC-MSMS was performed on a Hewlett-Packard 5890 gas chromatograph interfaced to a VG Autospec Ultima Q mass spectrometer. The gas chromatograph was equipped with a fused silica capillary column (60 m x 0.25 mm) coated with CP-Sil 5CB-MS (film thickness 0.25 µm). The carrier gas was helium. The gas chromatograph was programmed from 60°C to 200°C at a rate of 15°C/min and then at 1.5°C/min to 310°C (10 min). The mass spectrometer was operated at 70 eV with a source temperature of 250°C. Dissociation of the parent ions was induced by collision with argon (collision energy 18-20 eV). The parent ion to daughter ion transitions were analysed with 20 ms settling and 80-100 ms sampling periods. Total cycle time was 1020 ms.

*Gas chromatography-isotope ratio mass spectrometry (GC-IRMS).* The DELTA-C GC-IRMS-system used is in principal similar to the DELTA-S system described by Hayes et al. (1990). For analysis of the isoprenoid alkanes the gas chromatograph (Hewlett-Packard 5890) was equipped with a fused silica capillary column (25 m x 0.32 mm) coated with CP-Sil 5 (film thickness 0.12 µm). Diacholestanes were analysed using a CP-Sil 5CB-MS column (60 m x 0.25 mm) with a film thickness of 0.25 µm. Helium was used as the carrier gas. The oven temperature was programmed from 70°C to 130°C at 20°C/min, from 130°C to 310°C at 4°C/min and maintained at 310°C for 15 min. The  $\delta^{13}\text{C}$  values (vs PDB) were calculated by integrating the mass 44, 45 and 46 ion currents of the CO<sub>2</sub> peaks produced by combustion of the column effluent and those of CO<sub>2</sub> spikes with a known <sup>13</sup>C content which were directly led into the mass spectrometer at regular intervals. The  $\delta^{13}\text{C}$  values reported are averages of at least two measurements.

*Curie-point pyrolysis-gas chromatography (Py-GC).* Py-GC was performed with a Hewlett-Packard 5890 gas chromatograph using a FOM-3LX unit for pyrolysis. Decarbonated (6N HCl) and extracted sediments were applied to a ferromagnetic wire with a Curie-temperature of 610°C. The gas chromatograph, equipped with a cryogenic unit, was programmed from 0°C (5 min) to 310°C (5 min) at a rate of 3°C/min. Separation was achieved using a fused silica capillary column (25 m x 0.32 mm) coated with CP-Sil 5 (film thickness 0.4 µm). Helium was used as the carrier gas.

Curie-point pyrolysis-gas chromatography-mass spectrometry (Py-GC-MS) was performed using the same equipment and conditions as described above for the Py-GC in addition to a VG Autospec Ultima mass spectrometer operated at 70 eV with a mass range m/z 50-800 and a cycle time of 1.8 s (resolution 1000).

*Quantification.* Concentrations of C<sub>16</sub> and C<sub>18</sub>-C<sub>20</sub> regular isoprenoid alkanes and *n*-alkanes were determined by comparison of their peak areas in the FID-trace to that of the internal standard. Aryl- and diaryl isoprenoids were quantified by integration of their peaks in the m/z 133+134 mass chromatogram, and comparison with the peak area of the internal standard (2-methyl-2-(4,8,12-trimethyltridecyl)chroman) in the m/z 107+147 mass

chromatogram. Since these ions are the major fragment ions of both the (di)aryl isoprenoids and the internal standard, concentrations were not corrected for the different intensities of the fragment ions.

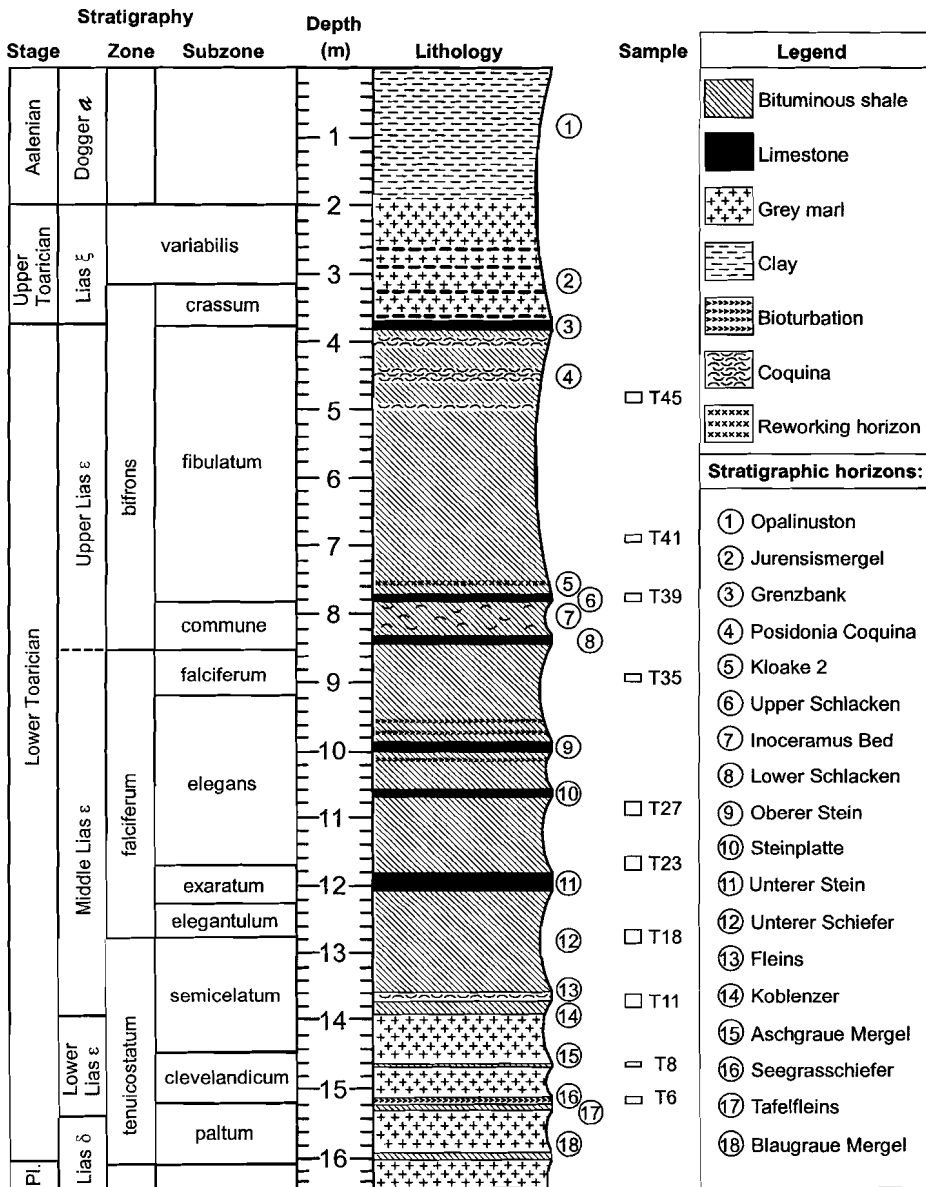


**Fig. 6.1.** Lithology and stratigraphic positions of the samples in a composite profile of sampling sites Dotternhausen (T18-T41) and Schömberg (T6-T11, T45) in SW Germany (Küspert, 1983).

## Results

### *Sample description and bulk data*

Samples are from the Dotternhausen-Schömberg area, near Tübingen, southwest Germany. Lithology and sample selection are given in Fig. 6.1. Sample T6 is the “Seegrasschiefer”, a bioturbation horizon of the type that is always present where bituminous shales grade into grey marls (Küspert, 1982). T8 and T11 are a bituminous marl and a grey marl, respectively. Samples T18, T23, T27 and T35 are thinly breaking, poorly laminated, uniformly dark grey shales. T39 is the “Upper Schlacken”, a homogeneous bituminous limestone. T41 and T45 are bituminous shales, the latter heavily weathered.

Total organic carbon content (TOC) varies between 1.3 and 10.5%. OM is marginally mature with a vitrinite reflectance of ca. 0.51% (Moldowan et al., 1986) and  $T_{\max}$  values ranging from 429 to 435°C (Table 6.1). There is no correlation between the Rock Eval Hydrogen Index (HI), which falls between 364 and 689, and the stable carbon isotopic composition of the kerogen ( $\delta^{13}\text{C}_{\text{TOC}}$ ), which ranges from -32.0 to -27.7‰ (Table 6.1).

### *Saturated hydrocarbons*

All saturated hydrocarbon fractions are dominated by  $\text{C}_{16}$  and  $\text{C}_{18}$ - $\text{C}_{20}$  regular isoprenoid alkanes and by series of  $n$ -alkanes maximising at  $n\text{-C}_{16}$  and  $n\text{-C}_{17}$  (e.g. Fig. 6.2). The  $n$ -alkanes do not show an odd-over-even carbon number predominance. Strictly, in samples T35 and T39 distributions of  $n$ -alkanes are bimodal, but the second maximum around  $n\text{-C}_{31}$  is subordinate (Fig. 6.2). Pristane/phytane (pr/ph) ratios vary between 1.5 and 2.8, and are considerably higher in T6, T8 and T11 than in the other samples (Table 6.1). Since the TOC normalised concentrations of biomarkers were found to largely depend on the yield of apolar fraction, concentrations were normalised on the apolar fraction. In general, linear and isoprenoid alkanes make up a rather constant part of the apolar fraction (Fig. 6.3a). It is

**Table 6.1.** Bulk data, molecular parameters and yields of the different fractions.

	T6	T8	T11	T18	T23	T27	T35	T39	T41	T45
TOC (%)	5.8	3.6	2.5	10.5	9.6	8.4	8.4	1.3	9.6	8.8
$T_{\max}$ (°C)	433	432	429	432	431	434	434	433	435	434
HI (mg HC/g TOC)	527	424	364	672	678	689	639	481	610	543
OI (mg $\text{CO}_2$ /g TOC)	12	17	21	10	10	11	9	10	11	27
$\delta^{13}\text{C}_{\text{TOC}}$ (‰)	-28.5	-28.5	-27.7	-32.0	-31.7	-28.5	-27.8	-29.6	-29.2	-29.5
bitumen <sup>a</sup>	58	84	76	94	110	110	88	87	77	83
asphaltenes <sup>a</sup>	2.2	11	n.d. <sup>b</sup>	2.3	7.6	10	13	n.d.	8.0	16
maltenes <sup>a</sup>	56	73	n.d.	92	100	100	74	n.d.	69	67
polars <sup>a</sup>	25	28	35	38	48	45	32	42	29	30
apolars <sup>a</sup>	26	34	8.4	42	41	44	32	34	29	22
pristane/phytane	2.75	2.49	2.31	1.68	1.45	1.71	1.99	2.14	1.89	1.84
20S/(S+R) cholestane	0.40	0.40	0.40	0.35	0.35	0.36	0.38	0.38	0.36	0.37

<sup>a</sup> in mg/g TOC

<sup>b</sup> not determined

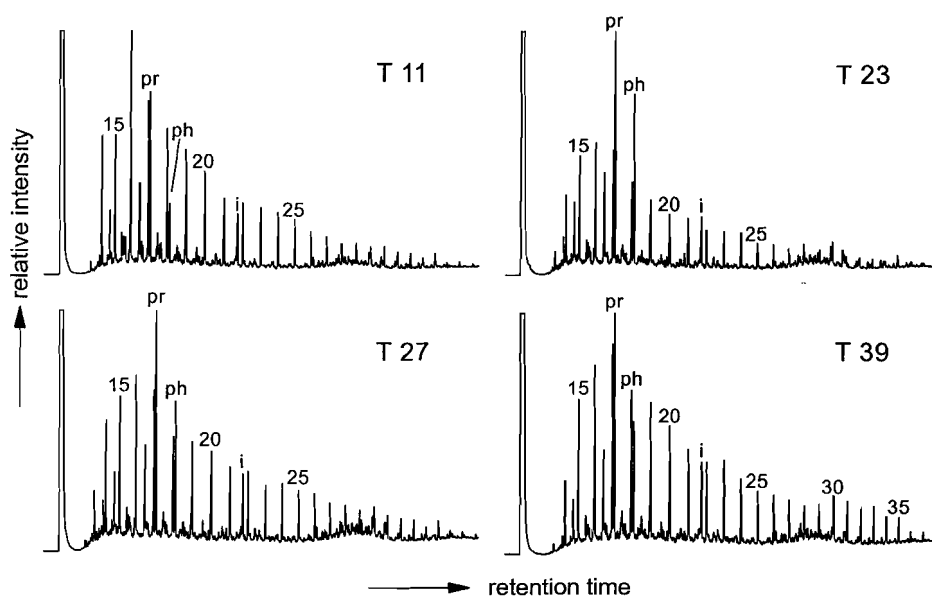


**Fig. 6.2.** Four typical GC-FID traces of saturated hydrocarbon fractions. Numbers correspond to number of carbon atoms; pr = pristane; ph = phytane; i = internal standard.

worthy of note though, that *n*-alkanes are relatively most abundant in the apolar fractions of T8 and T11 (Fig. 6.3a), whereas these two samples have the lowest HI (Table 6.1).

GC-MSMS analyses of the steroid mixtures indicate the presence of both regular- and rearranged  $C_{27}$ - $C_{30}$  desmethyl- and  $C_{28}$ - $C_{30}$  4-methyl steranes, including dinosterane, in all samples (e.g. Fig. 6.4). Ratios of desmethyl/4-methyl steranes, and distributions of desmethyl- ( $C_{27}>C_{28}>C_{29}>>C_{30}$ ) and 4-methyl steranes ( $C_{28}>>C_{29}\approx C_{30}$ ) exhibit no major differences among the samples. However, sterane distributions in T6, T8 and T11 have a less prominent 24-methylcholestane ( $C_{27}>>C_{28}\approx C_{29}>>C_{30}$ ), and a slightly higher  $C_{27}$  20S/(20S+20R) ratio (Table 6.1) than observed in the other samples. Assuming that the thermal history of the SW German Basin is similar to that of the Paris Basin, the range of 20S/(20S+20R) values observed corresponds to a maximum burial depth of less than 1500 m, which is below the zone of hydrocarbon generation (MacKenzie et al., 1980). The ratio of dia-/(dia- + regular) steranes is positively correlated with the ratio of clay/TOC, as discussed elsewhere (van Kaam-Peters et al., 1997a).

Series of  $C_{27}$  and  $C_{29}$ - $C_{35}$  hopanes, maximising at  $C_{30}$  and  $C_{31}$ , are present in all samples. The 22S/(22S+22R) ratios of the  $17\alpha,21\beta$ (H)-hopanes are at near equilibrium values (0.57-0.62; Peters and Moldowan, 1993). Relative to the steranes, hopanes are most abundant in samples T6, T8 and T11.

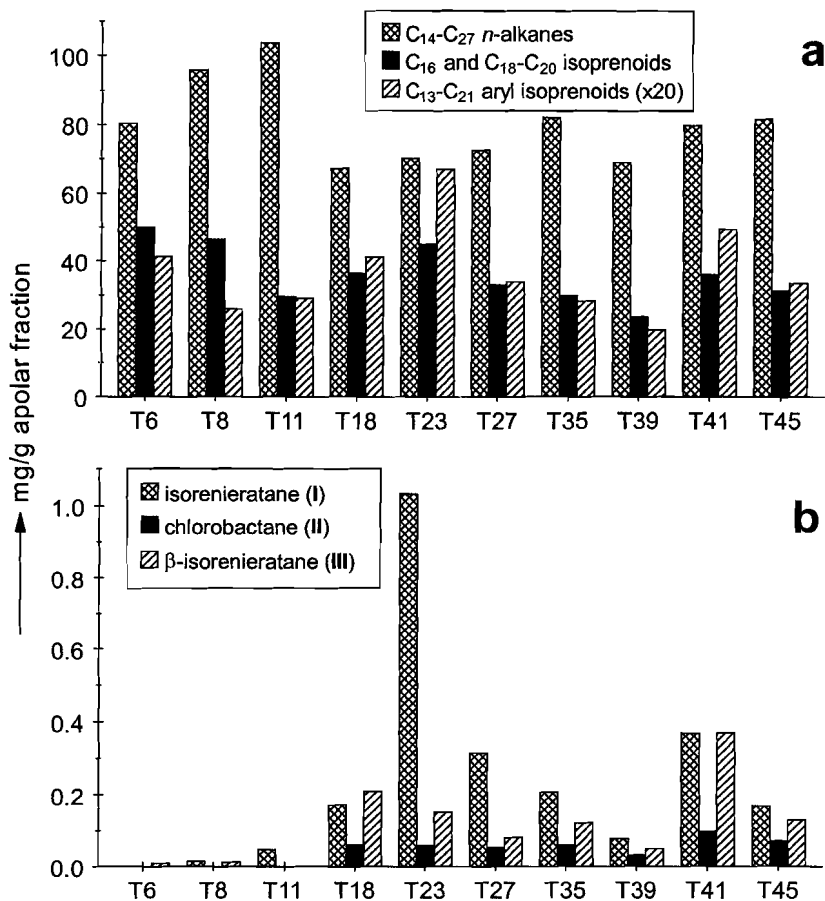


**Fig. 6.3.** Concentrations of (a) linear and acyclic isoprenoid alkanes and short-chain aryl isoprenoids and (b) isorenieratane, chlorobactane and  $\beta$ -isorenieratane.

### *Aromatic hydrocarbons*

The aromatic hydrocarbon fractions of all samples are dominated by mono- and tri-aromatic steroids, alkylbenzothiophenes, alkyl dibenzothiophenes and alkyl naphthalenes. Distributions of these compounds have been used as molecular parameters in oil-generation studies (Tissot et al., 1971; Radke and Willsch, 1991, 1994), or in studies addressing the maturation or environmental conditions during deposition of the rocks (Moldowan et al., 1986; Lichtfouse et al., 1994). Here we describe only the diagenetic derivatives of mono- and diaromatic carotenoids.

A series of C<sub>13</sub>-C<sub>21</sub> aryl isoprenoids with a trimethyl substitution pattern of the aromatic ring and with the usual low abundance of the C<sub>17</sub> member (cf. Summons and Powell, 1987) is present in all samples. Their concentrations are of the same order of magnitude in all samples except T23 and T41, where concentrations are higher (Fig. 6.3a).

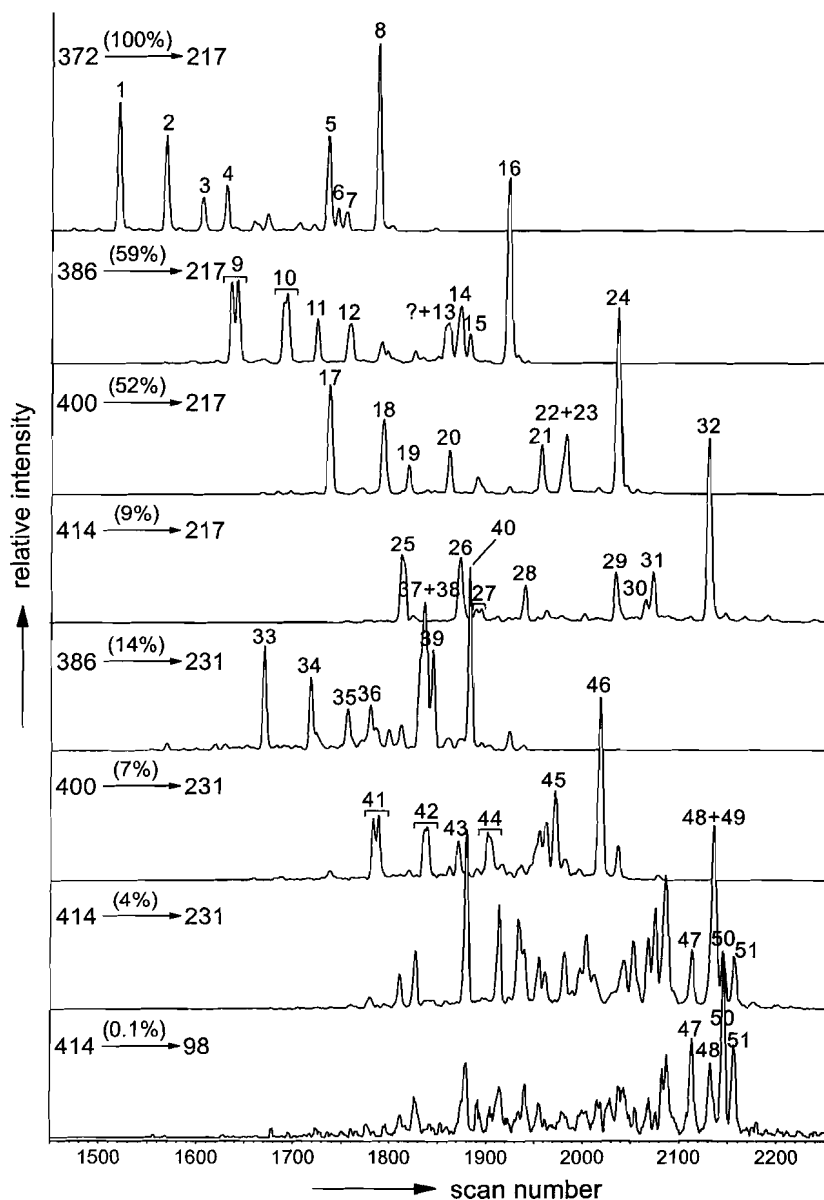


**Fig. 6.4.** Chromatograms showing desmethyl and 4-methyl sterane distributions in sample T41. The data were acquired by collisionally activated decomposition GC-MSMS. Each trace is identified with the masses of the parent and daughter ions, and the intensity of the base peak expressed as a percentage relative to the intensity of the 5 $\alpha$ -cholestane peak. Chromatograms were smoothed at 3 points of equal weight. Numbers refer to components listed in Table 6.2. The doublets of some of the diasteranes (e.g. compounds 9, 10, 41 and 42) are thought to represent 24S and 24R isomers.



**Table 6.2.** Steranes identified.

peak <sup>a</sup>	structure assignment	peak <sup>a</sup>	structure assignment
1	(20S)-13 $\beta$ ,17 $\alpha$ (H)-diacholestane <sup>b</sup>	27	(20R)-24-propyl-13 $\alpha$ ,17 $\beta$ (H)-diacholestane <sup>c</sup>
2	(20R)-13 $\beta$ ,17 $\alpha$ (H)-diacholestane <sup>b</sup>	28	(20S)-24-propyl-13 $\alpha$ ,17 $\beta$ (H)-diacholestane <sup>c</sup>
3	(20R)-13 $\alpha$ ,17 $\beta$ (H)-diacholestane <sup>b</sup>	29	24-propyl-5 $\beta$ -cholestane
4	(20S)-13 $\alpha$ ,17 $\beta$ (H)-diacholestane <sup>b</sup>	30	(20R)-24-propyl-5 $\alpha$ ,14 $\beta$ ,17 $\beta$ (H)-cholestane
5	5 $\beta$ -cholestane	31	(20S)-24-propyl-5 $\alpha$ ,14 $\beta$ ,17 $\beta$ (H)-cholestane
6	(20R)-5 $\alpha$ ,14 $\beta$ ,17 $\beta$ (H)-cholestane	32	24-propyl-5 $\alpha$ -cholestane
7	(20S)-5 $\alpha$ ,14 $\beta$ ,17 $\beta$ (H)-cholestane	33	(20S)-4 $\alpha$ -methyl-13 $\beta$ ,17 $\alpha$ (H)-diacholestane <sup>c</sup>
8	5 $\alpha$ -cholestane	34	(20R)-4 $\alpha$ -methyl-13 $\beta$ ,17 $\alpha$ (H)-diacholestane <sup>c</sup>
9	(20S)-24-methyl-13 $\beta$ ,17 $\alpha$ (H)-diacholestane <sup>c</sup>	35	(20R)-4 $\alpha$ -methyl-13 $\alpha$ ,17 $\beta$ (H)-diacholestane <sup>c</sup>
10	(20R)-24-methyl-13 $\beta$ ,17 $\alpha$ (H)-diacholestane <sup>c</sup>	36	(20S)-4 $\alpha$ -methyl-13 $\alpha$ ,17 $\beta$ (H)-diacholestane <sup>c</sup>
11	(20R)-24-methyl-13 $\alpha$ ,17 $\beta$ (H)-diacholestane <sup>c</sup>	37	4 $\alpha$ -methyl-5 $\beta$ -cholestane
12	(20S)-24-methyl-13 $\alpha$ ,17 $\beta$ (H)-diacholestane <sup>c</sup>	38	4 $\alpha$ -methyl-(20R)-5 $\alpha$ ,14 $\beta$ ,17 $\beta$ (H)-cholestane
13	24-methyl-5 $\beta$ -cholestane	39	4 $\alpha$ -methyl-(20S)-5 $\alpha$ ,14 $\beta$ ,17 $\beta$ (H)-cholestane
14	(20R)-24-methyl-5 $\alpha$ ,14 $\beta$ ,17 $\beta$ (H)-cholestane	40	4 $\alpha$ -methyl-5 $\alpha$ -cholestane
15	(20S)-24-methyl-5 $\alpha$ ,14 $\beta$ ,17 $\beta$ (H)-cholestane	41	(20S)-4 $\alpha$ ,24-dimethyl-13 $\beta$ ,17 $\alpha$ (H)-diacholestane <sup>c</sup>
16	24-methyl-5 $\alpha$ -cholestane	42	(20R)-4 $\alpha$ ,24-dimethyl-13 $\beta$ ,17 $\alpha$ (H)-diacholestane <sup>c</sup>
17	(20S)-24-ethyl-13 $\beta$ ,17 $\alpha$ (H)-diacholestane <sup>c</sup>	43	(20R)-4 $\alpha$ ,24-dimethyl-13 $\alpha$ ,17 $\beta$ (H)-diacholestane <sup>c</sup>
18	(20R)-24-ethyl-13 $\beta$ ,17 $\alpha$ (H)-diacholestane <sup>c</sup>	44	(20S)-4 $\alpha$ ,24-dimethyl-13 $\alpha$ ,17 $\beta$ (H)-diacholestane <sup>c</sup>
19	(20R)-24-ethyl-13 $\alpha$ ,17 $\beta$ (H)-diacholestane <sup>c</sup>	45	4 $\alpha$ ,24-dimethyl-5 $\beta$ -cholestane
20	(20S)-24-ethyl-13 $\alpha$ ,17 $\beta$ (H)-diacholestane <sup>c</sup>	46	4 $\alpha$ ,24-dimethyl-5 $\alpha$ -cholestane
21	24-ethyl-5 $\beta$ -cholestane	47	4 $\alpha$ ,23S,24S-trimethyl-5 $\alpha$ -cholestane <sup>d</sup>
22	(20R)-24-ethyl-5 $\alpha$ ,14 $\beta$ ,17 $\beta$ (H)-cholestane	48	4 $\alpha$ ,23S,24R-trimethyl-5 $\alpha$ -cholestane <sup>d</sup>
23	(20S)-24-ethyl-5 $\alpha$ ,14 $\beta$ ,17 $\beta$ (H)-cholestane	49	4 $\alpha$ -methyl-24-ethyl-5 $\alpha$ -cholestane
24	24-ethyl-5 $\alpha$ -cholestane	50	4 $\alpha$ ,23R,24R-trimethyl-5 $\alpha$ -cholestane <sup>d</sup>
25	(20S)-24-propyl-13 $\beta$ ,17 $\alpha$ (H)-diacholestane <sup>c</sup>	51	4 $\alpha$ ,23R,24S-trimethyl-5 $\alpha$ -cholestane <sup>d</sup>
26	(20R)-24-propyl-13 $\beta$ ,17 $\alpha$ (H)-diacholestane <sup>c</sup>		

<sup>a</sup> numbers refer to peaks indicated in Fig. 6.4<sup>c</sup> assuming the elution order to be similar to that of the diacholestanes<sup>b</sup> stereochemistry at C-20 after Sieskind et al. (1995)<sup>d</sup> stereochemistries at C-23 and C-24 after Moldowan (pers. comm., 1994)

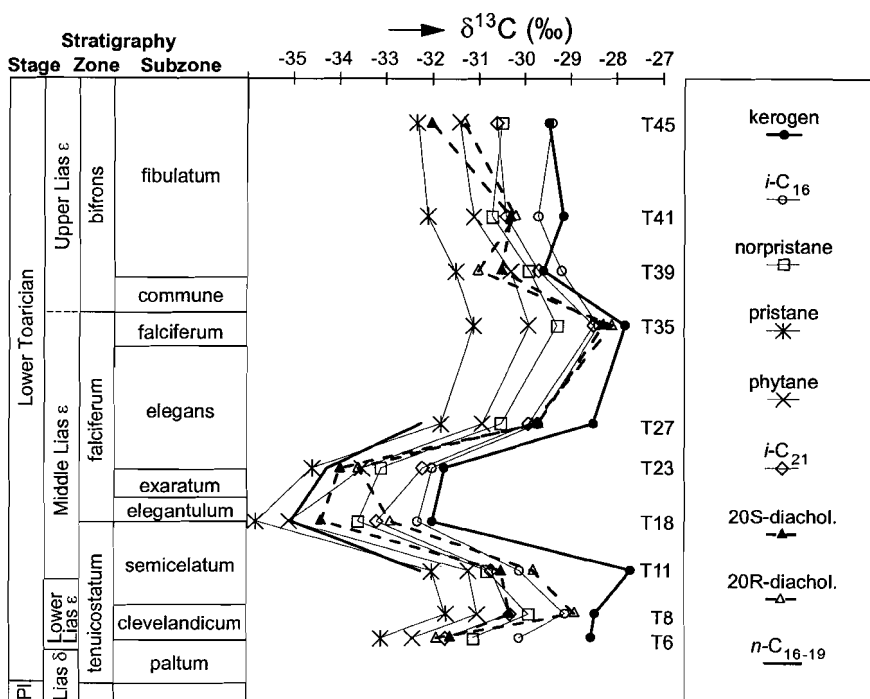


**Fig. 6.5.**  $\delta^{13}\text{C}$  values of kerogen, 2,6,10-trimethyltridecane ( $i\text{-C}_{16}$ ), norpristane, pristane, phytane, 2,6,10,14-tetramethylheptadecane ( $i\text{-C}_{21}$ ), (20S)-13 $\beta$ ,17 $\alpha$ (H)-diacholestane (20S-diachol.), (20R)-13 $\beta$ ,17 $\alpha$ (H)-diacholestane (20R-diachol.), and weighted average of  $\delta^{13}\text{C}$  of  $\text{C}_{16}\text{-C}_{19}$   $n$ -alkanes ( $n\text{-C}_{16-19}$ ) throughout the Lower Toarcian in SW Germany.

Depending on the sample, up to three carotenoid derivatives with an intact carbon skeleton are present. Unlike the short-chain derivatives, these  $\text{C}_{40}$  components are extremely low in samples T6, T8 and T11 (Fig. 6.3b). Concentrations of isorenieratane (**I**, see Appendix) are variable and show a distinct optimum in T23. Chlorobactane (**II**) is absent in T6, T8 and T11, and in the other samples its contribution to the apolar fraction is rather constant.  $\beta$ -Isorenieratane (**III**) was detected in all samples except T11, and it reaches its highest concentration in T41. It should be noted that the presence of chlorobactane and  $\beta$ -isorenieratane was not confirmed by coinjection with an authentic standard. Recently, two novel  $\text{C}_{40}$  carotenoid-derived compounds, **IV** and **V**, have been identified in sediments of a meromictic lake (Schaeffer et al., 1997), which, based on mass spectral data only, cannot be distinguished from chlorobactane (**II**) and  $\beta$ -isorenieratane (**III**), respectively.

#### *Molecular carbon isotope data*

The kerogens show a negative carbon isotope excursion in samples T18 and T23 (Fig. 6.5, Table 6.1), which is at the transition of the *tenuicostatum* and *falciferum* Zones, and at the transition of the *exaratum* and *elegans* Subzones, respectively. Immediately below the

**Table 6.3.** Stable carbon isotopic compositions of different biomarkers.

sample	<i>i</i> -C <sub>16</sub> <sup>a</sup>	norpristane	pristane	phytane	<i>i</i> -C <sub>21</sub> <sup>b</sup>	(20S)-13β,17α(H)- diacholestane	(20R)-13β,17α(H)- diacholestane
T6	-30.1 ± 0.1	-31.1 ± 0.1	-33.1 ± 0.1	-32.4 ± 0.1	-31.7 ± 0.5	-31.6 ± 0.1	-31.9 ± 0.5
T8	-29.1 ± 0.4	-29.9 ± 0.1	-31.7 ± 0.1	-31.0 ± 0.1	-30.3 ± 0.9	-30.3 ± 0.3	-28.9 ± 0.3
T11	-30.1 ± 0.2	-30.8 ± 0.2	-32.0 ± 0.2	-31.2 ± 0.2	-30.7 ± 0.5	-30.5 ± 0.2	-29.8 ± 1.3
T18	-32.3 ± 0.5	-33.6 ± 0.5	-35.8 ± 0.2	-35.1 ± 0.2	-33.2 ± 1.0	-34.4 ± 0.8	-32.9 ± 1.9
T23	-32.0 ± 0.3	-33.1 ± 0.3	-34.6 ± 0.3	-33.5 ± 0.3	-32.2 ± 0.2	-34.0 ± 0.1	-33.6 ± 1.2
T27	-29.7 ± 0.1	-30.5 ± 0.2	-31.8 ± 0.2	-30.9 ± 0.1	-29.9 ± 0.2	-29.7 ± 0.5	-29.8 ± 1.1
T35	-28.4 ± 0.2	-29.3 ± 0.9	-31.1 ± 0.3	-29.9 ± 0.1	-28.5 ± 0.9	-28.3 ± 0.4	-28.1 ± 0.3
T39	-29.2 ± 0.7	-29.9 ± 0.3	-31.5 ± 0.1	-30.3 ± 0.2	-29.7 ± 1.1	-30.5 ± 0.5	-31.0 ± 0.1
T41	-29.7 ± 0.3	-30.7 ± 0.5	-32.1 ± 0.3	-31.1 ± 0.4	-30.4 ± 0.5	-30.3 ± 0.6	-30.2 ± 0.3
T45	-29.4 ± 0.1	-30.5 ± 0.1	-32.3 ± 0.3	-31.4 ± 0.3	-30.6 ± 0.2	-32.0 ± 0.6	-31.3 ± 1.1

<sup>a</sup> 2,6,10-trimethyltridecane<sup>b</sup> 2,6,10,14-tetramethylheptadecane

excursion in T11, and well above the excursion in T35 (*falciferum* Subzone),  $\delta^{13}\text{C}_{\text{TOC}}$  is highest. Markedly, the  $\delta^{13}\text{C}$  values of the biomarkers follow a trend similar to that of  $\delta^{13}\text{C}_{\text{TOC}}$ , but with an offset of less than one to several per mil (Fig. 6.5, Tables 6.3, 6.4). In T6, T8 and T11, the offset is on average larger than in the other samples. An average offset of 3.3, 2.4, 1.6, 1.4 and 0.7‰ was calculated for pristane, phytane, norpristane, *i*-C<sub>21</sub> and *i*-C<sub>16</sub>, respectively. For the diacholestanes such an average was not determined, since they have less accurate  $\delta^{13}\text{C}$  values due to the fact that they elute at the beginning of a hump. The weighted average of  $\delta^{13}\text{C}$  of C<sub>16</sub>-C<sub>19</sub> *n*-alkanes, components abundantly present in algae (Gelpi et al., 1970), falls close to the  $\delta^{13}\text{C}$  values of pristane and phytane (Fig. 6.5).

Due to coelution and due to their relatively low abundance it was not possible to determine the  $^{13}\text{C}$  content of any of the aryl- and diaryl isoprenoids.

**Table 6.4.**  $\delta^{13}\text{C}$  values of free *n*-alkanes in samples T11-T27.

	T11 <sup>a</sup>	T18	T23	T27 <sup>a</sup>
<i>n</i> -C <sub>16</sub>	-30.6 ± 0.5	-34.6 ± 0.5	-34.4 ± 0.3	-31.7 ± 0.6
<i>n</i> -C <sub>17</sub>	-32.9 ± 0.6	-35.2 ± 0.1	-34.6 ± 0.3	-32.6 ± 0.4
<i>n</i> -C <sub>18</sub>	-32.8 ± 0.9	-35.2 ± 0.1	-34.0 ± 0.3	-32.4 ± 0.1
<i>n</i> -C <sub>19</sub>	-33.4 ± 0.7	-35.2 ± 0.2	-34.1 ± 0.1	-32.2 ± 0.7
<i>n</i> -C <sub>20</sub>	-33.5 ± 0.3	-35.2 ± 0.1	-34.2 ± 0.4	-32.8 ± 0.3
<i>n</i> -C <sub>21</sub>		-35.2 ± 0.1	-35.0 ± 0.6	
<i>n</i> -C <sub>22</sub>		-34.7 ± 0.4	-34.2 ± 0.5	
<i>n</i> -C <sub>23</sub>		-34.7 ± 0.1	-35.1 ± 0.7	
<i>n</i> -C <sub>24</sub>		-34.9 ± 0.1	-34.8 ± 1.3	
<i>n</i> -C <sub>25</sub>		-34.3 ± 0.1	-34.5 ± 1.4	
<i>n</i> -C <sub>26</sub>		-33.8 ± 0.9	-34.7 ± 1.2	
<i>n</i> -C <sub>27</sub>		-33.7 ± 0.1	-32.3 ± 0.3	
<i>n</i> -C <sub>28</sub>		-32.8 ± 0.1	-32.3 ± 0.2	
<i>n</i> -C <sub>29</sub>		-32.6 ± 0.4	-32.6 ± 0.9	
<i>n</i> -C <sub>30</sub>		-32.3 ± 1.8	-32.2 ± 1.5	
<i>n</i> -C <sub>31</sub>		-33.5 ± 0.1	-33.3 ± 0.8	

<sup>a</sup> C<sub>20+</sub> *n*-alkanes were contaminated

### *Kerogen pyrolysates*

The kerogen pyrolysates of all samples are predominantly composed of homologous series of *n*-alkanes and *n*-alkenes, and shorter series of alkylbenzenes, alkylthiophenes, alkylnaphthalenes and alkylbenzothiophenes (e.g. Fig. 6.6). Phenolic pyrolysis products, originating from lignins (Saiz-Jimenez and de Leeuw, 1984, 1986), are present in trace amounts only. The distributions of the individual compound classes are very similar in all samples, and differences among the pyrolysates mainly concern the relative abundances of the compound classes. It is noted, however, that the pyrolysate of sample T39 shows a drop in the *n*-alkane/*n*-alkene distribution at C<sub>17</sub>-C<sub>18</sub> (Fig. 6.6a), which is less conspicuous or absent in the other pyrolysates. As expected from their relatively low HI values (Table 6.1), pyrolysates of T8 and T11 are characterised by a relatively small contribution of *n*-alkanes and *n*-alkenes (e.g. Fig. 6.6c). The other pyrolysates show a higher, more or less constant ratio of *n*-alkane/*n*-alkene doublets over aromatic- and thiophenic pyrolysis products, but the

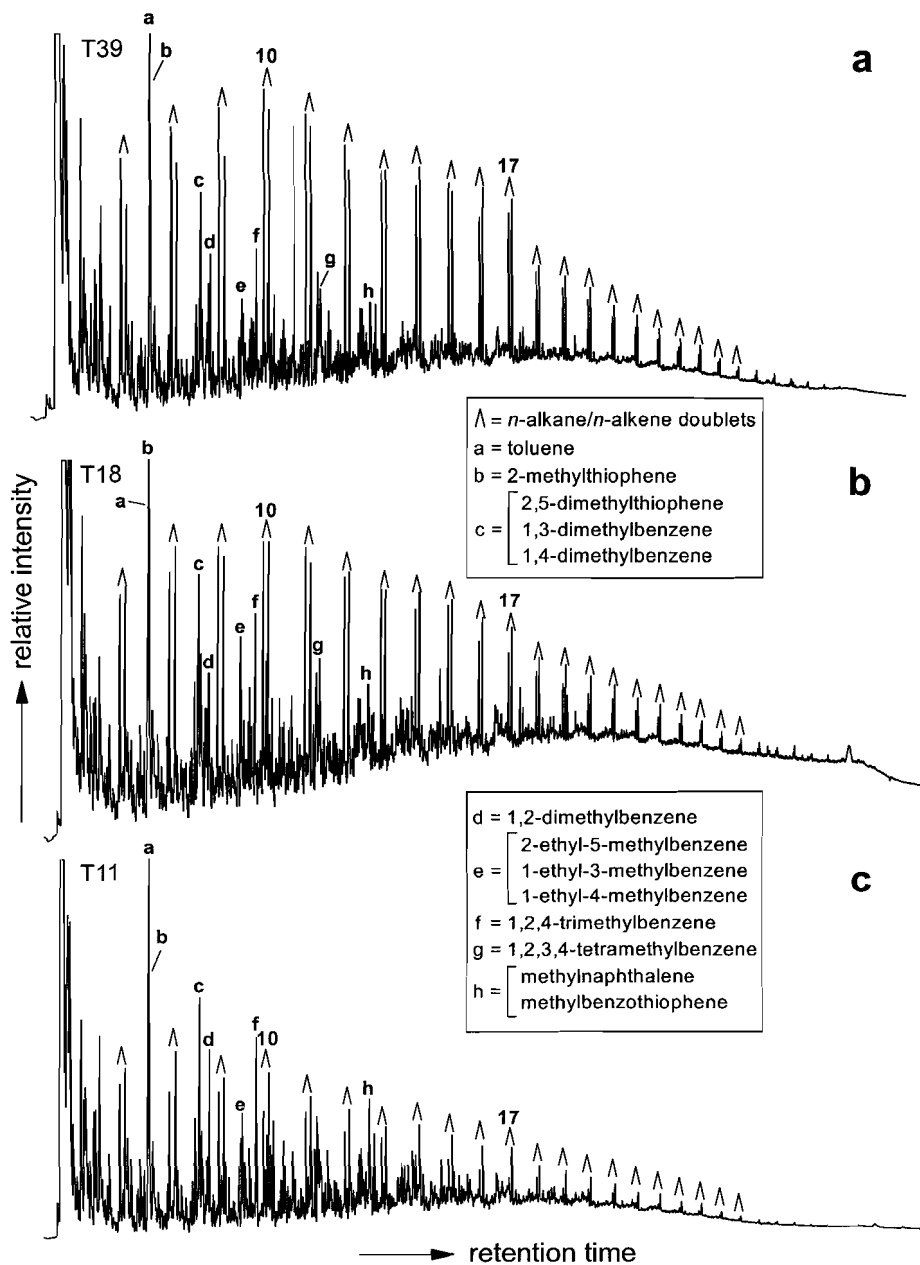


**Fig. 6.6.** Gas chromatograms of flash pyrolysates (Curie-temperature 610°C) of kerogens of samples (a) T39, (b) T18 and (c) T11.

proportions of aromatic and thiophenic compounds vary (Figs. 6.6a,b). The contribution of organic sulfur compounds to the pyrolysate is positively correlated with HI, and is greatest

in the pyrolysates of T18, T23, T27 and T35. These latter pyrolysates are also virtually identical.

## Discussion

In all samples, the proportion of terrestrial OM is small, as concluded from the small amounts of long-chain odd-numbered *n*-alkanes in the extracts (Eglinton et al., 1962) and the almost absence of phenolic compounds in the kerogen pyrolysates (Saiz-Jimenez and de Leeuw, 1984, 1986). The short-chain *n*-alkanes and steranes in the saturated hydrocarbon fractions (Fig. 6.2) are thus predominantly derived from algae (Gelpi et al., 1970; Volkman, 1986). Based on sterane distributions, pr/ph ratios and relative abundance of hopanes, samples in the *tenuicostatum* Zone (T6, T8 and T11) differ from those higher in the sedimentary sequence. The slightly different desmethyl sterane distribution of T6, T8 and T11 as opposed to the rest of the samples, may be related to the change in the assemblage of palynomorphs reported by Prauss et al. (1991). These authors, in their study of the *Posidonia* shales near Bisingen/Zimmern (SW Germany), report an almost complete replacement of dinocysts and acritarchs by prasinophytes at the *tenuicostatum/falciferum* transition. In this respect it is noteworthy that the relative abundance and distribution of 4-methyl steranes, components that are generally ascribed to dinoflagellates (de Leeuw et al., 1983; Summons et al., 1987, 1992), do not exhibit any changes along this transition. The succession dinocysts-acritarchs-prasinophytes was attributed to a decreasing salinity of the photic zone, ultimately leading to density stratification and anoxic conditions in at least the lower part of the water column (Prauss et al., 1991). In agreement with this, Moldowan et al. (1986) found the ratio of nickel to vanadium porphyrins to dramatically change within a narrow zone between T11 and T18. Samples from below this zone, characterised by high Ni/V ratios, were interpreted to have been deposited in a less reducing environment.

Isorenieratane (I), which is a marker for photic zone anoxia (PZA) (Sinninghe Damsté et al., 1993), was detected in all samples, but concentrations in samples from the *tenuicostatum* Zone (T6, T8, T11) are extremely low (Fig. 6.3b). To a certain extent, this is consistent with the findings of Prauss et al. (1991) and Moldowan et al. (1986), that the depositional environment was "less reducing" during the *tenuicostatum* Zone. The presence of isorenieratane in samples T6, T8 and T11 may seem to contradict the high Ni/V ratios reported by Moldowan et al. (1986) for these samples. However, since the complexation of nickel and vanadium to porphyrins is probably a reversible reaction sensitive to differences in Eh and pH (Lewan, 1984), the high Ni/V ratios in the TOC-rich shales from the *tenuicostatum* Zone (Moldowan et al., 1986) may not reflect the sedimentary conditions of the shales themselves, but instead be representative of pore water chemistry during deposition of the overlying marls.

In contrast to isorenieratane (I), chlorobactane (II) and  $\beta$ -isorenieratane (III), short-chain aryl isoprenoids are not low in samples from the *tenuicostatum* Zone (Fig. 6.3a). It was recently shown that these compounds, and also  $\beta$ -isorenieratane, can be formed from  $\beta$ -carotene (VI), and without knowing their  $\delta^{13}\text{C}$  values cannot be used as markers for PZA (Koopmans et al., 1996). Thus, although no  $\beta$ -carotene (VII) was detected, it may be that the short-chain aryl isoprenoids in T6, T8 and T11 are largely derived from  $\beta$ -carotene, whereas

short-chain aryl isoprenoids in the other samples originate from one or more of the aromatic carotenoids. Alternatively, short-chain aryl isoprenoids in T6, T8 and T11 also derive from aromatic carotenoids, but smaller amounts of C<sub>40</sub> derivatives survived due to differences in diagenesis. For example, if deposition of samples T6, T8 and T11 was followed by relatively long periods in which bottom waters were oxygenated, this may have led to selective degradation of the C<sub>40</sub> compounds.

Apart from the minor differences discussed above, the composition of the saturated hydrocarbon fraction is very similar in all samples, and differences that do occur show no correlation with  $\delta^{13}\text{C}_{\text{TOC}}$ . Differences among the kerogen pyrolysates are somewhat more pronounced, but do not correspond to changes in  $\delta^{13}\text{C}_{\text{TOC}}$  either. Moreover, exactly the pyrolysates of samples in the *falciferum* Zone (T18, T23, T27 and T35), which have very different  $\delta^{13}\text{C}_{\text{TOC}}$  values (Fig. 6.5), are most alike. This strongly suggests that contrary to the views of Jenkyns and Clayton (1986) and Prauss and Riegel (1989), the negative shift in  $\delta^{13}\text{C}_{\text{TOC}}$  cannot have resulted from changes in the composition of biota.

Of all  $\delta^{13}\text{C}$  values measured (Tables 6.3, 6.4), those of the diacholestanes are thought to best approximate the  $\delta^{13}\text{C}$  value of the "average algal lipid". As opposed to pristane and phytane, which may originate from both eukaryotic and prokaryotic sources, diacholestanes can only be derived from algae or heterotrophs grazing on them. Since the  $^{13}\text{C}$  contents of lipids from heterotrophs are not significantly different from those of their food source (Fry and Sherr, 1984; Grice et al., 1997), isotopic fractionation due to grazing can be neglected. In addition, diagenetic transformations of biomarkers involving the removal or transfer of hydrogen or methyl groups, are not accompanied by large isotopic fractionations either (Hauke et al., 1992; Freeman et al., 1994a; van Kaam-Peters et al., 1997b). This implies that the diacholestanes still bear their original primary producer  $\delta^{13}\text{C}$  value.

The  $\delta^{13}\text{C}$  values of 20S and 20R 13 $\beta$ ,17 $\alpha$ (H)-diacholestane follow a trend similar to that of  $\delta^{13}\text{C}_{\text{TOC}}$  (Fig. 6.5). Also, depending on carbon number, the  $\delta^{13}\text{C}$  values of the acyclic isoprenoids have an individual, almost constant offset from  $\delta^{13}\text{C}_{\text{TOC}}$  (Fig. 6.5). Assuming the classical mevalonate pathway for isoprenoid biosynthesis (e.g. Coolbear and Threlfall, 1989), differences in  $\delta^{13}\text{C}$  caused by different chain lengths of these isoprenoids, amount to 0.3‰ at most (Monson and Hayes, 1982). Based on this 0.3‰ margin, only norpristane and *i*-C<sub>21</sub> may be derived from a similar source, and each of the other isoprenoid alkanes is expected to have a different origin. However, new biosynthetic routes for the formation of isoprenoids have been found (e.g. Rohmer et al., 1993, 1996; Schwender et al., 1996), and much is still unknown about the isotope effects associated with biosynthesis. Therefore, caution is needed when inferring different sources based on stable carbon isotope data. In this respect it is noteworthy that differences as large as 6‰ were found between *n*-alkanes in a single leaf (Collister et al., 1994).

In samples from the *tenuicostatum* Zone (T6, T8, T11), the difference between  $\delta^{13}\text{C}_{\text{TOC}}$  and  $\delta^{13}\text{C}$  of the acyclic isoprenoids is somewhat larger than in the other samples (Fig. 6.5). Since these samples are also characterised by relatively abundant homohopanes, it is suggested that a greater part of the acyclic isoprenoids in these samples is derived from cyanobacteria. In that case, the offset between  $\delta^{13}\text{C}_{\text{TOC}}$  and  $\delta^{13}\text{C}$  of the diacholestanes should not differ among the samples. Unfortunately, due to the relatively large standard deviations of diacholestane  $\delta^{13}\text{C}$  values (Table 6.3), this could not be confirmed.

The fact that 20S and 20R 13 $\beta$ ,17 $\alpha$ (H)-diacholestane and other phytoplanktonic lipids, like pristane, phytane and short-chain *n*-alkanes (Goossens et al., 1984; Volkman, 1986; Volkman and Maxwell, 1986; Gelpi et al., 1970), exhibit an isotope excursion similar to that of  $\delta^{13}\text{C}_{\text{TOC}}$ , indicates that differences in  $\delta^{13}\text{C}_{\text{TOC}}$  are related to differences in  $[\text{CO}_2]_{\text{aq}}$  or  $\delta^{13}\text{C}_{\text{CO}_2}$  in the photic zone. Thus, unless the effect on  $\delta^{13}\text{C}_{\text{TOC}}$  of global organic carbon burial was outdone by the effect of regional changes in  $[\text{CO}_2]_{\text{aq}}$  or  $\delta^{13}\text{C}_{\text{CO}_2}$ , the Early Toarcian OAE was not a global event at all. Rather, the data seem to nicely fit the scenario of Küspert (1982) that during deposition of the low  $\delta^{13}\text{C}_{\text{TOC}}$  samples, isotopically light  $\text{CO}_2$ , released in the mineralisation of OM in stagnant bottom waters, was recycled into the photic zone.

If indeed recycling of  $\text{CO}_2$  has a large effect on  $\delta^{13}\text{C}_{\text{CO}_2}$  in the surface water, and thus on  $\delta^{13}\text{C}_{\text{TOC}}$ , it must have been that waters rich in organic-derived  $\text{CO}_2$  were at close distance from the photic zone during the lower part of the *falciferum* Zone. In cases that the oxic/anoxic interface was located in the photic zone, mixing of  $\text{CO}_2$  present in anoxic waters with relatively high  $[\text{CO}_2]_{\text{aq}}$  and low  $\delta^{13}\text{C}_{\text{CO}_2}$ , and  $\text{CO}_2$  present in surface waters with relatively low  $[\text{CO}_2]_{\text{aq}}$  and high  $\delta^{13}\text{C}_{\text{CO}_2}$ , must have been optimal. Since isorenieratane, indicating PZA, was detected in all samples, one could speculate that  $\delta^{13}\text{C}_{\text{TOC}}$  is related to the frequency or duration of PZA. The highly variable concentrations of isorenieratane (Fig. 6.3b), showing no correlation with  $\delta^{13}\text{C}_{\text{TOC}}$ , argue against this hypothesis. However, we cannot be sure that concentrations of isorenieratane properly reflect the intensity of  $\text{CO}_2$  recycling, since recycling of  $\text{CO}_2$  may already occur if the chemocline is just below the photic zone, in which case there is no ecological niche for the isorenieratane source organisms.

Interestingly, the difference between  $\delta^{13}\text{C}$  of the carbonate ( $\delta^{13}\text{C}_{\text{CARB}}$ ) and  $\delta^{13}\text{C}_{\text{TOC}}$  ( $\Delta\delta^{13}\text{C}_{\text{CARB-TOC}}$ ) is rather constant throughout the entire Early Toarcian sequence in the SW German Basin (Küspert, 1982), whereas Hollander et al. (1991), for the same stratigraphic interval in the Paris Basin, find  $\Delta\delta^{13}\text{C}_{\text{CARB-TOC}}$  to maximise in high TOC/low  $\delta^{13}\text{C}_{\text{TOC}}$  samples. Hollander et al. (1991) explain this by a more intense recycling of  $\text{CO}_2$ , leading to a higher  $[\text{CO}_2]_{\text{aq}}$  in the photic zone, in its turn inducing a larger isotopic fractionation by photoautotrophs, in the case of the Paris Basin section. This explanation is based on two assumptions: 1. The carbon isotopic fractionation associated with the formation of both skeletal and inorganically precipitated carbonate is much less dependent on  $[\text{CO}_2]_{\text{aq}}$  than the fractionation associated with photosynthesis. This justifies that changes in  $\Delta\delta^{13}\text{C}_{\text{CARB-TOC}}$  are interpreted in terms of changes in  $\Delta\delta^{13}\text{C}_{\text{CO}_2\text{-TOC}}$ . 2. The stable carbon isotopic composition of phytoplankton biomass largely depends on  $[\text{CO}_2]_{\text{aq}}$ . As for the first assumption, we agree (see e.g. Hayes et al., 1989), although one should not forget that (i) much is still unknown about the  $^{13}\text{C}$  content of skeletal carbonate in relation to  $\delta^{13}\text{C}_{\text{CO}_2}$  (Spero et al., 1991), (ii) to reconstruct  $\delta^{13}\text{C}_{\text{CO}_2}$  of the photic zone,  $\delta^{13}\text{C}_{\text{CARB}}$  should preferentially be measured on primary, planktonic carbonate (Hayes et al., 1989) and (iii) the carbon isotopic difference between dissolved  $\text{CO}_2$  and calcite is temperature dependent, the fractionation factor decreasing by ca. 1‰ over a temperature rise of 10°C (Mook et al., 1974). The second assumption, however, should be viewed with more caution. Obviously, it cannot be denied that e.g. in lake Greifen  $\Delta\delta^{13}\text{C}_{\text{CO}_2\text{-POC}}$  is lowest at times of high primary production and low  $[\text{CO}_2]_{\text{aq}}$  (Hollander and McKenzie, 1991). But this does not imply that the opposite, a high



$[\text{CO}_2]_{\text{aq}}$  leading to high  $\Delta\delta^{13}\text{C}_{\text{CO}_2\text{-POC}}$  is also true. Under conditions of low  $[\text{CO}_2]_{\text{aq}}$ , some algae can actively transport  $\text{CO}_2$  or even bicarbonate, which is significantly enriched in  $^{13}\text{C}$  relative to  $\text{CO}_2$ , by operating a " $\text{CO}_2$ -concentrating mechanism" (Burns and Beardall, 1987; Raven and Johnston, 1994). In that case, the carbon isotopic fractionation associated with photosynthesis ( $\epsilon_p$ ) is expected to be much reduced. Also, although  $\epsilon_p$  has frequently been reported to largely depend on  $[\text{CO}_2]_{\text{aq}}$  (e.g. Degens et al., 1968; Deuser et al., 1968; Calder and Parker, 1973; Kroopnick, 1974; Mizutani and Wada, 1982; Popp et al., 1989; Rau et al., 1989; Jasper and Hayes, 1990; Freeman and Hayes, 1992), differences as large as 5‰ were found for  $\delta^{13}\text{C}_{\text{POC}}$  in a region of the Indian Ocean characterised by nearly constant  $[\text{CO}_2]_{\text{aq}}$  (Rau et al., 1992). Furthermore, Laws et al. (1995) presented evidence that  $\epsilon_p$  is largely controlled not only by  $[\text{CO}_2]_{\text{aq}}$ , but also by the growth rate ( $\mu$ ) of the phytoplankton. For the marine diatom *Phaeodactylum tricornutum* and supposedly also for other algal species, a strong, linear, inverse relationship exists between  $\mu/[\text{CO}_2]_{\text{aq}}$  and  $\epsilon_p$  (Laws et al., 1995). Thus, an increase in  $[\text{CO}_2]_{\text{aq}}$  will lead to an increase in  $\epsilon_p$  only if this is not compensated for by an increase in  $\mu$ . Goericke et al. (1994), by modelling the diffusive uptake of  $\text{CO}_2$  with subsequent fixation *via* Rubisco and  $\beta$ -carboxylases, predicted  $\epsilon_p$  to be significantly influenced by also the cell size of the alga.

Considering the shallow position of the chemocline in the Black Sea (Repeta, 1993; Sinninghe Damsté et al., 1993), it was thought that if recycling of  $\text{CO}_2$  would ever have an effect on  $\delta^{13}\text{C}_{\text{TOC}}$ , this should currently be taking place in the Black Sea photic zone. Indeed, Goyet et al. (1991) report a large increase in  $[\text{CO}_2]_{\text{aq}}$  at depths below 40 m in the Black Sea. Starting from 17-21  $\mu\text{mol kg}^{-1}$  in the upper 40 m of the photic zone,  $[\text{CO}_2]_{\text{aq}}$  reaches 39  $\mu\text{mol kg}^{-1}$  already at a depth of 50 m, and 71  $\mu\text{mol kg}^{-1}$  at 65 m. Below 65 m,  $[\text{CO}_2]_{\text{aq}}$  gradually rises to reach a concentration of 95  $\mu\text{mol kg}^{-1}$  at 1500 m. Markedly, the large increase in  $[\text{CO}_2]_{\text{aq}}$  with depth in the 40 to 65 m interval, is accompanied by a decrease in  $\delta^{13}\text{C}_{\text{CO}_2}$  of only 0.6‰, and the overall decrease in  $\delta^{13}\text{C}_{\text{CO}_2}$  over the first 65 m amounts to only 4‰ (Freeman et al., 1994b). Therefore, if we want to explain the 4‰ difference in  $\delta^{13}\text{C}_{\text{TOC}}$  of the Early Toarcian shales by recycling of  $^{13}\text{C}$  depleted, organic-derived  $\text{CO}_2$ , the majority of biomass must have been produced at depths near the  $[\text{CO}_2]_{\text{aq}}$  maximum in the photic zone. The stable carbon isotope data reported by Fry et al. (1991) and Freeman et al. (1994b), show that in the modern Black Sea this is not the case. In the Black Sea,  $\delta^{13}\text{C}_{\text{POC}}$  was found to generally increase with depth (-25 to -22‰), with the exception of the -28.3‰ measured for a sample from 48 m (Fry et al., 1991). This 48 m sample has been suggested to represent a mixture of both heterotrophically altered material sinking from above and newly produced biomass of nitrifying bacteria (Fry et al., 1991; Freeman et al., 1994b). Considering the trend of increasing  $\delta^{13}\text{C}_{\text{POC}}$  with depth, however, it must be that most of the newly produced, isotopically light biomass decomposes rather quickly. Consequently, OM reaching the sea floor will largely bear the carbon isotopic signal of biomass produced in the upper part of the photic zone, where  $\text{CO}_2$  is largely derived from the atmosphere. The relatively high  $\delta^{13}\text{C}$  values of phytoplanktonic lipids in recent Black Sea sediments (Freeman et al., 1994b) are in agreement with this.

Altogether, our molecular data indicate that the negative excursion of  $\delta^{13}\text{C}_{\text{TOC}}$  originates from changes in  $\delta^{13}\text{C}_{\text{CO}_2}$  or  $[\text{CO}_2]_{\text{aq}}$  in the photic zone, but the reason for these

changes is not evident. The scenario of organic-derived CO<sub>2</sub> being regenerated back into the surface waters, favoured by Küspert (1982), has lost credibility, since, despite the occurrence of PZA, δ<sup>13</sup>C of OM in the water column and top sediments of the Black Sea is not significantly affected by CO<sub>2</sub> recycling. On the other hand, external factors like volcanic eruptions, forest fires or changes in the input of dissolved inorganic carbon (DIC) by rivers, do not provide good explanations either. With respect to the latter, stable carbon isotope analyses of the Great Lakes-St. Lawrence system have shown that δ<sup>13</sup>C of DIC (δ<sup>13</sup>C<sub>DIC</sub>) in tributary waters may partly be controlled by bacterial respiration, but DIC in the Great Lakes themselves is in isotopic equilibrium with atmospheric CO<sub>2</sub> (Yang et al., 1996). By analogy, δ<sup>13</sup>C<sub>DIC</sub> in the Lower Toarcian epicontinental seas is not likely to have been regulated by the inflow of river water DIC. As for eventual volcanic eruptions or forest fires, assuming that these led to enhanced concentrations of <sup>12</sup>CO<sub>2</sub> in the atmosphere, it is highly improbable that their impact was so profound in the SW German section and absent in the nearby Toarcian of NW Germany.

In our view, the negative excursion in δ<sup>13</sup>C<sub>TOC</sub> is still best explained by the CO<sub>2</sub> recycling hypothesis (Küspert, 1982). Possibly, the oxic/anoxic interface was even more shallow in the SW German Basin than it is today in the Black Sea. In that case, primary production perhaps could occur at depths where DIC is largely organic-derived. This would suggest that in the lower part of the *falciferum* Zone, during periods of water column stratification, only DIC in the very uppermost part (10 or 20 m?) of the photic zone was in isotopic equilibrium with CO<sub>2</sub> in the atmosphere.

## Conclusions

The OM in the Early Toarcian shales of the SW German Basin displays a negative carbon isotope excursion in the lower part of the *falciferum* Zone. Since the contribution of terrestrial OM is minor in all samples, this excursion cannot have resulted from differences in the ratio of terrestrial to marine OM. Biomarker distributions and kerogen pyrolysates exhibit only minor differences among the samples, and these do not correspond to differences in δ<sup>13</sup>C<sub>TOC</sub>. Therefore, changes in the composition of the planktonic community are not a likely cause for the excursion of δ<sup>13</sup>C<sub>TOC</sub> either.

The δ<sup>13</sup>C values of primary production and other markers follow a trend similar to that of δ<sup>13</sup>C<sub>TOC</sub> (Fig. 6.5), indicating that differences in δ<sup>13</sup>C<sub>TOC</sub> are related to differences in δ<sup>13</sup>C<sub>CO<sub>2</sub></sub> and/or [CO<sub>2</sub>]<sub>aq</sub>. This fits the hypothesis of Küspert (1982), that the negative carbon isotope excursion resulted from the recycling of isotopically light CO<sub>2</sub>, derived from the mineralisation of OM in stagnant bottom waters, into the surface water.

Isorenieratane, testifying to the occurrence of photic zone anoxia in the water column, was detected in all samples. Differences among the samples in the concentration of isorenieratane do not correspond to differences in δ<sup>13</sup>C<sub>TOC</sub>. This indicates that concentrations of isorenieratane are not a measure for the eventual influence of CO<sub>2</sub> recycling on δ<sup>13</sup>C<sub>TOC</sub>.

Literature data on the <sup>13</sup>C contents of organic and inorganic carbon in water column and sediments of the present-day Black Sea, show that, despite the occurrence of photic zone anoxia, suggesting good conditions for CO<sub>2</sub> recycling, sedimentary OM is mainly produced in the upper part of the photic zone, where CO<sub>2</sub> is largely derived from the atmosphere. In

other words, in the present-day Black Sea, eventual mixing of organic-derived CO<sub>2</sub> and atmospheric-derived CO<sub>2</sub> does not significantly influence δ<sup>13</sup>C of sedimentary OM. Despite this serious drawback of the CO<sub>2</sub> recycling hypothesis (Küspert, 1982), it is still believed to be the best explanation for the negative excursion of δ<sup>13</sup>C<sub>TOC</sub> in the SW German Toarcian shales. It is deemed unlikely that the shift in δ<sup>13</sup>C<sub>TOC</sub> was caused by external factors, like volcanic eruptions, forest fires or changes in the supply of DIC by rivers. Probably, during deposition of the low δ<sup>13</sup>C<sub>TOC</sub> shales, the chemocline was located at even shallower depths than observed in the Black Sea today.

Unless the effect of global organic carbon burial on δ<sup>13</sup>C<sub>TOC</sub> was negated by the more regional decrease in δ<sup>13</sup>C<sub>CO<sub>2</sub></sub> and/or increase in [CO<sub>2</sub>]<sub>aq</sub> in the SW German Basin, probably caused by recycling of organic-derived CO<sub>2</sub>, the Early Toarcian OAE is not a true global event.

**Acknowledgements.** We thank the Netherlands Organization for Scientific Research (NWO) for the PIONIER grant to JSSD and the studentship of HMEvKP. Shell International Petroleum Maatschappij BV financially supported the GC-IRMS facility. We thank Dr. J. Köster, Dr. R. Kreulen and R. Kloosterhuis for bulk analyses, and W.I.C. Rijpstra, M. Baas, M. Dekker and W. Pool for analytical assistance.

## References

- Barnard P.C. and Cooper B.S. (1981) Oils and source rocks of the North Sea area. In *Petroleum Geology of the Continental Shelf of North-West Europe* (ed. L.V. Illing and G.D. Hobson), pp. 169-175. London, Heyden and Son, Inst. Petroleum.
- Burns B.D. and Beardall J. (1987) Utilization of inorganic carbon by marine microalgae. *J. Exp. Mar. Biol. Ecol.* **107**, 75-86.
- Calder J.A. and Parker P.L. (1973) Geochemical implications of induced changes in C-13 fractionation by blue-green algae. *Geochim. Cosmochim. Acta* **37**, 133-140.
- Collister J.W., Rieley G., Stern B., Eglinton G. and Fry B. (1994) Compound-specific δ<sup>13</sup>C analyses of leaf lipids from plants with differing carbon dioxide metabolisms. *Org. Geochem.* **21**, 619-627.
- Coolbear T. and Threlfall D.R. (1989) Biosynthesis of terpenoid lipids. In *Microbial Lipids Vol. 2* (ed. C. Ratledge and S.G. Wilkinson), pp. 115-254. Academic Press, London.
- Degens E.T., Guillard R.R.L., Sackett W.M. and Hellebust J.A. (1968) Metabolic fractionation of carbon isotopes in marine plankton-I. Temperature and respiration experiments. *Deep Sea Research* **15**, 1-9.
- Deuser W.G., Degens E.T. and Guillard R.R.L. (1968) Carbon isotope relationships between plankton and sea water. *Geochim. Cosmochim. Acta* **32**, 657-660.
- Eglinton G., Hamilton R.J., Raphael R.A. and Gonzalez A.G. (1962) Hydrocarbon constituents of the wax coatings of plant leaves: a taxonomic survey. *Nature* **193**, 739-742.
- Espitalié J., Maxwell J.R., Chenet Y. and Marquis F. (1988) Aspects of hydrocarbon migration in the Mesozoic in the Paris Basin as deduced from an organic geochemical survey. In *Advances in Organic Geochemistry 1987* (ed. L. Mattavelli and L. Novelli). *Org. Geochem.* **13**, 467-481.
- Farrimond P., Eglinton G., Brassell S.C. and Jenkyns H.C. (1989) Toarcian anoxic event in Europe: an organic geochemical study. *Mar. Petr. Geol.* **6**, 136-147.
- Farrimond P., Stoddart D.P. and Jenkyns H.C. (1994) An organic geochemical profile of the Toarcian anoxic event in northern Italy. *Chem. Geol.* **111**, 17-33.
- Freeman K.H. and Hayes J.M. (1992) Fractionation of carbon isotopes by phytoplankton and estimates of ancient pCO<sub>2</sub> levels. *Global Biogeochem. Cycles* **6**, 185-198.

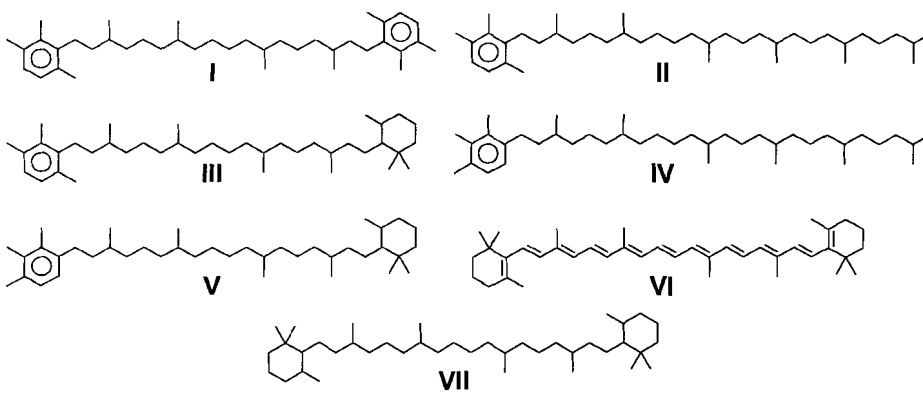
- Freeman K.H., Boreham C.J., Summons R.E. and Hayes J.M. (1994a) The effect of aromatization on the isotopic compositions of hydrocarbons during early diagenesis. *Org. Geochem.* **21**, 1037-1049.
- Freeman K.H., Wakeham S.G. and Hayes J.M. (1994b) Predictive isotopic biogeochemistry: Hydrocarbons from anoxic marine basins. *Org. Geochem.* **21**, 629-644.
- Fry B. and Sherr E.B. (1984)  $\delta^{13}\text{C}$  measurements as indicators of carbon flow in marine and freshwater ecosystems. *Contr. Mar. Sci.* **27**, 13-47.
- Fry B., Jannasch H., Molyneaux S.J., Wirsen C., Muramoto J. and King S. (1991) Stable isotope studies of the carbon, nitrogen, and sulfur cycles in the Black Sea and Cariaco Trench. *Deep-Sea Res.* **38**, Suppl. 2, S1003-1020.
- Gelpi E., Schneider H., Mann J. and Oró J. (1970) Hydrocarbons of geochemical significance in microscopic algae. *Phytochem.* **9**, 603-612.
- Goericke R., Montoya J.P. and Fry B. (1994) Physiology of isotopic fractionation in algae and cyanobacteria. In *Stable Isotopes in Ecology and Environmental Science* (ed. K. Lajtha and R.H. Michener), pp. 187-221. Blackwell Scientific Publications, Oxford.
- Goossens H., de Leeuw J.W., Schenck P.A. and Brassell S.C. (1984) Tocopherols as likely precursors of pristane in ancient sediments and crude oils. *Nature* **312**, 440-442.
- Goyet C., Bradshaw A.L. and Brewer P.G. (1991) The carbonate system in the Black Sea. *Deep-Sea Res.* **38**, Suppl. 2, S1049-1068.
- Grice K., Grossi V., Schouten S., Klein Breteler W., de Leeuw J.W. and Sinninghe Damsté J.S. (1997) The effects of zooplankton herbivory on the molecular structure, distribution and stable carbon isotopic composition of algal markers. In prep.
- Hallam A. (1981) A revised sea-level curve for the Early Jurassic. *J. Geol. Soc. London* **138**, 735-743.
- Hauke V., Graff R., Wehrung P., Trendel J.M. and Albrecht P. (1992a) Novel triterpene-derived hydrocarbons of arborane/fernane series in sediments. Part I. *Tetrahedron* **48**, 3915-3924.
- Hayes J.M., Popp B.N., Takigiku R. and Johnson M.W. (1989) An isotopic study of biogeochemical relationships between carbonates and organic carbon in the Greenhorn Formation. *Geochim. Cosmochim. Acta* **53**, 2961-2972.
- Hayes J.M., Freeman K.H., Popp B.N. and Hoham C.H. (1990) Compound-specific isotopic analyses: A novel tool for reconstruction of ancient biogeochemical processes. In *Advances in Organic Geochemistry 1989* (ed. B. Durand and F. Behar). *Org. Geochem.* **16**, 1115-1128.
- Hollander D.J. and McKenzie J.A. (1991)  $\text{CO}_2$  control on carbon isotope fractionation during aqueous photosynthesis: A paleo- $\text{pCO}_2$  barometer. *Geology* **19**, 929-932.
- Hollander D.J., Bessereau G., Belin S., Huc A.Y. and Houzay J.P. (1991) Organic matter in the Early Toarcian shales, Paris Basin, France: A response to environmental changes. *Rev. Inst. Français du Pétr.* **46**, 543-562.
- Jasper J.P. and Hayes J.M. (1990) A carbon isotope record of  $\text{CO}_2$  levels during the late Quaternary. *Nature* **347**, 462-464.
- Jenkyns H.C. (1985) The Early Toarcian and Cenomanian-Turonian Anoxic Events in Europe: comparisons and contrasts. *Geol. Rundschau* **74**, 505-518.
- Jenkyns H.C. (1988) The Early Toarcian (Jurassic) anoxic event: Stratigraphic, sedimentary, and geochemical evidence. *Am. J. Sci.* **288**, 101-151.
- Jenkyns H.C. and Clayton C.J. (1986) Black shales and carbon isotopes in pelagic sediments from the Tethyan Lower Jurassic. *Sedimentology* **33**, 87-106.
- Jenkyns H.C., Géczy B. and Marshall J.D. (1991) Jurassic manganese carbonates of central Europe and the Early Toarcian anoxic event. *J. Geol.* **99**, 137-149.
- Jenkyns H.C., Sarti M., Masetti D. and Howarth M.K. (1985) Ammonites and stratigraphy of Lower Jurassic black shales and pelagic limestones from the Belluno Trough, Southern Alps, Italy. *Eclogae. geol. Helvetiae* **78**, 299-311.
- van Kaam-Peters H.M.E., Köster J., van der Gaast S.J., Sinninghe Damsté J.S. and de Leeuw J.W. (1997a) The effect of clay minerals on diasterane/sterane ratios. In prep.

- van Kaam-Peters H.M.E., Schouten S., de Leeuw J.W. and Sinninghe Damsté J.S. (1997b) A molecular and carbon isotope biogeochemical study of biomarkers and kerogen pyrolysates of the Kimmeridge Clay Formation: Palaeoenvironmental implications. *Org. Geochem.* Accepted.
- Katz B.J. (1995) The Schistes Carton - the Lower Toarcian of the Paris Basin. In *Petroleum Source Rocks* (ed. B.J. Katz), pp. 89-110. Springer, Berlin.
- Kohnen M.E.L., Sinninghe Damsté J.S., Rijpstra W.I.C. and de Leeuw J.W. (1990) Alkylthiophenes as sensitive indicators of palaeoenvironmental changes: A study of a Cretaceous oil shale from Jordan. In *Geochemistry of Sulfur in Fossil Fuels* (ed. W.L. Orr and C.M. White), *ACS Symposium Series 429*, pp. 444-485. Amer. Chem. Soc., Washington.
- Koopmans M.P., Schouten S., Kohnen M.E.L. and Sinninghe Damsté J.S. (1996) Restricted utility of aryl isoprenoids as indicators for photic zone anoxia. *Geochim. Cosmochim. Acta* **60**, 4873-4876.
- Kroopnick P. (1974) Correlation between  $\delta^{13}\text{C}$  and  $\Sigma\text{CO}_2$  in surface water and atmosphere  $\text{CO}_2$ . *Earth Planet. Sci. Lett.* **22**, 217-240.
- Küspert W. (1982) Environmental changes during oil shale deposition as deduced from stable isotope ratios. In *Cyclic and Event Stratification* (ed. G. Einsele and A. Seilacher), pp. 482-501. Springer, Heidelberg.
- Küspert W. (1983) Faciestypen des Posidonienschiefers (Toarcium, Süddeutschland). Eine isotopengeologische, organisch-chemische und petrographische Studie. PhD thesis, Universität Tübingen, 232 pp.
- Laws E.A., Popp B.N., Bidigare R.R., Kennicutt M.C. and Macko S.A. (1995) Dependence of phytoplankton carbon isotopic composition on growth rate and  $[\text{CO}_2]_{\text{aq}}$ : Theoretical considerations and experimental results. *Geochim. Cosmochim. Acta* **59**, 1131-1138.
- de Leeuw J.W., Rijpstra W.I.C., Schenck P.A. and Volkman J.K. (1983) Free, esterified and residual bound sterols in Black Sea Unit 1 sediments. *Geochim. Cosmochim. Acta* **47**, 455-465.
- Lewan M.D. (1984) Factors controlling the proportionality of vanadium to nickel in crude oils. *Geochim. Cosmochim. Acta* **48**, 2231-2238.
- Lichtfouse E., Albrecht P., Béhar F. and Hayes J.M. (1994) A molecular and isotopic study of the organic matter from the Paris Basin, France. *Geochim. Cosmochim. Acta* **58**, 209-221.
- Loh H., Maul B., Prauss M. and Riegel W. (1986) Primary production, maceral formation and carbonate species in the Posidonia Shale of NW Germany. In *Biogeochemistry of Black Shales* (ed. E.T. Degens, P.A. Meyers and S.C. Brassell). Geol.-Paläont. Inst. Univ. Hamburg Mitt. **60**, 397-421.
- MacKenzie A.S., Patience R.L. and Maxwell J.R. (1980) Molecular parameters of maturation in the Toarcian shales, Paris Basin, France-I. Changes in the configurations of acyclic isoprenoid alkanes, steranes and triterpanes. *Geochim. Cosmochim. Acta* **44**, 1709-1721.
- Mizutani H. and Wada E. (1982) Effects of high atmospheric  $\text{CO}_2$  on  $\delta^{13}\text{C}$  of algae. *Origins of Life* **12**, 377-390.
- Moldowan J.M., Sundararaman P. and Schoell M. (1986) Sensitivity of biomarker properties to depositional environment and/or source input in the Lower Toarcian of SW-Germany. In *Advances in Organic Geochemistry 1985* (ed. D. Leythaeuser and J. Rullkötter). *Org. Geochem.* **10**, 915-926.
- Monson K.D. and Hayes J.M. (1982) Carbon isotopic fractionation in the biosynthesis of bacterial fatty acids. Ozonolysis of unsaturated fatty acids as a means of determining the intramolecular distribution of carbon isotopes. *Geochim. Cosmochim. Acta* **46**, 139-149.
- Mook W.G., Bommerson J.C. and Staverman W.H. (1974) Carbon isotope fractionation between dissolved bicarbonate and gaseous carbon dioxide. *Earth Planet. Sci. Lett.* **22**, 169-176.
- Oschmann W. (1995) The Posidonia Shales (Toarcian, Lower Jurassic) in SW-Germany. *Europal.* **8**, 44-53. Lyon.
- Peters K.E. and Moldowan J.M. (1993) The biomarker guide. Interpreting molecular fossils in petroleum and ancient sediments. Prentice Hall, New Jersey. pp. 363.
- Popp B.N., Takigiku R., Hayes J.M., Louda J.W. and Baker E.W. (1989) The post-Paleozoic chronology and mechanism of  $^{13}\text{C}$  depletion in primary marine organic matter. *Am. J. Sci.* **289**, 436-454.

- Prauss M. and Riegel W. (1989) Evidence from phytoplankton associations for causes of black shale formation in epicontinental seas. *N. Jb. Geol. Paläont. Mh.* **11**, 671-682.
- Prauss M., Ligouis B. and Luterbacher H. (1991) Organic matter and palynomorphs in the 'Posidonienschiefer' (Toarcian, Lower Jurassic) of southern Germany. In *Modern and Ancient Continental Shelf Anoxia* (ed. Tyson R.V. and Pearson T.H.), Geol. Soc. Lond. Spec. Publ. **58**, 335-351.
- Radke M. and Willsch H. (1991) Occurrence and thermal evolution of methylated benzo- and dibenzothiophenes in petroleum source rocks of western Germany. In *Organic Geochemistry: Advances and applications in energy and the natural environment* (ed. D.A.C. Manning), pp. 480-484. Manchester University Press.
- Radke M. and Willsch H. (1994) Extractable alkyldibenzothiophenes in Posidonia shale (Toarcian) source rocks: Relationship of yields to petroleum formation and expulsion. *Geochim. Cosmochim. Acta* **58**, 5223-5244.
- Rau G.H., Takahashi T. and Des Marais (1989) Latitudinal variation in plankton  $\delta^{13}\text{C}$ : Implications for  $\text{CO}_2$  and productivity in past oceans. *Nature* **341**, 516-518.
- Rau G.H., Takahashi T., Des Marais, Repeta D.J. and Martin J.H. (1992) The relationship between  $\delta^{13}\text{C}$  of organic matter and  $[\text{CO}_2]_{\text{aq}}$  in ocean surface water: Data from JGOFS site in the northeast Atlantic Ocean and a model. *Geochim. Cosmochim. Acta* **56**, 1413-1419.
- Raven J.A. and Johnston A.M. (1994) Algal DIC pumps and atmospheric  $\text{CO}_2$ . In *Regulation of Atmospheric  $\text{CO}_2$  and  $\text{O}_2$  by Photosynthetic Carbon Metabolism* (ed. N.E. Tolbert and J. Preiss), pp. 184-198. Oxford Univ. Press.
- Repeta D.J. (1993) A high resolution historical record of Holocene anoxygenic primary production in the Black Sea. *Geochim. Cosmochim. Acta* **57**, 4337-4342.
- Rohmer M., Knani M., Simonin P., Sutter B. and Sahn H. (1993) Isoprenoid biosynthesis in bacteria: A novel pathway for the early steps leading to isopentenyl diphosphate. *Biochem. J.* **295**, 517-524.
- Rohmer M., Seemann M., Horbach S., Bringer-Meyer S. and Sahn H. (1996) Glyceraldehyde 3-phosphate and pyruvate as precursors of isoprenic units in an alternative non-mevalonate pathway for terpenoid biosynthesis. *J. Am. Chem. Soc.* **118**, 2564-2566.
- Saiz-Jimenez C. and de Leeuw J.W. (1984) Pyrolysis-gas chromatography-mass spectrometry of isolated, synthetic and degraded lignins. In *Advances in Organic Geochemistry 1983* (ed. P.A. Schenck, J.W. de Leeuw and G.W.M. Lijmbach). *Org. Geochem.* **6**, 417-422.
- Saiz-Jimenez C. and de Leeuw J.W. (1986) Lignin pyrolysis products: Their structures and their significance as biomarkers. In *Advances in Organic Geochemistry 1985* (ed. D. Leythaeuser and J. Rullkötter). *Org. Geochem.* **10**, 869-876.
- Schaeffer P., Adam P., Wehrung P., Bernasconi S. and Albrecht P. (1997) Molecular and isotopic investigation of free and S-bound lipids from an actual meromictic lake (lake Cadagno, Switzerland). *Org. Geochem.* Submitted.
- Schlanger S.O., Arthur M.A., Jenkyns H.C. and Scholle P.A. (1987) The Cenomanian-Turonian Oceanic Anoxic Event, I. Stratigraphy and distribution of organic carbon-rich beds and the marine  $\delta^{13}\text{C}$  excursion. In *Marine Petroleum Source Rocks* (ed. J. Brooks and A.J. Fleet). *Geol. Soc. London Spec. Publ.* **26**, 373-402.
- Schwender J., Seemann M., Lichtenthaler H.K. and Rohmer M. (1996) Biosynthesis of isoprenoids (carotenoids, sterols, prenyl side-chains of chlorophylls and plastoquinone) via a novel pyruvate/glyceraldehyde 3-phosphate non-mevalonate pathway in the green alga *Scenedesmus obliquus*. *Biochem. J.* **316**, 73-80.
- Sinninghe Damsté J.S., Wakeham S.G., Kohlen M.E.L., Hayes J.M. and de Leeuw J.W. (1993) A 6,000-year sedimentary molecular record of chemocline excursions in the Black Sea. *Nature* **362**, 827-829.
- Spero H., Lerche I. and Williams D.F. (1991) Opening the carbon isotope "vital effect" black box, 2. Quantitative model for interpreting foraminiferal carbon isotope data. *Paleoceanography* **6**, 639-655.
- Summons R.E. and Powell T.G. (1987) Identification of aryl isoprenoids in source rocks and crude oils: Biological markers for the green sulphur bacteria. *Geochim. Cosmochim. Acta* **51**, 557-566.

- Summons R.E., Volkman J.K. and Boreham C.J. (1987) Dinosterane and other steroidal hydrocarbons of dinoflagellate origin in sediments and petroleum. *Geochim. Cosmochim. Acta* **51**, 3075-3082.
- Summons R.E., Thomas J., Maxwell J.R. and Boreham C.J. (1992) Secular and environmental constraints on the occurrence of dinosterane in sediments. *Geochim. Cosmochim. Acta* **56**, 2437-2444.
- Tissot B., Califet-Debyser Y., Deroo G. and Oudin J.L. (1971) Origin and evolution of hydrocarbons in early Toarcian shales. *Am. Assoc. Pet. Geol. Bull.* **55**, 2177-2193.
- Volkman J.K. (1986) A review of sterol markers for marine and terrigenous organic matter. *Org. Geochem.* **9**, 83-99.
- Volkman J.K. and Maxwell J.R. (1986) Acyclic isoprenoids as biological markers. In *Biological Markers in the Sedimentary Record* (ed. R.B. Johns), pp. 1-42. Elsevier, New York.
- Yang C., Telmer K. and Veizer J. (1996) Chemical dynamics of the "St. Lawrence" riverine system:  $\delta D_{H_2O}$ ,  $\delta^{18}O_{H_2O}$ ,  $\delta^{13}C_{DIC}$ ,  $\delta^{34}S_{sulfate}$ , and dissolved  $^{87}Sr/^{86}Sr$ . *Geochim. Cosmochim. Acta* **60**, 851-866.

## Appendix





## Chapter 7

### Occurrence of two novel benzothiophene hopanoid families in sediments.

#### Abstract

Two novel families of C<sub>34</sub>-C<sub>35</sub> benzothiophene hopanoids have been identified in laminated marlstones and limestones of Hauptdolomit (Germany, Upper Triassic), Calcaires en Plaquettes (France, Upper Jurassic) and Ghareb (Jordan, Upper Cretaceous) Formations. Structures were assigned on the basis of Raney nickel desulfurisation, deuteriated nickel boride desulfurisation, mass spectral data and GC behaviour. Based on quantitative analysis a precursor-product relationship between thiophene hopanoids and benzothiophene hopanoids seems likely. This means that the novel hopanoids are not formed by sulfur incorporation into benzohopanes, but instead cyclisation and aromatisation of the hopanoid side chain occur after sulfur incorporation.

#### Introduction

C<sub>30+</sub> hopanoid biomarkers are widespread in the geosphere. During diagenesis the precursor bacteriohopanepolyol derivatives (Rohmer et al., 1993) are subjected to different chemical reactions leading to a myriad of structures. For example, thiophene hopanoids (**I**, see Appendix), products of early diagenetic sulfur incorporation, have been reported by Valisolalao et al. (1984) and Sinninghe Damsté et al. (1989). Benzohopanes (**II**) are probably formed by side chain cyclisation and aromatisation (Hussler et al., 1984). Recently, it has become clear that side chain cyclisation and aromatisation of extended hopanoids can also give rise to a second series of benzohopanes with the aromatic ring condensed to the D- and E-ring (**III**) (Schaeffer et al., 1995). Here we report on two novel families of benzothiophene hopanoids (**IV,V**) which are diagenetically formed by both sulfur incorporation and aromatisation reactions.

#### Experimental

*Sample descriptions.* Laminated marlstones (TOC = 23.6%) and carbonates (TOC = 0.3%) of the Hauptdolomit Formation are from Norian (Upper Triassic) strata in the Northern Calcareous Alps. These sediments were deposited in restricted, subtidal areas of extended carbonate platforms surrounding the Tethys ocean (Köster et al., 1988). Samples were taken from outcrops near a former oil shale mine in the Isar valley (Schröfel, Bavaria/Germany).

Bituminous coccolithic limestones (TOC = 6.2%) of the Kimmeridgian (Upper Jurassic) Calcaires en Plaquettes Formation were taken from a quarry near the village of Orbagnoux (French Southern Jura, 50 km southwest of Geneva). These parallel laminites are found in a sedimentary sequence together with undulating laminites, massive limestones and

laminated limestones, all deposited in a lagoonal environment (Tribovillard et al., 1992; Bernier, 1984).

The organic-rich marlstones (TOC = 17.9%) of the Upper Cretaceous Ghareb Formation are from the El Lajjun deposit in Central Jordan. This near surface (i.e. exploitable by open-cast mining) deposit is located 100 km south of Amman. Sedimentation of the Ghareb oil shales took place in a number of restricted small basins on the edge of the Tethys ocean. Further geological background information on the El Lajjun deposit and other Ghareb oil shale deposits is given by Hufnagel (1984).

*Extraction and fractionation.* The powdered samples (ca. 100 g) were Soxhlet extracted with methanol (MeOH)/dichloromethane (DCM) (1:7.5, v/v) for 24 h. Asphaltenes were removed from the extracts by precipitation in *n*-heptane. Aliquots of the maltene fractions (ca. 250 mg), to which a mixture of four standards was added for quantitative analysis (Kohnen et al., 1990), were separated into two fractions using a column (25 cm x 2 cm; column volume 35 ml) packed with alumina (activated for 2.5 h at 150°C) by elution with hexane/DCM (9:1, v/v; 150 ml; "apolar fraction") and DCM/MeOH (1:1, v/v; 150 ml; "polar fraction"). Aliquots (ca. 10 mg) of the apolar fractions were further separated by argentation TLC (thin layer chromatography) using hexane as developer. The AgNO<sub>3</sub>-impregnated silica plates (20 x 20 cm; thickness 0.25 mm) were prepared by dipping them in a solution of 1% AgNO<sub>3</sub> in MeOH/H<sub>2</sub>O (4:1, v/v) for 45 s and subsequent activation at 120°C for 1 h. Four fractions (A1, R<sub>f</sub> = 0.85-1.00; A2, R<sub>f</sub> = 0.35-0.85; A3, R<sub>f</sub> = 0.06-0.35; A4, R<sub>f</sub> = 0-0.06) were scraped off the TLC plate and ultrasonically extracted with ethyl acetate (x3).

*Raney nickel desulfurisation.* The A3 fraction was dissolved in 4 ml ethanol together with 0.5 ml of a suspension of Raney nickel (0.5 g/ml ethanol) and refluxed under a nitrogen stream for 1.5 h. The desulfurisation products were isolated by centrifugation and subsequent extraction with DCM (x4). The combined extracts were washed (x3) against NaCl-saturated, double-distilled H<sub>2</sub>O, dried with MgSO<sub>4</sub> and evaporated to dryness. The extract was taken up into a small volume of ethyl acetate (2 mg extract/ml) to be analysed by GC and GC-MS.

*Desulfurisation using deuteriated nickel boride.* The A3 fraction was dissolved in 4 ml of a dry MeOD/tetrahydrofuran mixture (1:1, v/v). Subsequently, 100 mg of anhydrous NiCl<sub>2</sub> was added under a nitrogen stream. The solution was stirred and 100 mg NaBD<sub>4</sub> was added slowly. The reaction mixture was refluxed under a stream of nitrogen for 1 h. The desulfurisation products were isolated by centrifugation and subsequent extraction (x3) with a DCM/MeOH mixture (1:1, v/v). The combined extracts were then treated as above.

*Gas chromatography.* Gas chromatography (GC) was performed using a Carlo Erba 5300 or a Hewlett-Packard 5890 instrument, both equipped with an on-column injector. A fused silica capillary column (25 m x 0.32 mm) coated with CP Sil-5 (film thickness 0.12 µm) was used with helium as carrier gas. Compounds analysed on the Carlo Erba 5300 were detected by a flame ionisation detector (FID). Compounds analysed on the Hewlett-Packard 5890 were detected by both a flame ionisation detector (FID) and a sulfur-selective flame

photometric detector (FPD), applying a stream-splitter with a split ratio of FID:FPD = ca. 1:2. The samples were injected at 70°C and the oven was programmed to 130°C at 20°C/min and then at 4°C/min to 320°C, at which it was held for 15 min.

*Gas chromatography-mass spectrometry.* Gas chromatography-mass spectrometry (GC-MS) was carried out on a Hewlett-Packard 5890 gas chromatograph interfaced to a VG Autospec Ultima mass spectrometer operated at 70 eV with a mass range  $m/z$  50-800 and a cycle time of 1.8 s (resolution 1000). The gas chromatograph was equipped with a fused silica capillary column (25 m x 0.32 mm) coated with CP Sil-5 (film thickness 0.12  $\mu\text{m}$ ). Helium was used as carrier gas. The samples were injected at 60°C and the oven was programmed to 130°C at 20°C/min and then at 4°C/min to 320°C, at which it was held for 15 min.

*Quantification.* Benzohopanes **II** and thiophene hopanoids were quantified by integration of their peaks in the FID-trace and comparison with the internal standard. The most abundant members of the benzothiophene hopanoids and benzohopanes **III** were quantified in the same way. Remaining members of these series were quantified by integration of  $M^+$  and  $M^+-15$  mass chromatograms and comparison with the earlier established concentrations of the most abundant members, assuming that the relative contributions of these ions to the total ion current do not change significantly from one member to another.

## Results

GC and GC-MS analyses of diaromatic (A3) fractions of a marlstone and carbonate of the Hauptdolomit Formation, a marlstone of the Ghareb Formation and a coccolithic limestone of the Calcaires en Plaquettes Formation (CPF) revealed a number of novel compounds eluting at the end of the gas chromatograms (e.g. Fig. 7.1). The response on the sulfur-selective FPD indicated that they probably contain one sulfur atom, in accordance with the mass deficiency of the molecular ions and the  $M^+$ ,  $M^++1$  and  $M^++2$  distributions in their mass spectra. In the Ghareb marlstone only one of the novel compounds, characterised by the mass spectrum shown in Fig. 7.2c, was present. Upon Raney nickel desulfurisation this component disappeared and an equal amount of the  $C_{35}$  benzohopane **II** emerged. The benzohopane was identified by comparison of its mass spectrum with that published (Hussler et al., 1984). Since benzohopanes were absent in the original A3 fraction this established the benzohopane carbon skeleton of type **II** for the novel compound. Besides this compound, the coccolithic limestone of the CPF and the marlstone of the Hauptdolomit Formation contained a novel family of compounds characterised by the mass spectra shown in Figs. 7.3b,c. Raney nickel desulfurisation transformed them into the  $C_{34}$ - $C_{35}$  benzohopanes **III** recently identified by Schaeffer et al. (1995). Finally, the A3 fraction of the Hauptdolomit carbonate was desulfurised using deuteriated nickel boride (Schouten et al., 1993). This A3 fraction contained two members of each novel hopanoid family (for mass spectra see Figs. 7.2b,c and 7.3b,c), and also series of benzohopanes **II** and **III** (Fig. 7.1). These latter components usually end up in the A2 fraction. After desulfurisation the novel compounds had largely disappeared and the  $C_{35}$  and  $C_{34}$  members of benzohopanes **II** and **III**, respectively, had significantly increased (Fig. 7.1), which could be accounted for by the

decrease in concentration of the novel compounds. These desulfurisation experiments established the benzohopane carbon skeleton of type **II** for compounds with the mass spectra shown in Figs. 7.2b,c, and the benzohopane carbon skeleton of type **III** for compounds with the mass spectra shown in Figs. 7.3b,c.

The molecular ions at  $m/z$  488 and 502 in the mass spectra of the novel components indicate molecular formulae of  $C_{34}H_{48}S$  and  $C_{35}H_{50}S$ . This suggests the presence of a thiophene moiety condensed to the aromatic ring of both benzohopane isomers. Indeed, the mass spectra show a similarity with those of benzohopanenes **II** and **III** (Figs. 7.2a, 7.3a). Major fragments in the spectra of the novel hopanoids have shifted an equal number of mass

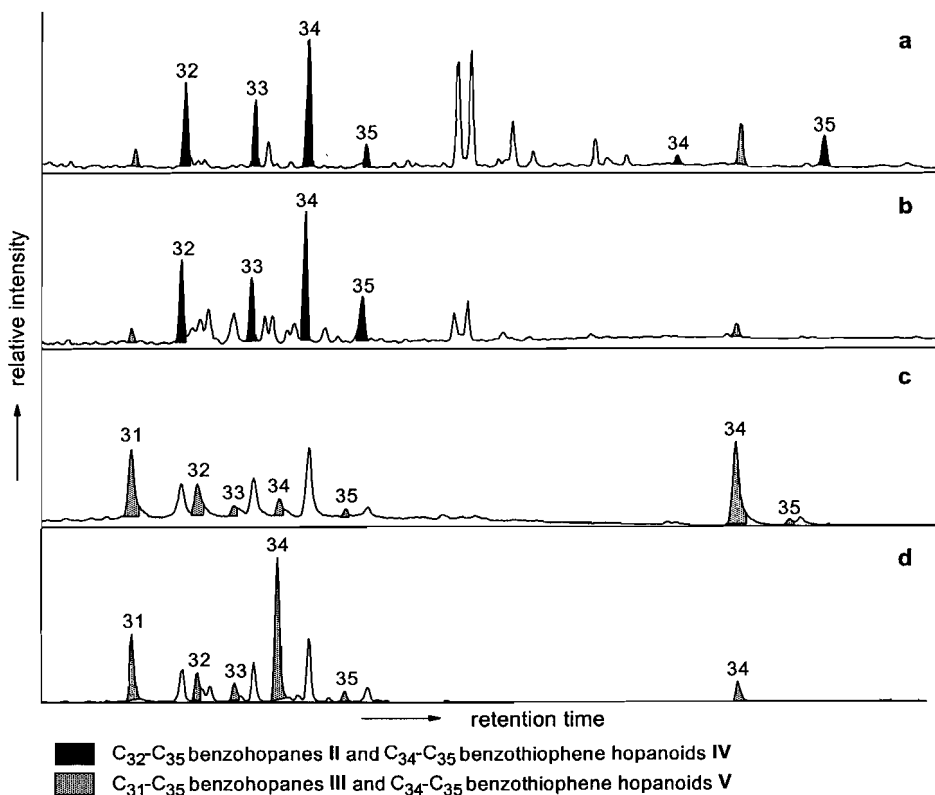


**Fig. 7.1.** Distributions of benzohopanenes and benzothiophene hopanoids in the A3 fraction of the Hauptdolomit carbonate before and after desulfurisation. FID trace (a) before and (b) after deuterated nickel boride desulfurisation. Summed mass chromatogram of  $m/z$  403 + 417 + 431 + 445 + 448 + 449 + 459 + 462 + 463 + 473 + 487 ( $M^+ - 15$  fragments of benzohopanenes **III** and benzothiophene hopanoids **V**) (c) before and (d) after deuterated nickel boride desulfurisation. Note that  $M^+ - 15$  fragments of benzohopanenes with only one or two deuterium atoms are not shown, because they coincide with  $M^+$  and  $M^+ + 1$  fragments of the more abundant benzohopanenes **II** and benzothiophene hopanoids **IV**.

units compared to the major fragments in the spectra of the resultant benzohopanes (see Hussler et al., 1984; Schaeffer et al., 1995) due to the presence of the thiophene group. The incorporated sulfur atom, thus, has little effect on the fragmentation pathway. Differences between the spectra of the benzohopanes and the novel hopanoids, besides the consistent shift of the major fragments, largely concern the relative intensities of the fragments. The spectra of the benzothiophene hopanoids are dominated by their molecular ions, whereas benzohopanes **II** and **III** have a base peak at  $m/z$  191 and  $M^+-15$  respectively, this latter probably mainly due to loss of the methyl group at position 18.

For every benzohopane skeleton two different benzothiophene hopanoid isomers (**IV-VII**) can be envisaged. Dreiding molecular models indicate that structures **VI** and **VII** experience far more steric stress than **IV** and **V**. Structure **VI** can probably be excluded as a possible isomer because of high ring stress. Mass spectral data, however, provide sufficient evidence to assign **IV** and **V** as the actual structures of the novel hopanoids. Their mass spectra are perfectly explained by these isomers (Figs. 7.2, 7.3), whereas for isomers **VI** and **VII** different fragmentations are expected. In case of isomer **VIIb** the  $M^+-15$  fragment is expected to be a major peak in its mass spectrum, because at both sides of the thiophene moiety,  $\beta$  cleavage will lead to loss of a methyl group, especially at position 18. Clearly the spectrum shown in Fig. 7.2c does not fit this feature. Isomers **VIIb,c** are rejected because they can not possibly account for the high intensity of the  $m/z$  228 and 242 peak (Figs. 7.3b,c). In addition,  $\beta$  cleavage at both sides of the thiophene moiety, especially at position 14, is expected to yield a  $M^+-15$  fragment that surpasses the molecular ion in intensity. This is clearly not the case (Figs. 7.3b,c).

Additional evidence for the structural positions of the sulfur atoms in the novel hopanoids was obtained from the mass spectra of the deuterated benzohopanes (Fig. 7.4) released by deuteriated nickel boride desulfurisation. Each of the released benzohopanes had incorporated four deuterium atoms. Because of coelution with the free benzohopanes, it was not possible to get pure spectra of the deuterated benzohopanes; it is, however, clear that the deuterium atoms are not located at the carbon atoms of the A-, B- or C-ring or their methyl substituents, nor at C-15 and C-16 of the type **II** compound. That is the fragments created by cleaving the D-ring and representing the E-ring plus adjoining atoms had gained four mass units, whereas, for example, mass fragment 191 did not shift (Fig. 7.4). This confirms the presence of a thiophene moiety condensed to the aromatic ring. Since the mass spectra of benzohopanes possessing less than 34 carbon atoms, and without any sulfur bearing equivalents, had not changed after the experiment, it is certain that in the procedure used hydrogen atoms of the aromatic ring do not exchange with deuterium.

The  $C_{36}$  ring A methylated benzothiophene hopanoid **VIII**, which elutes after the  $C_{35}$  benzothiophene hopanoid **IVb**, was tentatively identified in two of the samples. Its mass spectrum is nearly identical to that of **IVb**, except that it has a molecular ion at  $m/z$  516 instead of  $m/z$  502 and a major fragment at  $m/z$  205 instead of  $m/z$  191. Because on most columns  $2\beta$  methylated hopanoids elute close to their non-methylated analogues and  $3\beta$  methylated hopanoids have longer retention times (Rohmer et al., 1993, and references therein), the  $C_{36}$  ring A methylated benzothiophene hopanoid probably has a  $3\beta$  methyl substituent.

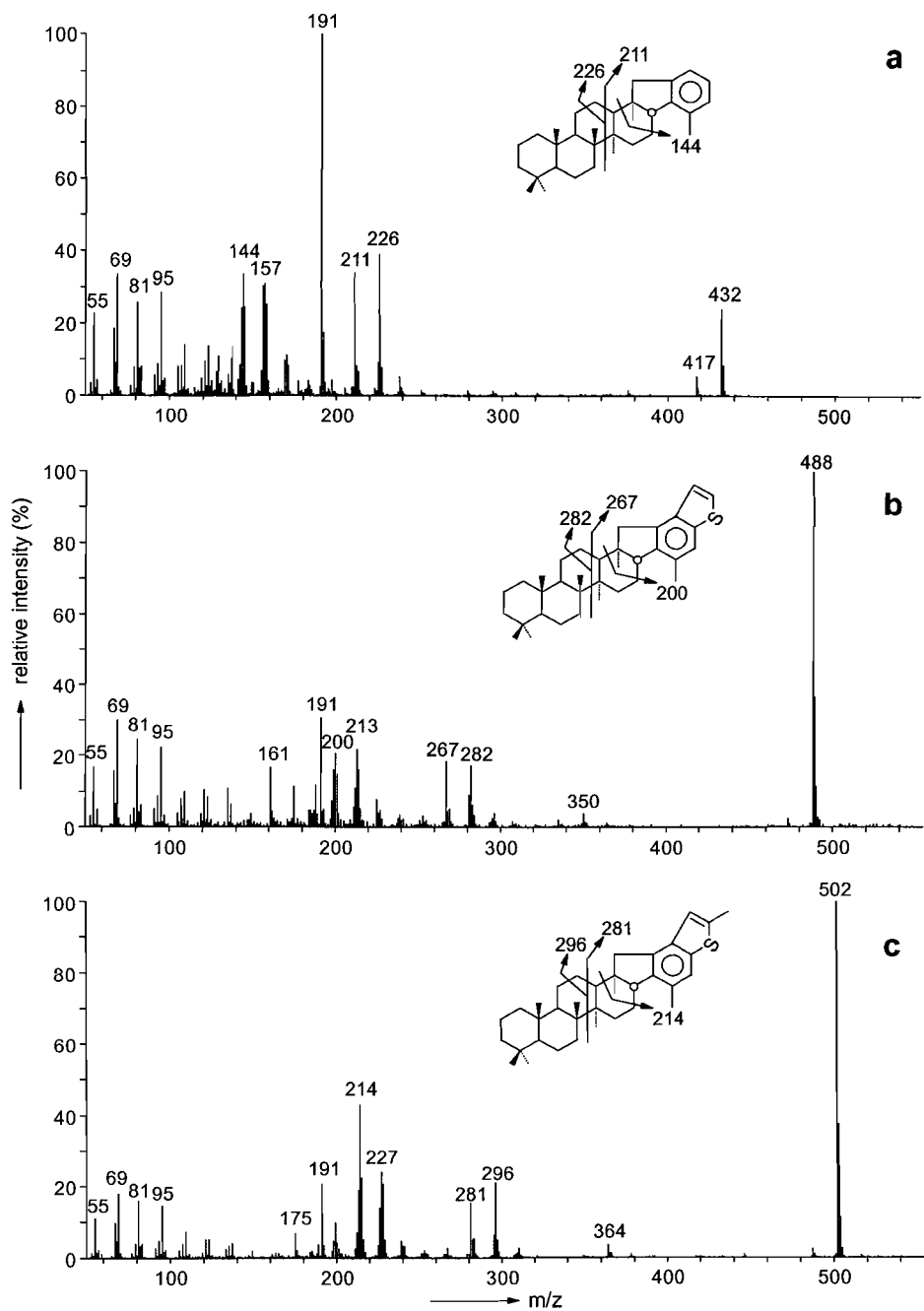


**Fig. 7.2.** Mass spectra of (a)  $C_{32}$  member of benzohopanes **II**, (b)  $C_{34}$  benzothiophene hopanoid **IVa**, (c)  $C_{35}$  benzothiophene hopanoid **IVb**.

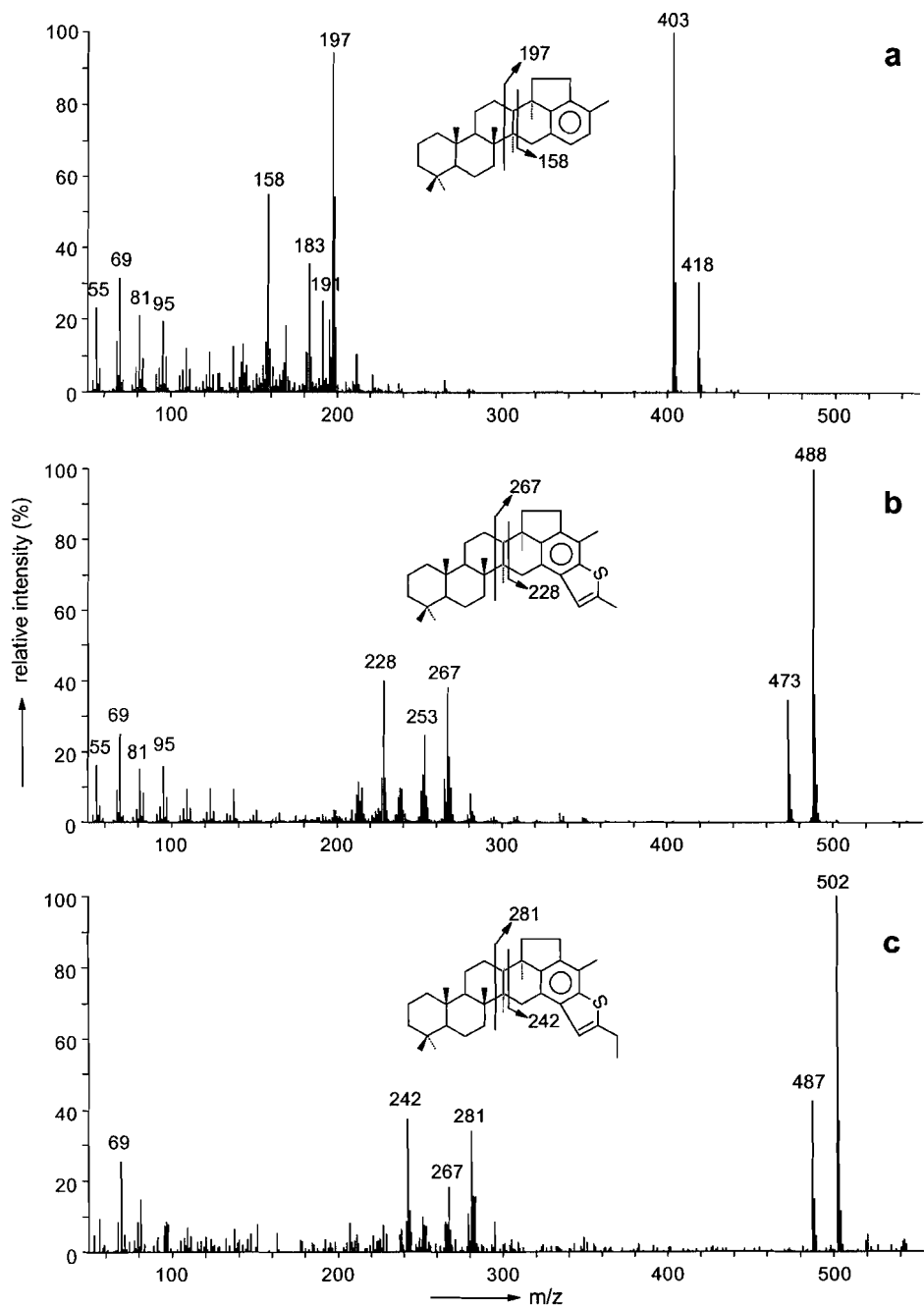


**Fig. 7.3.** Mass spectra of (a) C<sub>31</sub> member of benzohopanes **III**, (b) C<sub>34</sub> benzothiophene hopanoid **Vb** (c) C<sub>35</sub> benzothiophene hopanoid **Vc**.

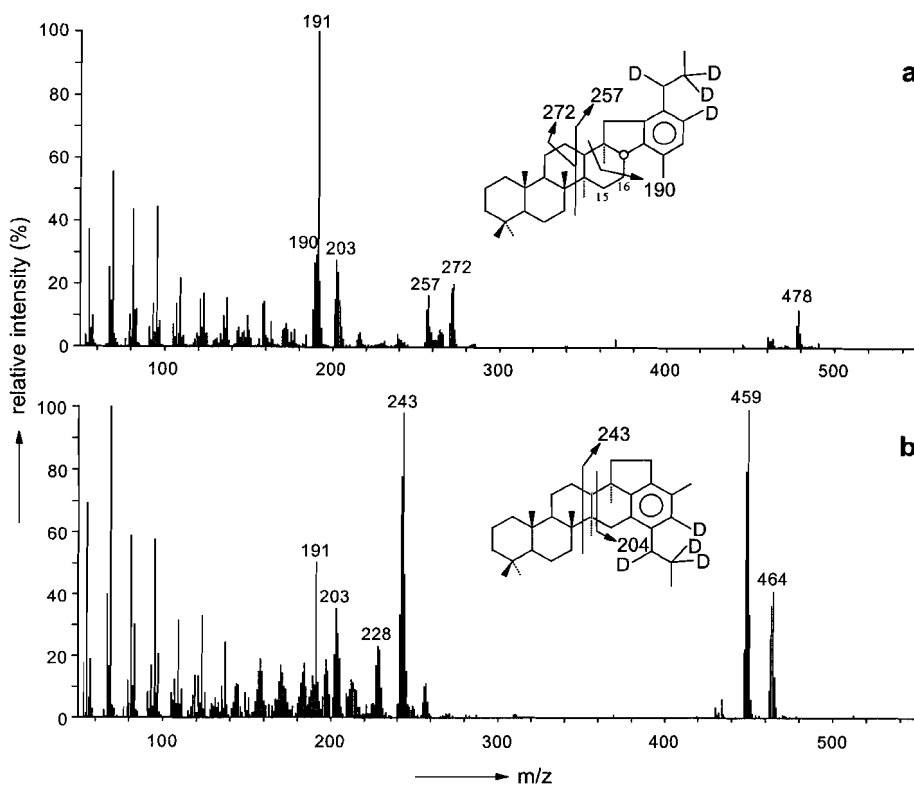


**Fig. 7.4.** Mass spectra of deuterated benzohopanes obtained after desulfurisation of novel benzothiophene hopanoids. (a) Deuterated  $C_{35}$  member of benzohopanes **II**. (b) Deuterated  $C_{34}$  member of benzohopanes **III**. Spectra were taken at one or two scans before peak maxima in order to reduce the signal of the coeluting non-deuterated benzohopanes.

## Discussion

The formation of benzothiophene hopanoids is structurally limited to the higher members of the homohopane series. At least 34 carbon atoms are required to form a benzothiophene hopanoid of type **IV**, and at least 33 to form the type **V** compounds. There are two pathways by which the benzothiophene hopanoids can be formed (Fig. 7.5). Either sulfur is incorporated into benzohopanes, or sulfur is incorporated prior to cyclisation and aromatisation of the hopanoid side chain. Because of the fixed position of a thiophene moiety in the side chain, subsequent cyclisation and aromatisation of the side chain can only lead to compounds **IVa,b** in the case of thiophene hopanoids **Ib,c**, and to compounds **Va-c** in the case of thiophene hopanoids **Id-f** (Fig. 7.5). For the same reason the  $C_{36}$  ring A methylated thiophene hopanoid **IX** can only give rise to benzothiophene hopanoid **VIII**.

In order to determine how the benzothiophene hopanoids were formed, their distributions were compared with those of the benzohopanes and thiophene hopanoids



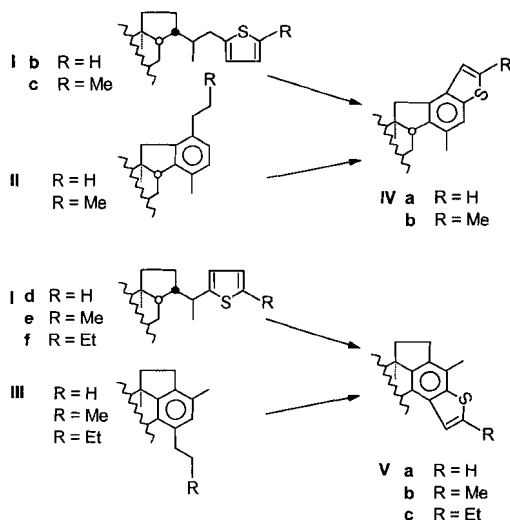


**Fig. 7.5.** Hypothetical precursor-product relationships in the formation of benzothiophene hopanoids.

within the same sample (Fig. 7.6). Distributions of  $C_{34}$ - $C_{35}$  benzohopanes of both types differ significantly from those of the corresponding benzothiophene hopanoids. On the other hand, the distributions of thiophene hopanoids resemble those of the benzothiophene hopanoids, suggesting a precursor-product relationship. The concentrations of benzothiophene hopanoids are substantially lower than those of the thiophene hopanoids, which may explain the apparent absence of benzothiophene hopanoids derived from some of the least abundant thiophene hopanoids. These data seem to indicate that the benzothiophene hopanoids are formed subsequent to or perhaps simultaneously with the process of sulfur incorporation.

Desulfurisation of the asphaltenes and polar fractions of the samples studied did not yield any benzohopane. This is also an indication that the benzothiophene hopanoids are not formed by sulfur incorporation into benzohopanes, otherwise there would be no reason why the benzohopanes are not incorporated via sulfur linkages into macromolecules. Finally, we favour a mechanism of sulfur incorporation prior to cyclisation and aromatisation, because sulfur incorporation is known to occur shortly after sediment deposition (e.g. Wakeham et al., 1995), whereas aromatisation usually takes place at a later stage of diagenesis.

The Hauptdolomit carbonate displays a hopanoid distribution somewhat different from the other samples (Fig. 7.6) i.e. most of its series are dominated by the  $C_{34}$  member, and the  $C_{34}$  benzothiophene hopanoid **IVa** is relatively abundant, but its presumed precursor, the  $C_{34}$  thiophene hopanoid **Ib**, was not identified. At present we cannot offer an explanation for this.

In the Jurf ed Darawish oil shales benzohopanes **II** can be detected, provided that at least some of the free hopanes have isomerised to the  $17\alpha,21\beta(H)$  configuration (Sinninghe Damsté et al., 1995). Therefore, these benzohopanes probably originated from  $17\alpha,21\beta(H)$  hopanes only. By analogy, benzothiophene hopanoids **IV** probably only derive from

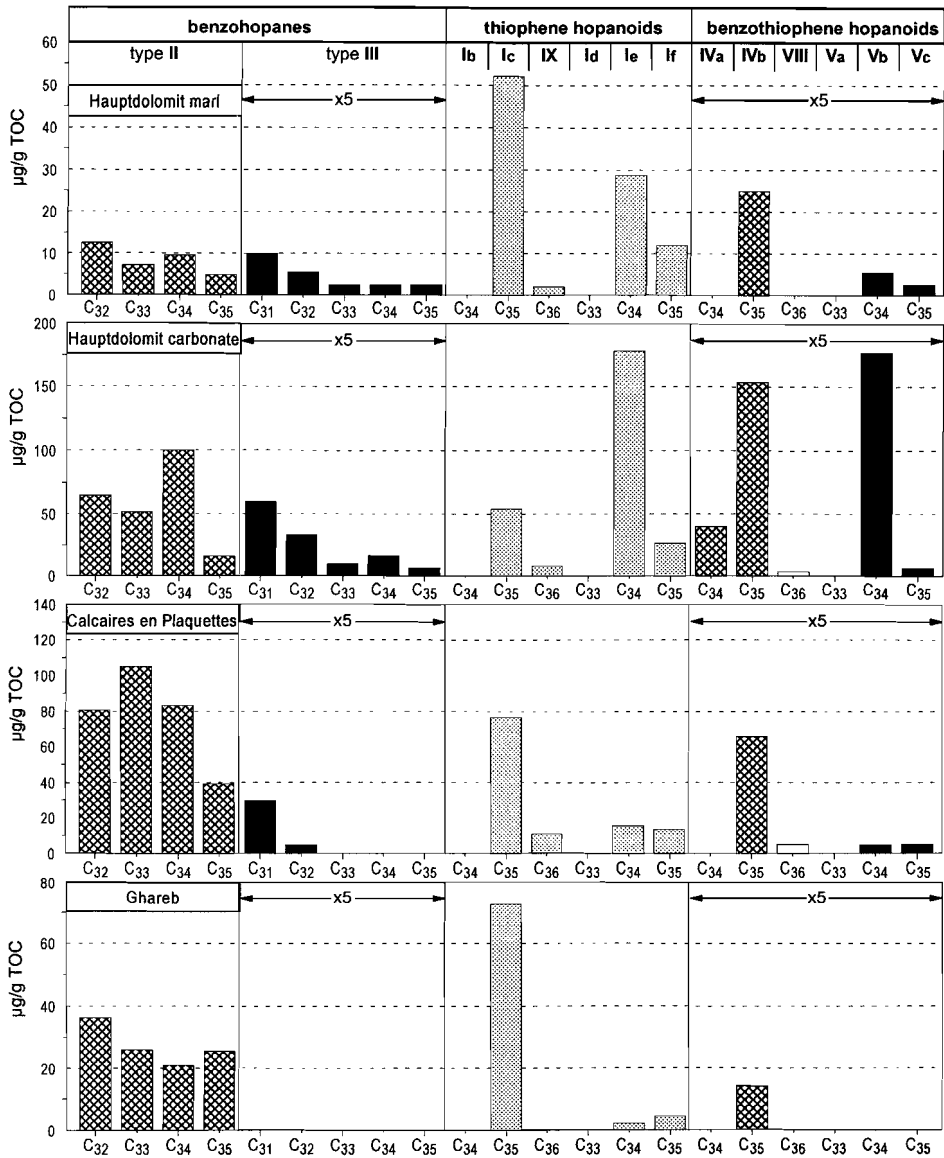


**Fig. 7.6.** The concentrations of benzohopanes, thiophene hopanoids and benzothiophene hopanoids in the four investigated samples.

$17\alpha,21\beta(H)$  thiophene hopanoids. In the four samples investigated the  $17\beta,21\alpha(H)$  and  $17\beta,21\beta(H)$  thiophene hopanoids are absent or minor compared to the  $17\alpha,21\beta(H)$  isomers.

Benzothiophene hopanoids have so far been identified in laminated marlstones and carbonates of the Hauptdolomit Formation (Upper Triassic, Northern Calcareous Alps), coccolithic limestones of the Calcaires en Plaquettes Formation (Upper Jurassic, France) and

El Lajjun oil shales of the Ghareb Formation (Upper Cretaceous, Jordan). The Jurf ed Darawish oil shales, studied by Kohnen et al. (1990), likewise the El Lajjun sediments belong to the Ghareb Formation. Therefore, these Jurf ed Darawish samples were re-examined for hopanoid biomarkers. It appeared that benzothiophene hopanoids were absent, and that thiophene hopanoids were different from those in the other samples. In the carbonate-rich facies of the Jurf ed Darawish sediments  $17\beta,21\beta(\text{H})$  thiophene hopanoids are highly dominant over their  $17\alpha,21\beta(\text{H})$  counterparts. Since benzothiophene hopanoids are thought to derive from  $17\alpha,21\beta(\text{H})$  thiophene hopanoids only, their absence here can be understood. In the more argillaceous facies, and in the phosphorite,  $17\alpha,21\beta(\text{H})$  thiophene hopanoids are more pronounced, but they are dominated by the  $\text{C}_{35}$  member with a terminal thiophene ring (**Ia**), which is not a potential precursor of the novel benzothiophene hopanoids. Nevertheless, thiophene hopanoid **Ic** is present and its presumed derivative **IVb** is not. This is possibly due to a lower maturity of the Jurf ed Darawish sediments as compared to the other samples. Alternatively, if thiophene hopanoids and benzothiophene hopanoids are simultaneously formed and not related to differences in maturity, the presence of **Ic** and the absence of **IVb** may be indicative of a precursor bacteriohopanepolyol derivative possessing such functionalities that enable the formation of a thiophene ring but have no potential to form a benzothiophene group. For example, dehydration of bacteriohopanepentol **Xa** (Rohmer et al., 1993) may yield a derivative containing one or more double bonds in the side chain plus a double bond at C-22(29) which, through isomerisation *via* tertiary carbon atoms, can move into the D- or E-ring. Such a derivative may be a precursor of predominantly benzothiophene hopanoids. On the contrary, dehydration of bacteriohopanetetrol **Xb** (Rohmer et al., 1993) will yield a derivative containing unsaturations only in the side chain, since isomerisation of the double bonds cannot proceed *via* C-31. Such a derivative may form thiophene hopanoids, whereas the formation of benzothiophene hopanoids may not be possible.

## Conclusions

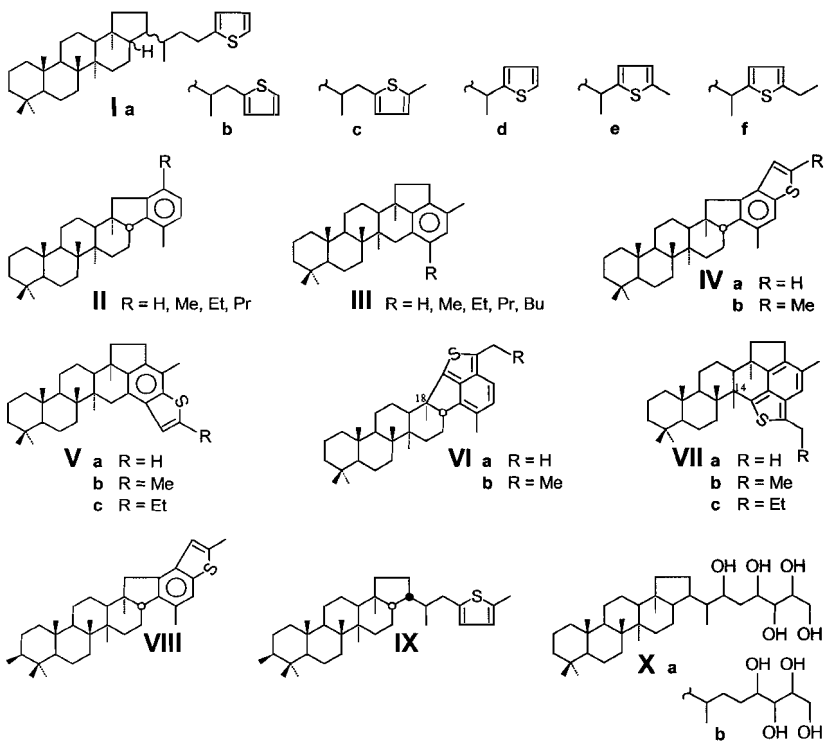
Two novel families of  $\text{C}_{34}$ - $\text{C}_{35}$  benzothiophene hopanoids have been tentatively identified in several laminated marlstones and limestones. These compounds are probably formed by side chain cyclisation and aromatisation of  $\text{C}_{34}$ - $\text{C}_{35}$  thiophene hopanoids. Apart from the availability of reduced inorganic sulfur species, a certain level of maturity may be required to form the novel hopanoids from their precursor bacteriohopanepolyol derivatives. However, if sulfur incorporation, cyclisation and aromatisation take place simultaneously, both thiophene hopanoids and benzothiophene hopanoids can be formed soon after organic matter deposition. In that case, the presence of benzothiophene hopanoids in sediments may be indicative of specific precursor bacteriohopanepolyol derivatives.

**Acknowledgements.** We thank the Netherlands Organization for Scientific Research (NWO) for the PIONIER grant to JSSD and the studentship of HMEvKP. We acknowledge W.I.C. Rijpstra, W. Pool and M. Dekker for analytical assistance. Dr. M.E.L. Kohnen (Koninklijke/Shell Exploratie en Productie Laboratorium) kindly provided the Orbagnoux sample. M.P. Koopmans and Dr. M.D. Lewan are thanked for data of the Ghareb sample.

## References

- Bernier P. (1984) Les formations carbonatées du Kimméridgien et du Portlandien dans le Jura méridional. Stratigraphie, micropaléontologie, sédimentologie. *Docum. Lab. Géol. Lyon* **92**, 803 pp.
- Hufnagel H. (1984) Die Ölschiefer Jordaniens. *Geol. Jb., Rh A* **75**, 295-311.
- Hussler G., Connan J. and Albrecht P. (1984) Novel families of tetra- and hexacyclic aromatic hopanoids predominant in carbonate rocks and crude oils. *Org. Geochem.* **6**, 39-49.
- Kohnen M.E.L., Sinninghe Damsté J.S., Rijpstra W.I.C. and de Leeuw J.W. (1990) Alkylthiophenes as sensitive indicators of palaeoenvironmental changes: A study of a Cretaceous oil shale from Jordan. In *Geochemistry of Sulfur in Fossil Fuels* (ed. W.L. Orr and C.M. White), *ACS Symposium Series 429*, pp. 444-485. Amer. Chem. Soc., Washington.
- Köster J., Wehner H. and Hufnagel H. (1988) Organic geochemistry and organic petrology of organic-rich sediments within the "Hauptdolomit" formation (Triassic, Norian) of the Northern Calcareous Alps. *Org. Geochem.* **13**, 377-386.
- Rohmer M., Bissere P. and Neunlist S. (1993) The hopanoids, prokaryotic triterpenoids and precursors of ubiquitous molecular fossils. In *Biological Markers in Sediments and Petroleum* (ed. J.M. Moldowan, P. Albrecht and R.P. Philp), Prentice-Hall, Inc., New Jersey, U.S.A., pp. 1-17.
- Schaeffer P., Adam P., Trendel J.-M., Albrecht P. and Connan J. (1995) A novel series of benzohopanes widespread in sediments. *Org. Geochem.* **23**, 87-89.
- Schouten S., Pavlovic D., Sinninghe Damsté J.S. and de Leeuw J.W. (1993) Nickel boride: An improved desulphurizing agent for sulphur-rich geomacromolecules in polar and asphaltene fractions. *Org. Geochem.* **7**, 901-909.
- Sinninghe Damsté J.S., Rijpstra W.I.C., de Leeuw J.W. and Schenck P.A. (1989) The occurrence and identification of series of organic sulphur compounds in oils and sediment extracts: II. Their presence in samples from hypersaline and non-hypersaline palaeoenvironments and possible application as source, palaeoenvironmental and maturity indicators. *Geochim. Cosmochim. Acta* **53**, 1323-1341.
- Sinninghe Damsté J.S., van Duin A.C.T., Hollander D., Kohnen M.E.L. and de Leeuw J.W. (1995) Early diagenesis of bacteriohopanepolyol derivatives: Formation of fossil homohopanoids. *Geochim. Cosmochim. Acta* **59**, 5141-5147.
- Tribovillard N., Gorin G.E., Belin S., Hopfgartner G. and Pichon R. (1992) Organic-rich biolaminated facies from a Kimmeridgian lagoonal environment in the French Southern Jura mountains - A way of estimating accumulation rate variations. *Palaeogeogr., Palaeoclimatol., Palaeoecol.* **99**, 163-177.
- Valisolalao J., Perakis N., Chappe B. and Albrecht P. (1984) A novel sulfur containing C<sub>35</sub> hopanoid in sediments. *Tetrahedron Lett.* **25**, No. 11, 1183-1186.
- Wakeham S.G., Sinninghe Damsté J.S., Kohnen M.E.L. and de Leeuw J.W. (1995) Organic sulfur compounds formed during early diagenesis in Black Sea sediments. *Geochim. Cosmochim. Acta* **59**, 521-533.

# Appendix



## Chapter 8

### The effect of clay minerals on diasterane/sterane ratios.

#### Abstract

To examine the effect of clay minerals on diasterane/sterane ratios, a quantitative study of source rock mineralogy was performed on two sample sets displaying a wide range of diasterane/sterane ratios. Diasterane/sterane ratios were found to be highly dependent on the availability of clay minerals, as revealed by their positive correlation with clay/TOC ratios. This correlation may explain the sometimes high diasterane/sterane ratios in oils derived from carbonate source rocks. Based on the concentrations of regular and rearranged steroids, it is proposed that in the sedimentary environment, diasterenes are partly reduced to diasteranes and partly degraded, in a ratio largely dependent on the availability of clay minerals. It is suggested that the hydrogen atoms required for reduction of the diasterenes are derived from the water in the interlayers of clay minerals.

#### Introduction

Mono- and diunsaturated sterenes are formed from their precursor steroids in an early stage of diagenesis (for a review see de Leeuw and Baas, 1986). Upon further maturation, limited double bond isomerisation and selective hydrogenation affords a mixture of mainly  $\Delta^2$ -,  $\Delta^4$ - and  $\Delta^5$ -sterenes (de Leeuw et al., 1989). These sterenes can be reduced to  $5\beta$ - and  $5\alpha$ -steranes, and the  $\Delta^4$ - and  $\Delta^5$ -sterenes can also be transformed into  $5\beta,14\beta$ -dimethyl-18,19-dinor- $8\alpha,9\beta,10\alpha$ -ster-13(17)-enes ( $\Delta^{13(17)}$ -diasterenes) *via* a backbone rearrangement (Fig. 8.1) (Rubinstein et al., 1975; Peakman and Maxwell, 1988). This backbone rearrangement, which is believed to be catalysed by clay minerals (Rubinstein et al., 1975; Sieskind et al., 1979), proceeds *via* a series of carbocation-alkene interconversions, and with increasing diagenesis, the initially formed 20R  $\Delta^{13(17)}$ -diasterenes undergo isomerisation at C-20, yielding a mixture of 20S and 20R isomers (Mackenzie et al., 1982; Brassell et al., 1984; Peakman et al., 1988). The laboratory hydrogenation of  $\Delta^{13(17)}$ -diasterenes produces mainly  $5\beta,14\beta$ -dimethyl-18,19-dinor- $8\alpha,9\beta,10\alpha,13\beta,17\alpha$ (H)-steranes ( $\beta\alpha$ -diasteranes) and a smaller amount of  $5\beta,14\beta$ -dimethyl-18,19-dinor- $8\alpha,9\beta,10\alpha,13\alpha,17\beta$ (H)-steranes ( $\alpha\beta$ -diasteranes) (Bauer et al., 1985; Sieskind et al., 1995).

Ratios of diasteranes over regular steranes are often used to differentiate between oils from argillaceous and carbonate source rocks. Low diasterane/sterane ratios are associated with anoxic, clay-poor, carbonate source rocks, whilst high ratios are generally found in petroleum derived from source rocks containing abundant clay minerals (Peters and Moldowan, 1993). There are several reports, however, on relatively abundant diasteranes in oils and bitumens of clay-poor limestones (e.g. Palacas et al., 1984; Connan et al., 1985; van Kaam-Peters et al., 1997b). Clark and Philp (1989) stated that in those cases where clay minerals are absent or low, diasterene formation takes place *via* an as yet unknown mechanism.

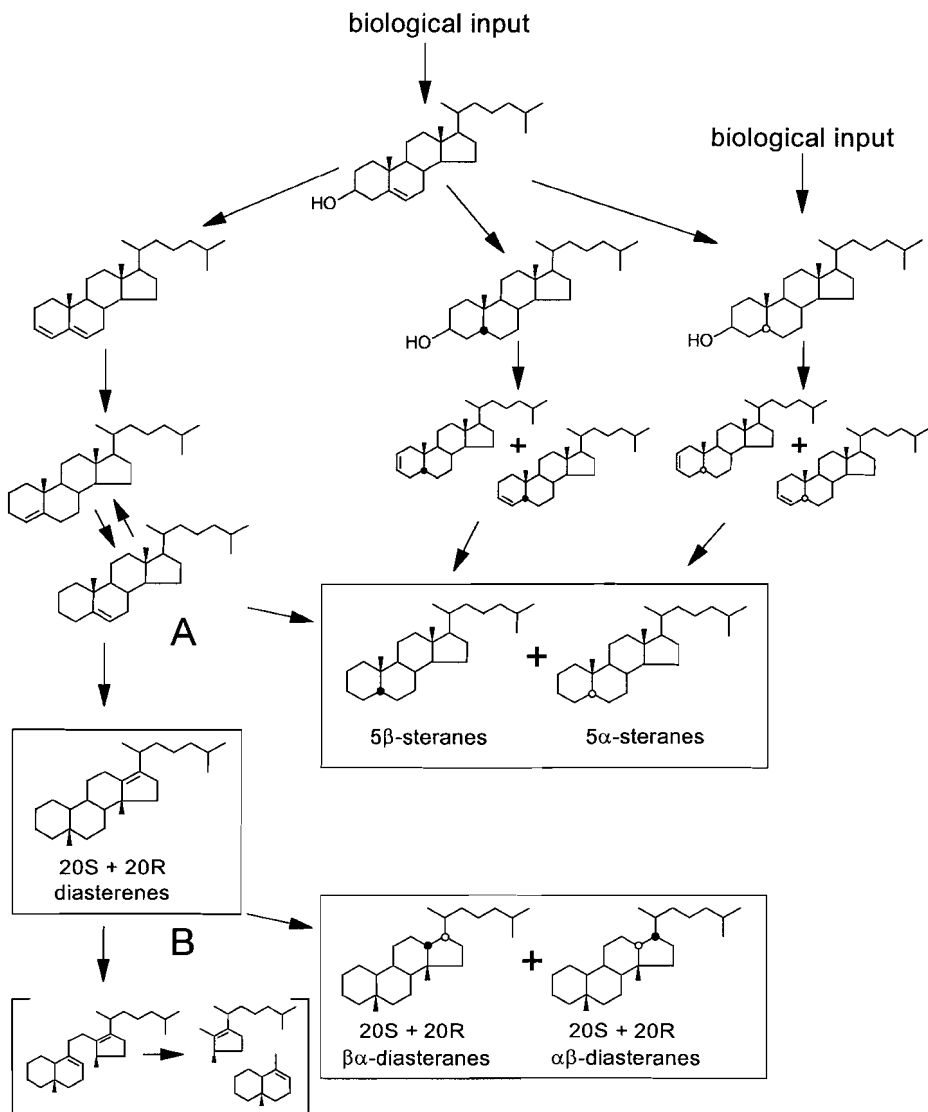


**Fig. 8.1.** Diagenetic pathways of  $\Delta^5$ -sterols and  $5\alpha$ (H)-stanols (partly from de Leeuw et al., 1989). Compounds between brackets are hypothetical and represent degradation products of  $\Delta^{13(17)}$ -diasterenes. A and B refer to branch points mentioned in the text.

In this study, we show that in samples from the Kimmeridge Clay Formation (KCF) in southern England and from Toarcian shales (TS) in southwestern Germany, the diasterane/sterane ratio is poorly correlated with the clay mineral content, but is strongly correlated with the ratio of clay mineral content to organic matter content. Our results may provide an explanation for the anomalously high diasteranes observed in some carbonate-

derived petroleum, and also suggest a major role for clay minerals in the reduction of  $\Delta^{13(17)}$ -diasterenes.

## Experimental

*Extraction and fractionation.* The work-up procedure of both sample sets has been described in detail elsewhere (van Kaam-Peters et al., 1997b,c). In short, the powdered rock samples were Soxhlet extracted using a mixture (7.5:1 v/v) of dichloromethane (DCM) and methanol (MeOH). Asphaltenes were precipitated in *n*-heptane. Maltene fractions of KCF samples were separated over a column packed with alumina by elution with hexane (saturated hydrocarbons), hexane/DCM (9:1 v/v) and DCM/MeOH (1:1 v/v). Maltene fractions of TS samples were separated over a similar column by elution with hexane/DCM (9:1 v/v) and DCM/MeOH (1:1 v/v), after which the hexane/DCM fractions were further separated over a column packed with AgNO<sub>3</sub> impregnated silicagel by elution with hexane (saturated hydrocarbons) and ethyl acetate (stripping). Sterane mixtures in the saturated hydrocarbon fractions were analysed by GC, GC-MS and GC-MSMS.

*Instrumental analyses.* X-ray powder diffraction (XRD), gas chromatography (GC), gas chromatography-mass spectrometry (GC-MS) and gas chromatography-mass spectrometry-mass spectrometry (GC-MSMS) were performed as described by van Kaam-Peters et al. (1997b).

*Molecular data.* Diacholestane/cholestane ratios were determined by integration of the relevant peaks in chromatograms of the *m/z* 372 to 217 transition measured by GC-MSMS. 5 $\alpha$ -Cholestane and  $\Delta^{13(17)}$ -diacholestanes were quantified by integration of their peaks in the *m/z* 217 and *m/z* 257 mass chromatograms, respectively, and comparison with the peak area of the internal standard (3-methyl-6-dideutero-henicosane) in the *m/z* 57 mass chromatogram. Concentrations of 5 $\alpha$ -cholestane and  $\Delta^{13(17)}$ -diacholestanes thus obtained were multiplied by 1.9 and 0.9, respectively, to correct for the different intensities of the fragment ions (determined from mass spectra of non-coeluting peaks).  $\beta\alpha$ -Diacholestanes were quantified by multiplying the (20S+20R  $\beta\alpha$ -diacholestane)/5 $\alpha$ -cholestane ratio by 4.0 (to correct for the different intensities of the 372 to 217 transitions) and by the concentration of 5 $\alpha$ -cholestane. This factor of 4.0 was determined by comparison of the relevant peaks in the GC-MSMS trace to those in the FID trace of sample D2.

*Mineralogical content.* Quartz and pyrite were quantified using XRD with CaF<sub>2</sub> as an external standard. Samples were mixed with 20% CaF<sub>2</sub> and the areas of the standard (111), quartz (101) and pyrite (200) peaks were compared to calibration curves. Carbonate contents of the KCF samples were calculated from TOC of the untreated sediment and TOC of the decalcified (6M HCl) sediment (TOC\*). TOC\* was determined by LECO analysis of a weighed amount of decalcified sediment. Carbonate contents of the TS samples were determined by weighing the powdered rocks before and after decalcification (6N HCl). The clay mineral content was calculated by difference from the amounts of carbonate, quartz,



**Table 8.1.** TOC and mineral contents (wt.%), clay/TOC and biomarker ratios of TS samples.

sample	TOC	carbonate	quartz	pyrite	clay <sup>a</sup>	clay/TOC	diasterane ratio <sup>b</sup>	$\beta\alpha$ -diasterane ratio <sup>c</sup>	20S/(S+R) cholestane	$\beta\beta/\alpha\alpha$ R cholestane <sup>d</sup>
T6	5.8	37	11	5	38	6.6	1.35	1.96	0.40	0.32
T8	3.6	30	12	12	41	11	1.48	2.17	0.40	0.33
T11	2.5	32	10	19	35	14	1.59	2.31	0.40	0.30
T18	10.5	22	14	27	21	2.0	0.63	0.82	0.35	0.21
T23	9.6	31	10	14	31	3.3	0.48	0.60	0.35	0.19
T27	8.4	44	9	16	19	2.3	0.70	0.90	0.36	0.22
T35	8.4	48	7	11	21	2.5	0.94	1.26	0.38	0.23
T39	1.3	82	3	16	neg. <sup>e</sup>	neg.	0.98	1.36	0.38	0.25
T41	9.6	37	7	9	32	3.4	0.87	1.15	0.36	0.23
T45	8.8	35	11	< 2	41	4.6	1.08	1.45	0.37	0.24

<sup>a</sup>  $100 - (\text{carbonate} + \text{quartz} + \text{pyrite} + (1.5 \times \text{TOC}))$

<sup>b</sup>  $(20\text{S}+20\text{R } \beta\alpha\text{- and } \alpha\beta\text{-diacholestane}) / (20\text{S}+20\text{R } 5\alpha\text{-cholestane and } 20\text{S}+20\text{R } 14\beta,17\beta(\text{H})\text{-cholestane})$

<sup>c</sup>  $(20\text{S}+20\text{R } \beta\alpha\text{-diacholestane}) / 5\alpha\text{-cholestane}$

<sup>d</sup>  $(20\text{S}+20\text{R } 14\beta,17\beta(\text{H})\text{-cholestane}) / 5\alpha\text{-cholestane}$

<sup>e</sup> negative value

pyrite and organic matter (OM), assuming that OM equals 1.5 x TOC. Pyrite contents of less than 2% were equated to zero.

## Results

*Sample description.* Lithology and stratigraphic positions of both sample sets are described elsewhere (van Kaam-Peters et al., 1997a,c). In short, the TS samples (T6-T45) originate from a 10 m interval of the Lower Toarcian of the Dotternhausen-Schömberg area in Germany. They consist of marls and shales and one carbonate, with TOC contents up to 10.5% (Table 8.1). The KCF samples (D1-D13) originate from a 60 m interval of the type section in Dorset, and consist of coccolithic limestones, diagenetic carbonates and shales, with TOC contents ranging from 0.6 to 52% (Table 8.2).

*Clay mineralogy.* The clay mineral composition as revealed by XRD, is quite similar in both sample sets. Kaolinite, illite and smectite-illite mixed layer clays are the dominant clay minerals, and except for samples D3 and D8, areas of their base peaks do not significantly differ from each other. In samples D3 and D8, kaolinite is relatively more abundant than in the other samples. In the TS samples also some chlorite is present.

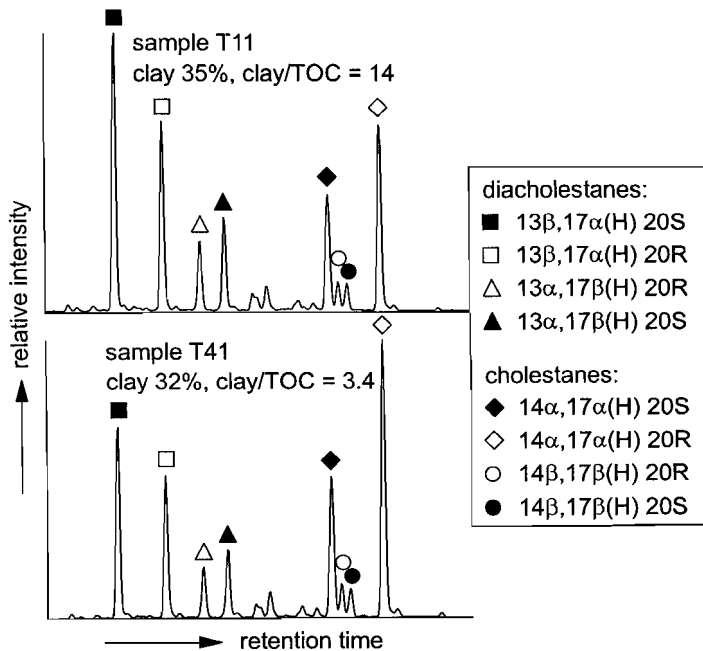


**Fig. 8.2.** GC-MSMS traces ( $m/z$  372  $\rightarrow$   $m/z$  217) showing the distributions of regular and rearranged cholestanes in two TS samples with similar clay contents but different clay/TOC ratios.

**Table 8.2.** TOC and mineral contents (wt.%), clay/TOC and biomarker ratios of KCF samples.

sample	TOC	carbonate	quartz	pyrite	clay <sup>a</sup>	clay/TOC	diasterane ratio <sup>b</sup>	$\beta\alpha$ -diasterane ratio <sup>c</sup>	20S/(S+R) $\Delta^{13(17)}$ -dia <sup>d</sup>	20S/(S+R) $\beta\alpha$ -dia <sup>e</sup>	20S/(S+R) $\alpha\beta$ -dia <sup>f</sup>	$\beta\alpha/(\beta\alpha+\alpha\beta)$ dia <sup>g</sup>
D1	4.5	93	< 1	< 2	< 1	0.1	0.17	0.21	0.44	0.53	0.45	0.74
D2	0.6	76	2	< 2	21	33	0.59	0.69	0.41	0.52	0.47	0.75
D3	7.0	85	1	< 2	3	0.5	0.15	0.20	0.37	0.47	0.44	0.73
D4	24.1	10	11	< 2	43	1.8	0.16	0.15	0.46	0.46	0.54	0.74
D5	18.2	0 <sup>h</sup>	16	< 2	57	3.1	0.29	0.34	0.39	0.50	0.49	0.70
D6	6.2	10	11	< 2	70	11	0.47	0.52	0.41	0.50	0.53	0.72
D7	2.1	86	2	< 2	9	4.5	0.30	0.34	0.42	0.52	0.53	0.75
D8	10.7	71	2	< 2	11	1.0	0.19	0.25	0.42	0.51	0.44	0.76
D9	52.1	17	2	< 2	3	0.1	0.11	0.14	0.38	0.51	0.56	0.75
D10	4.8	22	18	< 2	53	11	0.41	0.47	0.42	0.53	0.45	0.72
D11	10.8	25	12	< 2	47	4.4	0.37	0.41	0.41	0.49	0.51	0.75
D12	3.7	25	13	< 2	56	15	0.47	0.54	0.39	0.50	0.47	0.73
D13	7.4	30	15	< 2	44	5.9	0.37	0.40	0.41	0.50	0.47	0.73

<sup>a</sup> 100 - (carbonate + quartz + pyrite + (1.5 x TOC))

<sup>b</sup> (20S+20R  $\beta\alpha$ - and  $\alpha\beta$ -diacholestane)/(5 $\beta$ - and 5 $\alpha$ -cholestane and 20S+20R 14 $\beta$ ,17 $\beta$ (H)-cholestane)

<sup>c</sup> (20S+20R  $\beta\alpha$ -diacholestane)/5 $\alpha$ -cholestane

<sup>d</sup> 20S/(S+R)  $\Delta^{13(17)}$ -diacholestene

<sup>e</sup> 20S/(S+R)  $\beta\alpha$ -diacholestane

<sup>f</sup> 20S/(S+R)  $\alpha\beta$ -diacholestane

<sup>g</sup>  $\beta\alpha/(\beta\alpha+\alpha\beta)$  diacholestane

<sup>h</sup> XRD indicates some calcite

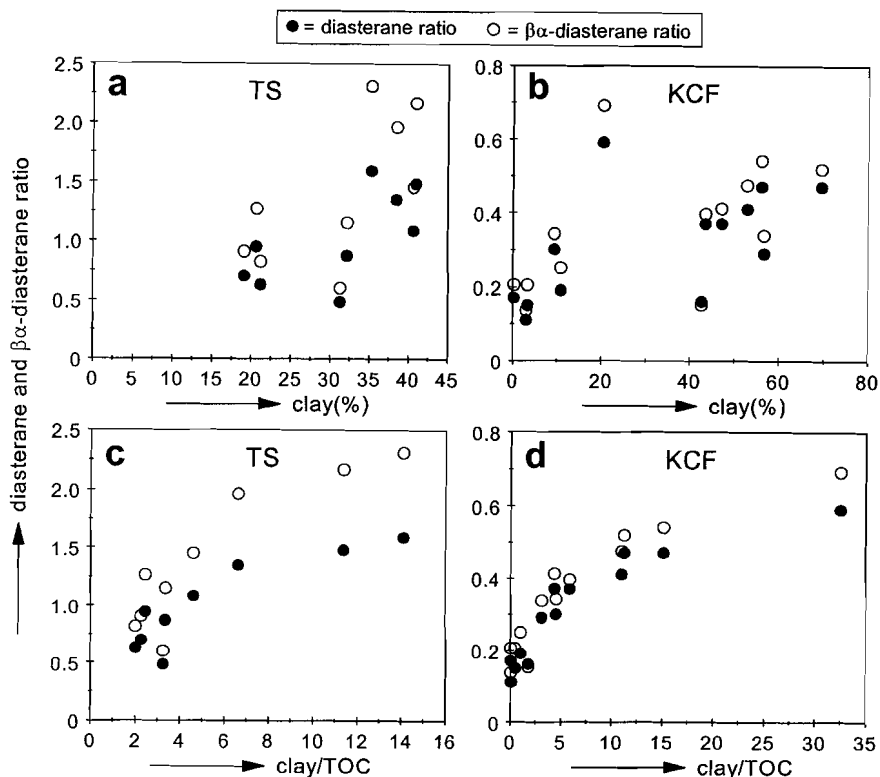


**Fig. 8.3.** Diasterane ratio (diacholestanes/cholestanes) and  $\beta\alpha$ -diasterane ratio ( $20S+20R$   $\beta\alpha$ -diacholestane/ $5\alpha$ -cholestane) as a function of clay content in samples from (a) Toarcian shales and (b) Kimmeridge Clay Formation. Diasterane and  $\beta\alpha$ -diasterane ratios as a function of clay/TOC in samples from (c) Toarcian shales and (d) Kimmeridge Clay Formation. Ratios were determined using GC-MSMS.

**Steroids.** Steroids in the hexane fractions of the TS samples are dominated by  $20S+20R$   $5\alpha,14\alpha,14\alpha(H)$ -steranes and  $20S+20R$   $\beta\alpha$ -diasteranes (e.g. Fig. 8.2).  $5\alpha,14\beta,14\beta(H)$ -steranes and  $\alpha\beta$ -diasteranes are present as well.  $\Delta^{13(17)}$ -diasterenes, which, following the fractionation scheme for the TS samples, end up in the ethyl acetate fraction, are absent. The  $20S/(S+R)$  ratios of  $\beta\alpha$ -diacholestane and  $\alpha\beta$ -diacholestane amount to  $0.58 \pm 0.01$ , and the  $(\beta\alpha)/(\beta\alpha+\alpha\beta)$  diacholestane ratios are constant at  $0.73 \pm 0.01$ . The  $20S/(S+R)$  and  $\beta\beta/\alpha\alpha R$  ratios of cholestane range from 0.35 to 0.40, and from 0.19 to 0.33, respectively (Table 8.1).

Steroids in the hexane fractions of the KCF samples are dominated by  $20R$   $5\alpha,14\alpha,17\alpha(H)$ -steranes,  $20S+20R$   $\Delta^{13(17)}$ -diasterenes, and  $20S+20R$   $\beta\alpha$ -diasteranes. Other steroids consist of  $5\beta,14\alpha,14\alpha(H)$ -steranes,  $5\alpha,14\beta,14\beta(H)$ -steranes and  $\alpha\beta$ -diasteranes. The  $20S/(S+R)$  ratios of  $\Delta^{13(17)}$ -diacholestene,  $\beta\alpha$ -diacholestane and  $\alpha\beta$ -diacholestane fall in the ranges 0.37-0.46, 0.46-0.53 and 0.44-0.56, respectively (Table 8.2). The  $\beta\alpha/(\beta\alpha+\alpha\beta)$  diacholestane ratio varies between 0.70 and 0.76.

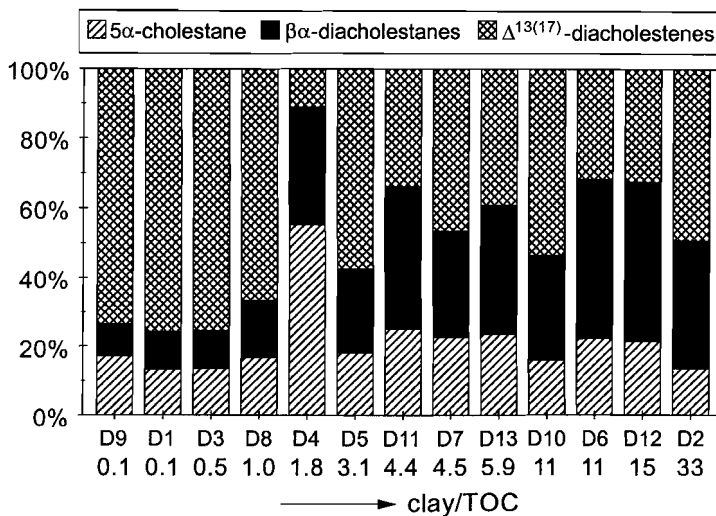


**Fig. 8.4.** Relative proportions of 5α-cholestane, 20S+20R βα-diacholestane and 20S+20R Δ<sup>13(17)</sup>-diacholestene in the KCF samples.

In both sample sets, the ratio of all rearranged cholestanes over all regular cholestanes, hereafter referred to as diasterane ratio, is not evidently correlated with clay content (Figs. 8.3a,b). However, diasterane ratios show a clear, positive correlation with clay/TOC ratios (Figs. 8.3c,d). In the TS samples, diasterane ratios are generally higher than in the KCF samples. For both sample sets also βα-diasterane ratios were determined, which are defined as (20S+20R βα-diacholestane)/5α-cholestane (Tables 8.1, 8.2). In general, βα-diasterane ratios are somewhat higher than diasterane ratios, and the difference between the two increases with increasing clay/TOC (Figs. 8.3c,d).

The relative abundance of Δ<sup>13(17)</sup>-diacholestenes in the KCF samples is consistently highest in samples with clay/TOC ratios of 1.0 and less (Fig. 8.4). There is no correlation between clay/TOC ratios and the relative abundance of Δ<sup>13(17)</sup>-diacholestenes in the other KCF samples.

## Discussion

The relatively wide range of diasterane ratios in lithologically similar samples of the TS has been ascribed to differences in the acidity and redox potential of the depositional environment (Moldowan et al., 1986). The positive correlation between the diasterane ratio and the clay/TOC ratio in the TS and KCF sample sets (Fig. 8.3c,d), however, indicates that different diasterane ratios in lithologically similar samples, can also be explained by differences in the availability of clay minerals. This availability, however, is not a matter of high or low clay mineral content, but of the amount of clay minerals relative to the amount of organic matter. In fact, the good correlation between the clay/TOC and diasterane ratios<sup>1</sup>

<sup>1</sup> Although this is only shown for C<sub>27</sub> steranes, a similar correlation exists for the higher homologues.

demonstrates that the formation of diasteranes is very sensitive to the presence of clay minerals. Moreover, it explains the high diasterane ratios in some of the carbonates (Tables 8.1, 8.2), and possibly also the anomalously high diasterane ratios in carbonate derived oils and extracts reported by others (e.g. Palacas et al., 1984; Connan et al., 1985).

In several downhole sequences of deep sea sediments, a gradual conversion of  $\Delta^4$ - and  $\Delta^5$ -sterenes to 20S and 20R  $\Delta^{13(17)}$ -diasterenes has been observed (Brassell et al., 1984). Therefore, the absence of  $\Delta^4$ - and  $\Delta^5$ -sterenes and the coexistence of steranes, diasterenes and diasteranes in the KCF samples, probably reflect a stage of diagenesis in which  $\Delta^{13(17)}$ -diasterenes are being transformed into diasteranes. The logical consequence would be that samples with high diasterane ratios (and high clay/TOC ratios) show relatively small amounts of diasterenes, and *vice versa*. However, this is certainly not so for samples with clay/TOC ratios of more than 1 (Fig. 8.4). Also, if all diasterenes in the KCF would ultimately end up as diasteranes, the resulting diasterane ratios would not at all exhibit a relationship with clay/TOC, in contrast to the data of the TS samples ( $\Delta^{13(17)}$ -diasterenes absent, and positive correlation between clay/TOC and diasterane ratios). Clay mineral composition is rather constant and can be excluded as a major factor influencing compound distributions. Therefore, it is suggested that during diagenesis, part of the  $\Delta^{13(17)}$ -diasterenes is hydrogenated and part is degraded (Fig. 8.1), in a ratio largely dependent on the clay/TOC ratio. The positive correlation between clay/TOC and diasterane ratios can then be understood as follows:

In many sediments,  $\Delta^4$ - and  $\Delta^5$ -sterenes are relatively abundant whilst  $\Delta^2$ - and other sterenes are absent or low (de Leeuw et al., 1989). This suggests that  $\Delta^4$ - and  $\Delta^5$ -sterenes are often the major source of 5 $\beta$ - and 5 $\alpha$ -steranes. Consequently, in the absence of diasteranes, the relative proportions of  $\Delta^{13(17)}$ -diasterenes and 5 $\beta$ - and 5 $\alpha$ -steranes are largely determined by the extent to which  $\Delta^4$ - and  $\Delta^5$ -sterenes are hydrogenated or undergo backbone rearrangement (branch point A in Fig. 8.1), and not by the hydrogenation of other sterenes. Since the backbone rearrangement is probably catalysed by clay minerals (Rubinstein et al., 1975; Sieskind et al., 1979), formation of  $\Delta^{13(17)}$ -diasterenes may increase in importance with increasing clay/TOC ratio. Alternatively, only minor amounts of clay minerals are required for rearrangement reactions to occur, and the balance between hydrogenation and backbone rearrangement of  $\Delta^4$ - and  $\Delta^5$ -sterenes largely depends on other sedimentary conditions. In either case, once sterenes are no longer present, the amount of steranes is more or less fixed, and  $\Delta^{13(17)}$ -diasterenes form the only substrate for diasterane formation. In a later stage of diagenesis (branch point B in Fig. 8.1), clay minerals probably participate in the reduction of  $\Delta^{13(17)}$ -diasterenes, possibly by donation of protons released by the dissociation of interlayer water (cf. Johns, 1979). Part of the  $\Delta^{13(17)}$ -diasterenes is probably degraded and disappears out of the analytical window or is not recognised as being steroidal-derived (Fig. 8.1). Thus, following this diagenetic scheme, diasterane ratios are largely determined by the dimensions of the carbon flows downstream of branch points A and B. The positive correlation between clay/TOC and diasterane ratios will be strongest if during early diagenesis (branch point A) clay minerals favour backbone rearrangement over reduction of  $\Delta^4$ - and  $\Delta^5$ -sterenes, and in a later stage of diagenesis (branch point B) they favour reduction over degradation of  $\Delta^{13(17)}$ -diasterenes. However, if the division of carbon flows at branch point A is more or less

constant, a positive correlation between clay/TOC and diasterane ratios can still be obtained through the reduction/degradation steps at branch point B.

Excluding sample D2, the range of clay/TOC values is similar in both sample sets, yet the range of diasterane ratios is much larger in the TS samples (Figs. 8.3c,d). This is partly explained by the fact that in the KCF samples diasterane formation has not yet been completed. In addition, the range of diasterane ratios ultimately obtained is partly determined by the extent to which  $\Delta^{13(17)}$ -diasterenes are formed (branch point A), and this may differ significantly between the sample sets. It is noted that at very high levels of thermal maturity, steranes may be degraded before diasteranes, leading to anomalously high diasterane ratios (Peters and Moldowan, 1993).

Markedly, the relative abundance of  $\Delta^{13(17)}$ -diasterenes is significantly lower in sample D4 than in the other KCF samples (Fig. 8.4). Also, sample D4 is the only sample in which diasterane ratios are higher than  $\beta\alpha$ -diasterane ratios (Table 8.2). It is tentatively suggested that these differences are related to differences in OM composition. Sample D4 is distinguished from the other KCF samples by its relatively high contents of acyclic isoprenoid hydrocarbons in both bitumen and kerogen (van Kaam-Peters et al., 1997a). This implies the presence in this sample of relatively high amounts of tertiary hydrogen atoms, which can be liberated relatively easily from their carbon skeletons. Thus, in addition to the protons released by the dissociation of water in clay mineral interlayers, protons may be supplied by the isoprenoidal organic matter, thereby facilitating hydrogenation reactions.

The proton-donating ability of clay minerals is known from several studies, and has been associated with hydrocarbon cracking (e.g. Fripiat et al., 1965; Fripiat and Cruz-Cumplido, 1974; Johns, 1979). To our knowledge, however, clay minerals have not yet been reported to function as a hydrogenating agent of sedimentary organic matter. It is recognised that our evidence for partial hydrogenation and partial degradation of  $\Delta^{13(17)}$ -diasterenes is inconclusive, but at present it seems the best way to reconcile the excellent correlation between clay/TOC and diasterane ratios, which cannot be a coincidence, with the 'random' proportions of  $\Delta^{13(17)}$ -diasterenes.

Finally, since the  $\beta\alpha/(\beta\alpha+\alpha\beta)$  diacholestane ratios are constant at  $0.73 \pm 0.01$  in all TS samples, the increasing difference between diasterane and  $\beta\alpha$ -diasterane ratios with increasing clay/TOC (Fig. 8.3c) must be due to differences in the sterane distributions only. Indeed, there are slight positive relationships between the diasterane ratio and the 20S/(S+R) and  $\beta\beta/\alpha\alpha$ R ratios of cholestane (Table 8.2). This suggests that also maturity parameters like 20S/(S+R) and  $\beta\beta/(\beta\beta+\alpha\alpha)$  sterane ratios (Peters and Moldowan, 1993) are sensitive to the availability of clay minerals. An influence of the mineral matrix on the epimerisation of steranes was also reported by Strachan et al. (1989). In the KCF samples, differences between diasterane and  $\beta\alpha$ -diasterane ratios are small, but show a positive correlation with clay/TOC as well (Fig. 8.3d). It could not be established if these differences are due to different sterane distributions, since in many instances, both 14 $\beta$ ,17 $\beta$ (H)-steranes and  $\alpha\beta$ -diasteranes were only slightly above the detection limit.

## Conclusions

1. In two different sets of rock samples, a clear, positive correlation exists between the diasterane ratio and the clay/TOC ratio. This finding provides an explanation for the sometimes anomalously high diasterane ratios in carbonate rocks.
2. Concentrations of regular and rearranged steroids in the KCF samples suggest that with increasing diagenesis,  $\Delta^{13(17)}$ -diasterenes are partly hydrogenated, yielding diasteranes, and partly degraded.
3. Whilst during early diagenesis high clay/TOC ratios may favour backbone rearrangement over reduction of  $\Delta^4$ - and  $\Delta^5$ -sterenes, our data indicate that in a later stage of diagenesis, high clay/TOC ratios favour the reduction of  $\Delta^{13(17)}$ -diasterenes over their degradation. It is suggested that through the dissociation of interlayer water, clay minerals are effective hydrogenating agents of  $\Delta^{13(17)}$ -diasterenes.
4. Maturity parameters like 20S/(S+R) and  $\beta\beta/(\beta\beta+\alpha\alpha)$  sterane ratios are also noticeably influenced by the availability of clay minerals.

**Acknowledgements.** We thank the Netherlands Organization for Scientific Research (NWO) for the PIONIER grant to JSSD and the studentship of HMEvKP. The TS samples were kindly provided by Dr. M. Schoell (Chevron Petroleum Technology Corp., California, USA). We thank M. Dekker and W. Pool (NIOZ), and A. Schulz (TUC) for analytical assistance.

## References

- Bauer P.E., Nelson D.A., Watt D.S., Reibenspies J.H., Anderson O.P., Seifert W.K. and Moldowan J.M. (1985) Synthesis of biological markers in fossil fuels. 4.  $C_{27}$ ,  $C_{28}$ , and  $C_{29}$   $13\beta,17\alpha(H)$ -diasteranes. *J. Org. Chem.* **50**, 5460-5464.
- Brassell S.C., McEvoy J., Hoffmann C.F., Lamb N.A., Peakman T.M. and Maxwell J.R. (1984) Isomerisation, rearrangement and aromatisation of steroids in distinguishing early stages of diagenesis. *Org. Geochem.* **6**, 11-23.
- Clark J.P. and Philp R.P. (1989) Geochemical characterization of evaporite and carbonate depositional environments and correlation of associated crude oils in the Black Creek Basin, Alberta. *Canadian Petroleum Geologists Bulletin* **37**, 401-416.
- Connan J., Bouroullec J., Dessort D. and Albrecht P. (1985) The microbial input in carbonate-anhydrite facies of a sabkha palaeoenvironment from Guatemala: a molecular approach. In *Advances in Organic Geochemistry 1985* (ed. D. Leythaeuser and J. Rullkötter). *Org. Geochem.* **10**, 29-50.
- Fripiat J.J. and Cruz-Cumplido M.I. (1974) Clays as catalysts for natural processes. *Ann. Rev. Earth Planet. Sci.* **2**, 239-256.
- Fripiat J.J., Telli A.M., Poncelet G. and Andre T. (1965) Thermodynamic properties of absorbed water molecules and electrical conduction in montmorillonites and silica. *J. Phys. Chem.* **69**, 2185-2197.
- Johns W.D. (1979) Clay mineral catalysis and petroleum generation. *Ann. Rev. Earth Planet. Sci.* **7**, 183-198.
- van Kaam-Peters H.M.E., Schouten S., Köster J. and Sinninghe Damsté J.S. (1997a) Palaeoclimatic control on the molecular and carbon isotopic composition of organic matter deposited in a Kimmeridgian euxinic shelf sea. *Geochim. Cosmochim. Acta*. Submitted.



- van Kaam-Peters H.M.E., Schouten S., de Leeuw J.W. and Sinninghe Damsté J.S. (1997b) A molecular and carbon isotope biogeochemical study of biomarkers and kerogen pyrolysates of the Kimmeridge Clay Formation: Palaeoenvironmental implications. *Org. Geochem.* Accepted.
- van Kaam-Peters H.M.E., Schouten S., Schoell M. and Sinninghe Damsté J.S. (1997c) Biomarker and compound-specific stable carbon isotope analysis of the Early Toarcian shales in SW Germany. In prep.
- de Leeuw J.W. and Baas M. (1986) Early-stage diagenesis of steroids. In *Biological Markers in the Sedimentary Record* (ed. R.B. Johns), pp. 101-123. Elsevier, Amsterdam.
- de Leeuw J.W., Cox H.C., van Graas G., van de Meer F.W., Peakman T.M., Baas J.M.A. and van de Graaf B. (1989) Limited double bond isomerisation and selective hydrogenation of sterenes during early diagenesis. *Geochim. Cosmochim. Acta* **53**, 903-909.
- Mackenzie A.S., Brassell S.C., Eglinton G. and Maxwell J.R. (1982) Chemical fossils: The geological fate of steroids. *Science* **217**, 491-504.
- Moldowan J.M., Sundararaman P. and Schoell M. (1986) Sensitivity of biomarker properties to depositional environment and/or source input in the Lower Toarcian of SW-Germany. In *Advances in Organic Geochemistry 1985* (ed. D. Leythaeuser and J. Rullkötter). *Org. Geochem.* **10**, 915-926.
- Palacas J.G., Anders D.E. and King J.D. (1984) South Florida Basin - A prime example of carbonate source rocks of petroleum. In *Petroleum Geochemistry and Source Rock Potential of Carbonate Rocks* (ed. J.G. Palacas). *AAPG Studies in Geology* **18**, 71-96.
- Peakman T.M. and Maxwell J.R. (1988) Early diagenetic pathways of steroid alkenes. In *Advances in Organic Geochemistry 1987* (ed. L. Mattavelli and L. Novelli). *Org. Geochem.* **13**, 583-592.
- Peakman T.M., Ellis K. and Maxwell J.R. (1988) Acid-catalysed rearrangements of steroid alkenes. Part 2. A re-investigation of the backbone rearrangement of cholest-5-ene. *J. Chem. Soc. Perkin Trans. I*, 1071-1075.
- Peters K.E. and Moldowan J.M. (1993) *The Biomarker Guide: Interpreting Molecular Fossils in Petroleum and Ancient Sediments*. Prentice Hall, New Jersey.
- Rubinstein I., Sieskind O. and Albrecht P. (1975) Rearranged sterenes in a shale: Occurrence and simulated formation. *J. Chem. Soc., Perkin Trans. I*, 1833-1836.
- Sieskind O., Joly G. and Albrecht P. (1979) Simulation of the geochemical transformations of sterols: superacid effect of clay minerals. *Geochim. Cosmochim. Acta* **43**, 1675-1679.
- Sieskind O., Kintzinger J.P., Metz B. and Albrecht P. (1995) Structure determination of diacholestanes. Their geochemical significance. *Tetrahedron* **51**, 2009-2022.
- Strachan M.G., Alexander R., van Bronswijk W. and Kagi R.I. (1989) Source and heating rate effects upon maturity parameters based on ratios of 24-ethylcholestane diastereomers. *J. Geochem. Explor.* **31**, 285-294.

## Publications

Parts of this thesis have appeared or will appear in the following publications:

- van Kaam-Peters H.M.E. and Sinninghe Damsté J.S., accepted for publication in *Org. Geochem.* (Chapter 2)
- van Kaam-Peters H.M.E., Rijpstra W.I.C., de Leeuw J.W. and Sinninghe Damsté J.S., submitted for publication in *Org. Geochem.* (Chapter 3)
- van Kaam-Peters H.M.E., Schouten S., de Leeuw J.W. and Sinninghe Damsté J.S., accepted for publication in *Org. Geochem.* (Chapter 4)
- van Kaam-Peters H.M.E., Schouten S., Köster J. and Sinninghe Damsté J.S., submitted for publication in *Geochim. Cosmochim. Acta* (Chapter 5)
- van Kaam-Peters H.M.E., Schouten S., Schoell M. and Sinninghe Damsté J.S., manuscript in preparation (Chapter 6)
- van Kaam-Peters H.M.E., Köster J., de Leeuw J.W. and Sinninghe Damsté J.S., *Org. Geochem.* **23**, 607-615 (Chapter 7)
- van Kaam-Peters H.M.E., Köster J., van der Gaast S.J., Sinninghe Damsté J.S. and de Leeuw J.W., manuscript in preparation (Chapter 8)

## Dankwoord

Behalve de laatste paar maanden voor het voltooien van dit proefschrift, waarin mijn dagelijkse bezigheden bijna uitsluitend bestonden uit schrijven, heb ik altijd met veel plezier aan mijn promotie-onderzoek gewerkt. Dit valt voor een deel te verklaren door de liefde voor het vak, maar zeker ook door de prettige samenwerking met vele NIOZ-ers van binnen en buiten de afdeling MBT. Deze pagina wil ik daarom gebruiken om iedereen te bedanken die mijn verblijf op het NIOZ (en de TESO-boot) tot een zowel leerzame als aangename tijd hebben gemaakt.

Lieve Fred, hoewel je altijd liever op de achtergrond blijft, ga ik hier toch enige regels speciaal aan jou wijden. Velen weten waarschijnlijk niet dat ik een aantal malen heb overwogen mijn promotie-onderzoek af te breken vanwege de geringe vooruitzichten op een vaste baan in het wetenschappelijk onderzoek. Jij hebt me altijd gestimuleerd door te gaan, “want dit is wat je leuk vindt”, zei je. Heel erg bedankt daarvoor!

## Curriculum Vitae

Ik ben geboren op 31 mei 1963 in Doesburg. Mijn middelbare schooltijd heb ik doorgebracht op het Pius X College in Beverwijk, waar ik in 1981 het atheneum B diploma behaalde. Na een jaar bouwkunde te hebben gestudeerd aan de Hogere Technische School in Haarlem, besloot ik een hogere beroepsopleiding analytische chemie te volgen aan het Bakhuis Roozeboom Instituut in Beverwijk. Deze opleiding rondde ik af in 1985. Later dat jaar verhuisde ik naar Engeland om Environmental Sciences te gaan studeren aan de University of Southampton. Om in aanmerking te komen voor studiefinanciering was het noodzakelijk om 6 maanden in Engeland te hebben gewerkt. Ik vond een baan als serveerster en begon in 1986 de studie. Vanwege een wijziging in het studiefinancieringsstelsel, was ik genoodzaakt de studie voortijdig te beëindigen. De daarop volgende anderhalf jaar heb ik als chemisch analiste voor een uitzendburo gewerkt (bij het Rijksinstituut voor de Zuivering van Afvalwater in IJmuiden en bij ingenieursburo Oranjewoud in Driehuis). De interesse voor de aardwetenschappen bleef bestaan en zodoende ving ik in 1988 aan met de studie Fysische Geografie en Bodemkunde aan de Universiteit van Amsterdam. In 1989 ben ik getrouwd met Fred van Kaam en werd onze zoon Niels geboren. In 1991 kregen we onze dochter Cinta. In oktober 1992 behaalde ik het doctoraal examen Fysische Geografie en 3 maanden later trad ik in dienst als Onderzoeker in Opleiding bij de vakgroep Organische Geochemie van de Technische Universiteit Delft (thans afdeling Mariene Biogeochemie en Toxicologie van het Nederlands Instituut voor Onderzoek der Zee).